frontiers | Research Topics

Applications of herbal medicine to control cardiovascular disease

Edited by
Rong Lu and Hai-dong Guo

Published in
Frontiers in Pharmacology

ISSN 1664-8714
ISBN 978-2-8325-3014-6
DOI 10.3389/978-2-8325-3014-6

About Frontiers

Frontiers is more than just an open access publisher of scholarly articles: it is a pioneering approach to the world of academia, radically improving the way scholarly research is managed. The grand vision of Frontiers is a world where all people have an equal opportunity to seek, share and generate knowledge. Frontiers provides immediate and permanent online open access to all its publications, but this alone is not enough to realize our grand goals.

Frontiers journal series

The Frontiers journal series is a multi-tier and interdisciplinary set of open-access, online journals, promising a paradigm shift from the current review, selection and dissemination processes in academic publishing. All Frontiers journals are driven by researchers for researchers; therefore, they constitute a service to the scholarly community. At the same time, the *Frontiers journal series* operates on a revolutionary invention, the tiered publishing system, initially addressing specific communities of scholars, and gradually climbing up to broader public understanding, thus serving the interests of the lay society, too.

Dedication to quality

Each Frontiers article is a landmark of the highest quality, thanks to genuinely collaborative interactions between authors and review editors, who include some of the world's best academicians. Research must be certified by peers before entering a stream of knowledge that may eventually reach the public - and shape society; therefore, Frontiers only applies the most rigorous and unbiased reviews. Frontiers revolutionizes research publishing by freely delivering the most outstanding research, evaluated with no bias from both the academic and social point of view. By applying the most advanced information technologies, Frontiers is catapulting scholarly publishing into a new generation.

What are Frontiers Research Topics?

Frontiers Research Topics are very popular trademarks of the *Frontiers journals series*: they are collections of at least ten articles, all centered on a particular subject. With their unique mix of varied contributions from Original Research to Review Articles, Frontiers Research Topics unify the most influential researchers, the latest key findings and historical advances in a hot research area.

Find out more on how to host your own Frontiers Research Topic or contribute to one as an author by contacting the Frontiers editorial office: frontiersin.org/about/contact

Applications of herbal medicine to control cardiovascular disease

Topic editors

Rong Lu — Shanghai University of Traditional Chinese Medicine, China

Hai-dong Guo — Shanghai University of Traditional Chinese Medicine, China

Citation

Lu, R., Guo, H.-d., eds. (2023). *Applications of herbal medicine to control cardiovascular disease*. Lausanne: Frontiers Media SA.

doi: 10.3389/978-2-8325-3014-6

Table of contents

frontiers | Frontiers in Pharmacology

TYPE Review
PUBLISHED 30 September 2022
DOI 10.3389/fphar.2022.997598

OPEN ACCESS

EDITED BY
Rong Lu,
Shanghai University of Traditional Chinese Medicine, China

REVIEWED BY
Suresh Kumar,
Punjabi University, India
Agnieszka Barbara,
University of Life Sciences of Lublin, Poland

*CORRESPONDENCE
Yabin Zhou,
zhouyabin@hotmail.com
Zhiping Liu,
liuzhiping@hljucm.net

†These authors have contributed equally to this work and share first authorship

SPECIALTY SECTION
This article was submitted to Ethnopharmacology, a section of the journal Frontiers in Pharmacology

RECEIVED 19 July 2022
ACCEPTED 16 September 2022
PUBLISHED 30 September 2022

CITATION
Meng T, Li X, Li C, Liu J, Chang H, Jiang N, Li J, Zhou Y and Liu Z (2022), Natural products of traditional Chinese medicine treat atherosclerosis by regulating inflammatory and oxidative stress pathways.
Front. Pharmacol. 13:997598.
doi: 10.3389/fphar.2022.997598

Natural products of traditional Chinese medicine treat atherosclerosis by regulating inflammatory and oxidative stress pathways

Tianwei Meng[1†], Xinghua Li[1†], Chengjia Li[1†], Jiawen Liu[1†], Hong Chang[2], Nan Jiang[1], Jiarui Li[1], Yabin Zhou[3*] and Zhiping Liu[4*]

[1]Graduate School, Heilongjiang University of Chinese Medicine, Harbin, Heilongjiang, China, [2]Department of Pharmacy, Baotou Medical College, Baotou, Inner Mongolia, China, [3]Department of Cardiovascular Medicine, First Affiliated Hospital of Heilongjiang University of Chinese Medicine, Harbin, Heilongjiang, China, [4]Respiratoy Disease Department, First Affiliated Hospital of Heilongjiang University of Chinese Medicine, Harbin, Heilongjiang, China

Atherosclerosis (AS) is a prevalent arteriosclerotic vascular disease that forms a pathological basis for coronary heart disease, stroke, and other diseases. Inflammatory and oxidative stress responses occur throughout the development of AS. Treatment for AS over the past few decades has focused on administering high-intensity statins to reduce blood lipid levels, but these inevitably damage liver and kidney function over the long term. Natural medicines are widely used to prevent and treat AS in China because of their wide range of beneficial effects, low toxicity, and minimal side effects. We searched for relevant literature over the past 5 years in databases such as PubMed using the keywords, "atherosclerosis," "traditional Chinese medicine," "natural medicines," "inflammation," and "oxidative stress." We found that the PI3K/AKT, TLR4, JAK/STAT, Nrf2, MAPK, and NF-κB are the most relevant inflammatory and oxidative stress pathways in AS. This review summarizes studies of the natural alkaloid, flavonoid, polyphenol, saponin, and quinone pathways through which natural medicines used to treat AS. This study aimed to update and summarize progress in understanding how natural medicines treat AS *via* inflammatory and oxidative stress-related signaling pathways. We also planned to create an information base for the development of novel drugs for future AS treatment.

KEYWORDS

atherosclerosis, natural medicines, inflammatory factor, receptor, pathological mechanism

Introduction

Atherosclerosis (AS) is a chronic progressive inflammatory disease (Zhu et al., 2018). It is the main pathological basis of cardiovascular and cerebrovascular diseases such as coronary heart disease, myocardial infarction, acute coronary syndrome, and stroke (Marchio et al., 2019). Statistics have indicated that the global population of patients with carotid plaque has increased from 513 to 816 million between 2000 and 2023, and the prevalence of carotid stenosis has increased by 59.13% (Song P. et al., 2020). This is due to population aging, smoking, unhealthy dietary habits, and other factors. According to a recent report from the World Health Organization (WHO), cardiovascular disease remains the leading cause of death worldwide (GBD 2017 DALYs and HALE Collaborators, 2018). Stabilizing and reversing plaque are considered important strategies for treating atherosclerotic cardiovascular disease (ASCVD), and anti-inflammatory and antioxidant strategies have also become mainstream (Steven et al., 2019).

Inflammation and oxidative stress are the important pathological features of ASCVD (Yuan et al., 2019). The occurrence and development of inflammation are closely associated with oxidative stress. Abnormal vasodilation caused by low-density lipoprotein (LDL) produced during oxidative stress is an initiating factor in the inflammatory response of AS. Simultaneously elevated levels of oxidative stress and inflammatory responses mediate damage to the vascular endothelium, which recruits monocytes to differentiate into macrophages, absorbs oxidized low-density lipoprotein (ox-LDL) and slowly transforms into foam cells, which are early signs of AS formation (Varghese et al., 2018; Marchio et al., 2019; Poznyak et al., 2020). Foam cells further propagate and amplify the inflammatory response, stimulating platelet aggregation and adhesion to damaged vascular endothelium. This further promotes the formation of AS plaques.

The inflammatory and oxidative stress responses involved in AS development are associated with abnormalities in several signal transduction pathways. The abnormal regulation of various signaling pathways in the vascular intima leads to atypical expression of inflammatory factors and proinflammatory mediators. These induce the continuous production of reactive oxygen species (ROS) and oxidative stress, and finally forms AS. This article reviews the known inflammatory and oxidative stress-related, phosphatidylinositol 3-kinase/protein kinase B (PI3K/AKT), Toll-like receptor 4 (TLR4), Janus kinase signal transducer and activator of transcription (JAK/STAT), nuclear factor erythroid 2–related factor 2 (Nrf2), mitogen-activated protein kinase (MAPK), and nuclear factor kappa-light-chain-enhancer of activated B cell (NF-κB) signaling pathways that are involved in the pathological process of AS. The structure and function of these pathways and their roles in AS pathogenesis are emphasized herein.

Antiplatelet drugs and statins are currently the most prevalent drugs for the clinical treatment of ASCVD (Kishore et al., 2018). Anakinra and canakinumab both block interleukin (IL)-1β, and tocilizumab blocks IL-6 that are inflammatory factors involved in the occurrence and development of AS and synthetic antioxidants such as probucol reduced cholesterol levels (Chistiakov et al., 2018; Gluba-Brzózka et al., 2021). However, the high cost and side effects of long-term drugs presently on the market and synthetic drugs under development have clarified that suitable alternatives are urgently needed. Traditional Chinese medicine (TCM) has a history of thousands of years, and it plays a key role in the prevention and treatment of cardiovascular diseases. Natural medicines including TCM have the advantages of low toxicity and side effects and are widely applicable. However, TCM also has the characteristics of multiple components and targets that function concurrently or synergistically in the treatment of diseases. However, the complex mechanisms of these components and targets are difficult to fully explain, and systematic reviews of the relevant pathways of natural products with which to treat AS are scant. We searched the PubMed, SciFinder, and Web of Science databases. Here, we summarize the inflammatory and oxidative stress signaling pathways involved in the pathological process of AS, and systematically review current progress in natural products that can treat AS through acting on these pathways. The advantages and disadvantages of the experimental design of natural TCM products acting on AS is discussed, and in-depth insights are provided for followup investigation.

Classical signaling pathway

The occurrence and development of AS are affected by processes such as the inflammatory response, oxidative stress, hemodynamics, cholesterol metabolism, angiogenesis, and foam cells. Abnormal activation of different signaling pathways directly or indirectly interferes with different AS stages. Here, we summarize the inflammatory and oxidative stress pathways involved in AS. Understanding the factors and pathways that contribute to AS pathology can inform future experimental and clinical studies. Figure 1 shows a schema of the signaling pathways.

PI3K/AKT signaling pathway

The signaling pathway consists of PI3K and its downstream molecule, PKB/AKT (Qin et al., 2021). Various extracellular signals trigger intracellular P13K to activate PKB/AKT, and AKT is a major downstream molecule of the PI3K signaling pathway (Zhao et al., 2021) that functions in promoting metabolism, proliferation, survival, growth, and angiogenesis. Activation of the PI3K/AKT signaling pathway inhibits the

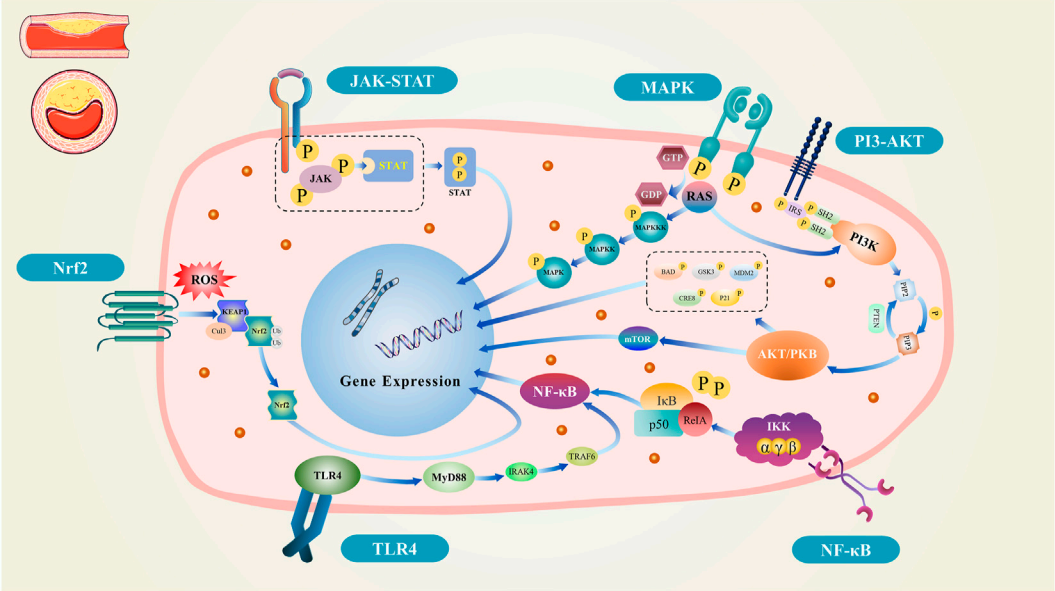

FIGURE 1
Schematic diagram of the signal pathway.

expression of proinflammatory factors caused by NF-κB and transforms the phenotype of microglia from pro, to anti-inflammatory. This activated pathway inhibits neuroinflammation mediated by proinflammatory microglia and attenuates inflammatory responses (Xu et al., 2018). In contrast, activated AKT further activates Nrf2, prevents Kelch-like ECH-associated protein 1 (Keap1) from coupling with it, promotes antioxidant response element (ARE) binding to it, and enhances the expression of antioxidant proteins (Li J. et al., 2021).

Phosphatidylinositol 3-kinase/protein kinase B (PI3K/AKT) signaling pathways mainly influence the development of AS by regulating inflammatory immunity and chemokines. The PI3K/AKT signaling pathway mediates dendritic cells to intervene in immune responses, thereby initiating inflammatory immunity (Monaci et al., 2021). Chemokines are also affected by the PI3K/AKT signaling pathway, prompting inflammatory cell activation and the regulation of macrophage polarization. The activation of inflammatory cells is significantly attenuated or disappears in macrophages without PI3K. Macrophages with AKT2-knockout have decreased levels of inflammatory factors, decreased cell migration ability, and foam cell formation, as well as increased cholesterol efflux. This leads to macrophage polarization towards the M2 type, which enhances plaque stability (Graves and Milovanova, 2019). The PI3K/AKT signaling pathway is also involved in lipid metabolism in endothelial cells. Inhibiting the PI3K/AKT signaling pathway reduces lipid deposition in vascular smooth muscle cells (VSMCs), increases lipid efflux, improves blood lipid metabolism disorders, and reduces the probability of plaque formation (Pi et al., 2021). Activation of the PI3K/AKT signaling pathway inhibits VSMC migration and reduces platelet adhesion. These results are attributed to the regulation of many important platelet responses by PI3K and its downstream effector AKT, such as changes in platelet shape, irreversible platelet aggregation, and increased thrombus volume (Sun et al., 2018).

TLR4 signaling pathway

As an important pattern recognition receptor of the Toll-like receptor (TLR) family involved in the inflammatory response, TLR4 is distributed in vascular endothelial cells, neutrophils, mononuclear macrophages, pancreatic islet endocrine cells, cardiomyocytes, and dendritic cells. All of these cells can form a bridge between innate and acquired immunity (Vijay, 2018). After TLR4 binds to specific ligands, it transmits stimulatory signals to the nucleus by activating a series of downstream protein cascades. This series of signal transductions promotes the activation of various immune response genes namely, nuclear factor kappa B (NF-κB), transcription factor complex activator protein-1 (AP-1), and interferon regulatory factors (IRFs) and induces the expression of various cytokines and adhesion molecules associated with the inflammatory response. This has become recognized as a pathogenic mechanism of AS (Kim et al., 2018). Oxidative stress and cellular damage activate TLR4, leading to the expression of inflammatory mediators (Zhu et al., 2021).

Toll-like receptor 4 (TLR4) has numerous ligands that are involved in the formation and development of AS. Lipopolysaccharide (LPS) upregulates the expression of lectin-like oxidized low-density lipoprotein receptor-1 (LOX-1) through the TLR4 signaling pathway, prompting macrophages to engulf oxidized lipids and convert them into foam cells that aggregate and increase plaque areas. In addition, LPS is involved in degradation of the extracellular matrix and weakening of the fibrous cap, which increases plaque instability and promotes plaque rupture (Jongstra-Bilen et al., 2017; Ciesielska et al., 2021). Oxidized LDL upregulates matrix metalloproteinase-9 (MMP-9) through the TLR4 signaling pathway, prompting macrophages to express a series of inflammatory factors and accelerate plaque rupture (Li T. et al., 2021). Furthermore, TLR4 downregulates the expression of ATP-binding cassette transporter G (ABCG1) and induces lipid accumulation and the infiltration of inflammatory cells into vascular smooth muscle, thereby mediating AS formation (Cao et al., 2018). Therefore, as a mediator of lipid metabolism, immune response, and chronic inflammation, a TLR4 deficiency significantly reduces the expression of proinflammatory factors while reducing lipid and macrophage components in AS plaques.

JAK/STAT signaling pathway

The Janus kinase-signal transducer and activator of transcription (JAK/STAT) signaling pathway is an essential multifunctional cascade of cytokine and growth hormone receptor signals (Owen et al., 2019). It is involved in regulating gene expression and cellular physiological processes. Janus kinase binds to extracellular transmembrane receptors and cytokines, consequently promoting JAK activation and tyrosine phosphorylation. Activated JAK binding to its receptor activates signal transducers and transcriptional activators in the cytoplasm, resulting in the tyrosine phosphorylation of STAT and the formation of homologous or heterologous dimers in the nucleus. Janus kinase then binds to the DNA sequence of the target gene promoter in the nucleus for specific gene expression (Herrera and Bach, 2019; Xu et al., 2020).

The JAK/STAT signaling pathway can mediate AS formation from various aspects, such as vascular endothelial cell (VEC) dysfunction, vascular smooth muscle (VSMC) proliferation and migration, and inflammatory cell infiltration (Hossain et al., 2021). The activation, proliferation, and migration of endothelial cells are the basis for the generation of new blood vessels, and immature new blood vessels can lead to AS plaque instability and even rupture. The proliferation and migration of endothelial cells is completed by the induction of vascular endothelial growth factor (VEGF), and the JAK/STAT signaling pathway is the main pathway of intracellular VEGF signaling (Bernal et al., 2021). Inhibiting this pathway can reverse VSMC proliferation and migration into a static state and inhibit the synthesis of many inflammatory mediators. Additionally, JAK/STAT signaling molecules are have been identified in AS plaques and inflammation-stimulated vascular cells. A lack of STATs in vascular endothelial cells or inflammatory cells can inhibit AS plaque formation (Tang et al., 2020). Inhibiting the JAK/STAT signaling pathway can antagonize LPS-induced AS (Hashimoto et al., 2020). Suppressors of cytokine signaling (SOCS) in the JAK/STAT pathway reduce STAT activity and inhibit subsequent proinflammatory responses. Moreover, SOCS can combine with various inflammatory factors to limit the inflammatory response of the vascular intima, thus inhibiting the occurrence of AS (Lopez-Sanz et al., 2018).

Nrf2 signaling pathway

The nuclear transcription factor Nrf2 contains seven domains (Neh1, Neh2, Neh3, Neh4, Neh5, Neh6 and Neh7) and is ubiquitous in organs that consume oxygen. It regulates various antioxidant protein genes (Alam et al., 2017) and the activities of various antioxidant enzymes through the antioxidant damage pathway. These antioxidant enzymes protect cells by reducing oxidative stress damage and inflammatory responses in several ways (He et al., 2020).

As a central regulator of intracellular redox homeostasis, the Nrf2 signaling pathway maintains a balanced intracellular redox process, which is crucial for anti-AS as well as cardiovascular and cerebrovascular protection (Chen and Maltagliati, 2018). Deletion Nrf2 or its disordered activation aggravates the cytotoxicity of oxidative stressors, cause oxidative damage to the vascular wall, and eventually leads to AS (Alonso-Piñeiro et al., 2021). The formation of AS not only damages the arterial vascular endothelium, but also destabilizes homeostasis of the intracellular milieu (Saha et al., 2020). Furthermore, lipid accumulation in the arterial intima recruits numerous inflammatory cells to the vascular endothelium, leading to the sustained production of cytokines and reactive oxygen species (ROS). The Nrf2 signaling pathway protects vascular endothelial cells from oxidative stress damage, participates in the regulation of macrophages, reduces intracellular lipid accumulation, and inhibits foam cell formation (Robledinos-Antón et al., 2019). Therefore, the Nrf2 signaling pathway exerts antioxidant action by protecting the vascular endothelium, reducing lipid accumulation, and inhibiting inflammation, thus diminishing AS development.

MAPK signaling pathway

The important MAPK signaling pathway mediates extracellular signals and reaction information transmission between cells and nuclei. This pathway mainly comprises extracellular signal-regulated kinase (ERK), c-Jun N-terminal

protein kinase (JNK), and p38 mitogen-activated protein kinase (p38MAPK) (Zhang L. et al., 2019). The hub of this signaling pathway is MAPK that when activated, phosphorylates nuclear transcription factors, cytoskeletal proteins, and enzymes. Activation of the MAPK signaling pathway is associated with the release of various inflammatory cytokines and oxidative stress and it is mainly involved in the cellular inflammatory response and apoptosis under stress (Guo et al., 2021).

Atherosclerosis is closely associated with activation of the MAPK signaling pathway. This pathway is affected by oxidative stress-mediated endothelial dysfunction and the expression of proinflammatory factors that affect the occurrence and development of AS. When the MAPK signaling pathway is activated by ox-LDL, MAPK phosphorylation in the blood produces abundant ROS, which promote the MAPK signaling pathway to induce monocyte accumulation in the arterial wall, reduce the secretion of collagen and other matrices by vascular smooth muscle cells, and elicit cytotoxicity (Gong et al., 2019). This leads to foam cell necrosis in vascular plaque, resulting in AS plaque fragmentation and the eventual formation of thrombus in blood vessels. Therefore, blocking the ROS/MAPK signaling pathway is one mechanism through which oxidative stress-mediated endothelial dysfunction is alleviated and foam cell formation is prevented (Geng et al., 2018; Fang et al., 2021). The activation of MAPK is driven by inflammation. Stimulation of intermittent hypoxia/reoxygenation (IHR) can activate the MAPK pathway in endothelial cells and induce the expression of proinflammatory cytokines (Ryan et al., 2007). Conversely, specific MAPK inhibitors reduce the IHR-induced expression of proinflammatory factors. Intervention in the MAPK signaling pathway can also modulate the degree of intimal proliferation, platelet activation, and apoptosis (Jeon et al., 2021), all of which are key factors in AS formation.

NF-κB signaling pathway

The NF-κB transcription factor family comprises homodimeric or heterodimeric subunits of the Rel family, including Rel (p65), NF-κB1 (p50), NF-κB2 (p52), RelB, and c-Rel. Activation of the IκB kinase (IKK) complex initiates NF-κB pathway signals (Mulero et al., 2019; Poma, 2020). Under the action of inflammatory factors, NF-κB, which is a normal cytoplasmic component, is transferred to the nucleus where it binds to the κB sequence in the promoter region of the relevant target gene sequence and induces the expression of proinflammatory cytokines, adhesion molecules, chemokines, matrix metalloproteinases, and acute-phase proteins associated with inflammation (Mitchell and Carmody, 2018).

Nuclear factor-kappa B is the most widely studied key regulator of inflammatory responses, as it participates in the initiation and development of AS lesions and plays a key role in the disease process. It participates in all stages of AS, from plaque formation to rupture, by regulating the activation of endothelial cells and the expression of proinflammatory factors (Zhong et al., 2018). Nuclear

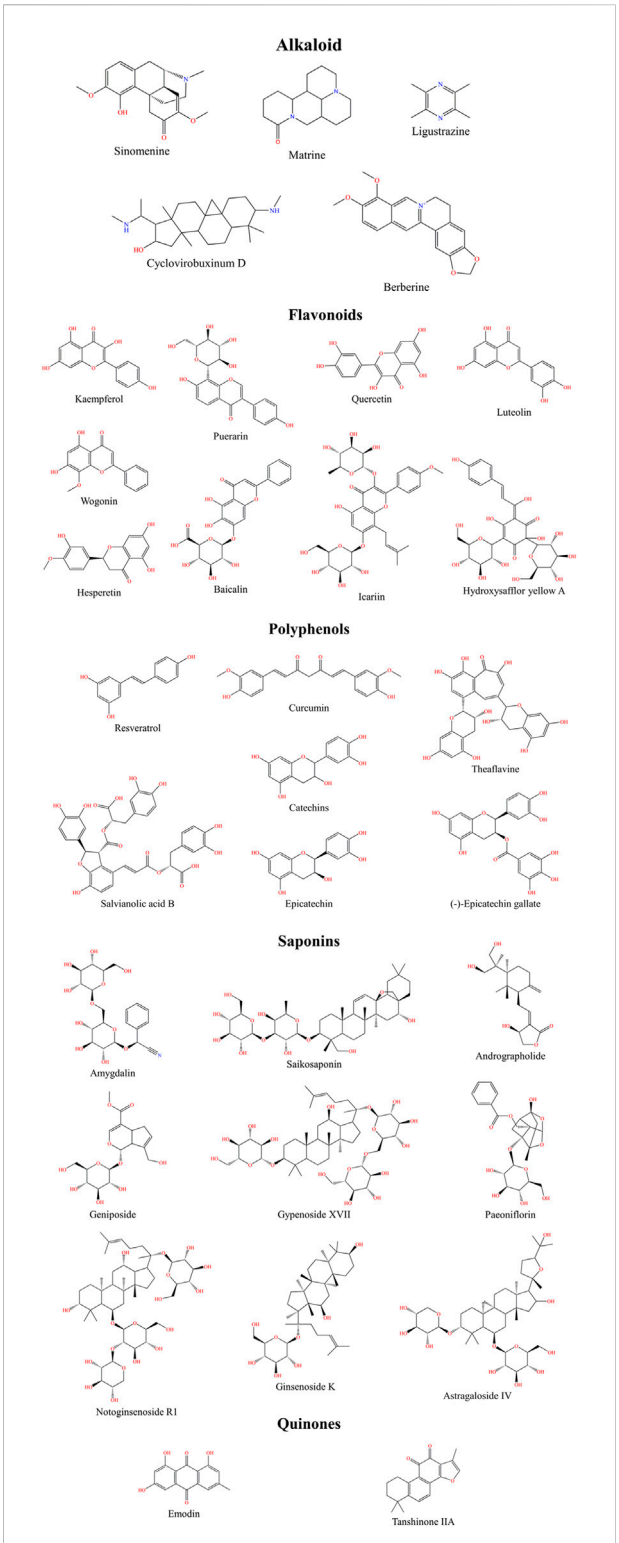

FIGURE 2
Natural medicine chemical structural formula.

factor-kappa B accelerates the growth of lipid plaques and promotes inflammatory responses by regulating the expression of cytokines such as IL-1β, tumor necrosis alpha (TNF-α), and interferon gamma (INF-γ) (Chen et al., 2018). The NF-κB signaling pathway regulates the invasion and colonization of inflammatory cells in vascular walls, changes the composition of the extracellular matrix, and promotes the migration of smooth muscle cells (Zhang Q. et al., 2021). Nuclear factor-kappa B is also an oxidative stress-sensitive transcription factor. Intracellular ROS directly mediate the upregulation of NF-κB. After IκB is phosphorylated, activated NF-κB enters the nucleus and initiates inflammatory responses (Wu et al., 2018a). These directly lead to the inflammatory and pro-apoptotic responses of vascular endothelial cells, which drive the progression of AS.

Natural medicines for atherosclerosis

Traditional Chinese Medicines are natural and offer unique advantages for treating cardiovascular diseases. They regulate lipid metabolism, resist lipid peroxidation, inhibit the proliferation and migration of VSMCs, are anti-inflammatory and anticoagulant, and protect vascular endothelial cells. TCMs can block the occurrence and development of AS through different signaling pathways. Therefore, we reviewed the effects and mechanisms of various natural medicines on AS from the perspectives of anti-inflammatory and antioxidant properties. Figure 2 shows the chemical structure of a natural medicine.

Alkaloids

Alkaloids are a ubiquitous class of organic compounds containing nitrogen and have complex cyclic structures, and alkaline properties (Ghorbani et al., 2021). Alkaloids are divided structurally into piperidines, isoquinolines, quinolone alkaloids, indoles, terpenes, and steroids. Alkaloids are the active components of many Chinese herbal medicines, due to their powerful antitumor, anti-inflammatory, antibacterial, antiviral, and insecticidal properties. Some of them have been applied to treat cardiovascular diseases (Liu et al., 2019). For example, Cyclovirobuxinum D extracted from the TCM plant *Buxus sinica var. Parvifolia* M. Cheng can protect blood vessels and the heart by activating the JAK/STAT signaling pathway, reducing nitric oxide (NO) release and intracellular NO (iNOS) expression, and inducing macrophages to participate in the initiation and regulation of immune inflammation (Guo et al., 2014). Matrine inhibits the NF-κB/MAPK signaling pathway and the production of ROS in human aortic smooth muscle cells (HASMCs), which subsequently decreases the expression of inflammatory TNF-α(Wang et al., 2021). Matrine can inhibit activation of the TLR4 signaling pathway, promote macrophage polarization towards M2, and reduce the expression of elevated DNA methyltransferase in macrophages. This further inhibits oxidative stress, which slows AS progression (Cui et al., 2022). Sinomenine extracted from the TCM *Sinomenium acutum* (Thunb.) Rehder&E.H.Wilson regulates lipid metabolism, reduces intracellular cholesterol levels, alters TLR4 and NF-κB signaling pathways, downregulates the expression of inflammatory factors, and inhibits oxidative stress and vascular inflammation (Geng et al., 2021). Ligustrazine significantly expression TLR4 inhibits in blood vessels (Yang L. et al., 2021) and block the activation and nuclear translocation of NF-κB and Nrf2(Li Y. et al., 2019), consequently inhibiting monocyte adhesion to the endothelium. Ligustrazine simultaneously affects platelet aggregation, secretion, and adhesion by inhibiting the PI3K/AKT pathway, thus exerting an anti-platelet activation effect (Li L. et al., 2019). Berberine promotes intimal growth repair and reduces or stabilizes plaques, which is associated with mobilizing arterial intimal inflammatory and immune factors to regulate the PI3K/AKT signaling pathway (Song and Chen, 2021).

Flavonoids

Many plants produce flavonoids as secondary metabolites. Flavonoids have a benzo-γ-pyranone parent nucleus and comprise isoflavones, flavanones, flavanols, and cyanidin chlorides according to their chemical structures (Badshah et al., 2021; Wen et al., 2021). Flavonoids have antioxidant, anti-inflammatory, and anticancer properties, and protect the cardiovascular system (Ciumărnean et al., 2020). Kaempferol reduces ox-LDL and inhibits intracellular ROS production Therefore, activation of the G protein-coupled estrogen receptor (GPER) and PI3K/AKT/Nrf2 pathways is enhanced, which in turn inhibits inflammation and apoptosis, reduces lipid levels and restores vascular morphology (Feng et al., 2021). Quercetin blocks expression of the NF-κB signaling pathway by inhibiting the upregulation of VCAM-1, ICAM-1, and E-selectin in HASMCs. It prevents the chemotaxis of endothelial cells to monocytes and their adhesion, protects endothelial cells, and delays the occurrence and development of AS (Chen et al., 2020). Puerarin is a hydroxyisoflavonoid extracted from the TCM *Puerariae Lobata* (Willd.) Ohwi. It activates the PI3K/AKT/eNOS signaling pathway and simultaneously inhibits the NF-κB signaling pathway, resulting in downregulated tissue factor (TF) expression in human umbilical vein endothelial cells (HUVECs), and ultimately inhibiting thrombosis (Deng et al., 2017). Icariin inhibits ROS generation by inhibiting the NF-κB/MAPK signaling pathway and upregulating the activity of the Nrf2 signaling pathway, thus inhibiting the transcription of cell adhesion factors and

chemokines. This mechanism inhibits the inflammatory response and antioxidative stress by significantly reducing the expression of factors and inhibiting plaque formation in blood vessels (Hu et al., 2016; Luo et al., 2022). Luteolin exerts anti-AS effects by downregulating expression of the cytokines VCAM-1 and TNF-α, thus reducing oxidative stress and inflammatory response. This is associated with its inhibition of the TNF-α-mediated feedback system and downregulation of the NF-κB/MAPK pathway (Xia et al., 2014; Jia et al., 2015). The main extract of the TCM *Carthamus tinctorius* L. is Hydroxysafflower yellow A, which inhibits the formation of foam cells, reduces the inflammation of blood vessel walls, maintains the integrity of the structure and function of endothelial cells, and inhibits platelet aggregation. These mechanisms are achieved by regulating the TLR4 signaling pathway, oxidative stress, and lipid metabolism (Xue et al., 2021). Baicalin (Wu et al., 2018b), wogonin (Wu et al., 2019), and hesperitin (Olumegbon et al., 2022) inhibit plaque formation *via* anti-inflammatory and anti-oxidative stress mechanisms, and play roles in protecting blood vessels.

Polyphenols

Polyphenolic compounds are a diverse group of plant components with several phenolic hydroxyl groups in their molecular structures, including flavonoids, tannins, phenolic acids, and anthocyanins (Singla et al., 2019). Polyphenols have anti-inflammatory and antioxidant capabilities that help to treat cardiovascular diseases (Fraga et al., 2019). Resveratrol is a natural cardioprotective polyphenol (Cheng et al., 2020) that acts on many of the pathways described herein to inhibit lipid peroxidation, antiplatelet aggregation, and inflammation (Pan et al., 2016; Zhang M. et al., 2019; Chen et al., 2022; Ji et al., 2022). Curcumin, extracted from *Curcuma longa* L, downregulates levels of proteins associated with the NF-κB signaling pathway by inhibiting the synthesis of cellular proteins required for cytomegalovirus replication. This results in proinflammatory cytokine inhibition and enhanced antioxidant enzyme activity. Curcumin also reduces lipid deposition and cardiovascular inflammatory damage (Lv et al., 2020). Theaflavine increases the activity of various antioxidant enzymes, reduces the activity of monoamine oxidases (MAO) and the lipid peroxide malondialdehyde (MDA), and upregulates the Nrf2 signaling pathway in vascular endothelial cells. This mechanism protects HUVECs from cholesterol-induced oxidative damage and inhibits AS plaque formation and changes in aortic histology (Zeng et al., 2021). Salvianolic acid B attenuates ox-LDL or LPS-induced inflammatory cytokines in cells and improves lipid deposition in the aorta. This is achieved by inhibiting phosphorylation of the MAPK/NF-κB signaling pathway (Zhang et al., 2022b). Catechin (Starzonek et al., 2019), epicatechin (Morrison et al., 2014) and (-)-epicatechin gallate extracted from the leaves of *Camellia sinensis* (L.) Kuntze help to stabilize AS plaques through the NF-κB signaling pathway and (-)-epicatechin gallate regulates lipid metabolism and improves foam cells through the MAPK/TLR4 signaling pathway (Li W. et al., 2021).

Saponins

Triterpenoid and steroidal saponins are glycosides that are ubiquitous in plants and have antitumor, anti-inflammatory, immunomodulatory, antiviral, and antifungal properties (Juang and Liang, 2020; Yang Y. et al., 2021). Ginsenoside K regulates the expression of macrophage scavenger receptor class A1 (SR-A1), ATP Binding Cassette Subfamily A Member 1 (ABCA1), and ATP Binding Cassette Subfamily G Member 1 (ABCG1) through the NF-κB/MAPK signaling pathway, reduces lipid accumulation in macrophages, inhibits the transformation of macrophages to foam cells, and blocks ox-LDL-induced inflammatory responses and foam cell formation (Lu et al., 2020). *Gynostemma pentaphyllum* (Thunb.) Makino, regulates the expression of aortic cell apoptosis and oxidative stress-related proteins by activating the PI3K/AKT signaling pathway, while downregulated mitochondrial fission proteins results in anti-inflammatory effects and reduced inflammatory factor expression. This in turn reduces endothelial cell shedding and aortic intima thickening (Song N. et al., 2020). Andrographolide downregulates inflammatory factor levels by altering the phenotype of macrophages, thus inhibiting activation of the NF-κB pathway. Andrographolide improves endothelial cell systolic and diastolic dysfunction by reducing endothelin (ET)-1 and thromboxane (TX) A2, levels and increasing levels of NO and prostaglandin (PG) I2. It plays a role in delaying the inflammatory damage caused by coronary heart disease and in protecting arterial plaques (Shu et al., 2020). Paeoniflorin, is a terpene glycoside extracted from *Paeonia lactiflora* Pall. That has anti-inflammatory effects. It downregulates expression of the downstream regulatory protein myeloid differentiation primary response 88 (MyD88) in the TLR4 pathway, thus inhibiting the transcriptional activity of NF-kB and downregulating proinflammatory factor expression (Li et al., 2017). Paeoniflorin blocks the MAPK/NF-κB signaling pathway, then exerts anti-AS effects by inhibiting ox-LDL production during VSMC proliferation and migration, reducing inflammatory cytokine secretion and inhibiting foam cell formation (Li et al., 2018). Geniposide inhibits the polarization of M1 macrophages through the MAPK signaling pathway, which inhibits induction of inflammatory IL-1β and induces a phenotype similar to that of M2 macrophages under M1 differentiation conditions.

TABLE 1 Regulatory effects of natural compounds of traditional Chinese medicine on AS-related signaling pathways.

Categories	Active ingredient	Plants	Extract method		Signaling pathways	Ref
			In Vivo	*In Vitro*		
Alkaloid	Cyclovirobuxinum D	*Buxus sinica var. Parvifolia* M. Cheng	–	RAW264.7 cells	JAK/STAT	Guo et al. (2014)
	Matrine	*Sophora flavescens* Aiton	–	HAVSMCs	NF-κB/MAPK	Wang et al. (2021)
			–	Macrophages	TLR4	Cui et al. (2022)
	Sinomenine	*Sinomenium acutum* (Thunb.) Rehder&E.H.Wilson	SD rats	–	TLR4/NF-κB	Geng et al. (2021)
	Ligustrazine	*Ligusticum chuanxiong* Hort	SD rats	–	NF-κB/Nrf2	Li Y. et al. (2019)
			SD rats	–	TLR4/NF-κB	Yang L. et al. (2021)
			SD rats	–	PI3K/AKT	Li L. et al. (2019)
	Berberine	*Coptis chinensis* Franch	$ApoE^{-/-}$ mice	–	PI3K/AKT	Song and Chen, (2021)
Flavonoids	Kaempferol	*Centella asiatica* (L.) Urb	$ApoE^{-/-}$ mice	–	PI3K/AKT/Nrf2	Feng et al. (2021)
	Quercetin	*Belamcanda chinensis* (L.) Redouté	–	HUVECs	NF-κB	Chen et al. (2020)
	Puerarin	*Puerariae Lobata* (Willd.) Ohwi	–	HUVECs	PI3K/AKT/NF-κB	Deng et al. (2017)
	Icariin	*Epimedium brevicornum* Maxim	Wistar rats	–	MAPK	Hu et al. (2016)
			SD rats	–	NF-κB/MAPK/Nrf2	Luo et al. (2022)
	Luteolin	*Clematis hexapetala* Pall	–	EA.hy926 cells	NF-κB	Jia et al. (2015)
			–	HUVECs	NF-κB/MAPK	Xia et al. (2014)
	Hydroxysafflor yellow A	*Carthamus tinctorius* L	$ApoE^{-/-}$ mice	–	TLR4	Xue et al. (2021)
	Baicalin	*Scutellaria baicalensis* Georgi	$ApoE^{-/-}$ mice	–	NF-κB/MAPK	Wu et al. (2018b)
	Wogonin		–	HUVECs	MAPK	Wu et al. (2019)
	Hesperetin	*Citrus reticulata* Blanco	Wistar rats	–	NF-κB/Nrf2	Olumegbon et al. (2022)
Polyphenols	Resveratrol	*Reynoutria japonica* Houtt	$ApoE^{-/-}$ mice	–	PI3K/AKT	Ji et al. (2022)
			–	HAVSMCs	TLR4	Chen et al. (2022)
			–	HUVECs	JAK/STAT/TLR4/NF-κB	Zhang M. et al. (2019)
			–	HUVECs	NF-kB/MAPK	Pan et al. (2016)
	Curcumin	*Curcuma longa* L	$ApoE^{-/-}$ mice	–	NF-κB	Lv et al. (2020)
	Theaflavine	*Camellia sinensis* (L.) Kuntze	$ApoE^{-/-}$ mice	HUVECs	Nrf2	Zeng et al. (2021)
	Salvianolic acid B	*Salvia miltiorrhiza* Bunge	LDLR −/− Mice	–	NF-κB/MAPK	Zhang et al. (2022b)
	Catechin	*Camellia sinensis* (L.) Kuntze	–	Macrophages	NF-κB	Starzonek et al. (2019)
	Epicatechin		$ApoE^{-/-}$ mice	–	NF-κB	Morrison et al. (2014)
	(-)-Epicatechin gallate		–	VSMCs	TLR4/NF-κB/MAPK	Li W. et al. (2021)
Saponins	Ginsenoside K	*Panax ginseng* C. A. Mey	–	RAW264.7 cells	NF-kB/MAPK	Lu et al. (2020)
	Gypenoside XVII	*Gynostemma pentaphyllum* (Thunb.) Makino	$ApoE^{-/-}$ mice	–	PI3K/AKT	Song N. et al. (2020)
	Andrographolide	*Andrographis paniculata* (Burm. f.) Nees	C57BL/6 mice	–	NF-κB	Shu et al. (2020)
	Paeoniflorin	*Paeonia lactiflora* Pall	SD rats	–	TLR4/NF-κB	Li et al. (2017)
			–	VSMCs	NF-κB/MAPK	Li et al. (2018)

(Continued on following page)

TABLE 1 (*Continued*) Regulatory effects of natural compounds of traditional Chinese medicine on AS-related signaling pathways.

Categories	Active ingredient	Plants	Extract method		Signaling pathways	Ref
			In Vivo	*In Vitro*		
	Geniposide	*Gardenia jasminoides* J. Ellis	New Zealand rabbits	–	MAPK	Jin et al. (2020)
	Geniposide and Notoginsenoside R1	*Gardenia jasminoides* J. Ellis and *Panax notoginseng* (Burkill) F. H. Chen	ApoE$^{-/-}$ mice	–	Nrf2	Liu et al. (2021)
	Amygdalin	*Eriobotrya japonica* (Thunb.) Lindl	ApoE$^{-/-}$ mice	–	NF-κB/MAPK	Wang et al. (2020)
	Astragaloside IV	*Astragalus membranaceus var. mongholicus* (Bunge) P. K. Hsiao	LDLR −/− Mice	–	NF-κB/MAPK	Zhang et al. (2022a)
	Saikosaponin	*Bupleurum chinense* DC.	–	HAVSMCs	MAPK	Yang et al. (2017)
Quinones	Emodin	*Rheum palmatum* L	ApoE$^{-/-}$ mice	–	JAK/STAT	Luo et al. (2021)
			–	VSMCs	MAPK	Pang et al. (2015)
	Tanshinone IIA	*Salvia miltiorrhiza* Bunge	ApoE$^{-/-}$ mice	–	TLR4/NF-κB	Chen et al. (2019)

Geniposide participates in M2 macrophage polarization by enhancing the expression of inflammatory factors such as Nuclear Receptor Subfamily four Group A Member 1 (NR4A1), cluster of differentiation 14 (CD14), and IL-10. It inhibits and stabilizes AS plaques (Jin et al., 2020). Geniposide combined with Panax notoginsenoside R1 inhibits the secretion of serum inflammatory and oxidative stress factors by inducing activation of the Nrf2 signaling pathway and synergistically reduces blood lipid levels and inhibits plaque formation (Liu et al., 2021). Other natural saponins, such as amygdalin (Wang et al., 2020), astragaloside IV(Zhang et al., 2022a), and saikosaponin (Yang et al., 2017) can also protect against AS plaques by modulating the MAPK/NF-κB signaling pathway and reducing inflammatory factors and oxidative stress responses.

Quinones

Quinones comprise benzoquinone, naphthoquinone, phenanthrenequinone, and anthraquinone, all of which are ubiquitous in plants (Zhang L. et al., 2021). Emodin is an anthraquinone extracted from *Rheum palmatum* L. (Cui et al., 2020) that reduces ROS generation and attenuates homocysteine-activated MAPK phosphorylation. It also significantly increases the content of SOCS3 and decreases the contents of phosphorylated JAK kinase two and phosphorylated STAT, thus blocking the JAK/STAT signaling pathway and exerting anti-AS effects (Pang et al., 2015; Luo et al., 2021). Tanshinone IIA from *Salvia miltiorrhiza* Bunge is an active constituent of the diterpene phenanthrene quinone and has anti-inflammatory, antioxidant, and other biological effects (Xu et al., 2020). Tanshinone IIA might exert immunomodulatory, anti-inflammatory, and anti-AS effects by regulating the TLR4/MyD88/NF-κB signaling pathway (Chen et al., 2019).

Conclusion and outlook

Atherosclerosis is the most prevalent type of arteriosclerotic vascular disease worldwide. It causes narrowing or even occlusion of the arterial lumen, which impedes the blood supply, resulting in ischemic pathological changes in corresponding organs (Wolf and Ley, 2019). The occurrence of AS is affected by many factors, among which inflammation and oxidative stress play crucial roles. The PI3K/AKT, TLR4, JAK/STAT, MAPK, and NF-κB pathways play roles in amplifying signaling during AS formation, and reducing the phosphorylation of the molecules in these pathways helps to alleviate the release of inflammatory factors, thus inhibiting the occurrence of AS. As the main antioxidant stress signaling pathway, Nrf2 plays a key role in restoring the physiological oxidative/antioxidative balance and protecting blood vessels from oxidative stress damage. Elevated intracellular Nrf2 levels can inhibit the pathological factors that mediate AS formation. Therefore, anti-inflammatory and antioxidant properties are crucial for AS treatment. Many natural medicines including TCM confer advantages and development prospects in terms of anti-inflammatory and anti-oxidative stress. This article described natural medicines including alkaloids, flavonoids, polyphenols, saponins, and quinones, all of which act on these pathways and confer beneficial therapeutic effects on AS. Most of them, including matrine, kaempferol, and resveratrol, act on several signaling pathways. We found that these natural drugs not only play an anti-AS role from anti-inflammatory and antioxidant perspectives but also inhibit the formation of

vascular plaque and protect the intima of vessels by repairing the vascular endothelium, inhibiting the formation of foam cells, and controlling platelet activation. Table 1 shows the mechanisms of action through which natural medicines can help to treat AS.

Natural medicines including TCM play multi-target, multi-path, and multi-linked regulatory roles in the treatment of AS. However, the nature of the investigative methodology and content remain problematic. The extraction and purification of natural medicines are relatively complex and affected by the environment, non-standardized products, medicinal material quality, and technological processes (Lefebvre et al., 2021). Traditional Chinese and other natural medicines do not rely on a single or specific type of active ingredient to exert therapeutic effects; they rather exert synergistic effects of numerous components acting on many pathways and targets. The pathogenesis of AS is complex and diverse, involving mechanisms of cytokine linkage to signaling pathways, cascade reactions of cytokines induced by these pathways, and interactions among signaling pathways (Libby, 2021). Therefore, the effects of natural medicines on these mechanisms and the intermediary mediators involved are important. Most mechanistic studies have focused on animal research and molecular biological approaches, whereas clinical research involving humans mostly remains at the level of blood sample analysis, and the methodology is relatively simple. However, AS is not easy to cure and the treatment cycle is long. Therefore, clinical studies of humans are needed to evaluate damage to metabolic organs, especially the liver and kidneys.

The formation of AS is the result of the cooperative actions of many mechanisms, and the inflammatory response and oxidative stress always run through the pathological formation of AS. TCM offers unique advantages for the prevention and treatment of AS. However, studies of most AS models are still in their infancy, and the upstream and downstream molecules in the pathways of some drug targets have not been specifically investigated. In addition, TCM exerts therapeutic effects through numerous targets and pathways, and formulae comprising several TCMs is the essence of TCM culture. This review explains only TMC compounds, which is one-sided. The mechanisms of TCM action and its compounds in the treatment of AS awaits discovery and validation by subsequent investigators. With the further development of biotechnology, such as bioinformatics analysis and network pharmacology (Fu et al., 2020; Zhou et al., 2020), an increasing number of active compounds with anti-AS effects in TCM will be discovered, providing more effective diagnostic tests and ideas for treating ASCVD using TCM.

Author contributions

YZ and ZL conceived the study; TM, XL, CL, and JL collected, analyzed, and interpreted the relevant literatures; HC, JL, and NJ drew all the figures and tables; TM wrote the manuscript; XL, JL, YZ and ZL supervised the study and revised the manuscript. The final version of the manuscript was read and approved by all authors.

Funding

This article is supported by the National Natural Science Foundation of China (82060784) and 2019 Heilongjiang University of Chinese Medicine Research Fund Project (2019BS04).

Conflict of interest

The authors declare that the research was conducted in the absence of any commercial or financial relationships that could be construed as a potential conflict of interest.

Publisher's note

All claims expressed in this article are solely those of the authors and do not necessarily represent those of their affiliated organizations, or those of the publisher, the editors and the reviewers. Any product that may be evaluated in this article, or claim that may be made by its manufacturer, is not guaranteed or endorsed by the publisher.

References

Alam, M. M., Okazaki, K., Nguyen, L. T. T., Ota, N., Kitamura, H., Murakami, S., et al. (2017). Glucocorticoid receptor signaling represses the antioxidant response by inhibiting histone acetylation mediated by the transcriptional activator NRF2. *J. Biol. Chem.* 292 (18), 7519–7530. doi:10.1074/jbc.M116.773960

Alonso-Piñeiro, J. A., Gonzalez-Rovira, A., Sánchez-Gomar, I., Moreno, J. A., and Durán-Ruiz, M. C. (2021). Nrf2 and heme oxygenase-1 involvement in atherosclerosis related oxidative stress. *Antioxidants (Basel)* 10 (9), 1463. doi:10.3390/antiox10091463

Badshah, S. L., Faisal, S., Muhammad, A., Poulson, B. G., Emwas, A. H., and Jaremko, M. (2021). Antiviral activities of flavonoids. *Biomed. Pharmacother.* 140, 111596. doi:10.1016/j.biopha.2021.111596

Bernal, S., Lopez-Sanz, L., Jimenez-Castilla, L., Prieto, I., Melgar, A., La Manna, S., et al. (2021). Protective effect of suppressor of cytokine signalling 1-based therapy in experimental abdominal aortic aneurysm. *Br. J. Pharmacol.* 178 (3), 564–581. doi:10.1111/bph.15330

Cao, X. J., Zhang, M. J., Zhang, L. L., Yu, K., Xiang, Y., Ding, X., et al. (2018). TLR4 mediates high-fat diet induced physiological changes in mice via attenuating PPARγ/ABCG1 signaling pathway. *Biochem. Biophys. Res. Commun.* 503 (3), 1356–1363. doi:10.1016/j.bbrc.2018.07.048

Chen, Q. M., and Maltagliati, A. J. (2018). Nrf2 at the heart of oxidative stress and cardiac protection. *Physiol. Genomics* 50 (2), 77–97. doi:10.1152/physiolgenomics.00041.2017

Chen, S., Ye, J., Chen, X., Shi, J., Wu, W., Lin, W., et al. (2018). Valproic acid attenuates traumatic spinal cord injury-induced inflammation via STAT1 and NF-κB pathway dependent of HDAC3. *J. Neuroinflammation* 15 (1), 150. doi:10.1186/s12974-018-1193-6

Chen, Z., Gao, X., Jiao, Y., Qiu, Y., Wang, A., Yu, M., et al. (2019). Tanshinone IIA exerts anti-inflammatory and immune-regulating effects on vulnerable atherosclerotic plaque partially via the TLR4/MyD88/NF-κB signal pathway. *Front. Pharmacol.* 10, 850. doi:10.3389/fphar.2019.00850

Chen, T., Zhang, X., Zhu, G., Liu, H., Chen, J., Wang, Y., et al. (2020). Quercetin inhibits TNF-α induced HUVECs apoptosis and inflammation via downregulating NF-kB and AP-1 signaling pathway *in vitro*. *Med. Baltim.* 99 (38), e22241. doi:10.1097/md.0000000000022241

Chen, J., Liu, Y., Liu, Y., and Peng, J. (2022). Resveratrol protects against ox-LDL-induced endothelial dysfunction in atherosclerosis via depending on circ_0091822/miR-106b-5p-mediated upregulation of TLR4. *Immunopharmacol. Immunotoxicol.*, 1–10. doi:10.1080/08923973.2022.2093740

Cheng, C. K., Luo, J. Y., Lau, C. W., Chen, Z. Y., Tian, X. Y., and Huang, Y. (2020). Pharmacological basis and new insights of resveratrol action in the cardiovascular system. *Br. J. Pharmacol.* 177 (6), 1258–1277. doi:10.1111/bph.14801

Chistiakov, D. A., Melnichenko, A. A., Grechko, A. V., Myasoedova, V. A., and Orekhov, A. N. (2018). Potential of anti-inflammatory agents for treatment of atherosclerosis. *Exp. Mol. Pathol.* 104 (2), 114–124. doi:10.1016/j.yexmp.2018.01.008

Ciesielska, A., Matyjek, M., and Kwiatkowska, K. (2021). TLR4 and CD14 trafficking and its influence on LPS-induced pro-inflammatory signaling. *Cell. Mol. Life Sci.* 78 (4), 1233–1261. doi:10.1007/s00018-020-03656-y

Ciumărnean, L., Milaciu, M. V., Runcan, O., Vesa Ș, C., Răchișan, A. L., Negrean, V., et al. (2020). The effects of flavonoids in cardiovascular diseases. *Molecules* 25 (18), E4320. doi:10.3390/molecules25184320

Cui, Y., Chen, L. J., Huang, T., Ying, J. Q., and Li, J. (2020). The pharmacology, toxicology and therapeutic potential of anthraquinone derivative emodin. *Chin. J. Nat. Med.* 18 (6), 425–435. doi:10.1016/s1875-5364(20)30050-9

Cui, Q., Du, H., Ma, Y., Wang, T., Zhu, H., Zhu, L., et al. (2022). Matrine inhibits advanced glycation end products-induced macrophage M1 polarization by reducing DNMT3a/b-mediated DNA methylation of GPX1 promoter. *Eur. J. Pharmacol.* 926, 175039. doi:10.1016/j.ejphar.2022.175039

Deng, H. F., Wang, X. L., Sun, H., and Xiao, X. Z. (2017). Puerarin inhibits expression of tissue factor induced by oxidative low-density lipoprotein through activating the PI3K/Akt/eNOS pathway and inhibiting activation of ERK1/2 and NF-κB. *Life Sci.* 191, 115–121. doi:10.1016/j.lfs.2017.10.018

Fang, S., Sun, S., Cai, H., Zou, X., Wang, S., Hao, X., et al. (2021). IRGM/Irgm1 facilitates macrophage apoptosis through ROS generation and MAPK signal transduction: Irgm1 (+/-) mice display increases atherosclerotic plaque stability. *Theranostics* 11 (19), 9358–9375. doi:10.7150/thno.62797

Feng, Z., Wang, C., YueJinMeng, Q., Wu, J., et al. (2021). Kaempferol-induced GPER upregulation attenuates atherosclerosis via the PI3K/AKT/Nrf2 pathway. *Pharm. Biol.* 59 (1), 1106–1116. doi:10.1080/13880209.2021.1961823

Fraga, C. G., Croft, K. D., Kennedy, D. O., and Tomás-Barberán, F. A. (2019). The effects of polyphenols and other bioactives on human health. *Food Funct.* 10 (2), 514–528. doi:10.1039/c8fo01997e

Fu, Y., Ling, Z., Arabnia, H., and Deng, Y. (2020). Current trend and development in bioinformatics research. *BMC Bioinforma.* 21 (, 538. doi:10.1186/s12859-020-03874-y

GBD 2017 DALYs and HALE Collaborators (2018). Global, regional, and national disability-adjusted life-years (DALYs) for 359 diseases and injuries and healthy life expectancy (HALE) for 195 countries and territories, 1990-2017 : a systematic analysis for the Global Burden of Disease Study 2017. *Lancet* 392 (10159), 1859–1922. doi:10.1016/s0140-6736(18)32335-3

Geng, J., Yang, C., Wang, B., Zhang, X., Hu, T., Gu, Y., et al. (2018). Trimethylamine N-oxide promotes atherosclerosis via CD36-dependent MAPK/JNK pathway. *Biomed. Pharmacother.* 97, 941–947. doi:10.1016/j.biopha.2017.11.016

Geng, P., Xu, X., and Gao, Z. (2021). Sinomenine suppress the vitamin D3 and high fat induced atherosclerosis in rats via suppress of oxidative stress and inflammation. *J. Oleo Sci.* 70 (12), 1815–1828. doi:10.5650/jos.ess21255

Ghorbani, N., Sahebari, M., Mahmoudi, M., Rastin, M., Zamani, S., and Zamani, M. (2021). Berberine inhibits the gene expression and production of proinflammatory cytokines by mononuclear cells in rheumatoid arthritis and healthy individuals. *Curr. Rheumatol. Rev.* 17 (1), 113–121. doi:10.2174/1573397116666200907111303

Gluba-Brzózka, A., Franczyk, B., Rysz-Górzyńska, M., Ławiński, J., and Rysz, J. (2021). Emerging anti-atherosclerotic therapies. *Int. J. Mol. Sci.* 22 (22), 12109. doi:10.3390/ijms222212109

Gong, L., Lei, Y., Liu, Y., Tan, F., Li, S., Wang, X., et al. (2019). Vaccarin prevents ox-LDL-induced HUVEC EndMT, inflammation and apoptosis by suppressing ROS/p38 MAPK signaling. *Am. J. Transl. Res.* 11 (4), 2140–2154.

Graves, D. T., and Milovanova, T. N. (2019). Mucosal immunity and the FOXO1 transcription factors. *Front. Immunol.* 10, 2530. doi:10.3389/fimmu.2019.02530

Guo, D., Li, J. R., Wang, Y., Lei, L. S., Yu, C. L., and Chen, N. N. (2014). Cyclovirobuxinum D suppresses lipopolysaccharide-induced inflammatory responses in murine macrophages *in vitro* by blocking JAK-STAT signaling pathway. *Acta Pharmacol. Sin.* 35 (6), 770–778. doi:10.1038/aps.2014.16

Guo, W., Li, H., Lou, Y., Zhang, Y., Wang, J., Qian, M., et al. (2021). Tyloxapol inhibits RANKL-stimulated osteoclastogenesis and ovariectomized-induced bone loss by restraining NF-κB and MAPK activation. *J. Orthop. Transl.* 28, 148–158. doi:10.1016/j.jot.2021.01.005

Hashimoto, R., Kakigi, R., Miyamoto, Y., Nakamura, K., Itoh, S., Daida, H., et al. (2020). JAK-STAT-dependent regulation of scavenger receptors in LPS-activated murine macrophages. *Eur. J. Pharmacol.* 871, 172940. doi:10.1016/j.ejphar.2020.172940

He, F., Antonucci, L., and Karin, M. (2020). NRF2 as a regulator of cell metabolism and inflammation in cancer. *Carcinogenesis* 41 (4), 405–416. doi:10.1093/carcin/bgaa039

Herrera, S. C., and Bach, E. A. (2019). JAK/STAT signaling in stem cells and regeneration: from Drosophila to vertebrates. *Development* 146 (2), dev167643. doi:10.1242/dev.167643

Hossain, E., Li, Y., and Anand-Srivastava, M. B. (2021). Role of the JAK2/STAT3 pathway in angiotensin II-induced enhanced expression of Giα proteins and hyperproliferation of aortic vascular smooth muscle cells. *Can. J. Physiol. Pharmacol.* 99 (2), 237–246. doi:10.1139/cjpp-2020-0415

Hu, Y., Sun, B., Liu, K., Yan, M., Zhang, Y., Miao, C., et al. (2016). Icariin attenuates high-cholesterol diet induced atherosclerosis in rats by inhibition of inflammatory response and p38 MAPK signaling pathway. *Inflammation* 39 (1), 228–236. doi:10.1007/s10753-015-0242-x

Jeon, B. R., Irfan, M., Lee, S. E., Lee, J. H., and Rhee, M. H. (2021). Rumex acetosella inhibits platelet function via impaired MAPK and phosphoinositide 3-kinase signaling. *Chin. J. Integr. Med.* 28, 802–808. doi:10.1007/s11655-021-2873-0

Ji, W., Sun, J., Hu, Z., and Sun, B. (2022). Resveratrol protects against atherosclerosis by downregulating the PI3K/AKT/mTOR signaling pathway in atherosclerosis model mice. *Exp. Ther. Med.* 23 (6), 414. doi:10.3892/etm.2022.11341

Jia, Z., Nallasamy, P., Liu, D., Shah, H., Li, J. Z., Chitrakar, R., et al. (2015). Luteolin protects against vascular inflammation in mice and TNF-alpha-induced monocyte adhesion to endothelial cells via suppressing IKBα/NF-κB signaling pathway. *J. Nutr. Biochem.* 26 (3), 293–302. doi:10.1016/j.jnutbio.2014.11.008

Jin, Z., Li, J., Pi, J., Chu, Q., Wei, W., Du, Z., et al. (2020). Geniposide alleviates atherosclerosis by regulating macrophage polarization via the FOS/MAPK signaling pathway. *Biomed. Pharmacother.* 125, 110015. doi:10.1016/j.biopha.2020.110015

Jongstra-Bilen, J., Zhang, C. X., Wisnicki, T., Li, M. K., White-Alfred, S., Ilaalagan, R., et al. (2017). Oxidized low-density lipoprotein loading of macrophages downregulates TLR-induced proinflammatory responses in a gene-specific and temporal manner through transcriptional control. *J. Immunol.* 199 (6), 2149–2157. doi:10.4049/jimmunol.1601363

Juang, Y. P., and Liang, P. H. (2020). Biological and pharmacological effects of synthetic saponins. *Molecules* 25 (21), E4974. doi:10.3390/molecules25214974

Kim, E., Yoon, J. Y., Lee, J., Jeong, D., Park, J. G., Hong, Y. H., et al. (2018). TANK-binding kinase 1 and Janus kinase 2 play important roles in the regulation of mitogen-activated protein kinase phosphatase-1 expression after toll-like receptor 4 activation. *J. Cell. Physiol.* 233 (11), 8790–8801. doi:10.1002/jcp.26787

Kishore, S. P., Blank, E., Heller, D. J., Patel, A., Peters, A., Price, M., et al. (2018). Modernizing the World health organization list of essential medicines for preventing and controlling cardiovascular diseases. *J. Am. Coll. Cardiol.* 71 (5), 564–574. doi:10.1016/j.jacc.2017.11.056

Lefebvre, T., Destandau, E., and Lesellier, E. (2021). Selective extraction of bioactive compounds from plants using recent extraction techniques: A review. *J. Chromatogr. A* 1635, 461770. doi:10.1016/j.chroma.2020.461770

Li, H., Jiao, Y., and Xie, M. (2017). Paeoniflorin ameliorates atherosclerosis by suppressing TLR4-mediated NF-κB activation. *Inflammation* 40 (6), 2042–2051. doi:10.1007/s10753-017-0644-z

Li, W., Zhi, W., Liu, F., Zhao, J., Yao, Q., and Niu, X. (2018). Paeoniflorin inhibits VSMCs proliferation and migration by arresting cell cycle and activating HO-1

through MAPKs and NF-κB pathway. *Int. Immunopharmacol.* 54, 103–111. doi:10.1016/j.intimp.2017.10.017

Li, L., Chen, H., Shen, A., Li, Q., Chen, Y., Chu, J., et al. (2019a). Ligustrazine inhibits platelet activation via suppression of the Akt pathway. *Int. J. Mol. Med.* 43 (1), 575–582. doi:10.3892/ijmm.2018.3970

Li, Y., Zhu, Z., Zhang, T., and Zhou, Y. (2019b). Ligustrazine attenuates inflammation and oxidative stress in a rat model of arthritis via the Sirt1/NF-κB and Nrf-2/HO-1 pathways. *Arch. Pharm. Res.* 42 (9), 824–831. doi:10.1007/s12272-018-1089-0

Li, J., Wang, T., Liu, P., Yang, F., Wang, X., Zheng, W., et al. (2021a). Hesperetin ameliorates hepatic oxidative stress and inflammation via the PI3K/AKT-Nrf2-ARE pathway in oleic acid-induced HepG2 cells and a rat model of high-fat diet-induced NAFLD. *Food Funct.* 12 (9), 3898–3918. doi:10.1039/d0fo02736g

Li, T., Li, X., Liu, X., Yang, J., and Ma, C. (2021b). The elevated expression of TLR4 and MMP9 in human abdominal aortic aneurysm tissues and its implication. *BMC Cardiovasc. Disord.* 21 (1), 378. doi:10.1186/s12872-021-02193-1

Li, W., Yu, J., Xiao, X., Li, W., Zang, L., Han, T., et al. (2021c). The inhibitory effect of (-)-Epicatechin gallate on the proliferation and migration of vascular smooth muscle cells weakens and stabilizes atherosclerosis. *Eur. J. Pharmacol.* 891, 173761. doi:10.1016/j.ejphar.2020.173761

Libby, P. (2021). The changing landscape of atherosclerosis. *Nature* 592 (7855), 524–533. doi:10.1038/s41586-021-03392-8

Liu, C., Yang, S., Wang, K., Bao, X., Liu, Y., Zhou, S., et al. (2019). Alkaloids from traditional Chinese medicine against hepatocellular carcinoma. *Biomed. Pharmacother.* 120, 109543. doi:10.1016/j.biopha.2019.109543

Liu, X., Xu, Y., Cheng, S., Zhou, X., Zhou, F., He, P., et al. (2021). Geniposide combined with notoginsenoside R1 attenuates inflammation and apoptosis in atherosclerosis via the AMPK/mTOR/Nrf2 signaling pathway. *Front. Pharmacol.* 12, 687394. doi:10.3389/fphar.2021.687394

Lopez-Sanz, L., Bernal, S., Recio, C., Lazaro, I., Oguiza, A., Melgar, A., et al. (2018). SOCS1-targeted therapy ameliorates renal and vascular oxidative stress in diabetes via STAT1 and PI3K inhibition. *Lab. Invest.* 98 (10), 1276–1290. doi:10.1038/s41374-018-0043-6

Lu, S., Luo, Y., Sun, G., and Sun, X. (2020). Ginsenoside compound K attenuates ox-LDL-mediated macrophage inflammation and foam cell formation via autophagy induction and modulating NF-κB, p38, and JNK MAPK signaling. *Front. Pharmacol.* 11, 567238. doi:10.3389/fphar.2020.567238

Luo, N., Fang, J., Wei, L., Sahebkar, A., Little, P. J., Xu, S., et al. (2021). Emodin in atherosclerosis prevention: Pharmacological actions and therapeutic potential. *Eur. J. Pharmacol.* 890, 173617. doi:10.1016/j.ejphar.2020.173617

Luo, Z., Dong, J., and Wu, J. (2022). Impact of Icariin and its derivatives on inflammatory diseases and relevant signaling pathways. *Int. Immunopharmacol.* 108, 108861. doi:10.1016/j.intimp.2022.108861

Lv, Y. L., Jia, Y., Wan, Z., An, Z. L., Yang, S., Han, F. F., et al. (2020). Curcumin inhibits the formation of atherosclerosis in ApoE(-/-) mice by suppressing cytomegalovirus activity in endothelial cells. *Life Sci.* 257, 117658. doi:10.1016/j.lfs.2020.117658

Marchio, P., Guerra-Ojeda, S., Vila, J. M., Aldasoro, M., Victor, V. M., and Mauricio, M. D. (2019). Targeting early atherosclerosis: A focus on oxidative stress and inflammation. *Oxid. Med. Cell. Longev.* 2019, 8563845. doi:10.1155/2019/8563845

Mitchell, J. P., and Carmody, R. J. (2018). NF-κB and the transcriptional control of inflammation. *Int. Rev. Cell Mol. Biol.* 335, 41–84. doi:10.1016/bs.ircmb.2017.07.007

Monaci, S., Coppola, F., Giuntini, G., Roncoroni, R., Acquati, F., Sozzani, S., et al. (2021). Hypoxia enhances the expression of RNASET2 in human monocyte-derived dendritic cells: Role of PI3K/AKT pathway. *Int. J. Mol. Sci.* 22 (14), 7564. doi:10.3390/ijms22147564

Morrison, M., van der Heijden, R., Heeringa, P., Kaijzel, E., Verschuren, L., Blomhoff, R., et al. (2014). Epicatechin attenuates atherosclerosis and exerts anti-inflammatory effects on diet-induced human-CRP and NFκB *in vivo*. *Atherosclerosis* 233 (1), 149–156. doi:10.1016/j.atherosclerosis.2013.12.027

Mulero, M. C., Huxford, T., and Ghosh, G. (2019). NF-κB, IκB, and IKK: Integral components of immune system signaling. *Adv. Exp. Med. Biol.* 1172, 207–226. doi:10.1007/978-981-13-9367-9_10

Olumegbon, L. T., Lawal, A. O., Oluyede, D. M., Adebimpe, M. O., Elekofehinti, O. O., and H, I. U. (2022). Hesperetin protects against diesel exhaust particles-induced cardiovascular oxidative stress and inflammation in Wistar rats. *Environ. Sci. Pollut. Res. Int.* 29, 52574–52589. doi:10.1007/s11356-022-19494-3

Owen, K. L., Brockwell, N. K., and Parker, B. S. (2019). JAK-STAT signaling: A double-edged sword of immune regulation and cancer progression. *Cancers (Basel)* 11 (12), E2002. doi:10.3390/cancers11122002

Pan, W., Yu, H., Huang, S., and Zhu, P. (2016). Resveratrol protects against TNF-α-induced injury in human umbilical endothelial cells through promoting sirtuin-1-induced repression of NF-KB and p38 MAPK. *PLoS One* 11 (1), e0147034. doi:10.1371/journal.pone.0147034

Pang, X., Liu, J., Li, Y., Zhao, J., and Zhang, X. (2015). Emodin inhibits homocysteine-induced C-reactive protein generation in vascular smooth muscle cells by regulating PPARγ expression and ROS-ERK1/2/p38 signal pathway. *PLoS One* 10 (7), e0131295. doi:10.1371/journal.pone.0131295

Pi, S., Mao, L., Chen, J., Shi, H., Liu, Y., Guo, X., et al. (2021). The P2RY12 receptor promotes VSMC-derived foam cell formation by inhibiting autophagy in advanced atherosclerosis. *Autophagy* 17 (4), 980–1000. doi:10.1080/15548627.2020.1741202

Poma, P. (2020). NF-κB and disease. *Int. J. Mol. Sci.* 21 (23), E9181. doi:10.3390/ijms21239181

Poznyak, A., Grechko, A. V., Poggio, P., Myasoedova, V. A., Alfieri, V., and Orekhov, A. N. (2020). The diabetes mellitus-atherosclerosis connection: The role of lipid and glucose metabolism and chronic inflammation. *Int. J. Mol. Sci.* 21 (5), E1835. doi:10.3390/ijms21051835

Qin, W., Cao, L., and Massey, I. Y. (2021). Role of PI3K/Akt signaling pathway in cardiac fibrosis. *Mol. Cell. Biochem.* 476 (11), 4045–4059. doi:10.1007/s11010-021-04219-w

Robledinos-Antón, N., Fernández-Ginés, R., Manda, G., and Cuadrado, A. (2019). Activators and inhibitors of NRF2: A review of their potential for clinical development. *Oxid. Med. Cell. Longev.* 2019, 9372182. doi:10.1155/2019/9372182

Ryan, S., McNicholas, W. T., and Taylor, C. T. (2007). A critical role for p38 map kinase in NF-kappaB signaling during intermittent hypoxia/reoxygenation. *Biochem. Biophys. Res. Commun.* 355 (3), 728–733. doi:10.1016/j.bbrc.2007.02.015

Saha, S., Buttari, B., Panieri, E., Profumo, E., and Saso, L. (2020). An overview of Nrf2 signaling pathway and its role in inflammation. *Molecules* 25 (22), E5474. doi:10.3390/molecules25225474

Shu, J., Huang, R., Tian, Y., Liu, Y., Zhu, R., and Shi, G. (2020). Andrographolide protects against endothelial dysfunction and inflammatory response in rats with coronary heart disease by regulating PPAR and NF-κB signaling pathways. *Ann. Palliat. Med.* 9 (4), 1965–1975. doi:10.21037/apm-20-960

Singla, R. K., Dubey, A. K., Garg, A., Sharma, R. K., Fiorino, M., Ameen, S. M., et al. (2019). Natural polyphenols: Chemical classification, definition of classes, subcategories, and structures. *J. AOAC Int.* 102 (5), 1397–1400. doi:10.5740/jaoacint.19-0133

Song, T., and Chen, W. D. (2021). Berberine inhibited carotid atherosclerosis through PI3K/AKTmTOR signaling pathway. *Bioengineered* 12 (1), 8135–8146. doi:10.1080/21655979.2021.1987130

Song, N., Jia, L., Cao, H., Ma, Y., Chen, N., Chen, S., et al. (2020a). Gypenoside inhibits endothelial cell apoptosis in atherosclerosis by modulating mitochondria through PI3K/Akt/Bad pathway. *Biomed. Res. Int.* 2020, 2819658. doi:10.1155/2020/2819658

Song, P., Fang, Z., Wang, H., Cai, Y., Rahimi, K., Zhu, Y., et al. (2020b). Global and regional prevalence, burden, and risk factors for carotid atherosclerosis: a systematic review, meta-analysis, and modelling study. *Lancet. Glob. Health* 8 (5), e721–e729. doi:10.1016/s2214-109x(20)30117-0

Starzonek, J., Roscher, K., Blüher, M., Blaue, D., Schedlbauer, C., Hirz, M., et al. (2019). Effects of a blend of green tea and curcuma extract supplementation on lipopolysaccharide-induced inflammation in horses and ponies. *PeerJ* 7, e8053. doi:10.7717/peerj.8053

Steven, S., Frenis, K., Oelze, M., Kalinovic, S., Kuntic, M., Bayo Jimenez, M. T., et al. (2019). Vascular inflammation and oxidative stress: Major triggers for cardiovascular disease. *Oxid. Med. Cell. Longev.* 2019, 7092151. doi:10.1155/2019/7092151

Sun, M., Liu, C., Zhao, N., Meng, K., and Zhang, Z. (2018). Predictive value of platelet aggregation rate in postpartum deep venous thrombosis and its possible mechanism. *Exp. Ther. Med.* 15 (6), 5215–5220. doi:10.3892/etm.2018.6116

Tang, Y., Liu, W., Wang, W., Fidler, T., Woods, B., Levine, R. L., et al. (2020). Inhibition of JAK2 suppresses myelopoiesis and atherosclerosis in apoe(-/-) mice. *Cardiovasc. Drugs Ther.* 34 (2), 145–152. doi:10.1007/s10557-020-06943-9

Varghese, J. F., Patel, R., and Yadav, U. C. S. (2018). Novel insights in the metabolic syndrome-induced oxidative stress and inflammation-mediated atherosclerosis. *Curr. Cardiol. Rev.* 14 (1), 4–14. doi:10.2174/1573403x13666171009112250

Vijay, K. (2018). Toll-like receptors in immunity and inflammatory diseases: Past, present, and future. *Int. Immunopharmacol.* 59, 391–412. doi:10.1016/j.intimp.2018.03.002

Wang, Y., Jia, Q., Zhang, Y., Wei, J., and Liu, P. (2020). Amygdalin attenuates atherosclerosis and plays an anti-inflammatory role in ApoE knock-out mice and bone marrow-derived macrophages. *Front. Pharmacol.* 11, 590929. doi:10.3389/fphar.2020.590929

Wang, G., Ji, C., Wang, C., Liu, Z., Qu, A., and Wang, H. (2021). Matrine ameliorates the inflammatory response and lipid metabolism in vascular smooth muscle cells through the NF-κB pathway. *Exp. Ther. Med.* 22 (5), 1309. doi:10.3892/etm.2021.10744

Wen, K., Fang, X., Yang, J., Yao, Y., Nandakumar, K. S., Salem, M. L., et al. (2021). Recent research on flavonoids and their biomedical applications. *Curr. Med. Chem.* 28 (5), 1042–1066. doi:10.2174/0929867327666200713184138

Wolf, D., and Ley, K. (2019). Immunity and inflammation in atherosclerosis. *Circ. Res.* 124 (2), 315–327. doi:10.1161/circresaha.118.313591

Wu, Y., Su, S. A., Xie, Y., Shen, J., Zhu, W., and Xiang, M. (2018a). Murine models of vascular endothelial injury: Techniques and pathophysiology. *Thromb. Res.* 169, 64–72. doi:10.1016/j.thromres.2018.07.014

Wu, Y., Wang, F., Fan, L., Zhang, W., Wang, T., Du, Y., et al. (2018b). Baicalin alleviates atherosclerosis by relieving oxidative stress and inflammatory responses via inactivating the NF-κB and p38 MAPK signaling pathways. *Biomed. Pharmacother.* 97, 1673–1679. doi:10.1016/j.biopha.2017.12.024

Wu, Y. H., Chuang, L. P., Yu, C. L., Wang, S. W., Chen, H. Y., and Chang, Y. L. (2019). Anticoagulant effect of wogonin against tissue factor expression. *Eur. J. Pharmacol.* 859, 172517. doi:10.1016/j.ejphar.2019.172517

Xia, F., Wang, C., Jin, Y., Liu, Q., Meng, Q., Liu, K., et al. (2014). Luteolin protects HUVECs from TNF-α-induced oxidative stress and inflammation via its effects on the Nox4/ROS-NF-κB and MAPK pathways. *J. Atheroscler. Thromb.* 21 (8), 768–783. doi:10.5551/jat.23697

Xu, X., Zhang, A., Zhu, Y., He, W., Di, W., Fang, Y., et al. (2018). MFG-E8 reverses microglial-induced neurotoxic astrocyte (A1) via NF-κB and PI3K-Akt pathways. *J. Cell. Physiol.* 234 (1), 904–914. doi:10.1002/jcp.26918

Xu, H., Li, H., Zhu, P., Liu, Y., Zhou, M., and Chen, A. (2020). Tanshinone IIA ameliorates progression of CAD through regulating cardiac H9c2 cells proliferation and apoptosis by miR-133a-3p/EGFR Axis. *Drug Des. devel. Ther.* 14, 2853–2863. doi:10.2147/dddt.S245970

Xue, X., Deng, Y., Wang, J., Zhou, M., Liao, L., Wang, C., et al. (2021). Hydroxysafflor yellow A, a natural compound from *Carthamus tinctorius* L. with good effect of alleviating atherosclerosis. *Phytomedicine.* 91, 153694. doi:10.1016/j.phymed.2021.153694

Yang, L., Liu, J., and Qi, G. (2017). Mechanism of the effect of saikosaponin on atherosclerosis *in vitro* is based on the MAPK signaling pathway. *Mol. Med. Rep.* 16 (6), 8868–8874. doi:10.3892/mmr.2017.7691

Yang, L., Lian, Z., Zhang, B., Li, Z., Zeng, L., Li, W., et al. (2021a). Effect of ligustrazine nanoparticles on Th1/Th2 balance by TLR4/MyD88/NF-κB pathway in rats with postoperative peritoneal adhesion. *BMC Surg.* 21 (1), 211. doi:10.1186/s12893-021-01201-7

Yang, Y., Laval, S., and Yu, B. (2021b). Chemical synthesis of saponins. *Adv. Carbohydr. Chem. Biochem.* 79, 63–150. doi:10.1016/bs.accb.2021.10.001

Yuan, T., Yang, T., Chen, H., Fu, D., Hu, Y., Wang, J., et al. (2019). New insights into oxidative stress and inflammation during diabetes mellitus-accelerated atherosclerosis. *Redox Biol.* 20, 247–260. doi:10.1016/j.redox.2018.09.025

Zeng, J., Deng, Z., Zou, Y., Liu, C., Fu, H., Gu, Y., et al. (2021). Theaflavin alleviates oxidative injury and atherosclerosis progress via activating microRNA-24-mediated Nrf2/HO-1 signal. *Phytother. Res.* 35 (6), 3418–3427. doi:10.1002/ptr.7064

Zhang, L., Zhang, Y., Wu, Y., Yu, J., Zhang, Y., Zeng, F., et al. (2019a). Role of the balance of akt and MAPK pathways in the exercise-regulated phenotype switching in spontaneously hypertensive rats. *Int. J. Mol. Sci.* 20 (22), E5690. doi:10.3390/ijms20225690

Zhang, M., Xue, Y., Chen, H., Meng, L., Chen, B., Gong, H., et al. (2019b). Resveratrol inhibits MMP3 and MMP9 expression and secretion by suppressing TLR4/NF-κB/STAT3 activation in ox-LDL-treated HUVECs. *Oxid. Med. Cell. Longev.* 2019, 9013169. doi:10.1155/2019/9013169

Zhang, L., Zhang, G., Xu, S., and Song, Y. (2021a). Recent advances of quinones as a privileged structure in drug discovery. *Eur. J. Med. Chem.* 223, 113632. doi:10.1016/j.ejmech.2021.113632

Zhang, Q., Liu, J., Duan, H., Li, R., Peng, W., and Wu, C. (2021b). Activation of Nrf2/HO-1 signaling: An important molecular mechanism of herbal medicine in the treatment of atherosclerosis via the protection of vascular endothelial cells from oxidative stress. *J. Adv. Res.* 34, 43–63. doi:10.1016/j.jare.2021.06.023

Zhang, Y., Du, M., Wang, J., and Liu, P. (2022a). Astragaloside IV relieves atherosclerosis and hepatic steatosis via MAPK/NF-κB signaling pathway in LDLR(-/-) mice. *Front. Pharmacol.* 13, 828161. doi:10.3389/fphar.2022.828161

Zhang, Y., Feng, X., Du, M., Ding, J., and Liu, P. (2022b). Salvianolic acid B attenuates the inflammatory response in atherosclerosis by regulating MAPKs/NF-κB signaling pathways in LDLR-/- mice and RAW264.7 cells. *Int. J. Immunopathol. Pharmacol.* 36, 3946320221079468. doi:10.1177/03946320221079468

Zhao, X., Ren, Y., Ren, H., Wu, Y., Liu, X., Chen, H., et al. (2021). The mechanism of myocardial fibrosis is ameliorated by myocardial infarction-associated transcript through the PI3K/Akt signaling pathway to relieve heart failure. *J. Int. Med. Res.* 49 (7), 3000605211031433. doi:10.1177/03000605211031433

Zhong, L., Simard, M. J., and Huot, J. (2018). Endothelial microRNAs regulating the NF-κB pathway and cell adhesion molecules during inflammation. *Faseb J.* 32 (8), 4070–4084. doi:10.1096/fj.201701536R

Zhou, Z., Chen, B., Chen, S., Lin, M., Chen, Y., Jin, S., et al. (2020). Applications of network pharmacology in traditional Chinese medicine research. *Evid. Based. Complement. Altern. Med.* 2020, 1646905. doi:10.1155/2020/1646905

Zhu, Y., Xian, X., Wang, Z., Bi, Y., Chen, Q., Han, X., et al. (2018). Research progress on the relationship between atherosclerosis and inflammation. *Biomolecules* 8 (3), E80. doi:10.3390/biom8030080

Zhu, K., Zhu, X., Sun, S., Yang, W., Liu, S., Tang, Z., et al. (2021). Inhibition of TLR4 prevents hippocampal hypoxic-ischemic injury by regulating ferroptosis in neonatal rats. *Exp. Neurol.* 345, 113828. doi:10.1016/j.expneurol.2021.113828

Glossary

The following abbreviations are used in this document:

ABCA1 ATP-binding cassette transporter A1
ABCG1 ATP-binding cassette transporter G1
AKT Proteinkinase B
AP-1 Activation protein-1
ARE Antioxidant response element
AS Atherosclerosis
ASCVD Atherosclerotic Cardiovascular Disease
eNOS Endothelial Nitric Oxide Synthases
ERK Extracellular signal-regulated kinase
ET-1 Endothelin-1
GPER G protein-coupled estrogen receptor
HASMCs Human aortic smooth muscle cells
ICAM-1 Intercellular cell adhesion molecule-1
IHR Intermittent hypoxia/reoxygenation
IL Interleukin
iNOS Inducible Nitric Oxide Synthase
IRFs Interferon regulatory factors
JAK Janus Kinase
JNK c-Jun N-terminal protein kinase
LOX-1 lectin-like oxidized low-density lipoprotein re-ceptor-1
LPS lipopolysaccharide
MAO Monoamine oxidases
MAPK Mitogen-Activated Protein Kinase
MDA Malondialdehyde
MMP-9 Matrix metalloproteinase-9
MyD88 Myeloiddifferentiationfactor88
NF-κB Nuclear Factor Kappa-B
NO Nitric oxide
NR4A1 Nuclear Receptor Subfamily 4 Group A Member 1
Nrf2 Nuclear Factor E2-Related Factor2
ox-LDL Oxidized low-density lipoprotein
p38MAPK p38 mitogen-activated protein kinase
PGI2 Prostaglandin-I-2
PI3K PhosphoInositide-3 Kinase
ROS Reactive oxygen species
SOCS Suppressors of cytokine signaling
SR-A1 Class A1 scavenger receptor
STAT Signal Transducer And Activator Of Transcription
TCM Traditional chinese medicine
TF Tissue factor
TLR4 Toll Like Receptor 4
TNF-α Tumor necrosis factor-α
TXA2 Thromboxane A2
VCAM-1 Vascular Cell Adhesion Molecule 1
VECs Vascular endothelial cells
VEGF Vascular endothelial growth factor
VSMCs Vascular smooth muscle cells
WHO World Health Organization.

frontiers | Frontiers in Pharmacology

TYPE Review
PUBLISHED 18 October 2022
DOI 10.3389/fphar.2022.1013740

OPEN ACCESS

EDITED BY
Jie Liu,
Zunyi Medical University, China

REVIEWED BY
Shangfu Xu,
Zunyi Medical University, China
Liping Shu,
Guizhou Medical University, China
Peng Cao,
Nanjing University of Chinese Medicine, China

*CORRESPONDENCE
Yuezhen Xue,
yzxue@imcb.a-star.edu.sg
Hai-dong Guo,
hdguo@shutcm.edu.cn

SPECIALTY SECTION
This article was submitted to Ethnopharmacology, a section of the journal Frontiers in Pharmacology

RECEIVED 07 August 2022
ACCEPTED 03 October 2022
PUBLISHED 18 October 2022

CITATION
Wang Y, Xue Y and Guo H-d (2022), Intervention effects of traditional Chinese medicine on stem cell therapy of myocardial infarction. *Front. Pharmacol.* 13:1013740. doi: 10.3389/fphar.2022.1013740

Intervention effects of traditional Chinese medicine on stem cell therapy of myocardial infarction

Yu Wang[1], Yuezhen Xue[2]* and Hai-dong Guo[1,3]*

[1]Academy of Integrative Medicine, Shanghai University of Traditional Chinese Medicine, Shanghai, China, [2]Institute of Molecular and Cell Biology (IMCB), Agency for Science, Technology and Research (A*STAR), Singapore, Singapore, [3]Department of Anatomy, School of Basic Medicine, Shanghai University of Traditional Chinese Medicine, Shanghai, China

Cardiovascular diseases are the leading cause of global mortality, in which myocardial infarction accounts for 46% of total deaths. Although good progress has been achieved in medication and interventional techniques, a proven method to repair the damaged myocardium has not yet been determined. Stem cell therapy for damaged myocardial repair has evolved into a promising treatment for ischemic heart disease. However, low retention and poor survival of the injected stem cells are the major obstacles to achieving the intended therapeutic effects. Chinese botanical and other natural drug substances are a rich source of effective treatment for various diseases. As such, numerous studies have revealed the role of Chinese medicine in stem cell therapy for myocardial infarction treatment, including promoting proliferation, survival, migration, angiogenesis, and differentiation of stem cells. Here, we discuss the potential and limitations of stem cell therapy, as well as the regulatory mechanism of Chinese medicines underlying stem cell therapy. We focus on the evidence from pre-clinical trials and clinical practices, and based on traditional Chinese medicine theories, we further summarize the mechanisms of Chinese medicine treatment in stem cell therapy by the commonly used prescriptions. Despite the pre-clinical evidence showing that traditional Chinese medicine is helpful in stem cell therapy, there are still some limitations of traditional Chinese medicine therapy. We also systematically assess the detailed experimental design and reliability of included pharmacological research in our review. Strictly controlled animal models with multi-perspective pharmacokinetic profiles and high-grade clinical evidence with multi-disciplinary efforts are highly demanded in the future.

KEYWORDS

traditional Chinese medicine, stem cells, myocardial infarction, survival, migration

Introduction

Cardiovascular diseases (CVDs), principally ischemic heart disease (IHD) and stroke, are the leading cause of mortality globally (Roth et al., 2020). Moreover, myocardial infarction (MI) accounts for 46% of all deaths attributed to CVDs (Tsao et al., 2022). MI-induced blood insufficiency leads to myocardial necrosis and fibrotic scar formation,

which eventually causes arrhythmias, ventricular dysfunction, and post-infarction congestive heart failure (Henry et al., 2021). Because of the limited capability of myocardial self-regeneration, the damages are typically irreversible (Tzahor and Poss, 2017). Although good progress has been achieved in medication and interventional techniques such as primary coronary angioplasty, a proven strategy to repair the damaged myocardium has not yet been determined.

Novel methods have been identified for promoting myocardial regeneration by injecting stem cells into the infarcted heart (Miao et al., 2017). Stem cells act as undifferentiated cells, which can divide and differentiate into numerous mature cell types with specialized functions (Bacakova et al., 2018). Stem cells are mainly classified into two groups: embryonic stem cells (ESCs), pluripotent stem cells originating from the internal cellular mass of the blastocyst, and adult stem cells (ASCs) presenting in different tissues throughout the body after development (Lagarkova, 2019). However, most stem cells have defects in the treatment of MI, including low survival rate, immune exclusion, and low differentiation efficiency (Laplane and Solary, 2019). Due to this potential limitation, there has been significant interest in understanding the factors determining the survival of transplanted stem cells (Miao et al., 2017). Moreover, the hostile ischemic environment, rich in inflammation factors; free radicals generated by oxidative stress, and hypoxic areas further limit the efficiency of stem cell-based therapy (Fu et al., 2021).

Overcoming these limitations can improve the efficacy of stem cell therapy for heart diseases. One such strategy is to genetically manipulate the expression of critical genes involved in cell survival. Pro-survival genes such as *Akt*, *Bcl-2*, and *SDF-1* improve stem cell viability after transplantation but with little efficacy (Penn and Mangi, 2008). Other strategies for improving the survival of transplanted stem cells in the ischemic myocardium have been developed, such as genetic modification of transplanted stem cells, stem cell transplantation in combination with growth factor delivery, and cell therapy using various scaffolds (Kim et al., 2013; Afjeh-Dana et al., 2022). A third and more critical strategy for myocardial infarction therapy is to promote angiogenesis and endothelial cell growth in the infarcted heart (Gu et al., 2015). However, only a portion of the stem cells successfully differentiates into cardiomyocytes but distributes in the less ischemic boundary zone. Therefore, transplanted stem cells are unable to form functional cardiac tissues, making the transplantation of stem cells for MI therapy less than optimal.

Chinese botanical and other natural drug substances are a major aspect of traditional Chinese medicine (TCM) and are a rich source of unique chemicals. As such, numerous studies have revealed the role of Chinese medicine in stem cell therapy for MI treatment, including promoting proliferation (Zhu et al., 2017), differentiation (Li et al., 2006), migration (Liu et al., 2013), angiogenesis (Guo et al., 2014), and survival (Cao et al., 2016) of stem cells. Here, we discuss the potential and limitations of stem cell therapy and the regulatory mechanism of Chinese medicines underlying stem cell therapy. We focus on the evidence derived from pre-clinical trials and clinical practices and summarize the theoretical basis for the efficacy of TCM from the perspective of stem cells.

Potential and limitations of stem cell therapy for treating myocardial infarction

Different sources of stem and progenitor cells, including ESCs and ASCs, have been validated for their ability to promote cardiac regeneration and repair (Rigaud et al., 2020). The therapeutic effects of unselected bone marrow cells (BMCs) (Fisher et al., 2014), hematopoietic stem cells (HSCs) (Shafei et al., 2018), mesenchymal stem cells (MSCs) (Ulus et al., 2020), resident cardiac stem cells (RCSCs) (Makkar et al., 2012), and induced pluripotent stem cells (iPSCs) (Drowley et al., 2016) have gained progression in basic translational and clinical applications. Moreover, skeletal myoblasts (SMs) (Menasché et al., 2008) and adipose-derived stem cells (ADSCs) (Davy et al., 2015) constitute other cell populations that may be suitable for cardiac repair. However, each cell category has its practical limitations and translational disadvantages (Figure 1). We discuss these in detail in the following sections.

Potential and limitations of embryonic stem cells and induced pluripotent stem cell therapy

Although ESCs possess some distinctive advantages in cardiac repair, including their pluripotency, which means that they can differentiate into all types of cells, there are still ethical and regulatory concerns (Lo and Parham, 2009; Khan et al., 2015). More importantly, the risk of malignancies further limits ESC-based treatments (Madigan and Atoui, 2018). Although some methods to inhibit tumorigenesis have been used, reliable approaches to modulate and control differentiation in a controllable and efficient manner are still scarce (Carvalho et al., 2015). In addition, ESCs trigger severe immune rejection following allogeneic application (Samak and Hinkel, 2019). iPSCs are a promising alternative to ESCs in regenerative medicine, which can be redifferentiated from adult somatic cells (e.g., fibroblasts, epidermal cells, and hemocytes) using reprogramming techniques (Hynes et al., 2015). iPSC technology has been developed for auto-transplantation, bypassing ethical concerns associated with destroying fertilized embryos, and without an immune response (Faiella and Atoui, 2016). Moreover, unlike ASCs, which partly differentiate into a limited number of cell types, the iPSCs have a great potential to give rise to all lineages of cells (Chamberlain, 2016). While iPSCs

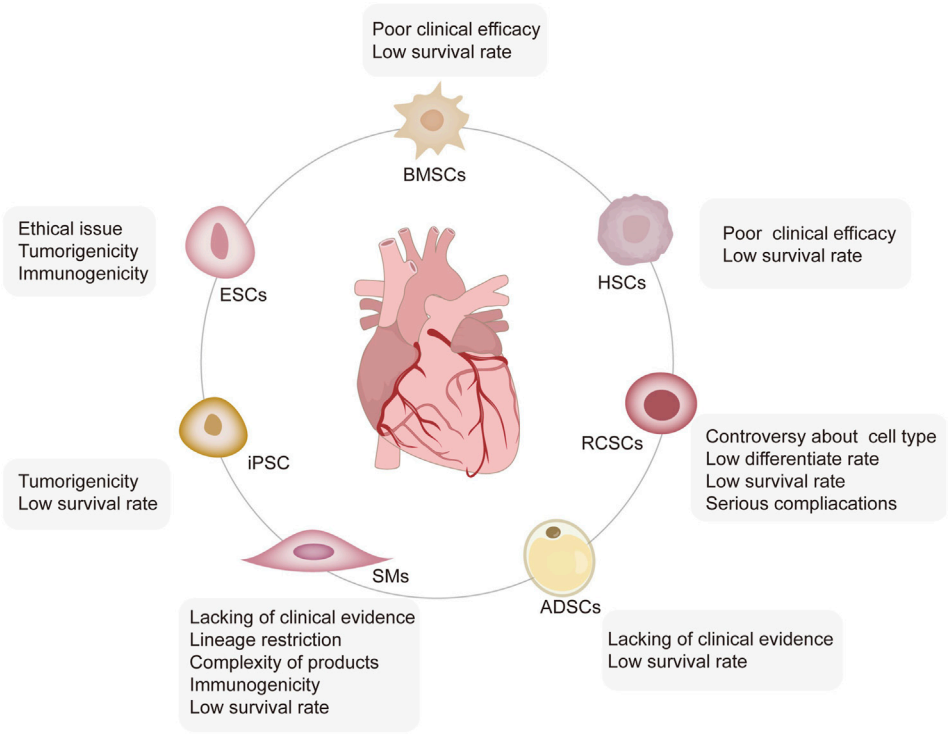

FIGURE 1
Limitations of stem cell-based therapy. Five types of stem cells, including ESCs, iPSCs, HSCs, RCSCs, ADSCs, and SMs, are involved in MI treatment, each of which has its limitations. ESCs face severe ethical issues with high tumorigenic and immunogenic characteristics; iPSCs have a high rate of tumorigenicity and a low survival rate. BMSCs and HSCs are characterized by self-renewal, no tumorigenicity, low immunogenicity, and strong immunomodulatory ability. However, their low survival rate leads to poor clinical efficacy. The biological functions of the subgroups of RCSCs have not been well detected yet, and the low survival rate, low differentiation rate, and even severe complications limit their application. SMs have lineage restrictions and thus, are unable to produce new cardiomyocytes. Moreover, the complexity, immunogenicity, and low survival of autologous SM products limited their wide application.

give full play to the advantage of ESCs and ASCs, safety issues with these cells need to be addressed before they can be used in clinical settings. The property of infinite proliferation in iPSCs is a double-edged sword because if cells keep proliferating even after transplantation, they may result in tumors (Malchenko et al., 2014). Therefore, finding the best source of stem cells has always been one of the main problems in this field.

Potential and limitations of bone marrow mesenchymal stem cell therapy

One of the most promising cardiac cell-based therapies is unselected BMCs therapy, which has clinical surveillance for up to 5 years (Fisher et al., 2018). BMCs have some advantages for clinical application, including the ease of procurement and harvesting *ex vivo*, a sufficient number, and purity, and both have the properties of stem and progenitor cells (Haider, 2018). However, the results of clinical trials suggested that the effectiveness of BMCs is usually modest and less than the expectations of the originally intended result (Wollert et al., 2017; Zhang et al., 2021). In a randomized clinical trial, BMC intracoronary transplantation in acute myocardial infarction (AMI) patients did not increase the left ventricular ejection fraction (LVEF), and only a slight improvement in myocardial perfusion was observed in the BMC group (Grajek et al., 2010).

Therefore, more studies focused on the different subgroups of BMCs, which are divided into two populations, HSCs and non-HSCs.

Potential and limitations of hematopoietic stem cell therapy

As for HSCs, markers of CD133 and CD34 are generally adopted to select specific cell populations, and $CD34^+$ cells possess more endothelial lineage-phenotype cells than $CD133^+$ cells, considered “early” endothelial progenitor cells (EPCs) in HSCs (Chen et al., 2021a). A randomized controlled trial compared the LVEF after MI between unsorted and $CD34^+$/

CXCR4$^+$-sorted BMCs (Tendera et al., 2009). After 6 months, a 3% increase in the LVEF was observed in patients treated, as discussed previously, whereas the control group remained unchanged. The CARDIO133 phase III clinical trial was designed to evaluate the effect of intra-myocardial injection of CD133$^+$-sorted BMCs in cardiac repair (Nasseri et al., 2014). The results showed that CD133$^+$-sorted BMCs improved regional scar perfusion but did not affect LV function. Presumably, this occurred because of the low baseline levels of HSCs, which limit their efficacy. Taken together, despite the diversity and therapeutic potential of BMC-based therapy, the clinical response of this therapy leaves great room for improvement; incorporating different combinations of biomarkers to reinforce the cellular repair capacity needs to be studied in the future.

Potential and limitations of mesenchymal stem cell therapy

MSCs, non-HSCs in bone marrow or adipose tissue, represent another potential selection for stem cell-based therapy. MSCs play an essential role in MI therapy because of their unique properties, including the ability to differentiate into cardiomyocytes (although controversial) (Wang et al., 2015), immunomodulatory property (Eldaly et al., 2022), anti-fibrotic activity (Li et al., 2015), and promotion of angiogenesis (Gao et al., 2017). Regarding differentiation ability, the combined treatment of MSCs and exogenous Jagged1 activated Notch1 signaling and caused multilineage differentiation (Ding et al., 2015). Moreover, the overexpression of miRNA1-2 in mouse MSCs promotes the differentiation of MSCs into cardiomyocyte-like cells through activation of the Wnt/β-catenin signaling pathway (Shen et al., 2017). However, it is widely acknowledged that the central effect of MSCs in the treatment of MI relies on the paracrine effect and not on the differentiation of MSCs into cardiomyocytes (Guo et al., 2020).

Bone marrow-derived MSCs (BMSCs), one of the adult pluripotent stem cells with great differentiation potential, low immunogenicity, and immune regulatory abilities, regulate different pathways of immune cells in a paracrine way (Bulati et al., 2020). BMSCs have great clinical application value and broad prospects due to their characteristics. However, the therapeutic efficacy of BMSC-based therapy *in vivo* remains a challenge. Previous studies have consistently indicated the poor survival of BMSCs after transplantation; about 90% of BMSCs died within the first 4 days (Zhao et al., 2019). Some researchers showed that BMSCs have a low survival rate in the cardiac environment, and most transplanted cells may disappear soon after transplantation (van der Spoel et al., 2011; Blocki et al., 2015; Li et al., 2016). When BMSCs are transplanted to ischemic zones, a hostile cardiac microenvironment, with a major proportion of reactive oxygen species (ROS), hypoxia, inflammation, fibrosis, and oxidative stress limit their survival potential (Lin et al., 2020). Currently, autologous and allogeneic BMSC transplantations are under investigation, whereas their therapeutic efficacy remains uncertain. In a clinical trial, 69 patients with AMI who underwent successful percutaneous coronary intervention (PCI) were transferred to receive an intracoronary infusion of BMSCs and saline. The results showed that BMSCs, at least in part, improved cardiac function without deaths (Chen et al., 2004). In another randomized, controlled trial, patients with ST-elevation AMI after reperfusion treatment within 12 h were randomly divided into BMSC-injection or standard medical treatment groups (Gao et al., 2013). BMSC-based treatment improved cardiac function and myocardial viability within the infarct area after 6 months in both groups compared with baseline; however, no significant difference was evident between these groups. The clinical benefits of BMSC-based therapy in patients with MI need further investigation and re-evaluation.

Moreover, adipose tissue also serves as a source of MSCs named ADSCs. Accumulating studies suggest that the effects of ADSCs are majorly related to paracrine action rather than trans-differentiation. The exosomes isolated from ADSCs attenuated cardiac injury after MI by activating the S1P/SK1/S1PR1 signaling pathway and increasing macrophage transition to the M2 phenotype (Deng et al., 2019). It was reported that conditional medium (CM) containing miR-221/222 from ADSCs significantly reduced cardiac apoptosis and fibrosis by reducing PUMA and ETS-1 expression, respectively (Lee et al., 2021). Meanwhile, miR-93-5p-encapsulating exosomes from ADSCs protected the myocardium by inhibiting autophagy and inflammatory response (Liu et al., 2018). Moreover, ADSCs-SIRT1-exosomes can recruit EPCs to the infarct area through Nrf2/CXCL12/CXCR7 signaling (Huang et al., 2020). However, clinical evidence remains scarce.

Potential and limitations of resident cardiac stem cell therapy

The adult mammalian heart has traditionally been thought of as a terminally differentiated organ, and cardiomyocytes have limited ability to regenerate for a long time (Windmueller et al., 2020). Nevertheless, RCSCs have been found and isolated in adult mammalian hearts, with multiple phenotypes, and they exhibit self-renewal capacity and multilineage potential, including differentiation into cardiomyocytes, smooth muscle cells, and endothelial cells under suitable conditions (Valiente-Alandi et al., 2016). Indeed, they are an appropriate candidate for cardiac regeneration therapy, for they are intrinsically programmed to form cardiac tissues and differentiate into parenchymal cells and coronary vessels rapidly upon activation (Uygur and

Lee, 2016). Multiple subtypes of RCSCs are classified through surface markers and transcription genes, including c-kit$^+$ RCSCs, Sca-1$^+$ RCSCs, Islet-1$^+$ RCSCs, side population RCSCs, and cardiosphere-derived CSCs (Li et al., 2019a). However, until now, whether RCSCs population extracted based on markers are of different types or whether they present a co-primitive cell type as the originator of these cells remains unclear. Moreover, the biological functions of the subgroups of RCSCs have not been well detected yet. There are still tremendous controversies about whether RCSCs can differentiate into a functional myocardium, especially after the retracted studies of Piero Anversa (Beltrami et al., 2003). It was reported that although c-kit$^+$ RCSCs cannot differentiate into new cardiomyocytes directly, they can improve heart function through an immune response by recruiting the accumulation of CCR2$^+$ and CX3CR1$^+$ macrophages (Vagnozzi et al., 2020). Challenges still remain regarding the future direction of RCSCs before bringing them into clinical practice. For instance, difficulty in autogenous cell isolation and the low survival rate of RCSCs in infarcted hearts limited their application. Moreover, numerous complications have been discussed after RCSC implantation (Eschenhagen et al., 2017). It is essential to explore novel methods to improve homing, survival, proliferation, and differentiation of RCSCs in injured hearts.

Potential and limitations of skeletal myoblast therapy

SMs are commonly isolated from muscle tissues and suffer *ex vivo* expansion for MI treatment. Pre-clinical evidence has proved their repair effects in MI (Imanishi et al., 2011). Furthermore, some Phase I clinical trials have generated exciting results for the therapeutic efficiency of SMs in MI, suggesting an increasingly global and regional LVEF, and improvement in cardiac tissue viability in the infarct areas (Herreros et al., 2003; Siminiak et al., 2004; Dib et al., 2009). However, the results of the Phase II MAGIC trial showed that myoblast injections in patients with depressed LV function failed to improve their heart function and increased the number of early postoperative arrhythmic events (Menasché et al., 2008). The other limitations of SMs are summarized as follows. First, the most severe drawback of SM-based therapy may be their lineage restriction and inability to produce new cardiomyocytes (Terajima et al., 2014). Second, the complexity of autologous SM products limits their wide application (Ponsuksili et al., 2022). Third, the immunogenicity of SMs increases the risk and complications in clinical treatments. Lastly, SMs also have a low survival rate; up to 90% of SMs die over the first days after engraftment, and the myoblast-transplanted human heart confirms the scarcity of persisting myotubes in scar tissues (Skuk and Tremblay, 2019).

Regulatory mechanism of Chinese medicines underlying stem cell therapy

To overcome the limitations of stem cell therapy, researchers have applied various methods to find approaches to enhance its efficacy for MI. Therein, Chinese medicines stand out due to their high efficiency and low toxicity, offering a feasible approach to compensate for the disadvantages of stem cell therapy. Based on TCM theory, Zhang et al. studied the related research about stem cells and kidney essence, found their similarity in the origin of life and physiological function, and provided new ideas for the research on the basic theory of TCM (Zhang and Zhang, 2018). Moreover, they further refined the view of "kidney properties" activating blood and removing stasis and clarified that stem cells were the material basis of "kidney properties" (Zhang et al., 2016). Next, we discuss how Chinese medicines improve the efficacy of stem cell therapy in TCM theories. More importantly, we will categorize TCM in prescription, botanical and other natural drug substances, pure compounds; and experiments *in vivo* and *in vitro* to better understand the mechanisms of TCM treatment in MI. We have summarized the mechanism of Chinese medicines for stem cell therapy in Figure 2 and Table 1, 2.

Chinese medicines promote the proliferation of stem cells by tonifying the spleen and kidney, nourishing qi and blood

The regenerative potential of stem cells is directly proportional to the number of available stem cells and their proliferation ability (Hedderich et al., 2020). Among these stem cells, BMSCs can differentiate into various lineages without risk of immunological rejection, so they have been mostly applied in stem cell transplantation. With developments in chemical purification technologies and mass spectrometry, the active compounds of numerous Chinese medicine formulas have been successfully purified, and their effects on BMSC proliferation have been detected.

For instance, Si–Wu decoction (SDE), a classic blood-tonifying formula in TCM, has been adopted for clinical treatment in China for centuries. Zeng H. P. et al., extracted the active ingredients of this formula using ethyl acetate/chloroform to explore its proliferation-promoting effects on BMSCs (Zeng et al., 2008). A total of 20 compounds were obtained, and ligustilide displayed the best proliferation-promoting effect. Palmitic acid methyl ester and stearic acid ethyl were also responsible for promoting the proliferation of BMSCs. Extractions with 0.3 mg/ml concentration had a better efficacy of BMSCs proliferation than bFGF, a common positive control in this area. Furthermore, another constituent of flavonoids from the *Epimedium brevicornu* Maxim. [Berberidaceae] (EBM), icariin (ICA), also facilitated the proliferation of BMSCs by

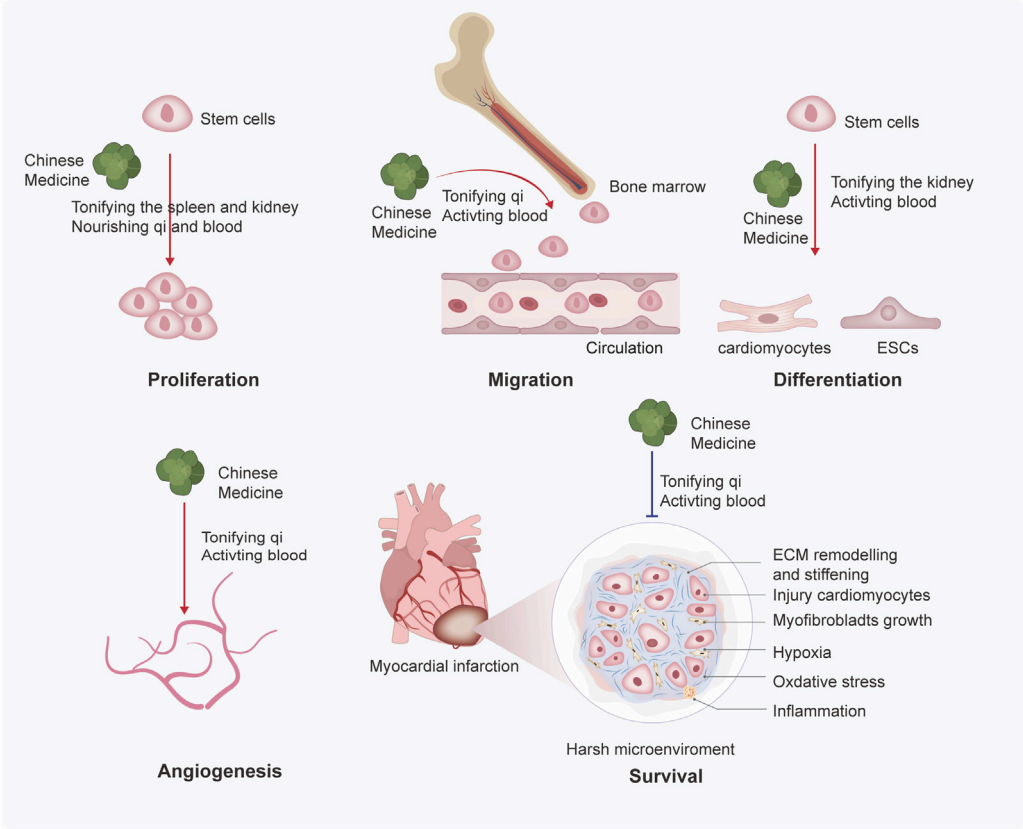

FIGURE 2
Mechanisms of Chinese medicines based on TCM theory enhance the efficacy of stem cell therapy. Chinese medicine promotes the proliferation, migration, differentiation, angiogenesis, and survival of stem cells. Through the summary analysis from commonly used prescriptions, the mechanisms based on TCM theory may be finally inferred as follows: 1) Chinese medicine promotes the proliferation of stem cells by tonifying the spleen and kidneys, nourishing qi and blood; 2) Chinese medicine promotes migration of stem cells by tonifying the qi and activating blood; 3) Chinese medicine promotes differentiation of stem cells by tonifying the kidney and activating blood; and) Chinese medicine promotes angiogenesis and survival by tonifying qi and activating blood.

activating ERK and p38 MAPK signaling pathways, and regulating their downstream transcription factors Elk1 and c-Myc (Qin et al., 2015). Several studies found the active components of Plastrum testudinis [Testudinidae] (PT) were able to promote BMSCs proliferation (Chen et al., 2007; Wang et al., 2012a). Further mechanism studies suggested that myristate is the main active component of PT, and it can increase the release of bone morphogenetic protein 4 (BMP4) from BMSCs in a time- and dose-dependent manner (Chen et al., 2009). Buzhong Yiqi decoction (BYD), a tonic formula of TCM, and its active compound, hexadecanoic acid (HA), was responsible for promoting the proliferation of BMSCs (Chen et al., 2010). Moreover, astragaloside, a compound from qi-replenishing Chinese medicine, promoted differentiation and proliferation, inhibited apoptosis, and reduced the inflammatory effects of BMSCs (Zhu et al., 2017).

ADSCs are believed to be a suitable cell source of regenerative treatment for their self-renewal capacity and multilineage differentiation. Chinese medicine also exhibits proliferation-promoting action in ADSCs. Rehmannia glutinosa oligosaccharide (RGO), an extract from Chinese medicine, has been proven to increase proliferation and relieve H_2O_2-induced apoptosis of ADSCs by the paracrine secretion of VEGF and HGF (Zhang et al., 2012). These studies have now allowed for refinement in the understanding of TCM with respect to pharmacological regulation of proliferation of stem cells and may be helpful to stem cell biology and therapy.

In summary, according to the TCM theory—"Kidney dominated bone marrow" (Gu et al., 2019), Chinese medicines used in promoting the proliferation of stem cells are mainly kidney-tonifying medicines such as ICA and PT or blood-nourishing medicines such as ligustilide and RGO. To a certain extent, this conforms to the mechanism of the inadequate number of stem cells in modern medicine and provides an integrative theoretical foundation for the proliferation of stem cells.

TABLE 1 Summary of prescriptions on stem cell therapy.

Prescriptions	Dose & Duration	Experimental subject	Effect
Guanxin Danshen formulation (冠心丹参方)[a]	100 mg/kg/d, 28 d	SD male rats	Promoting survival of BMSCs (Han et al., 2019)
Taohong Siwu decoction (桃红四物汤)[a]	1.13 g/ml/250 g/d (concentrated extraction), 28 d	SD male rats	Decreasing mitochondrial fission (Luo et al., 2019)
Xuefu Zhuyu decoction (血府逐瘀汤)[a]	5%, 10%, and 15%-drug serum	rEPC	Induced angiogenesis through EPC activation (Gao et al., 2010)
Shuangxinfang (双心方)[a]	1 ml/100 g, 3, 7, and 14 d	Male SD rats	Promoting mobilization of BMSCs (Wang et al., 2019)
Shuanglong formula (双龙方)[a]	1 μg/ml, 24 h	rMSCs	Promoting differentiation of BMSCs (Fan et al., 2010)
Tongxinluo (通心络)[a]	50 mg/kg/d, 7 d	Chinese mini pigs	Promoting survival and differentiation of MSCs (Qian et al., 2007)
	50–400 μg/ml, 6 h	rMSCs	Inhibiting apoptosis of MSCs (Li et al., 2014)
	400 μg/ml (pre-treat), 24 h	SD rats	Promoting cardiac repair combined with Exo (Xiong et al., 2022a; Xiong et al., 2022b)
Danhong injection (丹红注射液)[a]	1.5 ml/kg/d, 28 d (ip)	Male C57BL/6J mice	Promoting mobilization and angiogenesis of BMSCs (Chen et al., 2018)
Xuesaitong injection (血塞通注射液)[a]	150 mg/kg/d, 1, 7, and 14 d (ip)	Female and male Wistar rats	Promoting mobilization of BMSCs (Zhang et al., 2011)
Si–Wu decoction (四物汤)[a]	0.03–0.3 mg/ml, 72 h	rMSCs	Promoting proliferation of BMSCs (Zeng et al., 2008)
Gu Ben Pei Yuan San (固本培元散)[a]	5% and 10% drug powder mixed in feed for 7 d, 1 m, and 2 m	Male C57BL/6J mice	Promoting differentiation of iPSCs (Cui et al., 2019)

[a]The compositions of the prescriptions are presented in Supplementary Table S1.

Chinese medicines promote the mobilization and migration of stem cells by tonifying the qi and activating blood

Stem cells need to be recruited to infarct areas after reaching a certain number. TCM promotes the mobilization and migration of stem cells as well. Several BMSC-mobilizing factors, including transforming growth factor-β (TGF-β), tumor necrosis factor-α (TNF-α), stromal-derived factor-1 (SDF-1), and hepatocyte growth factor (HGF), can promote the migration of BMSCs and induce cardiac repair (Yu et al., 2015; Sun et al., 2018). Guanxin Danshen (GXDS) formulation with the preparation of dripping pills, which mainly activates blood in various diseases, increased SDF-1 levels in the infarcted area and enhanced the migration of BMSCs (Han et al., 2019). Shuangxinfang aqueous extract (Wang et al., 2019) and classical TCM prescriptions derived from the Danshen decoction and Baihe Dihuang decoction promoted the mobilization of BMSCs, inhibited the inflammatory response, and improved heart function after AMI. As a new dosage form of TCM, TCM injection (TCMI) is an important step in the modernizing of TCM. Danhong injection (DHI) increased the residence of BMSCs in cardiac tissue by regulating the SDF1/CXCR4 signaling (Chen et al., 2018). Moreover, the aqueous extract of *Ligusticum striatum* DC. [Apiaceae] and *Paeonia lactiflora* Pall. [Paeoniaceae] protected cardiomyocytes by promoting angiogenesis and mobilization of stem cells (Shi et al., 2019). Consequently, TCM prescriptions for promoting blood circulation or removing blood stasis are useful in promoting the migration of stem cells and the treatment of MI. Meanwhile, the specific blood-activating compounds are investigated as follows.

Tanshinone IIA (TIIA)- and astragaloside IV-stimulated BMSCs showed enhanced capacities of homing to ischemic myocardium partially by upregulation of the CXCR4 expression (Xie et al., 2013). Panax notoginseng saponins (PNS) combined with G-CSF to promote c-kit$^+$ BMSCs from the marrow into blood circulation and mobilized their "homing" to the infarction sites (Zhang et al., 2011). Further studies revealed that PNS increased the mobilization of progenitor cells *via* SDF-1α-CXCR4 interaction, thus decreasing the sizes of atherosclerotic plaques (Liu et al., 2013) as well as resveratrol (RSV) (Hong et al., 2015). Additionally, acupuncture is an important part of TCM and plays an essential role in stem cell mobilization as well. Recently, we have demonstrated that electro-acupuncture can repair myocardial damage by regulating the SDF-1/CXCR4 axis (Zhao et al., 2022).

Chinese medicines promote the differentiation of stem cells by tonifying the kidney and activating blood

The most important suggested mechanism of stem cell therapy is a substitution of injured cells by brand new stem cells, which needs successful differentiation in infarct areas (Müller et al., 2018). Nevertheless, in all cases, the

TABLE 2 Summary of natural drug substances on stem cell therapy.

Botanical and other natural drug substances	Compounds and metabolite	Dose and duration	Experimental subject	Effect
Astragalus mongholicus Bunge (Huang Qi)	Astragaloside IV	0.1–2 μg/ml (pre-treat), 72 h	SD rats; mMSCs	Promoting mobilization of BMSCs (Xie et al., 2013)
		20–50 mg/kg/d, 14 d; 10–160 μmol/L, 72 h	SD rats; rHUVECs	Promoting angiogenesis (Cheng et al., 2019)
	Astragaloside	5–500 ng/ml, 24–48 h	rMSCs	Promoting proliferation of MSCs (Zhu et al., 2017)
Epimedium brevicornu Maxim. (Yin Yang Huo)	Icariin	20–320 μg/L, 72 h	rBMSCs	Promoting proliferation of BMSCs *via* activating ERK and p38 MAPK (Qin et al., 2015)
Plastrum testudinis (PT, Gui Ban)	Fatty acid, fatty acid esters, and steroid	0.01–3 mg/ml, 24 h-5 d	rMSCs	Promoting proliferation of BMSCs (Chen et al., 2007)
	Fatty acid, fatty acid esters, and steroid	0.03–3 mg/ml, 24 h-5 d	rMSCs	Promoting proliferation of BMSCs (Wang et al., 2012a)
	Cholesterol myristate	30–300 μg/ml 72 h, 1 d, 3 d	rMSCs	Promoting proliferation of BMSCs (Chen et al., 2009)
Rehmannia glutinosa (Gaertn.) DC. (Di Huang)	Rehmannia glutinosa oligosaccharide (RGO)	1–400 mg/L, 72 h	hADMSCs	Promoting survival of ADSCs (Zhang et al., 2012)
Codonopsis pilosula (Franch.) Nannf. (Dang Shen)	—	10 mg/300 g, 10 d; 0.5 mg/ml, 10 d	Male Wistar rats; ES	Promoting differentiation of ESCs (Wang et al., 2021)
Panax ginseng C.A.Mey. (Ren Shen)	Ginsenosides Re	135 mg/kg, 28 d	Male Wistar rats	Inhibiting fibrosis (Yu et al., 2020)
Ligusticum striatum DC. (Chuan Xiong); *Paeonia lactiflora* Pall. (Shao Yao)	—	55 mg/kg/d, 21 d	Male C57BL/6J mice	Promoting mobilization and angiogenesis of BMSCs (Shi et al., 2019)
Paeonia lactiflora Pall. (Shao Yao)	Total paeony glucosides (TPGs)	5–40 μg/ml, 24 h	rH9c2	Preserving antioxidant defense (Luo et al., 2013)
Geum japonicum var. chinense F.Bolle	The angiogenic and cardiomyogenic fractions were mixed as myocardial repair fraction	0.3 mg, 30 d; 20–80 μg/ml, 72 h	SD rats; HCAEC	Promoting angiogenesis and cardiomyogenesis (Li et al., 2006)
	Cardiogenin	0.3 mg/kg/d, 14 d; 10 μg/ml, 4 d	SD rats; rMSCs	Promoting differentiation of BMSCs (Cheng et al., 2009)
		2 mg/kg/d, 14 d	SD rats	Promoting differentiation of BMSCs (Lin et al., 2012)
Salvia miltiorrhiza Bunge (Dan Shen)	Salvianolic acid B	10 μmol/L, 28 d; 1–100 μmol/L 24 h	Female SD rats; rMSCs	Promoting proliferation, differentiation, and angiogenesis of BMSCs (Guo et al., 2014)
		80, 160 mg/kg, 30 d; 5–20 ng/ml, 24 h	Male KM mice; CFs	Inhibiting fibrosis (Gao et al., 2019)
	Tanshinone IIA	0.1–2 μg/ml, 72 h	SD rats; mMSCs	Promoting mobilization of BMSCs (Xie et al., 2013)
		0.1–2 μg/ml, 72 h		
		1.5 mg/kg/d, 28 d; 10 μM, 24 h	SD rats; rCFs	Inhibiting fibrosis (Chen et al., 2021b)
Panax notoginseng (Burkill) F.H. Chen (San Qi)	Notoginsenoside R1	267 ng/kg (nanoparticle), 48 h 0.1–1,000 μg/ml, 2 h	BALB/c nude mice, C57BL/6 mice; H9C2, rCMs	Improving cardiac function (Li et al., 2022)
	Total panax notoginsenosides	0.1–100 μg/ml, 10 d	rBMSCs	Promoting angiogenesis of BMSCs (Zheng et al., 2013)
Scutellaria baicalensis Georgi (Huang Qin)	Baicalin	5–500 ng/ml, 24–48 h	rMSCs	Promoting proliferation of MSCs (Zhu et al., 2017)
/	Resveratrol	25 mg/kg/day, 28 d	Male C57BL6J mice	Promoting mobilization of BMSCs (Hong et al., 2015)
/	Hexadecanoic acid	3–30 μg/ml, 72 h	rMSCs	Promoting proliferation of BMSCs (Chen et al., 2010)

differentiation efficiency of stem cells is low, limiting the progression of stem cell differentiation in stem cell therapy (Bian et al., 2019). Due to its importance, TCM has been widely used for the differentiation of stem cells.

For example, *Geum japonicum* var. Chinense F. Bolle [Rosaceae] (GJ), usually used in the Miao ethnic minority group, promoted the cardiogenic differentiation capability of BMSCs, thus repairing infarcted hearts (Cheng et al., 2009). Further studies have shown that cardiogenin is the main active compound of GJ, which stimulates the processes of angiogenesis and cardiomyogenesis (Li et al., 2006; Lin et al., 2012). The Shuanglong formula (SLF) composed of ginsenosides Rg1 and salvianolic acid B (SalB) promoted BMSCs into cardiomyocyte-like cells (Fan et al., 2010). Therein, SalB (Guo et al., 2014), a water-soluble component of *Salvia miltiorrhiza* Bunge [Lamiaceae] induced BMSCs to differentiate into vascular endothelial cells (VECs), but not cardiomyocytes, improving angiogenesis and heart function after BMSC transplantation mainly through a paracrine effect. Long-term oral intake of Gu Ben Pei Yuan San (GBPYS) powder significantly improved cardiac function by promoting the division of both cardiomyocytes and iPSC-derived cardiomyocytes *in vitro*. Oral intake of GBPYS improved heart repair after myocardial damage in adult mice (Cui et al., 2019). GBPYS feeding for 3 months had no apparent toxicity to the liver, kidneys, and blood in normal mice, suggesting the relative safety of TCM treatment. Moreover, the extracts from *Codonopsis pilosula* (Franch.) Nannf. [Campanulaceae] promoted the cardiogenic differentiation of ESCs (Wang et al., 2021).

In conclusion, replenishing qi and activating blood is the basic therapeutic principle of TCM in regulating stem cell differentiation. In addition, electrical stimulation enhanced the efficiency of cardiac differentiation into iPSCs and promoted cardiomyocyte maturation (Ma et al., 2018). In fact, ESCs and iPSCs can differentiate into spontaneously beating cardiomyocytes, while ASCs can only be differentiated into cardiac cell types of expression of cardiomyocytic markers (Gurusamy et al., 2018). However, small molecular compounds facilitate the trans-differentiation of fibroblasts into cardiomyocytes directly (Fu et al., 2015) or induced ASCs to iPSCs (Guan et al., 2022). Thus, identifying potential natural drug compounds may provide new methods for developing regenerative therapeutic strategies.

Chinese medicines promote angiogenesis of stem cells by tonifying qi and activating blood

MI inflicts massive damage to the coronary microcirculation, resulting in vascular disintegration and rarefication of capillaries in the ischemia area (Wu et al., 2021). Cardiac repair after MI involves complex angiogenesis, which starts in the infarct border region and expands to the infarct core. TCM facilitates angiogenesis in the infarct zone through several mechanisms.

EPCs serve as endogenous repair cells to counteract endothelial cell damage, substitute dysfunctional endothelium, and repair tissue after MI (Berger et al., 2013). Xuefu Zhuyu decoction (XFZYD) induced the angiogenesis of EPCs and promoted capillary tube formation (Gao et al., 2010). BMSCs have a strong ability to promote angiogenesis, and TCM combined with them to enhance the process of angiogenesis. DHI (Chen et al., 2018) and PNS (Zheng et al., 2013) increased the expression of VEGF-A of BMSCs in the marginal zone of infarction. The combination of *Ligusticum striatum* DC. [Apiaceae], *Paeonia lactiflora* Pall. [Paeoniaceae] (Shi et al., 2019), and SalB (Guo et al., 2014) protected the ischemic myocardium through angiogenesis. Astragaloside IV (AS-IV) promoted angiogenesis and cardio-protection after MI by activating the PTEN/PI3K/Akt signaling pathway (Cheng et al., 2019).

Chinese medicines promote the survival of stem cells under the cardiac microenvironment by tonifying qi and activating blood

The efficacy of stem cell-based therapy is based on the survival of stem cells, as well as on the alteration of phenotype and biology that may take place on these cells after engraftment (Franchi et al., 2020). The post-ischemic myocardial microenvironment, characterized by inflammation, oxidative stress, hypoxia, and fibrosis, may inhibit the survival of stem cells (Wei et al., 2016). TCM can protect stem cells by countering the hostile cardiac microenvironment.

Tongxinluo (TXL) is extracted and concentrated from a group of botanical and other natural drug substances, including *Panax ginseng* C.A. Mey. [Araliaceae], *Paeonia lactiflora* Pall. [Paeoniaceae], *Cinnamomum camphora* (L.), J. Presl [Lauraceae], and Ziziphus jujuba Mill. [Rhamnaceae], which benefits qi and performs the function of blood activation (Qi et al., 2015). It could induce the survival and differentiation of BMSCs through the inhibition of apoptosis, oxidative stress, less fibrosis, and inflammatory cell infiltration with more surviving myocardium (Qian et al., 2007; Li et al., 2014; Xiong et al., 2022a). Moreover, TXL-pretreated BMSCs significantly improved cardiac repair through the exosomal transfer of miR-146a-5p by the IRAK1/NF-κB p65 pathway, which may have the potential for clinical translation (Xiong et al., 2022b). In addition, the GXDS formulation increased the number of injected BMSCs in the infarct area by decreasing cell apoptosis and promoting angiogenesis in the peri-infarction and infarction area (Han et al., 2019). Total paeony glucosides (TPGs) extracted from the roots of *Paeonia lactiflora* Pall. [Paeoniaceae] alleviated the dysfunction of cardiomyoblast by preserving antioxidant defense

(Luo et al., 2013). Moreover, SalB (Gao et al., 2019) and ginsenoside Re (Yu et al., 2020) inhibited the fibrosis process of the myocardial *via* regulating TGF-β/Smads signal pathways, whereas tanshinone IIA showed anti-fibrosis action by inhibiting oxidative stress (Chen et al., 2021b). Tetramethylpyrazine/ligustrazine (TMP) increased the survival rate of ADSCs, probably inducing the expression of transcription factors associated with fat formation, including peroxisome proliferator-activated receptor γ (PPARγ), CCAAT/enhancer-binding protein α, and Alu (Zhou et al., 2020). Our previous work has also shown that Taohong Siwu decoction (THSWD) aqueous extract improved the local ischemic microenvironment by decreasing mitochondrial fission after MI (Luo et al., 2019). Moreover, we designed a nanoparticle of MSN-Notoginsenoside R1 (NGR1)-CD11 b antibody, which enhanced the targeting of NGR1 *via* activation of AKT and MAPK signaling pathways and might provide a new method for targeted drug delivery systems for the MI (Li et al., 2022). Taken together, TCM promotes the survival of stem cells by ameliorating hostile microenvironment in infarction areas, including remodeling inflammation microenvironment, fibrosis microenvironment, hypoxia microenvironment, oxidative stress microenvironment, and angiogenesis microenvironment.

Deficiencies of Chinese medicines in stem cell therapy

Although the pre-clinical evidence shows that TCM is helpful in stem cell therapy, further mechanisms involved in TCM have not been thoroughly investigated. We systematically assessed the detailed experimental design and reliability of included pharmacological research in our review according to the consensus of the best practice in research (Heinrich et al., 2020). Of the total 37 MI studies, 10 *in vitro,* 12 *in vivo*, and 15 *in vivo* and *in vitro* studies, *only* one *study* provided patient-relevant results. Among these 37 studies, only one study evaluated the toxicity of TCM (Cui et al., 2019), and three studies used positive control (Zeng et al., 2008; Zhang et al., 2011; Gao et al., 2019). Overall, the majority of the studies present specific experimental details and verify the effectiveness of TCM treatment. However, the putative TCM efficacy based on pre-clinical studies may not be accurate and comprehensive enough.

Pharmacokinetic (PK) studies are essential to build concentration-activity/toxicity and promote target identification of Chinese medicine (Yan et al., 2018). TCM PK routines include five dimensions: 1) system analysis of chemical substances using liquid chromatograph mass spectrometry (LC–MS) together with the utilization of data in available chemical databases; 2) identification of the absorbed prototypes, absorbed metabolites, and unabsorbed constituents of TCM *in vivo*; 3) comprehensive study of the therapeutic mechanisms of TCM; 4) establishment of the qualitative and quantitative pharmacokinetics–pharmacodynamics (PK–PD) patterns by multidimensional data and mathematical modeling; and 5) validation of the main compounds and targets by gene-editing technology (Xu et al., 2021). Most studies in this review have met the basic requirements of PK studies. For example, silica gel column chromatography was used to identify the extraction of Si–Wu decoction (Zeng et al., 2008), and GC–MS was adopted to analyze the active compounds of Plastrum testudinis [Testudinidae] (Chen et al., 2007) and Buzhong Yiqi decoction (Chen et al., 2010). However, the plasma drug PK involves absorption, distribution, metabolism, and excretion of TCM in the body which has not been directly examined in these studies. TCM may perform a synergistic function in treating MI in combination with stem cell-based therapy by regulating the multi-targets through various signaling pathways. Strictly controlled animal models with multi-perspective pharmacokinetic evaluation need urgent investigation.

In addition, the efficacy of TCM in stem cell therapy still lacks high-grade clinical evidence. Zhang et al. (2020) systematically reviewed the effect of TCM on patients with MI, but the evidence from clinical trials was insufficient to assess the effect of TCM on patients with MI. Further rigorously designed random clinical trials with a large cohort of patients are required to verify or discover the efficacy of TCM in treating MI. Multi-disciplinary efforts are highly demanded to translate TCM-based treatment into a more persuasive proof of clinical efficacy.

Moreover, the side effects of TCM in stem cell therapy cannot be ignored. SMB, a commonly used botanical drug for MI treatment, is considered relatively safe and well tolerated during the treatment (Wang et al., 2012b). However, SMB injection may cause body weight loss and even increase the total bilirubin level and focal inflammation in a dose-dependent manner. In a cohort study, 30,180 patients were recruited to evaluate the adverse events of SMB, and the results showed that SMB might cause rashes, pruritus, platelet count abnormalities, and palpitations (Jia et al., 2019). Nevertheless, the most adverse events of SM were mild to moderate and cleared up after SM treatment withdrawal. *Carthamus tinctorius* L. [Asteraceae], with the efficacy of activating blood and resolving stasis, led to acute liver failure (ALF) in a few patients (de Ataide et al., 2018). In addition, the kidney-tonifying botanical drug, *Cullen corylifolium* (L.) Medik. [Fabaceae], caused ALF as well (Li et al., 2019b). Moreover, pre-treatment of umbilical cord-derived mesenchymal stem cells (UC-MSCs) with asarinin significantly promotes the immunosuppressive effects of MSC after HSC transplantation (He et al., 2021), whereas it may have multiple cytotoxic effects, including arrhythmia, respiratory center depression, hepatotoxicity, and nephrotoxicity (Jeong et al., 2018). These are Chinese

medicines commonly used in the clinical practice of MI; thus, attention must be paid when using these botanical drugs. First, it is recommended to take botanical drugs following the doctors' instructions with a moderate dose. Second, processing (Paozhi) through steaming, boiling, stewing, refined honey, stir-frying, and calcining can directly reduce the contents of toxic constituents (Wu et al., 2018). Eventually, this not only alleviates the side effect of TCM but also improves oral absorption and bioavailability by using modern methods and materials to modify the TCM dosage form, such as lipid nanocarriers, polymeric nanocarriers, inorganic nanocarriers, and hybrid nanocarriers (Liu and Feng, 2015).

Conclusion

Stem cell-based therapy after MI has made excellent progress in the last decade, whereas its drawbacks, such as low survival rate, low differentiation rate, and strong immunogenicity, severely limited the clinical application of this therapy. Our review showed that TCM has a great potential to compensate for the limitation of stem cells and can thus work together in preventing and treating MI. Based on TCM theories, we further summarized the mechanisms of Chinese medicine treatment in stem cell therapy by the commonly used prescriptions discussed previously. It seems that the role of TCM differs in different stages of stem cell therapy: 1) during the proliferation of stem cells, TCM mainly functions by tonifying the spleen and kidneys, nourishing qi and blood; 2) during the migration of stem cells, TCM mainly functions by tonifying the qi and activating blood; 3) during the differentiation of stem cells, TCM mainly functions by tonifying the kidneys and activating blood; and 4) when stem cells reach the infarct region, TCM can protect them even under hostile microenvironments by tonifying the qi and activating blood. In conclusion, tonifying the spleen and kidneys, replenishing qi, and activating blood are the basic therapeutic principles of TCM throughout the stem cell therapy. The principles allow us to choose the appropriate Chinese medicines in different stages of stem cell therapy for a more defined and precise functional study.

Author contributions

YW and H-DG conceived the structure of the manuscript. YW wrote the manuscript and constructed the figures. YX and H-DG reviewed and revised the manuscript. All authors read and approved the final manuscript.

Funding

This work was supported by grants from the National Natural Science Foundation of China (82174120, 81970991), Natural Science Foundation of Shanghai (No. 21ZR1463100), Shanghai Talent Development Funding Scheme (No. 2019090), and Program of Shanghai Academic Research Leader (22XD1423400).

Conflict of interest

The authors declare that the research was conducted in the absence of any commercial or financial relationships that could be construed as a potential conflict of interest.

Publisher's note

Supplementary material

The Supplementary Material for this article can be found online at: https://www.frontiersin.org/articles/10.3389/fphar.2022.1013740/full#supplementary-material

SUPPLEMENTARY TABLE S1
Composition of TCM prescription.

References

Afjeh-Dana, E., Naserzadeh, P., Moradi, E., Hosseini, N., Seifalian, A. M., and Ashtari, B.(2022). Stem cell differentiation into cardiomyocytes: Current methods and emerging approaches. *Stem Cell. Rev. Rep.* 18 (6). doi:10.1007/s12015-021-10280-1

Bacakova, L., Zarubova, J., Travnickova, M., Musilkova, J., Pajorova, J., Slepicka, P., et al. (2018). Stem cells: Their source, potency and use in regenerative therapies with focus on adipose-derived stem cells - a review. *Biotechnol. Adv.* 36 (4), 1111–1126. doi:10.1016/j.biotechadv.2018.03.011

Beltrami, A. P., Barlucchi, L., Torella, D., Baker, M., Limana, F., Chimenti, S., et al. (2003). Adult cardiac stem cells are multipotent and support myocardial regeneration. *Cell.* 114 (6), 763–776. doi:10.1016/s0092-8674(03)00687-1

Berger, S., Aronson, D., Lavie, P., and Lavie, L. (2013). Endothelial progenitor cells in acute myocardial infarction and sleep-disordered breathing. *Am. J. Respir. Crit. Care Med.* 187 (1), 90–98. doi:10.1164/rccm.201206-1144OC

Bian, X., Ma, K., Zhang, C., and Fu, X. (2019). Therapeutic angiogenesis using stem cell-derived extracellular vesicles: An emerging approach for treatment of ischemic diseases. *Stem Cell. Res. Ther.* 10 (1), 158. doi:10.1186/s13287-019-1276-z

Blocki, A., Beyer, S., Dewavrin, J. Y., Goralczyk, A., Wang, Y., Peh, P., et al. (2015). Microcapsules engineered to support mesenchymal stem cell (MSC) survival and proliferation enable long-term retention of MSCs in infarcted myocardium. *Biomaterials* 53, 12–24. doi:10.1016/j.biomaterials.2015.02.075

Bulati, M., Miceli, V., Gallo, A., Amico, G., Carcione, C., Pampalone, M., et al. (2020). The immunomodulatory properties of the human amnion-derived mesenchymal stromal/stem cells are induced by INF-γ produced by activated lymphomonocytes and are mediated by cell-to-cell contact and soluble factors. *Front. Immunol.* 11, 54. doi:10.3389/fimmu.2020.00054

Cao, Y., Wang, J., Su, G., Wu, Y., Bai, R., Zhang, Q., et al. (2016). Anti-myocardial ischemia effect of Syringa pinnatifolia Hemsl. by inhibiting expression of cyclooxygenase-1 and -2 in myocardial tissues of mice. *J. Ethnopharmacol.* 187, 259–268. doi:10.1016/j.jep.2016.04.039

Carvalho, E., Verma, P., Hourigan, K., and Banerjee, R. (2015). Myocardial infarction: Stem cell transplantation for cardiac regeneration. *Regen. Med.* 10 (8), 1025–1043. doi:10.2217/rme.15.63

Chamberlain, S. J. (2016). Disease modelling using human iPSCs. *Hum. Mol. Genet.* 25 (R2), R173–r181. doi:10.1093/hmg/ddw209

Chen, C., Dai, P., Nan, L., Lu, R., Wang, X., Tian, Y., et al. (2021). Isolation and characterization of endothelial progenitor cells from canine bone marrow. *Biotech. Histochem.* 96 (2), 85–93. doi:10.1080/10520295.2020.1762001

Chen, D. F., Du, S. H., Zhang, H. L., Li, H., Zhou, J. H., Li, Y. W., et al. (2009). Autocrine BMP4 signaling involves effect of cholesterol myristate on proliferation of mesenchymal stem cells. *Steroids* 74 (13-14), 1066–1072. doi:10.1016/j.steroids.2009.08.008

Chen, D. F., Li, X., Xu, Z., Liu, X., Du, S. H., Li, H., et al. (2010). Hexadecanoic acid from Buzhong Yiqi decoction induced proliferation of bone marrow mesenchymal stem cells. *J. Med. Food* 13 (4), 967–970. doi:10.1089/jmf.2009.1293

Chen, D. F., Zeng, H. P., Du, S. H., Li, H., Zhou, J. H., Li, Y. W., et al. (2007). Extracts from Plastrum testudinis promote proliferation of rat bone-marrow-derived mesenchymal stem cells. *Cell. Prolif.* 40 (2), 196–212. doi:10.1111/j.1365-2184.2007.00431.x

Chen, J., Wei, J., Huang, Y., Ma, Y., Ni, J., Li, M., et al. (2018). Danhong injection enhances the therapeutic efficacy of mesenchymal stem cells in myocardial infarction by promoting angiogenesis. *Front. Physiol.* 9, 991. doi:10.3389/fphys.2018.00991

Chen, R., Chen, W., Huang, X., and Rui, Q. (2021). Tanshinone IIA attenuates heart failure via inhibiting oxidative stress in myocardial infarction rats. *Mol. Med. Rep.* 23 (6), 404. doi:10.3892/mmr.2021.12043

Chen, S. L., Fang, W. W., Qian, J., Ye, F., Liu, Y. h., Shan, S. j., et al. (2004). Improvement of cardiac function after transplantation of autologous bone marrow mesenchymal stem cells in patients with acute myocardial infarction. *Chin. Med. J.* 117 (10), 1443–1448.

Cheng, L., Chen, H., Yao, X., Qi, G., Liu, H., Lee, K., et al. (2009). A plant-derived remedy for repair of infarcted heart. *PLoS One* 4 (2), e4461. doi:10.1371/journal.pone.0004461

Cheng, S., Zhang, X., Feng, Q., Chen, J., Shen, L., Yu, P., et al. (2019). Astragaloside IV exerts angiogenesis and cardioprotection after myocardial infarction via regulating PTEN/PI3K/Akt signaling pathway. *Life Sci.* 227, 82–93. doi:10.1016/j.lfs.2019.04.040

Cui, B., Zheng, Y., Zhou, X., Zhu, J., Zhuang, J., Liang, Q., et al. (2019). Repair of adult mammalian heart after damages by oral intake of Gu ben Pei yuan san. *Front. Physiol.* 10, 607. doi:10.3389/fphys.2019.00607

Davy, P. M., Lye, K. D., Mathews, J., Owens, J. B., Chow, A. Y., Wong, L., et al. (2015). Human adipose stem cell and ASC-derived cardiac progenitor cellular therapy improves outcomes in a murine model of myocardial infarction. *Stem Cells Cloning* 8, 135–148. doi:10.2147/SCCAA.S86925

de Ataide, E. C., Reges Perales, S., de Oliveira Peres, M. A., Bastos Eloy da Costa, L., QuarellaF.Valerini, F. G., et al. (2018). Acute liver failure induced by Carthamus tinctorius oil: Case reports and literature review. *Transpl. Proc.* 50 (2), 476–477. doi:10.1016/j.transproceed.2018.01.010

Deng, S., Zhou, X., Ge, Z., Song, Y., Wang, H., Liu, X., et al. (2019). Exosomes from adipose-derived mesenchymal stem cells ameliorate cardiac damage after myocardial infarction by activating S1P/SK1/S1PR1 signaling and promoting macrophage M2 polarization. *Int. J. Biochem. Cell. Biol.* 114, 105564. doi:10.1016/j.biocel.2019.105564

Dib, N., Dinsmore, J., Lababidi, Z., White, B., Moravec, S., Campbell, A., et al. (2009). One-year follow-up of feasibility and safety of the first U.S., randomized, controlled study using 3-dimensional guided catheter-based delivery of autologous skeletal myoblasts for ischemic cardiomyopathy (CAuSMIC study). *JACC. Cardiovasc. Interv.* 2 (1), 9–16. doi:10.1016/j.jcin.2008.11.003

Ding, R., Jiang, X., Ha, Y., Wang, Z., Guo, J., Jiang, H., et al. (2015). Activation of Notch1 signalling promotes multi-lineage differentiation of c-kit(POS)/NKX2.5(POS) bone marrow stem cells: Implication in stem cell translational medicine. *Stem Cell. Res. Ther.* 6 (1), 91. doi:10.1186/s13287-015-0085-2

Drowley, L., Koonce, C., Peel, S., Jonebring, A., Plowright, A. T., Kattman, S. J., et al. (2016). Human induced pluripotent stem cell-derived cardiac progenitor cells in phenotypic screening: A transforming growth factor-β type 1 receptor kinase inhibitor induces efficient cardiac differentiation. *Stem Cells Transl. Med.* 5 (2), 164–174. doi:10.5966/sctm.2015-0114

Eldaly, A. S., Mashaly, S. M., Fouda, E., Emam, O. S., Aglan, A., Abuasbeh, J., et al. (2022). Systemic anti-inflammatory effects of mesenchymal stem cells in burn: A systematic review of animal studies. *J. Clin. Transl. Res.* 8 (4), 276–291.

Eschenhagen, T., Bolli, R., Braun, T., Field, L. J., Fleischmann, B. K., Frisen, J., et al. (2017). Cardiomyocyte regeneration: A consensus statement. *Circulation* 136 (7), 680–686. doi:10.1161/CIRCULATIONAHA.117.029343

Faiella, W., and Atoui, R. (2016). Therapeutic use of stem cells for cardiovascular disease. *Clin. Transl. Med.* 5 (1), 34. doi:10.1186/s40169-016-0116-3

Fan, X., Li, X., Lv, S., Wang, Y., Zhao, Y., and Luo, G. (2010). Comparative proteomics research on rat MSCs differentiation induced by Shuanglong Formula. *J. Ethnopharmacol.* 131 (3), 575–580. doi:10.1016/j.jep.2010.07.036

Fisher, S. A., Brunskill, S. J., Doree, C., Taggart, D. P., and Martin-Rendon, E. (2014). Stem cell therapy for chronic ischaemic heart disease and congestive heart failure. *Cochrane Database Syst. Rev.* 12 (4), Cd007888. doi:10.1002/14651858.CD007888.pub3

Fisher, S. A., Doree, C., Mathur, A., Taggart, D. P., and Martin-Rendon, E. (2018). Cochrane corner: Stem cell therapy for chronic ischaemic heart disease and congestive heart failure. *Heart* 104 (1), 8–10. doi:10.1136/heartjnl-2017-311684

Franchi, F., Ramaswamy, V., Olthoff, M., Peterson, K. M., Paulmurugan, R., and Rodriguez-Porcel, M. (2020). The myocardial microenvironment modulates the biology of transplanted mesenchymal stem cells. *Mol. Imaging Biol.* 22 (4), 948–957. doi:10.1007/s11307-019-01470-y

Fu, X., He, Q., Tao, Y., Wang, M., Wang, W., Wang, Y., et al. (2021). Recent advances in tissue stem cells. *Sci. China. Life Sci.* 64 (12), 1998–2029. doi:10.1007/s11427-021-2007-8

Fu, Y., Huang, C., Xu, X., Gu, H., Ye, Y., Jiang, C., et al. (2015). Direct reprogramming of mouse fibroblasts into cardiomyocytes with chemical cocktails. *Cell. Res.* 25 (9), 1013–1024. doi:10.1038/cr.2015.99

Gao, D., Wu, L. Y., Jiao, Y. H., Chen, W. y., Chen, Y., Kaptchuk, T. J., et al. (2010). The effect of Xuefu Zhuyu Decoction on *in vitro* endothelial progenitor cell tube formation. *Chin. J. Integr. Med.* 16 (1), 50–53. doi:10.1007/s11655-010-0050-y

Gao, H., Bo, Z., Wang, Q., Luo, L., Zhu, H., and Ren, Y. (2019). Salvanic acid B inhibits myocardial fibrosis through regulating TGF-β1/Smad signaling pathway. *Biomed. Pharmacother.* 110, 685–691. doi:10.1016/j.biopha.2018.11.098

Gao, L. R., Pei, X. T., Ding, Q. A., Chen, Y., Zhang, N. K., Chen, H. Y., et al. (2013). A critical challenge: Dosage-related efficacy and acute complication intracoronary injection of autologous bone marrow mesenchymal stem cells in acute myocardial infarction. *Int. J. Cardiol.* 168 (4), 3191–3199. doi:10.1016/j.ijcard.2013.04.112

Gao, X. R., Xu, H. J., Wang, L. F., Liu, C. B., and Yu, F. (2017). Mesenchymal stem cell transplantation carried in SVVYGLR modified self-assembling peptide promoted cardiac repair and angiogenesis after myocardial infarction. *Biochem. Biophys. Res. Commun.* 491 (1), 112–118. doi:10.1016/j.bbrc.2017.07.056

Grajek, S., Popiel, M., Gil, L., Breborowicz, P., Lesiak, M., Czepczynski, R., et al. (2010). Influence of bone marrow stem cells on left ventricle perfusion and ejection fraction in patients with acute myocardial infarction of anterior wall: Randomized clinical trial: Impact of bone marrow stem cell intracoronary infusion on improvement of microcirculation. *Eur. Heart J.* 31 (6), 691–702. doi:10.1093/eurheartj/ehp536

Gu, F., Jiang, J., Wang, S., Feng, T., Zhou, Y., Ma, Y., et al. (2019). An experimental research into the potential therapeutic effects of Anti-Osteoporosis Decoction and Yougui Pill on ovariectomy-induced osteoporosis. *Am. J. Transl. Res.* 11 (9), 6032–6039.

Gu, M., Mordwinkin, N. M., Kooreman, N. G., Lee, J., Wu, H., Hu, S., et al. (2015). Pravastatin reverses obesity-induced dysfunction of induced pluripotent stem cell-derived endothelial cells via a nitric oxide-dependent mechanism. *Eur. Heart J.* 36 (13), 806–816. doi:10.1093/eurheartj/ehu411

Guan, J., Wang, G., Wang, J., Zhang, Z., Fu, Y., Cheng, L., et al. (2022). Chemical reprogramming of human somatic cells to pluripotent stem cells. *Nature* 605 (7909), 325–331. doi:10.1038/s41586-022-04593-5

Guo, H. D., Cui, G. H., Tian, J. X., Lu, P. P., Zhu, Q. C., Lv, R., et al. (2014). Transplantation of salvianolic acid B pretreated mesenchymal stem cells improves cardiac function in rats with myocardial infarction through angiogenesis and paracrine mechanisms. *Int. J. Cardiol.* 177 (2), 538–542. doi:10.1016/j.ijcard.2014.08.104

Guo, Y., Yu, Y., Hu, S., Chen, Y., and Shen, Z. (2020). The therapeutic potential of mesenchymal stem cells for cardiovascular diseases. *Cell. Death Dis.* 11 (5), 349. doi:10.1038/s41419-020-2542-9

Gurusamy, N., Alsayari, A., Rajasingh, S., and Rajasingh, J. (2018). Adult stem cells for regenerative therapy. *Prog. Mol. Biol. Transl. Sci.* 160, 1–22. doi:10.1016/bs.pmbts.2018.07.009

Haider, K. H. (2018). Bone marrow cell therapy and cardiac reparability: Better cell characterization will enhance clinical success. *Regen. Med.* 13 (4), 457–475. doi:10.2217/rme-2017-0134

Han, X. J., Li, H., Liu, C. B., Luo, Z. R., Wang, Q. L., Mou, F. F., et al. (2019). Guanxin Danshen Formulation improved the effect of mesenchymal stem cells transplantation for the treatment of myocardial infarction probably via enhancing the engraftment. *Life Sci.* 233, 116740. doi:10.1016/j.lfs.2019.116740

He, H., Yang, T., Li, F., Zhang, L., and Ling, X. (2021). A novel study on the immunomodulatory effect of umbilical cord derived mesenchymal stem cells pretreated with traditional Chinese medicine Asarinin. *Int. Immunopharmacol.* 100, 108054. doi:10.1016/j.intimp.2021.108054

Hedderich, J., El Bagdadi, K., Angele, P., Grassel, S., Meurer, A., Straub, R. H., et al. (2020). Norepinephrine inhibits the proliferation of human bone marrow-derived mesenchymal stem cells via β2-adrenoceptor-mediated ERK1/2 and PKA phosphorylation. *Int. J. Mol. Sci.* 21 (11), E3924. doi:10.3390/ijms21113924

Heinrich, M., Appendino, G., Efferth, T., Furst, R., Izzo, A. A., Kayser, O., et al. (2020). Best practice in research - overcoming common challenges in phytopharmacological research. *J. Ethnopharmacol.* 246, 112230. doi:10.1016/j.jep.2019.112230

Henry, T. D., Tomey, M. I., Tamis-Holland, J. E., Thiele, H., Rao, S. V., Menon, V., et al. (2021). Invasive management of acute myocardial infarction complicated by cardiogenic shock: A scientific statement from the American heart association. *Circulation* 143 (15), e815–e829. doi:10.1161/CIR.0000000000000959

Herreros, J., Prósper, F., Perez, A., Gavira, J. J., Garcia-Velloso, M. J., Barba, J., et al. (2003). Autologous intramyocardial injection of cultured skeletal muscle-derived stem cells in patients with non-acute myocardial infarction. *Eur. Heart J.* 24 (22), 2012–2020. doi:10.1016/j.ehj.2003.09.012

Hong, W., Tatsuo, S., Shou-Dong, W., Qian, Z., Jian-Feng, H., Jue, W., et al. (2015). Resveratrol upregulates cardiac SDF-1 in mice with acute myocardial infarction through the deacetylation of cardiac p53. *PLoS One* 10 (6), e0128978. doi:10.1371/journal.pone.0128978

Huang, H., Xu, Z., Qi, Y., Zhang, W., Zhang, C., Jiang, M., et al. (2020). Exosomes from SIRT1-overexpressing ADSCs restore cardiac function by improving angiogenic function of EPCs. *Mol. Ther. Nucleic Acids* 21, 737–750. doi:10.1016/j.omtn.2020.07.007

Hynes, K., Menichanin, D., Bright, R., IvanovSki, S., Hutmacher, D. W., GronthoS, S., et al. (2015). Induced pluripotent stem cells: A new frontier for stem cells in dentistry. *J. Dent. Res.* 94 (11), 1508–1515. doi:10.1177/0022034515599769

Imanishi, Y., Miyagawa, S., Saito, A., Kitagawa-Sakakida, S., and Sawa, Y. (2011). Allogenic skeletal myoblast transplantation in acute myocardial infarction model rats. *Transplantation* 91 (4), 425–431. doi:10.1097/TP.0b013e3182052bca

Jeong, M., Kim, H. M., Lee, J. S., Choi, J. H., and Jang, D. S. (2018). (-)-Asarinin from the roots of asarum sieboldii induces apoptotic cell death via caspase activation in human ovarian cancer cells. *Molecules* 23 (8), E1849. doi:10.3390/molecules23081849

Jia, Q., Zhu, R., Tian, Y., Chen, B., Li, R., Li, L., et al. (2019). Salvia miltiorrhiza in diabetes: A review of its pharmacology, phytochemistry, and safety. *Phytomedicine* 58, 152871. doi:10.1016/j.phymed.2019.152871

Khan, M., Nickoloff, E., Abramova, T., Johnson, J., Verma, S. K., Krishnamurthy, P., et al. (2015). Embryonic stem cell-derived exosomes promote endogenous repair mechanisms and enhance cardiac function following myocardial infarction. *Circ. Res.* 117 (1), 52–64. doi:10.1161/CIRCRESAHA.117.305990

Kim, S. W., Kim, H. W., Huang, W., Okada, M., Welge, J. A., Wang, Y., et al. (2013). Cardiac stem cells with electrical stimulation improve ischaemic heart function through regulation of connective tissue growth factor and miR-378. *Cardiovasc. Res.* 100 (2), 241–251. doi:10.1093/cvr/cvt192

Lagarkova, M. A. (2019). Such various stem cells. *Biochemistry.* 84 (3), 187–189. doi:10.1134/S0006297919030015

Laplane, L., and Solary, E. (2019). Towards a classification of stem cells. *Elife* 8, e46563. doi:10.7554/eLife.46563

Lee, T. L., Lai, T. C., Lin, S. R., Chen, Y. C., Pu, C. M., Lee, I. T., et al. (2021). Conditioned medium from adipose-derived stem cells attenuates ischemia/reperfusion-induced cardiac injury through the microRNA-221/222/PUMA/ETS-1 pathway. *Theranostics* 11 (7), 3131–3149. doi:10.7150/thno.52677

Li, A., Gao, M., Zhao, N., Li, P., Zhu, J., and Li, W. (2019). Acute liver failure associated with fructus Psoraleae: A case report and literature review. *BMC Complement. Altern. Med.* 19 (1), 84. doi:10.1186/s12906-019-2493-9

Li, H., Zhu, J., Xu, Y. W., Mou, F. F., Shan, X. L., Wang, Q. L., et al. (2022). Notoginsenoside R1-loaded mesoporous silica nanoparticles targeting the site of injury through inflammatory cells improves heart repair after myocardial infarction. *Redox Biol.* 54, 102384. doi:10.1016/j.redox.2022.102384

Li, L., Chen, X., Wang, W. E., and Zeng, C., (2016). How to improve the survival of transplanted mesenchymal stem cell in ischemic heart? *Stem Cells Int.* 2016, 9682757. doi:10.1155/2016/9682757

Li, M., Yu, C. M., Cheng, L., Wang, M., Gu, X., Lee, K. H., et al. (2006). Repair of infarcted myocardium by an extract of Geum japonicum with dual effects on angiogenesis and myogenesis. *Clin. Chem.* 52 (8), 1460–1468. doi:10.1373/clinchem.2006.068247

Li, N., Yang, Y. J., Cui, H. H., Zhang, Q., Jin, C., Qian, H. Y., et al. (2014). Tongxinluo decreases apoptosis of mesenchymal stem cells concentration-dependently under hypoxia and serum deprivation conditions through the AMPK/eNOS pathway. *J. Cardiovasc. Pharmacol.* 63 (3), 265–273. doi:10.1097/FJC.0000000000000044

Li, X., Zhao, H., Qi, C., Zeng, Y., Xu, F., and Du, Y. (2015). Direct intercellular communications dominate the interaction between adipose-derived MSCs and myofibroblasts against cardiac fibrosis. *Protein Cell.* 6 (10), 735–745. doi:10.1007/s13238-015-0196-7

Li, Z., Solomonidis, E. G., Meloni, M., Taylor, R. S., Duffin, R., Dobie, R., et al. (2019). Single-cell transcriptome analyses reveal novel targets modulating cardiac neovascularization by resident endothelial cells following myocardial infarction. *Eur. Heart J.* 40 (30), 2507–2520. doi:10.1093/eurheartj/ehz305

Lin, M., Liu, X., Zheng, H., Huang, X., Wu, Y., Huang, A., et al. (2020). IGF-1 enhances BMSC viability, migration, and anti-apoptosis in myocardial infarction via secreted frizzled-related protein 2 pathway. *Stem Cell. Res. Ther.* 11 (1), 22. doi:10.1186/s13287-019-1544-y

Lin, X., Peng, P., Cheng, L., Chen, S., Li, K., Li, Z. Y., et al. (2012). A natural compound induced cardiogenic differentiation of endogenous MSCs for repair of infarcted heart. *Differentiation.* 83 (1), 1–9. doi:10.1016/j.diff.2011.09.001

Liu, J., Jiang, M., Deng, S., Lu, J., Huang, H., Zhang, Y., et al. (2018). miR-93-5p-Containing exosomes treatment attenuates acute myocardial infarction-induced myocardial damage. *Mol. Ther. Nucleic Acids* 11, 103–115. doi:10.1016/j.omtn.2018.01.010

Liu, Y., and Feng, N. (2015). Nanocarriers for the delivery of active ingredients and fractions extracted from natural products used in traditional Chinese medicine (TCM). *Adv. Colloid Interface Sci.* 221, 60–76. doi:10.1016/j.cis.2015.04.006

Liu, Y., Hao, F., Zhang, H., Cao, D., Lu, X., and Li, X. (2013). Panax notoginseng saponins promote endothelial progenitor cell mobilization and attenuate atherosclerotic lesions in apolipoprotein E knockout mice. *Cell. Physiol. biochem.* 32 (4), 814–826. doi:10.1159/000354484

Lo, B., and Parham, L. (2009). Ethical issues in stem cell research. *Endocr. Rev.* 30 (3), 204–213. doi:10.1210/er.2008-0031

Luo, C., Wang, H., Chen, X., Cui, Y., Li, H., Long, J., et al. (2013). Protection of H9c2 rat cardiomyoblasts against oxidative insults by total paeony glucosides from Radix Paeoniae Rubrae. *Phytomedicine* 21 (1), 20–24. doi:10.1016/j.phymed.2013.08.002

Luo, Z. R., Li, H., Xiao, Z. X., Shao, S. J., Zhao, T. T., Zhao, Y., et al. (2019). Taohong siwu decoction exerts a beneficial effect on cardiac function by possibly improving the microenvironment and decreasing mitochondrial fission after myocardial infarction. *Cardiol. Res. Pract.* 2019, 5198278. doi:10.1155/2019/5198278

Ma, R., Liang, J., Huang, W., Guo, L., Cai, W., Wang, L., et al. (2018). Electrical stimulation enhances cardiac differentiation of human induced pluripotent stem cells for myocardial infarction therapy. *Antioxid. Redox Signal.* 28 (5), 371–384. doi:10.1089/ars.2016.6766

Madigan, M., and Atoui, R. (2018). Therapeutic use of stem cells for myocardial infarction. *Bioeng. (Basel)* 5 (2), E28. doi:10.3390/bioengineering5020028

Makkar, R. R., Smith, R. R., Cheng, K., Malliaras, K., Thomson, L. E., Berman, D., et al. (2012). Intracoronary cardiosphere-derived cells for heart regeneration after myocardial infarction (CADUCEUS): A prospective, randomised phase 1 trial. *Lancet* 379 (9819), 895–904. doi:10.1016/S0140-6736(12)60195-0

Malchenko, S., Xie, J., de Fatima Bonaldo, M., Vanin, E. F., Bhattacharyya, B. J., Belmadani, A., et al. (2014). Onset of rosette formation during spontaneous neural differentiation of hESC and hiPSC colonies. *Gene* 534 (2), 400–407. doi:10.1016/j.gene.2013.07.101

Menasché, P., Alfieri, O., Janssens, S., McKenna, W., Reichenspurner, H., Trinquart, L., et al. (2008). The myoblast autologous grafting in ischemic cardiomyopathy (MAGIC) trial: First randomized placebo-controlled study of myoblast transplantation. *Circulation* 117 (9), 1189–1200. doi:10.1161/CIRCULATIONAHA.107.734103

Miao, C., Lei, M., Hu, W., Han, S., and Wang, Q. (2017). A brief review: The therapeutic potential of bone marrow mesenchymal stem cells in myocardial infarction. *Stem Cell. Res. Ther.* 8 (1), 242. doi:10.1186/s13287-017-0697-9

Müller, P., Lemcke, H., and David, R. (2018). Stem cell therapy in heart diseases - cell types, mechanisms and improvement strategies. *Cell. Physiol. biochem.* 48 (6), 2607–2655. doi:10.1159/000492704

Nasseri, B. A., Ebell, W., Dandel, M., Kukucka, M., Gebker, R., Doltra, A., et al. (2014). Autologous CD133+ bone marrow cells and bypass grafting for regeneration of ischaemic myocardium: The Cardio133 trial. *Eur. Heart J.* 35 (19), 1263–1274. doi:10.1093/eurheartj/ehu007

Penn, M. S., and Mangi, A. A. (2008). Genetic enhancement of stem cell engraftment, survival, and efficacy. *Circ. Res.* 102 (12), 1471–1482. doi:10.1161/CIRCRESAHA.108.175174

Ponsuksili, S., Murani, E., Hadlich, F., Perdomo-Sabogal, A., Trakooljul, N., Oster, M., et al. (2022). Genetic regulation and variation of expression of miRNA and mRNA transcripts in fetal muscle tissue in the context of sex, dam and variable fetal weight. *Biol. Sex. Differ.* 13 (1), 24. doi:10.1186/s13293-022-00433-3

Qi, K., Li, L., Li, X., Zhao, J., Wang, Y., You, S., et al. (2015). Cardiac microvascular barrier function mediates the protection of Tongxinluo against myocardial ischemia/reperfusion injury. *PLoS One* 10 (3), e0119846. doi:10.1371/journal.pone.0119846

Qian, H. Y., Yang, Y. J., Huang, J., Gao, R. l., Dou, K. f., Yang, G. s., et al. (2007). Effects of Tongxinluo-facilitated cellular cardiomyoplasty with autologous bone marrow-mesenchymal stem cells on postinfarct swine hearts. *Chin. Med. J.* 120 (16), 1416–1425. doi:10.1097/00029330-200708020-00008

Qin, S., Zhou, W., Liu, S., Chen, P., and Wu, H. (2015). Icariin stimulates the proliferation of rat bone mesenchymal stem cells via ERK and p38 MAPK signaling. *Int. J. Clin. Exp. Med.* 8 (5), 7125–7133.

Rigaud, V. O. C., Hoy, R., Mohsin, S., and Khan, M. (2020). Stem cell metabolism: Powering cell-based therapeutics. *Cells* 9 (11), E2490. doi:10.3390/cells9112490

Roth, G. A., Mensah, G. A., Johnson, C. O., Addolorato, G., Ammirati, E., Baddour, L. M., et al. (2020). Global burden of cardiovascular diseases and risk factors, 1990-2019: Update from the GBD 2019 study. *J. Am. Coll. Cardiol.* 76 (25), 2982–3021. doi:10.1016/j.jacc.2020.11.010

Samak, M., and Hinkel, R. (2019). Stem cells in cardiovascular medicine: Historical overview and future prospects. *Cells* 8 (12), E1530. doi:10.3390/cells8121530

Shafei, A. E., Ali, M. A., Ghanem, H. G., Shehata, A. I., Abdelgawad, A. A., Handal, H. R., et al. (2018). Mechanistic effects of mesenchymal and hematopoietic stem cells: New therapeutic targets in myocardial infarction. *J. Cell. Biochem.* 119 (7), 5274–5286. doi:10.1002/jcb.26637

Shen, X., Pan, B., Zhou, H., Liu, L., Lv, T., Zhu, J., et al. (2017). Differentiation of mesenchymal stem cells into cardiomyocytes is regulated by miRNA-1-2 via WNT signaling pathway. *J. Biomed. Sci.* 24 (1), 29. doi:10.1186/s12929-017-0337-9

Shi, W. L., Zhao, J., Yuan, R., Lu, Y., Xin, Q. Q., Liu, Y., et al. (2019). Combination of Ligusticum chuanxiong and radix Paeonia promotes angiogenesis in ischemic myocardium through Notch signalling and mobilization of stem cells. *Evid. Based. Complement. Altern. Med.* 2019, 7912402. doi:10.1155/2019/7912402

Siminiak, T., Kalawski, R., Fiszer, D., Jerzykowska, O., Rzezniczak, J., Rozwadowska, N., et al. (2004). Autologous skeletal myoblast transplantation for the treatment of postinfarction myocardial injury: phase I clinical study with 12 months of follow-up. *Am. Heart J.* 148 (3), 531–537. doi:10.1016/j.ahj.2004.03.043

Skuk, D., and Tremblay, J. P. (2019). Myotubes formed de novo by myoblasts injected into the scar of myocardial infarction persisted for 16 Years in a patient: Importance for regenerative medicine in degenerative myopathies. *Stem Cells Transl. Med.* 8 (3), 313–314. doi:10.1002/sctm.18-0202

Sun, Y., Zhang, J., Qian, N., Sima, G., Zhang, J., Zhong, J., et al. (2018). Comparison of the osteogenic differentiation of orofacial bone marrow stromal cells prior to and following marsupialization in patients with odontogenic cyst. *Mol. Med. Rep.* 17 (1), 988–994. doi:10.3892/mmr.2017.7949

Tendera, M., Wojakowski, W., Ruzyłło, W., Chojnowska, L., Kepka, C., Tracz, W., et al. (2009). Intracoronary infusion of bone marrow-derived selected CD34+CXCR4+ cells and non-selected mononuclear cells in patients with acute STEMI and reduced left ventricular ejection fraction: Results of randomized, multicentre myocardial regeneration by intracoronary infusion of selected population of stem cells in acute myocardial infarction (REGENT) trial. *Eur. Heart J.* 30 (11), 1313–1321. doi:10.1093/eurheartj/ehp073

Terajima, Y., Shimizu, T., Tsuruyama, S., Sekine, H., Ishii, H., Yamazaki, K., et al. (2014). Autologous skeletal myoblast sheet therapy for porcine myocardial infarction without increasing risk of arrhythmia. *Cell. Med.* 6 (3), 99–109. doi:10.3727/215517913X672254

Tsao, C. W., Aday, A. W., Almarzooq, Z. I., Alonso, A., Beaton, A. Z., Bittencourt, M. S., et al. (2022). Heart disease and stroke statistics-2022 update: A report from the American heart association. *Circulation* 145 (8), e153–e639. doi:10.1161/CIR.0000000000001052

Tzahor, E., and Poss, K. D. (2017). Cardiac regeneration strategies: Staying young at heart. *Science* 356 (6342), 1035–1039. doi:10.1126/science.aam5894

Ulus, A. T., Mungan, C., Kurtoglu, M., Celikkan, F. T., Akyol, M., Sucu, M., et al. (2020). Intramyocardial transplantation of umbilical cord mesenchymal stromal cells in chronic ischemic cardiomyopathy: A controlled, randomized clinical trial (HUC-heart trial). *Int. J. Stem Cells* 13 (3), 364–376. doi:10.15283/ijsc20075

Uygur, A., and Lee, R. T. (2016). Mechanisms of cardiac regeneration. *Dev. Cell.* 36 (4), 362–374. doi:10.1016/j.devcel.2016.01.018

Vagnozzi, R. J., Maillet, M., Sargent, M. A., Khalil, H., Johansen, A. K. Z., Schwanekamp, J. A., et al. (2020). An acute immune response underlies the benefit of cardiac stem cell therapy. *Nature* 577 (7790), 405–409. doi:10.1038/s41586-019-1802-2

Valiente-Alandi, I., Albo-Castellanos, C., Herrero, D., Sanchez, I., and Bernad, A. (2016). Bmi1 (+) cardiac progenitor cells contribute to myocardial repair following acute injury. *Stem Cell. Res. Ther.* 7 (1), 100. doi:10.1186/s13287-016-0355-7

van der Spoel, T. I., Jansen of Lorkeers, S. J., Agostoni, P., van Belle, E., Gyongyosi, M., Sluijter, J. P. G., et al. (2011). Human relevance of pre-clinical studies in stem cell therapy: Systematic review and meta-analysis of large animal models of ischaemic heart disease. *Cardiovasc. Res.* 91 (4), 649–658. doi:10.1093/cvr/cvr113

Wang, C., Hou, J., Du, H., Yan, S., Yang, J., Wang, Y., et al. (2019). Anti-depressive effect of Shuangxinfang on rats with acute myocardial infarction: Promoting bone marrow mesenchymal stem cells mobilization and alleviating inflammatory response. *Biomed. Pharmacother.* 111, 19–30. doi:10.1016/j.biopha.2018.11.113

Wang, J. N., Kan, C. D., Lee, L. T., Huang, L. L. H., Hsiao, Y. L., Chang, A. H., et al. (2021). Herbal extract from Codonopsis pilosula (franch.) Nannf. Enhances cardiogenic differentiation and improves the function of infarcted rat hearts. *Life (Basel)* 11 (5), 422. doi:10.3390/life11050422

Wang, M., Liu, J., Zhou, B., Xu, R., Tao, L., Ji, M., et al. (2012). Acute and sub-chronic toxicity studies of Danshen injection in Sprague-Dawley rats. *J. Ethnopharmacol.* 141 (1), 96–103. doi:10.1016/j.jep.2012.02.005

Wang, T. T., Chen, W., Zeng, H. P., and Chen, D. F. (2012). Chemical components in extracts from Plastrum testudinis with proliferation-promoting effects on rat mesenchymal stem cells. *Chem. Biol. Drug Des.* 79 (6), 1049–1055. doi:10.1111/j.1747-0285.2012.01361.x

Wang, X., Zhen, L., Miao, H., Sun, Q., Yang, Y., Que, B., et al. (2015). Concomitant retrograde coronary venous infusion of basic fibroblast growth factor enhances engraftment and differentiation of bone marrow mesenchymal stem cells for cardiac repair after myocardial infarction. *Theranostics* 5 (9), 995–1006. doi:10.7150/thno.11607

Wei, R., Yang, J., Gao, M., Wang, H., Hou, W., Mu, Y., et al. (2016). Infarcted cardiac microenvironment may hinder cardiac lineage differentiation of human embryonic stem cells. *Cell. Biol. Int.* 40 (11), 1235–1246. doi:10.1002/cbin.10679

Windmueller, R., Leach, J. P., Babu, A., Zhou, S., Morley, M. P., Wakabayashi, A., et al. (2020). Direct comparison of mononucleated and binucleated cardiomyocytes reveals molecular mechanisms underlying distinct proliferative competencies. *Cell. Rep.* 30 (9), 3105–3116. e4. doi:10.1016/j.celrep.2020.02.034

Wollert, K. C., Meyer, G. P., Müller-Ehmsen, J., Tschope, C., Bonarjee, V., Larsen, A. I., et al. (2017). Intracoronary autologous bone marrow cell transfer after myocardial infarction: The BOOST-2 randomised placebo-controlled clinical trial. *Eur. Heart J.* 38 (39), 2936–2943. doi:10.1093/eurheartj/ehx188

Wu, X., Reboll, M. R., Korf-Klingebiel, M., and Wollert, K. C. (2021). Angiogenesis after acute myocardial infarction. *Cardiovasc. Res.* 117 (5), 1257–1273. doi:10.1093/cvr/cvaa287

Wu, X., Wang, S., Lu, J., Jing, Y., Li, M., Cao, J., et al. (2018). Seeing the unseen of Chinese herbal medicine processing (paozhi): Advances in new perspectives. *Chin. Med.* 13, 4. doi:10.1186/s13020-018-0163-3

Xie, J., Wang, H., Song, T., Wang, Z., Li, F., Ma, J., et al. (2013). Tanshinone IIA and astragaloside IV promote the migration of mesenchymal stem cells by up-regulation of CXCR4. *Protoplasma* 250 (2), 521–530. doi:10.1007/s00709-012-0435-1

Xiong, Y., Tang, R., Xu, J., Jiang, W., Gong, Z., Zhang, L., et al. (2022). Sequential transplantation of exosomes and mesenchymal stem cells pretreated with a combination of hypoxia and Tongxinluo efficiently facilitates cardiac repair. *Stem Cell. Res. Ther.* 13 (1), 63. doi:10.1186/s13287-022-02736-z

Xiong, Y., Tang, R., Xu, J., Jiang, W., Gong, Z., Zhang, L., et al. (2022). Tongxinluo-pretreated mesenchymal stem cells facilitate cardiac repair via exosomal transfer of miR-146a-5p targeting IRAK1/NF-κB p65 pathway. *Stem Cell. Res. Ther.* 13 (1), 289. doi:10.1186/s13287-022-02969-y

Xu, H., Zhang, Y., Wang, P., Zhang, J., Chen, H., Zhang, L., et al. (2021). A comprehensive review of integrative pharmacology-based investigation: A paradigm shift in traditional Chinese medicine. *Acta Pharm. Sin. B* 11 (6), 1379–1399. doi:10.1016/j.apsb.2021.03.024

Yan, R., Yang, Y., and Chen, Y. (2018). Pharmacokinetics of Chinese medicines: Strategies and perspectives. *Chin. Med.* 13, 24. doi:10.1186/s13020-018-0183-z

Yu, L., Tu, Q., Han, Q., Zhang, L., Sui, L., Zheng, L., et al. (2015). Adiponectin regulates bone marrow mesenchymal stem cell niche through a unique signal transduction pathway: An approach for treating bone disease in diabetes. *Stem Cells* 33 (1), 240–252. doi:10.1002/stem.1844

Yu, Y., Sun, J., Liu, J., Wang, P., and Wang, C. (2020). Ginsenoside Re preserves cardiac function and ameliorates left ventricular remodeling in a rat model of myocardial infarction. *J. Cardiovasc. Pharmacol.* 75 (1), 91–97. doi:10.1097/FJC.0000000000000752

Zeng, H. P., Wang, T. T., Chen, W., Wang, C. Y., Chen, D. F., and Shen, J. G. (2008). Characterization of chemical components in extracts from Si-Wu decoction with proliferation-promoting effects on rat mesenchymal stem cells. *Bioorg. Med. Chem.* 16 (9), 5109–5114. doi:10.1016/j.bmc.2008.03.024

Zhang, J. S., He, Q. Y., Huang, T., and Zhang, B. X. (2011). Effects of panax notoginseng saponins on homing of C-kit+ bone mesenchymal stem cells to the infarction heart in rats. *J. Tradit. Chin. Med.* 31 (3), 203–208. doi:10.1016/s0254-6272(11)60043-5

Zhang, J., Zhang, B., Zhu, H., and Zhang, Y. (2016). Insight into stem cells, microenvironment and methods for promoting blood circulation and removing stasis. *Chin. J. Tissue Eng. Res.* 20 (23), 3484–3490. doi:10.3969/j.issn.2095-4344.2016.23.021

Zhang, J., and Zhang, B. (2018). Research on identity between kidney essence and stem cells. *Chin. Archives Traditional Chin. Med.* 36 (2), 326–328. doi:10.13193/j.issn.1673-7717.2018.02.017

Zhang, R., Yu, J., Zhang, N., Li, W., Wang, J., Cai, G., et al. (2021). Bone marrow mesenchymal stem cells transfer in patients with ST-segment elevation myocardial infarction: Single-blind, multicenter, randomized controlled trial. *Stem Cell. Res. Ther.* 12 (1), 33. doi:10.1186/s13287-020-02096-6

Zhang, X. Y., Sun, Y., Yang, X. Y., Hu, J. Y., Zheng, R., Chen, S. Q., et al. (2020). Effect of Chinese medicine on No or slow reflow after percutaneous coronary intervention in myocardial infarction patients: A systematic review and meta-analysis. *Chin. J. Integr. Med.* 26 (3), 227–234. doi:10.1007/s11655-019-2703-9

Zhang, Y., Wang, Y., Wang, L., Qin, Y., Chen, T., Han, W, et al. (2012). Effects of Rehmannia glutinosa oligosaccharide on human adipose-derived mesenchymal stem cells *in vitro*. *Life Sci.* 91, 1323–1327. doi:10.1016/j.lfs.2012.10.015

Zhao, L., Chen, S., Yang, P., Cao, H., and Li, L. (2019). The role of mesenchymal stem cells in hematopoietic stem cell transplantation: Prevention and treatment of graft-versus-host disease. *Stem Cell. Res. Ther.* 10 (1), 182. doi:10.1186/s13287-019-1287-9

Zhao, T. T., Liu, J. J., Zhu, J., Li, H., Wang, Y. C., Zhao, Y., et al. (2022). SDF-1/CXCR4-Mediated stem cell mobilization involved in cardioprotective effects of electroacupuncture on mouse with myocardial infarction. *Oxid. Med. Cell. Longev.* 2022, 4455183. doi:10.1155/2022/4455183

Zheng, H., Liu, C., Ou, Y., Zhang, Y., and Fu, X. (2013). Total saponins of Panax notoginseng enhance VEGF and relative receptors signals and promote angiogenesis derived from rat bone marrow mesenchymal stem cells. *J. Ethnopharmacol.* 147 (3), 595–602. doi:10.1016/j.jep.2013.03.043

Zhou, J., Zhang, J., Wu, L., Zhu, F., and Xu, H. (2020). Tetramethylpyrazine/ligustrazine can improve the survival rate of adipose-derived stem cell transplantation. *Ann. Plast. Surg.* 84 (3), 328–333. doi:10.1097/SAP.0000000000002146

Zhu, L., Liu, Y. J., Shen, H., Gu, P. Q., and Zhang, L. (2017). Astragalus and baicalein regulate inflammation of mesenchymal stem cells (MSCs) by the mitogen-activated protein kinase (MAPK)/ERK pathway. *Med. Sci. Monit.* 23, 3209–3216. doi:10.12659/msm.902441

Glossary

CVDs cardiovascular diseases
MI myocardial infarction
IHD ischemic heart disease
ESCs embryonic stem cells
ASCs adult stem cells
TCM traditional Chinese medicine
BMCs bone marrow cells
HSCs hematopoietic stem cells
MSCs mesenchymal stem cells
RCSCs resident cardiac stem cells
iPSCs induced pluripotent stem cells
SMs skeletal myoblasts
ADSCs adipose-derived stem cells
AMI acute myocardial infarction
LVEF left ventricular ejection fraction
EPCs endothelial progenitor cells
BMSCs bone mesenchymal stem cells
ROS reactive oxygen species
PCI percutaneous coronary intervention
CM conditional medium
SDE Si–Wu decoction
EBM epimedium brevicornum Maxim
ICA icariin
PT Plastrum testudinis
BMP4 bone morphogenetic protein 4
FP Fructus Psoraleae
BYD Buzhong Yiqi decoction
HA hexadecanoic acid
SalB salvianolic acid B
RGO Rehmannia glutinosa oligosaccharide
APS Angelica polysaccharides
SMSCs skeletal muscle satellite cells
TCMI TCM injection
DI Danshen injection
TGF-β transforming growth factor-β
TNF-α tumor necrosis factor-α
SDF-1 stromal-derived factor-1
HGF hepatocyte growth factor
GXDS Guanxin Danshen
CHSIBA Shen invigorating and blood activating
DHI Danhong injection
SMB Salvia miltiorrhiza Bunge
YWHR Yiqi Wenyang Huoxue recipe
TIIA Tanshinone IIA
PNS Panax notoginseng saponins
RSV resveratrol
MK Musk ketonem
GJ Geum japonicum
SLF Shuanglong formula
VECs vascular endothelial cells
XZD Xuefu Zhuyu decoction
GBPYS Gu Ben Pei Yuan San
CMECs Cardiac microvascular endothelial cells
QLC Qiliqiangxin capsule
XFZYD Xuefu Zhuyu decoction
TXL Tongxinluo
TPG Total paeony glucosides
TMP Tetramethylpyrazine
PPARγ peroxisome proliferator-activated receptor γ
AS-IV astragaloside IV
THSWD Taohong Siwu decoction
NGR1 Notoginsenoside R1
RCT random clinical trials
ALF acute liver failure
UC-MSC umbilical cord-derived mesenchymal stem cells

frontiers | Frontiers in Pharmacology

TYPE Systematic Review
PUBLISHED 24 November 2022
DOI 10.3389/fphar.2022.1027131

OPEN ACCESS

EDITED BY
Rong Lu,
Shanghai University of Traditional Chinese Medicine, China

REVIEWED BY
Guang Chen,
Beijing University of Chinese Medicine, China
Alan Wu,
University of California, San Francisco, United States

*CORRESPONDENCE
Wei Zhu,
13826260112@163.com
Banghan Ding,
13682238225@139.com

†These authors have contributed equally to this work and share first authorship

SPECIALTY SECTION
This article was submitted to Ethnopharmacology, a section of the journal Frontiers in Pharmacology

RECEIVED 24 August 2022
ACCEPTED 27 October 2022
PUBLISHED 24 November 2022

CITATION
Wu Y, Li S, Li Z, Mo Z, Luo Z, Li D, Wang D, Zhu W and Ding B (2022), Efficacy and safety of Shenfu injection for the treatment of post-acute myocardial infarction heart failure: A systematic review and meta-analysis. *Front. Pharmacol.* 13:1027131. doi: 10.3389/fphar.2022.1027131

Efficacy and safety of Shenfu injection for the treatment of post-acute myocardial infarction heart failure: A systematic review and meta-analysis

Yanhua Wu[1,2,3†], Shuang Li[4†], Zunjiang Li[5†], Zhaofan Mo[5†], Ziqing Luo[6], Dongli Li[1,2,3], Dawei Wang[7], Wei Zhu[2*] and Banghan Ding[1,2,3*]

[1]The Second Affiliated Hospital of Guangzhou University of Chinese Medicine, Guangzhou, China, [2]Guangdong Provincial Hospital of Chinese Medicine, Guangzhou, China, [3]State Key Laboratory of Emergency of Chinese Medicine, Guangdong Provincial Hospital of Chinese Medicine, Guangzhou, China, [4]The First Clinical College of Guangzhou University of Chinese Medicine, Guangzhou, China, [5]The Second Clinical College of Guangzhou University of Chinese Medicine, Guangzhou, China, [6]Animal Experiment Centre of Guangzhou University of Chinese Medicine, Guangzhou, China, [7]Shunde Hospital of Guangzhou University of Chinese Medicine, Guangzhou, China

Objective: This systematic review and meta-analysis aimed to investigate the adjuvant effect and safety of Shenfu injection (SFI) on the treatment of post-acute myocardial infarction heart failure (PAMIHF).

Methods: Seven databases were searched to identify randomized controlled trials (RCTs) associated with SFI and PAMIHF treatment from May 1990 to May 2022. Primary outcomes included NT-proBNP and left ventricular ejection fraction (LVEF), and secondary outcomes included total effective rate, BNP, heart rate (HR), cardiac output (CO), and adverse event (AE). The risk of bias evaluation was assessed by the ROB2 tool, meta-analysis, subgroup analysis, sensitivity analysis, and publication bias were conducted by RevMan5.3 software, and the Grade of Recommendations, Assessment, Development, and Evaluations (GRADE) system was used to evaluate the quality of evidence of meta results.

Results: A total of 36 studies with 3231 PAMIHF patients were included. The meta results suggested that adjuvant SFI therapy was superior to conventional medical therapy alone. It improved the total effective rate [RR = 1.33; 95% CI (1.25.1.40); $p < 0.00001$], increased LVEF [SMD = 0.98; 95% CI (0.71, 1.24); $p < 0.00001$], and decreased HR [SMD = −1.14; 95% CI (−1.28, −0.99); $p < 0.00001$]. In addition, adjuvant SFI therapy (9.73%, 66/678) had a rate of AE lower than that of conventional medical therapy alone (21.7%, 147/677) when regarding safety [RR = 0.45; 95% CI (0.35, 0.57); $p < 0.00001$]. The quality of the evidence for the outcomes was rated from "very low" to "moderate."

Conclusion: Adjuvant SFI therapy was safer to improve the total effective rate and the heart function of PAMIHF patients. However, well-designed RCTs were

needed to confirm the efficacy and safety of adjuvant SFI therapy in PAMIHF treatment due to the low quality of the evidence for the outcomes caused by a small sample size and unclear risk of bias existed in included studies.

Systematic Review Registration: https://www.crd.york.ac.uk/PROSPERO/display_record.php?RecordID=151856), identifier CRD42020151856.

KEYWORDS

acute myocardial infarction, heart failure, Shenfu injection, meta-analysis, systematic review, traditional Chinese medicine

1 Introduction

Acute myocardial infarction (AMI) is a clinical syndrome, and it is mainly characterized by chest pain, shortness of breath, sweating, and abnormal heart beating, due to sudden reduction of blood flow and imbalance between myocardial oxygen supply and demand (Sandoval and Jaffe, 2019). Heart failure (HF) is a syndrome mainly associated with systematic congestion and ultimately organ dysfunction due to hypoperfusion (Arrigo et al., 2020). HF, a common complication of AMI, is the major driver of long-term mortality, high medical costs, and 3–6 times of risk of death within 30 days (Song and Jin, 2021). Despite the remarkable advances in AMI treatment over the past 2 decades, incidence of post-acute myocardial infarction heart failure (PAMIHF) among hospitalized patients remains high ranging from 14% to 36%. Thus, new and alternative medical management of PAMIHF remains challenging and urgently needed (Bahit et al., 2018).

Shenfu injection (SFI) is a traditional Chinese medical formulation, and it is prepared from *Panax ginseng* C.A. Meyer (Araliaceae, *Ginseng radix et rhizoma*) and *Aconitμm carmichaelii Debx* (Ranunculaceae, *Aconiti radix*). 1ml of SFI is extracted from 0.1 g of *Panax ginseng* C.A. Meyer and 0.2 g of *Aconitμm carmichaelii Debx*. (Wang et al., 2021a). The main active ingredients of SFI were identified as ginsenosides and aconite alkaloids by combinatory liquid chromatography–mass spectrometric techniques (Wang et al., 2021a). SFI has been widely used in the treatment of cardiovascular and cerebrovascular diseases, especially in HF treatment (Su et al., 2018). It has the functions of improving organ perfusion, protecting myocardium and tissue damage during cerebral ischemia (Li et al., 2013), improving hemodynamics, dilating blood vessels (Li, 2017), anti-inflammatory effects (Li et al., 2019), etc. However, it still lacks evaluation on the efficacy and safety of SFI in the treatment of PAMIHF in terms of methodology and quality of evidence.

In this study, we aimed to elucidate the efficacy and safety of SFI as an adjunctive treatment for AMI-HF through the available evidence in practice. We mainly focused on clarifying whether SFI combined with conventional therapy had an adjuvant effect compared with conventional therapy alone and was as safe as conventional therapy.

2 Data and methods

2.1 The composition of SFI

Shenfu injection, comprising *Panax ginseng* C.A. Meyer (Araliaceae, *Ginseng radix et rhizoma*) and *Aconitμm carmichaelii Debx* (Ranunculaceae, *Aconiti radix*), is derived from the traditional Chinese medicine formula Shenfu decoction, which has been used in China for over hundreds of years. Several studies have reported the chemical profile of SFI using different methods; SFI mainly includes *Aconitine alkaloids*, *Ginsenosaponin*, *Aconitum alkaloids*, *Ginsenoside*, *Aconitine*, and *Hydrophilic compound* (for details, see Supplementary Table S1), among which ginsenosides and aconite alkaloids are identified as the main active ingredients of SFI (Yang et al., 2014; Gao et al., 2016; Li et al., 2016).

2.2 Database for search

Here, three English databases (MEDLINE *via* PubMed, EMBASE, and Web of science) and four Chinese databases [China National Knowledge Infrastructure (CNKI), WanFang Database, Chinese Biomedical Literature Database (CBM), and China Science and Technology Journal Database (VIP)] were searched from May 1990 to May 2022.

2.3 Criteria for studies included

2.3.1 Type of participants (P)

Patients aged more than 18 years who were diagnosed with AMI and HF according to the diagnostic criteria recognized in certain guidelines, literature, or certain books were included, regardless of nationality, gender, race, age, course of disease, and types of heart failure, STEMI NSTEMI, HFrEF, or HFpEF.

2.3.2 Type of interventions (I and C)

Control group: Conventional western medicine treatment, including low-salt diet, lipid lowering, vasodilator, diuretic, cardiotonic, oxygen inhalation, and restriction of fluid intake. Experimental group: SFI treatment plus the control group.

2.3.3 Type of outcome measures

Primary outcomes (O): ① Left ventricular ejection fraction (LVEF) and ② NT-proBNP; secondary outcomes: ① Total clinical effective rate (for definition, see Supplementary file S2), ② heart rate (HR), ③ cardiac output (CO), and ④ BNP; safety outcome: Adverse events.

2.3.4 Types of studies (S)

The studies were randomized controlled trials (RCTs).

2.4 Exclusion criteria

The exclusion criteria are as follows: ① repeated publications, ② pure theoretical research, ③ case report, and ④ not complete data.

2.5 Searching strategy

We searched studies with [Title/Abstract] by developing the search strategies of the combination of the MeSH terms (participants, intervention, comparison, outcomes, and study design), including P+1, P + I + C, P + I + C + O, and P + I + C + O + S. If the number of studies retrieved was small, we searched by P + I and then manually screened studies based on inclusion and exclusion criteria.

2.6 Data collection and analysis

2.6.1 Selection of studies

Two review authors independently screened titles and abstracts of studies identified by literature search according to the criteria of PICOS. Duplication was omitted using NoteExpress software. Then, another two authors extracted and summarized the data from the included studies. Discrepancies were resolved by consensus.

2.6.2 Data extraction and management

The details of studies were identified separately by two reviewers and were presented in a standardized table. Two authors independently extracted the data including the sample size, age, treatment details, criteria for AMI and AHF diagnosis, outcomes, and adverse events.

2.6.3 Evaluation of risk of bias

Two authors independently evaluated the methodological quality of the screened studies by using the ROB2 tool according to the instructions (https://methods.cochrane.org/bias/resources/rob-2-revised-cochrane-risk-bias-tool-randomized-trials). The specific criteria for risk of bias mainly included the following five aspects: randomization process, deviations from the intended interventions, missing outcome data, measurement of the outcome, and selection of the reported result. Quality assessments were rated as "high risk," "some concerns," or "unclear" risk of bias. All the authors discussed to address any discrepancies.

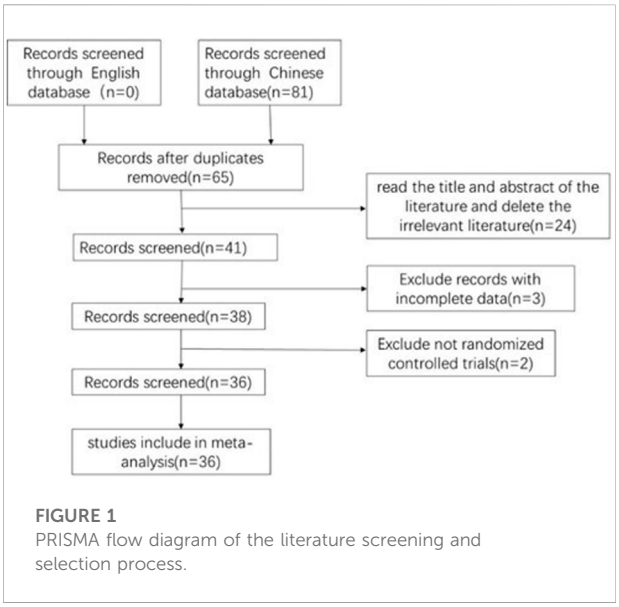

FIGURE 1
PRISMA flow diagram of the literature screening and selection process.

2.6.4 Data synthesis and analysis

The Review Manager Software tool (RevMan, v.5.3; The Cochrane Collaboration) was used to synthesize the data. We pooled the mean differences for dichotomous data with relative risk (RR) and 95% confidence intervals (CIs), while continuous data were pooled with standard mean difference (SMD) and 95% CI. When $I^2 \leq 75\%$, we used the fixed-effects model to synthesize the data. When $I^2 > 75\%$, we used the random-effects model to synthesize the data.

2.6.5 Sensitivity analysis

We aim to assess whether the conclusions were robust for the decision-making process, and we explored significant heterogeneity between studies by sensitivity analysis. When the analysis showed high heterogeneity, we performed a sensitivity analysis by removing a single study to observe whether the new effect size results and heterogeneity changed significantly.

2.7 Evidence confidence

The certainty of evidence was assessed by using the Graded Recommendation Assessment, Development, and Evaluations (GRADE) technique (https://www.gradepro.org/) according to risk of bias, indirectness, inconsistency, imprecision, and

publication bias. The level of evidence was classified as high, moderate, low, or very low.

3 Results

3.1 Results of RCT selection

A total of 147 related articles were initially detected. After excluding 82 replicate studies, 65 RCTs were included for further screening. After a detailed reading of the article titles and abstracts, 24 irrelevant studies, 3 studies with incomplete data, and 2 non-RCT studies were excluded. Finally, 36 studies were included (Mo and Zhao, 2002; Song et al., 2002; Zeng, 2005; Li et al., 2006; Guo et al., 2010; Li et al., 2010; Zhang, 2011; Zhi-Qing et al., 2011; Zhang et al., 2012; Guo et al., 2013; Zou, 2013; Guo, 2014; He and Sheng, 2014; Meng, 2014; Zong et al., 2014; Li, 2015; Xu et al., 2015; Li, 2016; Li and Chen, 2016; Sun, 2016; Zhao et al., 2016; Li and Hou, 2017; Wang and Qin, 2017; Wang et al., 2017; Yan et al., 2017; Wang, 2018; Wang et al., 2018; Zhang et al., 2018; Zhang and Zhang, 2018; Zhao, 2018; Fen et al., 2019; You and Wang, 2019; Zhang et al., 2019; Wang, 2020; Zhang, 2020; Wang, 2021), with a total of 3231 patients with PAMIHF for the systematic review and meta-analysis. Figure 1 describes the literature screening process and results, and details for search results are supplied in Supplementary File S1.

3.2 Characteristics of included RCTs

A total of 36 RCTs were conducted in China from 2002 to 2021, with sample sizes ranging from 46 to 334 and treatment durations ranging from 5 to 28 days, except for one study (Zou, 2013) that did not report the sustained time. In addition to two studies (Guo et al., 2013; Zhang et al., 2019) that did not mention the age, the mean age ranged from 46 to 76 years in other studies. In terms of the usage and dosage of SFI, three studies (Li et al., 2010; Zou, 2013; Zhang et al., 2018) did not report the dosage; the dosage of other studies varied from 20 to 100 ml. All the studies reported that SFI was diluted with 250–500 ml 5% dextrose, 100–500 ml 0.9% saline, or direct intravenous injection. Also, two studies (Zou, 2013; Zhang et al., 2018) did not record the usage, and one study (Wang and Qin, 2017) used the pump method. Moreover, eight studies (Zhi-Qing et al., 2011; Guo et al., 2013; Zou, 2013; Guo, 2014; Xu et al., 2015; Wang et al., 2017; Zhang et al., 2018; Zhang, 2020) did not report diagnostic criteria for AMI, and nine studies (Zhi-Qing et al., 2011; Guo et al., 2013; Zou, 2013; Guo, 2014; Xu et al., 2015; Sun, 2016; Wang et al., 2017; Zhang et al., 2018; Zhang, 2020) did not report diagnostic criteria for HF. The diagnostic criteria for AMI in one study (Li et al., 2006) were consistent with the literature (Sun and Fu, 2004). The diagnostic criteria for AMI in 15 studies (Mo and Zhao, 2002; Song et al., 2002; Zeng, 2005; Zhang, 2011; Zhang et al., 2012; Meng, 2014; Zong et al., 2014; Li and Chen, 2016; Sun, 2016; Zhao et al., 2016; Li and Hou, 2017; Wang, 2018; Wang et al., 2018; Fen et al., 2019; You and Wang, 2019) and the diagnostic criteria for HF in 23 studies (Mo and Zhao, 2002; Song et al., 2002; Zeng, 2005; Li et al., 2006; Guo et al., 2010; Zhang, 2011; Zhang et al., 2012; He and Sheng, 2014; Meng, 2014; Zong et al., 2014; Li, 2015; Li, 2016; Li and Chen, 2016; Zhao et al., 2016; Li and Hou, 2017; Wang and Qin, 2017; Yan et al., 2017; Wang, 2018; Wang et al., 2018; You and Wang, 2019; Zhang et al., 2019; Wang, 2020; Wang, 2021) met certain books (Chen, 1996; Wenwu, 2000; Chen, 2008). Diagnostic criteria for AMI in eight studies (Guo et al., 2010; Li et al., 2010; Li, 2015; Li, 2016; Wang and Qin, 2017; Yan et al., 2017; Zhang et al., 2019; Wang, 2020) were consistent with certain guidelines (Gao, 2001; Guidelines for the diagnosis and, 2010; Guidelines for the diagnosis and, 2015). Also, four studies (He and Sheng, 2014; Zhang and Zhang, 2018; Zhao, 2018; Wang, 2021) for AMI and two studies (Zhang and Zhang, 2018; Zhao, 2018) for HF had corresponding diagnostic criteria without mentioning the source of the reference. The diagnostic criteria for HF in two studies (Li et al., 2010; Fen et al., 2019) conformed to the NYHA classification, but did not mention the source of the relevant literature. A majority of patients in 11 studies (Mo and Zhao, 2002; Zeng, 2005; Zhang et al., 2012; Meng, 2014; Zong et al., 2014; Li, 2016; Sun, 2016; Zhao et al., 2016; Wang and Qin, 2017; Wang et al., 2018; Zhang and Zhang, 2018) received percutaneous coronary intervention (PCI). One study (Yan et al., 2017) mentioned that none of the patients received PCI treatment, and 24 studies did not record whether the patients received the PCI treatment or not. None of the studies reported the follow-up results. The essential characteristics of the included RCTs are listed in Table 1.

3.3 Risk of bias assessment

All included studies published complete data and did not report selective results, so the risk of missing outcome data, measurement of the outcome, and selection of the reported result was considered as "low". In addition, 13 (Zeng, 2005; Li et al., 2006; Zhang, 2011; Zou, 2013; Meng, 2014; Li, 2015; Li, 2016; Sun, 2016; Wang, 2018; Zhao, 2018; Wang, 2020; Zhang, 2020; Wang, 2021) articles had only one author, which led to a high risk of randomization process. In addition to these 13 studies, others studies did not state blind methods, so the risk of randomization process was considered to be some concerns. The risk of deviation was considered low because no deviation from the expected outcome was seen in any of the RCTs. Figure 2 presented the risk of bias results for the included RCTs.

TABLE 1 Characteristics of included RCTs investigating the adjunctive effect of Shenfu injection (SFI) on acute myocardial infarction and heart failure.

Included study (author/ year/ language)	Sample size (E/C)	Average age (E/C)	Duration	Interventions		Usage and dose	AHF diagnostic criteria	Adverse events	Outcome
				Experiment group	Control group				
Fen et al. (2019)	174/160	60.79 ± 9.73/ 61.43 ± 7.22	10 days	SFI plus CWT + E	CWT + E	Diluted in 5% GS 250ml, IVGTT	a	NR	②⑤⑨
Guo et al. (2010)	35/35	65.2 ± 14.2/ 63.7 ± 13.6	14 days	SFI plus CWT + rt-PA	CWT + rt-PA	Diluted in 0.9% NS 100ml, IVGTT	d	Death	⑨⑪
Guo et al. (2013)	30/30	NR	14 days	SFI plus CWT	CWT	Diluted in 5% GS/0.9% NS, IVGTT	NR	NR	①
Guo (2014)	40/40	73.70 ± 16.2/ 71.20 ± 14.6	14 days	SFI plus CWT	CWT	Diluted in 5% GS 100ml, IVGTT	NR	NR	①⑦⑨
He and Sheng (2014)	45/45	62.10 ± 2.4/ 60.13 ± 3.11	14 days	SFI plus CWT	CWT	Diluted in 0.9% NS 100ml, IVGTT (2 times/d)	NR	Death	①②⑤⑥⑨⑪
Li et al. (2006)	37/36	63.7 ± 18.6/ 59.8 ± 17.2	14 days	SFI plus CWT	CWT	IVGTT	e	NR	⑨
Li et al. (2010)	58/34	68.2 ± 9.3/ 67.8 ± 10.7	14 days	SFI plus CWT	CWT	IVGTT	d	NR	②③⑧⑪
Li (2015)	32/32	63.50 ± 11.2/ 63.20 ± 11.50	14 days	SFI plus CWT	CWT	Diluted in 0.9% NS 100ml, IVGTT (2 times/d)	g	Death	①②⑤⑥⑨⑪
Li (2016)	32/32	62.73 ± 8.23/ 62.73 ± 8.23	<14 days	SFI plus CWT + D	CWT + D	IVGTT	g	Death	⑧
Li and Chen (2016)	23/23	68.60 ± 2.60/ 68.70 ± 2.60	14 days	SFI plus CWT	CWT	Diluted in 5% GS 200ml, IVGTT	i	Bleeding	①②⑥⑦⑨⑪
Li and Hou (2017)	31/31	66.38 ± 10.69/ 67.41 ± 11.98	14 days	SFI plus CWT	CWT	Diluted in 0.9% NS 100ml, IVGTT	d	Death, SMI, bleeding, blood clots, arrhythmia	①②⑥⑧⑪
Meng (2014)	30/30	46.3 ± 11.9/ 46.7 ± 12.1	5 days	SFI plus CWT + Du	CWT + Du	IVGTT	i	NR	①②⑦⑪
Mo and Zhao (2002)	36/38	55.3 ± 15.6/ 54.9 ± 12.7	7 days	SFI plus CWT	CWT	Diluted in 5% GS/0.9% NS 250ml, IVGTT	l	NR	①⑨
Song et al. (2002)	24/24	56.23 ± 4.53/ 54.81 ± 4.37	20 days	SFI plus CWT + Du	CWT + Du	Diluted in 5% GS 250ml, IVGTT	m	Tachycardia, Hypertension, Ventricular Premature	①②⑧
Sun (2016)	31/31	65.3 ± 5.1/ 67.1 ± 5.3	7 days	SFI plus CWT + rhBNP	CWT + rhBNP	Diluted in 5% GS 250ml, IVGTT	a	Low blood pressure	⑧⑩
Wang and Qin (2017)	64/64	59.7 ± 14.3/ 58.2 ± 13.6	7 days	SFI plus CWT + D	CWT + D	pump	g	Arrhythmia	①⑧⑪
Wang et al. (2017)	44/44	72.79 ± 10.56/ 72.09 ± 10.62	14 days	SFI plus CWT + Simvastatin	CWT + Simvastatin	IVGTT	NR	NR	②③⑤⑪
Wang (2018)	58/58	60.8 ± 2.5/ 64.8 ± 2.5	7 days	SFI plus rhBNP	rhBNP	Diluted in 5% GS 250–500ml, IVGTT	f	Low blood pressure, arrhythmia	②③

(Continued on following page)

TABLE 1 (*Continued*) Characteristics of included RCTs investigating the adjunctive effect of Shenfu injection (SFI) on acute myocardial infarction and heart failure.

Included study (author/ year/ language)	Sample size (E/C)	Average age (E/C)	Duration	Interventions		Usage and dose	AHF diagnostic criteria	Adverse events	Outcome
				Experiment group	Control group				
Wang et al. (2018)	31/31	64.8 ± 2.5/ 60.8 ± 2.5	7 days	SFI plus CWT + rhBNP	CWT + rhBNP	Diluted in 5% GS 250ml, IVGTT	NR	Low blood pressure, arrhythmia	②③⑤⑧⑩⑪
Wang (2020)	37/37	65.78 ± 5.52/ 65.13 ± 5.39	7 days	SFI plus Lyophilized rhBNP	Lyophilized rhBNP	Diluted in 5% GS 250ml, IVGTT	d	NR	②⑤
Wang (2021)	33/32	73 ± 12.8/ 72 ± 13.6	10 days	SFI plus CWT	CWT	Diluted in 5–10% GS 250–500ml, IVGTT	NR	NR	①②⑨
Zhi-Qing et al. (2011)	37/33	75.8 ± 12.3/ 74.3 ± 11.5	14 days	SFI plus CWT	CWT	Diluted in 5% GS/0.9% NS, IVGTT	NR	Low blood pressure, arrhythmia, infection	①②⑧⑪
Xu et al. (2015)	36/38	55.3 ± 15.6/ 54.9 ± 12.7	7 days	SFI plus CWT	CWT	Diluted in 5% GS/0.9% NS 250ml, IVGTT	NR	NR	①⑨
Yan et al. (2017)	40/40	61.68 ± 7.54/ 62.03 ± 7.66	21 days	SFI plus CWT	CWT	Diluted in 0.9% NS 500ml, IVGTT	d	NR	①②
You and Wang (2019)	38/38	54.67 ± 9.68/ 52.35 ± 10.27	7 days	SFI plus Lyophilized rhBNP	Lyophilized rhBNP	Diluted in 5% GS 250ml, IVGTT	b	NR	①⑤
Zeng (2005)	54/56	57.6 ± 15.2/ 56.8 ± 15.7	10 days	SFI plus CWT	CWT	Diluted in 5% GS/0.9% NS 250ml, IVGTT	k	NR	①
Zhang (2011)	37/37	54.2/55.7	14 days	SFI plus CWT	CWT	Diluted in 5% GS, IVGTT	j	Death	①
Zhang et al. (2012)	39/39	61 ± 13/ 61 ± 12	12 days	SFI plus CWT	CWT	Diluted in 0.9% NS 100ml, IVGTT	NR	NR	①⑪
Zhang et al. (2018)	122/122	70.47 ± 5.39/ 70.33 ± 5.26	14 days	SFI plus CWT	CWT	NR	NR	NR	⑨
Zhang and Zhang (2018)	38/38	63.32 ± 1.78/ 63.91 ± 5.86	28 days	SFI plus CWT + aspirin	CWT + aspirin	Diluted in 0.9% NS 500ml, IVGTT	NR	NR	①②⑦⑧⑨
Zhang et al. (2019)	33/32	NR	10 days	SFI plus CWT	CWT	IVGTT	c	High heart rate	②⑤⑪
Zhang (2020)	50/50	65.39 ± 3.61/ 65.32 ± 3.32	NR	SFI plus rhBNP	rhBNP	Diluted in 5% GS 250–500ml, IVGTT	NR	NR	①
Zhao et al. (2016)	31/31	68 ± 5/68 ± 5	7 days	SFI plus CWT + rhBNP	CWT + rhBNP	Diluted in 5% GS 250ml, IVGTT	a	Low blood pressure, arrhythmia	②③⑤⑧⑩
Zhao (2018)	60/60	63.6 ± 3.9/ 65.6 ± 4.1	14 days	SFI plus CWT	CWT	Diluted in 5% GS 250ml, IVGTT	NR	NR	①②⑦⑧⑨
Zong et al. (2014)	52/53	65.32 ± 12.12/ 65.31 ± 11.37	14 days	SFI plus CWT	CWT	Diluted in 5% GS 250ml, IVGTT	a	NR	①②⑧⑪
Zou (2013)	36/36	70 ± 4.6/ 70 ± 4.6	NR	SFI plus CWT	CWT	NR	NR	NR	①⑦⑧⑨

E/C: experimental group/control group; SFI: Shenfu injection; CWT: conventional western treatment; E: enoxaparin sodium; rt-PA: reverse transcriptase PA; Du: dobutamine; D: dopamine; M: metoprolol; rhBNP: recombined human; NR: not report. ①:Total effective rate; ②:LVEF: left ventricular ejection fraction; ③:LVEDD: left ventricular end-diastolic dimension; ④:SV: stroke volume; ⑤:NT-proBNP: N-terminal pro-B-type natriuretic peptide; and ⑥: adverse events; cardiac index; heart rate; cardiac output; serum creatinine; and BNP. a. WHO, diagnostic criteria; b. (Zhao, 2017); c: (Guidelines for the diagnosis and, 2015); d: (Gao, 2001); e: (Sun and Fu, 2004); f: (Luo and Lin, 2013); g: (Guidelines for the diagnosis and, 2010); h: (Randhawa et al., 2014); i: (Chen, 2008); j: (Wenwu, 2000); k: (Wang, 2002); l: (Chen, 1995); and m (Chen, 1996):

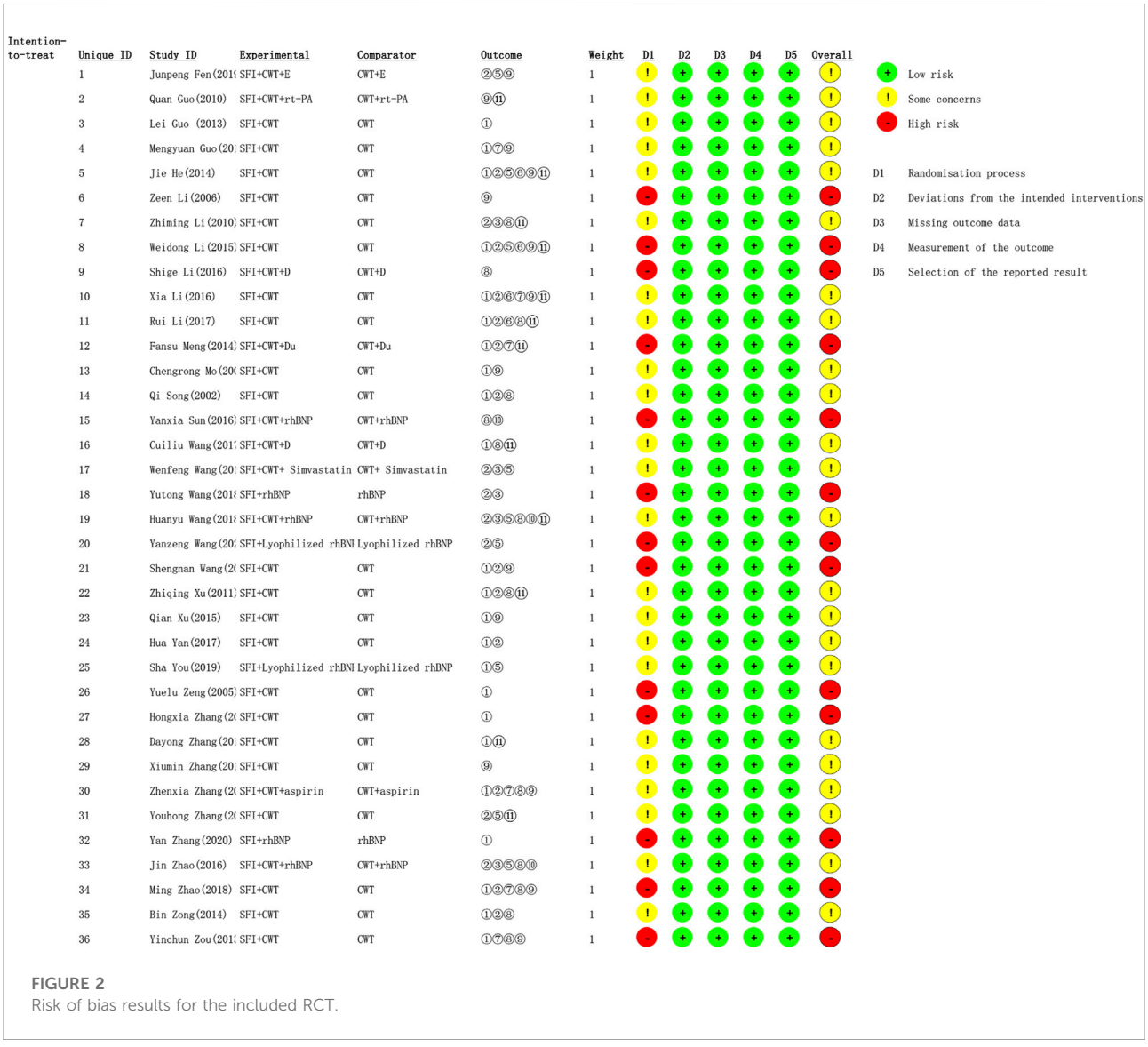

Unique ID	Study ID	Experimental	Comparator	Outcome	Weight	D1	D2	D3	D4	D5	Overall
1	Junpeng Fen(201	SFI+CWT+E	CWT+E	②⑤⑨	1	!	+	+	+	+	!
2	Quan Guo(2010)	SFI+CWT+rt-PA	CWT+rt-PA	⑨⑪	1	!	+	+	+	+	!
3	Lei Guo (2013)	SFI+CWT	CWT	①	1	!	+	+	+	+	!
4	Mengyuan Guo(20	SFI+CWT	CWT	①⑦⑨	1	!	+	+	+	+	!
5	Jie He(2014)	SFI+CWT	CWT	①②⑤⑥⑨⑪	1	!	+	+	+	+	!
6	Zeen Li(2006)	SFI+CWT	CWT	⑨	1	-	+	+	+	+	-
7	Zhiming Li(2010)	SFI+CWT	CWT	②③⑧⑪	1	!	+	+	+	+	!
8	Weidong Li(2015)	SFI+CWT	CWT	①②⑤⑥⑨⑪	1	-	+	+	+	+	-
9	Shige Li(2016)	SFI+CWT+D	CWT+D	⑧	1	-	+	+	+	+	-
10	Xia Li(2016)	SFI+CWT	CWT	①②⑥⑦⑨⑪	1	!	+	+	+	+	!
11	Rui Li(2017)	SFI+CWT	CWT	①②⑥⑧⑪	1	!	+	+	+	+	!
12	Fansu Meng(2014)	SFI+CWT+Du	CWT+Du	①②⑦⑪	1	-	+	+	+	+	-
13	Chengrong Mo(20(	SFI+CWT	CWT	①⑨	1	!	+	+	+	+	!
14	Qi Song(2002)	SFI+CWT	CWT	①②⑧	1	!	+	+	+	+	!
15	Yanxia Sun(2016)	SFI+CWT+rhBNP	CWT+rhBNP	⑧⑩	1	-	+	+	+	+	-
16	Cuiliu Wang(201	SFI+CWT+D	CWT+D	①⑧⑪	1	!	+	+	+	+	!
17	Wenfeng Wang(20	SFI+CWT+ Simvastatin	CWT+ Simvastatin	②③⑤	1	!	+	+	+	+	!
18	Yutong Wang(201	SFI+rhBNP	rhBNP	②③	1	-	+	+	+	+	-
19	Huanyu Wang(201	SFI+CWT+rhBNP	CWT+rhBNP	②③⑤⑧⑩⑪	1	!	+	+	+	+	!
20	Yanzeng Wang(20	SFI+Lyophilized rhBNI	Lyophilized rhBNP	②⑤	1	-	+	+	+	+	-
21	Shengnan Wang(2(	SFI+CWT	CWT	①②⑨	1	-	+	+	+	+	-
22	Zhiqing Xu(2011)	SFI+CWT	CWT	①②⑧⑪	1	!	+	+	+	+	!
23	Qian Xu(2015)	SFI+CWT	CWT	①⑨	1	!	+	+	+	+	!
24	Hua Yan(2017)	SFI+CWT	CWT	①②	1	!	+	+	+	+	!
25	Sha You(2019)	SFI+Lyophilized rhBNI	Lyophilized rhBNP	①⑤	1	!	+	+	+	+	!
26	Yuelu Zeng(2005)	SFI+CWT	CWT	①	1	-	+	+	+	+	-
27	Hongxia Zhang(2(	SFI+CWT	CWT	①	1	-	+	+	+	+	-
28	Dayong Zhang(20	SFI+CWT	CWT	①⑪	1	!	+	+	+	+	!
29	Xiumin Zhang(20	SFI+CWT	CWT	⑨	1	!	+	+	+	+	!
30	Zhenxia Zhang(2(	SFI+CWT+aspirin	CWT+aspirin	①②⑦⑧⑨	1	!	+	+	+	+	!
31	Youhong Zhang(2(	SFI+CWT	CWT	②⑤⑪	1	!	+	+	+	+	!
32	Yan Zhang(2020)	SFI+rhBNP	rhBNP	①	1	-	+	+	+	+	-
33	Jin Zhao(2016)	SFI+CWT+rhBNP	CWT+rhBNP	②③⑤⑧⑩	1	!	+	+	+	+	!
34	Ming Zhao(2018)	SFI+CWT	CWT	①②⑦⑧⑨	1	-	+	+	+	+	-
35	Bin Zong(2014)	SFI+CWT	CWT	①②⑧	1	!	+	+	+	+	!
36	Yinchun Zou(201	SFI+CWT	CWT	①⑦⑧⑨	1	-	+	+	+	+	-

FIGURE 2
Risk of bias results for the included RCT.

3.4 Meta-analysis results

3.4.1 Primary outcome measures of measures of NT-proBNP

Nine studies (He and Sheng, 2014; Li, 2015; Zhao et al., 2016; Wang et al., 2017; Wang et al., 2018; Fen et al., 2019; You and Wang, 2019; Zhang et al., 2019; Wang, 2020) involving 915 patients reported NT-proBNP outcomes. A random-effects model was used for meta-analysis because of high heterogeneity between studies ($p < 0.00001$, $I^2 = 98\%$). The sensitivity analyses did not find sources of heterogeneity. A meta regression analysis further explored that sample size, duration, age, type of disease, and usage were not the source of heterogeneity ($p > 0.05$, As Table 2 showed; for details see

TABLE 2 Meta regression analysis on the results of NT-proBNP.

_ES	Coefficient	Std. err	t	P>|t|	[95% conf. interval]	
Sample size	3.073344	6.531287	0.47	0.662	−15.06041	21.2071
Duration	−1.869973	4.332006	−0.43	0.688	−13.89755	10.1576
Usage	4.739137	6.534725	0.73	0.508	−13.40417	22.88244
Age	.8875687	6.558093	0.14	0.899	−17.32062	19.09576
_cons	−9.010748	9.910538	−0.91	0.415	−36.52681	18.50532

Sample size <50, 50–200, and ≥200 were categorized as 0, 1, and 2, respectively. Duration was categorized as 1, 2, 3, and 0, respectively, when duration<7, 7–14, ≥14 days, and no mention duration. Usage was categorized as 1, 2, 3, and 0, respectively, when it was 100 ml, 200 ml, more than 250 ml, and was no mention. Age was categorized as 0 and one when the average of participates was < 60 or ≥ 60 years old. Type of diseases was categorized as 0 and one when patients suffer from acute myocardial infarction with heart failure, accompanied without or with other disease. As for NT-proBNP, patients in the included studies suffer from acute myocardial infarction with heart failure, accompanied without or with other disease; thus, it could not be included in Meta regression analysis.

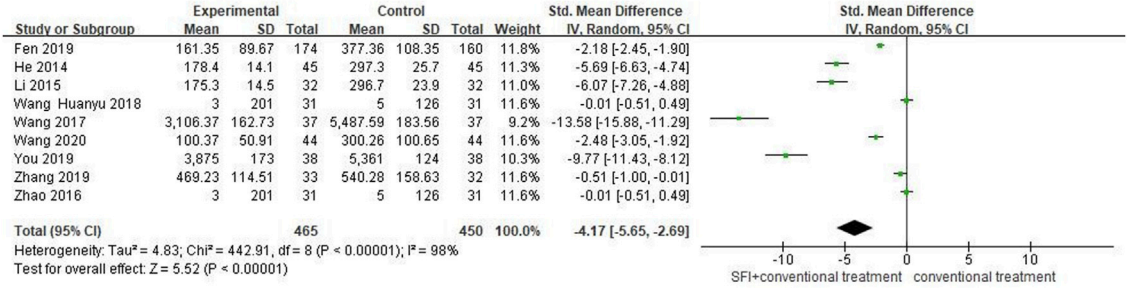

FIGURE 3
Forest plot of NT-proBNP.

Supplementary Table S5). Despite lacking the source of high heterogeneity, the meta results showed that the combination of SFI and conventional medical therapy improved NT-proBNP in PAMIHF patients better than conventional medical therapy alone [SMD = −4.17; 95% CI (−5.65, −2.69); p < 0.00001, Figure 3]; thus, future rigorous RCTs with large sample were required to confirm this meta result.

3.4.2 Primary outcome measures of LVEF

A total of 21 studies (Song et al., 2002; Li et al., 2010; Zhi-Qing et al., 2011; Zou, 2013; Guo, 2014; He and Sheng, 2014; Meng, 2014; Li, 2015; Li and Chen, 2016; Zhao et al., 2016; Li and Hou, 2017; Wang et al., 2017; Yan et al., 2017; Wang, 2018; Wang et al., 2018; Zhang and Zhang, 2018; Zhao, 2018; Fen et al., 2019; Zhang et al., 2019; Wang, 2020; Wang, 2021) involving 1826 patients reported LVEF. A random-effects model was used for meta-analysis because of high heterogeneity between studies (p < 0.00001, I^2 = 90%). The results of the meta-analysis showed that the combination of SFI and conventional medical therapy improved LVEF better [RR = 1.18; 95% CI (0.85, 1.51); p < 0.00001, Figure 4]. The sensitivity analysis showed six studies (Zou, 2013; He and Sheng, 2014; Meng, 2014; Li, 2015; Wang et al., 2017; Fen et al., 2019) that significantly reduced the heterogeneity to 84%. Compared with other studies, two studies (He and Sheng, 2014; Li, 2015) had treatment frequency of twice a day, which may lead to high heterogeneity between studies. The meta regression analysis further explored that sample size, duration, type of diseases, age, and usage were not the main source of heterogeneity (p > 0.05; as shown in Table 3;for detail see Supplementary Table S5). Although, after the sensitivity analysis, the heterogeneity was still high, and the results showed that SFI combined with conventional medical therapy significantly improved LVEF in patients with PAMIHF [SMD = 0.98; 95% CI (0.71.1.24); p < 0.00001, Figure 4], while it required future high quality RCTs with large sample to update this meta result due to its high heterogeneity.

3.4.3 Secondary outcome measures of total effective rate

A total of 22 studies (Mo and Zhao, 2002; Song et al., 2002; Zeng, 2005; Zhang, 2011; Zhi-Qing et al., 2011; Zhang et al., 2012; Guo et al., 2013; Guo, 2014; He and Sheng, 2014; Meng, 2014; Zong et al., 2014; Li, 2015; Xu et al., 2015; Li and Chen, 2016; Li and Hou, 2017; Wang and Qin, 2017; Yan et al., 2017; Zhang and Zhang, 2018; Zhao, 2018; You and Wang, 2019; Zhang, 2020;

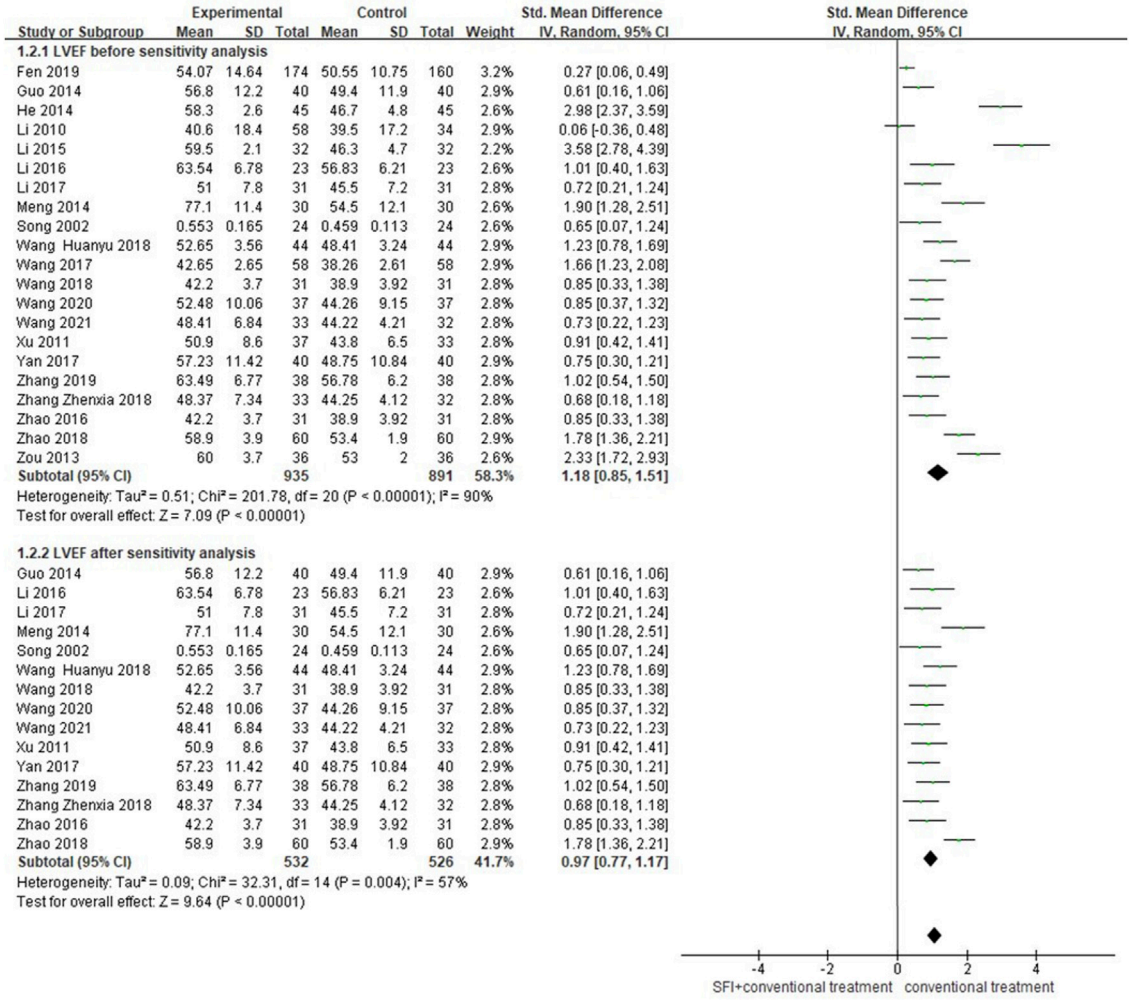

FIGURE 4
Forest plot of LVEF.

TABLE 3 Meta regression analysis on the results of LVEF.

_ES	Coefficient	Std. err	t	P>|t|	[95% conf. interval]	
Sample size	−0.270454	0.5496324	−0.49	0.630	−1.441968	0.9010597
Duration	−0.0132916	0.3310933	0.04	0.696	−0.7190003	0.6924171
Usage	−0.2900352	0.1525484	−1.90	0.077	−0.6151843	0.035114
Age	−0.239398	0.7126366	−0.34	0.742	−1.758347	1.279551
Type of disease	−1.349708	0.6562594	−2.06	0.058	−2.748492	0.0490755
_cons	2.114263	0.8478154	2.49	0.025	0.3071875	3.921339

Sample size <50, 50–200, and ≥200 were categorized as 0, 1, and 2, respectively. Duration was categorized as 1.2, 3, and 0, respectively, when duration<7, 7–14,≥14 days, and no mention duration. Usage was categorized as 1, 2, 3, and 0, respectively, when it was 100 ml, 200 ml, more than 250 ml, and was no mention. Age was categorized as 0 and one when the average of participates was < 60 or ≥ 60 years old. Type of diseases was categorized as 0 and one when patients suffer from acute myocardial infarction with heart failure, accompanied without or with other disease.

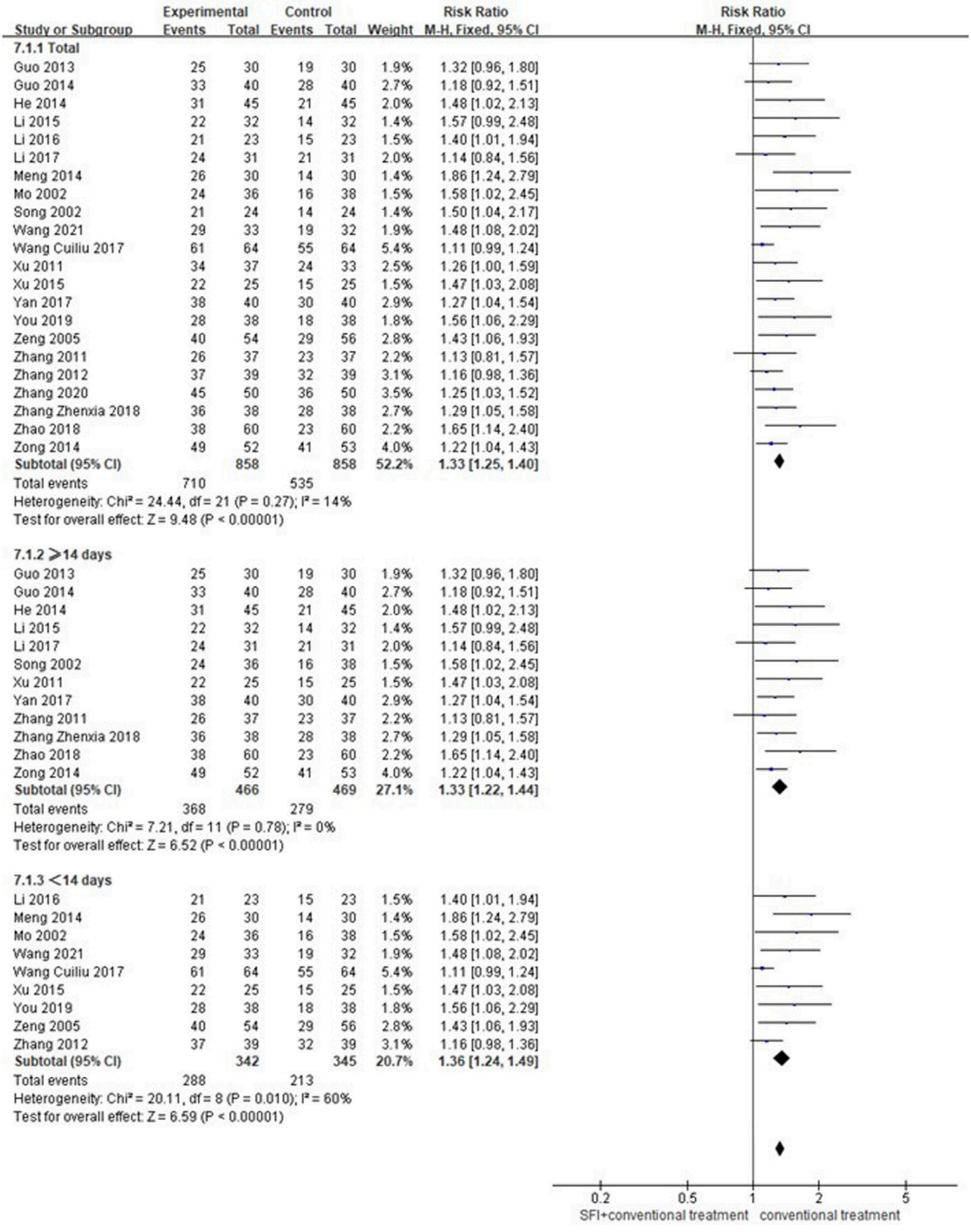

FIGURE 5
Forest plot of the total effective rate.

Wang, 2021) involving 1716 patients reported the total effective rate. Due to low heterogeneity ($p = 0.97$, $I^2 = 0\%$) between-study, a fixed-effects model was used for meta-analysis. As shown in Figure 5, the results showed that the combination of SFI and conventional medication was superior to improve the total effective rate compared with conventional medication alone [RR = 1.33; 95% CI (1.25, 1.40); $p < 0.00001$]. The subgroup analysis according to the SFI dose showed < 14 days [RR =

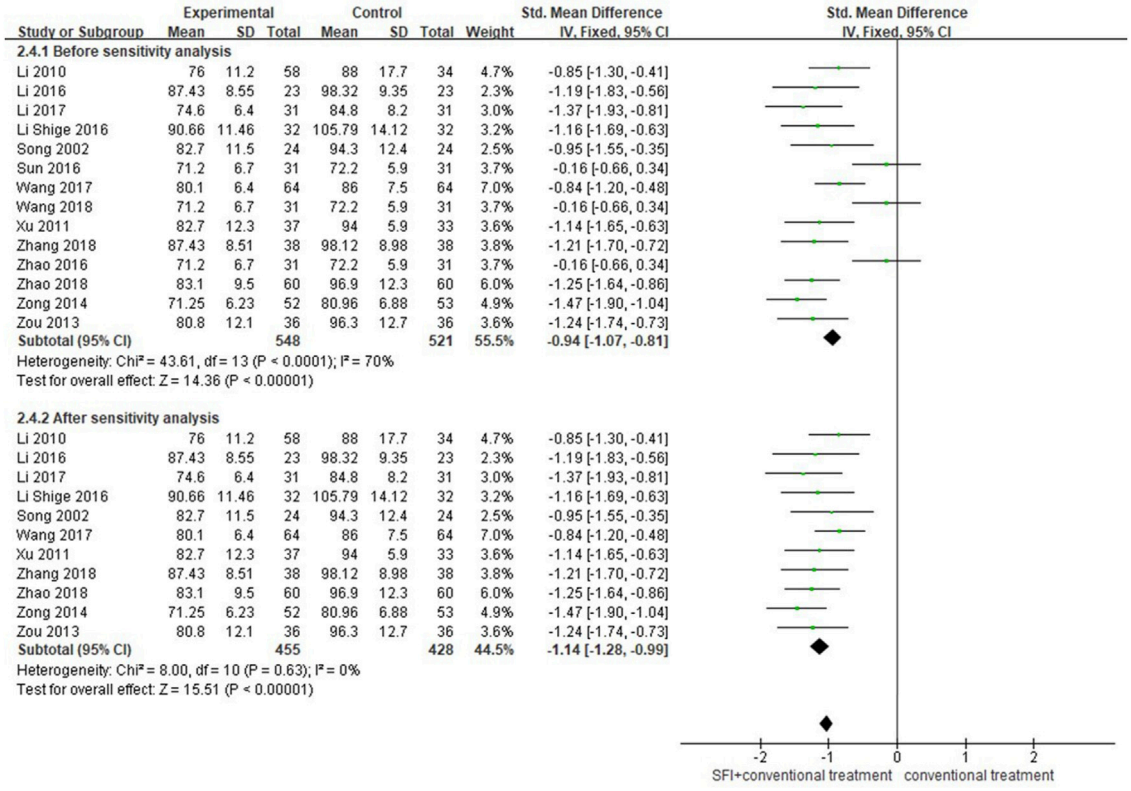

FIGURE 6
Forest plot of HR.

1.33; 95% CI (1.22, 1.44); $p < 0.00001$] and ≥ 14 days [RR = 1.36; 95% CI (1.24, 1.49); $p < 0.00001$; Figure 5] both improved the total effective rate better than that of conventional medication alone.

3.4.4 Secondary outcome measures of heart rate

A total of 14 studies (Song et al., 2002; Li et al., 2010; Zhi-Qing et al., 2011; Zou, 2013; Zong et al., 2014; Li, 2016; Li and Chen, 2016; Sun, 2016; Zhao et al., 2016; Li and Hou, 2017; Wang et al., 2017; Wang et al., 2018; Zhang and Zhang, 2018; Zhao, 2018) involving 1069 patients reported the results of HR. The random-effects model was used for meta-analysis as there existed high heterogeneity between studies ($p < 0.00001$, $I^2 = 70\%$). After excluding three studies by using the sensitivity analysis, the heterogeneity between studies was significantly reduced to 0%. As shown in Table 1, rh-BNP plus conventional therapy was used in both the SFI group and conventional therapy groups of these three studies (Sun, 2016; Zhao et al., 2016; Wang, 2018), which may lead to heterogeneity. After the sensitivity analysis, the results showed that adjunctive use of SFI decreased the HR better than conventional medicine treatment alone [SMD = −1.14; 95% CI (−1.28, −0.99); $p < 0.00001$; Figure 6].

3.4.5 Secondary outcome measures of cardiac output

A total of 12 studies (Mo and Zhao, 2002; Li et al., 2006; Guo et al., 2010; Zou, 2013; Guo, 2014; He and Sheng, 2014; Li, 2015; Li and Chen, 2016; Zhang and Zhang, 2018; Zhao, 2018; Fen et al., 2019; Wang, 2021) involving 1164 patients reported the results of cardiac output (CO). The random-effects model was used for meta-analysis as there existed high heterogeneity between studies ($p < 0.00001$, $I^2 = 98\%$). The sensitivity analyses did not find sources of heterogeneity. The results showed that CO of PAMIHF patients was improved better by combined used of SFI and conventional medicine treatment [SMD = 3.15; 95% CI (2.04.4.25); $p < 0.00001$, Figure 7].

3.4.6 Secondary outcome measures of BNP

A total of 13 studies (Guo et al., 2010; Li et al., 2010; Zhi-Qing et al., 2011; Zhang et al., 2012; He and Sheng, 2014; Meng, 2014; Zong et al., 2014; Li, 2015; Li and Chen, 2016; Li and Hou, 2017; Wang and Qin, 2017; Wang et al., 2017; Zhang et al., 2019) involving 1018 patients reported the value of BNP. A random-effects model was used for meta-analysis because of high heterogeneity between studies ($p < 0.00001$, $I^2 = 96\%$). The sensitivity analyses did not find sources of heterogeneity. The

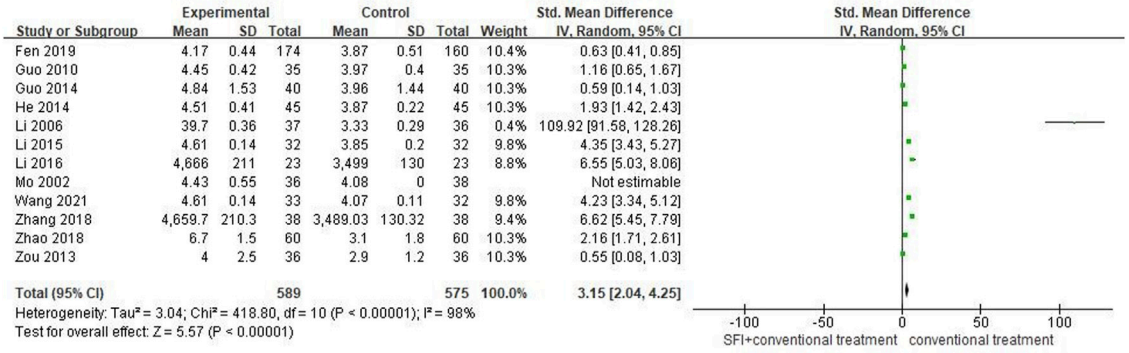

FIGURE 7
Forest plot of CO.

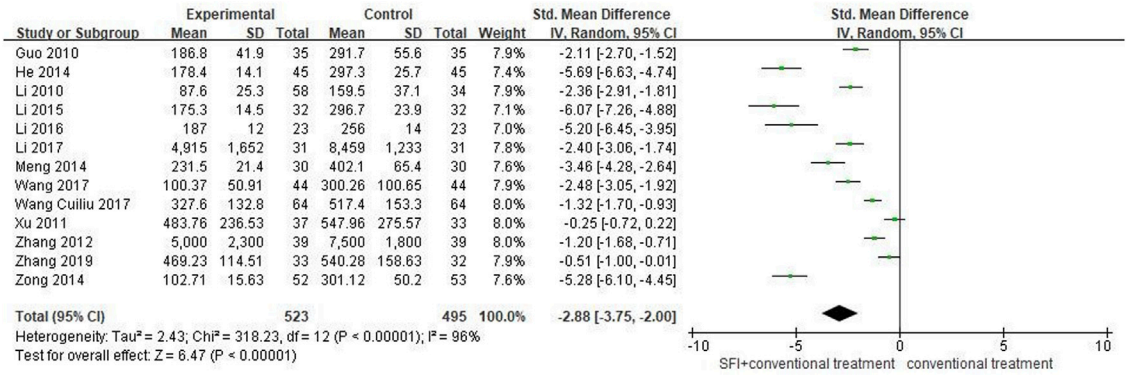

FIGURE 8
Forest plot of BNP.

results showed that the combination of SFI and conventional medical therapy improved BNP in PAMIHF patients better than conventional medical therapy alone [SMD = −2.88; 95% CI (−3.75, −2.00); $p < 0.00001$, Figure 8].

3.5 Safety of adverse events comparison

A total of 18 studies (Mo and Zhao, 2002; Song et al., 2002; Zeng, 2005; Guo et al., 2010; Zhang, 2011; Zhi-Qing et al., 2011; He and Sheng, 2014; Li, 2015; Li, 2016; Li and Chen, 2016; Sun, 2016; Zhao et al., 2016; Li and Hou, 2017; Wang and Qin, 2017; Wang et al., 2017; Wang, 2018; Wang et al., 2018; Zhang et al., 2019) involving 1055 patients reported the adverse events rate. The fixed-effects model was used for meta-analysis as there existed little heterogeneity between studies ($p = 0.38$, $I^2 = 7\%$). The meta-analysis results showed that SFI combined with conventional medical therapy had a lower adverse event rates [RR = 0.45; 95% CI (0.35, 0.57); $p < 0.00001$, Figure 9], indicating that SFI combined with conventional treatment (9.73%, 66/678) was safer than conventional treatment alone (21.7%, 147/677).

3.6 Results of publication bias assess

We assessed publication bias for the total effective rate, LVEF, NT-proBNP, BNP, CO, HR, and adverse effect outcomes. As Figure 10 showed, the funnel plot indicted that no publication bias existed in the results of total effective rate, LVEF, HR, and adverse events as the distribution of bubbles was relatively concentrated and was not scattered on the funnel boundary. The Egger and Begg analysis suggested that no published bias existed in the results of adverse events and HR (both $p > 0.05$), while they indicated published bias existed in the

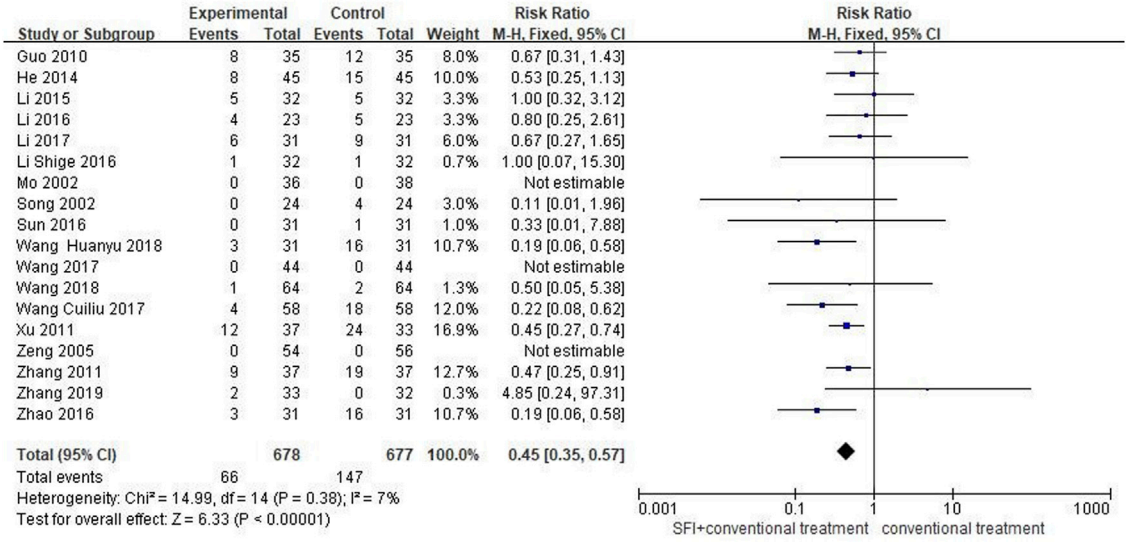

FIGURE 9
Forest plot of adverse events comparison.

results of LVEF and the total effective rate (both $p < 0.05$). However, we could not rule out the possibility of existing selective reporting of results because clinical trial registration or study protocol information was not available.

3.7 The quality of the evidence

We used the GRADE approach to assess the quality of evidence for the meta outcomes, which was rated from "very low" to "moderate". They were downgraded mainly due to small sample size and unclear risk of bias for selected studies in our meta results, as shown in Table 4.

4 Discussion

SFI has shown satisfactory clinical efficacy such as favorable neurological outcome in patients with return of spontaneous circulation after in-hospital cardiac arrest (Zhang et al., 2017; Shao et al., 2020). SFI also presents apparent effects in improving microcirculatory perfusion in patients with septic shock, and its mechanism may be related with the inhibition of endothelial dysfunction (Wang et al., 2022). Studies has shown that SFI could prevent sepsis-induced myocardial injury by inhibiting mitochondrial apoptosis (Xu et al., 2020) and attenuating lipopolysaccharide-induced myocardial inflammation (Chen et al., 2020), and it might regulate the expression of adenosine receptors to improve the myocardial ischemia–reperfusion postconditioning (Wang et al., 2021b). This systematic review and meta-analysis included 36 RCTs suggested that SFI combined with conventional western medicine had an adjunctive effect on the treatment of PAMIHF patients, which could better improve the total effective rate, LVEF, and HR. In addition, it was safer to decrease the adverse events rate compared with conventional therapy alone.

4.1 The adjunctive effect of SFI in treating AMI-HF

SFI has shown satisfactory clinical efficacy in the treatment of cardiovascular disease. AMI is a common acute pathological process, which can cause direct damage to the structure and function of the heart and then lead to acute HF. Because of tissue hypoperfusion and decreased coronary blood flow in PAMIHF patients, it aggravates myocardial damage, leads to increased heart rate, compensatory hypoperfusion and finally promotes myocardial remodeling (Wang, 2020). Cardiogenic shock is an extreme manifestation of PAMIHF and the leading cause of death in the AMI setting. The only treatment to reduce the mortality of patients with cardiogenic shock is early revascularization (Bahit et al., 2018). SFI could reduce the pre-load and post-load of the heart by acting on cell channels, avoiding the aggravation of myocardial hypoxia damage, promoting the repair of myocardial cells, and improving the cardiac pathology process (Wang, 2021). SFI combined with other Chinese patent medicines could inhibit the infiltration of inflammatory cells and improve hemodynamics by promoting cardiac function, reducing cardiomyocytes destruction, reducing

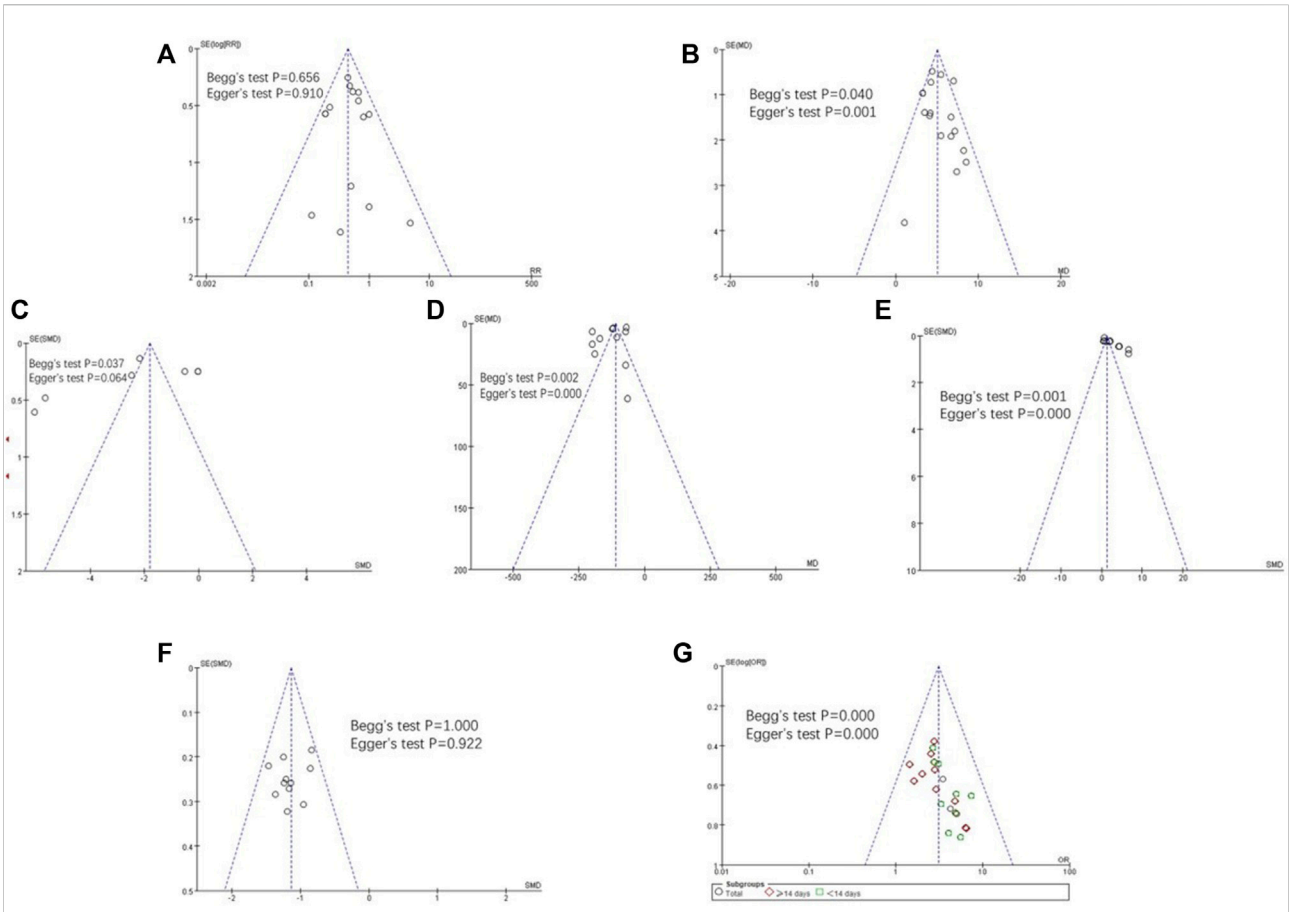

FIGURE 10
Funnel plot for publication bias assessment. **(A)** Adverse events publishes biased assessment, **(B)** LVEF publication bias assessment, **(C)** NT-proBNP publication bias assessment, **(D)** BNP publication bias assessment, **(E)** CO publishes biased assessment, **(F)** HR publishes biased assessment, and **(G)**total effective rate publication bias assessment.

collagen synthesis, inhibiting myocardial fibrosis, and ventricular remodeling (Gao et al., 2019). In our study, it also showed that SFI combined with conventional drug therapy improved the total effective rate, LVEF, and HR, which was consistent with previous results of published clinical studies. Interestingly, the results showed that adjunctive use of SFI showed satisfactory results regardless of treatment duration (≥14 days or <14 days) and also improved the NT-proBNP, BNP, and CO better.

4.2 The safety of SFI in conjunction with conventional medicine in treating AHF

In terms of clinical safety, a total of 9.7% (66/678) of adverse reactions occurred in the SFI group, while 21.7% (147/677) of adverse reactions occurred in the conventional treatment group, including nausea, vomiting, hypotension, hypertension, slow HR, and arrhythmia. With moderate safety assessment evidence, 18 studies (Mo and Zhao, 2002; Song et al., 2002; Zeng, 2005; Guo et al., 2010; Zhang, 2011; Zhi-Qing et al., 2011; He and Sheng, 2014; Li, 2015; Li, 2016; Li and Chen, 2016; Sun, 2016; Zhao et al., 2016; Li and Hou, 2017; Wang and Qin, 2017; Wang et al., 2017; Wang, 2018; Wang et al., 2018; Zhang et al., 2019) reported adverse effects, and we tentatively put forward the following arguments: combination therapy of SFI for PAMIHF was safer than conventional medicine alone. However, we still needed further eligible pivotal clinical trials to validate the safety of SFI as the risk of bias assessment of part of the RCTs was recorded as 'unclear'.

4.3 The assessment of bias risk and evidence's confidence on the meta results

We validated credible clinical evidence for our results by assessing risk of bias and confidence in the evidence. The final results indicated that detailed information on selection bias, blinding performance, and blinded outcome assessment were

TABLE 4 Summary of findings by the Grading Recommendations Assessment, Development, and Evaluations (GRADE) methods.

Outcomes	No. of participants (studies)	Quality of the evidence (GRADE)	Relative effect (95%CI)	Anticipated absolute effects* (95% CI)	
				Risk with [conventional medicine]	Risk with [SM injection]
Total effective rate	1716 (22 RCTs)[d]	⊕⊕⊕○ Moderate[a] risk of bias (-2[a])	RR 3.16 (2.50–4.00)	624 per 1,000	1000 per 1,000 (1,000 to 1,000)
LVEF	1564 (17 RCTs)[d]	⊕○○○ Very low[a,b] risk of bias (-2[a]) Inconsistency (-2[b])	-	The mean LVEF was 0	MD 4.98 higher (4.51 higher to 5.46 higher)
NT-proBNP	219 (3 RCTs)[d]	⊕○○○ Very low[a,c] Risk of bias (-2[a]) Inconsistency (-1[b])	-	The mean nT-proBNP was 0	MD 119.56 lower (125.95 lower to 113.17 lower)
LVEFD	328 (4 RCTs)[d]	⊕○○○ Very low[a,c] Risk of bias (-2[a]) Inconsistency (-1[b])	-	The mean LVEFD was 0	MD 5.84 lower (6.54 lower to 5.13 lower)
BNP	1018 (13 RCTs)[d]	⊕⊕○○ Low[a,b] Risk of bias (-2[a]) Imprecision (-1[e])	-	The mean BNP was 0	MD 109.48 lower (113.66 lower to 105.29 lower)
CI	258 (4 RCTs)[d]	⊕○○○ Very low[a,c] Risk of bias (-2[a]) Inconsistency (-1[b])	-	The mean CI was 0	MD 0.78 higher (0.57 higher to 0.99 higher)
HR	755 (10 RCTs)[d]	⊕⊕⊕○ Moderate[a] Risk of bias (-2[a])	-	The mean heart rate was 0	MD 11.34 lower (12.75 lower to 9.93 lower)
CO	451 (6 RCTs)[d]	⊕⊕○○ Low[a] Risk of bias (-2[a])	-	The mean cardiac output was 0	MD 0.55 higher (0.5 higher to 0.61 higher)
Adverse events	1355 (18 RCTs)[d]	⊕⊕⊕○ Moderate[a] Risk of bias (-2[a])	RR 0.45 (0.35–0.57)	217 per 1,000	98 per 1,000 (76–124)

*__The risk in the intervention group__ (and its 95% confidence interval) is based on the assumed risk in the comparison group and the __relative effect__ of the intervention (and its 95% CI)

CI: confidence interval; **MD:** mean difference; **RR:** risk ratio

GRADE working group grades of evidence

High certainty: we are very confident that the true effect lies close to that of the estimate of the effect

Moderate certainty: we are moderately confident in the effect estimate: the true effect is likely to be close to the estimate of the effect, but there is a possibility that it is substantially different

Low certainty: our confidence in the effect estimate is limited: the true effect may be substantially different from the estimate of the effect

Very low certainty: we have very little confidence in the effect estimate: the true effect is likely to be substantially different from the estimate of effect

[a]The performance bias were high in the studies.
[b]The direction of the effect is different as I^2>75%.
[c]The sample size was too small.
[d]None of the studies stated whether there was follow-up.

lacking in some of the included studies (Table 2), which may have contributed to the effect of exaggeration and reporting bias of selected outcomes. In addition, the confidence of the evidence varies from very low to moderate quality from the GRADE assessment (Table 4), and the main reasons for downgrading of evidence were risk of bias, inconsistency, imprecision, and publication bias. Thus, as the quality of the included RCTs varied, future larger RCTs with improved methodological quality were expected to further update the results of this systematic review and meta results.

4.4 Implications on prospective research and limitations of the present study

This study was the first systematic review and meta-analysis to summarize and evaluate the adjunctive efficacy and safety of SFI in patients with PAMIHF. Our findings suggested that SFI was safer to improve cardiac function and the total effective rate in PAMIHF. This study was designed in accordance with the high standard of methodological quality of the systematic review 2 (AMSTAR 2) by comprehensively identifying relevant literature, which improved the accuracy and clinical applicability of the systematic review.

However, there still existed limitations in this study. First, this study included 36 RCT clinical trials, most of which were small-scale clinical trials without scientific calculation before trials, and they also lacked enough follow-up time to clearly observe the long-term curative effect of SFI. Second, the quality of the part of the included studies was poor. All the studies lacked specific information about blind methods, including allocation blind, evaluation blind, or experimenter blind. Third, random grouping methods varied, few studies clearly stated that they adopted random number table method for random grouping, and most studies did not provide specific random grouping method or other methods. Fourth, the duration of treatment and the doses of SFI in the included studies were different; thus, subgroup analysis could not be performed to rule out the high heterogeneity due to unavailability of the data. In addition, due to the fact that the control group involved different conventional drug treatments, heterogeneity between studies may vary from each other. Finally, included studies in our meta-analysis were all conducted in China, which limited the generalizability of our results. Owing to the low to moderate quality of the included studies, the results should be more cautious until further rigorously trials were designed to validate the efficacy of SFI as adjuvant therapy for PAMIHF, strengthen, and update the results of the current meta-results.

In the future, the related research needs to be further improved from the following aspects: 1) the trials should be designed strictly according to the Combined Criteria for Trials Reporting (CONSORT) statements, 2) the trials should have enough follow-up time to clearly observe the long-term and short-term curative effect, 3) the sample size of the study should be large enough with scientific calculation before starting the trials, 4) there should be a clear scheme of random grouping and distribution blinding, and 5) the duration and usage of SFI should be unified to reduce the heterogeneity between studies. The curative effect and adverse reactions of SFI should be fully reported and comprehensively evaluated.

5 Conclusion

In conclusion, this meta-analysis suggested that SFI combined with conventional therapy was safer to significantly improve total effective rate and cardiac function in PAMIHF but due to very low to moderate quality of the meta-results evidence, which was mainly downgraded for small sample size and unclear risk of bias existed in selected studies; thus, high-quality-designed RCTs were also required for further confirmation on the efficacy and safety of adjunctive SFI therapy.

Data availability statement

The original contributions presented in the study are included in the article/Supplementary Material; further inquiries can be directed to the corresponding authors.

Author contributions

YW, SL, ZM, and ZL were involved in conceptualization, methodology, investigation, and writing—original draft. YW and SL helped with methodology, investigation, and formal analysis. ZM and ZL were involved in investigation, validation, data collection, and visualization. ZL, DL, and ZL performed data collection and validation. BD, DW, and WZ were involved in conceptualization, funding acquisition, supervision, writing—review and editing, and project administration. All authors contributed to the article and approved the submitted version.

Funding

This study was supported by the Department of Science and Technology of Guangdong Province (No. 2021A1515012224); clinical effect evaluation of Kuanxiong aerosol on patients with “chest tightness and pain” in emergency: an open, randomized, controlled study [HT 2020-0974(KY)]; joint project of Guangzhou City and College of Guangzhou Science and Technology Bureau (202201020296); and Special Research on Traditional Chinese Medicine Science and Technology of Traditional Chinese Medicine in Guangdong Province (YN2019MJ11).

Conflict of interest

The authors declare that the research was conducted in the absence of any commercial or financial relationships that could be construed as a potential conflict of interest.

Publisher's note

All claims expressed in this article are solely those of the authors and do not necessarily represent those of their affiliated organizations, or those of the publisher, the editors, and the reviewers. Any product that may be evaluated in this article, or claim that may be made by its manufacturer, is not guaranteed or endorsed by the publisher.

Supplementary material

The Supplementary Material for this article can be found online at: https://www.frontiersin.org/articles/10.3389/fphar.2022.1027131/full#supplementary-material

References

Arrigo, M., Jessup, M., Mullens, W., Reza, N., Shah, A. M., Sliwa, K., et al. (2020). Acute heart failure. *Nat. Rev. Dis. Prim.* 6 (1), 16. doi:10.1038/s41572-020-0151-7

Bahit, M. C., Kochar, A., and Granger, C. B. (2018). Post-myocardial infarction heart failure. *JACC. Heart Fail.* 6 (3), 179–186. doi:10.1016/j.jchf.2017.09.015

Chen, G. (1995). *Modern emergency medicine*. Guangdong: Guangdong Science and Technology Press.

Chen, H. (1996). *Internal medicine people's*. Beijing: Health Publishing House.

Chen, R. J., Rui, Q. L., Wang, Q., Tian, F., Wu, J., and Kong, X. Q. (2020). Shenfu injection attenuates lipopolysaccharide-induced myocardial inflammation and apoptosis in rats. *Chin. J. Nat. Med.* 18 (3), 226–233. doi:10.1016/S1875-5364(20)30025-X

Chen, Z. (2008). *Internal medicine people's*. Beijing: Health Publishing House.

Fen, J., Liang, M., Wang, Y., et al. (2019). Efficacy analysis of Shenfu injection combined with enoxaparin sodium in the treatment of acute myocardial infarction complicated with heart failure. *Drug Eval. Res.* 42 (10), 2057–2061. doi:10.7501/j.issn.1674-6376.2019.10.028

Gao, R. (2001). Guidelines for the diagnosis and treatment of acute myocardial infarction. *China Circ. Mag.* (06), 407–422.

Gao, S., Li, L., Li, L., Ni, J., Guo, R., Mao, J., et al. (2019). Effects of the combination of tanshinone IIA and puerarin on cardiac function and inflammatory response in myocardial ischemia mice. *J. Mol. Cell. Cardiol.* 137, 59–70. doi:10.1016/j.yjmcc.2019.09.012

Gao, W., Qi, L. W., Liu, C. C., Wang, R., Li, P., and Yang, H. (2016). An improved method for the determination of 5-hydroxymethylfurfural in Shenfu injection by direct analysis in real time-quadrupole time-of-flight mass spectrometry. *Drug Test. Anal.* 8 (7), 738–743. doi:10.1002/dta.1838

Guidelines for the diagnosis Guidelines for the diagnosis and treatment of acute ST-segment elevation myocardial infarction. *Chin. J. Cardiovasc. Dis.*, 2010(08), 675–690.

Guidelines for the diagnosis Guidelines for the diagnosis and treatment of acute ST-segment elevation myocardial infarction. *Chin. J. Cardiovasc. Dis.*, 2015, 43 (05), 380–393.

Guo, L., Wang, Q., Cao, Y., Liu, J. W., Wu, C. H., et al. (2013). Shenfu injection in the treatment of 30 cases of acute left heart failure after acute myocardial infarction. *Mod. distance Educ. traditional Chin. Med. China* 11 (18), 47. doi:10.3969/j.issn.1672—2779.2013.18.034

Guo, M. (2014). Observation of curative effect of Shenfu injection in adjuvant treatment of ST-segment elevation acute myocardial infarction complicated with acute left heart failure.

Guo, Q., Fang, B., Chen, H., Tian, Y., Zhang, Y. L., Chen, B. J., et al. (2010). "Clinical observation on Shenfu injection in treating 35 cases of heart failure after acute myocardial infarction," in 2010 National Conference on Critical Illness and Emergency Medicine of Integrated Traditional Chinese and Western Medicine.

He, J., and Sheng, G. (2014). *Clinical analysis of Shenfu injection in the treatment of acute myocardial infarction complicated with heart failure*. Beijing: Chinese Modern Doctor.

Li, J., Yu, W., Zhang, W., et al. (2013). Clinical application progress of Shenfu injection in the treatment of cardiovascular and cerebrovascular diseases. *Med. Rev.* 19 (15), 2808–2810. doi:10.3969/j.issn.1006-2084.2013.15.039

Li, P., Lv, B., Jiang, X., Wang, T., Ma, X., Chang, N., et al. (2016). Identification of NF-κB inhibitors following Shenfu injection and bioactivity-integrated UPLC/Q-TOF-MS and screening for related anti-inflammatory targets *in vitro* and *in silico*. *J. Ethnopharmacol.* 194, 658–667. doi:10.1016/j.jep.2016.10.052

Li, R., and Hou, A. (2017). Clinical study on Shenfu injection in treating acute myocardial infarction combined with pump failure. *Clin. J. Traditional Chin. Med.* 29 (11), 1874–1877. doi:10.16448/j.cjtcm.2017.0622

Li, S. (2016). *Clinical study on Shenfu injection in the treatment of acute myocardial infarction complicated with cardiogenic shock after PCI*. Hubei: Asia Pacific Traditional Medicine.

Li, W. (2015). *Shenfu injection in the treatment of acute myocardial infarction and heart failure*. Zhangjiakou: Xinglin Traditional Chinese Medicine.

Li, X., and Chen, Y. (2016). The effect of Shenfu injection on improving cardiac function in patients with acute myocardial infarction complicated with heart failure and its curative effect analysis. *Med. Rev.* 22 (15), 3108–3111. doi:10.3969/j.issn.1006-2084.2016.15.057

Li, X. (2017). The use of traditional Chinese medicine injection in cardiovascular and cerebrovascular drugs. *Clin. Med. Res. Pract.* 2 (21), 102–103.

Li, Y., Chen, Y., Yang, L., Wu, R. Y., Yan, X. J., Nie, P., et al. (2019). Research progress on the material basis and mechanism of action of Shenfu injection in the treatment of cardiovascular and cerebrovascular diseases. *New Chin. Med. Clin. Pharmacol.* 30 (04), 499–503. doi:10.19378/j.issn.1003-9783.2019.04.017

Li, Z., Feng, X. B., Tang, S. L., and Wang, S. F. (2006). Pathways of mercury emissions to atmosphere from closed municipal landfills. *New Chin. Med.* 27 (06), 19–23.

Li, Z., Hu, Q., Mao, Y., Li, H. J., et al. (2010). Effect of Shenfu injection combined with conventional therapy on heart failure in elderly patients with myocardial infarction. *Chin. J. Integr. Med.* 30 (09), 996–998.

Luo, Y., and Lin, X. (2013). Effects of recombinant human brain natriuretic peptide on heart rate variability in patients with acute decompensated heart failure. *J. Pract. Med.* 29 (02), 291–293. doi:10.3969/j.issn.1006-5725.2013.02.052

Meng, F. (2014). Clinical observation of Shenfu injection in the treatment of acute extensive anterior myocardial infarction complicated with left heart failure. *Chin. Med. Emerg.* 23 (11), 2002–2031. doi:10.3969/j.issn.1004-745X.2014.11.015

Mo, C., and Zhao, K. (2002). Shenfu injection adjuvant treatment of 36 cases of acute myocardial infarction complicated with heart failure. *Chin. J. Integr. Med.* (11), 812.

Randhawa, M. S., Dhillon, A. S., and Desai, M. Y. (2014). Incremental use of biomarkers and electrocardiogram in differentiating takotsubo cardiomyopathy from acute myocardial infarction: A potential way to go. *J. Card. Fail.* 20 (4), 292–293. doi:10.1016/j.cardfail.2014.01.015

Sandoval, Y., and Jaffe, A. S. (2019). Type 2 myocardial infarction: JACC review topic of the week. *J. Am. Coll. Cardiol.* 73 (14), 1846–1860. doi:10.1016/j.jacc.2019.02.018

Shao, F., Li, H., Li, D., and Li, C. (2020). Effects of Shenfu injection on survival and neurological outcome after out-of-hospital cardiac arrest: A randomised controlled trial. *Resuscitation* 150, 139–144. doi:10.1016/j.resuscitation.2019.11.010

Song, Q., Li, Z., Zhang, X., Cheng, S., et al. (2002). Clinical observation of Shenfu injection in the treatment of 48 cases of acute myocardial infarction complicated with heart failure. *J. Jining Med. Coll.* (01), 53–54.

Song, Y., and Jin, L. (2021). Research progress on predictors of heart failure after acute myocardial infarction. *Chin. J. Evid. Based Cardiovasc Med. Oct.* 13 (10), 2021. doi:10.3969/j.issn.1674-4055.2021.10.34

Su, W., Hong, F., and Yang, S. (2018). New progress of Shenfu injection on prevention and treatment of cardiovascular and cerebrovascular diseases. *J. Nanchang Univ. Med. Ed.* 58 (05), 85–89. doi:10.13764/j.cnki.ncdm.2018.05.019

Sun, J., and Fu, X. (2004). Diagnosis and treatment of acute myocardial infarction with ST segment elevation. *Clin. meta* (03), 131–134.

Sun, Y. (2016). Clinical treatment and efficacy evaluation of recombinant human brain natriuretic peptide combined with Shenfu injection in the treatment of acute myocardial infarction with acute heart failure. *Contemp. Med.* 22 (15), 144–145. doi:10.3969/j.issn.1009-4393.2016.15.097

Wang, C. L., and Qin, L. J. (2017). Clinical observation of Shenfu injection combined with continuous intravenous injection of dopamine in the treatment of acute myocardial infarction combined with pump failure after PCI. *J. Guangxi Univ. Traditional Chin. Med.* 20 (02), 7–9.

Wang, H., Zhang, F., Zhang, L., Li, T. T., Zhang, M. L., et al. (2018). Efficacy evaluation of recombinant human brain natriuretic peptide combined with Shenfu injection in the treatment of acute myocardial infarction with acute heart failure. *J. Bengbu Med. Coll.* 43 (01), 59–64. doi:10.13898/j.cnki.issn.1000-2200.2018.01.018

Wang, J. (2002). *Internal medicine people's*. Beijing: Health Publishing House.

Wang, J., Wang, X., Wan, W., Guo, Y., Cui, Y., Liu, W., et al. (2021). Effects of Shenfu injection on myocardial adenosine receptors in rats with myocardial ischemia-reperfusion postconditioning. *Hum. Exp. Toxicol.* 40 (12), S300–S309. doi:10.1177/09603271211041668

Wang, S., Liu, G., Chen, L., Xu, X., Jia, T., Zhu, C., et al. (2022). Effects of Shenfu injection on sublingual microcirculation in septic shock patients: A randomized controlled trial. *Shock* 58, 196–203. doi:10.1097/SHK.0000000000001975

Wang, S. (2021). The effect of Shenfu injection in adjuvant treatment of acute myocardial infarction complicated with heart failure. *Inn. Mong. Tradit. Chin. Med.* 40 (04), 127–129.

Wang, W., Jin, D., Zhang, Y., Zhao, J., Zhang, N., Wang, P. F., et al. (2017). Clinical study of simvastatin combined with Shenfu injection in the treatment of heart failure in patients with acute myocardial infarction complicated by diabetes. *Liaoning J. Traditional Chin. Med.* 44 (04), 791–793.

Wang, X., Miao, H., Yan, Y., Guo, R., Gong, W., He, Y., et al. (2021). Effect of Shenfu injection on reperfusion injury in patients undergoing primary percutaneous coronary intervention for st segment elevation myocardial infarction: A pilot randomized clinical trial. *Front. Cardiovasc. Med.* 8, 736526. doi:10.3389/fcvm.2021.736526

Wang, Y. (2020). Effects of Shenfu injection + freeze-dried recombinant human brain natriuretic peptide on cardiac function in patients with acute myocardial infarction and acute heart failure. *Heilongjiang Med. Sci.*

Wang, Y. (2018). Short-term efficacy and safety observation of recombinant human brain natriuretic peptide combined with Shenfu injection in the treatment of acute myocardial infarction complicated with heart failure. *World J. Integr. Med.* 13 (01), 108–111.

Wenwu, Z. (2000). *Emergency medicine people's*. Beijing: Health Publishing House.

Xu, P., Zhang, W. Q., Xie, J., Wen, Y. S., Zhang, G. X., and Lu, S. Q. (2020). Shenfu injection prevents sepsis-induced myocardial injury by inhibiting mitochondrial apoptosis. *J. Ethnopharmacol.* 261, 113068. doi:10.1016/j.jep.2020.113068

Xu, Q., Guo, Z., Chan, C. O., Mok, D. K. W., Yi, L. Z., and Chau, F. T. (2015). Identifying bioactive components in natural products through chromatographic fingerprint. *Anal. Chim. Acta* 13 (18), 45–55. doi:10.1016/j.aca.2015.02.030

Yan, H., Hu, Z., and Xu, G. (2017). Effects of Shenfu injection on left ventricular remodeling and cardiac function in patients with early acute myocardial infarction. *J. Mod. Integr. Med.* 26 (01), 52–54. doi:10.3969/j.issn.1008-8849.2017.01.017

Yang, H., Liu, L., Gao, W., Liu, K., Qi, L. W., and Li, P. (2014). Direct and comprehensive analysis of ginsenosides and diterpene alkaloids in Shenfu injection by combinatory liquid chromatography-mass spectrometric techniques. *J. Pharm. Biomed. Anal.* 92, 13–21. doi:10.1016/j.jpba.2013.12.041

You, S., and Wang, Y. (2019). Curative effect of Shenfu injection on acute myocardial infarction complicated with acute heart failure and its effect on hemorheology and neuroendocrine hormones. *Huaxia Med.* 32 (01), 53–57. doi:10.19296/j.cnki.l008-2409.2019-01-015

Zeng, Y. (2005). Shenfu injection in adjuvant treatment of 54 cases of acute myocardial infarction complicated with heart failure. *Chin. J. Pract. Rural Dr.* (01), 31–32.

Zhang, D., Wang, Y., Qiu, Y., Hu, B., Hu, T., Liu, S. T., et al. (2012). Study on the treatment of acute myocardial infarction complicated with heart failure by Shenfu injection. *Liaoning J. Traditional Chin. Med.* 39 (11), 2225–2227.

Zhang, H. (2011). Observation on the curative effect of Shenfu injection in the treatment of heart failure after acute myocardial infarction. *Chin. Folk. Med.* 20 (05), 75.

Zhang, Q., Li, C., Shao, F., Zhao, L., Wang, M., and Fang, Y. (2017). Efficacy and safety of combination therapy of Shenfu injection and postresuscitation bundle in patients with Return of spontaneous circulation after in-hospital cardiac arrest: A randomized, assessor-blinded, controlled trial. *Crit. Care Med.* 45 (10), 1587–1595. doi:10.1097/CCM.0000000000002570

Zhang, X., Wu, Y., Huang, W., Zhu, L. R., Li, J., et al. (2018). Effects of Shenfu injection on the levels of inflammatory factors in patients with acute myocardial infarction and heart failure. *Smart health* 4 (12), 123–124.

Zhang, Y., Cheng, R., Shang, Y., Shang, Y. D., Qu, X. Y., Wang, T. T., et al. (2019). Observation of Shenfu injection in the treatment of acute myocardial infarction complicated with heart failure. *Chin. Med. Emergencies*. doi:10.3969/j.issn.1004-745X.2019.02.037

Zhang, Y. (2020). Effect of recombinant human brain natriuretic peptide combined with Shenfu injection in the treatment of acute myocardial infarction with acute heart failure. *Chin. J. Misdiagnosis* 15 (02), 61–62.

Zhang, Z., and Zhang, Y. (2018). Effects of Shenfu injection combined with PCI on cardiac function and prognosis in patients with acute myocardial infarction complicated with cardiac insufficiency. *Clin. Med. Res. Pract.* 3 (29), 134–136.

Zhao, J., Zhao, Q., and Wu, T. (2016). Efficacy evaluation of recombinant human brain natriuretic peptide combined with Shenfu in the treatment of acute myocardial infarction complicated with pump failure. *J. Mod. Integr. Med.* 25 (13), 1413–1416. doi:10.3969/j.issn.1008-8849.2016.13.015

Zhao, M. (2018). To observe the long-term clinical efficacy of Shenmai injection in the treatment of patients with heart failure after acute myocardial infarction. *Health big Vis.* (1), 35–36.

Zhao, S. (2017). Effect of Shenfu injection combined with non-invasive positive pressure ventilation on patients with acute ST-segment elevation myocardial infarction complicated with cardiogenic shock. *Henan Med. Res.* 26 (08), 1430–1431. doi:10.3969/j.issn.1004-437X.2017.08.045

Zhi-Qing, X., Jing, H., Ying, H., Zhang, D. F., et al. (2011). Observation on the curative effect of Shenfu injection in the treatment of acute left heart failure after acute myocardial infarction. *Chin. J. Integr. Traditional Chin. West. Med. First Aid* 18 (5), 287–289. doi:10.3969/j.issn.1008—9691.2011.05.012

Zong, B., Wang, H., and Zong, X. (2014). Clinical study of Shenfu injection in the treatment of acute myocardial infarction in patients with heart failure after emergency PCI. *Chin. J. Traditional Chin. Med.* 29 (11), 3640–3642.

Zou, Y. (2013). *Clinical analysis of Shenfu injection in the treatment of acute myocardial infarction complicated with heart failure*. Chinese Medicine Guide.

frontiers | Frontiers in Pharmacology

TYPE Original Research
PUBLISHED 09 January 2023
DOI 10.3389/fphar.2022.1103557

OPEN ACCESS

EDITED BY
Rong Lu,
Shanghai University of Traditional Chinese Medicine, China

REVIEWED BY
Da-Zhuo Shi,
Xiyuan Hospital, China Academy of Chinese Medical Sciences, China
Shuzhen Guo,
Beijing University of Chinese Medicine, China

*CORRESPONDENCE
Chao Li,
lichao71795@hotmail.com

†These authors have contributed equally to this work and share first authorship

SPECIALTY SECTION
This article was submitted to Ethnopharmacology, a section of the journal Frontiers in Pharmacology

RECEIVED 20 November 2022
ACCEPTED 29 December 2022
PUBLISHED 09 January 2023

CITATION
Zhang M-X, Huang X-Y, Song Y, Xu W-L, Li Y-L and Li C (2023), *Astragalus propinquus* schischkin and *Salvia miltiorrhiza* bunge promote angiogenesis to treat myocardial ischemia *via* Ang-1/Tie-2/FAK pathway.
Front. Pharmacol. 13:1103557.
doi: 10.3389/fphar.2022.1103557

Astragalus propinquus schischkin and *Salvia miltiorrhiza* bunge promote angiogenesis to treat myocardial ischemia *via* Ang-1/Tie-2/FAK pathway

Mu-Xin Zhang[1†], Xue-Ying Huang[2†], Yu Song[3], Wan-Li Xu[4], Yun-Lun Li[3] and Chao Li[3*]

[1]First Clinical Medical College, Shandong University of Traditional Chinese Medicine, Jinan, China, [2]College of Pharmacy, Shandong University of Traditional Chinese Medicine, Jinan, China, [3]Innovative Institute of Chinese Medicine and Pharmacy, Shandong University of Traditional Chinese Medicine, Jinan, China, [4]College of Traditional Chinese Medicine, Shandong University of Traditional Chinese Medicine, Jinan, China

Astragalus propinquus Schischkin and *Salvia miltiorrhiza* Bunge (AS) have been clinically used as adjunctive drugs in the treatment of myocardial ischemia (MI). However, the effect and mechanism of AS on MI have yet to be fully recognized. Here, we explored the cardioprotective effect of their combined use, and the mechanism of promoting angiogenesis through pericyte recruitment. Our data revealed that AS reduced MI and protects cardiac function. AS-treated MI mice exhibited reduced ST-segment displacement and repolarization time, increased ejection fraction, and less BNP and NT-proBNP expression. Pathological studies showed that, AS reduced the area of infarcted myocardium and slowed down the progress of cardiac remodelling and fibrosis. In addition, AS increased the content of platelet-derived growth factor receptors β (PDGFR-β), platelet endothelial cell adhesion molecule-1 (CD31) and angiogenesis-related proteins including vascular endothelial cadherin (VE-cadherin), Vascular Endothelial Growth Factor (VEGF) and transforming growth factor β (TGF-β). Moreover, these botanical drugs upregulated the expression of Angiopoietin-1 (Ang-1), phosphorylated angiopoietin-1 receptor (p-Tie-2), focal adhesion kinase (FAK) and growth factor receptor bound protein 7 (GRB7), indicating that the cardioprotection-related angiogenesis effect was related to pericyte recruitment, which may be through Ang-1/Tie-2/FAK pathway. In summary, AS can treat MI by protecting cardiac function, attenuating cardiac pathological changes, and hindering the progression of heart failure, which is related to angiogenesis after pericyte recruitment. Therefore, AS at a certain dose can be a promising treatment for MI with broad application prospects.

KEYWORDS

angiogenesis, myocardial ischemia, pericyte recruitment, astragalus propinquus, Salvia miltiorrhiza

1 Introduction

MI, a disease of the blood vessels that supply the heart muscle, occurs when blood flow through one or more of coronary arteries is decreased, preventing the heart muscle from receiving enough oxygen (Wang et al., 2013). According to the World Health Organization (WHO), MI is one of the top three causes of years of life lost due to premature death globally. Patients with MI should have access to appropriate technology and medication. However, the most widely used therapy for

restoring blood supply after MI is also facing defects. The incidence of insufficient reflow in infarcted area after percutaneous coronary intervention (PCI) was 46%, and the MI of patients receiving coronary artery bypass graft (CABG) was only reduced by 30%. (Qiu et al., 2017; Doenst et al., 2019). Therefore, angiogenesis is a promising therapeutic strategy to partially restore myocardial perfusion.

Angiogenesis, the derivation of new capillaries from existing capillary venules, has the ability to improve blood supply to ischemic areas after MI (Fan et al., 2006; Bu et al., 2020). This therapeutic effect is inseparable from the action of pericytes, the elongated supporting cells of the blood vessel wall (Armulik et al., 2005). Under normal physiological conditions, pericytes are distributed along endothelial cells and inhibit excessive angiogenesis (Tang et al., 2017). Following MI, the myocardium is affected by hypoxia and glucose deprivation, resulting in the release of pericytes from the vessel wall (Teichert et al., 2017). Endothelial cells isolated from pericytes have the ability to proliferate and migrate under the action of VEGF-A from pericytes, thereby enabling the generation of new capillaries (Franco et al., 2011). In addition to the early stages of angiogenesis, pericyte recruitment is also involved in maintaining the stability of newly formed blood vessels. After a certain degree of angiogenesis, pericytes return to the vicinity of endothelial cells to cover the new blood vessels, thereby stabilizing the new blood vessels and promoting their maturation (Dobaczewski et al., 2004; Stratman et al., 2010). Futhermore, pericytes derived TGF-β to inhibit the immortal proliferation of endothelial cells (Winkler et al., 2010). Therefore, therapeutic angiogenesis plays a crucial role in the treatment of MI. Unfortunately, there is a lack of cost-effective, controllable, and reproducible methods to promote angiogenesis by modulating pericyte recruitment. In this context, botanical drugs may be a proven complementary and alternative therapy.

Botanical drugs have been used clinically for more than 5,000 years with a systematic theoretical basis that guarantees their efficacy. Notably, a growing number of studies have shown that many natural medicines are powerful inducers of angiogenesis (Bernas, 2003). *Astragalus propinquus* Schischkin [*Leguminosae*; Astragalus membranaceus radix et rhizoma] and *Salvia miltiorrhiza* Bunge [*Lamiaceae*; Salviae miltiorrhizae radix et rhizoma] are both one of the most popular botanical drugs in the world, they can also be used as a drug pair to improve blood circulation, protect ischemia-reperfusion injury, and improve cardiac function in mice with MI (Li et al., 2008; Ma et al., 2013; Fu et al., 2014; Li et al., 2018). Accumulating evidence suggests that *Astragalus propinquus* Schischkin and *Salvia miltiorrhiza* Bunge can play a protective role against MI. However, their combined effect of promoting angiogenesis by regulating pericyte recruitment is yet to be elucidated. In this paper, a left anterior descending coronary artery ligation (LAD)-induced MI mouse model was employed and treated with *Astragalus propinquus* Schischkin and *Salvia miltiorrhiza* Bunge. The purpose of this study was to explore the effect of the above drug pair on protecting cardiac function and angiogenesis after MI, and to elucidate the relationship with pericyte recruitment in a targeted manner.

2 Materials and methods

2.1 Preparation of AS

Astragalus propinquus Schischkin (HuangQi in Chinese pharmacopoeia, family *Leguminosae*) granules and *Salvia miltiorrhiza* Bunge (DanShen in Chinese pharmacopoeia, family *Lamiaceae*) granules were purchased from Beijing Kangrentang Pharmaceutical Co., Ltd. (Beijing, China). According to the manufacturing standard of Chinese formula granules, 2500 g *Astragalus propinquus* Schischkin was boiled with water, filtered and concentrated into clear extract (the extraction rate of dry extract ranged from 22% to 40%). An appropriate amount of excipients was added. These extracts were dried (or dried, crushed), mixed, granulated, and made into 1000 g. 2000 g *Salvia miltiorrhiza* Bunge was boiled with water, filtered and concentrated into clear extract (the extraction rate of dry extract ranged from 31% to 49%). An appropriate amount of excipients was added. These extracts were dried (or dried, crushed), mixed, granulated, and made into 1000 g. Therefore, 1 g of *Astragalus propinquus* Schischkin formula granules are equivalent to 2.5 g of the botanical drugs, and 1 g of *Salvia miltiorrhiza* Bunge formula granules are equivalent to 2 g of the botanical drugs. According to the drug instructions and Chinese Pharmacopoeia, the chemical profiles of *Astragalus propinquus* Schischkin and *Salvia miltiorrhiza* Bunge were attached to the supplementary materials. The above granules were dissolved in .9% NaCl and stored at 4° in the dark.

2.2 Animals

7-week-old male C57BL/6J normal and MI mice were purchased from Vital River Laboratory Animal Technology Co. (Beijing, China) and used in the following experiments. The animal experiments were performed in accordance with the Guide for the Care and Use of Laboratory Animals (published by the US National Institutes of Health) and were approved by the Institutional Animal Care and Research Advisory Committee of the Shandong University of Traditional Chinese Medicine. All mice were housed under SPF laboratory conditions with water and food temperature of 22°C ± 2°C and maintained a 12-h light/dark cycle throughout the experiment. The above mice were divided into 3 groups, (n = 8 rats per group), as follows: 1) Control group: Normal mice received LAD sham operation and were gavaged with .9% NaCl (2 mL kg^{-1}); 2) Model group: MI mice were gavaged with .9% NaCl (2 mL kg^{-1}); 3) AS group: MI mice were gavaged with *Astragalus propinquus* Schischkin and *Salvia miltiorrhiza* Bunge decoction extract (2 mL·kg-1), which is equivalent to 1.875 g/kg of *Astragalus propinquus* Schischkin and .9375 g/kg of *Salvia miltiorrhiza* Bunge. After 6 weeks of intragastric administration, 3 groups of mice were used for subsequent experiments.

2.3 ECG and ultrasonic cardiogram

Mice were anesthetized by inhalation of isoflurane at an initial infusion concentration of 2%, increased to 5% after 3 min, induction of anesthesia was completed within 5 min, and maintained at a concentration of 1% thereafter. The limbs and head of mice were fixed on a wooden mouse board in a supine position, and then four small metal syringe needles were inserted subcutaneously into the limbs. The ECG changes in the limbs were recorded with RM6240E multichannel physiological signal acquisition system (Shanghai, Xinruan, China), recorded from lead I. M-mode images of the left ventricle were obtained by a

small animal ultrasound instrument (Xuzhou China) to determine percentage ejection fraction (EF), short axis shortening of the left heart asphyxia (FS), left ventricular end diastolic volume (LVvol; d), left ventricular end systolic volume (LVvol; s), left asphyxiating end diastolic diameter (LVID; d) and left ventricular end systolic diameter (LVID; s).

2.4 TTC staining

The mouse heart tissues were frozen at—80°C for 10 min, and then cut into five 2 mm thick slices along the transverse axis. The heart slices were immersed in 1% TTC solution and dyed at 37°C for half an hour. Next, the hearts were placed in order and photographed. The normal heart tissues were red, and the infarcted areas were grayish white. ImageJ software was used to calculate the area of myocardial infarction.

2.5 H&E staining

Mouse heart tissue was stored at −20°C for 30 min and cut into 2 mm thick sections, which were then stained with H&E. The staining results were observed under a microscope to detect ischemic myocardium.

2.6 Masson staining

Mouse heart tissue was fixed with 3% glutaraldehyde fixative (pH 7.2–7.4) for 24 h, and the aortic sinus was cut into 5 μm serial paraffin sections. Masson (Nanjing Jiancheng Technology Co., Ltd., Nanjing, China) was performed to determine collagen fiber content. The staining results were observed under a fluorescence microscope for pathological analysis and analysed semi-quantitatively based on the collagen volume fraction (CVF, percentage of collagen-positive blue area to total tissue area) using ImageJ software.

2.7 Immunohistochemical (IHC) staining

Mouse heart tissues were fixed in 4% paraformaldehyde and embedded in paraffin to cut into 5 μm sections. The sections were blocked in blocking buffer at room temperature and then incubated with CD31: (1:100, ab24590, Abcam), PDGFR-β: (1:100, #3169, Cell Signaling) at 4° for 12 h according to the instructions. After washing the sample sections, the sections were incubated with the secondary antibody for 1.5 h at room temperature. The staining results were observed under a microscope to explore the recruitment of pericytes around endothelial cells.

2.8 Immunofluorescence (IF) staining

The mouse heart sections were first treated with EDTA Antigen Retrieval Solution (C1033, Solarbio) according to the instructions, and incubated with .5% Triton X-100 for 30 min. After being blocked with 3% BSA for 30 min, the mouse heart slices were incubated with FAK (1:500, 66258-1-lg, Proteintech) at 4°C overnight. CoraLite488 combined Goat Anti Mouse IgG (H + L) (1:500, SA00013-1, Proteintech) was used as a secondary antibody to incubate the slices in dark at room temperature for 50 min. The slices were dropped with DAPI containing anti fluorescence attenuation sealing agent (S2110, Solarbio), and visualized using a fluorescent microscope.

2.9 Enzyme-linked immunosorbent assay (ELISA)

Blood samples were collected and left to stand for 30 min, then were centrifuge for 15 min at 3000r at 4°C. BNP, NT-ProBNP, Ang-1, Ang-2 and Tie-2 in the supernatant was measured using the Mouse ELISA Kit (Elabscience, Wuhan, China). The absorbance was recorded at 450 nm with a plate reader. Based on the standard curve OB values of the samples, the corresponding BNP, NT-ProBNP, Ang-1, Ang-2 and Tie-2 were calculated.

2.10 Western blotting

The mice myocardial tissues were lysed with RIPA buffer (R0020, Solarbio), with protease inhibitor (.1% phenylmethanesulfonyl fluoride (PMSF) (P0100, Solarbio)). Protein concentrations were measured using a BCA protein assay kit (Interchim, Montluçon, France). The proteins were separated by 10% SDS-polyacrylamide gel electrophoresis (SDS-PAGE), and the resulting protein bands were transferred onto PVDF membranes. After blocking with 5% fat-free dry milk in Tris-buffered saline containing .1% Tween-20 for 2 h, the membranes were incubated with the following primary antibodies overnight at 4°C: Collagen 1 (1:1000, #72026, Cell Signaling), matrix metalloproteinase-9 (MMP9) (1:1000, 10375-2-AP, Proteintech), PDGFR-β (1:1000, 13449-1-ap, Proteintech), NG2 (1:1000, #4226, Cell Signaling), VE-cadherin (1:1000, ab33168, Abcam), VEGF (1:1000, 19003-1-ap, Proteintech), TGF-β (1:1000, 21898-1-ap, Proteintech), Ang-1 (1:1000, ab183701, Abcam), Ang-2 (1:1000, ab155106, Abcam), phospho-Tie-2 (1:1000, #4226, Cell Signaling), GRB7 (1:1000, 10045-1-Ig, Proteintech), FAK (1:1000, ab40794, Abcam) and β-actin (1:1000, 66009-1-lg, Proteintech). Then, the membranes were incubated with horseradish peroxidase-conjugated secondary antibodies at room temperature for 1 h. The protein bands were visualized using an ECL Substrate (Thermo Fisher Scientific), and the quantification of the average densities of the protein bands was performed using the ImageJ software.

2.11 RNA isolation and quantitative-PCR (q-PCR)

The total RNA in mouse heart tissues was extracted with TriZol. After the concentration was determined, the RNA was reverse transcribed into cDNA using SPARKscript II RT Plus Kit (AG0304, SparkJade). SYBR Green qPCR Mix (Ah0104, SparkJade) was used to amplify the target gene, and the reaction system was 10 μL. Roche LightCycle 480II was used for qPCR experiments. The

10.3389/fphar.2022.1103557

TABLE 1 The primer sequences for Collagen 1, MMP9 and β-actin.

Gene of interest	Species	Sequence (5′-3′)
Collagen 1	Mouse	Forward: CCCTGGTCCCTCTGGAAATG
		Reverse: GGACCTTTGCCCCCTTCTTT
MMP9	Mouse	Forward: TAGATCATTCCAGCGTGCCG
		Reverse: GCTTAGAGCCACGACCATACA
β-actin	Mouse	Forward: GGCTGTATTCCCCTCCATCG
		Reverse: CCAGTTGGTAACAATGCC ATGT

primer sequences for Collagen 1, MMP9 and β-actin were listed in Table 1.

2.12 Statistical analysis

Data from at least three independent experiments were analyzed using Graphpad 7 software (GraphPad Software, La Jolla, CA, United States) and are expressed as the mean ± standard deviation (SD). Two groups of data were compared using an independent samples *t*-test, while multiple groups were compared using one-way ANOVA with Bonferroni's multiple comparison *post hoc* test. *p*-values <.05 were considered statistically significant.

3 Results

3.1 AS reduces MI and protects cardiac function

At baseline, there was no significant difference in ECG between model group and AS group, whereas ST segment of the two groups was higher than that of the control group, indicating that the MI mouse model was successfully established.

In clinical practice, electrocardiography has been used for more than a century to detect MI and drug effects (Yan et al., 2003). Therefore, we first carried out mouse ECG detection. After 6 weeks of intervention, the ECG of the model group showed the most significant ST segment shift (i.e., the magnitude of distortion) and the longest time interval for repolarization abnormalities (i.e., ST segment integration). (Figure 1A). These results suggest that MI affects cellular depolarization and repolarization processes, resulting in decreased cardiomyocyte resting potential, production of pathological ionic currents, and opening of ATP-K channels, thereby affecting T wave morphology and duration (Yan et al., 2003). In the AS group, these ischemia indicators were partially restored, suggesting that the botanical drugs could alleviate the damage caused by MI to a certain extent.

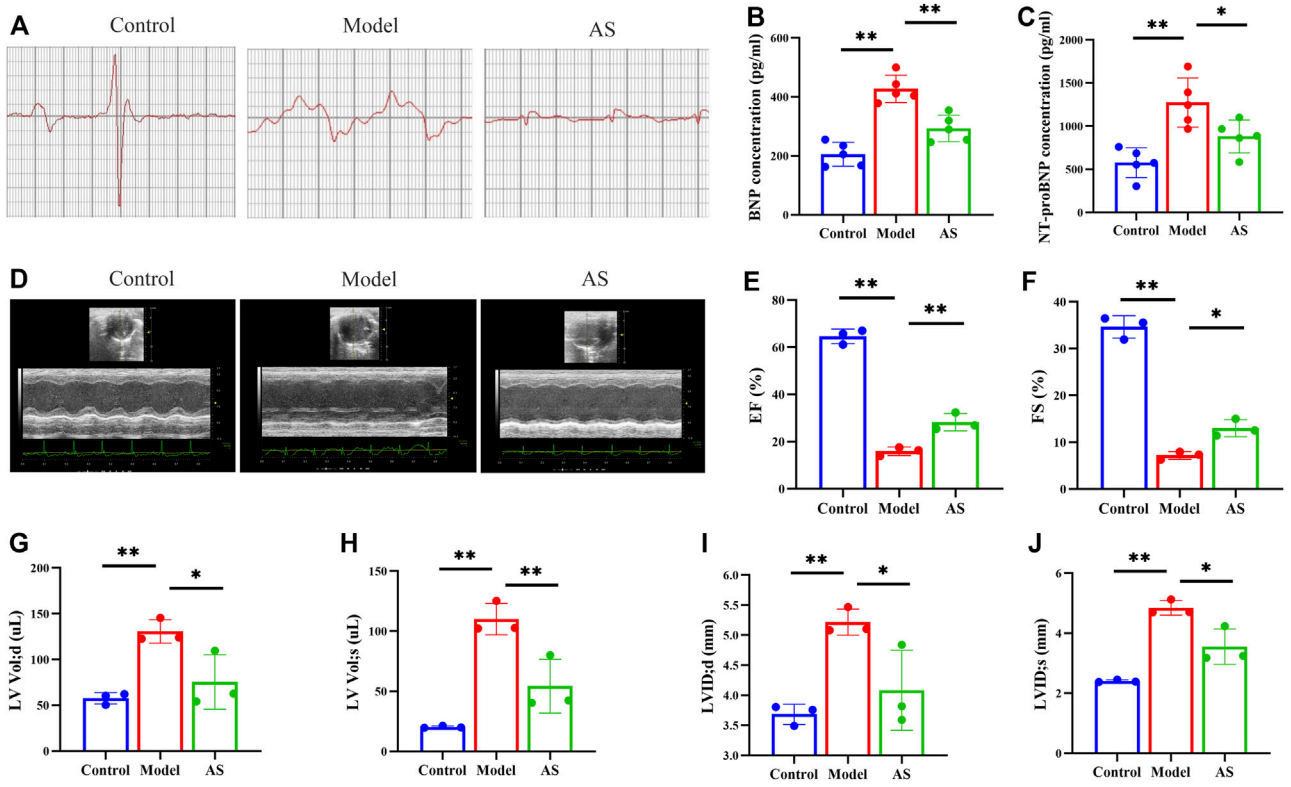

FIGURE 1
AS reduces MI and protects cardiac function. **(A)** Representative images of Mice electrocardiogram. **(B)** Quantitative analysis of BNP concentration, n = 5. **(C)** Quantitative analysis of NT-proBNP concentration, n = 5. **(D)** Representative images of mice echocardiography. **(E)** Quantitative analysis of EF (%), n = 3. **(F)** Quantitative analysis of FS (%), n = 3. **(G)** Quantitative analysis of LVVd; d (uL), n = 3. **(H)** Quantitative analysis of LVVd; s (uL), n = 3. **(I)** Quantitative analysis of LVID; d (mm), n = 3. **(J)** LVID; s (mm), n = 3. Results are expressed as mean ± SD, $^{**}p < .001$, $^{*}p < .05$.

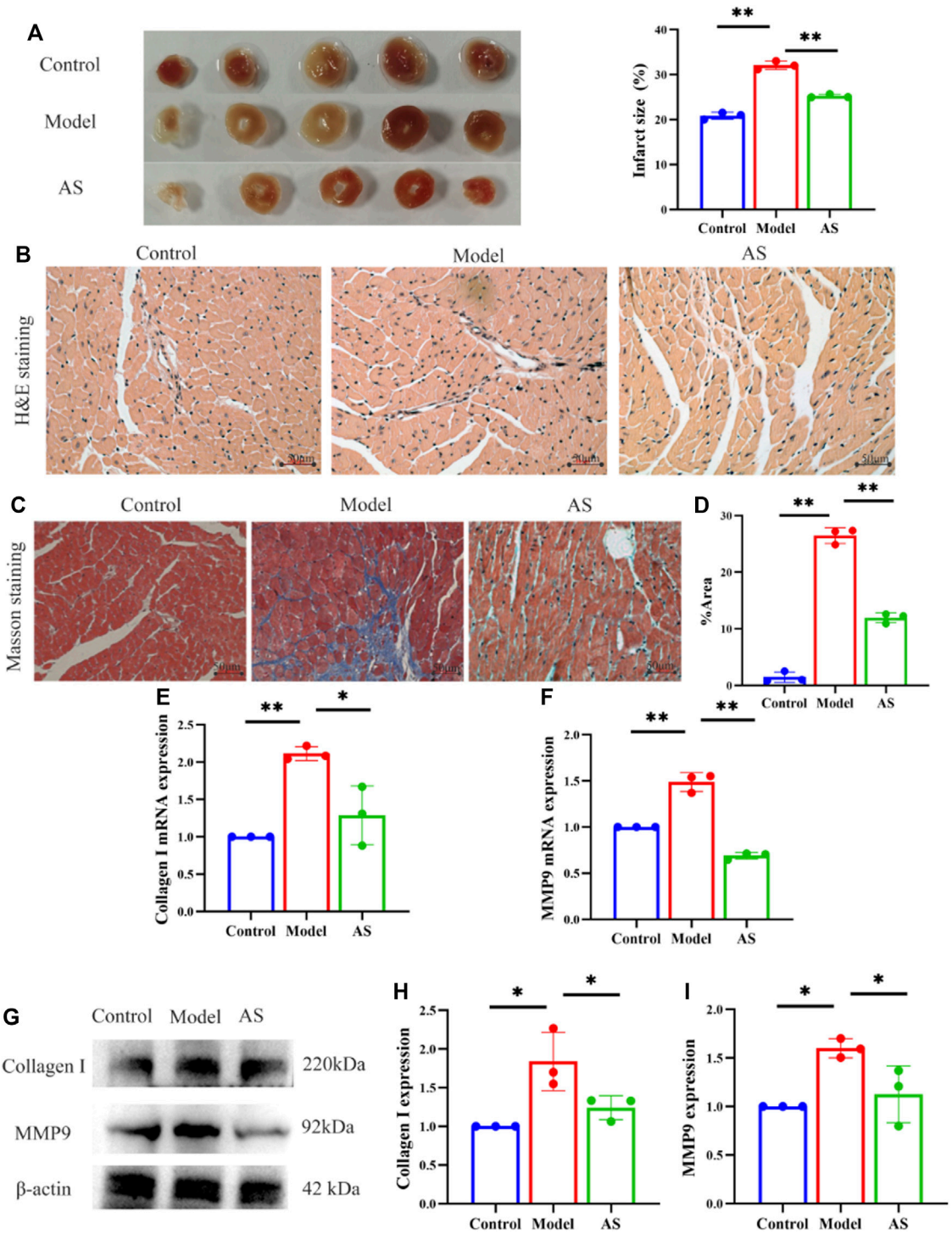

FIGURE 2
AS attenuates myocardial pathological injury. **(A)** Representative images and calculated infarct size of the myocardium of mice. **(B)** Representative images of H&E staining. **(C)** Representative images of Masson staining. **(D)** Fibrosis area as percentage, results are expressed as mean ± SD, n = 3, $^{**}p < .01$. **(E)** Quantitative analysis of Collagen I mRNA, results are expressed as mean ± SD, n = 3, $^{**}p < .01$, $^{*}p < .05$. **(F)** Quantitative analysis of MMP9 mRNA, results are expressed as mean ± SD, n = 3, $^{**}p < .01$. **(G)** Western blot analysis of Collagen I and MMP9 expression in mice. **(H)** Quantitative analysis of Collagen I, results are expressed as mean ± SD, n = 3, $^{*}p < .05$. **(I)** Quantitative analysis of MMP9, results are expressed as mean ± SD, n = 3, $^{*}p < .05$.

Then, echocardiography in short-axis M-mode mode was performed (Figure 1D). The results showed that there was improvement in EF, FS (Figures 1E, F) and significant reductions in LVVol; d, LVVol; s, LVID; d, LVID; s (Figures 1G–J) in AS mice compared to the model.

Since cardiac function was preserved after AS intervention in MI mice, the next goal was to determine whether AS could slow disease progression and delay the onset of heart failure. To accomplish this, two markers of heart failure, BNP and NT-ProBNP, were measured by ELISA.

The serum expression levels of these two indicators are of great significance, not only reflecting cardiovascular defects, but also their severity (Maries and Manitiu, 2013). Previous studies have confirmed that the levels of BNP and NT-proBNP are positively correlated with the risk of death, which can effectively evaluate the prognosis and drug treatment effects of MI mice (Nunez et al., 2008). As shown in Figures 1B, C, the levels of BNP and NT-ProBNP in control group were maintained at a low level, while those in model group were significantly increased due to ischemia. At the same time, the expressions of BNP and NT-ProBNP in AS group were lower than those in model group, indicating that the botanical drugs played a protective role.

3.2 AS attenuates myocardial pathological injury

To investigate the mitigating effect of AS on cardiac pathological changes after MI, histological staining was performed. TTC staining showed that after LAD operation, the MI area of mice increased to 31%, while after AS intervention, the index decreased to 25%. (Figure 2A).

On this basis, we observed the pathological damage of MI in mice from a more microscopic level. After HE staining of myocardial tissue under light microscope, it was found that the structure of blood vessels in the control group was normal, and the myocardial fibers were arranged neatly. In the model group, the arrangement of myocardial fibers was disordered, the vascular wall was edema, and inflammatory cell infiltration was seen around the blood vessels. Compared with the model group, the myocardial fibers in the AS group were still neatly arranged, and the vascular wall edema and inflammatory cell infiltration were reduced (Figure 2B).

In addition, Masson staining showed that the cardiomyocytes in control group were red-stained, with normal size, neat arrangement, clear structure, and almost no blue-stained collagen fibers. In the model group, the structure of myocardial cells was disordered, with extensive blue staining of collagen fibers, which was more obvious near blood vessels. And cardiomyocytes were divided into strips or islands by collagen fibers. AS treatment reduced myocardial fiber rupture and collagen deposition, resulting in a lower proportion of myocardial fibrosis than model group (Figures 2C, D).

In order to further examine the antagonistic effect of AS on myocardial fibrosis after MI, collagen 1 and MMP9 were measured from the RNA and protein layers. Collagen 1 is considered to be the decisive factor leading to myocardial fibrosis, and MMP9 has also been proved to be an important reason for extracellular matrix remodeling after MI, which are closely related to left ventricular remodeling (Garcia et al., 2005; Wang et al., 2014). Consistent with the results of cardiac staining, AS intervention can reduce the expression of collagen 1 and MMP9 induced by MI to some extent. These indicate that AS can reduce myocardial pathological damage after MI by inhibiting myocardial fibrosis (Figures 2E–I).

3.3 AS regulates pericyte recruitment and promotes angiogenesis

Whether AS can treat MI by promoting angiogenesis through pericyte recruitment? We further confirmed this by measuring the expression of NG2 and PDGFR-β, which are markers of pericytes. NG2 is expressed in microvascular pericytes in neovascularization and can mediate the communication between pericytes and endothelial cells. Therefore, NG2 is an important factor to promote endothelial cell migration and morphogenesis in the early stage of neovascularization (Fukushi et al., 2004). PDGF receptor signaling pathway plays a key role in pericytes recruitment during angiogenesis (Lindahl et al., 1997). WB results showed that in the model group, the expression of NG2 and PDGFR-β decreased. In contrast, the expression increased after AS treatment, (Figure 3A), which indicate that pericytes are recruited near endothelial cells for proliferation and migration.

After pericytes are collected around endothelial cells, they secrete VEGF to act on endothelial cells and promote the stability and maturation of new blood vessels. Pericytes and endothelial cells can also co-secrete TGF- β. In addition, VE-cadherin can maintain the adhesion between cells and the integrity of new blood vessels. As shown in Figure 3B, AS can mitigate the decline of VEGF, TGF-β and VE-cadherin caused by MI.

We further provided solid evidence through IHC. The cells stained with brownish yellow containing PDGFR-β and CD31 decreased significantly in model group, and recovered in AS group (Figures 3C, D). These evidences indicate that AS can treat MI by promoting angiogenesis through pericyte recruitment.

3.4 AS regulates Ang-1/Tie-2/FAk pathway

Since AS can promote pericyte recruitment and angiogenesis, the next goal is to determine how AS can promote angiogenesis in the heart after MI. Thus, classical angiogenic proteins, Ang-1, Ang-2 and p-Tie-2 were detected. As shown in Figure 4A, the expression of p-Tie-2 in model group was lower than that in normal group, while that in AS group was higher than that in model group. In contrast to p-Tie-2, Ang-2 was most expressed in the model group. Compared with the model group, the expression of Ang-2 in AS group was lower. Notably, the expression of Ang-1 increased after MI, and the intervention of AS can enhance this rising trend. We further explored by ELISA and got the same trend as the WB results above (Figure 4B).

In order to investigate the downstream pathway of Ang-1/Tie-2, we explored the expression of GRB7 and FAK in mice. Compared with LAD sham operated mice, the levels of GRB7 and FAK in model group mice decreased significantly. Treatment of MI mice with AS increased the production of GRB7 and FAK (Figure 4C). And in Figures 4D, I, F showed the same results.

4 Discussion

Angiogenesis is a new therapeutic direction for MI, and we propose that two botanical drugs, *Astragalus propinquus* Schischkin and *Salvia miltiorrhiza* Bunge, can promote angiogenesis through pericyte recruitment. Therefore, we took the sham-operated mice as control group, the LAD mice as model group, and the LAD mice gavaged with extracts of *Astragalus propinquus* Schischkin and *Salvia miltiorrhiza* Bunge as AS group. The first objective of this study was to determine the extent of cardioprotection after MI by AS. The results of ECG and echocardiography showed that compared with the model group, the ST segment injury degree and abnormal

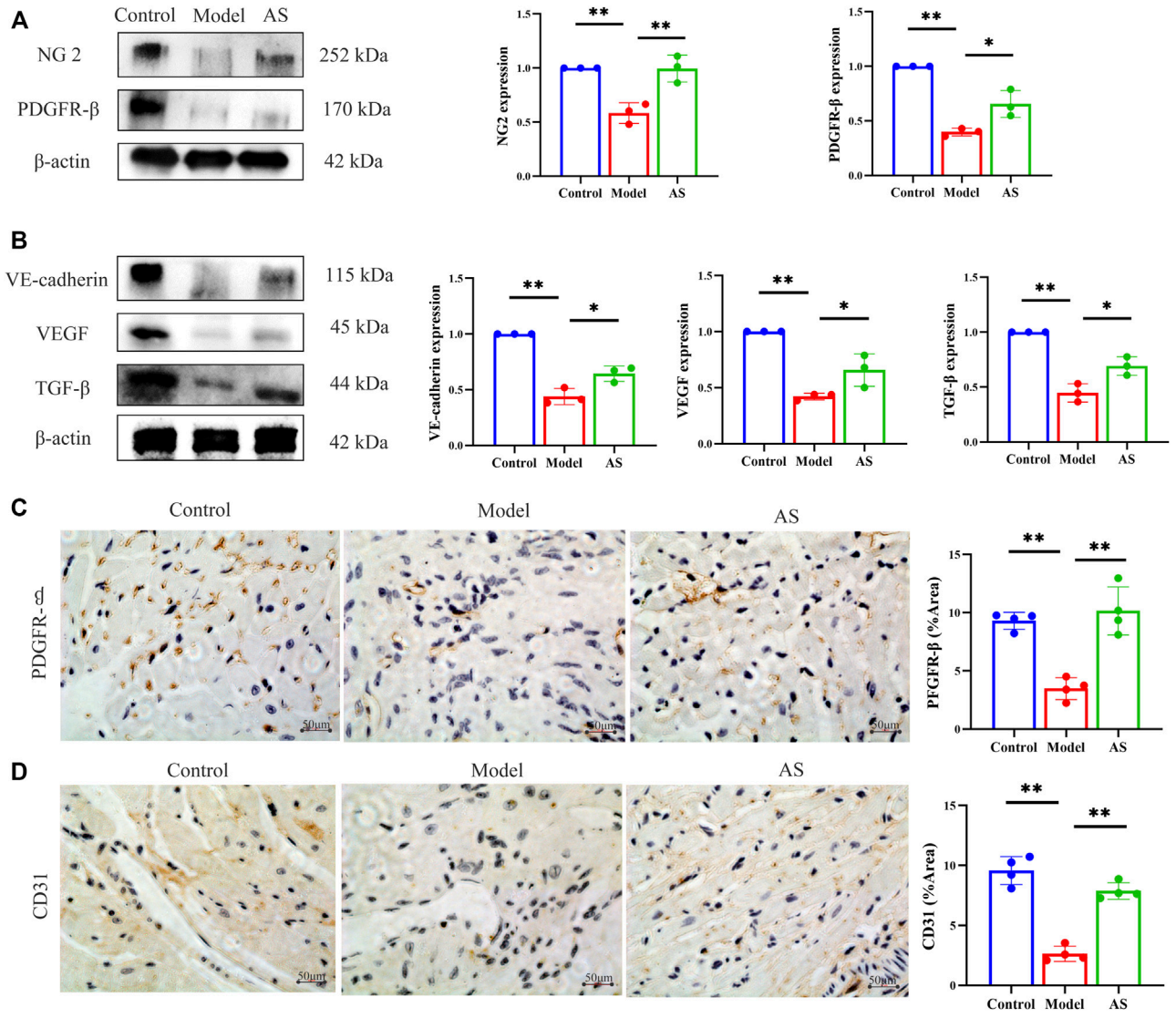

FIGURE 3
AS activates pericyte recruitment and promotes angiogenesis in MI mice. **(A)** Protein level of NG 2 and PDGFR-β, results are expressed as mean ± SD, n = 3, $^{**}p < .01$, $^{*}p < .05$. **(B)** Protein level of VE-cadherin, VEGF and TGF-β, results are expressed as mean ± SD, n = 3, $^{**}p < .01$, $^{*}p < .05$. **(C)** IHC staining, the brownish-yellow region is PDGFR-β, results are expressed as mean ± SD, n = 4, $^{**}p < .01$. **(D)** IHC staining, the brownish-yellow region is CD31, results are expressed as mean ± SD, n = 4, $^{**}p < .01$.

repolarization time in the AS group were reduced, and the EF, FS, LVVol; d, LVVol; s, LVID; d, LVID; s were recovered. Next, we performed an ELISA to test for BNP and NT-proBNP, and the lower values compared to the model group indicated that AS intervention could slow the progression of heart failure. Further cardiac pathology analysis demonstrated a smaller infarct size, a more stable cardiac structure and a reduced collagen deposition in AS group, when compared to model group. Further research found that the pericyte-specific marker PDGFR-β, NG2 and endothelial cell-specific marker CD31 in AS group rebounded. In addition, the angiogenesis related proteins VE cadherin, VEGF and TGF- β also increased after AS intervention compared with the model group, indicating that the effects of AS in the treatment of MI were related to pericyte recruitment and angiogenesis. Finally, Western blotting and IF results showed that AS played the role as described above through Ang-1/Tie-2/FAK pathway.

Interestingly, the results showed that AS upregulated the expression of Ang-1 and downregulated the expression of Ang-2. Ang-1 and Ang-2, which are secreted proteins that bind Tie-2 receptors, have the ability to regulate vascular maturation (Dumont et al., 1992; Korhonen et al., 1992). Ang-1 mainly promotes vascular maturation and maintains homeostasis, while Ang-2 can break vascular homeostasis and allow angiogenesis or regression. (Maisonpierre et al., 1997; Kim et al., 2000a). Previous studies have shown that Ang-1 overexpression can normalize the immature vascular system and increase the generation of new blood vessels, which is accompanied by a significant improvement in the density of capillaries and arterioles induced by ischemia in the heart infarction region (Chen and Stinnett, 2008). Therefore, we conclude that after MI, the stress response caused by ischemia and hypoxia increased the expression of Ang-1 in mice, and the

10.3389/fphar.2022.1103557

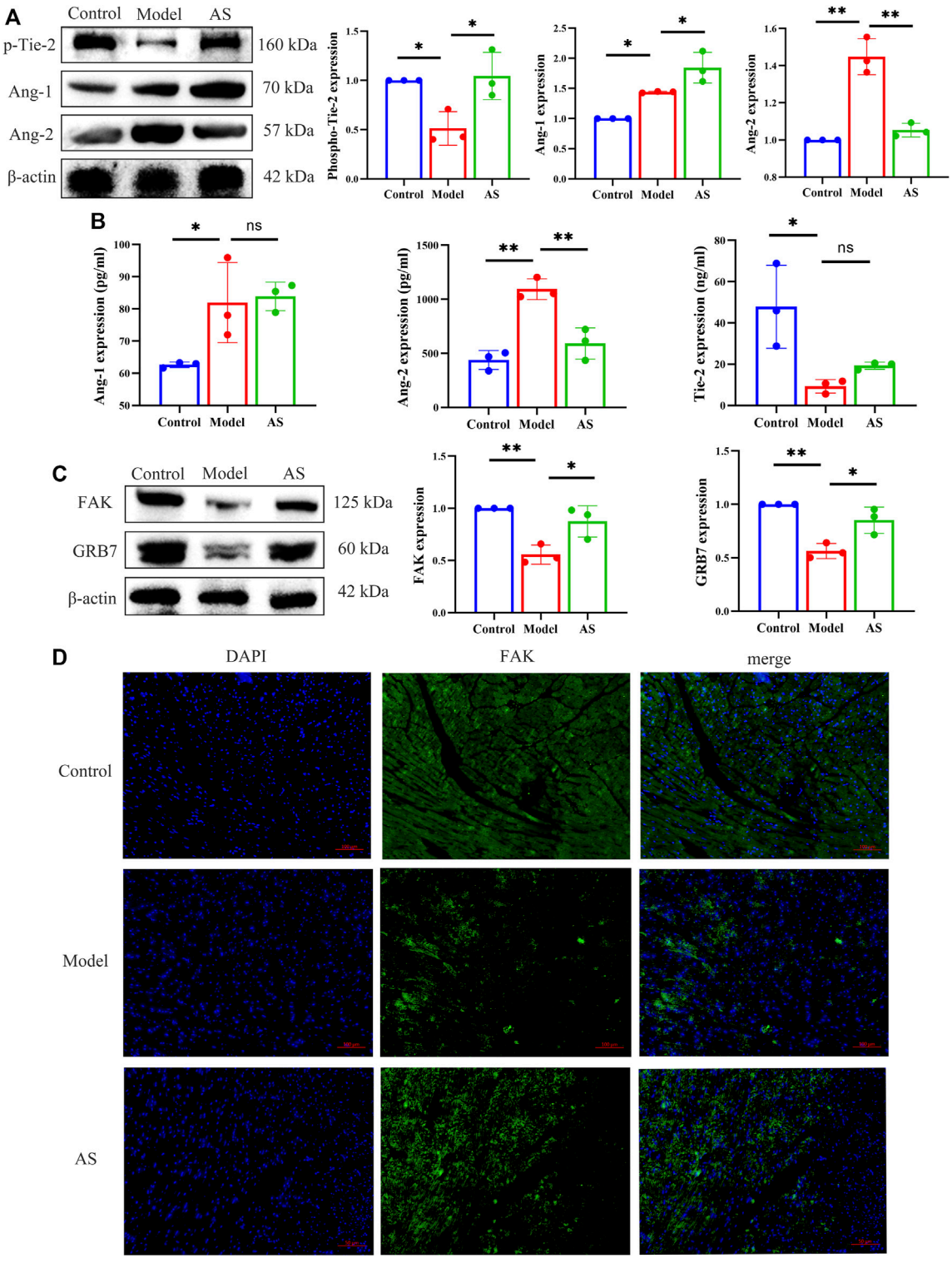

FIGURE 4
AS regulates Ang-1/Tie-2/FAk pathway. **(A)** Protein level of p-Tie-2, Ang-1 and Ang-2, results are expressed as mean ± SD, n = 3, $^{**}p < .01$, $^{*}p < .05$. **(B)** Quantitative analysis of Ang-1, Ang-2 and p-Tie-2 concentration, n = 3. Results are expressed as mean ± SD, $^{**}p < .001$, $^{*}p < .05$, ns indicates not significant. **(C)** Protein level of FAK and GRB7, results are expressed as mean ± SD, n = 3, $^{**}p < .01$, $^{*}p < .05$. **(D)** IF staining, the green region is FAK, results are expressed as mean ± SD, n = 3, $^{**}p < .01$, $^{*}p < .05$.

regulatory mechanism of the heart tried to antagonize MI damage through spontaneous angiogenesis. In this case, AS expands this trend of angiogenesis and further increased the expression of Ang-1. In addition, Ang-2 is also highly expressed in MI mice. Studies have shown that Ang-2 begin to express on the second day after MI, reaches the peak on the third day, and remains at the peak level

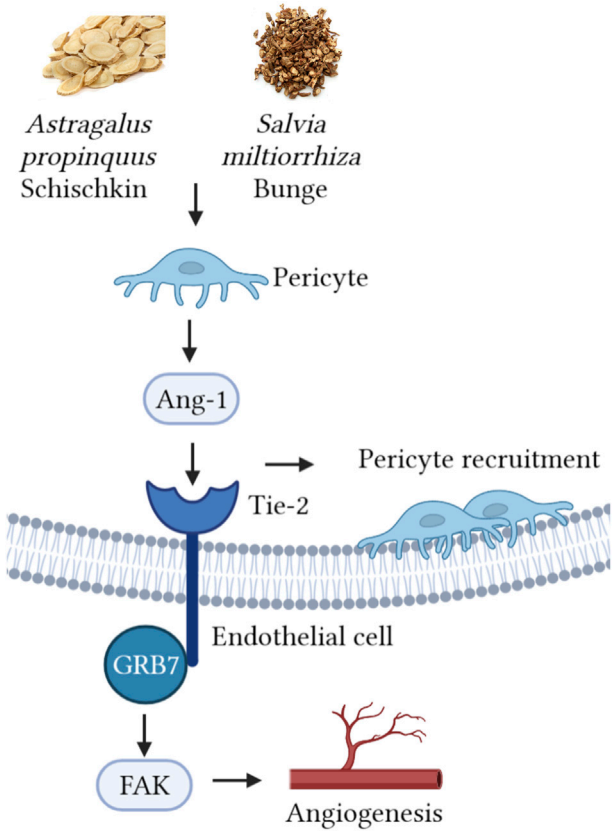

FIGURE 5
Astragalus propinquus Schischkin and *Salvia miltiorrhiza* Bunge regulate pericyte recruitment and promote angiogenesis to treat MI *via* Ang-1/Tie-2/FAk pathway.

until the seventh day (Lee et al., 2018). This may be related to Ang-2's ability to start angiogenesis, because in the case of high concentration of Ang-2, it can be used as an agonist of angiogenesis (Kim et al., 2000b; Wakui et al., 2006). It is worth noting that during acute MI, Ang-1 and Ang-2 exist at the same time, which will cause Ang-2 to antagonize Ang-1/Tie-2 signal and aggravate cardiac hypoxia (Lee et al., 2018). As a consequence, we speculate that after MI, the expression of Ang-2 increases to start the process of angiogenesis, and the application of AS weakens the expression of Ang-2, thereby weakening its negative effect against the maturation and stability of neovascularization.

Furthermore, as an antigen of Tie2, GRB7 can activate FAK to promote angiogenesis. FAK, a cycloplasmic tyrosine kinas, is a downstream protein of Ang-1 and Tie-2. Previous studies have shown that the interaction between Tie-2 and FAK is related to cell migration (Lamalice et al., 2007). Under the control of Tie-2 promoter and enhancer, FAK can promote angiogenesis in ischemic model (Peng et al., 2004). At the same time, Ang-1 can promote the phosphorylation of FAK (Kim et al., 2000c). In addition, the interaction between FAK and GRB7 is also related to stress response, which may also affect angiogenesis (Tsai et al., 2008).

We further focused on the active ingredients of AS. Previous studies have shown that *Astragalus propinquus* Schischkin and its main active components astragaloside IV and astragalus polysaccharide can exert cardioprotective effects *in vitro* and *in vivo*, which are specifically manifested in inhibiting myocardial cell death, reducing oxidative stress, reducing autophagosome accumulation, reducing myocardial fibrosis. and myocardial remodeling, thereby improving cardiac function and reducing cardiac ischemia-reperfusion injury (Ma et al., 2013; Liu et al., 2018; Jiang et al., 2019; Huang et al., 2021; Zhang et al., 2022). *Salvia miltiorrhiza* Bunge, with tanshinone IIa, salvianolic acid A and B as the main active ingredients, has also been proven to prevent and treat MI, cardiac hypertrophy and cardiac fibrosis (Li et al., 2018). Specifically, *Salvia miltiorrhiza* Bunge extract can regulate the accumulation of free fatty acids in ischemic myocardium (Sun et al., 2021), inhibit the expression of endothelial cell adhesion molecules (Jin et al., 2009), and improve ischemia-reperfusion microcirculation disorders and target organ damage (Han et al., 2008). Furthermore, the combination of *Astragalus propinquus* Schischkin and *Salvia miltiorrhiza* Bunge widely used in China and can enhance the effect on MI.

In this study, we focused on the synergistic ability of AS, explored their effect on promoting angiogenesis after MI, and innovatively pointed out the relationship between botanical drugs and pericyte recruitment. As shown in Figure 5, we speculate that this therapeutic effect is related to the regulation of the pericyte Ang-1/Tie-2/FAK paracrine loop by the botanical drugs. However, this study has some limitations. In the *in vivo* experiment, we only used the single dose recommended by the drug manual, which conforms to the specifications of Chinese Pharmacopoeia, but the concentration gradient was not set. This is an early exploration, and we aim to explore the effect of AS on promoting angiogenesis after MI and its possible mechanism. Based on the 4R rules (Reduce, refine, replace—Responsibility), we simplified the experimental procedures in order to reduce the pain or discomfort caused to animals, reduce the frequency and harm of inhuman use, and improve animal welfare. In the follow-up study, we will explore the relationship between dose and efficacy, screen out the main effective components of *Astragalus propinquus* Schischkin and *Salvia miltiorrhiza* Bunge, and further explore their mechanisms through *in vivo* and *in vitro* experiments. We expect that the effect of *Astragalus propinquus* Schischkin and *Salvia miltiorrhiza* Bunge on promoting angiogenesis can be applied to clinical practice and provide new complementary and alternative therapies for patients with MI.

5 Conclusion

Taken together, we demonstrate the efficacy of AS on MI at a single dose. AS has a positive effect on protecting cardiac function, hindering myocardial pathological changes, and slowing down the process of heart failure, which is achieved by regulating the recruitment of pericytes, thereby promoting angiogenesis. Our findings provide new complementary and alternative options for the future treatment of MI.

Data availability statement

The raw data supporting the conclusion of this article will be made available by the authors, without undue reservation.

Ethics statement

The animal study was reviewed and approved by Institutional Animal Care and Research Advisory Committee of the Shandong University of Traditional Chinese Medicine.

Author contributions

M-XZ: Investigation, validation, writing—Original draft X-YH: Investigation, validation, writing—Original draft YS: Validation W-LX: Project administration Y-LL: Conceptualization, writing—Review and editing CL: Conceptualization, funding acquisition, writing—Review and editing. All authors read and approved the final manuscript.

Funding

This work was supported by Natural Science Foundation of Shandong Province [grant number ZR2020QH305], Shandong Young Scientific and Technological Talents Promotion Project [grant number SDAST 2021qt08] and Youth Program of National Natural Science Foundation of China [grant number 82004276].

Conflict of interest

The authors declare that the research was conducted in the absence of any commercial or financial relationships that could be construed as a potential conflict of interest.

Publisher's note

All claims expressed in this article are solely those of the authors and do not necessarily represent those of their affiliated organizations, or those of the publisher, the editors and the reviewers. Any product that may be evaluated in this article, or claim that may be made by its manufacturer, is not guaranteed or endorsed by the publisher.

Supplementary material

The Supplementary Material for this article can be found online at: https://www.frontiersin.org/articles/10.3389/fphar.2022.1103557/full#supplementary-material

References

Armulik, A., Abramsson, A., and Betsholtz, C. (2005). Endothelial/pericyte interactions. *Circ. Res.* 97, 512–523. doi:10.1161/01.RES.0000182903.16652.d7

Bernas, G. (2003). Angiotherapeutics from natural products: From bench to clinics? *Clin. Hemorheol. Microcirc.* 29, 199–203.

Bu, L., Dai, O., Zhou, F., Liu, F., Chen, J. F., Peng, C., et al. (2020). Traditional Chinese medicine formulas, extracts, and compounds promote angiogenesis. *Biomed. Pharmacother.* 132, 110855. doi:10.1016/j.biopha.2020.110855

Chen, J. X., and Stinnett, A. (2008). Ang-1 gene therapy inhibits hypoxia-inducible factor-1alpha (HIF-1alpha)-prolyl-4-hydroxylase-2, stabilizes HIF-1alpha expression, and normalizes immature vasculature in db/db mice. *Diabetes* 57, 3335–3343. doi:10.2337/db08-0503

Dobaczewski, M., Akrivakis, S., Nasser, K., Michael, L. H., Entman, M. L., and Frangogiannis, N. G. (2004). Vascular mural cells in healing canine myocardial infarcts. *J. Histochem Cytochem* 52, 1019–1029. doi:10.1369/jhc.3A6210.2004

Doenst, T., Haverich, A., Serruys, P., Bonow, R. O., Kappetein, P., Falk, V., et al. (2019). PCI and CABG for treating stable coronary artery disease: JACC Review topic of the week. *J. Am. Coll. Cardiol.* 73, 964–976. doi:10.1016/j.jacc.2018.11.053

Dumont, D. J., Yamaguchi, T. P., Conlon, R. A., Rossant, J., and Breitman, M. L. (1992). tek, a novel tyrosine kinase gene located on mouse chromosome 4, is expressed in endothelial cells and their presumptive precursors. *Oncogene* 7, 1471–1480.

Fan, T. P., Yeh, J. C., Leung, K. W., Yue, P. Y. K., and Wong, R. N. S. (2006). Angiogenesis: From plants to blood vessels. *Trends Pharmacol. Sci.* 27, 297–309. doi:10.1016/j.tips.2006.04.006

Franco, M., Roswall, P., Cortez, E., Hanahan, D., and Pietras, K. (2011). Pericytes promote endothelial cell survival through induction of autocrine VEGF-A signaling and Bcl-w expression. *Blood* 118, 2906–2917. doi:10.1182/blood-2011-01-331694

Fu, J., Wang, Z., Huang, L., Zheng, S., Wang, D., Chen, S., et al. (2014). Review of the botanical characteristics, phytochemistry, and pharmacology of Astragalus membranaceus (Huangqi). *Phytother. Res.* 28, 1275–1283. doi:10.1002/ptr.5188

Fukushi, J., Makagiansar, I. T., and Stallcup, W. B. (2004). NG2 proteoglycan promotes endothelial cell motility and angiogenesis via engagement of galectin-3 and alpha3beta1 integrin. *Mol. Biol. Cell* 15, 3580–3590. doi:10.1091/mbc.e04-03-0236

Garcia, R. A., Brown, K. L., Pavelec, R. S., Go, K. V., Covell, J. W., and Villarreal, F. J. (2005). Abnormal cardiac wall motion and early matrix metalloproteinase activity. *Am. J. Physiol. Heart Circ. Physiol.* 288, H1080–H1087. doi:10.1152/ajpheart.00860.2004

Han, J. Y., Fan, J. Y., Horie, Y., Miura, S., Cui, D. H., Ishii, H., et al. (2008). Ameliorating effects of compounds derived from Salvia miltiorrhiza root extract on microcirculatory disturbance and target organ injury by ischemia and reperfusion. *Pharmacol. Ther.* 117, 280–295. doi:10.1016/j.pharmthera.2007.09.008

Huang, K. Y., Yu, Y. W., Liu, S., Zhou, Y. Y., Wang, J. S., Peng, Y. P., et al. (2021). A single, acute astragaloside IV therapy protects cardiomyocyte through attenuating superoxide anion-mediated accumulation of autophagosomes in myocardial ischemia-reperfusion injury. *Front. Pharmacol.* 12, 642925. doi:10.3389/fphar.2021.642925

Jiang, M., Ni, J., Cao, Y., Xing, X., Wu, Q., and Fan, G. (2019). Astragaloside IV attenuates myocardial ischemia-reperfusion injury from oxidative stress by regulating succinate, lysophospholipid metabolism, and ROS scavenging system. *Oxid. Med. Cell Longev.* 2019, 9137654. doi:10.1155/2019/9137654

Jin, Y. C., Kim, C. W., Kim, Y. M., Nizamutdinova, I. T., Ha, Y. M., Kim, H. J., et al. (2009). Cryptotanshinone, a lipophilic compound of Salvia miltiorrriza root, inhibits TNF-alpha-induced expression of adhesion molecules in HUVEC and attenuates rat myocardial ischemia/reperfusion injury *in vivo*. *Eur. J. Pharmacol.* 614, 91–97. doi:10.1016/j.ejphar.2009.04.038

Kim, I., Kim, H. G., Moon, S. O., Chae, S. W., So, J. N., Koh, K. N., et al. (2000). Angiopoietin-1 induces endothelial cell sprouting through the activation of focal adhesion kinase and plasmin secretion. *Circ. Res.* 86, 952–959. doi:10.1161/01.res.86.9.952

Kim, I., Kim, H. G., So, J. N., Kwak, H. J., and Koh, G. Y. (2000). Angiopoietin-1 regulates endothelial cell survival through the phosphatidylinositol 3'-Kinase/Akt signal transduction pathway. *Circ. Res.* 86, 24–29. doi:10.1161/01.res.86.1.24

Kim, I., Kim, J. H., Moon, S. O., Kwak, H. J., Kim, N. G., and Koh, G. Y. (2000). Angiopoietin-2 at high concentration can enhance endothelial cell survival through the phosphatidylinositol 3'-kinase/Akt signal transduction pathway. *Oncogene* 19, 4549–4552. doi:10.1038/sj.onc.1203800

Korhonen, J., Partanen, J., Armstrong, E., VaahtokAri, A., Elenius, K., JalkanenM., et al. (1992). Enhanced expression of the tie receptor tyrosine kinase in endothelial cells during neovascularization. *Blood* 80, 2548–2555. doi:10.1182/blood.v80.10.2548.bloodjournal80102548

Lamalice, L., Le Boeuf, F., and Huot, J. (2007). Endothelial cell migration during angiogenesis. *Circ. Res.* 100, 782–794. doi:10.1161/01.RES.0000259593.07661.1e

Lee, S. J., Lee, C. K., Kang, S., Park, I., Kim, Y. H., Kim, S. K., et al. (2018). Angiopoietin-2 exacerbates cardiac hypoxia and inflammation after myocardial infarction. *J. Clin. Invest.* 128, 5018–5033. doi:10.1172/JCI99659

Li, M. H., Chen, J. M., Peng, Y., Wu, Q., and Xiao, P. G. (2008). Investigation of Danshen and related medicinal plants in China. *J. Ethnopharmacol.* 120, 419–426. doi:10.1016/j.jep.2008.09.013

Li, Z. M., Xu, S. W., and Liu, P. Q. (2018). Salvia miltiorrhizaBurge (danshen): A golden herbal medicine in cardiovascular therapeutics. *Acta Pharmacol. Sin.* 39, 802–824. doi:10.1038/aps.2017.193

Lindahl, P., Johansson, B. R., Leveen, P., and Betsholtz, C. (1997). Pericyte loss and microaneurysm formation in PDGF-B-deficient mice. *Science* 277, 242–245. doi:10.1126/science.277.5323.242

Liu, D., Chen, L., Zhao, J., and Cui, K. (2018). Cardioprotection activity and mechanism of Astragalus polysaccharide *in vivo* and *in vitro*. *Int. J. Biol. Macromol.* 111, 947–952. doi:10.1016/j.ijbiomac.2018.01.048

Ma, X., Zhang, K., Li, H., Han, S., Ma, Z., and Tu, P. (2013). Extracts from Astragalus membranaceus limit myocardial cell death and improve cardiac function in a rat model of myocardial ischemia. *J. Ethnopharmacol.* 149, 720–728. doi:10.1016/j.jep.2013.07.036

Maisonpierre, P. C., Suri, C., Jones, P. F., Bartunkova, S., Wiegand, S. J., Radziejewski, C., et al. (1997). Angiopoietin-2, a natural antagonist for Tie2 that disrupts *in vivo* angiogenesis. *Science* 277, 55–60. doi:10.1126/science.277.5322.55

Maries, L., and Manitiu, I. (2013). Diagnostic and prognostic values of B-type natriuretic peptides (BNP) and N-terminal fragment brain natriuretic peptides (NT-pro-BNP). *Cardiovasc J. Afr.* 24, 286–289. doi:10.5830/CVJA-2013-055

Nunez, J., Nunez, E., Robles, R., Bodi, V., Sanchis, J., Carratala, A., et al. (2008). Prognostic value of brain natriuretic peptide in acute heart failure: Mortality and hospital readmission. *Rev. Esp. Cardiol.* 61, 1332–1337. doi:10.1016/s1885-5857(09)60062-1

Peng, X., Ueda, H., Zhou, H., Stokol, T., Shen, T. L., Alcaraz, A., et al. (2004). Overexpression of focal adhesion kinase in vascular endothelial cells promotes angiogenesis in transgenic mice. *Cardiovasc Res.* 64, 421–430. doi:10.1016/j.cardiores.2004.07.012

Qiu, M., Li, Y., Li, J., Xu, K., Jing, Q., Dong, S., et al. (2017). Impact of six versus 12 months of dual antiplatelet therapy in patients with drug-eluting stent implantation after risk stratification with the residual SYNTAX score: Results from a secondary analysis of the I-LOVE-IT 2 trial. *Catheter Cardiovasc Interv.* 89, 565–573. doi:10.1002/ccd.26948

Stratman, A. N., Schwindt, A. E., Malotte, K. M., and Davis, G. E. (2010). Endothelial-derived PDGF-BB and HB-EGF coordinately regulate pericyte recruitment during vasculogenic tube assembly and stabilization. *Blood* 116, 4720–4730. doi:10.1182/blood-2010-05-286872

Sun, L., Jia, H., Yu, M., Yang, Y., Li, J., Tian, D., et al. (2021). Salvia miltiorrhiza and Pueraria lobata, two eminent herbs in Xin-Ke-Shu, ameliorate myocardial ischemia partially by modulating the accumulation of free fatty acids in rats. *Phytomedicine* 89, 153620. doi:10.1016/j.phymed.2021.153620

Tang, L., Pan, W., Zhu, G., Liu, Z., Lv, D., and Jiang, M. (2017). Total flavones of abelmoschus manihot enhances angiogenic ability both *in vitro* and *in vivo*. *Oncotarget* 8, 69768–69778. doi:10.18632/oncotarget.19264

Teichert, M., Milde, L., Holm, A., Stanicek, L., Gengenbacher, N., Savant, S., et al. (2017). Pericyte-expressed Tie2 controls angiogenesis and vessel maturation. *Nat. Commun.* 8, 16106. doi:10.1038/ncomms16106

Tsai, N. P., Ho, P. C., and Wei, L. N. (2008). Regulation of stress granule dynamics by Grb7 and FAK signalling pathway. *EMBO J.* 27, 715–726. doi:10.1038/emboj.2008.19

Wakui, S., Yokoo, K., Muto, T., Suzuki, Y., Takahashi, H., Furusato, M., et al. (2006). Localization of Ang-1, -2, Tie-2, and VEGF expression at endothelial-pericyte interdigitation in rat angiogenesis. *Lab. Invest.* 86, 1172–1184. doi:10.1038/labinvest.3700476

Wang, X., Lv, H., Gu, Y., Wang, X., Cao, H., Tang, Y., et al. (2014). Protective effect of lycopene on cardiac function and myocardial fibrosis after acute myocardial infarction in rats via the modulation of p38 and MMP-9. *J. Mol. Histol.* 45, 113–120. doi:10.1007/s10735-013-9535-2

Wang, Y. B., Liu, Y. F., Lu, X. T., Yan, F. F., Wang, B., Bai, W. W., et al. (2013). Rehmannia glutinosa extract activates endothelial progenitor cells in a rat model of myocardial infarction through a SDF-1 α/CXCR4 cascade. *PLoS One* 8, e54303. doi:10.1371/journal.pone.0054303

Winkler, E. A., Bell, R. D., and Zlokovic, B. V. (2010). Pericyte-specific expression of PDGF beta receptor in mouse models with normal and deficient PDGF beta receptor signaling. *Mol. Neurodegener.* 5, 32. doi:10.1186/1750-1326-5-32

Yan, G. X., Lankipalli, R. S., Burke, J. F., Musco, S., and Kowey, P. R. (2003). Ventricular repolarization components on the electrocardiogram: Cellular basis and clinical significance. *J. Am. Coll. Cardiol.* 42, 401–409. doi:10.1016/s0735-1097(03)00713-7

Zhang, X., Qu, H., Yang, T., Liu, Q., and Zhou, H. (2022). Astragaloside IV attenuate MI-induced myocardial fibrosis and cardiac remodeling by inhibiting ROS/caspase-1/GSDMD signaling pathway. *Cell Cycle* 21, 2309–2322. doi:10.1080/15384101.2022.2093598

Glossary

Ang-1 Angiopoietin-1
Ang-2 Angiopoietin-2
AS *Astragalus propinquus* Schischkin and Salvia miltiorrhiza Bunge
BNP Brain Natriuretic Peptide
CABG coronary artery bypass graft
CD31 platelet endothelial cell adhesion molecule-1
ECG Electrocardiogram
EF ejection fraction
ELISA Enzyme-linked Immunosorbent Assay
FAK focal adhesion kinase
FS short axis shortening of the left heart asphyxia
GRB7 growth factor receptor bound protein 7
H&E Hematoxylin and eosin
IF immunofluorescence
IHC immunohistochemistry
LAD left anterior descending coronary artery ligation
LVID; d left asphyxiating end diastolic diameter
LVID; s left ventricular end systolic diameter
LVvol; d left ventricular end diastolic volume
LVvol; s left ventricular end systolic volume
MI myocardial ischemia
MMP9 matrix metalloproteinase-9
NT-proBNP N-terminal Pro-brain Natriuretic Peptide
PCI percutaneous coronary intervention
PDGFR-β platelet-derived growth factor receptors β
p-Tie-2 phosphorylated angiopoietin-1 receptor
TGF-β transforming growth factor β
q-PCR RNA isolation and quantitative-PCR
SD standard deviation
TTC Triphenyl tetrazolium chloride
VE-cadherin vascular endothelial cadherin
VEGF Vascular Endothelial Growth Factor
WHO World Health Organization

frontiers | Frontiers in Pharmacology

TYPE Clinical Trial
PUBLISHED 10 January 2023
DOI 10.3389/fphar.2022.1014410

OPEN ACCESS

EDITED BY
Rong Lu,
Shanghai University of Traditional Chinese Medicine, China

REVIEWED BY
Yonggang Zhang,
Sichuan University, China
Jianxin Chen,
Beijing University of Chinese Medicine, China
Xingjiang Xiong,
China Academy of Chinese Medical Sciences, China
Lin Li,
China-Japan Friendship Hospital, China

*CORRESPONDENCE
Hao Xu,
xuhaotcm@hotmail.com

†These authors have contributed equally to this work and share first authorship

SPECIALTY SECTION
This article was submitted to Ethnopharmacology, a section of the journal Frontiers in Pharmacology

RECEIVED 08 August 2022
ACCEPTED 29 December 2022
PUBLISHED 10 January 2023

CITATION
Xu X, Tian W, Duan W, Pan C, Huang M, Wang Q, Yang Q, Wen Z, Tang Y, Xiong Y, Zhu Z, Liu Y, Wei D, Qi W, Ouyang X, Ying S, Wang X, Zhou Z, Li X, Cui Y, Yang S and Xu H (2023), Quanduzhong capsules for the treatment of grade 1 hypertension patients with low-to-moderate risk: A multicenter, randomized, double-blind, placebo-controlled clinical trial. *Front. Pharmacol.* 13:1014410. doi: 10.3389/fphar.2022.1014410

Quanduzhong capsules for the treatment of grade 1 hypertension patients with low-to-moderate risk: A multicenter, randomized, double-blind, placebo-controlled clinical trial

Xuan Xu[1,2,3†], Wende Tian[1,2,4†], Wenhui Duan[1,2], Chaoxin Pan[5], Mingjian Huang[5], Qinggao Wang[5], Qinghua Yang[5], Zhihao Wen[5], Yu Tang[6], Yao Xiong[6], Zhiyun Zhu[6], Yuanyuan Liu[6], Dan Wei[6], Wenqiang Qi[6], Xiaochao Ouyang[6], Shaozhen Ying[6], Xiaohua Wang[6], Zhigang Zhou[7], Xiaofeng Li[7], Yu Cui[7], Shuyin Yang[7] and Hao Xu[1,2]*

[1]Xiyuan Hospital, China Academy of Chinese Medical Sciences, Beijing, China, [2]National Clinical Research Center for Chinese Medicine Cardiology, Xiyuan Hospital, China Academy of Chinese Medical Sciences, Beijing, China, [3]The Eighth Hospital of Baotou, Baotou, China, [4]Graduate School, China Academy of Chinese Medical Sciences, Beijing, China, [5]The First Affiliated Hospital of Guangxi University of Chinese Medicine, Guangxi, China, [6]Jiangxi Provincial People's Hospital, Nanchang, Jiangxi Province, China, [7]Jiangxi Puzheng Pharmaceutical Co, Ltd., Jiangxi, China

Background: Duzhong [DZ (*Eucommia ulmoides* Oliv.)] is regarded as a traditional Chinese medicine with a history dating back more than 2000 years. This herb is considered a nourishing herb in China and is commonly used as a tonic to strengthen muscles and bones, nourish the kidneys and liver, and soothe miscarriages. Moreover, there is evidence that DZ is capable of regulating blood pressure (BP), and several compounds isolated from DZ have been shown to have a BP-lowering effect. Quanduzhong capsules contain an extract of DZ [*Eucommia ulmoides* Oliv. (Eucommiaceae; Eucommiae cortex)] that is effective in treating hypertension. This multicenter, randomized, double-blind, placebo-controlled clinical trial sought to evaluate the clinical efficacy of Quanduzhong capsules in the treatment of low-to-moderate risk grade 1 hypertension patients.

Materials and methods: A total of 60 patients from 3 centers with documented low-to-moderate risk grade 1 hypertension were randomly assigned in a 1:1 ratio to the test group or the control group. After a 1 week lead-in period using sham Quanduzhong capsules, all patients who met the entry criteria (29 cases in the test group and 29 cases in the control group) entered the 4 week test period. The test group took Quanduzhong capsules, and the control group continued to take sham Quanduzhong capsules. The primary endpoints [24-h mean systolic blood pressure

Abbreviations: ALD, aldosterone; Ang II, angiotensin II; ADR, adverse drug reaction; AEs, adverse events; ANOVA, analysis of variance; BP, blood pressure; β2m, β2-microglobulin; CV, coefficient of variation; CI, confidence interval; CMH, Cochran–Mantel–Haenszel; DBP, diastolic blood pressure; DZ, Duzhong; FAS, full analysis set; GAP, Good Agricultural Practice; HPLC, high-performance liquid chromatography; Hcy, homocysteine; K-W, Kruskal–Wallis; PRA, plasmatic renin activity; PPS, per protocol set; RAAS, renin-angiotensin-aldosterone; SBP, systolic blood pressure; SS, safety set; SD, standard deviation; TCM, Traditional Chinese medicine; UK: unknown; WHOQOL-BREF, WHO Quality of Life-BREF; 24-h ABPM, 24-h ambulatory blood pressure monitoring.

(SBP) and diastolic blood pressure (DBP) determined *via* 24-h ambulatory blood pressure monitoring (ABPM); office SBP and DBP] and secondary endpoints [mean arterial pressure; mean pulse; daytime mean SBP and DBP; nocturnal mean SBP and DBP; SBP and DBP load; area under the blood pressure (BP) curve; morning peak BP; early morning SBP and DBP; smoothness index of SBP and DBP; 24 h BP mean coefficient of variation (CV); percentage of patients with circadian restoration in ABPM; home BP; quality of life evaluated by WHO Quality of Life-BREF questionnaire; grading and quantitative evaluation of hypertension symptoms; values of plasmatic renin activity, angiotensin II, aldosterone, β-2 microglobulin and homocysteine] were assessed following the treatment. Drug-related adverse events and adverse drug reactions were also compared.

Results: After a 4 week test period, a significant difference in the DBP CV between the two groups was observed (−2.49 ± 4.32 vs. 0.76 ± 4.3; $p < .05$). Moreover, the mean office SBP change was −7.62 ± 9.32 mmHg, and the mean DBP change was −4.66 ± 6.03 ($p < .05$). Among the three subjects with abnormal homocysteine levels in the test group, homocysteine levels decreased by 6.23 ± 9.15 μmol/L after treatment. No differences were observed between the two groups in any other indicators. After 4 weeks of treatment, there were no significant differences between the groups in terms of safety indicators ($p > .05$). No abnormal vital signs (except BP) or severe liver or renal function impairment were observed during the treatment periods; in addition, adverse events and drug reactions were mild.

Conclusion: Treatment with Quanduzhong capsules reduced office SBP and DBP as well as DBP CV determined by 24-h ambulatory BP monitoring in patients with grade 1 hypertension at low-to-moderate risk.

Clinical Trial Registration: https://www.chictr.org.cn/showproj.aspx?proj=32531, identifier ChiCTR1900021699.

KEYWORDS

quanduzhong capsule, traditional Chinese medicine, grade 1 hypertension, low-to-moderate risk, randomized controlled trial

1 Introduction

Hypertension is a complex and multifactorial disease. Stroke and cardiovascular and kidney diseases all have a pathogenesis that is closely related to high blood pressure (BP) (Ettehad et al., 2016; Joint Committee for Guideline Revision, 2018). Hypertension, as a pandemic, has become the most critical and significant public health problem. Moreover, approximately one billion people worldwide suffer from hypertension, and less than a fifth have it under control, according to the World Health Organization (Hypertension, 2021).

Hypertension is defined as office systolic BP (SBP) values ≥140 mmHg and/or diastolic BP (DBP) values ≥90 mmHg (Williams et al., 2018). Currently, antihypertension medication still serves as a primary option for treating hypertension. It is still debated whether low-to-moderate risk grade 1 hypertension (140–159/90–99 mmHg) patients should immediately start treatment with antihypertensive drugs because older trials of "mild hypertension" included patients with BP levels potentially higher than those who were defined as having grade 1 hypertension or high risk for hypertension (Morales Salinas et al., 2017).

Furthermore, the potential adverse reactions of antihypertensive medication, such as headache, dizziness, orthostatic hypotension and decreased sexual function, limit their clinical application, especially in patients with grade 1 hypertension (Xiong et al., 2013a). Thus, looking for alternative therapies to control BP is necessary in the early stage of hypertension. Traditional Chinese medicine (TCM) has attracted much attention in recent years. Integrating TCM with Western medicine significantly improves the therapeutic effectiveness of hypertension treatment compared to Western medicine alone (Mohammed et al., 2023). Songling Xuemaikang capsules are beneficial for essential hypertension because they can lower BP and relieve hypertensive symptoms and they are well tolerated (Meng et al., 2022). A meta-analysis showed that Zhen Gan Xi Feng decoction, a traditional Chinese herbal formula, is effective in improving BP and hypertension-related symptoms (Xiong et al., 2013b). Recently, a Chinese herbal formula consisting of gastrodia-uncaria granules was shown to be efficacious for patients with masked hypertension in a randomized, placebo-controlled trial (Zhang et al., 2020).

The Quanduzhong capsules contain Duzhong [DZ (*Eucommia ulmoides* Oliv.)], which is a marketed formula well known for its antihypertensive effect. As shown by Zhang et al. (Zhang and Wei, 2018), the clinical curative effect of Quanduzhong capsules on renal hypertension is remarkable, as it can improve renal function and regulate BP circadian rhythm. Recently, Zhang et al. (Zhang et al., 2022a) observed the clinical effect of Quanduzhong capsules on new-onset mild hypertension. The patients in this study were treated for 6 months; 48 patients in the test group were given enalapril maleate tablets and Quanduzhong capsules, and 29 patients in the control group were given enalapril maleate tablets alone. The total effective rate of the test group was 97.92%, and the total effective rate of the control group was 85.42% (Zhang et al., 2022a). The clinical curative

rate in the test group was higher ($p = .027$). A randomized controlled trial conducted by Jiang et al. (Jiang et al., 2022) confirmed that Quanduzhong capsules can lower office BP in patients with mild hypertension and kidney deficiency syndrome. The test group was given Quanduzhong capsules, and the control group received sham Quanduzhong capsules (Jiang et al., 2022). Compared with the BP values in the control group, the SBP and DBP in the test group decreased after 12 weeks of treatment ($p < .05$) (Jiang et al., 2022).

However, prior studies examining the efficacy of Quanduzhong capsules in treating hypertension were single-center studies or were not placebo-controlled. In addition, risk factors for hypertension were not taken into consideration. Therefore, we conducted a multicenter, randomized, double-blind, placebo-controlled clinical trial to assess the efficacy and safety of Quanduzhong capsules in grade 1 hypertension with low-to-moderate risk.

2 Materials and methods

2.1 Study design

This multicenter, randomized, placebo-controlled trial was conducted at three hospitals across mainland China, including Xiyuan Hospital, The First Affiliated Hospital of Guangxi University of Chinese Medicine, and Jiangxi Provincial People's Hospital. Twenty patients were enrolled in each hospital. Our study, which was registered in the Chinese Clinical Trial Registry (ChiCTR1900021699), complies with the principles of the Declaration of Helsinki and Good Clinical Practice guidelines, and the ethics committee at each participating hospital approved the protocol. An independent data and safety monitoring committee blinded to treatment allocation oversaw the trial. The study was reported according to the CONSORT guidelines (Schulz et al., 2010).

2.2 Participant inclusion and exclusion criteria

Male and female patients between the ages of 30 and 75 years who were diagnosed with essential low-to-moderate risk grade 1 hypertension (140–159/90–99 mmHg) were eligible for participation. The subjects volunteered to participate in this trial and signed the informed consent form. Patients were excluded if they 1) were known or suspected to be allergic to the test drug and its components; 2) had malignant hypertension, hypertensive emergencies, hypertensive crisis, or hypertensive encephalopathy; 3) had secondary hypertension, including but not limited to the following diseases: unilateral or double renal artery, polycystic kidney disease, hyperaldosteronism, aortic coarctation, Cushing's syndrome, or pheochromocytoma; 4) had the following comorbid diseases: acute myocardial infarction within 6 months, cerebrovascular accident, transient ischemic attack, large aneurysm or dissection aneurysm, unstable angina, grade II-IV (NYHA classification) history of heart failure, grade II or above atrioventricular block, sick sinus syndrome, bradycardia (heart rate <50 beats/min), or malignant or potentially malignant arrhythmias such as atrial fibrillation; 5) had serious liver, kidney or blood system diseases or malignant tumors; 6) had gastrointestinal lesions or gastrointestinal surgery such as gastrointestinal resection, active gastrointestinal inflammation, ulcers or gastrointestinal bleeding in the past 1 year; 7) had a reversed circadian rhythm or irregular sleep pattern; 8) were pregnant, were lactating, or had future plans for child bearing in 6 months; 9) had a history of alcohol or drug abuse 10) had neurological or mental disorders and could not or were unwilling to cooperate 11) were unable to participate in this research; and 12) had participated in other clinical trials 3 months prior.

2.3 Plant and drug preparation

Quanduzhong capsules are a China Food and Drug Administration-approved drug that contain an extraction of *Eucommia ulmoides* Oliv. [Eucommiaceae; Eucommiae cortex]. Each capsule of 0.48 g is equivalent to 2.5 g of crude drug. The crude drug was obtained from DZ Good Agricultural Practice (GAP) bases established by Jiangxi Puzheng Pharmaceutical Co., Ltd., in Jinggangshan and Jishui in Jiangxi Province, China. Quanduzhong capsules for the present clinical trial were prepared by Jiangxi Puzheng Pharmaceutical Co., Ltd., Jiangxi Province, China (production batch number: 180401; inspection order number: CP054180401).

With the cork removed, a total of 2500 g DZ was crushed into fine powder, 250 g of which was saved for later use, and the remainder was crushed, heated, refluxed with 85% ethanol for 2 h, and filtered, and the ethanol was recovered. The liquid medicine was stored for later use. Then, medicinal dregs were decocted twice with water, each time for an hour, and the decoctions were then combined and filtered. Once the filtrate had been combined with the abovementioned liquid medicine, it was concentrated into a paste with a relative density of 1.30 g/mL (80°C) by decompression; the paste was mixed with the 250 g fine powder mentioned above and soluble starch, then dried, crushed, sieved, and packed into 1000 capsules. Therefore, extractions were performed using ethanol extraction first, followed by water extraction. The Quanduzhong capsules contained a crude drug powder, which was improved by innovative micropowder technology to ensure uniformity and stability of the extraction and to ensure that the active ingredients were dispersed properly when taken, thus maximizing efficacy. The unfilled gelatin capsules used in this batch of products were made by Suzhou Capsule Co., Ltd. (production batch number: 12863878; material number: YF033-18012501).

The appearance of the sham capsules were indistinguishable in color, shape, size, packaging, smell, and taste from the Quanduzhong capsules, which were supplied by Jiangxi Puzheng Pharmaceutical Co., Ltd., China (production batch number: 180401; material number: CP054180701).

2.4 LC-MS/MS analysis of quanduzhong capsules

For LC-MS/MS analysis, 0.3 g Quanduzhong capsule powder was added to 25 mL deionized water and ultrasonically dissolved for 30 min. Then, 1 ml of the solution was taken, diluted 100 times, separated by high-speed centrifugation, and filtered through a 0.22 μm filter membrane.

The identification experiment was performed using ultra-performance liquid chromatography-quadrupole-time of flight (UPLC-Q-TOF) mass spectrometry (MS) [AB SCIEX Triple TOF

5600 + mass spectrometer system (AB SCIEX, Foster City, CA, United States)]. A C_{18} column (100 × 2.1 mm, 1.8 μm) was used with a flow rate of 0.25 ml/min. The mobile phases used were A) acetonitrile and B) 0.1% aqueous formic acid under the following gradient elution: 10% A from 0.1 to 2 min; 10%–25% A from 2 to 5 min; 25%–40% A from 5 to 15 min; 40%–90% A from 15 to 23 min; 90% A from 23 to 27 min. The electrospray ionization (ESI) source was used in negative ion mode. For the compounds of interest, a scan range of m/z 120–1500 was chosen. Other conditions were as follows: atomization temperature, 600°C; spray voltage, −4500 V; declustering potential, −80 V. MS data were collected in TOF-MS-IDA-MS/MS mode.

2.5 Randomization, intervention and masking

In each center, 20 patients were randomly assigned using a block randomization method in a 1:1 ratio to the test group or control group. After checking for eligibility during screening, subjects were allocated numbers in chronologic order. First, each participant took three sham Quanduzhong capsules twice daily for 1 week. After the sham lead-in period, all patients who met the entry criteria were allowed to enter the next 4 week test period. During the 4 week test period, the test group took three Quanduzhong capsules twice daily, and the control group continued to take sham Quanduzhong capsules. In addition, all randomized patients adopted similar lifestyle interventions throughout the trials. A two-level blinding method was set up, with the first level being by group (group A and group B) according to case number and the second level being by treatment (Quanduzhong capsules and sham). All investigators, data collectors, and patients were masked to the treatment allocation.

2.6 Outcomes

The primary outcome measures were 24-h mean SBP and DBP determined *via* 24-h ambulatory blood pressure monitoring (ABPM) and office SBP and DBP. The secondary efficacy measures were mean arterial pressure, mean pulse, daytime mean SBP and DBP, nocturnal mean SBP and DBP, SBP and DBP load, area under the BP curve, morning peak BP, early morning SBP and DBP, smoothness index of SBP and DBP, 24 h BP mean CV, percentage of patients with circadian restoration in ABPM, home BP, quality of life evaluated by WHO Quality of Life-BREF (WHOQOL-BREF) questionnaire, grading and quantitative evaluation of hypertension symptoms, as well as values of plasmatic renin activity (PRA), angiotensin II (Ang II), aldosterone (ALD), β_2-microglobulin (β_2m) and homocysteine (Hcy).

2.7 Safety measures

The clinical laboratory tests included routine blood and urine parameters, as well as liver and kidney function examinations. The measured vital signs included pulse, body temperature, and respiratory rate. In addition, adverse events (AEs) were recorded at any time of occurrence during the trial. An AE was categorized as related (definitely, probably, or possibly) or not related (unlikely or not related) to the study drug (Ren et al., 2012; Belknap et al., 2017). An adverse drug reaction (ADR) was defined as an AE that was considered related to the study drug.

2.8 Statistical analysis

The full analysis set (FAS), per protocol set (PPS), and safety set (SS) were included for analysis by SAS software, version 9.4 (SAS Institute). All hypothesis tests were two-sided, with $\alpha = 0.05$; thus, results where $p < .05$ were considered statistically significant. All results are presented with a 95% confidence interval (95% CI). Measurement data are expressed as the mean, standard deviation (SD), median, Q1 (25th percentile), Q3 (75th percentile), and maximum and minimum values. Descriptive statistics were calculated as frequencies to express count data; inferential statistics and the corresponding *p* values were calculated. Depending on the type of variable and its distribution in measurement data, the Kruskal–Wallis (K-W) test and analysis of variance (ANOVA) were used to compare characteristics between groups; comparisons of exams among groups were performed by Fisher's exact test or the chi-square test for descriptive statistics; the Cochran–Mantel–Haenszel (CMH) test was used for grade data. Primary efficacy measures were analyzed by ANCOVA with the baseline as a covariate. The chi-square test was used to compare the incidence of adverse events and reactions between the two groups.

3 Results

3.1 Identification of the main compounds in quanduzhong capsules

A total of 51 chromatographic peaks of Quanduzhong capsules were identified by LC–MS/MS. The total ion chromatogram (TIC) and base peak chromatogram (BPC) are shown in Figures 1, 2. Supplementary Table S1 shows the results of the chemical components in Quanduzhong capsules.

3.2 Demographic and baseline characteristics

A total of 60 patients were enrolled at 3 centers (Xiyuan Hospital, The First Affiliated Hospital of Guangxi University of Chinese Medicine, and Jiangxi Provincial People's Hospital) from June 2018 to June 2020. The flow chart of this study is presented in Figure 3. Sixty patients were randomized to the test group (n = 30) or the control group (n = 30). Over the course of this study, there was a 1 week sham lead-in period and a 4 week test period. After the sham lead-in period, two patients were excluded who did not meet the inclusion criteria. Overall, 51 (85%) patients completed the study, and 9 (15%) patients did not. Specifically, two patients from Jiangxi Provincial People's Hospital and one patient from The First Affiliated Hospital of Guangxi University of Chinese Medicine discontinued treatment because of unsatisfactory therapeutic effects; three patients from The First Affiliated Hospital of Guangxi University of Chinese Medicine were lost to follow-up because of the COVID-19 epidemic; two patients from Xiyuan Hospital were lost to follow-up for personal reasons; and one patient from The First Affiliated Hospital of Guangxi University of Chinese Medicine was excluded because of incorrect inclusion. The FAS included 58 (97%) patients, with 29 from the test group and 29 from the control group. The PPS

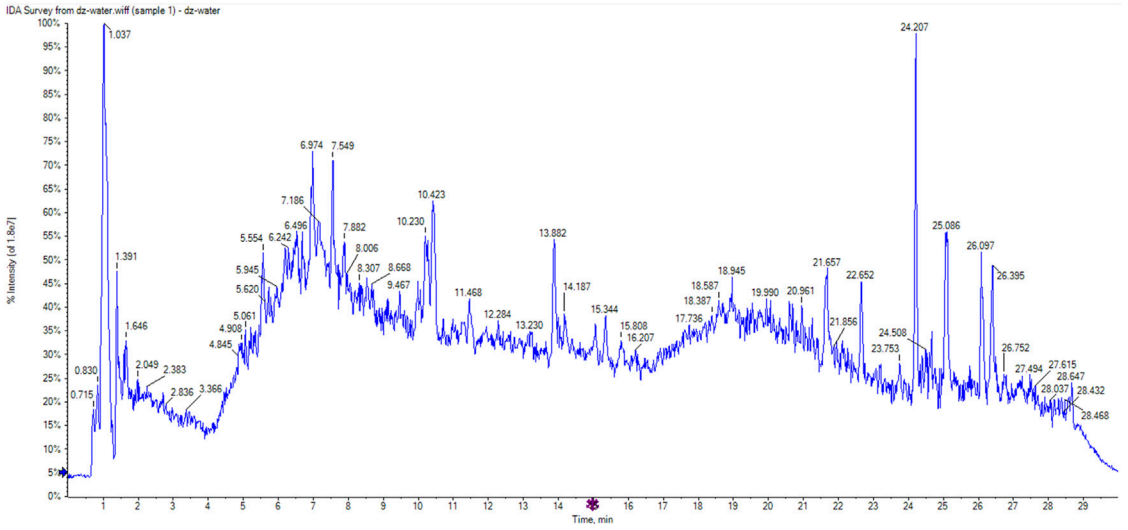

FIGURE 1
TIC of Quanduzhong capsules.

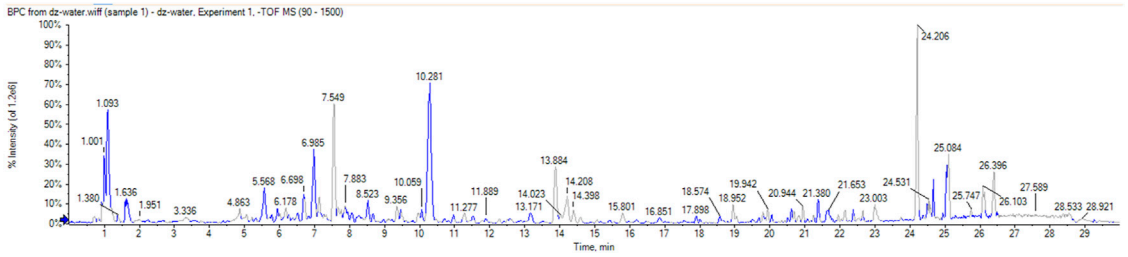

FIGURE 2
BPC of Quanduzhong capsules.

included 51 (85%) patients, with 29 from the test group and 22 from the control group.

Baseline characteristics were comparable across the test and control groups and are presented in Table 1. Of all 58 subjects, 19 were women and 39 were men. The mean age of the subjects was 52.78 years. The mean height was 165.30 cm. The mean weight was 69.36 kg. Fifty-four patients were of Chinese Han ethnicity. In addition, 30 subjects were at low risk and 28 were at moderate risk. Two subjects had a history of drug or other allergies. Twenty-three patients had a history of other diseases. Forty-five patients received no treatment with medicine or non-pharmaceutical therapies within the last 3 months. In addition, eight male patients were smokers (1 in the test group and seven in the control group). There were no significant differences in baseline characteristics between the test and control groups ($p > .05$), except for smoking ($p = .02$).

3.3 Efficacy

3.3.1 ABPM index analysis

As the primary outcome, changes in the 24-h mean SBP and DBP are presented in Table 2 and Figure 4; in the test group, the 24-h mean SBP decreased by 2.52 ± 12.09 mmHg, and the 24-h mean DBP decreased by 1.17 ± 6.65 mmHg; in the control group, the 24-h mean SBP decreased by 1.93 ± 9.63 mmHg, and the 24-h mean DBP decreased by 0.41 ± 7.26 mmHg. The differences in SBP and DBP between the test and control groups were not significant ($p > .05$).

Various other indices of 24-h ABPM presented as secondary outcomes are shown in Tables 2, 3 and Figure 5. For FAS (results were consistent with the PPS), at baseline in the test and control groups, the CV of DBP by ABPM was 14.83 ± 5.04 and 13.32 ± 3.31, respectively. After 4 weeks, the CV values were 12.45 ± 2.93 and 14.07 ± 2.8; the difference values were −2.49 ± 4.32 and 0.76 ± 4.3. The CV of DBP after the test period decreased in the test group and increased in the control group, and the differences between the two groups were significant ($p = .01$). For the CV of SBP, the difference values between baseline and 4 weeks later were −1.65 ± 3.41 (test group) and 0.37 ± 2.83 (control group), but the differences were not significant ($p = .07$). The changes in CV are shown in Figure 5. In addition, as shown in Table 2, other 24-h ABPM values, such as the mean BP, mean arterial pressure, mean pulse, daytime BP, nocturnal BP, early morning and morning peak BP, area under the BP curve and smoothness index, were not found to be significantly different between the two groups. The percentage of patients with circadian restoration

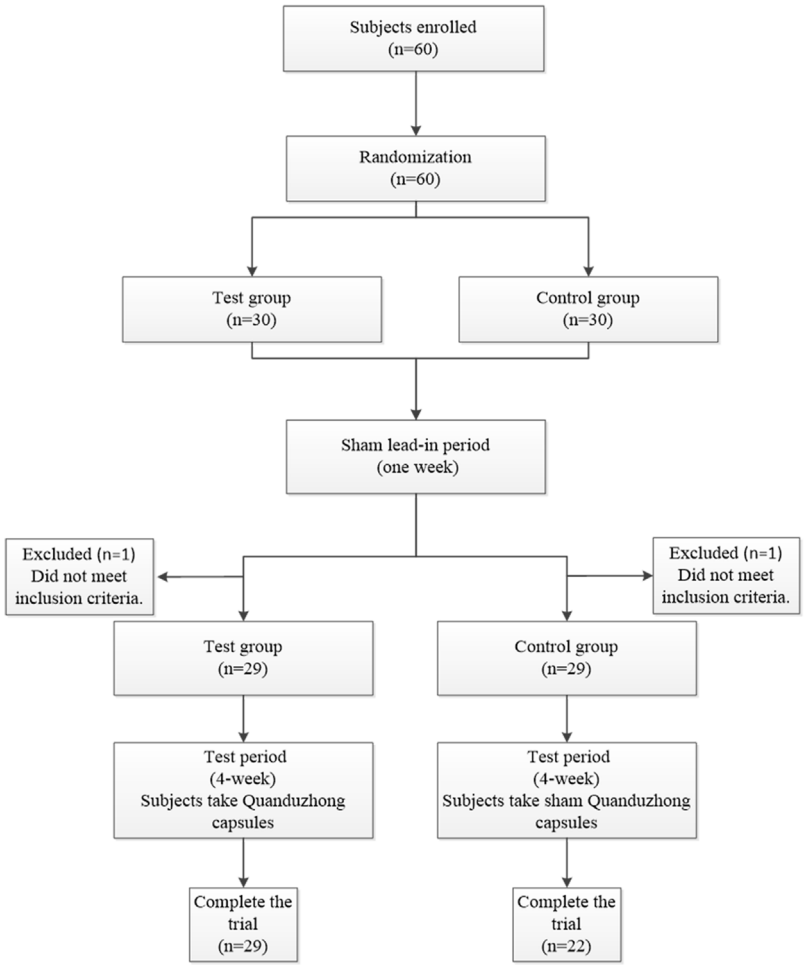

FIGURE 3
Flow chart of the study.

is listed in Table 3. The test group was 9.09%/9.09% (FAS/PPS), and the control group was 10%/25% (FAS/PPS); there were no significant differences ($p > .05$).

3.3.2 Office BP

Office SBP and DBP were other primary outcomes. At baseline, there were no statistically significant differences between the two groups. After 4 weeks of treatment, the SBP and DBP in both groups were decreased. In the FAS, SBP decreased 7.62 ± 9.32 mmHg in the test group and decreased 3.55 ± 7.55 mmHg in the control group, and DBP decreased 4.66 ± 6.03 mmHg and 0.38 ± 6.65 mmHg, respectively. The difference in SBP and DBP between the two groups was significant ($p < .05$). In PPS, the difference in DBP between the two groups was significant ($p = .03$), but no significant difference was found in SBP ($p = .13$) (Table 4; Figure 6).

3.3.3 Home BP and other outcomes

After 4 weeks of treatment, for home BP, the normotensive test group comprised 18 (62.07%) subjects in the FAS and 18 (62.07%) subjects in the PPS, while the normotensive control group comprised 11 (37.93%) subjects in the FAS and 7 (31.82%) subjects in the PPS. In addition, the number (percentage) of subjects in the test group who experienced a decrease in home BP was 19 (65.52%) in the FAS and 19 (65.52%) in the PPS, while in the control group, the number (percentage) of subjects was 15 (51.72%) in the FAS and 11 (50%) in the PPS, but there were no significant differences between the two groups ($p > .05$). Changes observed in home BP after treatment are shown in Table 5, and there were no significant differences.

Regarding the quality-of-life evaluation, which was performed using the WHOQOL-BREF questionnaire, and the grading and quantitative evaluation of hypertension symptoms, no significant differences were found between the two groups, either at baseline or after 4 weeks of treatment.

Regarding laboratory indicators, a few participants had abnormal baseline results, so we decided to describe the results and not to perform hypothesis testing. In the test group, there were no patients with baseline abnormal PRA, Ang II, or ALD. In the control group, one patient had abnormal PRA with a value of 42.78 pg/ml; after 4 weeks of treatment, the value was 20.99 pg/ml. One patient had abnormal Ang II, and the baseline and 4 week values were 923.97 pg/ml and 1012.28 pg/ml, respectively. There was one patient who was found to have abnormal ALD in the control group; the baseline value was 310.81 pg/ml with no change after 4 weeks. The results of β_2m and Hcy are shown in Table 6.

TABLE 1 Baseline characteristics of the study subjects.

Characteristics	Test group	Control group	*p*
Age—yrs	53.76 ± 11.29	51.79 ± 9.49	.48
Sex			.78
Male	20	19	
Female	9	10	
Ethnicity			.61
Han	26	28	
Other ethnic groups	3	1	
Risk			.29
Low risk	17	13	
Moderate risk	12	16	
High risk	0	0	
Height (cm)	165.07 ± 6.24	165.52 ± 8.58	.82
Weight (kg)	67.81 ± 10.17	70.9 ± 13.12	.32
History of drug or other allergies			.49
Yes	0	2	
No	29	27	
History of other diseases			.42
Yes	10	13	
No	19	16	
Treatment with medicine or non-pharmaceutical therapies within 3 months			.34
Yes	8	5	
No	21	24	
Smoking or not			.02
Currently smoking	1	7	
1–9 cigarettes per day	0	4	
≥10 cigarettes per day	1	3	
Quit smoking	0	1	
Never smoked	28	21	

4 Safety

No abnormal vital signs (except BP) or severe liver or renal function impairment were observed during the treatment periods. As shown in Supplementary Table S2, in the SS analysis (n = 59), 22 (37.29%) patients experienced 23 AEs, and 15 ADRs were reported in 14 (23.73%) patients. In addition, AEs were confirmed in 12 (40%) patients from the test group and 10 (34.48%) from the control group; 8 (26.67%) patients in the test group and 6 (20.69%) patients in the control group experienced ADRs. AEs and ADRs were not significantly different between groups (AE, p = .66; ADR, p = .59) (Supplementary Table S3). In our study, both AEs and ADRs were mild, without leading to unblinding. No patients withdrew from the trial. Detailed information is listed in Supplementary Tables S4, S5.

5 Discussion

Our results demonstrated that treatment with Quanduzhong capsules can result in a greater reduction in office BP and in the DBP CV of 24-h ABPM compared with placebo. There is general agreement that patients with grade 2 or 3 hypertension should be treated with antihypertensive drugs and lifestyle interventions. In addition, guidelines consistently recommend that patients with grade 1 hypertension who are at high cardiovascular risk or who have hypertension-mediated organ damage should be treated with BP-lowering medication. It has been less consistent regarding whether BP-lowering drugs should be prescribed to patients with grade 1 hypertension and low-to-moderate risk; that is, the benefit of antihypertensive medication in individuals with grade 1 hypertension with low-to-moderate risk is controversial, so there is room for alternative therapies (Zanchetti, 2015). TCM plays a significant role in this field. A recent meta-analysis reported that long-term variability in BP is associated with cardiovascular and mortality outcomes (Stevens et al., 2016). Thus, decreasing BP variability is essential in the treatment of hypertension. The efficacy of Quanduzhong capsules in reducing the CV of DBP was demonstrated in our study. Many Chinese herbal formulae have also been found to reduce the CV of BP; these include Qingxuanjiangya decoction, Niuhuangjiangya pills, and Banxia Baizhu Tianma decoction, which are used for treating liver fire/liver-yang hyperactivity pattern and phlegm-fluid retention pattern in hypertensive patients (Xiong et al., 2013a).

For Hcy, the baseline values of three patients were abnormal in the test and control groups. After 4 weeks, the Hcy level in the test group was significantly lower than that in the control group. Thus, treatment with Quanduzhong capsules may be associated with a decrease in Hcy levels. However, we cannot draw firm conclusions given our small

TABLE 2 Changes in 24-h ABPM values.

	FAS difference value			PPS difference value		
	Test group	Control group	*p*	Test group	Control group	*p*
24-h MSBP	−2.52 ± 12.09	−1.93 ± 9.63	.58	−2.52 ± 12.09	−2.55 ± 11.04	.71
24-h MDBP	−1.17 ± 6.65	−0.41 ± 7.26	.34	−1.17 ± 6.65	−0.55 ± 8.38	.41
24-h MAP	−1.69 ± 8.38	−1 ± 7.97	.37	−1.69 ± 8.38	−1.32 ± 9.18	.48
24-h MP	1.89 ± 7	2.04 ± 5.85	.90	1.96 ± 7.13	2.75 ± 6.7	.70
Daytime MSBP	−2 ± 17.28	−1.93 ± 10.62	.39	−2 ± 17.28	−2.55 ± 12.2	.45
Daytime MDBP	−1.76 ± 6.84	−0.24 ± 7.83	.16	−1.76 ± 6.84	−0.32 ± 9.04	.22
Daytime MAP	−2.31 ± 8.72	−0.66 ± 8.63	.17	−2.31 ± 8.72	−0.86 ± 9.96	.23
Daytime MP	1.41 ± 7.44	1.79 ± 6.06	.72	1.46 ± 7.59	2.5 ± 7.09	.47
N MSBP	1.68 ± 12.91	−0.93 ± 14.47	.79	1.74 ± 13.15	−1.23 ± 16.7	.79
N MDBP	1.64 ± 8.49	−0.86 ± 11	.63	1.7 ± 8.64	−1.14 ± 12.69	.78
N MAP	1.36 ± 9.72	−0.9 ± 11.97	.83	1.41 ± 9.9	−1.18 ± 13.81	.88
N MP	2.5 ± 6.52	3.11 ± 8.02	.77	2.71 ± 6.75	4.35 ± 9.26	.51
SBP Load	−4.76 ± 16.52	−1.99 ± 18.5	.27	−4.96 ± 16.84	−2.79 ± 22	.36
DBP Load	−1.88 ± 16.77	2.25 ± 22.48	.27	−1.96 ± 17.12	3.16 ± 26.74	.33
SBP AUC	−46.48 ± 481.94	−68.28 ± 288.28	.90	−46.48 ± 481.94	−90 ± 329.78	.99
DBP AUC	−22.66 ± 296.52	−30.83 ± 196.16	.73	−22.66 ± 296.52	−40.64 ± 225.58	.77
Early morning SBP	−3.19 ± 15.67	−1.71 ± 10.9	.26	−3.54 ± 19.41	−2.94 ± 13.68	.29
Early morning DBP	−2.11 ± 12.95	−0.63 ± 7.43	.18	−2.68 ± 14.4	−0.02 ± 8.98	.03
Morning peak BP	−5.85 ± 14.67	−1.67 ± 15.55	.40	−6.31 ± 16.53	−3.83 ± 18.57	.32
Smoothness index in SBP	−0.02 ± 0.13	−0.03 ± 0.08	.82	−0.02 ± 0.13	−0.04 ± 0.09	.89
Smoothness index in DBP	0.01 ± 0.12	−0.01 ± 0.08	.82	0.01 ± 0.12	−0.02 ± 0.09	.87

FAS = the full analysis set; PPS = the per protocol set; MSBP = mean systolic blood pressure; MDBP = mean diastolic blood pressure; MAP = mean arterial pressure; MP = mean pulse; N = nocturnal; AUC = area under the BP, curve.

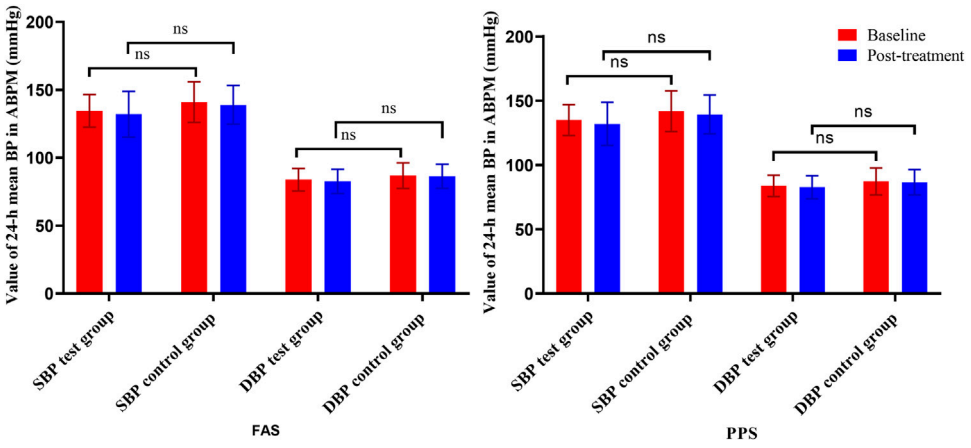

FIGURE 4
Changes in the 24-h mean BP from ABPM (left is FAS; right is PPS). *Note: ns = non-significant.*

TABLE 3 Percentage of patients with circadian restoration.

	FAS/PPS		
	Test group	Control group	*p*
Non-dipper hypertension in baseline	11/11	10/4	
Dipper hypertension after treatment (%)	1 (9.09)/1 (9.09)	1 (10)/1 (25)	1/.48

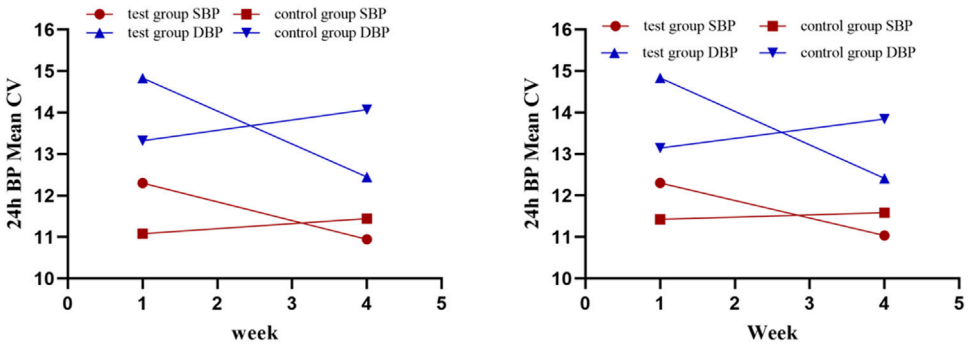

FIGURE 5
24-h BP mean CV (left is FAS; right is PPS).

TABLE 4 Changes in office BP (FAS, PPS).

	FAS			PPS		
	Test group	Control group	*p*	Test group	Control group	*p*
MSBP in baseline	144.69 ± 7.31	147.1 ± 7.55	.22	144.69 ± 7.31	146.64 ± 8.26	.38
MDBP in baseline	90.31 ± 6.52	91.9 ± 5.95	.34	90.31 ± 6.52	91.5 ± 6.49	.52
MSBP in 4 weeks	137.07 ± 8.92	143.55 ± 9.73	.01	137.07 ± 8.92	141.96 ± 10.41	.08
MDBP in 4 weeks	85.66 ± 8.2	91.52 ± 8.75	.01	85.66 ± 8.2	91 ± 9.83	.04
Difference in SBP	−7.62 ± 9.32	−3.55 ± 7.55	.03	−7.62 ± 9.32	−4.68 ± 8.4	.13
Difference in DBP	−4.66 ± 6.03	−0.38 ± 6.65	.01	−4.66 ± 6.03	−0.5 ± 7.67	.03

sample size. The elevation of plasma Hcy is identified as an independent risk factor for cardiovascular disease and is associated with an increased risk of ischemic stroke (Ganguly and Alam, 2015; Koller et al., 2018; Yuan et al., 2021). Thus, this finding is worthy of further investigation.

"Syndrome" or "pattern" refers to a pathological state that manifests itself as a corresponding set of signs and symptoms, representative of a specific stage in the progression of the disease in TCM. There are various Chinese medicine patterns for hypertension, each with its own specific symptoms and constitutions, with dizziness or headache being the primary complaint. According to the "*Expert Consensus on Diagnosis and Treatment of Hypertension with Traditional Chinese Medicine*", the patterns of hypertension include kidney essence insufficiency, kidney yang deficiency, yin and yang deficiency, liver yang ascendant hyperactivity, liver yang and yin deficiency, etc. (Society of Cardiovascular Diseases and China Association of Chinese Medicine, 2019). The pathogenesis of hypertension is largely attributed to kidney deficiency, and tonifying the kidney has become a new strategy for reducing BP (Society of Cardiovascular Diseases and China Association of Chinese Medicine, 2019). As a classic pattern in TCM, kidney deficiency is characterized by feeling vexed, difficulty falling asleep, ringing in the ears, a cold feeling in the back, aversion to wind, and soreness in the lower back and knees. In East Asia, particularly in China, Korea, and Japan, DZ is commonly used as an herbal kidney-tonifying remedy to treat hypertension, either alone or in combination with other medications.

The Quanduzhong capsules used in our study consist of an extract of DZ bark. DZ belongs to the monotypic genus Eucommia (Cronquist, 1981), which has been used as a traditional medical therapy for approximately 2000 years. As an upper grade drug, DZ was first recorded in the Shen Nong Ben Cao Jing (Sheng Nong's herbal classic). The bark, leaves, seeds, and even male flowers of this plant are commonly used as medicine. DZ bark was documented in

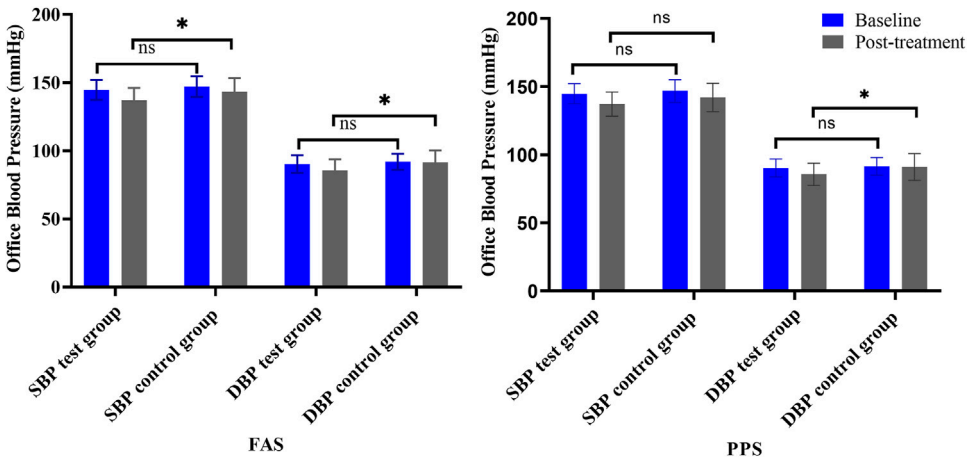

FIGURE 6
Changes in office BP (left is FAS; right is PPS). *Note: ns = non-significant. *p < .05* versus *posttreatment.*

TABLE 5 Changes in home BP from baseline to 4 weeks (FAS, PPS).

	FAS difference value			PPS difference value		
	Test group	Control group	*p*	Test group	Control group	*p*
SBP	−2.68 ± 9.8	−0.21 ± 11.35	.19	−2.78 ± 9.97	−0.24 ± 12.13	.25
DBP	−3.17 ± 11.8	−1.24 ± 9.08	.15	−3.28 ± 12	−1.41 ± 9.69	.22

TABLE 6 Changes in β_2m and Hcy.

	β_2m (mg/L)		Hcy (μmol/L)	
	Test group	Control group	Test group	Control group
N	4	3	3	8
Mean difference	−0.07 ± 0.18	−0.15 ± 1.39	−6.23 ± 9.15	−0.87 ± 2.03

the Pharmacopoeia Committee of the People's Republic of China 2020 for its effects of tonifying the liver and kidneys, strengthening muscles and bones, and calming fetuses; similar to DZ bark, DZ leaves nourish the liver and kidneys, strengthen the tendons and bones and are often employed as an alternative medicine. The medicinal properties of DZ include antihypertensive, antiinflammatory, antihyperlipidemic, antidiabetic, antioxidant, and antitumor properties (He et al., 2014; Shao et al., 2015; Zhang et al., 2022b).

The antihypertensive efficacy of DZ has been known for over 40 years, and evidence for the efficacy of DZ against hypertension was identified in modern pharmacological studies. (+)-Pinoresinol di-β-d-glucoside is the main antihypertensive pharmacological active compound, which was reported as early as 1970 (Sih et al., 1976). Recent studies have found that lignans, flavonoids, and iridoids from DZ exert hypotensive effects, potentially due to inhibiting oxidative stress, improving endothelial dysfunction, regulating the autonomic nervous system, activating ion channels, and regulating the renin-angiotensin-aldosterone (RAAS) system (Sih et al., 1976; Li et al., 2013; He et al., 2014; Hosoo et al., 2015). Both the bark and leaves of DZ exhibit these biological activities.

Several animal models and patients with hypertension are reported to have gut dysbiosis, characterized by reduced diversity and an abnormal structure (Sun et al., 2019). In a recent study by Yan D et al. (Yan et al., 2022), a high-salt diet and N (omega)-nitro-L-arginine methyl ester-induced hypertensive mice were treated with bark extract, which improved blood pressure, ameliorated kidney injury, decreased serum IL-6 and IL-17α as well as renal IL-17α, and restored gut microbiota diversity and composition. The potential gut bacteria involved in the antihypertensive action of DZ was suggested to be Parabacteroides strain XGB65, which exerted antihypertensive effects by lowering the levels of inflammatory cytokines such as renal IL-17α (Yan et al., 2022).

Antihypertensive effects have been shown for other parts of DZ. DZ leaves are effective against secondary hypertension, such as renal hypertension and salt-sensitive hypertension, as well as hypertension

caused by thoracic aortic endothelial dysfunction, high-fat diets, and oxidized low-density lipoprotein by regulating the Ras homolog family member A/Rho-associated protein kinase signaling and NO/soluble guanylate cyclase/cyclic guanosine monophosphate signaling pathways (Li et al., 2022). In spontaneously hypertensive rats, the male flower extract of DZ exhibited antihypertensive effects by targeting the angiotensin-converting enzyme 2/angiotensin (1–7)/Mas signaling pathway (Ding et al., 2020). In addition, DZ can lower BP when combined with other herbs. For example, DZ and Jili (Tribulus terrestris L.) inhibit the onset and progression of hypertension by regulating ferroptosis in vascular neuron cells by acting on proteins associated with neuroactive ligand–receptor interactions (Zhang et al., 2022b). Overall, DZ is considered a promising therapy for treating hypertension due to its extensive biological activities.

A previous study using approaches based on network robustness identified 21 possible active compounds in Quanduzhong capsules that may target 13 genes specifically expressed in glomeruli, including RAAS, lipid metabolism, immune response, and inflammatory response (Guo et al., 2019). In these biological processes, primary hypertension factors and kidney protection factors are implicated, demonstrating that Quanduzhong capsules may improve renal function and reduce hypertensive risk factors by inhibiting inflammation, reducing oxidative stress, and regulating metabolic homeostasis (Guo et al., 2019). There is, however, a need for further experimental verification of the molecular mechanisms involved in the BP-lowering effects of Quanduzhong capsules.

This study has some limitations that should be addressed in future studies. First, the sample was small, containing only 60 patients. Second, although recruited from three hospitals in China, all patients selected in this study were Chinese; thus, the broad representativeness is limited. Third, the 4-week study duration was short. A trial with a larger sample size and a longer course of treatment is needed in the future. Fourth, TCM patterns need to be incorporated into the inclusion criteria in future studies.

6 Conclusion

Treatment with Quanduzhong capsules was superior to placebo for reducing office SBP and DBP and the DBP CV of 24-h ABPM. As far as safety is concerned, Quanduzhong capsules did not result in any noticeable adverse effects compared to placebo.

Data availability statement

The original contributions presented in the study are included in the article/Supplementary Material, further inquiries can be directed to the corresponding author.

Ethics statement

The studies involving human participants were reviewed and approved by Ethic Committee of Xiyuan Hospital of China Academy of Chinese Medical Sciences (Ethical Approval Number: 2018XL006-6). The patients/participants provided their written informed consent to participate in this study.

Author contributions

HX conceived the concept for the study and was accountable for its design. XX and WT analyzed the data, normalized the figures, and wrote the original draft. XX, WD, CP and MH, QW, QY and ZW, YT, YX and ZZ, YL, DW and WQ, XO, SY, and XW collected the data. ZZ, XL, YC, SY, HX and XX reviewed and revised the manuscript. All the authors approved the final version and agreed to be accountable for all aspects of the work in ensuring that questions related to the accuracy or integrity of any part of the work are appropriately investigated and resolved.

Funding

A traditional Chinese medicine comprehensive anti-hypertensive ABC regimen for patients with grade 1 hypertension at low-moderate-risk: Study protocol for a prospective randomized controlled trial (GZY-KJS-2020–074).

Acknowledgments

The authors would like to thank the National Clinical Research Center for Chinese Medicine Cardiology for their support of this work.

Conflict of interest

ZZ, XL, YC and SY are employed by Jiangxi Puzheng Pharmaceutical Co., Ltd., China.

The remaining authors declare that the research was conducted in the absence of any commercial or financial relationships that could be construed as a potential conflict of interest.

The reviewer XX declared a shared parent affiliation with the authors XX, WT, WD and HX to the handling editor at the time of review.

Publisher's note

Supplementary material

The Supplementary Material for this article can be found online at: https://www.frontiersin.org/articles/10.3389/fphar.2022.1014410/full#supplementary-material

References

Belknap, R., Holland, D., Feng, P. J., Millet, J. P., Caylà, J. A., Martinson, N. A., et al.TB Trials Consortium iAdhere Study Team (2017). Self-administered versus directly observed once-weekly isoniazid and rifapentine treatment of latent tuberculosis infection: A randomized trial. *Ann. Intern Med.* 167 (10), 689–697. doi:10.7326/M17-1150

Cronquist, A. (1981). *An integrated system of classification of flowering plants*. New York: Columbia University Press.

Ding, Z. J., Liang, C., Wang, X., Yao, X., Yang, R. H., Zhang, Z. S., et al. (2020). Antihypertensive activity of Eucommia ulmoides Oliv: Male flower extract in spontaneously hypertensive rats. *Evid. Based Complement. Altern. Med.* 2020, 20206432173. doi:10.1155/2020/6432173

Ettehad, D., Emdin, C. A., Kiran, A., Anderson, S. G., Callender, T., Emberson, J., et al. (2016). Blood pressure lowering for prevention of cardiovascular disease and death: A systematic review and meta-analysis. *Lancet* 387 (10022), 957–967. doi:10.1016/S0140-6736(15)01225-8

Ganguly, P., and Alam, S. F. (2015). Role of homocysteine in the development of cardiovascular disease. *Nutr. J.* 14, 6. doi:10.1186/1475-2891-14-6

Guo, F., Zhang, W., Su, J., Xu, H., and Yang, H. (2019). Prediction of drug positioning for quan-du-zhong capsules against hypertensive nephropathy based on the robustness of disease network. *Front. Pharmacol.* 10, 49. doi:10.3389/fphar.2019.00049

He, X., Wang, J., Li, M., Hao, D., Yang, Y., Zhang, C., et al. (2014). Eucommia ulmoides Oliv.: Ethnopharmacology, phytochemistry and pharmacology of an important traditional Chinese medicine. *J. Ethnopharmacol.* 151 (1), 78–92. doi:10.1016/j.jep.2013.11.023

Hosoo, S., Koyama, M., Kato, M., Hirata, T., Yamaguchi, Y., Yamasaki, H., et al. (2015). The restorative effects of Eucommia ulmoides oliver leaf extract on vascular function in spontaneously hypertensive rats. *Molecules* 20 (12), 21971–21981. doi:10.3390/molecules201219826

Hypertension (2021). Available at:https://www.who.int/news-room/fact-sheets/detail/hypertension.

Jiang, L. J., Yang, Y., Tang, B. H., Wang, C. C., Zhang, Q. S., Xiang, K., et al. (2022). Randomized controlled trial of Quanduzhong capsule on reducing blood pressure in patients with essential hypertension with shen deficiency syndrome. *Chin. J. Integr. Traditional West. Med.* 42 (04), 431–437. doi:10.7661/j.cjim.20220302.092

Joint Committee for Guideline Revision (2018). 2018 Chinese guidelines for prevention and treatment of hypertension-A report of the revision committee of Chinese guidelines for prevention and treatment of hypertension. *J. Geriatr. Cardiol.* 16 (3), 182–241. doi:10.11909/j.issn.1671-5411.2019.03.014

Koller, A., Szenasi, A., Dornyei, G., Kovacs, N., Lelbach, A., and Kovacs, I. (2018). Coronary microvascular and cardiac dysfunction due to homocysteine pathometabolism; A complex therapeutic design. *Curr. Pharm. Des.* 24 (25), 2911–2920. doi:10.2174/1381612824666180625125450

Li, M., Zheng, Y., Deng, S., Yu, T., Ma, Y., Ge, J., et al. (2022). Potential therapeutic effects and applications of Eucommiae Folium in secondary hypertension. *J. Pharm. Anal.* 12 (5), 711–718. doi:10.1016/j.jpha.2021.10.004

Li, Z. Y., Gu, J., Yan, J., Wang, J. J., Huang, W. H., Tan, Z. R., et al. (2013). Hypertensive cardiac remodeling effects of lignan extracts from Eucommia ulmoides Oliv. bark--a famous traditional Chinese medicine. *Am. J. Chin. Med.* 41 (4), 801–815. doi:10.1142/S0192415X13500547

Meng, T., Wang, P., Xie, X., Li, T., Kong, L., Xu, Y., et al. (2022). Efficacy and safety of songling xuemaikang capsule for essential hypertension: A systematic review and meta-analysis of randomized controlled trials. *Phytomedicine* 107, 154459. doi:10.1016/j.phymed.2022.154459

Mohammed, S. A. D., Hanxing, L., Fang, L., Algradi, A. M., Alradhi, M., Safi, M., et al. (2023). Integrated Chinese herbal medicine with western medicine versus western medicine in the effectiveness of primary hypertension treatment: A systematic review and meta-analysis of randomized controlled trials. *J. Ethnopharmacol.* 300, 115703. doi:10.1016/j.jep.2022.115703

Morales Salinas, A., Coca, A., Olsen, M. H., Sanchez, R. A., Sebba-Barroso, W. K., Kones, R., et al. (2017). Clinical perspective on antihypertensive drug treatment in adults with grade 1 hypertension and low-to-moderate cardiovascular risk: An international expert consultation. *Curr. Probl. Cardiol.* 42 (7), 198–225. doi:10.1016/j.cpcardiol.2017.03.001

Ren, X., Liu, D., Ding, N., Huang, K., Xiong, Y., Du, G., et al. (2012). Safety evaluation of cephalosporins based on utilization and adverse drug events: Analysis of two databases in China. *Expert Opin. Drug Saf.* 11 (5), 689–697. doi:10.1517/14740338.2012.699037

Schulz, K. F., Altman, D. G., and Moher, D.CONSORT Group (2010). CONSORT 2010 statement: Updated guidelines for reporting parallel group randomised trials. *Trials* 11, 32. doi:10.1186/1745-6215-11-32

Shao, P., Zhang, J. F., Chen, X. X., and Sun, P. L. (2015). Microwave-assisted extraction and purification of chlorogenic acid from by-products of Eucommia Ulmoides Oliver and its potential anti-tumor activity. *J. Food Sci. Technol.* 52 (8), 4925–4934. doi:10.1007/s13197-014-1571-8

Sih, C. J., Ravikumar, P. R., Huang, F. C., Buckner, C., and Whitlock, H., Jr (1976). Letter: Isolation and synthesis of pinoresinol diglucoside, a major antihypertensive principle of Tu-Chung(Eucommia ulmoides, Oliver). *J. Am. Chem. Soc.* 98 (17), 5412–5413. doi:10.1021/ja00433a070

Society of Cardiovascular Diseases, China Association of Chinese Medicine (2019). Expert Consensus on Diagnosis and treatment of hypertension with traditional Chinese medicine. *Chin. J. Exp. Traditional Med. Formulae* 25 (15), 217–221. doi:10.13422/j.cnki.syfjx.20191521

Stevens, S. L., Wood, S., Koshiaris, C., Law, K., Glasziou, P., Stevens, R. J., et al. (2016). Blood pressure variability and cardiovascular disease: Systematic review and meta-analysis. *BMJ* 354, i4098. doi:10.1136/bmj.i4098

Sun, S., Lulla, A., Sioda, M., Winglee, K., Wu, M. C., Jacobs, D. R., et al. (2019). Gut microbiota composition and blood pressure. *Hypertension* 73 (5), 998–1006. doi:10.1161/HYPERTENSIONAHA.118.12109

Williams, B., Mancia, G., Spiering, W., Agabiti Rosei, E., Azizi, M., Burnier, M., et al.ESC Scientific Document Group (2018). 2018 ESC/ESH Guidelines for the management of arterial hypertension.Erratum in. *Eur. Heart JEur Heart J.* 3940 (335), 3021475–3023104. doi:10.1093/eurheartj/ehy339

Xiong, X., Yang, X., Feng, B., Liu, W., Duan, L., Gao, A., et al. (2013). Zhen gan xi feng decoction, a traditional Chinese herbal formula, for the treatment of essential hypertension: A systematic review of randomized controlled trials. *Evid. Based Complement. Altern. Med.* 2013, 982380. doi:10.1155/2013/982380

Xiong, X., Yang, X., Liu, Y., Zhang, Y., Wang, P., and Wang, J. (2013). Chinese herbal formulas for treating hypertension in traditional Chinese medicine: Perspective of modern science. *Hypertens. Res.* 36 (7), 570–579. doi:10.1038/hr.2013.18

Yan, D., Si, W., Zhou, X., Yang, M., Chen, Y., Chang, Y., et al. (2022). Eucommia ulmoides bark extract reduces blood pressure and inflammation by regulating the gut microbiota and enriching the Parabacteroides strain in high-salt diet and N(omega)-nitro-L-arginine methyl ester induced mice. *Front. Microbiol.* 13, 967649. doi:10.3389/fmicb.2022.967649

Yuan, S., Mason, A. M., Carter, P., Burgess, S., and Larsson, S. C. (2021). Homocysteine, B vitamins, and cardiovascular disease: A mendelian randomization study. *BMC Med.* 19 (1), 97. doi:10.1186/s12916-021-01977-8

Zanchetti, A. (2015). Do we over treat mild hypertension? *Expert Opin. Pharmacother.* 16 (8), 1121–1126. doi:10.1517/14656566.2015.1040761

Zhang, D. Y., Cheng, Y. B., Guo, Q. H., Shan, X. L., Wei, F. F., Lu, F., et al. (2020). Treatment of masked hypertension with a Chinese herbal formula: A randomized, placebo-controlled trial. *Circulation* 142 (19), 1821–1830. doi:10.1161/CIRCULATIONAHA.120.046685

Zhang, G. X., Song, X., Guo, L. L., and Zhao, J. W. (2022). An analysis of Quan Du Zhong capsules in the treatment of new-onset mild hypertension. *Chin. J. Clin. Ration. Drug Use* 15 (16), 54–56. doi:10.15887/j.cnki.13-1389/r.2022.16.016

Zhang, Q., Yang, J., Yang, C., Yang, X., and Chen, Y. (2022). Eucommia ulmoides oliver-tribulus terrestris L. Drug pair regulates ferroptosis by mediating the neurovascular-related ligand-receptor interaction pathway- A potential drug pair for treatment hypertension and prevention ischemic stroke. *Front. Neurol.* 13, 833922. doi:10.3389/fneur.2022.833922

Zhang, Z. Q., and Wei, J. R. (2018). Observation on clinical efficacy of complete Eucommia ulmoides capsules in the treatment of renal hypertension and their safety evaluation. *Chin. J. Ration. Drug Use* 15 (12), 73–77. doi:10.3969/j.issn.2096-3327.2018.12.022

frontiers | Frontiers in Pharmacology

TYPE Review
PUBLISHED 24 February 2023
DOI 10.3389/fphar.2023.1038906

OPEN ACCESS

EDITED BY
Hai-Dong Guo,
Shanghai University of Traditional Chinese Medicine, China

REVIEWED BY
Hui Cui,
Guangzhou University of Chinese Medicine, China
Peter Akah,
University of Nigeria, Nsukka, Nigeria

*CORRESPONDENCE
Ren Chaoxiang,
764793950@qq.com
Pei Jin,
peixjin@163.com

†These authors have contributed equally to this work

SPECIALTY SECTION
This article was submitted to Ethnopharmacology, a section of the journal Frontiers in Pharmacology

RECEIVED 07 September 2022
ACCEPTED 13 February 2023
PUBLISHED 24 February 2023

CITATION
Huajuan J, Xulong H, Bin X, Yue W, Yongfeng Z, Chaoxiang R and Jin P (2023), Chinese herbal injection for cardio-cerebrovascular disease: Overview and challenges. *Front. Pharmacol.* 14:1038906. doi: 10.3389/fphar.2023.1038906

Chinese herbal injection for cardio-cerebrovascular disease: Overview and challenges

Jiang Huajuan[1,2†], Huang Xulong[1,2†], Xian Bin[1,2], Wang Yue[1,2], Zhou Yongfeng[1,2], Ren Chaoxiang[1,2*] and Pei Jin[1,2*]

[1]State Key Laboratory of Southwestern Chinese Medicine Resources, Chengdu, China, [2]Pharmacy College, Chengdu University of Traditional Chinese Medicine, Chengdu, China

Cardio-cerebrovascular diseases are the leading cause of death worldwide and there is currently no optimal treatment plan. Chinese herbal medicine injection (CHI) is obtained by combining traditional Chinese medicine (TCM) theory and modern production technology. It retains some characteristics of TCM while adding injection characteristics. CHI has played an important role in the treatment of critical diseases, especially cardio-cerebrovascular diseases, and has shown unique therapeutic advantages. TCMs that promote blood circulation and remove blood stasis, such as *Salvia miltiorrhiza*, *Carthami flos*, *Panax notoginseng*, and *Chuanxiong rhizoma*, account for a large proportion of CHIs of cardio-cerebrovascular disease. CHI is used to treat cardio-cerebrovascular diseases and has potential pharmacological activities such as anti-platelet aggregation, anti-inflammatory, anti-fibrosis, and anti-apoptosis. However, CHIs have changed the traditional method of administering TCMs, and the drugs directly enter the bloodstream, which may produce new pharmacological effects or adverse reactions. This article summarizes the clinical application, pharmacological effects, and mechanism of action of different varieties of CHIs commonly used in the treatment of cardio-cerebrovascular diseases, analyzes the causes of adverse reactions, and proposes suggestions for rational drug use and pharmaceutical care methods to provide a reference for the rational application of CHIs for cardio-cerebrovascular diseases.

KEYWORDS

Chinese herbal injection, cardio-cerebrovascular diseases, clinical application, pharmacological effects, traditional Chinese medicine

Introduction

Cardio-cerebrovascular disease is one of the most serious diseases that threaten human health today; its morbidity and mortality rates have surpassed those of tumor diseases and now rank first (Liberale et al., 2021; Xu et al., 2022). The heart and brain are the most closely related organs physiologically, and brain tissue relies on blood circulation driven by the heart to maintain normal physiological functions. At the same time, cardiovascular and cerebrovascular diseases are pathologically based on vascular occlusion caused by atherosclerotic rupture related to blood lipid levels. When abnormal blood rheology occurs, atherosclerosis may involve multiple organs, particularly the heart and brain (Novo et al., 2014; Novo et al., 2019; Keeter et al., 2022). Furthermore, cardio-cerebrovascular diseases have the same pathological basis. Research data show that about 10%–45% of patients with heart disease may have a stroke, about 78.1%–90.2% of patients

with cerebrovascular disease have an abnormal electrocardiogram, and 12.7% can be complicated by cerebral infarction (Xu et al., 2021; Lu et al., 2022).

Although conventional Western medical treatments such as nitrates, statins, receptor blockers, clopidogrel, and aspirin have good effects on cardio-cerebrovascular diseases, there are still great risks, such as embolism and bleeding caused by excessive antithrombotics (Wang Y. et al., 2022; Sikora et al., 2022). Chinese herbal injections (CHIs) play an irreplaceable role in the treatment of cardio-cerebrovascular diseases and have economic and social benefits (Feng et al., 2021; Li et al., 2022b). An increasing number of doctors tend to use certain CHIs combined with conventional Western medicine to improve their therapeutic effect (Li et al., 2015a; Liu et al., 2016). As a new dosage form of traditional Chinese medicine (TCM) preparation, CHI not only has the characteristics of injection, but also retains the characteristics of TCM to a certain extent. Its active ingredients and modern pharmacological effects are clear, and it avoids degradation of the gastrointestinal tract and the first-pass effect of the liver following oral drug administration. The clinical application of CHI is more convenient, its effect is faster, and it plays an important role in the treatment of acute and severe diseases. The research and development of CHI varieties mainly focus on the treatment of cardio-cerebrovascular diseases, respiratory systems, and tumors; in particular, the therapeutic effect of cardio-cerebrovascular diseases has been recognized by doctors and patients. A total of 134 types of CHI have been listed, encompassing 158 types of raw materials for prescription decoction pieces, and the majority (56.7%) of medicinal materials are single-agent. The types and sales of CHI for the treatment of cardio-cerebrovascular diseases are the most numerous (Hao et al., 2020).

In terms of medicine composition, TCM to promote blood circulation and remove blood stasis accounts for a large proportion of CHI for cardio-cerebrovascular diseases, such as *Salvia miltiorrhiza*, *Carthami flos*, *Panax notoginseng*, and *Chuanxiong rhizoma* (Li et al., 2015a; Sun et al., 2022). Cardio-cerebrovascular diseases such as cerebral thrombosis and coronary heart disease are related to enhanced platelet function, blood thickening, and changes in hemodynamic characteristics (Gresele et al., 2021; Li et al., 2022c). In TCM, drugs that promote blood circulation and remove blood stasis dredge blood vessels and eliminate blood stasis, which can change the platelet function and hemodynamics of patients (Li D. et al., 2022). Patients with cardio-cerebrovascular diseases can use drugs to promote blood circulation and remove blood stasis to clear blocked blood vessels and improve blood supply. TCM for promoting blood circulation and removing blood stasis has unique advantages for the treatment of cardio-cerebrovascular diseases (Li et al., 2015a; Guo R. et al., 2020).

CHI for cardio-cerebrovascular diseases

The CHI clinically used for the treatment of cardio-cerebrovascular diseases includes extracts obtained from TCM or the effective parts and single components obtained by further purification. TCM prescription injections are obtained by extracting and purifying TCM prescriptions based on the compatibility of TCM. Among these, *S. miltiorrhiza*, *C. flos*, *P. notoginseng*, and *C. rhizoma* are important drugs developed for the treatment of cardio-cerebrovascular diseases. The details of each CHI were obtained from the Chinese Medicine Information Query Platform (https://www.dayi.org.cn/), as shown in Table 1.

Single TCM extract injection

CHI is prepared from a single component extracted and purified from Chinese herbal medicines such as PI. Puerarin is an isoflavone derivative with a crown expanding effect isolated from *Pueraria lobata radix*. Puerarin can be used to treat coronary heart disease, angina pectoris, and hypertension (Ma et al., 2022; Shao et al., 2022). Puerarin treatment causes an expansion of coronary blood vessels and cerebral blood vessels, improves local blood flow, improves microcirculation, inhibits platelet aggregation, reduces muscle oxygen consumption, and increases oxygen supply (Zeng et al., 2021; Chen D. et al., 2022; Lv et al., 2022).

CHI can be prepared from a single TCM extraction mixture, such as DSI, HHI, HQI, or DZXXI, as shown in Figure 1. DSI and SLI were prepared by extraction and purification of *S. miltiorrhiza*. *Salvia miltiorrhiza* promotes blood circulation, regulates menstruation, removes blood stasis, relieves pain, cools the blood, eliminates carbuncle, eliminates trouble, and soothes the nerves (Li H. et al., 2021; Wang SM. et al., 2022). Its main chemical components are danshensu, salvianolic acid, and tanshinone IIA, which can inhibit the activity of various coagulation factors and stimulate the plasmin system, thereby reducing thrombus formation and improving microcirculation. At the same time, *S. miltiorrhiza* has a good preventive effect on blood lipid metabolism by reducing the content of denatured lipoprotein, thereby preventing the development of atherosclerosis and reducing the incidence of cerebrovascular disease (Wang ZY. et al., 2022). *Salvia miltiorrhiza* can also reduce the content of oxygen free radicals produced by cardiovascular and cerebrovascular diseases, thereby protecting myocardial cells and brain tissue. In particular, Tanshinone IIA can increase the residence time of drugs in brain tissue (Zhong et al., 2021).

HHI and SYI were extracted and purified from the safflower. Safflower promotes blood circulation, removes stasis, relieves pain, and detoxifies blood. *Salvia miltiorrhiza* and safflower are essential medicines for promoting blood circulation and removing blood stasis (Orgah et al., 2020; Zhao et al., 2022). The main components of safflower are flavonoids, which are classified as quinoid chalcones, represented by hydroxysafflor yellow A, and common flavonoids, represented by kaempferol. The SYI was prepared by extracting the effective parts of the safflower. Safflower yellow can block platelet-activating factors, inhibit the release of serotonin, reduce peripheral resistance of blood vessels, expand cardiovascular and cerebrovascular vessels, inhibit platelet aggregation, significantly reduce blood viscosity and plasma viscosity, and improve the erythrocyte aggregation index; thus, blood platelet aggregation in the stasis model was reduced, and microcirculation disturbance was significantly improved. Prothrombin time following treatment with safflower yellow was delayed (Wang L. et al., 2021).

TABLE 1 CHIs for the treatment of cardio-cerebrovascular diseases.

Name	Composition of medicinal materials	Preparation process	Approved year	Main components	Clinical application	Pharmacological action	Dosage
Danhong injection (DHI)	*Salvia miltiorrhiza* Bunge [Lamiaceae; Salviae miltiorrhizae radix et rhizoma], *Carthamus tinctorius* L. [Compositae; Carthami Flos]	Soak Salviae miltiorrhizae radix et rhizoma twice in dilute ethanol and filter. Mix the dregs with Carthami Flos, add water, soak twice, combine the filtrate, add sodium chloride for injection to isotonicity, adjust pH to 6–7, filter, refrigerate for 24 h, add water for injection to the specified amount, filter, pot and sterilize	2002	Tanshinone IIA, danshensu, safflower yellow	Coronary heart disease, angina pectoris, myocardial infarction, blood stasis pulmonary heart disease, ischemic encephalopathy, cerebral thrombosis	Anti-inflammatory, antioxidant, anticoagulant, anti-apoptotic, protecting vascular endothelium, inhibiting platelet aggregation, reducing blood lipids	1. Intramuscular injection, 2–4 mL each dose, 1–2 times a day 2. Intravenous injection, 4 mL each dose, 1–2 times a day 3. Intravenous infusion, 20–40 mL each dose, 1–2 times a day
Honghua injection (HHI)	*Carthamus tinctorius* L. [Compositae; Carthami Flos]	Add water to Carthami Flos (500 g), and decoct three times. The concentrated solution is precipitated twice with ethanol, pH is adjusted with 50% sodium hydroxide solution. Then water is added for injection, after which it is filtered, potted, and sterilized	2012	Safflower yellow, kaempferol	Obliterative cerebrovascular disease, coronary heart disease, vasculitis	Anticoagulant, antiplatelet aggregation, coronary dilation	1. Treatment of occlusive cerebrovascular disease: intravenous drip, 15 mL each dose, once daily 2. Treatment of coronary heart disease: intravenous drip. 5–20 mL each dose, once daily 3. Treatment of vasculitis: intramuscular injection. 2.5–5 mL each dose, 1–2 times a day.
Safflower Yellow for Injection (SYI)	*Carthamus tinctorius* L. [Compositae; Carthami Flos]	Carthami Flos is extracted with water. The extract is concentrated and eluted by column chromatography, and the total safflower yellow is recovered as a solvent and concentrated and dried	2005	Hydroxysafflor yellow A; anhydrosafflor yellow B	Stable exertional angina	Inhibits arrhythmia, reduces infarct size, increases coronary blood flow, lowers blood pressure, slows heart rate, and reduces myocardial oxygen consumption	Intravenous infusion, 100 mg of safflower yellow for injection, added to 250 mL of 0.9% sodium chloride injection, intravenous infusion slowly, once daily; 14 days treatment course.
Danshen injection (DSI)	*Salvia miltiorrhiza* Bunge [Lamiaceae; Salviae miltiorrhizae radix et rhizoma]	Take 1,500 g of Salviae miltiorrhizae radix et rhizoma, add water and decoct three times, combine the decoction, concentrate, add ethanol to precipitate for two times, recover ethanol from the filtrate and concentrate to about 250 mL. Add water for injection to 400 mL and mix, adjust pH to 6.8 with 10% sodium hydroxide solution, boil for half an hour, filter, add water for injection to 1,000 mL and seal, sterilize.	2011	Tanshinone IIA and danshensu	Coronary heart disease, angina pectoris	The anticoagulant effect, promote fibrin degradation, improve myocardial ischemia, anti-atherosclerosis, anti-thrombotic	Intramuscular injection, 2–4 mL each dose, 1–2 times a day; intravenous injection, 4 mL each dose, 1–2 times a day; intravenous drip, 10–20 mL each dose, once daily
Xuesaitong injection (XSTI)		Notoginseng radix et rhizoma is crushed into a coarse powder, extracted with 70%	2001	Ginsenoside Rb1, ginsenoside Rg1,		Inhibit platelet aggregation and activation, antithrombotic,	

(Continued on following page)

10.3389/fphar.2023.1038906

TABLE 1 (*Continued*) CHIs for the treatment of cardio-cerebrovascular diseases.

Name	Composition of medicinal materials	Preparation process	Approved year	Main components	Clinical application	Pharmacological action	Dosage
	Panax notoginseng (Burkill) F.H.Chen [Araliaceae, Notoginseng radix et rhizoma]	ethanol and filtered. The filtrate is concentrated under reduced pressure, filtered, passed through a column of styrene-type non-polar copolymer macroporous adsorbent resin, and washed with water. The aqueous eluate is discarded after which it is eluted with 80% ethanol. The eluate is concentrated under reduced pressure, decolorized, refined, concentrated under reduced pressure to infusion and dried		panax notoginsenosides	Atherothrombotic cerebral infarction, cerebral embolism, central retinal vein occlusion	promote hematopoietic cell proliferation, lower blood lipids, and blood pressure, prevent atherosclerosis	1. Intramuscular injection: 100 mg once, 1–2 times daily 2. Intravenous infusion: 200–400 mg each dose, once daily.
Shenmai Injection (SMI)	*Panax ginseng* C.A.Mey. [Araliaceae, Ginseng Radix et Rhizoma Rubra], *Ophiopogon japonicus* (L.f) Ker-Gawl. [Lillaceae; Ophiopogonis radix]	Red ginseng and Ophiopogonis radix are extracted twice with water, and the decoction is concentrated and added to a solution of 101 clarifiers at 7% of the volume of the solution, stirred well, and left for several hours to produce flocculation in the extract. Then an equal amount of suspension aid 5% suspension is added and stirred well, centrifuged, dispensed and sterilized	2010	Ginsenosides Rb1, Rg1, Re	Shock, coronary heart disease, viral myocarditis, chronic pulmonary heart disease, neutropenia	Inhibit cardiovascular oxidative stress, regulate calcium balance, improve mitochondrial function and inhibit apoptosis, inhibit neuronal apoptosis, and maintain blood-brain barrier integrity after cerebral ischemia	1. Intramuscular injection of 2–4 mL once daily 2. Intravenous infusion, 20–100 mL each dose
Danshen Ligustrazine Injection (DLI)	*Salvia miltiorrhiza* Bunge [Lamiaceae; Salviae miltiorrhizae radix et rhizoma], *Ligusticum chuanxiong* Hort. [Apiaceae; Chuanxiong Rhizoma]	After taking Salviae miltiorrhizae radix et rhizoma by water extraction and treated using the stone sulfur method, ethanol is recovered by alcohol precipitation twice (the first time to make the alcohol content reach 60%, the second time to make the alcohol content reach 70%) to make a clear liquid containing 0.4 g of medicinal material per 1 mL. To adjust the pH value, as a backup solution, mix Chuanxiongzin hydrochloride, glycerol and the above solution evenly, add water for injection and adjust the pH value of the solution with a hydrochloric acid solution to make a total of 1,000 mL. The solution is filtered, sealed in 5 mL ampoule and sterilized (115°C, 30 min).	2002	Danshensu, ligustrazine hydrochloride	Obstructive cerebrovascular diseases, such as cerebral insufficiency, cerebral thrombosis, cerebral embolism, and other ischemic cardiovascular diseases, such as coronary heart disease, chest tightness, angina pectoris, myocardial infarction, ischemic stroke, thromboangiitis obliterans, etc.	Anti-platelet aggregation, dilate coronary arteries, reduce blood viscosity, accelerate the flow rate of red blood cells, improve microcirculation, and anti-myocardial ischemia and myocardial infarction effects	Intravenous infusion, diluted with 5%–10% glucose injection or normal saline 250–500 mL, 5–10 mL each dose
Puerarin Injection (PI)	*Pueraria* lobata (Willd.) Ohwi [Fabaceae; Radix Puerariae Lobatae]	Sterilized aqueous solution made of Puerarin with the appropriate amount of co-solvent.	2004	Puerarin	Coronary heart disease, angina pectoris, myocardial infarction, retinal artery, and vein occlusion, sudden deafness	Dilate coronary and cerebrovascular, reduce myocardial oxygen consumption, improve microcirculation and anti-platelet aggregation	Intravenous infusion, 200–400 mg each dose, add 250–500 mL of glucose injection for intravenous infusion, once daily, 10–20 days treatment course, can be used

(Continued on following page)

10.3389/fphar.2023.1038906

TABLE 1 (*Continued*) CHIs for the treatment of cardio-cerebrovascular diseases.

Name	Composition of medicinal materials	Preparation process	Approved year	Main components	Clinical application	Pharmacological action	Dosage
							continuously for 2–3 courses of treatment
Huangqi Injection (HQI)	*Astragalus mongholicus* Bunge [Fabaceae; Astragali Radix]	Take 2000 g of Astragali Radix, add water and decoct three times, each time for 1.5 h, combine the decoction, filter, concentrate the filtrate, precipitate with ethanol twice, refrigerate each time, recover the ethanol and concentrate, dilute with water for injection, refrigerate for 12 h, filter, concentrate the filtrate, let it cool, adjust the pH to 7.5 with 20% sodium hydroxide solution, boil, add 0.125% activated carbon, boil for 5 min, filter while hot, add water for injection to make 1,000 mL, filter, adjust the pH to 7.5 with 20% sodium hydroxide solution, filter, pot, sterilize. Add 0.125% activated carbon, boil for 5 min, filter out while hot, add water for injection to make 1,000 mL, filter out, then adjust pH to 7.5 with 20% sodium hydroxide solution, filter out, pot and sterilize	2010	Astragaloside IV	Viral myocarditis due to heart qi deficiency and blood stasis, heart insufficiency and hepatitis due to spleen deficiency and dampness	It has a positive inotropic effect on the heart, enhances myocardial contractility, increases coronary blood flow, protects myocardial cells, and improves cardiovascular function	Intramuscular injection, 2–4 mL each dose, 1–2 times daily. Intravenous infusion, 10–20 mL each dose, once daily.
Mailuoning Injection (MLNI)	*Achyranthes bidentata* Blume [Amaranthaceae; Achyranthis Bidentatae Radix]	The decoction is concentrated into semi-solid form and precipitated with ethanol, the alcoholic solution is recovered and extracted with ethyl acetate, and the extract is dissolved in distilled water, the aqueous solution is filtered with an appropriate amount of Tween 80% and 20% NaOH solution to adjust its pH value to 8.5–9.0, filtered, potted, and sterilized	2011	Artesinolide	Thromboangiitis obliterans, arteriosclerotic obliterans, cerebral thrombosis and sequelae, venous thrombosis	It can dilate small blood vessels, coronary arteries, and veins, increase vascular perfusion, enhance myocardial contractility, improve blood circulation, increase fibrinolytic activity, and improve blood rheology	Intravenous infusion, 10–20 mL each dose, once daily, 10–14 days treatment course, severe patients can use 2–3 courses of treatment continuously
	Scrophularia ningpoensis Hemsl. [Scrophulariaceae; Scrophulariae Radix], *Dendrobium nobile* Lindl. [Orchidaceae; Dendrobii Caulis]						
	Lonicera japonica Thunb. [Caprifoliaceae; Lonicerae japonicae flos]						
Xingnaojing injection (XNJI)	Artificial Moschus, *Gardenia jasminoides* Ellis [Rubiaceae; Gardeniae fructus], Borneolum syntheticum	Add water of about 1,500 mL to Curcumae radix and Gardeniae fructus for distillation, collect distillate (1,000 mL), add musk into the above distillate, distill, collect distillate (1,000 mL). Take Borneolum syntheticum and add 8 g of polysorbate 80, mix well, add into distillate, mix well,	2003	Muskone	Cerebral embolism, acute cerebral hemorrhage, craniocerebral trauma, acute alcoholism with the above symptoms	Improve the permeability of the blood-brain barrier, protect the structure of the blood-brain barrier, inhibit inflammation, reduce cerebral ischemia-reperfusion injury, and improve neurological function	1. Intramuscular injection, 2–4 mL each dose, 1–2 times a day 2. Intravenous infusion, 10–20 mL each dose

(Continued on following page)

10.3389/fphar.2023.1038906

TABLE 1 (*Continued*) CHIs for the treatment of cardio-cerebrovascular diseases.

Name	Composition of medicinal materials	Preparation process	Approved year	Main components	Clinical application	Pharmacological action	Dosage
		add 8 g of sodium chloride, stir to dissolve, mix well, filter, pot, and sterilize					
Xinmailong injection (XMLI)	*Periplaneta americana* (L.)	Dried *Periplaneta americana* powder is refluxed with 95% ethanol at 80°C for 1 h and filtered. The filtrate is concentrated to dryness under reduced pressure and the resulting extract is warmed and dissolved in 50 mL of distilled water and filtered. 5 mL of the filtrate is extracted and treated with strong alkaline anion exchange resin 717	2006	L-tryptophan, L-tyrosine, N-acetyldopamine	Adjuvant medication for chronic congestive heart failure caused by chronic pulmonary heart disease	Strengthen the heart, improve myocardial cell energy supply, expand coronary artery, increase coronary blood flow, inhibit oxygen free radicals mediated muscle damage, anti-arrhythmia	Each dose 5 mg/kg body weight, intravenous infusion, twice daily, with an interval of more than 6 h between the two doses. 5 days treatment course
Dazhu Hongjingtian injection (HJTI)	*Rhodiola wallichiana* (Hook.) S. H. Fu var. cholaensis (Praeg.) S.H.Fu [Crassulaceae; Rhodiola wallichiana var. cholaensis]	Take 1,670 g of Rhodiola wallichiana var. cholaensis, add water, and decoct three times, combine the decoction, and filter through. The filtrate is concentrated, ethanol is added to make the alcohol content reach 70%, it is stirred well, refrigerated for 24 h, filtered, the filtrate is combined, ethanol is recovered and concentrated, ethanol is added to make the content reach 85%, filtered, the filtrate is adjusted to pH 7.0, activated carbon is added and boiled for 30 min, refrigerated for 72 h, the filtrate is filtered by removing the carbon, the filtrate is filtered by ultra-column with a cut-off molecular weight of 10,000 g/mol. The filtrate is ultrafiltered by ultra-column with a cut-off molecular weight of 10,000, freeze-dried, and the lyophilized material is prepared by adding water for injection to 1,000 mL, filtered by microporous membrane, potted and sterilized	2006	Gallic acid, syringic acid, salidroside	Coronary heart disease stable angina pectoris	Reduced peripheral vascular resistance and coronary resistance, increased coronary blood flow, decreased myocardial oxygen consumption; decreased platelet aggregation rate; decreased whole blood viscosity and plasma viscosity	Intravenous infusion, 10 mL each dose, once daily. 10 days treatment course
Ginkgo Damo injection (GDI)	*Ginkgo biloba* L. [Ginkgoaceae; Ginkgo folium]	Take dipyridamole, dissolve in deionized water, dissolve evenly, add hydrochloric acid dropwise to adjust pH = 3–6, and centrifuge. Dissolve in 20%–90% ethanol, add activated carbon, raise the temperature to 50°C–80°C, stir for 0.5–3 h, filter and decarbonize, then add hydrochloric acid to adjust pH = 3–6. Mix dipyridamole and Ginkgo biloba extract and sterilize	2002	Ginkgo total flavonoids, dipyridamole	Coronary heart disease, thromboembolic disease	Dilate coronary blood vessels and cerebral blood vessels, improve symptoms and memory function of cerebral ischemia; inhibit platelet aggregation and platelet release	Intravenous infusion, adults take 10–25 mL each dose, twice daily
Shuxuening injection (SXNI)	*Ginkgo biloba* L. [Ginkgoaceae; Ginkgo folium]	Add anhydrous ethanol to the ginkgo extract, then dilute with 2000–3,000 mL of water for	2004		Ischemic cardiovascular and cerebrovascular diseases,	Dilate blood vessels and improve microcirculation	Intramuscular injection, 10 mL at a time, 1–2 times

(Continued on following page)

10.3389/fphar.2023.1038906

TABLE 1 (*Continued*) CHIs for the treatment of cardio-cerebrovascular diseases.

Name	Composition of medicinal materials	Preparation process	Approved year	Main components	Clinical application	Pharmacological action	Dosage
		injection. Add antioxidant and pH adjuster, add activated carbon for needles, keep warm and stir for 10 min, decarbonize and filter, filter through a microporous membrane, add water for injection to 3,000–6,000 mL in filtrate, and sterilize		Ginkgolide A, quercetin, isorhamnetin	coronary heart disease, angina pectoris, cerebral embolism, cerebral vasospasm		daily. Intravenous infusion, 20 mL per day
Salvia miltiorrhiza polyphenolate for injection (SLI)	*Salvia miltiorrhiza* Bunge [Lamiaceae; Salviae miltiorrhizae radix et rhizoma]	After the crushing of Salviae miltiorrhizae radix et rhizoma, it is extracted using hot water, filtered, and concentrated. The filtrate is adsorbed using macroporous resin and washed with water to remove impurities, the polyphenolic acid salt adsorbed on the macroporous resin is eluted with aqueous low-grade alcohol, the eluate is concentrated to a certain volume under reduced pressure and added to anhydrous ethanol alcohol precipitation, the supernatant is poured out and the precipitate is discarded, dried and crushed to obtain Salvia miltiorrhiza polyphenolate	2005	Salvia Polyphenolate	Coronary heart disease stable angina pectoris	Inhibit platelet aggregation, inhibit thrombosis	Intravenous infusion, 200 mg each dose, once daily, 2 weeks treatment course
Shenxiong Glucose Injection (SXI)	*Salvia miltiorrhiza* Bunge [Lamiaceae; Salviae miltiorrhizae radix et rhizoma], *Ligusticum chuanxiong* Hort. [Apiaceae; Chuanxiong Rhizoma]	Salviae miltiorrhizae radix et rhizoma is extracted using water and treated using the rock-sulfur method, then alcohol is used twice to recover ethanol and adjust the pH as a backup solution. The filtrate is mixed with ligustrazine and added to the water for injection, and the pH value of the solution is adjusted with hydrochloric acid	2002	Danshensu, Ligustrazine Hydrochloride	Occlusive cerebrovascular disease and other ischemic vascular diseases	Anti-platelet aggregation, dilate coronary arteries, reduce blood viscosity, accelerate the flow rate of red blood cells, improve microcirculation, and anti-myocardial ischemia and myocardial infarction	Intravenous infusion, once daily, 100–200 mL each dose
Dengzhan Xixin injection (DZXXI)	*Erigeron breviscapus* (Vant.) Hand.-Mazz. [Compositae; Erigerontis Herba]	Boil a decoction of Erigerontis Herba twice with water, combine decoction, filter, concentrate under reduced pressure, add ethanol until the alcohol content reaches 80%, filter, the filtrate is recovered ethanol under reduced pressure and concentrated, extracted with ethyl acetate shaking, the extract is concentrated under reduced pressure, the determination of the total flavonoid content. Take the appropriate amount of extract (containing 4.5 g of total flavonoids), add water for injection to dissolve, adjust pH to 8–8.5 with 5 mol/L sodium hydroxide solution, add water for injection and 0.1% activated carbon for injection, heat and boil for 30 min, filter, add 8 g of sodium chloride for injection	2015	Astragaloside, total caffeate	Chest pain, ischemic stroke, coronary heart disease angina pectoris	Inhibits oxygen free radicals in the body, increases the content of reducing substances and exerts an antioxidant effect; it can reduce blood viscosity and protect cell membranes, thereby reducing blood LPO and increasing SOD content	1. Intravenous injection, 20–40 mL each dose, 1–2 times a day 2. Intramuscular injection, 4 mL each dose, 2–3 times a day

(Continued on following page)

10.3389/fphar.2023.1038906

TABLE 1 (*Continued*) CHIs for the treatment of cardio-cerebrovascular diseases.

Name	Composition of medicinal materials	Preparation process	Approved year	Main components	Clinical application	Pharmacological action	Dosage
		and dissolve, add water for injection to 1,000 mL, filter, pot and sterilize					
Shengmai injection (SGMI)	*Panax ginseng* C.A.Mey. [Araliaceae; Ginseng Radix et Rhizoma Rubra], *Ophiopogon japonicus* (L.f) Ker-Gawl. [Lillaceae	Crush Ginseng Radix et Rhizoma Rubra into fine grains, extract with ethanol reflux 4–5 times, control the end point of extraction by thin layer method, combine the extracts, concentrate to a thick paste, add a sufficient quantity of water to 400 mL, stir well, refrigerate, filter through, filtrate for liquid preparation; collect 150 mL of distillate of Schisandrae Chinensis Fructus by water distillation, refrigerate, for liquid preparation, decoct the dregs with water three times, combine the decoctions and concentrate to a thick paste, add ethanol and concentrate to a thick paste, add water for injection to 200 mL, boil the filtrate with an appropriate amount of activated carbon for 30 min, cool slightly, filter to clarify for liquid preparation; make about 200 mL of a clear aqueous solution of maidenhair according to the preparation method of an aqueous solution of schisandra for liquid preparation. The above solution is mixed well, filtered, and the filtrate is added with water for injection to 1,000 mL, and the pH of the solution is adjusted to 7.5, filtered, potted, and sterilized.	2011	Ginsenosides Rb1, Rg1, Re, schisandrin A	Myocardial infarction, cardiogenic shock; septic shock	Improve microcirculation and anti-shock, reduce blood viscosity, anti-platelet aggregation	1. Intramuscular injection: 2–4 mL each dose, 1–2 times a day
	Ophiopogonis radix], *Schisandra chinensis* (Turcz.) Baill. [Magnoliaceae; Schisandrae Chinensis Fructus]						2. Intravenous infusion; 20–60 mL each dose

10.3389/fphar.2023.1038906

FIGURE 1
Single TCM extract injection; **(A)** Puerarin Injection; **(B)** Danshen injection; **(C)** Honghua injection; **(D)** Xuesaitong injection; **(E)** Shuxuening injection; **(F)** Xinmailong injection; **(G)** Dazhu Hongjingtian injection; **(H)** Huangqi injection.

XSTI were prepared from the total saponins of *Panax notoginseng*. *Panax notoginseng* promotes blood circulation, removes blood stasis, reduces swelling and calms pain, promotes hemostasis, and is nourishing. It is the main drug used to treat traumatic injuries (Wang et al., 2016; Yang et al., 2018). *Panax notoginseng* saponins have a wide range of effects, such as dilation of the coronary arteries, improvement of left ventricular diastolic function, and reduction the concentration of Ca^{2+} in cardiomyocytes. It can also inhibit platelet aggregation and promote fibrinolysis (Duan et al., 2018; Xu CC. et al., 2019).

SXNI was prepared from Ginkgo leaf extract and GDI was prepared by mixing *Ginkgo biloba* L. leaf extract and dipyridamole. *Ginkgo biloba* L. leaves contain active ingredients such as flavonoid glycosides and terpenoid lactones, including quercetin, kaempferol, bilobalide, and ginkgolide, which have functions such as promoting blood circulation and remove blood stasis, dredge collaterals, relieve pain, astringe the lungs, relieve asthma, reduce turbidity, and lower lipids (Tian et al., 2017; Liu et al., 2021). *Ginkgo biloba* L. leaves can be used for blood stasis blocking collaterals, chest pain and heart pain, stroke hemiplegia, lung deficiency, cough and asthma, and hyperlipidemia (Wang et al., 2021a; Li et al., 2021d; Liang et al., 2022). *Ginkgo biloba* L. leaves can effectively inhibit platelet-activating factors, abnormal platelet aggregation, and thrombosis and reduce blood lipids and viscosity (Sarkar et al., 2020; Li R. et al., 2021).

XMLI was prepared from the extract of the animal TCM *Periplaneta americana*. *Periplaneta americana* is a natural animal medicine that can eliminate inflammation and edema, promote wound healing, and improve immune function (Lin et al., 2019; Zeng et al., 2019; Liao et al., 2022; Pang et al., 2022). HJTI is prepared from an extract of the traditional Chinese medicine *Rhodiolae Crenulatae Radix et Rhizoma*. *Dazhu Rhodiolae* has pharmacological effects including protection of the heart and nerves, anti-fatigue, anti-aging, anti-radiation, and immune regulation (Fan et al., 2020; Li et al., 2021c; Chen Y. et al., 2022).

TCM prescription injection

The compatibility of TCM prescriptions to reduce toxicity and increase efficacy is a characteristic of the clinical application of TCM. Based on the compatibility and combination characteristics of TCM prescriptions, a batch of TCM prescription injections was innovatively developed, as shown in Figure 2. Danhong injection (DHI) is obtained by water extraction and alcohol precipitation of two medicinal materials, *S. miltiorrhiza* and safflower. *Salvia miltiorrhiza* and safflower are currently widely used as clinical medicines to promote blood circulation and remove blood stasis (Li M. et al., 2018). SMI was derived from Shendongyin in "Zhengyin Maizhi," written by Qin Jingming during the Ming

FIGURE 2
TCM Prescription Injection; **(A)** Danhong injection; **(B)** Mailuoning Injection; **(C)** Shengmai Injection; **(D)** Xiangdan injection; **(E)** Xingnaojing injection; **(F)** Shenmai injection; **(G)** Danshen Ligustrazine Injection; **(H)** Shenxiong Glucose Injection.

Dynasty. It is a TCM preparation composed of *red ginseng* and *Ophiopogonis radix*. It nourishes qi, removes qi, nourishes yin, promotes body fluids, and nourishes blood vessels (Yu JH. et al., 2019; Xu HM. et al., 2019). MLNI is a TCM prescription developed based on the classic medical prescription "Si Miao Yong An San" in "Yanfang Xinbian," guided by integrated traditional Chinese and Western medicine. It comprises *Lonicerae japonicae flos*, *Scrophulariae radix*, *Dendrobii caulis*, and *Achyranthis bidentatae radix*. Its functions include clearing heat, nourishing yin, promoting blood circulation, and removing blood stasis (Wang and Tian, 2014; Yang et al., 2015). XNJI was extracted from the Angong Niuhuang Pill, a classic first-aid prescription for stroke. It mainly consists of several TCM such as *Moschus*, *Borneolum syntheticum*, and *Gardeniae Fructus*. It is the only CHI approved in China for the treatment of acute cerebral hemorrhage and acute ischemic stroke in ambulances (Wang L. et al., 2022; Liu et al., 2022).

The DLI is one of the most commonly used injections in clinical practice. Unlike the traditional compatibility method, this injection combines the extract of *S. miltiorrhiza* with the active ingredients of *Ligusticum chuanxiong* (Xie et al., 2021; Ye et al., 2021). CHI is composed of the main active ingredients of these two medicinal materials. For example, SXI is composed of ligustrazine hydrochloride, the active ingredient of Chuanxiong, and Danshensu, the active ingredient of *S. miltiorrhiza* (Lu et al., 2020; Lu et al., 2021). Based on the classic drug pair theory of TCM, CHIs with effective active ingredients have been gradually developed. The injection obtained by combining the active ingredients has the advantages of a defined chemical composition, an evident pharmacological mechanism, and clinical indications.

Pharmacological effects of Chinese herbal injection in the cardio-cerebrovascular diseases

In recent years, based on the clinical application of CHIs, researchers have revealed their efficacy and mechanism of action through *in vitro* and *in vivo* pharmacological studies. Numerous studies have shown that CHIs for the treatment of cardio-cerebrovascular diseases have potential pharmacological activities, such as anti-platelet aggregation, anti-inflammatory, anti-fibrosis, and anti-apoptosis activities (Table 2; Figure 3).

Anti-platelet aggregation

DHI can inhibit inflammation and platelet aggregation, reduce immune response and peroxidation, and protect vascular endothelium and organ function, thus preventing and treating cardiovascular diseases (Zou et al., 2018; Bi et al., 2019). DHI can inhibit blood lipid levels and platelet aggregation rate in rats with hyperlipidemia. Meanwhile, thrombin time (TT), activated partial thrombin time (APTT), prothrombin time (PT), 6-K-

TABLE 2 Pharmacological effects of CHIs in the cardio-cerebrovascular diseases.

Diseases	Type of study	Drug	Experimental model	Dose range tested	Duration	Results	References
Ischemic stroke	*In vivo*	GHI	I/R injury	2.5, 5, 10 mL/kg	0, 6, 23 h	(−) NO; iNOS; MPO; IL-1β; TNF-α; CRP; ICAM-1; NF-κB p65	Ai et al. (2017)
Ischemic heart disease	*In vitro*	SMI + DSI	Hypoxia/reoxygenation and H_2O_2-induced cardiomyocyte injury	2.5, 5 and 10 μL/mL	10 h	(+) cell viability; ΔΨm; PI3K/Akt; Erk1/2	Li et al. (2019b)
						(−) CK; LDH; ROS; Ca^{2+}; cardiomyocyte injury	
Ischemic heart disease	*In vitro*	SMI	H9c2 cardiomyocytes were subjected to 12 h of hypoxia	1, 2.5, 5 μL/mL	24 h	(+) cell survival; ΔΨm; LC3, beclin 1, Parkin; Pink	Yu et al. (2019a)
						(−) mitochondrial mass and cytosolic Ca^{2+}; mPTP opening; impaired mitochondrial respiration	
Ischemic heart disease	*In vitro*	SMI	Myocardial cells following I/R	5 mL/L	24 h	(+) Ca^{2+}	Ye et al. (2015)
						(−) phosphorylated PLB; SERCA; aberrant apoptosis	
Cardiac toxicity induced by doxorubicin	*in vivo*	SMI	DOX-induced myocardial injury in C57BL/6 mice	2.5 mL/kg	6 days	(+) PI3K; p-Akt; p-GSK-3b; the ratio of L-OPA1 to S-OPA1; AMPK phosphorylation; DRP1	Li et al. (2020a)
						phosphorylation (−) mortality rate; levels of creatine kinase; creatine kinase-MB; Bax/Bcl-2; cleaved-Caspase3	
Stroke	*in vivo*	SMI	Middle cerebral artery occlusion (MCAO) rats	5 mL/kg	60 min after MCAO	(−) extravasation of FITC-albumin	Xu et al. (2019b)
						(+) flotillin-1; the translocation of occludin	
Myocardial infarction	*In vitro*	DLI	I/R and H/R	6.8, 20.4, 61.2 mg/kg	3 days	(+) cardiac function; Bcl-2/Bax ratio; Akt-eNOS	Huang et al. (2016)
						(−) myocardial infarct size; creatine kinase; lactate dehydrogenase; malondialdehyde levels; activation of caspase-3	
Stroke	*in vivo*	SLI	T1DM + MCAO rats	10.5, 21, 42 mg/kg	3 days	(+) brain microvasculature in ipsilateral; glucose uptake in the cortex; hippocampus; penumbra; HQ-1; HQO-1 and Nrf-2	Wang et al. (2017a)
						(−) RAGE, MMP9; inflammatory factors expression	
Atrial interstitial fibrosis and atrial fibrillation	*in vivo*	SLI	Rats underwent center anterior descending coronary artery ligation	10, 20 and 40 mg/kg	5 weeks	(+) cardiac function	Qiu et al. (2018)
						(−) center atrial enlargement and P-wave duration; atrial hypertrophy; TXNIP/NLRP3 inflammasome/IL-1β; IL-18 signal pathway; BNP, IL-6, CRP, and TGFβ1	
Cerebral vascular diseases	*in vivo*	SLI	I/R rat Model	21 mg/kg	24, 48, 72 h	(+) ZO-1 expression; BBB function	Zhao et al. (2019a)
						(−) brain leakage of Evans blue; phosphorylation of ERK1/2 and Akt	

(Continued on following page)

10.3389/fphar.2023.1038906

TABLE 2 (*Continued*) Pharmacological effects of CHIs in the cardio-cerebrovascular diseases.

Diseases	Type of study	Drug	Experimental model	Dose range tested	Duration	Results	References
Diabetes and hyperglycemia	*in vivo*	DSI	Fed a high sugar and fat diet mice	6 g/kg	24 weeks	(+) HO-1	Zhou et al. (2020)
						(−) KLF10 upregulation; ROS generation	
Spinal cord ischemia	*in vivo*	PL	Acute spinal I/R injury was conducted by aortic occlusion	50 mg/kg	2 days	(+) motor function	Tian et al. (2015)
						(−) spinal infarction volume; Cdk5 and p25 activities	
Ischemic heart disease	*In vivo*	PL	Isoproterenol-induced myocardial infarction mice	40 mg/kg	5 days	(+) ventricular wall infarction	Li et al. (2018b)
						(−) typical ST segment depression; incidence of mortality; levels of myocardial injury markers; inflammatory milieu; TNF-α; IL-1βandIL-6	
Ischemic heart disease	*In vivo*	HJTI	Myocardial ischemia model	2, 4 mL/kg	7 days	(+) ATP content; LC3-II; beclin	Zhang et al. (2017)
						(−) Oxidative Stress; apoptosis rate; caspase 3 expression; Bcl-2/Bax ratio; phos-ERK; phos-AKT	
Diabetic angiopathies	*In vitro*	HJTI	HG-stimulated A7r5 cells	10, 20, 40, 80, 160, or 320 mL/L	48 h	(+) p53; cleaved caspase-3; Bax/Bcl-2 ratio	Fan et al. (2019)
						(−) pAKT; MMP9; PCNA	
myocardial infarction	*In vivo*	SGMI	Myocardial ischemia-reperfusion (MIRI) injury	6, 12 mL/kg	4 days	(+) Bcl-2; VEGF	Liu et al. (2018b)
						(−) myocardial apoptosis; Bax; caspase 3	
Extremity ischemia-reperfusion injury	*in vivo*	MLN	Posterior limb I/R injury rabbits	1.5 mL/kg	24 h	(+) SOD activity	Wang and Tian (2014)
						(−) levels of 8-iso-PGF2a	
Ischemic heart disease	*in vivo*	SXNI	MIRI model	4.38, 8.75, 17.5 mg/kg	3 days	(+) the activity of antioxidant enzymes	Wang et al. (2019b)
						(−) infarct size of myocardial tissue; myocardial enzyme and TnI levels; myocardial damage; MDA level; GRP78, CRT, CHOP, and caspase-12 expression levels; inflammatory cytokines; procoagulant molecules; TLR4/NF-κB expression	
Ischemic myocardial infarction and ischemic stroke	*in vivo*	SXNI	MIRI model	2.5 mL/kg	24 h	(−) cerebral infarction area; cerebral edema; TWEAK; Fn14	Xiao et al. (2019)
Stroke	*in vivo*	SXNI	MCAO model	3 mL/kg	7 days	(+) survival rate	Li et al. (2020c)
						(−) cerebral infarction and edema volume; G-csf; MAC-1; E-selectin; MAC-1	
Acute myocardial infarction	*in vivo*	SXNI	MIRI model	12.5 mL/kg	24 h	(+) cardiac function; mitochondrial function	Li et al. (2019c)
						(−) infarct size	

(Continued on following page)

10.3389/fphar.2023.1038906

TABLE 2 (*Continued*) Pharmacological effects of CHIs in the cardio-cerebrovascular diseases.

Diseases	Type of study	Drug	Experimental model	Dose range tested	Duration	Results	References
Stroke	*In vitro*	SLI + XSTI	Oxygen-glucose deprivation/reperfusion (OGD/R) injury model	3.125; 6.25; 12.5; 25; 50 μg/mL	24 h	(+) TEER; expression of tight junctions (TJs) between cells; stabilize the basement membrane (BM) composition	Yuan et al. (2021)
						(−) permeability of Na-Flu; Ang-2; VEGF	
Stroke	*in vivo*	SLI + XSTI	MCAO/R	XST 100 mg/kg + SLI 21 mg/kg	3 days	(+) regional cerebral blood flow; SOD; CAT; GSH; Nrf-2, HO-1, NQO-1; the nuclear translocation of Nrf-2	Wang et al. (2018b)
						(−) neurological deficit scores; infarct volumes; the activation of both microglia and astrocytes in the hippocampus; MDA; ROS; Keap1	
Myocardial ischemia-reperfusion injury	*In vitro*	SMI	H_2O_2-induced oxidative stress model of cardiomyocytes	0.2, 1 and 5 μL/mL	12 h	(+) SOD; GSR; CAT; P-Akt	Zhu et al. (2019)
						(−) proliferation arrest and apoptosis; ROS; NADH; MDA; the overloads of cytoplasmic Ca^{2+} and mitochondrial Ca^{2+}; P-ERK1/2	
Ischemic myocardial infarction and ischemic stroke	*In vivo*	SXNI	Cerebral and myocardial I/R	2.5, 12.5 mL/kg	24 h	(+) cardiac function and coronary blood flow; myocardial infarction area	Lyu et al. (2018)
						(−) LDH, AST, CK-MB, and CK	
Ischemic stroke	*In vivo*	SXNI	Cerebral I/R model	3 mL/kg	7 days	(−) hippocampal neuronal apoptosis; the activation of Caspase-3 protein; Cleaved-Caspase-3	Lyu et al. (2018)
Ischemic stroke	*In vitro*	SXNI	HT-22 apoptosis caused by OGD/R	200 μg/mL	36 h	(−) the apoptosis rate; Bax and Cleaved-Caspase-3	Lyu et al. (2018)
Stroke	*In vivo*	SXNI	MCAO model	3 mL/kg	28 days	(+) repaired brain injury; BDNF and TrkB	Li et al. (2021e)
						(−) reduced neuronal apoptosis; level of p-Erk and Creb; GFAP	
ischemic stroke	*In vivo*	SXNI	MCAO model	1.83 mL/kg	72 h	(+) NOS3	Cui et al. (2020)
						(−) cerebral infarct volume; PTGS2 and CASP3	
heart failure	*In vitro*	XMLI	H9C2 rat cardiomyocytes	0.75 mg/mL	30 min	(−) phosphorylation of ERK1/2, AKT, and GSK3β; GATA4 in the nucleus	Qi et al. (2017)
Epirubicin-induced cardiotoxicity	*In vivo*	XMLI	Rats were intraperitoneally injected with epirubicin	125, 250, 500 mg/kg	14 h	(+) cardiac function; PKB/Akt; PI3K; Bcl_2	Li et al. (2016)
						(−) center ventricle dilatation; the accumulation of collagen; Mmp9; Tgfb1; cardiac-fibrotic remodeling; autophagy; accumulation of Beclin1 and autophagy-related 7; phosphorylated P38; Erk1/2	

(Continued on following page)

10.3389/fphar.2023.1038906

TABLE 2 (*Continued*) Pharmacological effects of CHIs in the cardio-cerebrovascular diseases.

Diseases	Type of study	Drug	Experimental model	Dose range tested	Duration	Results	References
Stroke	*In vivo*	XNJI	Cerebral I/R injury	5, 10, or 15 mL/kg	24 h	(+) Bcl2/Bax; p-PI3K/Akt; p-eNOS; NO	Zhang et al. (2018)
						(−) the scores of neurological deficits; cerebral infarct volume; attenuated neuronal impairments; leukoaraiosis; apoptosis	
Ischemic stroke	*In vivo*	XNJI	Cerebral I/R injury	10 and 15 mL/kg	24 h	(+) neurological scores and morphological changes; SIRT1	Qu et al. (2019)
						(−) cerebral infarct area; inflammatory mediator levels	
Ischemic stroke	*In vivo*	XNJI	MCAO	15 mL/kg	24 h	(+) survival percent; tight junction protein, occludin and ZO-1	Zhang et al. (2020b)
						(−) infarct area and ameliorate neurological deficits; leaking amount of Evans Blue; NLRP3; inflammatory response; BBB disruption and brain damage	
Stroke	*In vitro*	XSTI	H_2O_2-injured cardiac cells	80 mg/kg	7 days	(+) the activity of PDH; intracellular contents of acetyl-CoA and ATP	Zhao et al. (2017)
						(−) intracellular MDA release	
Persistent myocardial ischemia	*In vitro*	DHI	H9C2 cells treated with H/R	5, 10, 20, 40, 80, 100 μg/mL	24 h	(+) mitochondrial morphology with increased mitochondrial length; ATP levels and the oxygen-consumption rate (−) anti-apoptosis action; ROS generation; mitochondrial dysfunction with a decreased mitochondrial membrane potential	Zhang et al. (2020a)
Ischemic cerebrovascular disease	*In vivo*	DHI	MCAO	0.5, 1, and 2 mL/kg	24 h	(+) the brain function score; anti-apoptotic factor Bcl_2; PI3K-Akt signaling pathway	Feng et al. (2020)
						(−) brain tissue cell apoptosis; Bax, and Bim; apoptotic gene p53	
Ischemic heart disease	*In vivo*	DHI	Myocardial infarction model	1.5 mL/kg	28 days	(+) MSC survival rate and cardiac function; CXCR4; SDF-1	Chen et al. (2018)
						(−) myocardial infarct size; VEGF	

10.3389/fphar.2023.1038906

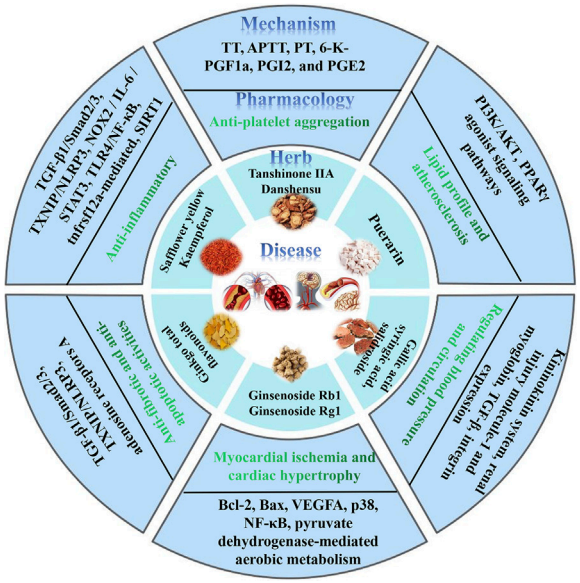

FIGURE 3
Data visualization of some Chinese herbal medicines, compounds, pharmacological effects, and mechanisms for the treatment of cardio-cerebrovascular diseases.

PGF1a, PGI2, and PGE2 mRNA expression were significantly increased after DHI treatment, while the expression of TXA2 was significantly decreased (Fan et al., 2018). Based on path analysis and CMAP query of microarray data, researchers have found that anti-inflammatory response and anti-platelet coagulation are the main mechanisms of XSTI against stroke (Wang et al., 2015).

Lipid profile and atherosclerosis

SXNI can effectively protect the brain and heart from I/R injury through the TNFRSF12a-mediated common pathway of atherosclerotic signaling and inflammatory responses (Lyu et al., 2018). DHI attenuates high-fat diet-induced atherosclerosis and macrophage lipid accumulation by modulating the PI3K/AKT pathway (Zhou et al., 2019). The effect of DHI on DC maturation and immune function induced by oxidized low-density lipoprotein is mainly through the activation of peroxisome proliferator-activated receptor γ (PPARγ) agonist signaling pathways (Liu et al., 2012).

Anti-inflammatory

SLI attenuates inflammatory responses in BMMs and HUVECs. GHI can significantly improve brain I/R injury in rats, which may be achieved by inhibiting inflammation. GHI significantly reduces serum nitric oxide (NO), inducible nitric oxide synthase (iNOS), myeloperoxidase (MPO), interleukin-1b (IL-1b), tumor necrosis factor-α (TNF-α), and C-reactive protein (CRP) levels (Ai et al., 2017). Salvianolate treats myocardial infarction by inhibiting the TGF-β1/Smad2/3 and TXNIP/NLRP3 inflammasome signaling pathways (Qiu et al., 2018). XSTI, when combined with aspirin and clopidogrel, can protect rats from focal cerebral I/R injury by inhibiting oxidative stress and inflammation and regulating the NOX2/IL-6/STAT3 pathway. SXNI can prevent myocardial I/R injury by reducing oxidative stress, inflammation, and thrombosis (Zhu et al., 2021). SXNI can reduce the levels of inflammatory cytokines in serum, the levels of procoagulant molecules in plasma, and the expression of TLR4/NF-κB in rats (Wang R. et al., 2019). SXNI effectively protects the brain and heart from I/R injury through a common tnfrsf12a-mediated pathway involved in atherosclerotic signaling and inflammatory responses (Lyu et al., 2018). XNJI ameliorates cerebral I/R injury by inhibiting SIRT1-mediated inflammatory response (Zhang YM. et al., 2020).

Anti-fibrotic and anti-apoptotic activities

Salvianolate reduces atrial fibrillation by inhibiting the TGF-β1/Smad2/3 and TXNIP/NLRP3 inflammasome signaling pathways in rats after myocardial infarction, thereby inhibiting atrial fibrosis (Qiu et al., 2018). DHI protects the heart of rats with myocardial infarction by resisting cardiomyocyte apoptosis and angiogenesis, and reducing myocardial fibrosis (Chen JR. et al., 2016). Pretreatment with SFI enhanced the expression of adenosine receptor A in a dose-dependent manner compared to that in the MI/R-post group (Wang et al., 2021b).

Myocardial ischemia and cardiac hypertrophy

SXNI preconditioning has a cardioprotective effect on myocardial I/R injury, manifested as a reduced infarct size, improved cardiac function, and improved mitochondrial function (Li T. et al., 2019). SMI reduces apoptosis and enhances angiogenesis after myocardial I/R injury in rats. SMI-driven reduction in apoptosis is associated with changes in the ratio of Bcl-2 to Bax expression, whereas treatment-induced angiogenesis is associated with enhanced vascular endothelial growth factor A (VEGFA) expression (Liu X. et al., 2018). XSTI attenuates myocardial I/R injury by enhancing pyruvate dehydrogenase-mediated aerobic metabolism (Zhao et al., 2017). DHI attenuates isoproterenol-induced cardiac hypertrophy by modulating p38 and NF-κB pathways (Zhou et al., 2019).

Cerebral ischemia

XSTI, when combined with freeze-dried sulfate injection, protects rats from focal cerebral I/R injury by inhibiting oxidative stress and the Nrf-2/Keap1 pathway (Wang FJ. et al., 2018). XNJI protects rats from cerebral I/R injury and alleviates blood-brain barrier damage by inhibiting the underlying mechanism of the NLRP3 inflammasome (Qu et al., 2019). DHI may reduce inflammation by maintaining the integrity of the brain-blood barrier and regulating TLR4-related signaling pathways, thereby effectively improving the prognosis of cerebral I/R injury (Qian et al., 2018).

Regulating blood pressure and circulation

DHI reduces vascular remodeling and upregulates the kallikrein-kinin system in spontaneously hypertensive rats (Yang XH. et al., 2017). DHI prevents hypertension-induced renal injury by downregulating the expression of renal injury molecules and myoglobin in spontaneously hypertensive rats (Orgah et al., 2018). HHI can affect connective tissue growth factor; transforming growth factor-β and integrin expression can regulate pulmonary artery remodeling, thus affecting the wall thickness of the pulmonary and myocardial arterioles, which is conducive to the control of pulmonary hypertension (Chen et al., 2021).

Clinical application of Chinese herbal injection in the cardio-cerebrovascular diseases

Most clinical trials of CHI for the treatment of cardio-cerebrovascular diseases have been conducted in China. In recent years, some scholars have collected relevant published randomized controlled trials for Bayesian network meta-analysis. We collected and summarized literature on the clinical application of CHIs to cardio-cerebrovascular diseases in recent years to provide a reference for the clinical use of CHIs in the treatment of cardio-cerebrovascular diseases, as shown in Figure 4.

Stroke

The present study conducted a network meta-analysis of randomized controlled trials on the efficacy of CHI in the treatment of acute cerebral infarction, including 64 studies with 6,225 participants involving 15 TCM injections. In terms of apparent efficiency, DHI is most likely the best treatment option. In terms of improving nerve damage, SXNI has the highest probability of being the best treatment option (Huang et al., 2022).

In a randomized controlled trial of SYI in the treatment of acute cerebral infarction, the National Institute of Health Stroke Scale score in the SYI group decreased, and the hemorheological indices of red blood cell deformation and aggregation were significantly improved. The prothrombin time was increased, fibrinogen, TNF-α, and IL-1β levels were increased, and IL-6 levels were decreased (Li et al., 2015b). In a Bayesian network meta-analysis of randomized controlled trials of Danshen class injection in the treatment of acute cerebral infarction, including 157 randomized controlled trials with a total of 15,570 patients, the results showed that tanshinone IIA sodium sulfonate injection plus Western medicine is clinically effective; it is superior to other drugs in terms of neurological impairment and activities of daily living. DSI and SLI performed excellently in improving blood rheology (Liu S. et al., 2019).

A study conducted A meta-analysis of randomized controlled trials on the efficacy and safety of PI in the treatment of acute ischemic stroke. The meta-analysis identified 35 randomized controlled trials with a total of 3,224 participants. The results showed that PI was superior to the control drug in terms of clinical effectiveness, and the neurological deficit was significantly improved (Zheng et al., 2017).

A systematic review and meta-analysis of XNJI in the treatment of acute ischemic stroke showed that XNJ plus conventional treatment alleviated neurological deficits in acute ischemic stroke. Compared to DHI combined with conventional treatment, XNJ combined with conventional therapy reduces mortality (Tian et al., 2021; Wang L. et al., 2022). The researchers meta-analyzed 29 studies with a total of 2,638 patients. Compared with conventional treatment, XNJI is more effective, significantly reduces hs-CRP levels, enhances activities of daily living, and alleviates hematoma and edema (Ma et al., 2020). In a meta-analysis of the clinical efficacy of XNJI in the treatment of cerebral infarction, 53 randomized controlled trials involving a total of 4,915 participants, the results showed that compared to traditional treatment alone, XNJI can significantly improve the total effective rate, daily life enhanced ability, reduced infarct size, reduced neurological damage. XNJ can improve hemorheology and reduce whole-blood viscosity, plasma viscosity, and hematocrit. XNJ can also reduce cholesterol and triglyceride levels (Ma et al., 2017).

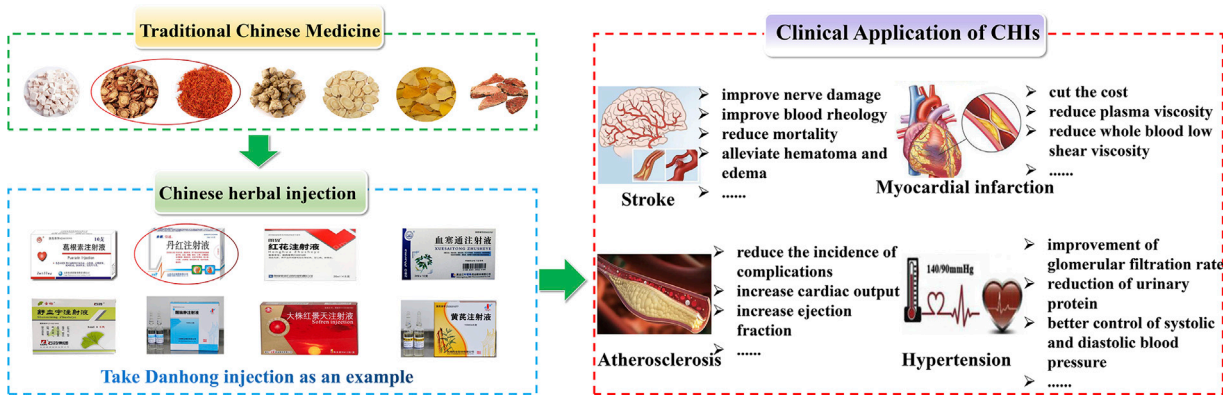

FIGURE 4
Clinical application of CHIs in cardio-cerebrovascular diseases, take Danhong injection as an example.

An efficacy and safety study of GDI in the treatment of ischemic stroke, with data from 39 trials including 3,182 ischemic stroke patients, showed that the general response of the neurological function in the conventional treatment and the GDI groups was significantly improved. The patients' hemorheology and blood lipid indexes were also significantly improved after combined treatment (Wang YS. et al., 2017; Xue et al., 2019).

Myocardial infarction and cardiomyopathy

Through a systematic review and meta-analysis of randomized controlled trials, some studies have compared the efficacy of DHI at different time points in the perioperative period of acute myocardial infarction. The analysis included 23 studies, all of which showed that the efficacy of the DHI was better (He et al., 2021). Some researchers have meta-analyzed GDI in the adjuvant treatment of angina pectoris, including 41 randomized controlled trials involving 4,462 patients. The combined application of GDI and Western medicine in the treatment of angina pectoris has a higher total effective rate and reduces plasma viscosity levels, fibrinogen, whole blood low shear viscosity, and whole blood high shear viscosity (Tan et al., 2018).

Some researchers have conducted a meta-analysis of 26 randomized controlled trials involving 3,447 participants to evaluate the therapeutic effect of XMLI on chronic heart failure. The results showed that XMLI plus conventional treatment improved the total efficacy rate. Compared with conventional treatment alone, XMLI combined with conventional treatment can increase left ventricular ejection fraction and 6-min walk distance, and reduce left ventricular end-diastolic diameter, serum brain natriuretic peptide, and N-terminal pro-brain natriuretic peptide (Lu et al., 2018). A randomized, double-blind, controlled study analyzed the effects of SMI on energy metabolism in patients with heart failure. The results showed that SMI improved patients' energy metabolism compared to the trimetazidine and control groups, as evidenced by changes in serum-free fatty acid, lactic acid, pyruvate, and branched-chain amino acid levels (Wang SM. et al., 2020). This was a randomized, double-blind, multicenter, placebo-controlled clinical study on the efficacy and safety of SMI in the treatment of patients with chronic heart failure. The improvement in the form 36 hearth survey score and TCM syndrome score was better than that in the control group, the use of SMI treatment was well tolerated, and there were no obvious safety issues (Xian et al., 2016). In a cost-effectiveness analysis of SYI for the treatment of stable angina pectoris in China, SYI combined with conventional therapy was a cost-effective treatment option compared with conventional therapy for unstable angina pectoris (Xuan et al., 2018). A network meta-analysis of CHIs in the treatment of pulmonary heart disease, which compared the efficacy of seven CHIs with Western medicine in the treatment of pulmonary heart disease, included 118 randomized controlled trials with 10,085 patients. The results showed that Shenfu injection, SMI, and Shenqi Fuzheng injection combined with Western medicine may be the best treatment for pulmonary heart disease (Wang KH. et al., 2020).

Atherosclerosis and coronary artery disease

A total of 53 qualified randomized controlled trials involving 6,401 patients were included in the treatment of acute coronary syndrome with DSI. The results showed that compared with Western medicine treatment alone, DSI combined with Western medicine treatment could significantly improve the curative effect (Guo SY. et al., 2020). A systematic review and meta-analysis of the efficacy of DHI combined with coronary revascularization in the treatment of acute coronary syndrome, included 14 studies involving 1,533 patients. DHI combined with surgical treatment of acute coronary syndrome can significantly improve acute coronary syndrome and reduce the incidence of complications after coronary intervention (Zou et al., 2018). SMI can effectively increase cardiac output, stroke volume, and ejection fraction in patients undergoing off-pump coronary artery bypass surgery, and improve the safety of anesthesia management (Liu QX. et al., 2018).

Hypertension and hypertrophy

Some researchers have conducted a meta-analysis of tanshinone IIA sulfonate sodium injection in the treatment of hypertensive nephropathy, including 16 trials involving 1,696 patients. Tanshinone IIA sodium sulfonate injection combined with angiotensin receptor blocker (ARB) therapy is more effective than ARB monotherapy in regulating hypertensive nephropathy, manifested as improvement of glomerular filtration rate and reduction of urinary protein, cystatin, urinary immunoglobulin G, and urinary transferrin. In addition, combination therapy allows for better control of systolic and diastolic blood pressure (Xu JY. et al., 2019).

Some researchers have investigated the efficacy of DHI combined with antihypertensive drugs for the treatment of hypertensive nephropathy. The meta-analysis included 15 studies and the results showed that DHI combined with antihypertensive drugs was more effective in reducing microalbuminuria than antihypertensive drugs alone. The drug has the advantage of lowering systolic blood pressure, diastolic blood pressure, and serum creatinine (Li YZ. et al., 2020).

Safety concerns, toxicity, and synergistic effects of CHIs

Although CHIs have been used clinically for many years and play an indispensable role in the treatment of cardio-cerebrovascular diseases, their adverse reactions have always been a focus of clinical attention. As the injection is a special dosage form, it is more likely to cause adverse reactions. CHIs are mostly complex systems containing many biologically active ingredients; therefore, the possibility of complex unforeseen effects will increase. Modern researchers have conducted extensive research on the safety of CHIs, including their quality control through chemical and biological methods. Through a pharmacokinetic study of CHIs, drug absorption, distribution, metabolism, and excretion *in vivo* were analyzed to evaluate their safety.

Adverse reactions to CHIs have always been the focus of attention. Scientific and reasonable quality control methods are crucial to ensure the stability and safety of their clinical application. Chemical and biological evaluation is the main of quality control methods for CHI. Because chemical components are critical to the efficacy of CHIs, component detection is the primary method for the quality control of CHI. For example, in the production process of SMI, its quality control index components were selected through the analysis of the component transfer process, and the quality control method of SMI injection was established (Zhao CX. et al., 2019). Quantitative analysis of SLI by 1H-qNMR and its quality control. qNMR can be used as a routine method for quality control of SLI and may be used for the quantification of diastereomers in other TCM preparations (Chen XL. et al., 2016). Rapid identification of the chemical constituents of DHI using liquid chromatography-mass spectrometry and precursor ion scanning enhanced liquid chromatography-tandem mass spectrometry (Li C. et al., 2019; Xu LL. et al., 2019). Rapid identification of chemical constituents in HJTI by liquid chromatography-quadrupole time-of-flight mass spectrometry (LC-Q-TOF-MS) can also be used to identify the chemical constituents of other *Rhodiola Rosea*-containing Chinese medicine formulations Element (Liu YN. et al., 2019). The phytochemical components of SXNI were identified using ultra-high-performance liquid chromatography-Q-precise mixed quadrupole orbital high-resolution mass spectrometry (UHPLC-Q-orbitrap HRMS) and nuclear magnetic resonance (NMR) techniques (Yu ST. et al., 2019). The detection of haptens in SXNI is based on human serum albumin fluorescence. A method for determining curcuminone, curcuminenol, curcuminenone, and gemmanone in XNJI was established based on a high-performance liquid chromatography-diode array (Pan et al., 2015).

Affected by the concept of "the higher the content of the index components, the better the quality," there are still many drawbacks to a single chemical evaluation. It is easy to cause the post-marketing TCM products to be "qualified" according to the current quality standards, but cases of excessive biological activity affecting the clinical treatment effect occur occasionally. Therefore, biological evaluation is indispensable for the quality control of CHIs. For example, HHI detects mass fluctuations by chemical fingerprinting (ultra-performance liquid chromatography-tandem mass spectrometry) and bioassays (including cell-based bio-atlas assays and enzymatic assays) to screen out abnormal samples of HHI, and 33 compounds have been identified in HHI (Feng et al., 2018). In addition, *in vitro* anticoagulant activity evaluations of seven HHI samples from different companies through *in vitro* anticoagulant activity tests (Wang KH. et al., 2018). The efficacy and consistency of different batches of XSTI were evaluated based on bioactive chemical markers. First, the chemical structure of the XSTI was systematically characterized. Second, through *in vivo* validation based on the adjusted efficacy score, Panax notoginsenoside R1, ginsenoside Rg1, Re, Rb1, and Rd were identified as bioactive chemical markers for XSTI treatment of cardio-cerebrovascular diseases to assess the consistency between the batches (Yang ZZ. et al., 2017).

Owing to the particularity of the administration of CHIs, their safety has always been a concern for everyone. Therefore, pharmacokinetic research and analysis of the absorption, distribution, metabolism, and excretion of CHIs *in vivo* are important. Some researchers have developed the pharmacokinetics of ligustrazine after single and multiple intravenous injections of Shenxiong glucose in rats. After single and multiple intravenous injections of SXG, the pharmacokinetics of ligustrazine in rats showed a linear relationship with a half-life of approximately 35 min. Ligustrazine is easily distributed in organs with high perfusion and almost disappears from the organs 90 min after injection (Wang Q. et al., 2019). Pharmacokinetic study of salvianolic acid and ligustrazine in rat plasma after intravenous administration of DLI. The results showed that the elimination half-life ($t_{1/2}$), $AUC_{0\text{-}t,}$ and C_o in the tanshinol group were 30%–40% higher than those in the tanshinol ligustrazine injection group (Jiao et al., 2020). Some researchers have investigated the distribution kinetics of puerarin in the hippocampus of rats treated with puerarin injection after acute focal cerebral ischemia. The AUC of puerarin in the embolic hippocampus ($AUC_{0-120min}$) was higher than that in the normal hippocampus. The average dwell time was higher than that of a normal hippocampus (Kong et al., 2019).

The content and pharmacokinetic analysis of borneol and muskone after the intravenous administration of XNJI in rats were determined by GC-MS/MS. At 8 and 1.5 h after intravenous injection of XNJ, the concentrations of borneol and muskone were 10 and 2.5 ng/mL (Song et al., 2017). Some researchers have also identified biologically active anti-angiogenic components targeting tumor endothelial cells in SMI through multi-dimensional pharmacokinetics, and protopanaxadiol (PPD) ginsenoside (Rb1, Rb2, Rb3, Rc, and Rd) concentrations were higher than those of protopanaxadiol (Rg1 and Re) and oleanane types (Rb1, Rb2, Rb3, Rc, and Rd). Among the PPD-type ginsenosides, Rd showed the highest concentration in tumors and TECs after repeated injections. *In vivo* bioactivity results showed that Rd inhibited neovascularization in tumors, normalized tumor vascular architecture, and enhanced the antitumor effect of 5-fluorouracil in xenografted mice. Furthermore, Rd inhibited endothelial cell migration and tube formation *in vitro*. In conclusion, Rd may be an important active form that exerts antiangiogenic effects on tumors after SMI treatment (Zhong et al., 2020).

Re-evaluation of the post-marketing safety of CHIs is also important to ensure the safety of clinical medication. Some researchers have evaluated the factors influencing suspected allergic reactions and systemic adverse reactions after SXNI. A randomized controlled study and cohort study were conducted on adverse drug reactions to SXNI using a computer database. When SXNI was used in combination with the chemical drugs, the adverse reaction rate was 4.36%. The incidence of allergic reactions to SXNI is also affected by the drug, treatment time, single dose, indications, and off-label use (Wang C. et al., 2018).

Perspectives and challenges

The theory of TCM is summed up with long-term human experience, and its basis is oral or external administration. CHI has changed the traditional administration of TCM, which may produce new pharmacological effects or adverse reactions. In most cases, traditional medicine has limited guidance on the compatibility and proportion of CHIs. In addition, CHIs have the characteristics

of a single component and multiple components, and exist as a single herb or prescription. Most CHI herbal studies are unclear, and pharmacology, pharmacokinetics, adverse reactions, and mechanisms of action research are not sufficiently thorough. In recent years, based on the multi-component and multi-target characteristics of CHIS, researchers have revealed the material basis of the efficacy of CHIS and its mechanism of action in treating diseases through network pharmacology, metabolomics, transcriptomics, and other technologies (Wang Z. et al., 2021). In addition, a large sample multicenter clinical trial of CHIS is conducive to ensuring the safety and effectiveness of its clinical application (Jiang et al., 2019; Cao et al., 2022; Yan et al., 2022).

Research on pharmaceutical preparations for CHIs is scarce. The technical requirements set standardized requirements for the pharmaceutical research content of CHIs, such as raw materials, excipients, preparation technology, and quality standards. Compared with oral TCM preparations, the quality of raw materials for CHIs should be higher, and the medicinal parts, origin (including origin processing), harvest season, storage conditions, and production of raw materials should be fixed. In terms of the preparation process, developers should fully explain the rationality of the process and comprehensively consider the impact of the process on the safety, effectiveness, and quality controllability of CHIs.

CHIs should have higher quality standards to ensure the safety and effectiveness of clinical use; therefore, quality research is very important in the research and development process of CHIs. Quality research includes literature research, chemical composition research, qualitative and quantitative analysis methods, and biological quality control methods. The quality control items of CHIs should consider the injection characteristics and sensitively reflect changes in drug quality (Wang N. et al., 2018; Tu et al., 2021). It is important to establish the pharmacodynamic material basis of CHIs and to rapidly detect harmful components to ensure safety and effectiveness (Bu et al., 2018; Zang et al., 2018).

Conclusion

Compared with TCM preparations, CHIs avoid degradation of the gastrointestinal tract and the first-pass effect of the liver during traditional administration. The clinical application of CHI is more convenient, and its onset is faster. CHIs have been used clinically for many years and have played an important role in the treatment of acute and severe cardio-cerebrovascular diseases. However, some adverse reactions occur as a result of its complexity and deficiencies in development and production. These issues can be addressed by expanding the scope of our research. Through research, the main components of the injection can be determined and quality control oversight can be carried out so that the quality standard can be controlled. At the same time, further research on the mechanism of action and pharmacokinetics can reveal the scientific connotation of CHIs. In addition to standardizing clinical use and strengthening supervision, CHIs have broad application prospects.

Author contributions

JH performed the research and drafted the manuscript. RC, HX, ZY, XB, and WY proposed amendments to the manuscript. PJ helped to coordinate support and funding. All authors read and approved the final manuscript.

Funding

The research work was financially supported by the National Natural Science Foundation of China (U19A2010), the Sichuan Province Science and Technology Planning Project (2021YFYZ0012-5) and the national multidisciplinary innovation team project of traditional Chinese medicine (ZYYCXTD-D-202209).

Acknowledgments

We would like to thank PJ and Chaomei Fu for their guidance on the selection of this paper. We would like to thank Editage (www.editage.cn) for English language editing.

Conflict of interest

The authors declare that the research was conducted in the absence of any commercial or financial relationships that could be construed as a potential conflict of interest.

Publisher's note

References

Ai, J., Wan, H., Shu, M., Zhou, H., Zhao, T., Fu, W., et al. (2017). Guhong injection protects against focal cerebral ischemia-reperfusion injury via anti-inflammatory effects in rats. *Arch. Pharm. Res.* 40 (5), 610–622. doi:10.1007/s12272-016-0835-4

Bi, C., Li, P. L., Liao, Y., Rao, H. Y., Li, P. B., Yi, J., et al. (2019). Pharmacodynamic effects of Dan-hong injection in rats with blood stasis syndrome. *Biomed. Pharmacother.* 118, 109187. doi:10.1016/j.biopha.2019.109187

Bu, Y., Hu, Q., Xu, K., Xie, X., and Wang, S. (2018). Improved cell membrane bioaffinity sample pretreatment technique with enhanced stability for screening of potential allergenic components from traditional Chinese medicine injections. *J. Mater Chem. B* 6 (4), 624–633. doi:10.1039/c7tb02768k

Cao, X., Liu, H., Zhou, M., Chen, X., and Long, D. (2022). Comparative efficacy of five Chinese medicine injections for treating dilated cardiomyopathy with heart failure: A bayesian network meta-analysis. *J. Ethnopharmacol.* 282, 114604. doi:10.1016/j.jep.2021.114604

Chen, A. F., Ding, S. B., Kong, L. L., Xu, J. P., He, F., Ru, C. H., et al. (2021). Safflower injection inhibits pulmonary arterial remodeling in a monocrotaline-induced pulmonary arterial hypertension rat model. *Zeitschrift Fur Naturforschung Sect. C-a J. Biosci.* 76 (1-2), 27–34. doi:10.1515/znc-2020-0004

Chen, D., Zhang, H. F., Yuan, T. Y., Sun, S. C., Wang, R. R., Wang, S. B., et al. (2022a). Puerarin-V prevents the progression of hypoxia- and monocrotaline-induced pulmonary hypertension in rodent models. *Acta Pharmacol. Sin. Physiol.* 43(9), 2325–2339. doi:10.1038/s41401-022-00865-y

Chen, J. R., Cao, W. J., Asare, P. F., Lv, M., Zhu, Y., Li, L., et al. (2016a). Amelioration of cardiac dysfunction and ventricular remodeling after myocardial infarction by danhong injection are critically contributed by anti-TGF-beta-mediated fibrosis and angiogenesis mechanisms. *J. Ethnopharmacol.* 194, 559–570. doi:10.1016/j.jep.2016.10.025

Chen, J., Wei, J., Huang, Y., Ma, Y., Ni, J., and Li, M. (2018). Danhong injection enhances the therapeutic efficacy of mesenchymal stem cells in myocardial infarction by promoting angiogenesis. *Ther. Efficacy Mesenchymal Stem Cells Myocard. Infarct. by Promot. Angiogenesis. Front Physiol*, 9, 991. doi:10.3389/fphys.2018.00991

Chen, X. L., Guo, Y. J., Hu, Y. J., Yu, B. Y., and Qi, J. (2016b). Quantitative analysis of highly similar salvianolic acids with 1 H qNMR for quality control of traditional Chinese medicinal preparation Salvianolate Lyophilized Injection. *J. Pharm. Biomed. Analysis* 124, 281–287. doi:10.1016/j.jpba.2016.02.016

Chen, Y., Tang, M., Yuan, S., Fu, S., Li, Y., Li, Y., et al. (2022b). Rhodiola rosea: A therapeutic candidate on cardiovascular diseases. *Oxidative Med. Cell. Longev.* 2022, 1348795. doi:10.1155/2022/1348795

Cui, Q., Zhang, Y. L., Ma, Y. H., Yu, H. Y., Zhao, X. Z., Zhang, L. H., et al. (2020). A network pharmacology approach to investigate the mechanism of Shuxuening injection in the treatment of ischemic stroke. *J. Ethnopharmacol.* 257, 112891. doi:10.1016/j.jep.2020.112891

Duan, L., Xiong, X. J., Hu, J. Y., Liu, Y. M., and Wang, J. (2018). Efficacy and safety of oral Panax notoginseng saponins for unstable angina patients: A meta-analysis and systematic review. *Phytomedicine* 47, 23–33. doi:10.1016/j.phymed.2018.04.044

Fan, F., Yang, L., Li, R., Zou, X., Li, N., Meng, X., et al. (2020). Salidroside as a potential neuroprotective agent for ischemic stroke: A review of sources, pharmacokinetics, mechanism and safety. *Biomed. Pharmacother.* 129, 110458. doi:10.1016/j.biopha.2020.110458

Fan, H., Li, M., Yu, L., Jin, W., Yang, J., Zhang, Y., et al. (2018). Effects of Danhong Injection on platelet aggregation in hyperlipidemia rats. *J. Ethnopharmacol.* 212, 67–73. doi:10.1016/j.jep.2017.10.017

Fan, Z., Guo, C., Zhang, Y., Yao, J., Liao, L., and Dong, J. (2019). Hongjingtian injection inhibits proliferation and migration and promotes apoptosis in high glucose-induced vascular smooth muscle cells. *Drug Des. Devel Ther.* 13, 4115–4126. doi:10.2147/DDDT.S220719

Feng, C., Wan, H., Zhang, Y., Yu, L., Shao, C., He, Y., et al. (2020). Neuroprotective effect of danhong injection on cerebral ischemia-reperfusion injury in rats by activation of the PI3K-akt pathway. *Front. Pharmacol.* 11, 298. doi:10.3389/fphar.2020.00298

Feng, L., Wu, X. J., Cao, T., and Wu, B. (2021). The efficacy and safety of Xuesaitong injection combined with Western medicines in the treatment of ischemic stroke: An updated systematic review and meta-analysis. *Ann. Palliat. Med.* 10 (9), 9523–9534. doi:10.21037/apm-21-1828

Feng, W. W., Zhang, Y., Tang, J. F., Zhang, C. E., Dong, Q., Li, R. Y., et al. (2018). Combination of chemical fingerprinting with bioassay, a preferable approach for quality control of Safflower Injection. *Anal. Chim. Acta* 1003, 56–63. doi:10.1016/j.aca.2017.11.069

Gresele, P., Guglielmini, G., Del Pinto, M., Calabro, P., Pignatelli, P., Patti, G., et al. (2021). Peripheral arterial disease has a strong impact on cardiovascular outcome in patients with acute coronary syndromes: From the START antiplatelet registry. *Int. J. Cardiol.* 327, 176–182. doi:10.1016/j.ijcard.2020.10.079

Guo, R., Li, L., Su, J., Li, S., Duncan, S. E., Liu, Z. H., et al. (2020a). Pharmacological activity and mechanism of tanshinone IIA in related diseases. *Drug Des. Dev. Ther.* 14, 4735–4748. doi:10.2147/DDDT.S266911

Guo, S. Y., Wu, J. R., Ni, M. W., Jia, S. S., Zhang, J. Y., Zhou, W., et al. (2020b). Comparative efficacy of danshen class injections for treating acute coronary syndrome: A multidimensional bayesian network meta-analysis of randomized controlled trials. *Front. Pharmacol.* 11, 1260. doi:10.3389/fphar.2020.01260

Hao, L. J., L, A. H., and S, J. Y. (2020). Statistical analysis of raw materials of traditional Chinese medicine injections and their prescriptions. *Mod. Chin. Tradit. Med.* 3 (22), 322–331.

He, Q. Y., Yu, X. Y., Xiao, Z., Sun, X., Zhu, W. F., Yi, X. Q., et al. (2021). Comparison of the efficacy of danhong injections at different time-points during the perioperative period of acute myocardial infarction: A systematic review and meta-analysis of randomized controlled trials. *Front. Pharmacol.* 12, 643446. doi:10.3389/fphar.2021.643446

Huang, P. Y., Chen, Y., Zhang, H. B., Chen, B. J., Zhao, S., Feng, Y. C., et al. (2022). Comparative efficacy of Chinese herbal injections for septic shock: A bayesian network meta-analysis of randomized controlled trials. *Front. Pharmacol.* 13, 850221. doi:10.3389/fphar.2022.850221

Huang, W., Yang, Y., Zeng, Z., Su, M., Gao, Q., and Zhu, B. (2016). Effect of Salvia miltiorrhiza and ligustrazine injection on myocardial ischemia/reperfusion and hypoxia/reoxygenation injury. *Mol. Med. Rep.* 14 (5), 4537–4544. doi:10.3892/mmr.2016.5822

Jiang, C., Shen, J., Shou, D., Wang, N., Jing, J., Zhang, G., et al. (2019). Identification of high-risk patients for ADR induced by traditional Chinese medicine injection: A nested case-control study. *Sci. Rep.* 9 (1), 16721. doi:10.1038/s41598-019-53267-2

Jiao, W. J., Lei, Z., Zhao, X., Wang, K., Ma, A. L., Du, L., et al. (2020). Pharmacokinetic study of tanshinol and ligustrazine in rat plasma after intravenous administration of tanshinol and Danshen Chuanxiongqin Injection. *Biomed. Chromatogr.* 34 (9), e4869. doi:10.1002/bmc.4869

Keeter, W. C., Ma, S., Stahr, N., Moriarty, A. K., and Galkina, E. V. (2022). Atherosclerosis and multi-organ-associated pathologies. *Seminars Immunopathol.* 44 (3), 363–374. doi:10.1007/s00281-022-00914-y

Kong, H., Zhang, G. L., Cheng, J. J., Shi, R. F., Zhang, M. L., Cao, P., et al. (2019). Distribution kinetics of puerarin in rat hippocampus after acute local cerebral ischemia. *J. Pharm. Biomed. Analysis* 164, 196–201. doi:10.1016/j.jpba.2018.10.038

Li, C., Yang, J. H., Tong, X., Zhao, C., He, Y., and Wan, H. T. (2019a). Precursor ion scan enhanced rapid identification of the chemical constituents of Danhong injection by liquid chromatography-tandem mass spectrometry: An integrated strategy. *J. Chromatogr. A* 1602, 378–385. doi:10.1016/j.chroma.2019.04.023

Li, D., Li, Y., Yang, S., Yu, Z., Xing, Y., and Wu, M. (2022a). Mechanism and potential target of blood-activating Chinese botanical drugs combined with anti-platelet drugs: Prevention and treatment of atherosclerotic cardiovascular diseases. *Front. Pharmacol.* 13, 811422. doi:10.3389/fphar.2022.811422

Li, H., Gao, C., Liu, C., Liu, L., Zhuang, J., Yang, J., et al. (2021a). A review of the biological activity and pharmacology of cryptotanshinone, an important active constituent in Danshen. *Biomed. Pharmacother.* 137, 111332. doi:10.1016/j.biopha.2021.111332

Li, H., Mao, Y., Zhang, Q., Han, Q., Man, Z., Zhang, J., et al. (2016). Xinmailong mitigated epirubicin-induced cardiotoxicity via inhibiting autophagy. *J. Ethnopharmacol.* 192, 459–470. doi:10.1016/j.jep.2016.08.031

Li, H. Q., Wei, J. J., Xia, W., Li, J. H., Liu, A. J., Yin, S. B., et al. (2015a). Promoting blood circulation for removing blood stasis therapy for acute intracerebral hemorrhage: A systematic review and meta-analysis. *Acta Pharmacol. Sin.* 36 (6), 659–675. doi:10.1038/aps.2014.139

Li, L. J., Li, Y. M., Qiao, B. Y., Jiang, S., Li, X., Du, H. M., et al. (2015b2015). The value of safflower yellow injection for the treatment of acute cerebral infarction: A randomized controlled trial. *Evidence-Based Complementary Altern. Med.* 2015, 1–6. doi:10.1155/2015/478793

Li, L., Li, J., Wang, Q., Zhao, X., Yang, D., Niu, L., et al. (2020a). Shenmai injection protects against doxorubicin-induced cardiotoxicity via maintaining mitochondrial homeostasis. *Front. Pharmacol.* 11, 815. doi:10.3389/fphar.2020.00815

Li, L., Sha, Z., Wang, Y., Yang, D., Li, J., Duan, Z., et al. (2019b). Pre-treatment with a combination of Shenmai and Danshen injection protects cardiomyocytes against hypoxia/reoxygenation- and H2O2-induced injury by inhibiting mitochondrial permeability transition pore opening. *Exp. Ther. Med.* 17 (6), 4643–4652. doi:10.3892/etm.2019.7462

Li, M., Zhou, J., Jin, W. F., Li, X. H., and Zhang, Y. Y. (2018a). Danhong injection combined with t-PA improves thrombolytic therapy in focal embolic stroke. *Front. Pharmacol.* 9. doi:10.3389/fphar.2018.00308

Li, R., Xia, Z., Li, B., Tian, Y., Zhang, G., Li, M., et al. (2021b). Advances in supercritical carbon dioxide extraction of bioactive substances from different parts of Ginkgo biloba L. *Molecules* 26 (13), 4011. doi:10.3390/molecules26134011

Li, T., Zhang, Y., Tian, J., Yang, L., and Wang, J. (2019c). Ginkgo biloba pretreatment attenuates myocardial ischemia-reperfusion injury via mitoBKCa. *Am. J. Chin. Med.* 47 (5), 1057–1073. doi:10.1142/S0192415X1950054X

Li, X., Guo, K., Zhang, R., Wang, W., Sun, H., Yague, E., et al. (2022b). Exploration of the mechanism of salvianolic acid for injection against ischemic stroke: A research based on computational prediction and experimental validation. *Front. Pharmacol.* 13, 894427. doi:10.3389/fphar.2022.894427

Li, X., Guo, T., Feng, Q., Bai, T., Wu, L., Liu, Y., et al. (2022c). Progress of thrombus formation and research on the structure-activity relationship for antithrombotic drugs. *Eur. J. Med. Chem.* 228, 114035. doi:10.1016/j.ejmech.2021.114035

Li, X., Yuan, T., Chen, D., Chen, Y., Sun, S., Wang, D., et al. (2018b). Cardioprotective effects of puerarin-V on isoproterenol-induced myocardial infarction mice is associated with regulation of PPAR-Ɣ/NF-κB pathway. *Molecules* 23 (12), 3322. doi:10.3390/molecules23123322

Li, Y., Cai, M., Mao, G. X., Shu, Q. F., Liu, X. B., and Liu, X. L. (2021c). Preclinical evidence and possible mechanisms of Rhodiola rosea L. and its components for ischemic stroke: A systematic review and meta-analysis. *Front. Pharmacol.* 12, 736198. doi:10.3389/fphar.2021.736198

Li, Y., Xu, C., Wang, H., Liu, X., Jiang, L., Liang, S., et al. (2021d). Systems pharmacology reveals the multi-level synergetic mechanism of action of Ginkgo biloba L. leaves for cardiomyopathy treatment. *J. Ethnopharmacol.* 264, 113279. doi:10.1016/j.jep.2020.113279

Li, Y. Z., Yan, S. H., Qian, L. C., Wu, L. H., Zheng, Y. W., and Fang, Z. Y. (2020b). Danhong injection for the treatment of hypertensive nephropathy: A systematic review and meta-analysis. *Front. Pharmacol.* 11, 909. doi:10.3389/fphar.2020.00909

Li, Z., Wang, H., Xiao, G., Du, H., He, S., Feng, Y., et al. (2021e). Recovery of post-stroke cognitive and motor deficiencies by Shuxuening injection via regulating hippocampal BDNF-mediated Neurotrophin/Trk Signaling. *Biomed. Pharmacother.* 141, 111828. doi:10.1016/j.biopha.2021.111828

Li, Z., Xiao, G., Lyu, M., Wang, Y., He, S., Du, H., et al. (2020c). Shuxuening injection facilitates neurofunctional recovery via down-regulation of G-CSF-mediated granulocyte adhesion and diapedesis pathway in a subacute stroke mouse model. *Biomed. Pharmacother.* 127, 110213. doi:10.1016/j.biopha.2020.110213

Liang, H., Yuan, X., Sun, C., Sun, Y., Yang, M., Feng, S., et al. (2022). Preparation of a new component group of Ginkgo biloba leaves and investigation of the antihypertensive effects in spontaneously hypertensive rats. *Biomed. Pharmacother.* 149, 112805. doi:10.1016/j.biopha.2022.112805

Liao, Q., Pang, L., Li, J. J., Zhang, C., Li, J. X., Zhang, X., et al. (2022). Characterization and diabetic wound healing benefits of protein-polysaccharide complexes isolated from an animal ethno-medicine *Periplaneta americana* L. *Int. J. Biol. Macromol.* 195, 466–474. doi:10.1016/j.ijbiomac.2021.12.018

Liberale, L., Ministrini, S., Carbone, F., Camici, G. G., and Montecucco, F. (2021). Cytokines as therapeutic targets for cardio- and cerebrovascular diseases. *Basic Res. Cardiol.* 116 (1), 23. doi:10.1007/s00395-021-00863-x

Lin, S. S., Liu, C. X., Wang, X. L., and Mao, J. Y. (2019). Intervention mechanisms of Xinmailong injection, a Periplaneta americana extract, on cardiovascular disease: A systematic review of basic researches. *Evid. Based Complement. Altern. Med.* 2019, 8512405. doi:10.1155/2019/8512405

Liu, G., Lin, J., Zhang, L., Gao, Q., Wang, Z., Chang, Z., et al. (2022). Uncovering the mechanism of the xingnaojing injection against ischemic stroke using a combined network pharmacology approach and gut microbiota analysis. *Evid. Based Complement. Altern. Med.* 2022, 5886698. doi:10.1155/2022/5886698

Liu, H. Y., Wang, S. J., Sun, A. J., Huang, D., Wang, W., Zhang, C. Y., et al. (2012). Danhong inhibits oxidized low-density Lipoprotein–Induced immune maturation of dentritic cells via a peroxisome proliferator activated receptor <I>γ</I>–Mediated pathway. *J. Pharmacol. Sci.* 119 (1), 1–9. doi:10.1254/jphs.11226fp

Liu, L., Wang, Y., Zhang, J., and Wang, S. (2021). Advances in the chemical constituents and chemical analysis of Ginkgo biloba leaf, extract, and phytopharmaceuticals. *J. Pharm. Biomed. Anal.* 193, 113704. doi:10.1016/j.jpba.2020.113704

Liu, Q. X., Wu, H. Y., Wang, J. J., and Li, X. M. (2018a). Effects of Shenmai injection on the values of CO, SV, and ef in patients undergoing off-pump coronary artery bypass graft: A randomized, clinical trial. *Medicine* 97 (10), e0085. doi:10.1097/MD.0000000000010085

Liu, S., Wang, K. H., Duan, X. J., Wu, J. R., Zhang, D., Liu, X. K., et al. (2019a). Efficacy of danshen class injection in the treatment of acute cerebral infarction: A bayesian network meta-analysis of randomized controlled trials. *Evidence-Based Complementary Altern. Med.* 2019, 1–12. doi:10.1155/2019/5814749

Liu, X. T., Ren, P. W., Peng, L., Kang, D. Y., Zhang, T. L., Wen, S., et al. (2016). Effectiveness and safety of ShenXiong glucose injection for acute ischemic stroke: A systematic review and GRADE approach. *BMC Complement. Altern. Med.* 16, 68. doi:10.1186/s12906-016-1038-8

Liu, X., Tan, W., Yang, F., Wang, Y., Yue, S., Wang, T., et al. (2018b). Shengmai injection reduces apoptosis and enhances angiogenesis after myocardial ischaemia and reperfusion injury in rats. *Biomed. Pharmacother.* 104, 629–636. doi:10.1016/j.biopha.2018.04.180

Liu, Y. N., Chen, C. H., Qiu, J. W., Fang, Z. B., Wu, H. B., Zhang, X. X., et al. (2019b). Characterization of the chemical constituents in Hongjingtian injection by liquid chromatography quadrupole time-of-flight mass spectrometry. *Biomed. Chromatogr.* 33 (3), e4446. doi:10.1002/bmc.4446

Lu, D. Y., Sun, J., Zheng, J., Zheng, L., Xue, W. N., Li, C., et al. (2021). Shenxiong glucose injection inhibits H2O2-induced H9c2 cell apoptosis by activating the ERK signaling pathway. *Biomed. Pharmacother.* 143, 112114. doi:10.1016/j.biopha.2021.112114

Lu, D., Zhang, Y., Xue, W., Sun, J., Yang, C., Lin, C., et al. (2020). Shenxiong glucose injection protects H9c2 cells from CoCl2-induced oxidative damage via antioxidant and antiapoptotic pathways. *Nat. Product. Commun.* 15 (4), 1934578X2092005. doi:10.1177/1934578x20920054

Lu, X. F., Liu, Z. Y., Cui, Q. M., Liu, F. C., Li, J. X., Niu, X. G., et al. (2022). A polygenic risk score improves risk stratification of coronary artery disease: A large-scale prospective Chinese cohort study. *Eur. Heart J.* 43 (18), 1702–1711. doi:10.1093/eurheartj/ehac093

Lu, X. H., Zhang, L., Wang, J. B., Liu, H. H., Li, H. T., Zhou, H. Q., et al. (2018). Clinical efficacy and safety of Xinmailong injection for the treatment of chronic heart failure: A meta-analysis. *Front. Pharmacol.* 9, 810. doi:10.3389/fphar.2018.00810

Lv, J. Y., Shi, S. Q., Zhang, B. X., Xu, X., Zheng, H. R., Li, Y. M., et al. (2022). Role of puerarin in pathological cardiac remodeling: A review. *Pharmacol. Res.* 178, 106152. doi:10.1016/j.phrs.2022.106152

Lyu, M., Cui, Y., Zhao, T., Ning, Z., Ren, J., Jin, X., et al. (2018). Tnfrsf12a-Mediated atherosclerosis signaling and inflammatory response as a common protection mechanism of shuxuening injection against both myocardial and cerebral ischemia-reperfusion injuries. *Front. Pharmacol.* 9, 312. doi:10.3389/fphar.2018.00312

Ma, R. S., Zhao, L. C. Y., Zhao, Y. M., and Li, Y. (2022). Puerarin action on stem cell proliferation, differentiation and apoptosis: Therapeutic implications for geriatric diseases. *Phytomedicine* 96, 153915. doi:10.1016/j.phymed.2021.153915

Ma, X., Wang, T., Wen, J. X., Wang, J., Zeng, N., Zou, W. J., et al. (2020). Role of Xingnaojing Injection in treating acute cerebral hemorrhage A systematic review and meta-analysis. *Medicine* 99 (15), e19648. doi:10.1097/MD.0000000000019648

Ma, X., Yang, Y. X., Chen, N. A., Xie, Q., Wang, T., He, X., et al. (2017). Meta-analysis for clinical evaluation of xingnaojing injection for the treatment of cerebral infarction. *Front. Pharmacol.* 8, 485. doi:10.3389/fphar.2017.00485

Novo, G., Sansone, A., Rizzo, M., Guarneri, F. P., Pernice, C., and Novo, S. (2014). High plasma levels of endothelin-1 enhance the predictive value of preclinical atherosclerosis for future cerebrovascular and cardiovascular events: A 20-year prospective study. *J. Cardiovasc. Med.* 15 (9), 696–701. doi:10.2459/JCM.0000000000000121

Novo, S., Carita, P., Lo Voi, A., Muratori, I., Tantillo, R., Corrado, E., et al. (2019). Impact of preclinical carotid atherosclerosis on global cardiovascular risk stratification and events in a 10-year follow-up: Comparison between the algorithms of the framingham heart study, the European SCORE and the Italian 'progetto cuore. *J. Cardiovasc. Med.* 20 (2), 91–96. doi:10.2459/JCM.0000000000000740

Orgah, J. O., He, S., Wang, Y., Jiang, M., Wang, Y., Orgah, E. A., et al. (2020). Pharmacological potential of the combination of Salvia miltiorrhiza (Danshen) and Carthamus tinctorius (Honghua) for diabetes mellitus and its cardiovascular complications. *Pharmacol. Res.* 153, 104654. doi:10.1016/j.phrs.2020.104654

Orgah, J. O., Wang, M., Yang, X. H., Wang, Z. L., Wang, D. D., Zhang, Q., et al. (2018). Danhong injection protects against hypertension-induced renal injury via down-regulation of myoglobin expression in spontaneously hypertensive rats. *Kidney & Blood Press. Res.* 43 (1), 12–24. doi:10.1159/000486735

Pan, W. D., Yang, L. X., Feng, W. H., Lin, L. M., Li, C., Liu, W. W., et al. (2015). Determination of five sesquiterpenoids in Xingnaojing injection by quantitative analysis of multiple components with a single marker. *J. Sep. Sci.* 38 (19), 3313–3323. doi:10.1002/jssc.201500494

Pang, L., Liao, Q., Zou, L., Zhang, C., Nie, X., Yi, Z. W., et al. (2022). Two glycoproteins from medicinal insect *Periplaneta americana* (L.) promote diabetic wound healing via macrophage polarization modulation. *Int. J. Biol. Macromol.* 209, 2130–2141. doi:10.1016/j.ijbiomac.2022.04.193

Qi, J., Yu, J., Tan, Y., Chen, R., Xu, W., Chen, Y., et al. (2017). Mechanisms of Chinese Medicine Xinmailong's protection against heart failure in pressure-overloaded mice and cultured cardiomyocytes. *Sci. Rep.* 7, 42843. doi:10.1038/srep42843

Qian, J., Zhao, X. P., Wang, W. T., Zhang, S. J., Hong, Z. P., Chen, X. L., et al. (2018). Transcriptomic study reveals recovery of impaired astrocytes contribute to neuroprotective effects of danhong injection against cerebral ischemia/reperfusion-induced injury. *Front. Pharmacol.* 9, 250. doi:10.3389/fphar.2018.00250

Qiu, H., Liu, W., Lan, T., Pan, W., Chen, X., Wu, H., et al. (2018). Salvianolate reduces atrial fibrillation through suppressing atrial interstitial fibrosis by inhibiting TGF-β1/Smad2/3 and TXNIP/NLRP3 inflammasome signaling pathways in post-MI rats. *Phytomedicine* 51, 255–265. doi:10.1016/j.phymed.2018.09.238

Qu, X-Y., Zhang, Y-M., Tao, L-N., Gao, H., Zhai, J-H., Sun, J-M., et al. (2019). XingNaoJing injections protect against cerebral ischemia/reperfusion injury and alleviate blood-brain barrier disruption in rats, through an underlying mechanism of NLRP3 inflammasomes suppression. *Chin. J. Nat. Med.* 17 (7), 498–505. doi:10.1016/S1875-5364(19)30071-8

Sarkar, C., Quispe, C., Jamaddar, S., Hossain, R., Ray, P., Mondal, M., et al. (2020). Therapeutic promises of ginkgolide A: A literature-based review. *Biomed. Pharmacother.* 132, 110908. doi:10.1016/j.biopha.2020.110908

Shao, H., Huang, Y., Xu, D., Huang, S., and Tong, R. (2022). A systematic review and meta-analysis on the efficacy of puerarin injection as adjunctive therapy for unstable angina pectoris. *Front. Cardiovasc. Med.* 9, 763567. doi:10.3389/fcvm.2022.763567

Sikora, J., Karczmarska-Wodzka, A., Bugieda, J., and Sobczak, P. (2022). The importance of platelets response during antiplatelet treatment after ischemic stroke-between benefit and risk: A systematic review. *Int. J. Mol. Sci.* 23 (3), 1043. doi:10.3390/ijms23031043

Song, Y. F., Chu, Y., Ma, X. H., Zheng, H. R., Bai, X. L., Zhou, S. P., et al. (2017). GC-MS/MS method for the determination and pharmacokinetic analysis of borneol and muscone in rat after the intravenous administration of Xingnaojing injection. *J. Sep. Sci.* 40 (21), 4264–4271. doi:10.1002/jssc.201700341

Sun, W., Zhang, L. S., Fang, Z. R., Han, L. F., Wang, Q. Y., Leng, Y. Z., et al. (2022). Shuxuetong injection and its peptides enhance angiogenesis after hindlimb ischemia by activating the MYPT1/LIMK1/Cofilin pathway. *J. Ethnopharmacol.* 292, 115166. doi:10.1016/j.jep.2022.115166

Tan, D., Wu, J. R., Cui, Y. Y., Zhao, Y., Zhang, D., Liu, S., et al. (2018). Ginkgo leaf extract and dipyridamole injection as adjuvant treatment for angina pectoris: A meta-analysis of 41 randomized controlled trials. *Chin. J. Integr. Med.* 24 (12), 930–937. doi:10.1007/s11655-018-2557-6

Tian, F., Xu, L. H., Wang, B., Tian, L. J., and Ji, X. L. (2015). The neuroprotective mechanism of puerarin in the treatment of acute spinal ischemia-reperfusion injury is linked to cyclin-dependent kinase 5. *Neurosci. Lett.* 584, 50–55. doi:10.1016/j.neulet.2014.09.049

Tian, J. F., Liu, Y., and Chen, K. J. (2017). Ginkgo biloba extract in vascular protection: Molecular mechanisms and clinical applications. *Curr. Vasc. Pharmacol.* 15 (6), 532–548. doi:10.2174/1570161115666170713095545

Tian, Z. Y., Feng, L. D., Xie, Y., Xu, D. H., Zhang, C. Y., Kong, L. B., et al. (2021). Chinese herbal medicine xingnaojing injection for acute ischemic stroke: An overview of systematic reviews and meta-analyses. *Front. Pharmacol.* 12, 659408. doi:10.3389/fphar.2021.659408

Tu, Y., Li, L., Wang, Z., and Yang, L. (2021). Advances in analytical techniques and quality control of traditional Chinese medicine injections. *J. Pharm. Biomed. Anal.* 206, 114353. doi:10.1016/j.jpba.2021.114353

Wang, C., Shi, Q. P., Ding, F., Jiang, X. D., Tang, W., Yu, M. L., et al. (2018a). Reevaluation of the post-marketing safety of Shuxuening injection based on real-world and evidence-based evaluations. *Drug Des. Dev. Ther.* 12, 757–767. doi:10.2147/DDDT.S156000

Wang, D. J., and Tian, H. (2014). Effect of Mailuoning injection on 8-iso-prostaglandin F2 alpha and superoxide dismutase in rabbits with extremity ischemia-reperfusion injury. *J. Surg. Res.* 192 (2), 464–470. doi:10.1016/j.jss.2014.06.008

Wang, F., He, Q., Wang, J., Yuan, Q., Guo, H., Chai, L., et al. (2017a). Neuroprotective effect of salvianolate lyophilized injection against cerebral ischemia in type 1 diabetic rats. *BMC Complement. Altern. Med.* 17 (1), 258. doi:10.1186/s12906-017-1738-8

Wang, F. J., Wang, S. X., Chai, L. J., Zhang, Y., Guo, H., and Hu, L. M. (2018b). Xueshuantong injection (lyophilized) combined with salvianolate lyophilized injection protects against focal cerebral ischemia/reperfusion injury in rats through attenuation of oxidative stress. *Acta Pharmacol. Sin.* 39 (6), 998–1011. doi:10.1038/aps.2017.128

Wang, J., Chen, X. L., Bai, W. R., Wang, Z. Z., Xiao, W., and Zhu, J. B. (2021a). Study on mechanism of Ginkgo biloba L. Leaves for the treatment of neurodegenerative diseases based on network pharmacology. *Neurochem. Res.* 46 (7), 1881–1894. doi:10.1007/s11064-021-03315-z

Wang, J., Wang, X. H., Wan, W. P., Guo, Y. Y., Cui, Y. F., Liu, W. B., et al. (2021b). Effects of Shenfu injection on myocardial adenosine receptors in rats with myocardial ischemia-reperfusion postconditioning. *Hum. Exp. Toxicol.* 40 (12), S300–S309. doi:10.1177/09603271211041668

Wang, K. H., Li, S. F., Zhao, Y., Li, H. X., and Zhang, L. W. (2018c). *In vitro* anticoagulant activity and active components of safflower injection. *Molecules* 23 (1), 170. doi:10.3390/molecules23010170

Wang, K. H., Wu, J. R., Wang, H. J., Duan, X. J., Zhang, D., Wang, Y. Z., et al. (2020a). Comparative efficacy of Chinese herbal injections for pulmonary heart disease: A bayesian network meta-analysis of randomized controlled trials. *Front. Pharmacol.* 11, 634. doi:10.3389/fphar.2020.00634

Wang, L., Botchway, B. O. A., and Liu, X. (2021c). The repression of the HMGB1-TLR4-NF-κb signaling pathway by safflower yellow may improve spinal cord injury. *Front. Neurosci.* 15, 803885. doi:10.3389/fnins.2021.803885

Wang, L., Fan, X., Chen, Y., Liang, X., Shen, W., and Zhang, Y. (2022a). Efficacy and safety of xingnaojing injection for emergency treatment of acute ischemic stroke: A systematic review and meta-analysis. *Front. Pharmacol.* 13, 839305. doi:10.3389/fphar.2022.839305

Wang, L. L., Yu, Y. R., Yang, J. H., Zhao, X. P., and Li, Z. (2015). Dissecting Xuesaitong's mechanisms on preventing stroke based on the microarray and connectivity map. *Mol. Biosyst.* 11 (11), 3033–3039. doi:10.1039/c5mb00379b

Wang, N., Li, Z. Y., Zheng, X. L., Li, Q., Yang, X., and Xu, H. (2018d). Quality assessment of kumu injection, a traditional Chinese medicine preparation, using HPLC combined with chemometric methods and qualitative and quantitative analysis of multiple alkaloids by single marker. *Molecules* 23 (4), 856. doi:10.3390/molecules23040856

Wang, Q., Sun, H. P., Yu, L., Ma, X. P., Jiang, B. P., Bi, H. Q., et al. (2019a). Pharmacokinetic behaviors of ligustrazine after single- and multiple-dose intravenous Shenxiong glucose injection in rats by high-performance liquid chromatography. *Naunyn-Schmiedebergs Archives Pharmacol.* 392 (5), 565–572. doi:10.1007/s00210-018-01608-9

Wang, R., Wang, M., Zhou, J., Ye, T., Xie, X., Ni, D., et al. (2019b). Shuxuening injection protects against myocardial ischemia-reperfusion injury through reducing oxidative stress, inflammation and thrombosis. *Ann. Transl. Med.* 7 (20), 562. doi:10.21037/atm.2019.09.40

Wang, S. M., Ye, L. F., and Wang, L. H. (2020b). Shenmai injection improves energy metabolism in patients with heart failure: A randomized controlled trial. *Front. Pharmacol.* 11, 459. doi:10.3389/fphar.2020.00459

Wang, S. M., Ye, L. F., and Wang, L. H. (2022b). Traditional Chinese medicine enhances myocardial metabolism during heart failure. *Biomed. Pharmacother.* 146, 112538. doi:10.1016/j.biopha.2021.112538

Wang, T., Guo, R. X., Zhou, G. H., Zhou, X. D., Kou, Z. Z., Sui, F., et al. (2016). Traditional uses, botany, phytochemistry, pharmacology and toxicology of Panax notoginseng (burk.) FH chen: A review. *J. Ethnopharmacol.* 188, 234–258. doi:10.1016/j.jep.2016.05.005

Wang, Y., Chen, W., Zhou, J., Wang, Y., Wang, H., and Wang, Y. (2022c). Nitrate metabolism and ischemic cerebrovascular disease: A narrative review. *Front. Neurology* 13, 735181. doi:10.3389/fneur.2022.735181

Wang, Y. S., Mu, H., Jiang, Y., Gao, Y. L., Liu, Z. H., Zhu, C. T., et al. (2017b). A systematic review and meta-analysis of randomized controlled clinical trials of Ginkgo leaf extract and dipyridamole injection combined with aspirin for the treatment of cerebral infarction. *Int. J. Clin. Exp. Med.* 10 (8), 11304–11313.

Wang, Z., Wan, H., Tong, X., He, Y., Yang, J., Zhang, L., et al. (2021d). An integrative strategy for discovery of functional compound combination from Traditional Chinese Medicine: Danhong Injection as a model. *Biomed. Pharmacother.* 138, 111451. doi:10.1016/j.biopha.2021.111451

Wang, Z. Y., Sun, Y. Z., Bian, L. H., Zhang, Y. L., Zhang, Y., Wang, C. G., et al. (2022d). The crosstalk signals of Sodium Tanshinone IIA Sulfonate in rats with cerebral ischemic stroke: Insights from proteomics. *Biomed. Pharmacother.*, 151.

Xian, S. X., Yang, Z. Q., Lee, J., Jiang, Z. P., Ye, X. H., Luo, L. Y., et al. (2016). A randomized, double-blind, multicenter, placebo-controlled clinical study on the efficacy and safety of Shenmai injection in patients with chronic heart failure. *J. Ethnopharmacol.* 186, 136–142. doi:10.1016/j.jep.2016.03.066

Xiao, G., Lyu, M., Wang, Y., He, S., Liu, X., Ni, J., et al. (2019). Ginkgo flavonol glycosides or ginkgolides tend to differentially protect myocardial or cerebral ischemia-reperfusion injury via regulation of TWEAK-fn14 signaling in heart and brain. *Front. Pharmacol.* 10, 735. doi:10.3389/fphar.2019.00735

Xie, F., Zhang, B., Dai, S., Jin, B., Zhang, T., and Dong, F. (2021). Efficacy and safety of Salvia miltiorrhiza (Salvia miltiorrhiza bunge) and ligustrazine injection in the adjuvant treatment of early-stage diabetic kidney disease: A systematic review and meta-analysis. *J. Ethnopharmacol.* 281, 114346. doi:10.1016/j.jep.2021.114346

Xu, C. C., Wang, W. W., Wang, B., Zhang, T., Cui, X. M., Pu, Y. Q., et al. (2019a). Analytical methods and biological activities of Panax notoginseng saponins: Recent trends. *J. Ethnopharmacol.* 236, 443–465. doi:10.1016/j.jep.2019.02.035

Xu, H. M., Liu, Y., Wang, D. S., and Zhang, Z. Q. (2019b). Shenmai injection maintains blood-brain barrier integrity following focal cerebral ischemia via modulating the expression and trafficking of occludin in lipid rafts. *J. Ethnopharmacol.* 237, 55–63. doi:10.1016/j.jep.2019.03.034

Xu, J. Y., Zhang, C. H., Shi, X. Q., Li, J., Liu, M., Jiang, W. M., et al. (2019c). Efficacy and safety of sodium tanshinone IIA sulfonate injection on hypertensive nephropathy: A systematic review and meta-analysis. *Front. Pharmacol.* 10, 1542. doi:10.3389/fphar.2019.01542

Xu, J., Zhang, X., Jin, A., Pan, Y., Li, Z., Meng, X., et al. (2022). Trends and risk factors associated with stroke recurrence in China, 2007-2018. *Jama Netw. Open* 5 (6), e2216341. doi:10.1001/jamanetworkopen.2022.16341

Xu, L. L., Shang, Z. P., Bo, T., Sun, L., Guo, Q. L., Qiao, X., et al. (2019d). Rapid quantitation and identification of the chemical constituents in Danhong Injection by liquid chromatography coupled with orbitrap mass spectrometry. *J. Chromatogr. A* 1606, 460378. doi:10.1016/j.chroma.2019.460378

Xu, Z., Lu, D., Yuan, J., Ren, M., Ma, R., Xie, Q., et al. (2021). Storax, A promising botanical medicine for treating cardio-cerebrovascular diseases: A review. *Front. Pharmacol.* 12, 785598. doi:10.3389/fphar.2021.785598

Xuan, J. W., Huang, M., Lu, Y. J., and Tao, L. B. (2018). Economic evaluation of safflower yellow injection for the treatment of patients with stable angina pectoris in China: A cost-effectiveness analysis. *J. Altern. Complementary Med.* 24 (6), 564–569. doi:10.1089/acm.2017.0284

Xue, P., Ma, Z. Y., and Liu, S. G. (2019). Efficacy and safety of Ginkgo leaf extract and dipyridamole injection for ischemic stroke: A systematic review and meta analysis. *Front. Pharmacol.* 10, 1403. doi:10.3389/fphar.2019.01403

Yan, Z., Feng, Z., Jiao, Z., Wang, G., Chen, C., and Feng, D. (2022). Safety of using traditional Chinese medicine injections in primary medical institutions: Based on the spontaneous reporting system 2016–2020 in henan Province, China. *Front. Pharmacol.* 13, 761097. doi:10.3389/fphar.2022.761097

Yang, B. R., Yuen, S. C., Fan, G. Y., Cong, W. H., Leung, S. W., and Lee, S. M. Y. (2018). Identification of certain Panax species to be potential substitutes for Panax notoginseng in hemostatic treatments. *Pharmacol. Res.* 134, 1–15. doi:10.1016/j.phrs.2018.05.005

Yang, W., Shi, Z., Yang, H. Q., Teng, J., Zhao, J., and Xiang, G. (2015). Mailuoning for acute ischaemic stroke. *Cochrane Database Syst. Rev.* 1, CD007028. doi:10.1002/14651858.CD007028.pub3

Yang, X. H., Orgah, J., Wang, D. D., Fan, G. W., Hu, J. Y., Han, J. H., et al. (2017a). Danhong injection reduces vascular remodeling and up-regulates the Kallikrein-kinin system in spontaneously hypertensive rats. *Sci. Rep.* 7, 4308. doi:10.1038/s41598-017-04661-1

Yang, Z. Z., Shao, Q., Ge, Z. W., Ai, N., Zhao, X. P., and Fan, X. H. (2017b). A bioactive chemical markers based strategy for quality assessment of botanical drugs: Xuesaitong injection as a case study. *Sci. Rep.* 7, 2410. doi:10.1038/s41598-017-02305-y

Ye, L. F., Zheng, Y. R., and Wang, L. H. (2015). Effects of Shenmai injection and its bioactive components following ischemia/reperfusion in cardiomyocytes. *Exp. Ther. Med.* 10 (4), 1348–1354. doi:10.3892/etm.2015.2662

Ye, T., Li, Y., Xiong, D., Gong, S., Zhang, L., Li, B., et al. (2021). Combination of Danshen and ligustrazine has dual anti-inflammatory effect on macrophages and endothelial cells. *J. Ethnopharmacol.* 266, 113425. doi:10.1016/j.jep.2020.113425

Yu, J. H., Li, Y. H., Liu, X. Y., Ma, Z., Michael, S., Orgah, J. O., et al. (2019a). Mitochondrial dynamics modulation as a critical contribution for Shenmai injection in attenuating hypoxia/reoxygenation injury. *J. Ethnopharmacol.* 237, 9–19. doi:10.1016/j.jep.2019.03.033

Yu, S. T., Li, J., Guo, L., Di, C. X., Qin, X. M., and Li, Z. Y. (2019b). Integrated liquid chromatography-mass spectrometry and nuclear magnetic resonance spectra for the comprehensive characterization of various components in the Shuxuening injection. *J. Chromatogr. A* 1599, 125–135. doi:10.1016/j.chroma.2019.04.008

Yuan, Q., Wang, J. X., Li, R. L., Jia, Z. Z., Wang, S. X., Guo, H., et al. (2021). Effects of salvianolate lyophilized injection combined with Xueshuantong injection in regulation of BBB function in a co-culture model of endothelial cells and pericytes. *Brain Res.* 1751, 147185. doi:10.1016/j.brainres.2020.147185

Zang, Q., Gao, Y., Huang, L., He, J., Lin, S., Jin, H., et al. (2018). Rapid and sensitive liquid chromatography-tandem mass spectrometric method for the quantitative determination of potentially harmful substance 5,5'-oxydimethylenebis (2-furfural) in traditional Chinese medicine injections. *Acta Pharm. Sin. B* 8 (2), 235–241. doi:10.1016/j.apsb.2017.11.002

Zeng, C., Liao, Q., Hu, Y., Shen, Y., Geng, F., and Chen, L. (2019). The role of *Periplaneta americana* (blattodea: Blattidae) in modern versus traditional Chinese medicine. *J. Med. Entomology* 56 (6), 1522–1526. doi:10.1093/jme/tjz081

Zeng, J., Zheng, S. Z., Chen, Y. Z., Qu, Y. M., Xie, J. Y., Hong, E. H., et al. (2021). Puerarin attenuates intracerebral hemorrhage-induced early brain injury possibly by PI3K/Akt signal activation-mediated suppression of NF-kappa B pathway. *J. Cell. Mol. Med.* 25 (16), 7809–7824. doi:10.1111/jcmm.16679

Zhang, L., Wang, Y., Li, C., Shao, C., Zhou, H., Yang, J., et al. (2020a). Dan hong injection protects against cardiomyocytes apoptosis by maintaining mitochondrial integrity through keap1/nuclear factor erythroid 2-related factor 2/JNK pathway. *Front. Pharmacol.* 11, 591197. doi:10.3389/fphar.2020.591197

Zhang, S., Zhang, L., Zhang, H., Fan, G., Qiu, J., Fang, Z., et al. (2017). Hongjingtian injection attenuates myocardial oxidative damage via promoting autophagy and inhibiting apoptosis. *Oxidative Med. Cell. Longev.* 2017, 6965739. doi:10.1155/2017/6965739

Zhang, Y. M., Qu, X. Y., Tao, L. N., Zhai, J. H., Gao, H., Song, Y. Q., et al. (2020b). XingNaoJing injection ameliorates cerebral ischaemia/reperfusion injury via SIRT1-mediated inflammatory response inhibition. *Pharm. Biol.* 58 (1), 16–24. doi:10.1080/13880209.2019.1698619

Zhang, Y. M., Qu, X. Y., Zhai, J. H., Tao, L. N., Gao, H., Song, Y. Q., et al. (2018). Xingnaojing injection protects against cerebral ischemia reperfusion injury via PI3K/Akt-Mediated eNOS phosphorylation. *Evid. Based Complement. Altern. Med.* 2018, 2361046. doi:10.1155/2018/2361046

Zhao, C., Li, X., Li, X., Xu, Y., Ma, M., Wang, S., et al. (2019a). Salvianolate lyophilized injection (SLI) strengthens blood-brain barrier function related to ERK1/2 and Akt signaling pathways. *Brain Res.* 1720, 146295. doi:10.1016/j.brainres.2019.06.014

Zhao, C. X., Liu, H., Miao, P. Q., Wang, H. E., Yu, H. S., Wang, C. H., et al. (2019b). A strategy for selecting "Q-Markers" of Chinese medical preparation via components transfer process analysis with application to the quality control of Shengmai injection. *Molecules* 24 (9), 1811. doi:10.3390/molecules24091811

Zhao, X., He, Y., Zhang, Y., Wan, H., Wan, H., and Yang, J. (2022). Inhibition of oxidative stress: An important molecular mechanism of Chinese herbal medicine (Astragalus membranaceus, Carthamus tinctorius L., radix Salvia miltiorrhizae, etc.) in the treatment of ischemic stroke by regulating the antioxidant system. *Oxidative Med. Cell. Longev.* 2022, 1425369. doi:10.1155/2022/1425369

Zhao, X., Zhang, F., and Wang, Y. (2017). Proteomic analysis reveals Xuesaitong injection attenuates myocardial ischemia/reperfusion injury by elevating pyruvate dehydrogenase-mediated aerobic metabolism. *Mol. Biosyst.* 13 (8), 1504–1511. doi:10.1039/c7mb00140a

Zheng, Q. H., Li, X. L., Mei, Z. G., Xiong, L., Mei, Q. X., Wang, J. F., et al. (2017). Efficacy and safety of puerarin injection in curing acute ischemic stroke A meta-analysis of randomized controlled trials. *Medicine* 96 (1), e5803. doi:10.1097/MD.0000000000005803

Zhong, C. J., Jiang, C., Ni, S. Y., Wang, Q. Z., Cheng, L. G., Wang, H., et al. (2020). Identification of bioactive anti-angiogenic components targeting tumor endothelial cells in Shenmai injection using multidimensional pharmacokinetics. *Acta Pharm. Sin. B* 10 (9), 1694–1708. doi:10.1016/j.apsb.2019.12.011

Zhong, C., Lin, Z., Ke, L., Shi, P., Li, S., Huang, L., et al. (2021). Recent research progress (2015-2021) and perspectives on the pharmacological effects and mechanisms of tanshinone IIA. *Front. Pharmacol.* 12, 778847. doi:10.3389/fphar.2021.778847

Zhou, J., Zhang, L., Zheng, B., Zhang, L., Qin, Y., Zhang, X., et al. (2020). Salvia miltiorrhiza bunge exerts anti-oxidative effects through inhibiting KLF10 expression in vascular smooth muscle cells exposed to high glucose. *J. Ethnopharmacol.* 262, 113208. doi:10.1016/j.jep.2020.113208

Zhou, M. X., Ren, P., Li, S. A., Kang, Q. F., Zhang, Y., Liu, W. H., et al. (2019). Danhong injection attenuates high-fat-induced atherosclerosis and macrophage lipid accumulation by regulating the PI3K/AKT insulin pathway. *J. Cardiovasc. Pharmacol.* 74 (2), 152–161. doi:10.1097/FJC.0000000000000691

Zhu, J., Ye, Q., Xu, S., Chang, Y. X., Liu, X., Ma, Y., et al. (2019). Shengmai injection alleviates H2O2induced oxidative stress through activation of AKT and inhibition of ERK pathways in neonatal rat cardiomyocytes. *J. Ethnopharmacol.* 239, 111677. doi:10.1016/j.jep.2019.01.001

Zhu, T., Meng, X. B., Dong, D. X., Zhao, L. Y., Qu, M. W., Sun, G. B., et al. (2021). Xuesaitong injection (lyophilized) combined with aspirin and clopidogrel protect against focal cerebral ischemic/reperfusion injury in rats by suppressing oxidative stress and inflammation and regulating the NOX2/IL-6/STAT3 pathway. *Ann. Palliat. Med.* 10 (2), 1650–1667. doi:10.21037/apm-20-1681

Zou, J. B., Zhang, X. F., Wang, J., Wang, F., Cheng, J. X., Yang, F. Y., et al. (2018). The therapeutic efficacy of danhong injection combined with percutaneous coronary intervention in acute coronary syndrome: A systematic review and meta-analysis. *Front. Pharmacol.* 9, 550. doi:10.3389/fphar.2018.00550

frontiers | Frontiers in Pharmacology

TYPE Original Research
PUBLISHED 23 March 2023
DOI 10.3389/fphar.2023.1127123

OPEN ACCESS

EDITED BY
Hai-dong Guo,
Shanghai University of Traditional Chinese Medicine, China

REVIEWED BY
Yafeng Li,
The Fifth Hospital of Shanxi Medical University, China
Xichun Pan,
Army Medical University, China

*CORRESPONDENCE
Yifan Yan,
yifan@cqtgmc.edu.cn
Yonghui Zhang,
zhangyonghui@cqtgmc.edu.cn

†These authors have contributed equally to this work

SPECIALTY SECTION
This article was submitted to Ethnopharmacology, a section of the journal Frontiers in Pharmacology

RECEIVED 19 December 2022
ACCEPTED 13 March 2023
PUBLISHED 23 March 2023

CITATION
Zhen C, Wu X, Zhang J, Liu D, Li G, Yan Y, He X, Miao J, Song H, Yan Y and Zhang Y (2023), *Ganoderma lucidum* polysaccharides attenuates pressure-overload-induced pathological cardiac hypertrophy.
Front. Pharmacol. 14:1127123.
doi: 10.3389/fphar.2023.1127123

Ganoderma lucidum polysaccharides attenuates pressure-overload-induced pathological cardiac hypertrophy

Changlin Zhen[1,2†], Xunxun Wu[3†], Jing Zhang[1,2], Dan Liu[1,2], Guoli Li[1,2], Yongbo Yan[4], Xiuzhen He[1,2], Jiawei Miao[1,2], Hongxia Song[1,2], Yifan Yan[1,2*] and Yonghui Zhang[1,2*]

[1]Chongqing Key Laboratory of Development and Utilization of Genuine Medicinal Materials in Three Gorges Reservoir Area, Chongqing, China, [2]Chongqing Engineering Research Center of Antitumor Natural Drugs, Chongqing Three Gorges Medical College, Chongqing, China, [3]School of Biomedical Science, Huaqiao University, Quanzhou, China, [4]The People's Hospital Affiliated to Chongqing Three Gorges Medical College, Chongqing, China

Pathological cardiac hypertrophy is an important risk factor for cardiovascular disease. However, drug therapies that can reverse the maladaptive process and restore heart function are limited. *Ganoderma lucidum* polysaccharides (GLPs) are one of the main active components of *G. lucidum* (*Ganoderma lucidum*), and they have various pharmacological effects. GLPs have been used as Chinese medicine prescriptions for clinical treatment. In this study, cardiac hypertrophy was induced by transverse aortic constriction (TAC) in mice. We found that GLPs ameliorate Ang II-induced cardiomyocyte hypertrophy *in vitro* and attenuate pressure overload–induced cardiac hypertrophy *in vivo*. Further research indicated that GLPs attenuated the mRNA levels of hypertrophic and fibrotic markers to inhibit cardiac hypertrophy through the PPARγ/PGC-1α pathway. Overall, these results indicate that GLPs inhibit cardiac hypertrophy through downregulating key genes for hypertrophy and fibrosis and attenuate pressure overload-induced pathological cardiac hypertrophy by activating PPARγ. This study provides important theoretical support for the potential of using GLPs to treat pathological myocardial hypertrophy and heart failure.

KEYWORDS

GLPs, heart function, PPARγ, PGC-1α, cardiac hypertrophy

1 Introduction

Cardiovascular disease is one of the major threats to human life and health, and cardiac hypertro-phy is an important contributor (Braunwald, 2015). Hypertension, aortic stenosis, and other conditions causing long-term increases in ventricular afterload are common risk factors for cardiac hypertrophy (Oldfield et al., 2020). Among the many ways to treat and prevent cardiac hypertrophy, medication is effective because of good patient compliance and low patient costs. Although current drug therapies are effective in relieving symptoms, their effects on disease prevention and reducing morbidity and mortality are limited. Therefore, finding new drugs by studying homologous medicine and food in detail could be key to inhibiting cardiac hypertrophy.

Cardiac hypertrophy is an adaptive response to mechanical stimuli, such as pregnancy, exercise training, and pressure overload, and it can be classified as pathological or physiological cardiac hypertrophy according to the different causes (Tham et al., 2015; Nakamura and

Sadoshima, 2018). Physiological cardiac hypertrophy, which is induced by pregnancy and athletic training, is reversible and does not lead to heart failure (Gibb et al., 2017). However, pathological cardiac hypertrophy, which is characterized by heart fibrosis and failure, is irreversible (Yang et al., 2020). In the pathogenesis of pathological cardiac hypertrophy, the cardiomyocyte area increases due to long-term high workload, leading to ventricular wall thickening; persistent pressure overload can lead to the heart entering a decompensated state with cardiomyocyte apoptosis and fibrosis, eventually leading to heart failure (Yang et al., 2021). Although many pathogenesis and molecular mechanisms of cardiac hypertrophy have been described, therapeutic strategies for preventing and managing this pathological process remain limited. Peroxisome proliferator-activated receptor gamma (PPARγ) and its coactivator 1α (PGC-1α) play critical roles in controlling cardiac metabolism (Marian and Braunwald, 2017; Li et al., 2018). PPARγ activation improves cardiac hypertrophy and cardiometabolic dysfunction (Wang et al., 2012; Ni et al., 2020). Relevant studies in rats fed a high-fat diet have confirmed that metformin can attenuate cardiac hypertrophy *via* the PPARγ signaling pathway (Liu et al., 2022). Other literature has reported that PPAR? signaling inhibits cardiac hypertrophy by activating autophagy (Yuan et al., 2017). Additionally, many traditional Chinese medicines have been shown to attenuate cardiac hypertrophy by upregulating PPAR? (Gao et al., 2018; Ni et al., 2020; Zhou et al., 2021). Moreover, activating PPARγ improved myocardial cell injury by reducing myocardial fibrosis and cardiomyocyte apoptosis induced by ischemia/reperfusion (Ma et al., 2017; Peng et al., 2017; Zhou et al., 2017). Therefore, the identification of potential PPARγ activators has great potential research value for the treatment of cardiac hypertrophy.

Ganoderma lucidum (*Ganoderma lucidum*) is a mushroom belonging to the Polyporaceae family of Basidiomycota, and it has been used as a traditional medicine for more than 2000 years, particularly in Asian countries; the fruiting bodies, culture mycelia, and spores of *G. lucidum* contain various bioactive chemicals, such as polysaccharides, triterpenes, and proteins (Gong et al., 2020). *Ganoderma lucidum* polysaccharides (GLPs) are one of the main active components, and they have various pharmacological effects. In fact, GLPs have protective anti-free radical effects and can reduce cell damage caused by mutagens, in addition to their immune enhancing and anti-tumor effects (Jiang et al., 2017; Huang et al., 2019; Zhang et al., 2021). Some studies have shown that GLPs can protect the cardiovascular system by preventing cardiomyocyte damage. GLPs protect the myocardium by reducing MDA, activating antioxidant enzymes (GSH-Px, CAT, SOD and NO) in heart tissue, and reducing lipid peroxidation in type 2 diabetic rats (Xue et al., 2010). Patients with coronary heart disease (CHD) treated with GLPs for 12 weeks had improved CHD symptoms and decreased mean blood pressure values (Yihuai et al., 2004). In patients with atrial fibrillation, GLPs were shown to have a cardioprotective effect, manifested by a significant decrease in systolic and diastolic blood pressure, heart rate, and inflammatory factors such as LDL-C, IL-1b, IL-6, hsCRP, and TNF-a (Rizal et al., 2020). However, little is known of the function of GLPs in cardiac hypertrophy.

Our study aims to determine whether GLPs treatment can ameliorate cardiac hypertrophy by using histopathological and molecular biology methods *in vivo* and *in vitro*. Furthermore, we will investigate the mechanism of GLPs regulating cardiac hypertrophy.

2 Materials and methods

2.1 Transverse aortic constriction

Transverse aortic constriction (TAC) was implemented as described previously (Jiang et al., 2014). In narcotized mice, the aorta was ligated with a ligation line that was tied tightly. The constrictive band was placed around the aortic arch between the innominate and the left common carotid arteries. In sham mice, the ligation was not performed.

2.2 Animals

Eight-week-old C57BL/6J male mice were obtained from CavensBiogle (Changzhou, China) and maintained in specific pathogen-free rooms at a constant temperature (20°C–26°C) and humidity (40%–70%). Additionally, they were maintained on a 12-h light/dark cycle and had free access to food (normal chow) and water. Mice were randomly assigned to each experimental group. GLPs were procured from ESITEBiogle (Chengdu, China; purity: UV ≥ 95%) and dissolved in sterile water. TAC was used to induce cardiac hypertrophy in the mice. In brief, in narcotized mice, a constrictive band was placed around the aortic arch between the innominate and left common carotid arteries. We determined the GLP and PPARγ inhibitor doses *in vivo* and *in vitro* by consulting the literature and performing preliminary experiments (Li et al., 2011; Ni et al., 2020; Hu et al., 2022). GLPs at a dose of 100 mg/kg/d were administered to the mice for 4 weeks *via* oral gavage. Simultaneously, the mice received intraperitoneal injections of the PPARγ inhibitor T0070907 at a dose of 1 mg/kg/d. The mice were placed randomly into the following experimental groups, with four animals in each group: Sham, TAC, Sham + GLPs, TAC + GLPs, and Sham + T0070907 + GLPs + TAC group. All animal experiments were performed with approval from the Institutional Animal Care and Use Committee of the Chongqing Three Gorges Medical College (no: A2022015).

2.3 Cell culture and treatments

H9C2 cells were cultured with 10% fetal bovine serum (Solarbio, Beijing, China), high-glucose-DMEM (Solarbio, Beijing, China) and antibiotics. GLPs were procured from SEITEbiogle (Chengdu, China). Angiotensin II was from Sigma (A9525, St. Louis, MO, United States). Antibodies against the following proteins were used: PPARγ (Abcam, ab272718, London, United Kingdom, 1:1000), PGC1α (Abcam, ab176328, London, United Kingdom, 1:1000), and β-actin (NCM Biotech, AB1020, Suzhou, Jiangsu, China, 1:1000). BCA protein assay kit was purchased from Beyotime (Shanghai, China), and T0070907 was obtained from Selleck (Houston, Texas, United States).

2.4 Echocardiography

The mice were anesthetized and imaged using a Vevo 3100 Ultrasound (Visual Sonics, Toronto, Ontario, Canada) after TAC or Sham surgery. The instrument instructions were followed to detect the end-diastolic diameter (LVID; d), left ventricular end-

systolic diameter (LVID; s), left ventricular ejection fraction (EF%), and fractional shortening (FS%) of the mouse hearts.

2.5 Histology

We flushed the mouse hearts with PBS and fixed them with 4% paraformaldehyde. As described in a previous study, the cross-sectional surface area of cardiomyocytes was measured by hematoxylin and eosin (H&E) staining (Hasan et al., 2018). Fifty cardiomyocytes were counted per heart, and the average area was calculated. Heart fibrosis was detected with Masson's trichrome (He et al., 2017).

2.6 Immunofluorescence microscopy

Immunofluorescence staining was performed as described previously (He et al., 2015b). In brief, after treatment with the indicated drugs, the cardiomyocytes were incubated with α-actinin (Proteintech, 11313-2-AP, Wuhan, Hubei, China, 1: 500), followed by AffiniPure donkey anti-rabbit IgG (H + L) fluorescent secondary antibody (Jackson ImmunoResearch, 1: 200). A fluorescence microscope was used to observe the cell area, and Image-Pro Plus software was used to quantify the cardiomyocyte area.

2.7 Western blotting

The cells and mouse heart tissue were homogenized in lysis buffer to extract whole-cell lysates, and the protein concentrations of the samples were determined by BCA kit. The cleavage products were examined by Western blotting assay as described previously (He et al., 2015a). The protein concentration of each sample was adjusted to the same level, and 10 μL of each sample was loaded into a gel for electrophoresis. The protein samples were then separated by SDS-PAGE, and the proteins in the gel were transferred electrically to a polyvinylidene fluoride (PVDF) membrane. Non-specific binding was blocked by incubating the membranes in 5% BSA. Afterwards, the PVDF membranes and antibodies were incubated at 4°C overnight, and the corresponding horseradish peroxidase secondary antibody (ZSGB-BIO, goat anti-rabbit ZB-2301) was added for 1 h. The membranes were washed, and the images were recorded and analyzed with a Bio-Rad Bole ChemiDoc MP Chemiluminescent Gel Imaging System. Antibodies against the following proteins were used: PPARγ (Abcam, ab272718, London, United Kingdom, 1:1000), PGC1α (Abcam, ab176328, London, United Kingdom, 1:1000), and β-actin (NCM Biotech, AB1020, Suzhou, Jiangsu, China, 1:1000).

2.8 Quantitative real time-PCR

Total RNA was extracted from mouse myocardial tissue and cardiomyocytes using Trizol (Beyotime, Shanghai, China) according to the manufacturer's instructions. cDNA was synthesized with a cDNA first-strand synthesis kit (Yeasen Biotech, Shanghai, China). An ABI 9500 Real-Time PCR system (Applied Biosystems, Carlsbad, United States) and Hieff UNICON® universal Blue qPCR SYBR Green Master Mix (Yeasen, Shanghai, China) were used to perform quantitative real-time PCR. Gapdh was used as an internal control. The relative mRNA expression was calculated with the $2^{-\triangle\triangle Ct}$ method. The primers used in the present study are listed in Table 1.

2.9 Statistical analyses

The data are presented as the mean ± SEM. Time course data were analyzed by repeated measures ANOVA, and significant differences were analyzed by one-way ANOVA followed by Bonferroni post-processing analysis. Comparisons between two

TABLE 1 Sequences of primers used in quantitative real-time polymerase chain reaction.

Gene name	Forward primer	Reverse primer
Anp (rat)	5'-GAGAAGATGCCGGTAGAAGATG-3'	R:5'-ACTTAGCTCCCTCTCTGAGG-3'
Bnp(rat)	5'-CTGCTGGAGCTGATAAGAGAAA-3'	5'-GCGCTGTCTTGAGACCTAA-3'
β-MHC(rat)	F:5'-CCAACACCAACCTATCCAA-3'	R:5'-GCCAATGTCACGGCTCTT-3'
Gapdh (rat)	F:5'-CATCTCCCTCACAATTCCATCC-3'	R:5'-GAGGGTGCAGCGAACTTTAT-3'
Anp (mouse)	F:5'-TCCGATAGATCTGCCCTCTT-3'	R:5'-CTCCAATCCTGTCAATCCTACC-3'
Bnp(mouse)	F:5'-ACCACCTTTGAAGTGATCCTATT-3'	R:5'-GCAAGTTTGTGCTCCAAGATAAG-3'
β-MHC(mouse)	F:5'-CCGAGTCCCAGGTCAACAA-3'	R:5'-CTTCACGGGCACCCTTGGA-3'
Gapdh (mouse)	F:5'-GTGGCAAAGTGGAGATTGTTG-3'	R:5'-CGTTGAATTTGCCGTGAGTG-3'
α-SMA (mouse)	F:5'-AGGGAGTGATGGTTGGAATG-3'	R:5'-GGTGATGATGCCGTGTTCTA-3'
Col1a1 (mouse)	F:5'-AGGCTTCAGTGGTTTGGATG-3'	R:5'-CACCAACAGCACCATCGTTA-3'
Col3a1 (mouse)	F:5'-CCCAACCCAGAGATCCCATT-3'	R:5'-GAAGCACAGGAGCAGGTGTAGA-3'
Fibronectin (mouse)	F:5'-CCGGTGGCTGTCAGTCAGA-3'	R:5'-CCGTTCCCACTGCTGATTTATC-3'

Anp, Atrial natriuretic peptide; BNP, b-type natriuretic peptide; β-MHC, β-myosin heavy chain; Col1a1, collagen I; Col3a1, collagen III; α-SMA, α-smooth muscle actin.

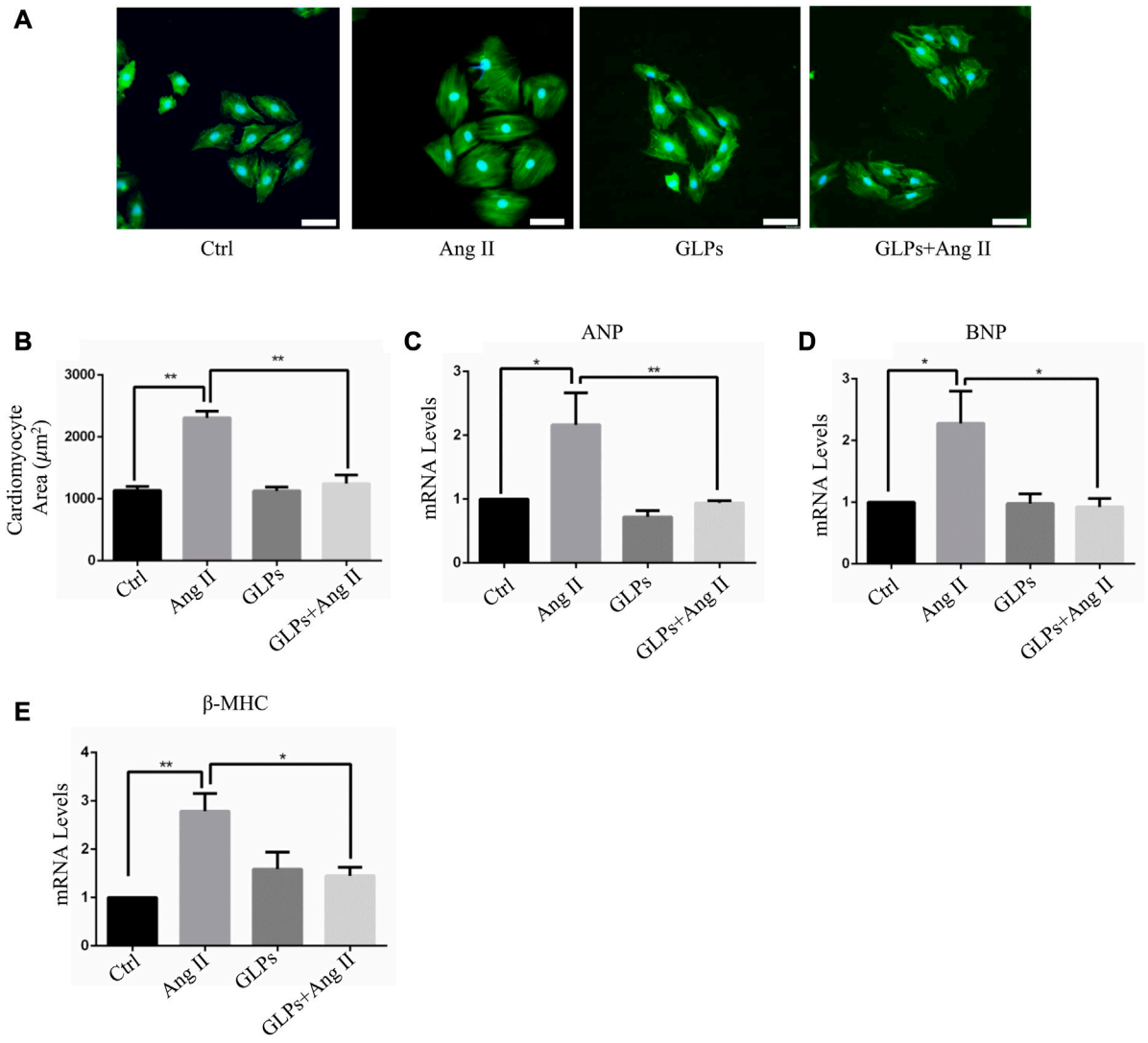

FIGURE 1
GLPs alleviate Ang II-induced hypertrophy in cardiomyocytes. **(A)** Representative images of cardiomyocytes treated with Ang II (1 μM) and GLPs (50 mg/mL) (green: α-actinin; blue: DAPI). Original magnification ×200, scale bars, 50 μM. **(B)** Quantification of cell surface areas (n = 50 + cells in each group). **(C)** Real-time PCR analysis of ANP gene expression in H9C2 cells treated with Ang II and GLPs (n = 3). **(D)** Real-time PCR analysis of BNP gene expression in H9C2 cells treated with Ang II and GLPs (n = 3). **(E)** Real-time PCR analysis of β-MHC gene expression in H9C2 cells treated with Ang II and GLPs (n = 3). All values represent the means ± SEM, *p < 0.05, **p < 0.01. Ctrl: control; Ang II: angiotensin II; ANP: atrial natriuretic peptide; BNP: B-type natriuretic peptide; β-MHC: β-myosin heavy chain; GLPs: *Ganoderma lucidum* polysaccharides.

groups were assessed using Student's t-test. A value of $p < 0.05$ was considered statistically significant.

3 Results

3.1 GLPs alleviated angiotensin II-induced cardiomyocyte hypertrophy

We first assessed the effect of GLPs on cardiomyocyte hypertrophy induced by angiotensin II (Ang II) in H9C2 cells. The cardiomyocyte area increased after Ang II treatment for 48 h (Figures 1A,B). However, compared with Ang II stimulation, GLPs decreased the cell size (Figures 1A,B). ANP, BNP, and β-MHC are widely considered molecular and biochemical markers of cardiac hypertrophy. Atrial natriuretic peptide (ANP) can reduce cardiac load by decreasing the amount of blood returned to the heart and maintaining cardiac function (Vesely et al., 1994). B-type natriuretic peptide (BNP) has effects similar to those of ANP (Mukoyama et al., 1991). Research has reported that cardiac hypertrophy is associated with increased ANP and BNP expression and changes in the β-myosin heavy chain (MHC) (Bernardo et al., 2010). Thus, we detected hypertrophic marker (ANP, BNP, and β-MHC) mRNA levels in H9C2 cells. Ang II treatment increased ANP, BNP, and β-MHC expression, but these changes were decreased in GLP-treated cardiomyocytes (Figures 1C–E). These data indicate that GLPs ameliorate Ang II-induced cardiomyocyte hypertrophy.

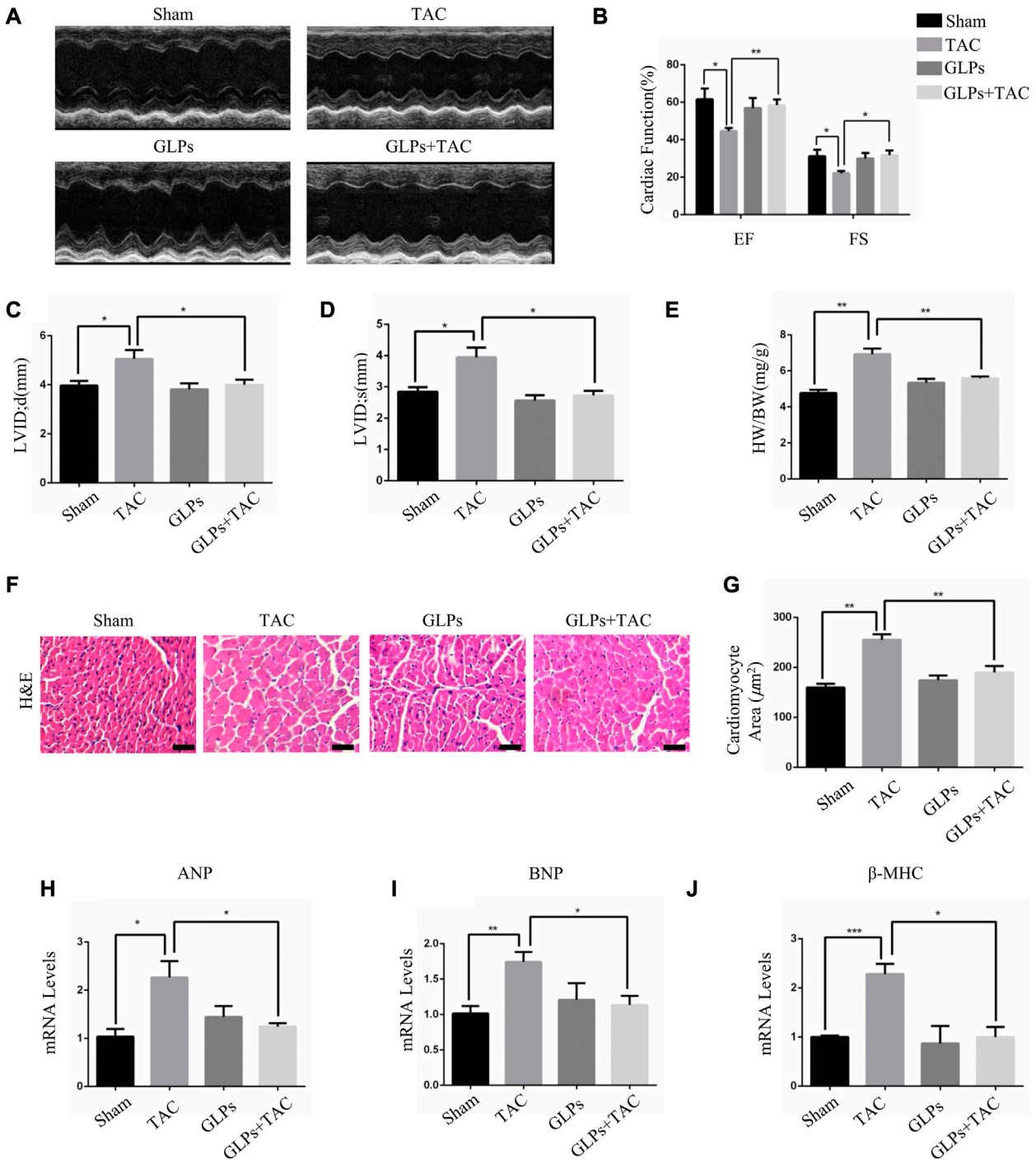

FIGURE 2
GLPs improve cardiac function and attenuate cardiac hypertrophy induced by TAC *in vivo*. **(A)** Representative M-mode echocardiographic tracings of the left ventricle for mice after sham operation or TAC surgery. **(B)** Quantification of the recovery of EF% and FS% in **(A)** (n = 4 per group). **(C)** Quantification of the LVID; d in **(A)**. **(D)** Quantification of the LVID; s in **(A)**. **(E)** Changes in the HW/BW ratio for WT and GLP mice after sham operation or TAC surgery (n = 4 per group). **(F)** Histological sections of hearts from WT and GLP mice after sham operation or TAC surgery were stained with H&E to analyze cardiomyocyte size. Original magnification, ×400, scale bars, 100 μM. **(G)** Quantification of cell surface areas (n = 50 + cells in each group). **(H–J)** Real-time PCR analysis of hypertrophic markers (ANP, BNP, and β-MHC) in WT and GLP mouse hearts after sham operation or TAC surgery (n = 4 per group). All values represent the means ± SEM, *p < 0.05, **p < 0.01. TAC: transverse aortic constriction; EF: ejection fraction; FS: fractional shortening; LVID; d: end-diastolic left ventricular internal dimension; LVID; s: end-systolic left ventricular internal dimension; HW/BW: heart weight/body weight; H&E: hematoxylin and eosin; GLPs: *Ganoderma lucidum* polysaccharides.

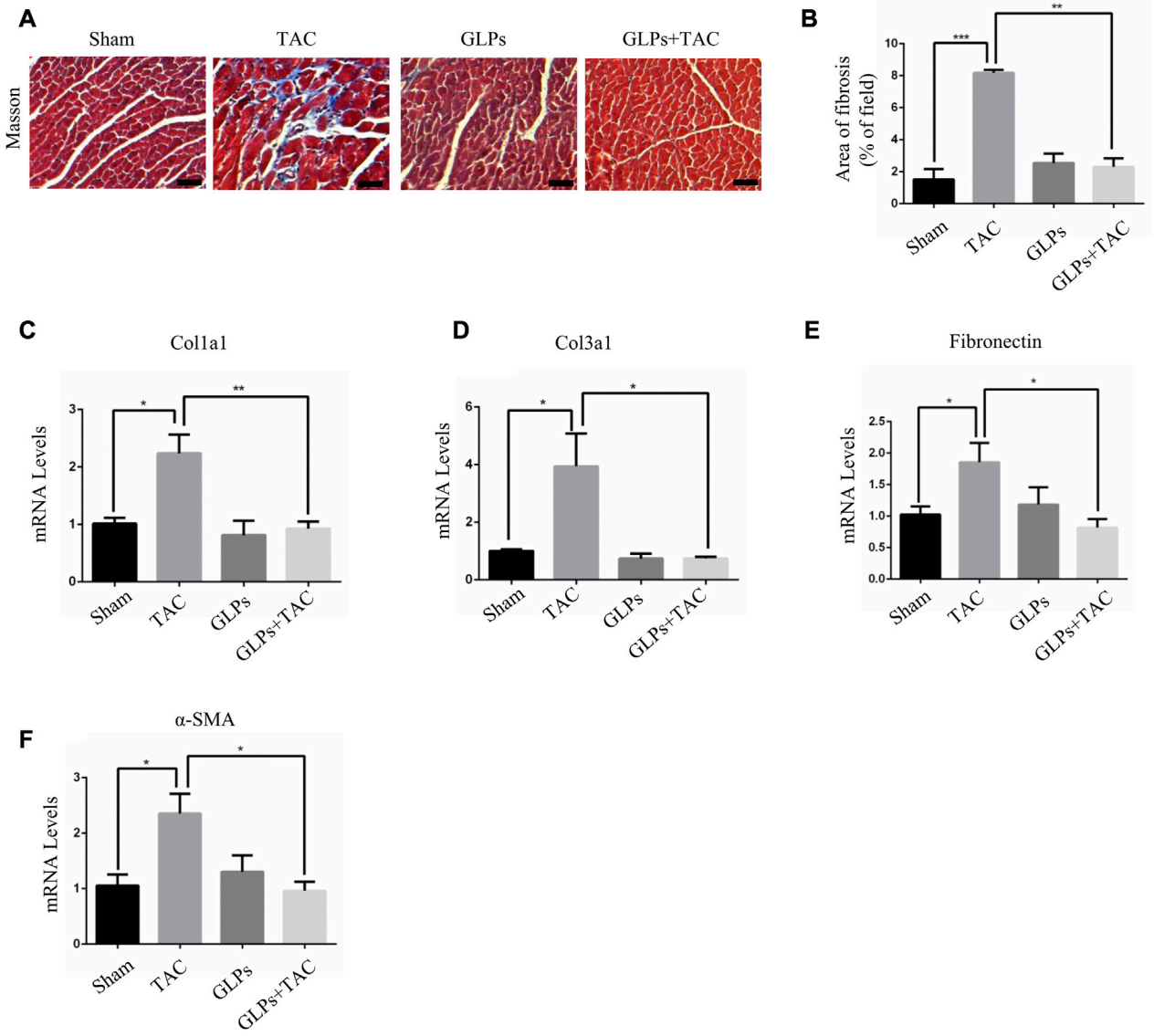

FIGURE 3
GLPs alleviate cardiac fibrosis induced by TAC *in vivo*. **(A)** Histological sections of hearts from WT and GLP mice after sham operation or TAC surgery were stained with Masson's trichrome to analyze collagen deposition. Original magnification, ×400, scale bars, 100 μM. **(B)** Statistical results of cardiac interstitial fibrosis (n = 4 per group). **(C–F)** Real-time PCR analysis of fibrotic markers (Col1a1, Col3a1, fibronectin, and α-SMA) in WT and GLP mouse hearts after sham operation or TAC surgery (n = 4 per group). All values represent the means ± SEM, *$p < 0.05$, **$p < 0.01$, ***$p < 0.001$. WT: wild-type; Col1a1: collagen I; Col3a1: collagen III; α-SMA: α-smooth muscle actin; GLPs: *Ganoderma lucidum* polysaccharides.

3.2 GLPs attenuated pressure overload–induced cardiac hypertrophy *in vivo*

In vivo, we used transverse aortic constriction (TAC)-induced cardiac hypertrophy to examine the potential role of GLPs in cardiac hypertrophy. After TAC operation, wild-type (WT) mice received an oral gavage of GLPs for 4 weeks. As demonstrated by the echocardiographs shown in Figures 2A–D, WT TAC mouse hearts exhibited a decreased hypertrophic phenotype, evidenced by reduced fractional shortening (FS%) and left ventricular ejection fraction (EF%) and increased end-systolic left ventricular internal dimension (LVID; s) and end-diastolic left ventricular internal dimension (LVID; d). However, GLP treatment prevented deteriorative cardiac hypertrophy as demonstrated by an increase in EF% and FS% and a decrease in LVID; s and LVID; d (Figures 2A–D). The GLP-stimulated group showed attenuated hypertrophic features and decreased heart weight/body weight (HW/BW) ratios (Figure 2E). In the histological analysis, H&E staining showed that the increased cardiomyocyte area induced by TAC was reversed by GLP treatment (Figures 2F,G). Furthermore, GLP treatment decreased the mRNA expression of hypertrophic markers (ANP, BNP, and β-MHC) *in vivo* (Figures 2H–J). Masson's

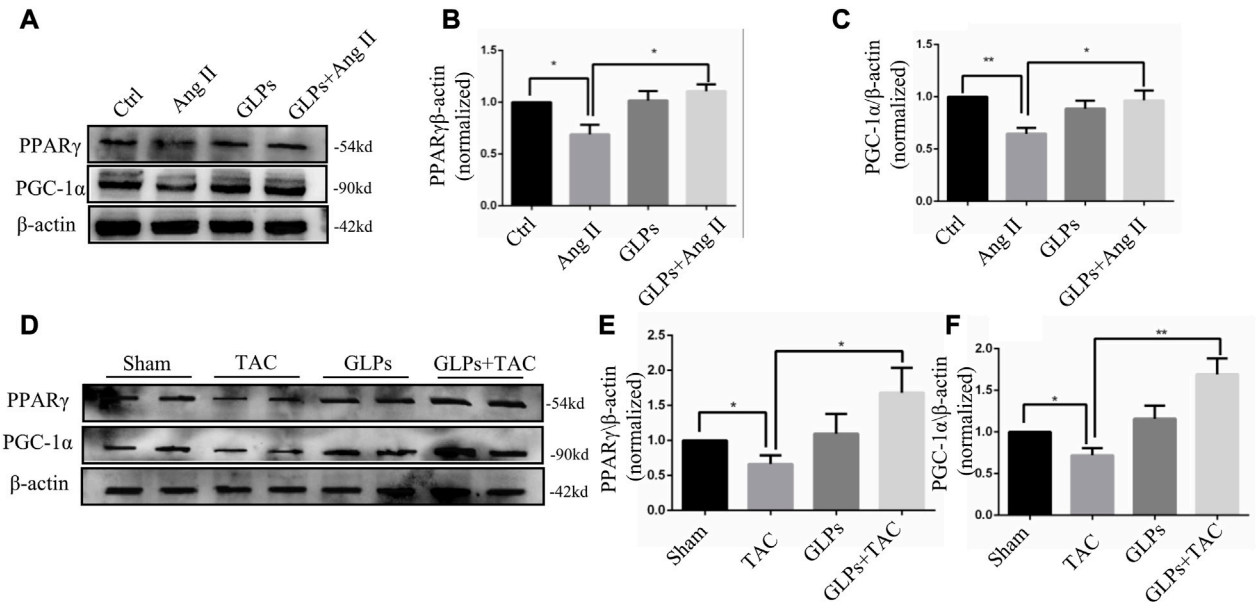

FIGURE 4
PPARγ and PGC-1α are upregulated by GLPs in both cardiomyocytes and mouse hearts. **(A)** Representative Western blot results for PPARγ and PGC-1α protein levels in extracts from H9C2 cells treated with Ang II (1 μM) and GLPs (50 mg/mL). **(B)** Quantification of the PPARγ protein levels shown in **(A)** (n = 3). **(C)** Quantification of the PGC-1α protein levels shown in **(A)** (n = 3). **(D)** Representative Western blot results for PPARγ and PGC-1α protein levels in WT and GLP mouse hearts after sham operation or TAC surgery. **(E)** Quantification of the PPARγ protein levels shown in **(D)** (n = 4). **(F)** Quantification of the PGC-1α protein levels shown in **(D)** (n = 4). All values represent the means ± SEM, *$p < 0.05$, **$p < 0.01$. TAC: transverse aortic constriction; Ang II: angiotensin II; PPAR γ: peroxisome proliferator-activated receptor gamma; PGC-1α: peroxisome proliferator-activated receptor gamma coactivator-1α.; GLPs: *Ganoderma lucidum* polysaccharides.

staining indicated that GLP treatment markedly inhibited cardiac fibrosis relative to that of WT TAC mice (Figures 3A,B). Next, to confirm the antifibrotic effect of GLPs, we measured mRNA levels of fibrotic genes (Col3a1, Col1a1, fibronectin, and α-SMA) by qRT-PCR. GLPs reduced the upregulation of fibrotic genes induced by TAC (Figures 3C–F). Taken together, these results show that GLPs alleviated cardiac hypertrophy, fibrosis, and failure after the TAC operation.

3.3 GLPs regulated PPARγ and PGC-1α in cardiomyocytes and mouse hearts

Studies have shown that cardiometabolic substrates are altered during cardiovascular disease (Wang et al., 2015; Liu et al., 2019). PPARγ and PGC-1α play important roles in stabilizing cardiac metabolism. Therefore, we assessed whether GLPs have an effect on PPARγ and PGC-1α signaling. The results showed that the protein expression levels of PPARγ and PGC-1α were decreased in the Ang II-stimulated group. In contrast, GLP treatment increased PPARγ and PGC-1α expression in the GLP-stimulated group (Figures 4A–C). Next, we examined PPARγ and PGC-1α expression in different mouse heart tissue samples. As shown in Figures 4D–F, PPARγ and PGC-1α levels were decreased in TAC mouse hearts, while PPARγ and PGC-1α levels were increased in GLP-stimulated mouse hearts. These results indicate that GLPs upregulated PPARγ and PGC-1α in both cardiomyocytes and mouse hearts.

3.4 GLPs alleviated cardiomyocyte hypertrophy through PPARγ activation

In this section, we explored whether GLP-regulated PPARγ activation is involved in the protective effects of GLPs against Ang II-stimulated cardiomyocyte hypertrophy. After using the PPAR γ inhibitor T0070907 (1 μM), PPAR γ protein expression was decreased (Figures 5A–C). As indicated by α-actinin immunostaining in cardiomyocytes, T0070907 (1 μM) reversed the protective effects of GLPs on cardiomyocyte hypertrophy induced by Ang II (Figures 5D,E). qRT-PCR results indicated that the decrease in hypertrophic gene mRNA levels induced by GLPs was abolished by treatment with T0070907 (Figures 5F–H). Altogether, these results indicate that GLPs alleviated cardiomyocyte hypertrophy through activating PPARγ.

3.5 GLPs inhibited pressure overload-induced cardiac hypertrophy through PPARγ activation

To explore the important role of PPARγ in the reversal of cardiac hypertrophy by GLPs, T0070907 (1 mg/kg/d) was administered to mice. As demonstrated by the echocardiographs shown in Figures 6A–D, GLP treatment inhibited cardiac hypertrophy and failure, evidenced by decreased LVID; s and LVID; d and increased EF% and FS%. However, T0070907 reversed the protective effects of GLPs on TAC-

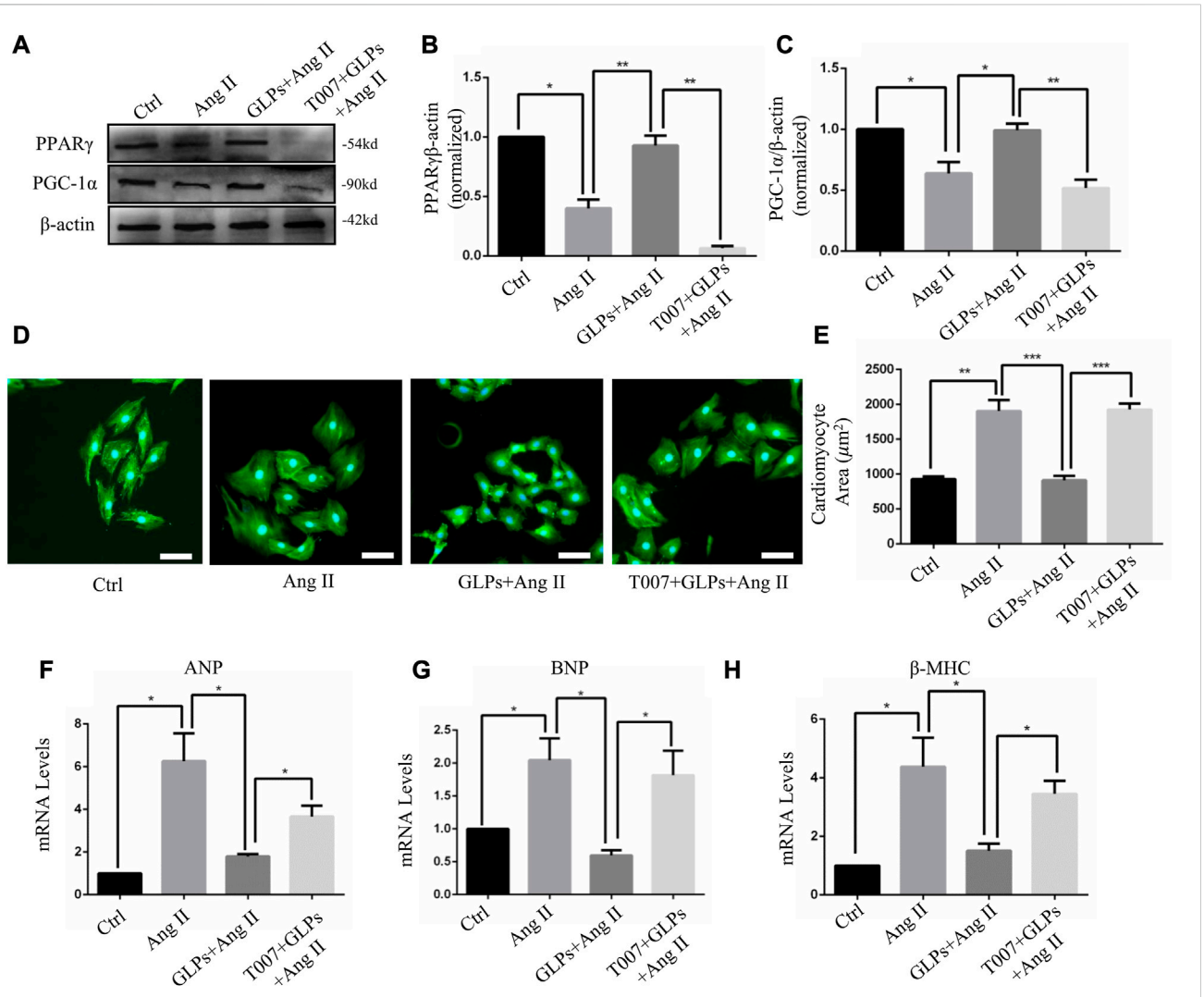

FIGURE 5
GLPs alleviate Ang II-induced cardiomyocyte hypertrophy *via* PPARγ. **(A)** Representative Western blot results for PPARγ and PGC-1α protein levels in extracts from H9C2 cell treated with Ang II (1 μM) and GLPs (50 mg/mL) and pre-treatment with T0070907 (1 μM-4 h). **(B)** Quantification of the PPARγ protein levels shown in **(B)** (n = 3). **(C)** Quantification of the PGC-1α protein levels shown in **(A)** (n = 3). **(D)** Representative images of cardiomyocytes treated with Ang II and GLPs and pre-treated with T0070907 (green: α-actinin; blue: DAPI). Original magnification, ×200, scale bars, 50 μM. **(E)** Quantification of cell surface areas (n = 50 + cells in each group). **(F)** Real-time PCR analysis of ANP gene expression in H9C2 cells treated with Ang II and GLPs and pre-treated with T0070907. **(G)** Real-time PCR analysis of BNP gene expression in H9C2 cells treated with Ang II and GLPs and pre-treated with T0070907 (n = 3). **(H)** Real-time PCR analysis of β-MHC gene expression in H9C2 cells treated with Ang II and GLPs and pre-treated with T0070907 (n = 3). All values represent the means ± SEM, *p < 0.05, **p < 0.01, ***p < 0.001. Ang II: angiotensin II; PPAR γ: peroxisome proliferator-activated receptor gamma; PGC-1α: peroxisome proliferator-activated receptor gamma coactivator-1α.; GLPs: *Ganoderma lucidum* polysaccharides; T007: T0070907.

induced cardiac hypertrophy and failure, indicated by increased LVID; s and LVID; d and decreased EF% and FS% (Figures 6A–D). An increased hypertrophic response and increased HW/BW ratios revealed that T0070907 abolished the protective effects of GLPs (Figure 6E). In addition, T0070907 inhibited the reversion effects of GLPs, evidenced by enlarged cell areas and increased expression of hypertrophic genes (ANP, BNP, and β-MHC) (Figures 6F–J). Masson's trichrome staining revealed that the antifibrotic effect of GLPs was blunted by the PPARγ inhibitor T0070907, evidenced by decreased interstitial fibrosis in T0070907-treated mice (Figures 7A,B). To further determine the antifibrotic effect of GLPs, we measured the mRNA levels of fibrosis-related genes (Col3a1, Col1a1, α-SMA, and fibronectin). T0070907 reversed the GLP-induced downregulation of fibrosis markers in TAC mice (Figures 7C–F). These results show that PPARγ is indispensable for the inhibitory effects of GLPs on cardiac hypertrophy, fibrosis, and failure induced by sustained pressure overload.

4 Discussion

For many cardiovascular diseases, cardiac hypertrophy is one of the most important potential pathogenic factors. However, pharmacological treatments to reverse the maladaptive processes and restore cardiac function are limited. Seeking new therapeutic methods and strategies has broad therapeutic prospects. *Ganoderma*

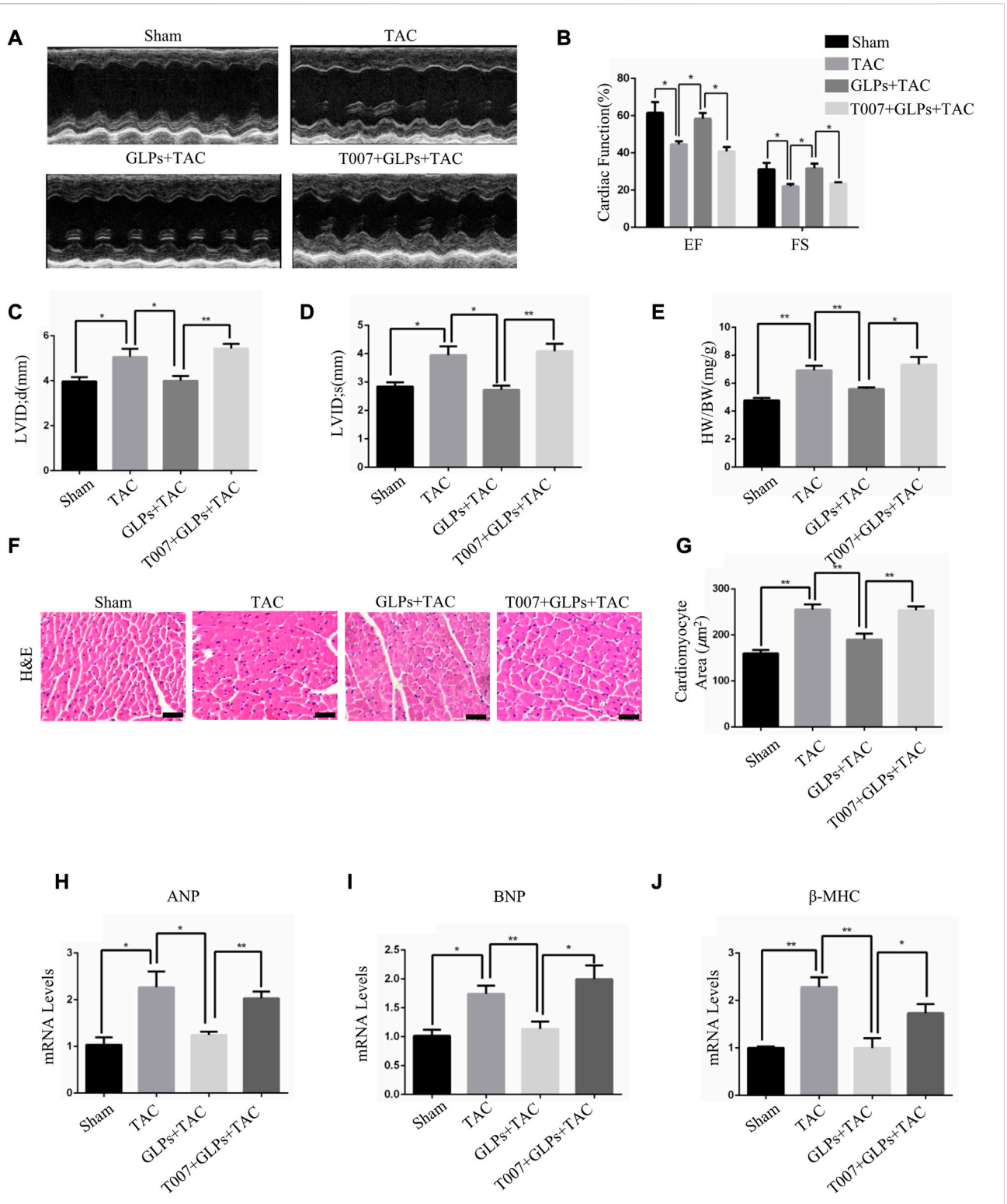

FIGURE 6
GLPs increase cardiac function and ameliorate cardiac hypertrophy *via* PPARγ. **(A)** Representative M-mode echocardiographic tracings of the left ventricle in mice after sham operation or TAC surgery. **(B)** Quantification of the recovery of EF% and FS% in **(A)** (n = 4 per group). **(C)** Quantification of the LVID; d in **(A)**. **(D)** Quantification of the LVID; s in **(A)**. **(E)** Changes in the HW/BW ratio for WT and GLP mice after sham operation or TAC surgery (n = 4 per group). **(F)** Histological sections of hearts from WT and GLP mice after sham operation or TAC surgery were stained with H&E to analyze cardiomyocyte size. Original magnification, ×400, scale bars, 100 μM. **(G)** Quantification of cell surface areas (n = 50 + cells in each group). **(H–J)** Real-time PCR analysis of hypertrophic markers (ANP, BNP, and β-MHC) in WT and GLP mouse hearts after sham operation or TAC surgery (n = 4 per group). All values represent the means ± SEM, *$p < 0.05$, **$p < 0.01$. TAC: transverse aortic constriction; EF: ejection fraction; FS: fractional shortening; LVID; d: end-diastolic left ventricular internal dimension; LVID; s: end-systolic left ventricular internal dimension; HW/BW: heart weight/body weight; H&E: hematoxylin and eosin; T007: T0070907; GLPs: *Ganoderma lucidum* polysaccharides.

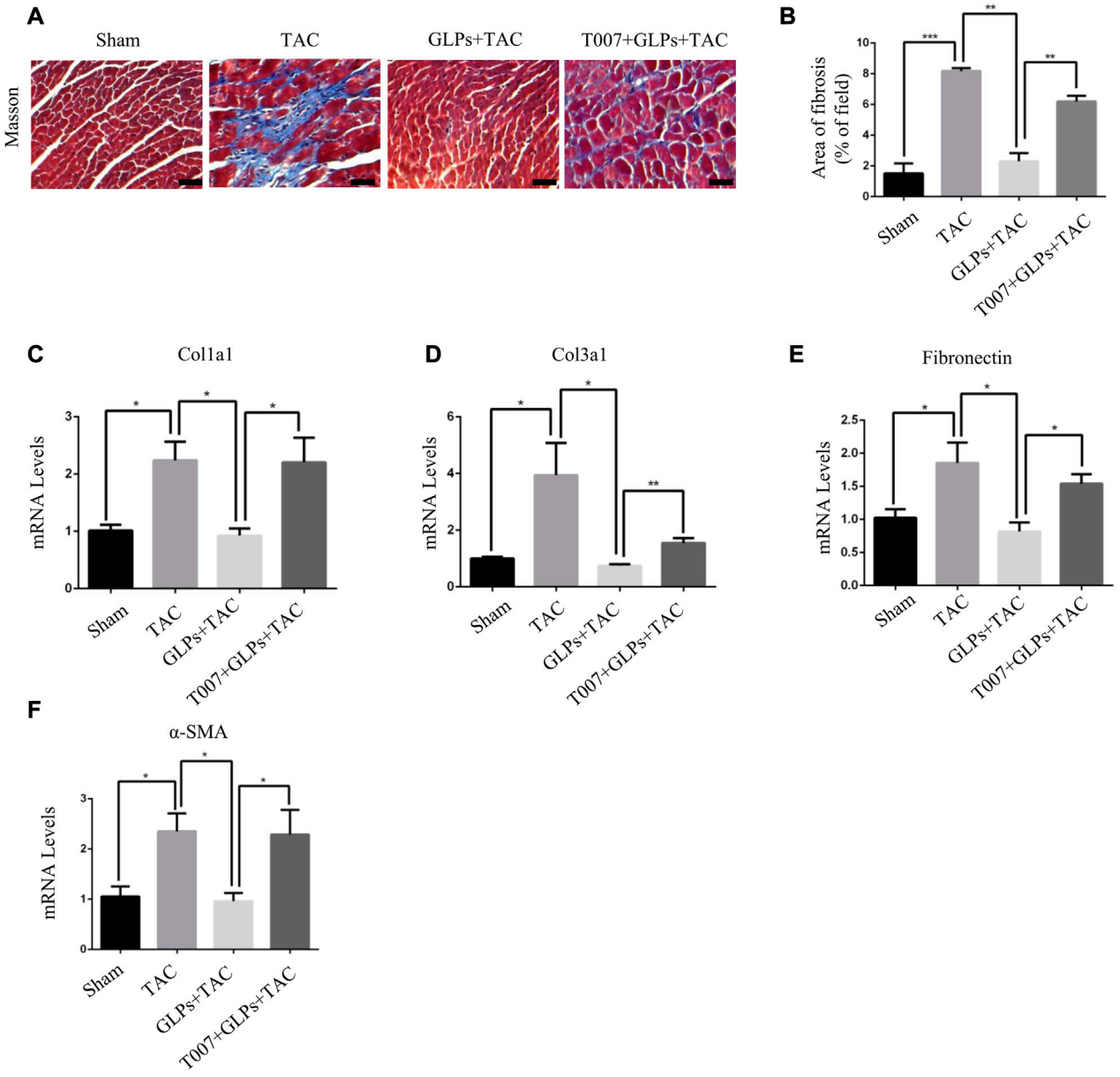

FIGURE 7
GLPs attenuate cardiac fibrosis induced by TAC *via* PPARγ *in vivo*. **(A)** Histological sections of hearts from WT and GLP mice after sham operation or TAC surgery were stained with Masson's trichrome to analyze collagen deposition. Original magnification, ×400, scale bars, 100 μM. **(B)** Statistical results for cardiac interstitial fibrosis (n = 4 per group). **(C–F)** Real-time PCR analysis of fibrotic markers (Col1a1, Col3a1, fibronectin, and α-SMA) in WT and GLP mouse hearts after sham operation or TAC surgery (n = 4 per group). All values represent the means ± SEM, *$p < 0.05$, **$p < 0.01$, ***$p < 0.001$. WT: wild-type; Col1a1: collagen I; Col3a1: collagen III; α-SMA: α-smooth muscle actin; T007: T0070907; GLPs: *Ganoderma lucidum* polysaccharides.

lucidum (*G. lucidum*), a rare traditional Chinese medicine, has been widely used in clinical treatment. *Ganoderma lucidum* polysaccharides (GLPs), the active ingredient of *G. lucidum*, have many positive health effects, including anti-tumor, blood pressure lowering, immunity regulation, and liver protection (Jiang et al., 2017; Li et al., 2018; Huang et al., 2019). In our study, we demonstrated that GLPs reversed pressure overload-induced cardiac hypertrophy. First, GLPs inhibited TAC-induced cardiac hypertrophy and fibrosis and rescued cardiac function. Second, GLPs upregulated PPARγ and PGC-1α expression *in vitro* and *in vivo*. Further experiments showed that PPARγ inhibitors blocked the cardioprotective effects of GLPs *in vitro* and *in vivo*.

Increased cardiomyocyte area, thickened ventricular wall, and altered hypertrophic gene expression are the main features of cardiac hypertrophy. Normal cardiac energy metabolism is essential for the maintenance of normal cardiac function, but metabolic disorders often occur in cardiomyocytes during compensatory cardiac growth. PGC-1α and PPARγ play important roles in controlling heart energy metabolism (Di et al., 2018). PPARγ belongs to the peroxisome proliferator-activated

receptor (PPAR) nuclear receptor family and is highly expressed in adipocytes, cardiomyocytes, and macrophages. Relevant studies have confirmed that PPARγ activation improved myocardial cell injury caused by ischemia/reperfusion (Zhou et al., 2017), reduced myocardial fibrosis (Ma et al., 2017), reduced cardiomyocyte apoptosis, and inhibited cardiac hypertrophy (Peng et al., 2017). Moreover, regulating PPARγ activation has important applications in clinical treatment. PPARγ activators have been used as hypoglycemic drugs in clinical practice (Wang et al., 2017). Our current study found that PPARγ expression was downregulated during Ang II stimulation in cardiomyocytes and TAC mouse hearts and upregulated during GLP treatment. Importantly, our experiments demonstrated that PPARγ inhibitors reversed the protective effects of GLPs in cardiomyocytes and *in vivo*. Thus, GLPs protect against pressure overload-induced cardiac hypertrophy through PPARγ activation.

Myocardial fibrosis often occurs during the pathogenesis of cardiac hypertrophy and cardiac remodeling (Kong et al., 2014; Segura et al., 2014). Decreasing fibroblast aggregation and activation during cardiac hypertrophy is crucial to slow fibrosis and improve cardiac function (Hou et al., 2013; Yang et al., 2018). In our study, GLPs significantly inhibited myocardial fibrosis, which manifested as reduced fibrosis areas and decreased expression levels of collagen markers. Moreover, a PPARγ inhibitor attenuated the anti-fibrotic effects of GLPs in TAC mice. These results suggest the potential therapeutic effects of GLPS on myocardial fibrosis.

This study has some limitations. The specific mechanism through which GLPs activate PPARγ and the relationship between PPARγ and PGC-1α remain unclear. Additionally, the molecular mechanism of how GLPs regulate cardiac hypertrophy is not well understood. Further studies are needed to elucidate the detailed mechanisms by which GLPs prevent pathological cardiac hypertrophy.

5 Conclusion

Overall, our study demonstrates that GLPs can protect against pressure overload-induced cardiac hypertrophy through PPARγ activation. The PPARγ inhibitor T0070907 reversed the protective effects of GLPs on cardiomyocyte hypertrophy. Furthermore, *in vivo*, T0070907 blocked the preventive effects of GLPs on cardiac hypertrophy and heart fibrosis. This study provides important theoretical support for the potential of GLPs in the treatment of pathological cardiac hypertrophy and expanding the use of GLP in the treatment of pathological cardiac hypertrophy and heart failure.

Data availability statement

The original contributions presented in the study are included in the article/supplementary material, further inquiries can be directed to the corresponding authors.

Ethics statement

The animal study was reviewed and approved by Institutional Animal Care and Use Committee of the Chongqing Three Gorges Medical College.

Author contributions

YoiY, YoZ, CZ, and XW conceived and designed the study. JiZ, DL, GL, YoY, XH, JM, and HS performed the experiments. CZ and XW acquired, analyzed and interpreted the data. YoY and YoZ conducted statistical analysis. YoY, YoZ, CZ, and XW confirmed the authenticity of all the raw data. All authors read and approved the final version of the manuscript.

Funding

This research was supported by the Science and Technology Research Program of Chongqing Municipal Education Commission (grant nos. KJQN202102701), Special Program for High-level Talents of Chongqing Three Gorges Medical College (grant nos.06020605008).

Conflict of interest

The authors declare that the research was conducted in the absence of any commercial or financial relationships that could be construed as a potential conflict of interest.

Publisher's note

References

Bernardo, B. C., Weeks, K. L., Pretorius, L., and McMullen, J. R. (2010). Molecular distinction between physiological and pathological cardiac hypertrophy: Experimental findings and therapeutic strategies. *Pharmacol. Ther.* 128 (1), 191–227. doi:10.1016/j.pharmthera.2010.04.005

Braunwald, E. (2015). The war against heart failure: The lancet lecture. *Lancet* 385 (9970), 812–824. doi:10.1016/S0140-6736(14)61889-4

Di, W., Lv, J., Jiang, S., Lu, C., Yang, Z., Ma, Z., et al. (2018). PGC-1: The energetic regulator in cardiac metabolism. *Curr. Issues Mol. Biol.* 28, 29–46. doi:10.21775/cimb.028.029

Gao, R. R., Wu, X. D., Jiang, H. M., Zhu, Y. J., Zhou, Y. L., Zhang, H. F., et al. (2018). Traditional Chinese medicine Qiliqiangxin attenuates phenylephrine-induced cardiac hypertrophy via upregulating PPARγ and PGC-1α. *Ann. Transl. Med.* 6 (8), 153. doi:10.21037/atm.2018.04.14

Gibb, A. A., Epstein, P. N., Uchida, S., Zheng, Y., McNally, L. A., Obal, D., et al. (2017). Exercise-induced changes in glucose metabolism promote physiological cardiac growth. *Circulation* 136 (22), 2144–2157. doi:10.1161/CIRCULATIONAHA.117.028274

Gong, X., Ji, M., Xu, J., Zhang, C., and Li, M. (2020). Hypoglycemic effects of bioactive ingredients from medicine food homology and medicinal health food species used in

China. *Crit. Rev. Food Sci. Nutr.* 60 (14), 2303–2326. doi:10.1080/10408398.2019.1634517

Hasan, P., Saotome, M., Ikoma, T., Iguchi, K., Kawasaki, H., Iwashita, T., et al. (2018). Mitochondrial fission protein, dynamin-related protein 1, contributes to the promotion of hypertensive cardiac hypertrophy and fibrosis in Dahl-salt sensitive rats. *J. Mol. Cell. Cardiol.* 121, 103–106. doi:10.1016/j.yjmcc.2018.07.004

He, C., Li, H., Viollet, B., Zou, M. H., and Xie, Z. (2015a). AMPK suppresses vascular inflammation *in vivo* by inhibiting signal transducer and activator of transcription-1. *Diabetes* 64 (12), 4285–4297. doi:10.2337/db15-0107

He, C., Medley, S. C., Hu, T., Hinsdale, M. E., Lupu, F., Virmani, R., et al. (2015b). PDGFRβ signalling regulates local inflammation and synergizes with hypercholesterolaemia to promote atherosclerosis. *Nat. Commun.* 6, 7770. doi:10.1038/ncomms8770

He, C., Medley, S. C., Kim, J., Sun, C., Kwon, H. R., Sakashita, H., et al. (2017). STAT1 modulates tissue wasting or overgrowth downstream from PDGFRβ. *Genes. Dev.* 31 (16), 1666–1678. doi:10.1101/gad.300384.117

Hou, X., Zhang, Y., Shen, Y. H., Liu, T., Song, S., Cui, L., et al. (2013). PPAR-gamma activation by rosiglitazone suppresses angiotensin II-mediated proliferation and phenotypictransition in cardiac fibroblasts via inhibition of activation of activator protein 1. *Eur. J. Pharmacol.* 715 (1-3), 196–203. doi:10.1016/j.ejphar.2013.05.021

Hu, Y., Wang, S. X., Wu, F. Y., Wu, K. J., Shi, R. P., Qin, L. H., et al. (2022). Effects and mechanism of ganoderma lucidum polysaccharides in the treatment of diabetic nephropathy in streptozotocin-induced diabetic rats. *Biomed. Res. Int.* 2022, 4314415. doi:10.1155/2022/4314415

Huang, Q., Li, L., Chen, H., Liu, Q., and Wang, Z. (2019). GPP (composition of ganoderma lucidum poly-saccharides and polyporus umbellatus poly-saccharides) enhances innate immune function in mice. *Nutrients* 11 (7), 1480. doi:10.3390/nu11071480

Jiang, D. S., Li, L., Huang, L., Gong, J., Xia, H., Liu, X., et al. (2014). Interferon regulatory factor 1 is required for cardiac remodeling in response to pressure overload. *Hypertension* 64 (1), 77–86. doi:10.1161/HYPERTENSIONAHA.114.03229

Jiang, D., Wang, L., Zhao, T., Zhang, Z., Zhang, R., Jin, J., et al. (2017). Restoration of the tumor-suppressor function to mutant p53 by Ganoderma lucidum polysaccharides in colorectal cancer cells. *Oncol. Rep.* 37 (1), 594–600. doi:10.3892/or.2016.5246

Kong, P., Christia, P., and Frangogiannis, N. G. (2014). The pathogenesis of cardiac fibrosis. *Cell. Mol. Life Sci.* 71 (4), 549–574. doi:10.1007/s00018-013-1349-6

Li, F., Zhang, Y., and Zhong, Z. (2011). Antihyperglycemic effect of ganoderma lucidum polysaccharides on streptozotocin-induced diabetic mice. *Int. J. Mol. Sci.* 12 (9), 6135–6145. doi:10.3390/ijms12096135

Li, L. F., Liu, H. B., Zhang, Q. W., Li, Z. P., Wong, T. L., Fung, H. Y., et al. (2018a). Comprehensive comparison of polysaccharides from ganoderma lucidum and G. Sinense: Chemical, antitumor, immunomodulating and gut-microbiota modulatory properties. *Sci. Rep.* 8 (1), 6172. doi:10.1038/s41598-018-22885-7

Li, Y., Liang, Y., Zhu, Y., Zhang, Y., and Bei, Y. (2018b). Noncoding RNAs in cardiac hypertrophy. *J. Cardiovasc Transl. Res.* 11 (6), 439–449. doi:10.1007/s12265-018-9797-x

Liu, Y., Zhang, Q., Yang, L., Tian, W., Yang, Y., Xie, Y., et al. (2022). Metformin attenuates cardiac hypertrophy *via* the HIF-1α/PPAR-γ signaling pathway in high-fat diet rats. *Front. Pharmacol.* 13, 919202. doi:10.3389/fphar.2022.919202

Liu, Z., Tian, H., Hua, J., Cai, W., Bai, Y., Zhan, Q., et al. (2019). A CRM1 inhibitor alleviates cardiac hypertrophy and increases the nuclear distribution of NT-PGC-1α in NRVMs. *Front. Pharmacol.* 10, 465. doi:10.3389/fphar.2019.00465

Ma, Z. G., Yuan, Y. P., Zhang, X., Xu, S. C., Wang, S. S., and Tang, Q. Z. (2017). Piperine attenuates pathological cardiac fibrosis via PPAR-γ/AKT pathways. *EBioMedicine* 18, 179–187. doi:10.1016/j.ebiom.2017.03.021

Marian, A. J., and Braunwald, E. (2017). Hypertrophic cardiomyopathy: Genetics, pathogenesis, clinical manifestations, diagnosis, and therapy. *Circ. Res.* 121 (7), 749–770. doi:10.1161/CIRCRESAHA.117.311059

Mukoyama, M., Nakao, K., Hosoda, K., Suga, S., Saito, Y., Ogawa, Y., et al. (1991). Brain natriuretic peptide as a novel cardiac hormone in humans. Evidence for an exquisite dual natriuretic peptide system, atrial natriuretic peptide and brain natriuretic peptide. *J. Clin. Invest.* 87 (4), 1402–1412. doi:10.1172/JCI115146

Nakamura, M., and Sadoshima, J. (2018). Mechanisms of physiological and pathological cardiac hypertrophy. *Nat. Rev. Cardiol.* 15 (7), 387–407. doi:10.1038/s41569-018-0007-y

Ni, G., Wang, K., Zhou, Y., Wu, X., Wang, J., Shang, H., et al. (2020). Citri reticulatae Pericarpium attenuates Ang II-induced pathological cardiac hypertrophy via upregulating peroxisome proliferator-activated receptors gamma. *Ann. Transl. Med.* 8 (17), 1064. doi:10.21037/atm-20-2118

Oldfield, C. J., Duhamel, T. A., and Dhalla, N. S. (2020). Mechanisms for the transition from physiological to pathological cardiac hypertrophy. *Can. J. Physiol. Pharmacol.* 98 (2), 74–84. doi:10.1139/cjpp-2019-0566

Peng, S., Xu, J., Ruan, W., Li, S., and Xiao, F. (2017). PPAR-Gamma activation prevents septic cardiac dysfunction via inhibition of apoptosis and necroptosis. *Oxid. Med. Cell. Longev.* 2017, 8326749. doi:10.1155/2017/8326749

Rizal, A., Sandra, F., Fadlan, M. R., and Sargowo, D. (2020). Ganoderma lucidum polysaccharide peptide reduce inflammation and oxidative stress in patient with atrial fibrillation. *Indonesian Biomed. J.* 12 (4), 384–389. doi:10.18585/inabj.v12i4.1244

Segura, A. M., Frazier, O. H., and Buja, L. M. (2014). Fibrosis and heart failure. *Heart Fail Rev.* 19 (2), 173–185. doi:10.1007/s10741-012-9365-4

Tham, Y. K., Bernardo, B. C., Ooi, J. Y., Weeks, K. L., and McMullen, J. R. (2015). Pathophysiology of cardiac hypertrophy and heart failure: Signaling pathways and novel therapeutic targets. *Arch. Toxicol.* 89 (9), 1401–1438. doi:10.1007/s00204-015-1477-x

Vesely, D. L., Douglass, M. A., Dietz, J. R., Gower, W. R., McCormick, M. T., Rodriguez-Paz, G., et al. (1994). Three peptides from the atrial natriuretic factor prohormone amino terminus lower blood pressure and produce diuresis, natriuresis, and/or kaliuresis in humans. *Circulation* 90 (3), 1129–1140. doi:10.1161/01.cir.90.3.1129

Wang, H., Bei, Y., Lu, Y., Sun, W., Liu, Q., Wang, Y., et al. (2015). Exercise prevents cardiac injury and improves mitochondrial biogenesis in advanced diabetic cardiomyopathy with PGC-1α and akt activation. *Cell. Physiol. Biochem.* 35 (6), 2159–2168. doi:10.1159/000374021

Wang, J., Song, Y., Zhang, Y., Xiao, H., Sun, Q., Hou, N., et al. (2012). Cardiomyocyte overexpression of miR-27b induces cardiac hypertrophy and dysfunction in mice. *Cell. Res.* 22 (3), 516–527. doi:10.1038/cr.2011.132

Wang, W., Zhou, X., Kwong, J. S. W., Li, L., Li, Y., and Sun, X. (2017). Efficacy and safety of thiazolidinediones in diabetes patients with renal impairment: A systematic review and meta-analysis. *Sci. Rep.* 7 (1), 1717. doi:10.1038/s41598-017-01965-0

Xue, H., Qiao, J., Meng, G., Wu, F., Luo, J., Chen, H., et al. (2010). Effect of Ganoderma lucidum polysaccharides on hemodynamic and antioxidation in T2DM rats. *Zhongguo Zhong Yao Za Zhi* 35 (3), 339–343. doi:10.4268/cjcmm20100318

Yang, D., Liu, H. Q., Tang, F. Y., NanGuo, Z., Yang, H. M., Zheng, T., et al. (2021). Critical roles of macrophages in pressure overload-induced cardiac remodeling. *J. Mol. Med. Official organ "Gesellschaft Deutscher Naturforscher und Arzte* 99 (1), 33–46. doi:10.1007/s00109-020-02002-w

Yang, D., Liu, H. Q., Liu, F. Y., Tang, N., Guo, Z., Ma, S. Q., et al. (2020). The roles of noncardiomyocytes in cardiac remodeling. *Int. J. Biol. Sci.* 16 (13), 2414–2429. doi:10.7150/ijbs.47180

Yang, M., Xiong, J., Zou, Q., Wang, D. D., and Huang, C. X. (2018). Chrysin attenuates interstitial fibrosis and improves cardiac function in a rat model of acute myocardial infarction. *J. Mol. Histol.* 49 (6), 555–565. doi:10.1007/s10735-018-9793-0

Yihuai, G., Guoliang, C., Xihu, D., Ye, J., and Zhou, S. (2004). A phase I/II study of ling zhi mushroom ganoderma lucidum (W.curt.:Fr.) lloyd (aphyllophoromycetideae) extract in patients with coronary heart disease. *Int. J. Med. Mushrooms* 6, 327–334. doi:10.1615/intjmedmushr.v6.i4.30

Yuan, S., Jin, J., Chen, L., Hou, Y., and Wang, H. (2017). Naoxintong/ppar**γ** signaling inhibits cardiac hypertrophy via activation of autophagy. *Evid. Based Complement. Altern. Med.* 2017, 3801976. doi:10.1155/2017/3801976

Zhang, Y., Feng, Y., Wang, W., Jia, L., and Zhang, J. (2021). Characterization and hepatoprotections of ganoderma lucidum polysaccharides against multiple organ dysfunction syndrome in mice. *Oxid. Med. Cell. Longev.* 2021, 9703682. doi:10.1155/2021/9703682

Zhou, H., Li, D., Zhu, P., Hu, S., Hu, N., Ma, S., et al. (2017). Melatonin suppresses platelet activation and function against cardiac ischemia/reperfusion injury via PPARγ/FUNDC1/mitophagy pathways. *J. Pineal Res.* 63 (4), e12438. doi:10.1111/jpi.12438

Zhou, Y., Yin, T., Shi, M., Chen, M., Wu, X., Wang, K., et al. (2021). Nobiletin attenuates pathological cardiac remodeling after myocardial infarction via activating PPAR*γ* and PGC1*α*. *PPAR Res.* 2021, 9947656. doi:10.1155/2021/9947656

frontiers | Frontiers in Pharmacology

TYPE Original Research
PUBLISHED 23 March 2023
DOI 10.3389/fphar.2023.1097407

OPEN ACCESS

EDITED BY
Mingxia Gu,
Cincinnati Children's Hospital Medical Center, United States

REVIEWED BY
Feihua Wu,
China Pharmaceutical University, China
Achuthan Raghavamenon,
Amala Cancer Research Centre, India

*CORRESPONDENCE
Malik Hassan Mehmood,
malikhassan.mehmood@gmail.com,
malikhassanmehmood@gcuf.edu.pk

SPECIALTY SECTION
This article was submitted to Ethnopharmacology, a section of the journal Frontiers in Pharmacology

RECEIVED 13 November 2022
ACCEPTED 23 February 2023
PUBLISHED 23 March 2023

CITATION
Ahmed MG, Mehmood MH, Mehdi S and Farrukh M (2023), *Caryopteris odorata* and its metabolite coumarin attenuate characteristic features of cardiometabolic syndrome in high-refined carbohydrate-high fat-cholesterol-loaded feed-fed diet rats. *Front. Pharmacol.* 14:1097407. doi: 10.3389/fphar.2023.1097407

Caryopteris odorata and its metabolite coumarin attenuate characteristic features of cardiometabolic syndrome in high-refined carbohydrate-high fat-cholesterol-loaded feed-fed diet rats

Mobeen Ghulam Ahmed, Malik Hassan Mehmood*, Shumaila Mehdi and Maryam Farrukh

Department of Pharmacology, Faculty of Pharmaceutical Sciences, Government College University of Faisalabad, Faisalabad, Pakistan

Caryopteris odorata (D. Don) B.L. Robinson (Verbenaceae family) is an aromaric shrub traditionally used to treat diabetes and related pathologies (diabetic foot ulcer), cancer/tumors, wound healing, and inflammation. It is enriched with flavonoids and phenolics like coumarins, quercetin, gallic acid, coumaric acid, stigmasterol, α-tocopherol, and iridoids. *C. odorata* has been reported as having α-glucosidase, anti-inflammatory, and anti-oxidant properties. Its effectiveness in preventing cardiometabolic syndrome has not yet been assessed. This study aims to investigate the potential efficacy of *C. odorata* and coumarin for characteristic features of cardiometabolic syndrome (CMS), including obesity, dyslipidemia, hyperglycemia, insulin resistance, and hypertension by using high-refined carbohydrate-high fat-cholesterol (HRCHFC)-loaded feed-fed rats. Chronic administration of *C. odorata* and coumarin for 6 weeks revealed a marked attenuation in body and organ weights, with a consistent decline in feed intake compared to HRCHFC diet fed rats. The test materials also caused a significant reduction in the blood pressure (systolic, diastolic, and mean) and heart rate of HRCHFC-diet fed rats. Improved glucose tolerance and insulin sensitivity tests were also observed in test material administered rats compare to only HRCHFC-diet fed rats. *C. odorata* and coumarin-treated animals produced a marked decline in serum FBG, TC, TG, LFTs, and RFTs, while an increase in serum HDL-C levels was noticed. *C. odorata* and coumarin also significantly modulated inflammatory biomarkers (TNFα, IL-6), adipokines (leptin, adiponectin, and chemerin), and HMG-CoA reductase levels, indicating prominent anti-inflammatory,

Abbreviations: ALT, alanine transaminase; AST, aspartate transaminase; CAT, catalase; CMS, cardiometabolic syndrome; CRP, c reactive protein; CVD, cardiovascular diseases; DBP, diastolic blood pressure; ELISA, enzyme-linked immunosorbent assay; HDL, high density lipoprotein; HMG-CoA reductase, (3-hydroxy-3-methyl-glutaryl-coenzyme A) reductase; HR, heart rate; HRCHFC, high refined-carbohydrate-high fat-cholesterol; IL-6, interlukin-6; IR, insulin resistance; LFTs, liver function tests; MBP, mean blood pressure; MDA, Malondialdehyde; NIBP, non-invasive blood pressure; RFTs, renal function tests; ROS, reactive oxygen species; SBP, systolic blood pressure; SOD, superoxide dismutase; TC, total cholesterol; TG, total triglycerides; TNF-α, tumor necrosis factor.

cholesterol-lowering, and anti-hyperglycemic potential. Administration of *C. odorata* and coumarin exhibited a marked improvement in oxidative stress markers (CAT, SOD, and MDA). Histopathological analysis of liver, heart, kidney, pancreas, aorta, and fat tissues showed a revival of normal tissue architecture in *C. odorata* and coumarin-treated rats compared to only HRCHFC-diet fed rats. These results suggest that *C. odorata* and coumarin possess beneficial effects against the characteristic features of CMS (obesity, insulin resistance, hypertension, and dyslipidemia) in HRCHFC feed-administered rats. These effects were possibly mediated through improved adipokines, glucose tolerance, and insulin sensitivity, the attenuation of HMG-CoA reductase and inflammatory biomarkers, and modulated oxidative stress biomarkers. This study thus demonstrates a rationale for the therapeutic potential of *C. odorata* and coumarin in CMS.

KEYWORDS

***Caryopteris odorata*, leptin, adiponectin, chemerin, diet induced cardiometabolic syndrome**

Introduction

Cardiometabolic syndrome (CMS) is a consolidation of metabolic anomalies characterized by central obesity, insulin resistance, hyperglycemia, hyperlipidemia, and hypertension (Ojetola et al., 2021). It is reaching pandemic levels and hence presents a serious global health concern (Agrawal et al., 2018). CMS prevalence varies and depends greatly upon population, gender, age, and race. It is directly proportional to the increased frequency of obesity, which is considered an underlying cause of CMS (Ojetola et al., 2021). It affects approximately 25% of the world's adult population. According to a survey conducted by the Dow University of Health Sciences, Karachi, Pakistan, ageing and unhealthy lifestyle practices have led to an upsurge in CMS risk factors which affect more than 51.8% adults—of these, 39.7% had hypertension, 29.7% had obesity, 23.1% diabetes, and 11.9% had dyslipidemia (Inam and Shah, 2019). Increased oxidative stress and inflammation are the key factors in obesity which lead to a sequential progression in insulin resistance (IR), type 2 diabetes, dyslipidemia, hepatic steatosis, and hypertension (Sharma et al., 2012), resulting in the development of CMS. Metabolic syndrome and chronic inflammation have an established association with increased adipocytokine (TNFα, IL-6, leptin, and chemerin) and decreased adiponectin levels (Nwakiban-Atchan et al., 2022).

Dietary habits and lifestyle modifications are known to ameliorate the risk factors of CMS for a limited duration. Similarly, weight reduction also attenuates cardiometabolic abnormalities; however, these modifications remain unsuccessful when practiced intermittently in established CMS. Pharmacological treatment involves the use of multiple therapeutic agents, but with increased cost, patient non-compliance, and adverse effects (Gutierrez-Salmean et al., 2014). Hence, there is an urgent need to develop multifactorial approaches to the treatment of CMS to probe its underlying causes. Due to the high prevalence of CMS, WHO recommends an increased use of medicinal herbs/plants to combat its characteristic features. Multiple evidence also indicates that medicinal plants and naturally derived compounds have great potential to combat CMS and related pathologies (Agrawal et al., 2018; De-Oliveira et al., 2021; Ojetola et al., 2021).

Caryopteris odorata (D. Don) B.L. Robinson, belonging to family Verbenaceae, mostly exists in tropical and subtropical climatic regions. The Verbenaceae family comprises of numerous important medicinal plants with a wide range of biological activities and potent phytochemical constituents. In Pakistan, around 35 species and 17 genera of this plant have been found (Shahzadi et al., 2013). It is a shrub which is found mostly in the subtropics or outer Himalayas of Pakistan, Bhutan, India, and Bangladesh. In Pakistan's traditional system of medicine, its powdered leaves and flowers are used to treat diabetes and associated pathologies like diabetic foot ulcer, tumors/cancer, wound healing, and general body aches (Abbasi et al., 2017; Joshi et al., 2019). It is used as fuel and fodder in northern areas of Pakistan. It has also been claimed to have antiulcer, antitumor, antidiarrhea, anti-inflammatory, antirheumatic, antihemorrhagic, and antitussive effects in Pakistan, China, and Mongolia (Frezza et al., 2019). It has been used for allergic reactions in Nepal (Bhattarai and Tamang, 2017).

The pharmacological effects of *C. odorata*, its derived iridoids, and the essential oils of its leaf, stem, and flower feature superodixe dismutase (SOD) and nitric oxide (NO) scavenging (Joshi et al., 2019), and antioxidant (Shahzadi et al., 2011; Shahzadi et al., 2012; Shahzadi et al., 2013; Abbasi M. A. et al., 2014; Singh et al., 2014; Joshi et al., 2019) and lipid peroxidation inhibitory activities (Shahzadi et al., 2011). It has also been reported to possess anti-inflammatory (Joshi et al., 2019), antimicrobial, antifungal, hemolytic (Abbasi M. et al., 2014; Singh et al., 2014), anti-urease, and anti-tyrosinase properties (Shahzadi et al., 2012). Furthermore, *C. odorata* has also shown enzyme inhibition potential against α-glucosidase, acetylcholinesterase, butylcholinestrase, and lipo-oxygenase (Shahzadi et al., 2013; Abbasi M. et al., 2014), thus providing indirect evidence for its use in diabetes, obesity, dyslipidemia, and hypertension. *C. odorata* has also been reported to be enriched with diverse phytoconstituents, including quercetin, gallic acid, cinnamic acid, vanillic acid, coumaric acid, ursolic acid, coumarins, and their derivative furanocoumarin (psoralen, methoxsalen, oxypeucedanin, isoimperatorin, and bergamottin) (Abbasi et al., 2017), stigmasterol, α-tocopherol, β-caryophyllene, α-and β-longipinene, α-humulene, caryophyllene

oxide, germacrene B and D, and α-bisabolol. Various iridoid glycosides (8-O-trans-cinnamoyl caryoptoside, 8-O-trans-cinnamoyl shanzhiside methyl ester, 8-O-trans-cinnamoyl mussaenoside, 8-O-caffeoyl massenoside) have also been isolated from *C. odorata*. These possess widespread cardiovascular protective, hepatoprotective, cholagogues, antihyperglycemic, analgesic, anti-inflammatory, anti-cancer, spasmolytic, antitumor, antiviral, immune modulator, and laxative (Shahzadi et al., 2013; Joshi et al., 2019) properties, thus providing support for the use of *C. odorata* in treating CMS. Despite the available precious pharmacological profile of *C. odorata,* no study has explored its pharmacological effects on CMS.

Coumarins owe their class name from *coumarou*, the vernacular name of the tonka bean (*Dipteryx odorata*). Coumarins were first isolated from the tonka bean by Vogel in 1820 (Bruneton, 1999). They are also referred as "plant-derived secondary metabolites". Coumarins (1,2-benzopyrone or o-hydroxycinamic acid-8-lactone) constitute a large class of phenolic substances; they are abundantly present in many plants like woodruff, tonka beans, cinnamon, green tea, honey, fruits (cloudberry, bilberry), celery, carrots, and chicory (Lake, 1999). Coumarin possesses anti-oxidant properties, which is evident from its ability to protect cells from oxidative damage and stress (Basile et al., 2009). It has also shown anti-inflammatory properties through stimulation of phagocytosis, enzyme production, and proteolysis to removes protein and edematous fluid from injured tissue sites (Piller, 1975). Coumarin inhibits COX and LOX enzymes, produces SOD (Fylaktakidou et al., 2004), and inhibits protein expression of NO synthase and COX-2 enzyme (Huang et al., 2012). It possesses promising therapeutic potential as an anticoagulant (Abdelhafez et al., 2010) and antithrombotic (Jain et al., 2013) agent for cardiovascular disorders. It has also been considered a vitamin K antagonist because of its potential to interfere with vitamin K cycle conversion (Hirsh et al., 2001). It displays an antihypertensive effect (Nguelefack-Mbuyo et al., 2008) through its smooth muscle relaxant actions (Mead et al., 1958). Coumarin is also known for its effectiveness in reducing left ventricular hypertrophy (Najmanova et al., 2015); it has peripheral and coronary vasodilatory efficacy (Gantimur et al., 1986) through platelet aggregation and NO-mediated system and has thus also been used to treat angina pectoris (Najmanova et al., 2015). Coumarin has also shown an antihyperglycemic effect (Murali et al., 2013). It has exhibited antihyperlipidemic action—possibly by activating the AMPK phosphorylation pathway and downregulating FAS and HMGR protein expression (Iwase et al., 2017; Li et al., 2017). Coumarin also possesses antiadipogenic effects. It is known to inhibit lipid accumulation and lipogenic-related gene expressions in 3T3-L1 adipocytes cells, possibly through the PPARγ pathway (Shin E. et al., 2010; Taira et al., 2017). Although coumarin has been studied in isolation and, in part, for its pharmacological effect in hypertension, diabetes, and dyslipidemia, no study has comprehensively ascertained its pharmacological effects against characteristic features of CMS using a rat model.

This study has been designed to provide a pharmacological basis for the protective potential of *C. odorata* and coumarin in CMS, including obesity, hyperglycemia, insulin resistance, hypertension, and dyslipidemia using HRCHFC-loaded diet-fed rats. This study also explains the possible mechanism(s) of *C. odorata* and coumarin for anti-oxidant, anti-hypertensive, anti-inflammatory, and HMG-CoA reductase inhibitory pathways. It thus presents sound evidence for the use of *C. odorata* in CMS. Furthermore, anti-obesity and insulin sensitizing effects have also been endorsed by the modulating potential of *C. odorata* and coumarin on adipokinin levels (leptin, adiponectin, and chemerin), and inflammatory (TNFα, IL-6) and oxidative stress biomarkers (CAT, SOD, MDA).

Novelty

- This is a pioneer study to show the effectiveness of *C. odorata* and coumarin in CMS induced by a HRCHFC-loaded diet.
- The quantification of obesity-related candid parameters including chemerin, leptin, adiponectin, and the inhibition of HMG-CoA reductase for the efficacy of *C. odorata* and coumarin in CMS.
- *C. odorata* and coumarin exhibit anti-inflammatory and antioxidant potential, which might reflect their effectiveness in CMS.

Materials and methods

Chemicals and drug

Coumarin ≥99% (HPLC), metformin, rosuvastatin, formaldehyde, and cholic acid were purchased from Sigma Aldrich (St. Louis, MA, United States). Cholesterol was bought from PanReac AppliChem (Ottoweg, Darmstadt, Germany). Additional ingredients, including sodium chloride (NaCl), dry powdered milk (Nido/Everyday, Nestle Ltd, Lahore, Pakistan), vegetable oil (Dalda oil, Unilever, Lahore, Pakistan), desi ghee (Pak pure, United Dairy Pharms, Lahore, Pakistan), and multivitamins (Metavit-Super, Batch# PM5483, Prix Pharmaceuticals (Pvt.) Ltd. Lahore, Pakistan), were purchased from respective commercial suppliers. Choker, highly refined wheat flour, fishmeal, molasses, and potassium metabisulfite were obtained from the local market in Faisalabad, Pakistan. All drug solutions and dilutions of the aqueous methanolic extract of *C. odorata* were prepared freshly on daily basis in distilled water. Stock solution of coumarin was prepared in 1% (v/v) dimethyl sulfoxide (DMSO) and 1% Tween-80 (w/v). All the chemicals and drugs used in this study were of analytical grade purity.

Plant collection, identification and preparation of extract

Whole plant material was obtained from Poonch, Azad Jammu Kashmir (AJK), Pakistan, in May 2020. Dr. Sardar Irfan Mehmood, Department of Botany, Govt. Boy's Degree College Abbasapur, Poonch AJK, Pakistan, identified and authenticated the plant material. The crude specimen was also submitted to the AJK Medicinal Plants Herbarium (AJKMPH) with issued Voucher no. AJKH: 437 for future reference. Whole plant of *C. odorata* was shade dried and ground into a fine powder in a mechanical grinder.

Approximately 1.5 kg of fine ground powder was soaked in methanol and distilled water (80:20) for 7 days at 25°C. The first filtrate was collected by passing soaked solution through muslin cloth followed by Whatman filter paper No.1. The maceration process was repeated thrice to obtain a sufficient quantity of extract. A rotary evaporator (Model: RE300 Stuart ® United Kingdom) was used to evaporate all of the filtrates. After air drying the final filtrate, the yield of *C. odorata* aqueous methanolic extract was 9% wt/wt.

Animals

Wistar albino rats weighing 180–220 g were used in this experiment. These were housed in an animal house at standard conditions of 12 h light and dark cycle, 55% relative humidity, and 22 ± 3°C temperature with free access to food and water. All the experiments were performed according to standard housing conditions and laboratory animal protocols as approved by the animal ethical review committee of GCU, Faisalabad No. IRB: 879 (Ref. No. GCUF/ERC/2279).

Quantitative analysis of *C. odorata*

Estimation of total flavonoid contents (TFC)

C. odorata extract (500 µL) was mixed with 2 ml of distilled water and 0.15 ml of $NaNo_2$ solution (5%). Next, 150 µL of 10% aluminum chloride ($AlCl_3$) solution with 4% sodium hydroxide solution were added into it. Total volume was made up to 5 ml with methanol. After incubation for 15 min, absorbance was measured at 510 nm. The findings were displayed as (mg/g QE) of catechin equivalent of the concentration of plant extract (Kumar and Roy, 2018).

Estimation of total phenolic contents (TPC)

C. odorata extract was prepared at 0.1 g/ml concentration, and 200 µL (two replicate) was poured in a test tube. Folin Ciocalteu reagent (6%) 1 ml and 0.8 ml of sodium carbonate (Na_2CO_3) solution (7.5% or 0.6 M) were added to the mixture. The test tube mixture was thoroughly mixed and incubated for 30 min. Absorbance was recorded at a wavelength of 765 nm or 725 nm. Total phenolic contents (TPC) were expressed as mg of gallic acid equivalent in milligram GAE/g of dry plant extract. Gallic acid was used as a reference control (Fetni et al., 2020).

DPPH (1,1-diphenyl-2picryl-hydrazyl) radical scavenging activity

The anti-oxidant potential of *C. odorata* extract was accessed using DPPH by following an earlier practiced method with slight modification (Fetni et al., 2020). To prepare fresh stock solution, 4 mg of DPPH was mixed with 100 ml methanol. A 3 ml aliquot was prepared with 2,800 µL of DPPH and 200 µL from different concentrations of *C. odorata* extract (500–6.25 µg/ml). This mixture was stored for 30 min in the dark at 25°C. OD (optical density) was noted at 517 nm. Methanol and DPPH were used as negative controls while, methanol was used as blank control. The antioxidant activity of quercetin (standard) was also evaluated. The % age inhibition of the DPPH radical scavenging capacity of the test samples was computed as: scavenging activity/DPPH % age inhibition = absorbance of negative control − absorbance of test sample/absorbance of negative control × 100.

Estimation of reducing power

A 10 µL test sample and 25 µL each of 1% potassium ferrocyanate (K_4 [Fe (CN)$_6$] ·3H_2O), 0.2 mM (pH = 6.6) phosphate buffer, and (10%) trichloroacetic acid were added to the test tube. It was then centrifuged to separate the supinated layer. Then, 8.5 µL of ferric chloride and 85 µL of distilled water were added. The mixture was incubated for 30 min and absorbance was recorded at a wavelength of 700 nm. The ferric reducing power of the sample was evaluated using following formula:

% age reducing power = A_o-At/A_o × 100 where A_o = negative control absorbance, At = test sample absorbance (Sharma et al., 2016).

Determination of H_2O_2 scavenging activity

Hydrogen peroxide (H_2O_2) (40 mM) solution was freshly prepared in 50 mM phosphate buffer (PBS) (pH = 7.4). Different concentrations of *C. odorata* extract and standard 10–200 µg/ml (50–100 µL) were added to the H_2O_2 solution (0.6 ml). After 10 min of incubation, the change in absorbance was measured from 30 s to 3 min at a wavelength of 230 nm. The % age of H_2O_2 scavenged by the sample was calculated using following formula:

% age of H_2O_2 scavenging activity = A_o -At/A_o × 100, where A_o = negative control absorbance, At = test sample absorbance (Sharma et al., 2016).

Finger print analysis by Fourier transform infrared (FTIR) spectroscopy

An ATR-FTIR spectrophotometer (Alpha-Bruker, Germany) was used for FTIR analysis of *C. odorata* extract. The sample was supplied with the projected ATR (Attenuated Total Reflectance) accessory system. ATR potassium bromide diamond crystal was thoroughly cleaned with alcohol during procedure. Around 10 mg of *C. odorata* extract was prepared and cautiously placed on the surface of the FTIR diamond crystal center. The spectrum was analyzed at an absorbance range of 400–4,000 cm^{-1} with a resolution of 4 cm^{-1} (Kumar and Roy, 2018).

High performance liquid chromatographic (HPLC) analysis

The quantifiable determination of flavonoids and phenolics present in *C. odorata* was conducted using the HPLC technique. A sample of *C. odorata* extract (50 mg) was prepared with methanol (24 ml), distilled water (16 ml), and hydrochloric acid (10 ml, 6 M). It was then incubated at 95°C for 2 h. The prepared solution was purified by membrane filter paper (nylon, 0.45 µm). A gradient reverse phase HPLC system (Shimadzu, Japan Model = SPD-10AV) was utilized to isolate the phenolics and flavonoids from *C. odorata*. The system was provided with C_{18} (shim-pack-CLC-ODS) 5 µm column (25 cm × 4.6 mm) attached with an UV-visible spectrophotometer detector

system and automatic injector for sampling. Separation of the valuable constituents was achieved through a gradient mobile phase (A: acetic acid and water; B: acetonitrile, 1 ml/min flow rate). Solvent B was used at a different gradient from time to time, like 15% for 0–15 min, 45% for 15–30 min, and 100% for 35–45 min. The compounds were detected at a preset wavelength of 280 nm and temperature of 25°C. Results were recorded by comparing (Rt) retention time with UV-visible peaks previously gained from the standard compound(s). Quantification was achieved by external standardization (Fetni et al., 2020).

Similarly, the standardization of coumarin was carried out in the isocratic mode using acetonitrile (40%)/water (60%); v/v. An injection volume of 20 µL with a flow rate of 0.5 ml/min was used at 274 nm UV detection. Quantification of coumarin in the plant sample was performed by an external standard method by comparison with coumarin (Sigma-Aldrich) as a standard. The stock solution of plant sample was prepared by mixing 224 mg of the dry extract in a 50 ml solution of methanol/water (80:20). The HPLC chromatogram was obtained using the same mobile phase and detection wavelength as for coumarin (Celeghini et al., 2001).

Preventive effect of *C. odorata* and coumarin on HRCHFC diet induced CMS

A high-refined carbohydrate-high fat-cholesterol loaded diet was used to induce CMS in animals (Agrawal et al., 2018).

Animal diet preparation

Two different types of diets were prepared for the study.

Standard diet (SD)

SD used the following composition for a 15 kg diet: chokar (5 kg), high-refined wheat flour (5 kg), dried powdered milk (2 kg), molasses (150 g), powdered fishmeal (2.25 kg), sodium chloride (75 g), potassium metabisulfite (15 g), vegetable oil (500 g), desi ghee (1 kg), and multivitamin (33 g). All the solid ingredients were ground and mixed to form palatable biscuits for the animals. Water was added in small quantities to make a soft composition (Aziz et al., 2013).

High-refined carbohydrate-high fat-cholesterol loaded diet (HRCHFC)

An earlier protocol was followed with minor modifications (Aziz et al., 2013). The HRCHFC diet comprised 20% protein, 35% carbohydrate, and 50% fat combined with cholesterol (2%w/w) and cholic acid (0.5% w/w).

Experimental design

Wistar albino rats were randomly allocated into eight different groups of six animals prior to dietary manipulation. The animals in Group 1 were considered the negative control and received a normal or standard diet, while the remaining groups, II–VIII, were administered the HRCHFC diet for 12–14 weeks. Group II was considered the disease control, receiving the HRCHFC diet only. The animals in Groups III–VI were further divided into different treatment groups. Group III was given metformin at 300 mg/kg/d, while group IV was administered metformin + rosuvastatin at (200 mg/kg/d + 1.5 mg/kg/d); these were considered the positive controls. Coumarin at 30 and 70 mg/kg was administered to Groups V and VI, serving as treatment. An aqueous methanolic extract of *C. odorata* (150 and 300 mg/kg) was administered to Groups VII and VIII as treatment. The treatment schedule was started orally from the eighth week of HRCHFC diet intake and continued until the study was terminated (Agrawal et al., 2018).

The doses of coumarin were selected from the results of our preliminary pilot experiment performed on few animals at given doses (appreciable effects were observed against developed parameters of CMS; data not shown) and the dose range of coumarin used in previous animal studies (Pari and Rajarajeswari, 2009) and doses exhibiting hepatic toxicity (Tasdemir et al., 2017).

Considering that the traditional dose of *C. odorata* plant used in human is 1 teaspoon thrice daily (Yaseen et al., 2015), the doses of *C. odorata* extract were selected on the basis of converting human doses to animal doses (Shin J. W. et al., 2010), and the effective dose range of similar species used in animal models (Ullah et al., 2019).

Body weight, feed intake and weight of different body organs

Body weights (g) were recorded at Weeks 0, 2, 4, 6, 8, 10, 12, and 14 to assess weight variation. Feed intake (g) was measured daily. Different organ weights (g) of the animals were calculated at the completion of study, such as the liver, heart, and kidney (Sasso et al., 2019).

Non-invasive measurement of blood pressure (NIBP) in conscious rats

Blood pressure was assessed by the tail cuff method in conscious rats. The systolic pressure of the conscious rats was recorded non-invasively using a tail cuff attached with a PowerLab data acquisition system (AD Instruments, Sydney, Australia) at an interval of 2 weeks. For estimation of blood pressure, the cuff sensor was attached to their tails by keeping the rat in a NIBP restrainer of appropriate size. The expected pressure (SBP, 200 mm Hg) was applied to the tail cuff by inflation followed by its gradual deflation. The intensified pulses were noted by PowerLab on Lab chart 7.0 running on a computer during inflation and deflation. Various hemodynamic parameters like systolic blood pressure (SBP), mean blood pressure (MBP), and heart rate (HR) were directly monitored by pulse tracing. Diastolic blood pressure (DBP) was measured by the formula DBP= (3MBP-SBP)/2. Blood pressure parameters were monitored at Weeks 0, 4, 8, 10, 12, and 14 of the diet in conscious rats. For each measurement, an average of 3–5 pressure readings was recorded (Senaphan et al., 2015).

Determination of fasting blood glucose (FBG), oral glucose tolerance test (OGTT), and insulin sensitivity/tolerance test (ITT)

Fasting blood glucose levels (FBG) were measured from overnight-fasted rats using a digital glucometer (EVOCHECK GM700S) at the end of treatment. During the 14th week of treatment, the animals were subjected to OGTT to measure the effect of *C. odorata* and coumarin administration on glucose metabolism. All rats had been fasted for 12 h. Afterwards, a glucose load (2 g/kg, p.o.) was administered to all test animals. Blood was drawn from their tail veins to assess the glucose levels in the test samples at 0, 30, 60, 90, and 120 min after glucose load through a digital glucometer (EVOCHECK GM700S). Insulin tolerance was tested at Day 5 before the animals were euthanized. ITT was conducted after 6 h of food deprivation. Blood glucose levels were verified in the animals at a fed state (0 min). Thence, 0.75 U/kg/animal weight of insulin (100 U/ml) was administered through intraperitoneal injection. Blood samples were drawn to assess glucose levels at 15, 30, 60, and 120 min by digital glucometer (EVOCHECK GM700S). Area under curves (AUC) was determined for each animal to calculate the mean for the whole study group (Sasso et al., 2019).

Biochemical analysis

After the 14th week of the experiment, the animals were starved for 18 h before being euthanized after deep anesthesia with isoflurane (5–10% v/wt) through inhalation in a closed chamber. Blood was drawn by cardiac puncture from each rat. The collected blood samples were then centrifuged at 4,000 rpm for 10 min to obtain the serum and stored at −80°C. Serum samples were preserved for further biochemical analysis (Javaid et al., 2021).

Assessment of lipid, liver, and kidney profile indices

The lipid profile including triglycerides (TG), high density lipoprotein (HDL), total cholesterol (TC), liver profile indices (aspartate aminotransferase (AST), alanine aminotransferase (ALT), and renal profile indices (urea and creatinine) were measured from isolated serum samples using commercial biochemical assay kits (Germany) as per the manufacturer's protocol. The results were shown in mg/dl and U/L (Sasso et al., 2019).

Determination of leptin, adiponectin, chemerin, and HMG-CoA reductase levels

Serum biomarkers for obesity, hyperlipidemia and insulin resistance, leptin (E-EL-R0582), adiponectin (E-EL-H6122), HMG-CoA reductase (E-EL-H2472) were sourced from Elabscience, United States, and chemerin (E-0864Ra) from BT LAB, Birmingham, United Kingdom; levels were analyzed by ELISA Kits as per manufacturer's instructions. 100 µL of serum (reaction mixture) in pre-coated wells with specific rat antibodies of LEP, ADP, HMG-CoA reductase, and CHEM, maintained at 37°C in an ELISA plate reader (DIA source, Germany), were taken. Responses were checked at 450 nm wavelength. 10 µL of serum leptin was taken and diluted 50-fold. The dilution factor was multiplied with sample OD. Serum adiponectin and chemerin levels were shown as pg/ml and ng/ml, respectively, while leptin and HMG-CoA reductase levels were expressed as ng/mL and pmol/ml, respectively (Della-Vedova et al., 2016).

Determination of inflammatory biomarkers (TNF-α and IL-6)

Serum concentration of TNF-α (E-EL-H0109) and IL-6 (E-EL-H0102) were determined using ELISA Kits (Elabscience Biotechnology CO. Ltd., United States) with sensitivity in the 7.6 pg/ml – 46.88 pg/ml range. Assays were performed as per manufacturer's protocol. The reaction mixture was provided 100 µL of serum in previously coated wells in the ELISA plate reader (DIA source, Germany) and kept at 37°C. The reactions were measured at an absorbance of 450 nm. The findings are presented as pg/ml or pg/mg (Adedapo et al., 2020).

Determination of oxidative stress biomarkers

The anti-oxidant potential of *C. odorata* and coumarin was analyzed by measuring the amount of catalase, superoxide dismutase, and malondialdehyde peroxidase in tissue homogenate. After 14 weeks, animals were starved for 18 h before being euthanized through deep anesthesia with isoflurane (5–10% v/wt) by inhalation in a closed chamber. Organs (liver, heart, kidney, and aorta) were removed and washed with ice-cold normal saline. These were stored at −80°C for further analysis. 100 mg of each organ was homogenized with 5 ml of tris-base/phosphate buffer solution (7.4 pH) and centrifuged at 2000 rpm for 15–20 min at 4°C. The supernatant layer was removed and stored at -80°C for further analysis. For catalase activity (CAT), 50 µL of different organ homogenates were mixed with freshly prepared H_2O_2 (30 mM, 1 ml) and 50 mM phosphate buffer (7.0 pH, 1.95 ml). Absorbance was measured at 240 nm. Catalase activity was estimated as units/g tissue. Superoxide dismutase (SOD) was estimated by following an earlier practiced method (Younis et al., 2018) where chromogen intensity was measured at an absorbance of 560 nm against blank. It was equated with the known SOD standard curve as units/mg. Lipid peroxidation/malondialdehyde peroxidase (MDA) levels were evaluated using the methodology of Adedapo et al. (2020).

Histological examination

The isolated tissues of heart (5 mm), liver, kidney, aorta, pancreas, and fat (5 µm) were dissected and fixed with 17% formalin. Different organ tissue sections were stained with hematoxylin and eosin. A microtome (Leica, Germany) was used to collect thin sections of organs to assess histopathological changes under a light microscope (ACCU-SCOPE 3001-LED Digital Microscope, United States) (Sasso et al., 2019).

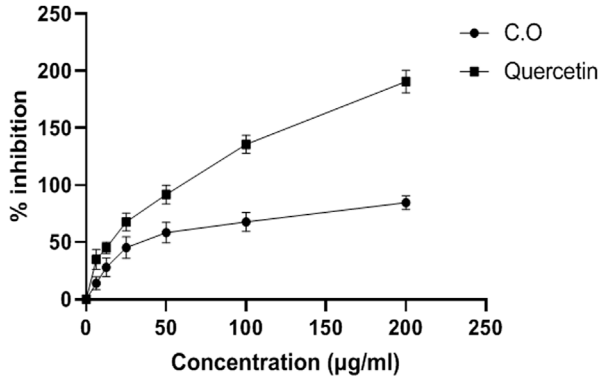

FIGURE 1
Antioxidant DPPH radical scavenging activity of aqueous methanolic extract of *C. odorata* (*in vitro*). Values are stated as mean ± SEM (n = 6).

Statistical analysis

The values were presented as mean ± SEM. The significance among results was tested using one-way analysis of variance (ANOVA) followed by Dunnett's test, and two-way ANOVA followed by Dunnett's test/ Bonferroni post doc test and unpaired *t*-test. Non-linear regression analysis was applied to compare concentration response curves. GraphPad Software 8.4.3 (Diego California United States) was used for statistical analysis and calculation to convert data into graphs.

Results

TFC and TPC

The equivalent contents of TF and TP were quantified using standard regression lines of catechin and gallic acid, respectively. TFC of *C. odorata* extract were 67.34 mg catechin/g DE and TPC were 86.82 mg GAE/g DE weight.

Antioxidant activities

Aqueous methanolic extract of *C. odorata* was found to be a promising reducing agent with an IC_{50} value of 78.38 ± 0.79 mg/ml. *C. odorata* extract showed 20.86 ± 0.87 U/mg protein of H_2O_2% inhibition. The DPPH % age activity of *C. odorata* extract is shown in Figure 1. *C. odorata* extract showed % age DPPH inhibition with maximum effect of 84.61% at 200 µg/ml concentration. The IC_{50} value was 29.78 µg/ml, similar to the effect of quercetin (IC_{50} value = 107.3 µg/ml).

FTIR analysis

Figure 2 depicts the spectrum of the FTIR analysis of *C. odorata* extract. The ATR-FTIR spectrum was interpreted in comparison with previous reported studies (Table 1). An infrared spectrum represents a fingerprint of a sample with absorption peaks which correspond to the frequencies of vibrations between the bonds of the atoms comprising the material. The absorption signals of 1–11 wave numbers in *C. odorata* FTIR-spectrum showed first peak at 3,245.75 cm^{-1}, which lies in the reference range of 3,000–3,600. This range represents possible stretching of C–H, O–H and N–H bands of alcohol, phenol, amine, or amide. The second peak of 2,938.41 cm^{-1} found in the 2,800–2,900 reference range indicates a C–H stretch of alkanes. The peak at 2,366.59 cm^{-1} and 2059.31 cm^{-1} at a 2000–2,500 reference range represents C≡N and C≡C bonds of alkynes and isothiocyanate. Peak 5 at 1,607.74 cm^{-1} of the 1,600–1706 range revealed the presence of amino acids. The peak of 1,521.24 at the 1,500–1,600 range finds N–H bonds of either carboxylic acid salt, amide of amino acids, or nitro compounds. The remaining peak at 1,442.22, 1,358.66, 1,245.68, 1,014.86, and 926.32 wavenumber (cm^{-1}) indicates the aromatic or phenyl group, amide I, phenol, alcohol or nitro, alkyl halide, acyl, or phenyl, ether or aliphatic phosphate, and the methylene (CH_2) group of isoprenoids as functional groups, respectively, as detailed in Figure 2 and Table 1.

HPLC analysis

The achieved chromatograms of *C. odorata* extract (Figures 3A, B) showed identified compounds as plant constituents. The HPLC profiles of the test materials were related to the standards. The quantitative results were presented in ppm, where quercetin (7.53), catechin (0.34), gallic acid (9.42), caffeic acid (8.75), ferulic acid (176.6), chologenic acid (3.23), syringic acid (0.58), p-coumaric acid (0.84), sinapic acid (0.39) (Figure 3A), and coumarins (416.24) (Figure 3B) were found as active ingredients of *C. odorata*. The observed retention times (rt) of these standards were 3.09, 3.56, 4.88, 12.06, 13.79, 15.14, 16.22, 17.43, and 26.59 min, respectively. Standard coumarin appeared with 5.63 min (rt) (Figure 3C), while it appeared in plant extract at a retention time of 5.58 min.

Effect of *C. odorata* and coumarin on body weight, feed intake, and weight of different body organs

Initially, rats in all groups did not show a significant ($p > 0.05$) difference in their body weight. However, HRCHFC-fed rats showed a significant ($p < 0.001$) rise at Weeks 10–14. Chronic administration of *C. odorata*, coumarin or positive controls to HRCHFC-fed rats markedly ($p < 0.001$) reduced weight gain at Weeks 12–14 of the study (Table 2). Similarly, *C. odorata* treatment caused a marked ($p < 0.001$) reduction in feed intake pattern at Weeks 11–14 compared to HRCHFC-fed rat data. Coumarin or positive controls groups showed a consistent pattern of feed intake at the start of experiment and showed significant ($p < 0.001$) reduction in daily diet intake at Weeks 12–14 of the study period compared to HRCHFC group data (Figure 4). Table 3 shows that HRCHFC-fed rats displayed a marked ($p < 0.001$) increase in liver and heart weight with no effect on kidney weight at end of the study. Significant ($p < 0.001$) reductions in liver and heart weight were seen in all treatment groups.

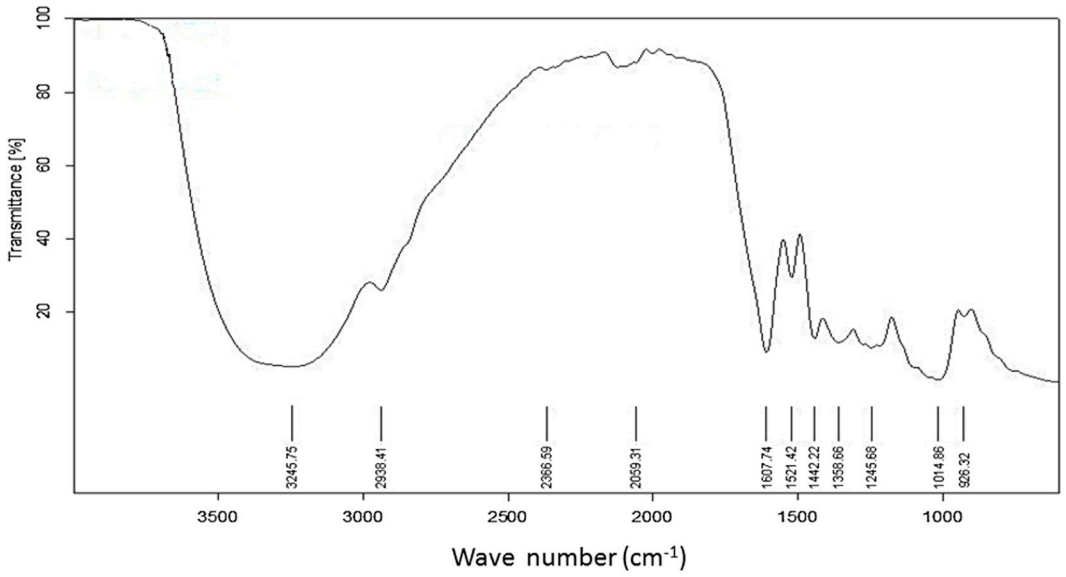

FIGURE 2
FTIR spectrum of aqueous methanolic extract of *C. odorata* studied at 400–4,000 cm^{-1} range.

TABLE 1 FTIR frequency range with peaks and functional groups present in aqueous methanolic extract of *C. odorata*.

No.	Wavenumber cm^{-1} (observed)	Wavenumber cm^{-1} (references)	Biomolecular assignment	Possible functional group	References
1	3,245.75	3,000–3,600	Stretching of C–H, O–H, and N–H bands	Water, phenols, protein, carbohydrates, alcohols, peroxides	Caunii et al. (2012), Cao et al. (2017)
2	2,938.41	2,800–2,900	C–H stretch	Lipids, metoxy derivatives (cis double bonds)	Caunii et al. (2012)
		2,970–2,950/2,880–2,860			
3	2,366.59, 2059.31	2000–2,500	C≡N, C≡C	Alkynes, isothiocyanate	Nandiyanto et al. (2019), Nnorom and Onuegbu (2019)
4	1,607.74	1,600–1760, 1,600–1706	Aromatic ring stretch, vibrations N-H, C=O, C–O, C–N, CNN	Aldehydes, cetones, esters, amino acids, fatty acids, and ester-like glycerides	Caunii et al. (2012), Hands et al. (2016), Tatarua L.D (2017)
5	1,521.24	1,500–1,600	N–H bending vibrations, carboxylic acid salt, amide	Amino acids	Caunii et al. (2012), Tatarua L.D (2017)
6	1,442.22	1,380–1,465	Stretching vibrations CO and C-C, prim, sec or teri OH, phenol	Amide II, phenyl groups	Hands et al. (2016)
7	1,358.66	1,315–1,384	CH_3/CH_2 bending	Amide I	Hands et al. (2016)
8	1,245.68	1,150–1,270	Tertiary amine, CN stretch, C-O vibrations	Acid or ester	Caunii et al. (2012), Tatarua (2017)
9	1,014.86	997–1,130	Aliphatic phosphates (P–O–C stretch)	(Mono-, oligo-, and carbohydrates) deoxyribose/ribose, DNA, RNA (PO^{2-})	Caunii et al. (2012), Hands et al. (2016)
		1,008–1,230	C–C stretch, C–H bend		
10	926.32	<1,000	Methylene– (CH2) n, trans-C–H, cis–C–H	Isoprenoids	Caunii et al. (2012)

Hypotensive effect of *C. odorata* and coumarin

The hypotensive effect of chronically-administered *C. odorata* and coumarin on systolic blood pressure, mean arterial pressure, diastolic blood pressure, and heart rate in HRCHFC-fed rats is evident in Tables 4 and 5. The results clearly showed that HRCHFC diet administration revealed a noticeable ($p < 0.001$) rise in SBP, MAP, and DBP, along with HR, at Weeks 12–14 of the study period compared to the control

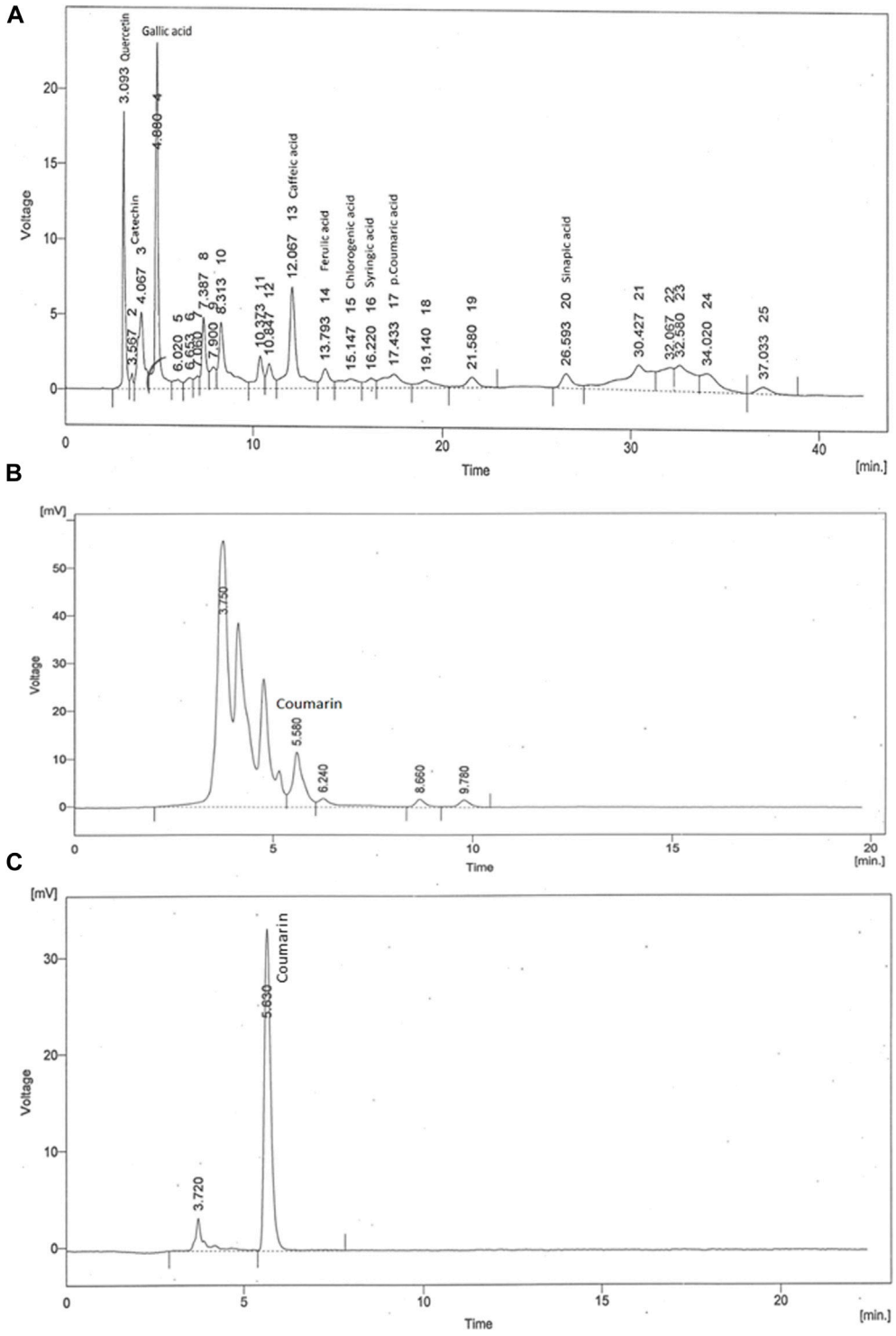

FIGURE 3
HPLC fingerprint of **(A)** aqueous methanolic extract of *C. odorata* in gradient mode, **(B)** aqueous methanolic extract of *C. odorata* in isocratic mode, and **(C)** standard coumarin.

rats. Subsequently, after 6 weeks of the treatment schedule, all treated rats manifested a significant ($p < 0.001$) decline in blood pressure (SBP, DBP, MBP) and HR at Weeks 10–14 of the study period compared to HRCHFC-fed rats. The hypotensive effect of *C. odorata* and coumarin were observed dose-dependent in SBP, MBP (10–14 weeks), and HR (12–14 weeks).

Effect of *C. odorata* and coumarin on fasting blood glucose (FBG), oral glucose tolerance (OGT), and insulin sensitivity tests (ITT)

Administration of *C. odorata* and coumarin significantly ($p < 0.001$) showed a dose-dependent reduction in elevated fasting blood

TABLE 2 Effect of *C. odorata* and coumarin administration on body weight in HRCHFC- diet induced CMS rats.

Parameter	Duration (W)	Groups							
		N	HRCHFC	HRCHFC + MET	HRCHFC + MET + ST	HRCHFC + COM-30	HRCHFC + COM-70	HRCHFC + CO-150	HRCHFC + CO-300
Body weight (g)	0	135.6 ± 9.0	139.6 ± 5.9	157.6 ± 6.6	146.0 ± 13.9	155.4 ± 10.7	137.2 ± 4.3	168.2 ± 3.8	127.4 ± 8.1
	2	143.2 ± 13.5	148.0 ± 7.5	167.2 ± 2.8	158.2 ± 10.0	167.8 ± 9.7	148.6 ± 5.8	179.0 ± 3.1	143.2 ± 6.9
	4	155.4 ± 12.7	164.4 ± 8.5	177.8 ± 4.0	176.2 ± 10.5	176.0 ± 12.1	154.8 ± 11.7	195.4 ± 5.7*	155.4 ± 6.7
	6	164.6 ± 14.3	184.0 ± 6.6	187.2 ± 12.3	182.6 ± 7.3	184.8 ± 13.0	166.8 ± 8.3	204.0 ± 7.7	162.4 ± 6.4
	8	183.8 ± 10.4	221.20 ± 8.5	194.0 ± 5.3	198.6 ± 7.0	194.8 ± 12.5	181.2 ± 6.5^{a*}	209.4 ± 8.2	185.2 ± 7.2
	10	196.0 ± 10.1^{c}	257.4 ± 0.4***	209.2 ± 13.9^{**b}	210.0 ± 7.8^{**b}	209.0 ± 9.9^{**b}	209.4 ± 22.4$^{**b/ns}$	218.8 ± 10.2^{*a}	201.8 ± 7.8$^{***c/ns}$
	12	201.4 ± 8.7^{c}	281.8 ± 6.8***	212.6 ± 11.7^{***c}	211.2 ± 9.1^{***c}	221.4 ± 13.1^{***c}	212.8 ± 25.6$^{***c/ns}$	220.6 ± 5.2^{***c}	202.8 ± 6.0$^{***c/α}$
	14	207.6 ± 7.2^{c}	308.0 ± 5.5***	223.2 ± 20.7^{***c}	218.8 ± 7.3^{***c}	224.0 ± 0.3^{***c}	214.4 ± 0.5$^{***c/γ}$	222.4 ± 4.7^{***c}	192.6 ± 5.8$^{***c/β}$

Effect of *C. odorata* and coumarin administration on body weight in HRCHFC-diet induced CMS rats. N: normal control; HRCHFC: high refined carbohydrate-high fat-cholesterol loaded diet induced CMS control; HRCHFC + MET: (metformin 300 mg/kg); HRCHFC + MET + ST: (metformin and rosuvastatin 200 mg/kg +1.5 mg/kg); HRCHFC + COM-30: (coumarin 30 mg/kg); HRCHFC + COM-70: (coumarin 70 mg/kg); HRCHFC + CO-150: (*C. odorata* 150 mg/kg); HRCHFC + CO-300: (*C. odorata* 300 mg/kg). Values are stated as mean ± SEM (n = 6), where ***p < 0.001, **p < 0.01, *p < 0.05 vs. normal control and ^{c}p < 0.001, ^{b}p < 0.01, and ^{a}p < 0.05 vs. CMS control group using two-way ANOVA followed by Bonferroni *post hoc* test. ns = non-significant, ^{γ}p < 0.001, ^{β}p < 0.01, ^{α}p < 0.05 shows effect of low vs. high dose of *C. odorata* and coumarin in treatment period (Student's t-test).

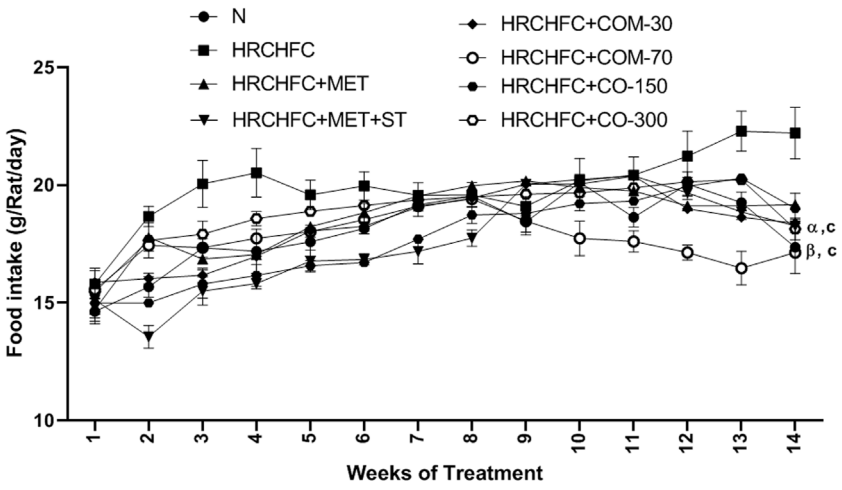

FIGURE 4
Effect of *C. odorata* and coumarin administration on feed intake in HRCHFC- diet induced CMS rats. N: normal control; HRCHFC: high refined carbohydrate-high fat-cholesterol loaded diet induced CMS control; HRCHFC + MET: (metformin 300 mg/kg); HRCHFC + MET + ST: (metformin and rosuvastatin 200 mg/kg + 1.5 mg/kg); HRCHFC + COM-30: (coumarin 30 mg/kg); HRCHFC + COM-70: (coumarin 70 mg/kg); HRCHFC + CO-150: (*C. odorata* 150 mg/kg); HRCHFC + CO-300: (*C. odorata* 300 mg/kg). Values are expressed as mean ± SEM (n = 6), where ***p < 0.001, **p < 0.01, *p < 0.05 vs. normal control and ^{c}p < 0.001, ^{b}p < 0.01 and ^{a}p < 0.05 vs. CMS control group using two-way ANOVA followed by Bonferroni *post hoc* test. ns = non-significant, ^{γ}p < 0.001, ^{β}p < 0.01, ^{α}p < 0.05 shows effect of low vs. high dose of *C. odorata* and coumarin (Student's t-test).

glucose in HRCHFC-fed rats (Table 3). These effects were comparable to standards. HRCHFC-fed rats exhibited notably (p < 0.05) impaired glucose tolerance against normal control rats. A remarkably (p < 0.001) faster disposal of glucose levels was noticed from circulation at 60, 90, and 120 min in *C. odorata* and coumarin-treated rats compared to HRCHFC-fed rats (Figure 5A). The AUC study revealed a significant difference in HRCHFC-fed rats compared to normal control rats (Figure 5B). The ITT results showed that, after 6 weeks of treatment with *C. odorata* and coumarin, significant (p < 0.001) differences in blood glucose

TABLE 3 Effect of *C. odorata* and coumarin administration on weight of various organs, feed intake, and fasting blood glucose level in HRCHFC-diet induced CMS rats.

Parameters	N	HRCHFC	HRCHFC + MET	HRCHFC + MET + ST	HRCHFC + COM-30	HRCHFC + COM-70	HRCHFC + CO-150	HRCHFC + CO-300
Liver. Wt. (g)	7.8 ± 0.1^{c}	13.9 ± 0.0***	11.5 ± 0.2***^{c}	8.9 ± 0.1 ***^{c}	10.7 ± 0.2***^{c}	8.8 ± 0.2***$^{c/\gamma}$	11.2 ± 0.4**^{c}	9.8 ± 0.5**$^{c/\alpha}$
Kidney. wt. (g)	0.98 ± 0.0	1.0 ± 0.0	1.1 ± 0.0	0.99 ± 0.0	0.94 ± 0.0	0.98 ± 0.0^{ns}	1.0 ± 0.0	0.99 ± 0.0^{ns}
Heart. wt. (g)	0.81 ± 0.0^{c}	1.3 ± 0.03***	0.86 ± 0.0^{c}	0.80 ± 0.0^{c}	0.82 ± 0.0^{c}	0.79 ± 0.0$^{c/ns}$	1.0 ± 0.0^{c}	0.95 ± 0.0$^{c/ns}$
Feed intake (g/rat/d)	17.1 ± 0.9^{c}	21.2 ± 0.5*	18.5 ± 0.0^{a}	17.5 ± 0.0^{b}	18.3 ± 0.0^{b}	17.6 ± 0.2$^{b/\alpha}$	17.9 ± 0.2^{b}	17.1 ± 0.2$^{c/\beta}$
FBG (mg/dl)	82.0 ± 6.3	134.6 ± 3.5**	87.6 ± 6.9^{c}	73.0 ± 4.7^{c}	95.3 ± 3.7^{c}	86.3 ± 0.8$^{c/\alpha}$	96.6 ± 4.0^{c}	79.6 ± 6.0$^{c/\alpha}$

Effect of *C. odorata* and coumarin administration on weight of various organs, feed intake, and fasting blood glucose (FBG) level in HRCHFC-diet induced CMS rats. Values are stated as mean ± SEM ($n = 6$), where ^{ns} = non-significant, ***$p < 0.001$, **$p < 0.01$, *$p < 0.05$ vs. normal control and $^{c}p < 0.001$, $^{b}p < 0.01$ and $^{a}p < 0.05$ vs. CMS control group using one-way ANOVA followed by Dunnett's test. ns = non-significant, $^{\gamma}p < 0.001$, $^{\beta}p < 0.01$, $^{\alpha}p < 0.05$ shows effect of low vs. high dose of *C. odorata* and coumarin (Student's t-test).

levels were analyzed following insulin administration. ITT showed notably ($p < 0.01$) lower responsiveness to insulin in HRCHFC-fed rats compared to normal rats. *C. odorata* and coumarin-treated rats showed marked ($p < 0.001$) insulin sensitivity compared to HRCHFC-fed rats. These results were verified by AUC analysis between treated groups during the experiment period (Figures 5C, D).

Effect of *C. odorata* and coumarin on serum biochemical markers

HRCHFC-fed rats showed a significant ($p < 0.001$) increase in serum triglycerides and total cholesterol (lipid biomarkers), aspartate transaminase, alanine transaminase (liver biomarker enzyme), urea, and creatinine (renal biomarkers) levels, while showing a notable reduction in serum high density lipoprotein cholesterol levels compared to the normal control group. However, concurrent treatment with *C. odorata*, coumarin, and positive controls produced a notable ($p < 0.001$) decline in serum TC, TG, ALT, AST, urea, and creatinine levels, while elevated HDL-C levels were observed compared to only HRCHFC-fed rats (Table 6).

Effect of *C. odorata* and coumarin on serum biomarkers of leptin, adiponectin, chemerin, and HMG-CoA reductase levels

The animals on the HRCHFC diet showed a marked ($p < 0.001$) elevation in serum leptin and chemerin levels and HMG-CoAreductase activity with serum leptin, chemerin and HMG-CoA reductase levels, while adiponectin levels were found to be decreased in diseased animals compared to the normal control group. After the sixth week of treatment with *C. odorata*, coumarin, and positive controls, there was a marked ($p < 0.001$) suppression in leptin and chemerin levels and HMG-CoAreductase activity with leptin, chemerin and HMG-CoA reductase levels, while a significant ($p < 0.001$) rise of adiponectin levels was observed in treated rats compared with data from only HRCHFC-fed rats (Figure 6).

Effect of *C. odorata* and coumarin on inflammatory biomarkers (TNF-α and IL-6)

HRCHFC-fed rats displayed a significant ($p < 0.001$) elevation in TNF-α and IL-6 levels versus the normal control group. However, oral treatment of *C. odorata* and coumarin to diseased animals produced a significant ($p < 0.001$) fall in serum TNF-α and IL-6 levels to normal values, comparable to positive controls (Figure 7).

Effect of *C. odorata* and coumarin on oxidative stress markers

Figure 8 shows the effect of *C. odorata* and coumarin supplementation on oxidative stress markers in liver, heart, kidney, and aorta tissue homogenates. *C. odorata* and coumarin-treated rats significantly ($p < 0.001$) raised catalase and superoxide dismutase enzymes in their livers, heart, kidneys, and aortas, which were found depleted in the organs of HRCHFC-fed rats. The detrimental effect of lipid peroxidation in HRCHFC-fed rats markedly ($p < 0.001$) decreased, representing an attenuation in MDA levels when treated with *C. odorata* and coumarin.

Effect on histopathology of organs

The histopathological examination of *C. odorata* and coumarin-treated liver tissues revealed a restored normal or intact texture of hepatocyte with a lesser appearance of fat deposition, reduced hepatic lesions, and necrosis with diminished inflammatory cells. A normal portal vein and dilation of sinusoids were observed in treated groups, while HRCHFC-fed rats caused degenerative and vacuolized hepatocytes, damaged hyaline with fat deposition, inflammatory cell infiltration, and congested sinusoids. The heart

TABLE 4 Effect of *C. odorata* and coumarin administration on systolic blood pressure (SBP), mean blood pressure (MBP), and diastolic blood pressure (DBP) in HRCHFC-diet induced CMS rats.

Parameters	Duration (W)	Groups							
		N	HRCHFC	HRCHFC + MET	HRCHFC + MET + ST	HRCHFC + COM-30	HRCHFC + COM-70	HRCHFC + CO-150	HRCHFC + CO-300
SBP (mmHg)	0	123.0 ± 1.5	122.3 ± 1.6	123.8 ± 2.7	119.0 ± 0.5	120.6 ± 1.2	115.3 ± 0.8^{a*}	121.96 ± 2.7	122.6 ± 1.9
	4	125.5 ± 0.8^{c}	149.9 ± 0.9***	145.2 ± 0.6***	144.4 ± 1.2***	149.7 ± 1.3***	144.1 ± 0.9***	144.4 ± 2.9***	145.8 ± 2.1***
	8	124.3 ± 0.7^{c}	178.9 ± 3.4***	176.6 ± 2.3***	176.3 ± 0.6***	177.7 ± 1.0***	174.7 ± 1.4***	176.0 ± 1.3***	175.7 ± 3.3***
	10	120.3 ± 0.9^{c}	180.0 ± 2.3***	139.4 ± 2.3^{***c}	134.0 ± 1.0^{***c}	155.3 ± 1.2^{***c}	158.2 ± 2.1$^{***c/ns}$	157.6 ± 3.7^{***c}	148.2 ± 2.0$^{***c/\alpha}$
	12	125.3 ± 0.9^{c}	181.9 ± 1.4***	129.3 ± 0.6^{c}	126.4 ± 1.0^{c}	136.8 ± 0.9^{***c}	119.6 ± 0.8$^{c/\gamma}$	126.2 ± 1.0^{c}	118.2 ± 2.4$^{*c/\alpha}$
	14	126.7 ± 0.7^{c}	182.4 ± 1.4***	119.6 ± 0.8^{*c}	117.3 ± 0.6^{**c}	108.7 ± 0.9^{***c}	103.2 ± 1.0$^{***c/\beta}$	112.8 ± 2.0^{***c}	99.1 ± 1.3$^{***c/\gamma}$
MBP (mmHg)	0	86.1 ± 1.6^{c}	97.4 ± 1.1***	95.2 ± 0.5**	87.4 ± 1.1^{c}	92.3 ± 1.6	90.2 ± 1.1^{a}	90.1 ± 1.2^{a}	94.4 ± 0.6**
	4	99.8 ± 0.5^{c}	115.5 ± 1.9***	119.1 ± 2.1***	119.3 ± 0.5***	118.3 ± 2.5***	114.6 ± 3.9***	117.5 ± 0.6***	113.4 ± 2.6***
	8	97.4 ± 1.1^{c}	124.2 ± 0.5***	123.7 ± 1.4***	125.5 ± 1.9***	124.6 ± 2.6***	125.6 ± 0.9***	125.4 ± 2.1***	124.9 ± 1.3***
	10	95.2 ± 0.0^{c}	125.8 ± 0.8***	105.2 ± 0.5^{***c}	106.3 ± 0.5^{***c}	109.3 ± 0.5^{***c}	115.3 ± 1.7$^{***c/\beta}$	117.4 ± 4.5^{***b}	118.5 ± 1.2$^{***a/ns}$
	12	93.4 ± 0.1^{c}	126.3 ± 0.5***	95.2 ± 0.5^{c}	95.6 ± 0.7^{c}	103.1 ± 1.1^{***c}	97.0 ± 1.5$^{c/\beta}$	107.6 ± 3.2^{***c}	100.1 ± 1.0$^{*c/\alpha}$
	14	92.3 ± 1.6^{c}	127.1 ± 0.6***	92.0 ± 1.4^{c}	100.1 ± 0.5^{**c}	94.8 ± 1.1^{c}	92.3 ± 0.0$^{c/\alpha}$	95.2 ± 0.6^{c}	87.2 ± 1.1$^{c/\gamma}$
DBP (mmHg)	0	67.6 ± 1.0^{c}	85.0 ± 0.4***	80.8 ± 0.7***	71.6 ± 0.5^{c}	78.1 ± 0.5^{***b}	77.6 ± 0.7^{***c}	74.2 ± 0.6^{**c}	80.3 ± 0.3^{***a}
	4	87.0 ± 0.9^{c}	98.3 ± 0.8***	106.0 ± 1.6^{***c}	106.7 ± 1.6^{***c}	102.5 ± 1.2***	99.9 ± 0.3***	104.0 ± 0.8^{***b}	97.2 ± 0.9***
	8	84.3 ± 2.0^{c}	96.5 ± 0.0***	97.1 ± 0.6***	100.7 ± 0.4***	98.7 ± 0.4***	101.6 ± 0.7^{***a}	100.4 ± 0.5***	99.5 ± 0.5***
	10	82.6 ± 0.0^{c}	98.3 ± 0.0***	88.1 ± 2.5^{*c}	92.5 ± 2.6^{***a}	86.2 ± 0.8^{c}	93.6 ± 0.6$^{***/\gamma}$	97.3 ± 1.1***	103.6 ± 0.8$^{***/\gamma}$
	12	77.4 ± 0.7^{c}	99.8 ± 0.4***	78.2 ± 0.4^{c}	80.2 ± 2.2^{c}	87.2 ± 0.6^{***c}	85.7 ± 3.2$^{***c/ns}$	98.3 ± 0.9^{***b}	91.0 ± 0.6$^{***c/\gamma}$
	14	75.1 ± 1.3^{c}	108.9 ± 1.7***	78.1 ± 0.0^{c}	91.2 ± 3.1^{***c}	87.8 ± 0.2^{***c}	86.3 ± 2.8$^{***c/ns}$	86.4 ± 0.4^{***c}	81.3 ± 0.8$^{**c/\beta}$

Effect of *C. odorata* and coumarin administration on systolic blood pressure (SBS), mean blood pressure (MBP) and diastolic blood pressure in HRCHFC-diet induced CMS rats. Values are stated as mean ± SEM ($n = 6$), where $^{***}p < 0.001$, $^{**}p < 0.01$, $^{*}p < 0.05$ vs. normal control and $^{c}p < 0.001$, $^{b}p < 0.01$ and $^{a}p < 0.05$ vs. CMS control group using two-way ANOVA followed by Bonferroni *post hoc* test. ns = non-significant, $^{\gamma}p < 0.001$, $^{\beta}p < 0.01$, $^{\alpha}p < 0.05$ shows effect of low vs. high dose of *C. odorata* and coumarin in treatment period (Student's t-test).

tissues of treated rats revealed non-infracted architecture or intact branches of myocardium, lesser cell infiltration, necrosis, and inflammation, and reduced edema with a restoration of myofibril integrity. Restored normal glomerulus with no hyperemia, normal basement membrane and capillaries, no shrinkage of the renal cortex, and absence of inflammatory cells was observed in the kidney tissues of treated rats, whereas the aortic tissues of treated groups presented significant progression of foam cells, repair of elastic fibers, and lessened fat deposition in the tunica media layer of the aorta. An organized pattern, normal architecture, and the regeneration and development of islets of Langerhans and β-cells were evident in the pancreatic tissue of *C. odorata* and coumarin-treated rats. The dilation of the intra-lobular duct and reduced inflammation of pancreatic tissue were also observed in treated groups. Treated rats reversed the size and number of adipocytes with less inflammation in the fat pad of the epididymal tissues (Figure 9).

TABLE 5 Effect of *C. odorata* and coumarin administration on heart rate in HRCHFC-diet induced CMS rats.

Groups									
Parameter	Duration (W)	N	HRCHFC	HRCHFC + MET	HRCHFC + MET + ST	HRCHFC + COM-30	HRCHFC + COM-70	HRCHFC + CO-150	HRCHFC + CO-300
Heart rate (BPM)	0	299.4 ± 11.6	309.1 ± 6.5	289.5 ± 7.5	304.6 ± 3.9	304.1 ± 7.3	308.4 ± 5.4	291.8 ± 11.4	295.4 ± 10.0
	4	314.2 ± 7.9^{c}	388.9 ± 5.8***	375.9 ± 5.7***	385.1 ± 7.6***	376.5 ± 5.1***	378.1 ± 6.1***	383.5 ± 7.0***	372.1 ± 11.8***
	8	328.9 ± 3.4^{c}	425.06 ± 2.2***	419.7 ± 3.4***	430.7 ± 3.0***	439.4 ± 0.5***	432.3 ± 2.0***	429.5 ± 8.2***	436.6 ± 5.2***
	10	319.7 ± 10.2^{c}	446.4 ± 2.0***	367.7 ± 5.6^{***c}	364.1 ± 9.9^{**c}	373.3 ± 9.9^{***c}	366.8 ± 7.5$^{***c/ns}$	383.6 ± 11.2^{***c}	379.7 ± 2.1$^{***c/ns}$
	12	320.9 ± 3.1^{c}	452.6 ± 0.9***	332.0 ± 8.3^{c}	326.6 ± 2.1^{c}	341.8 ± 0.3^{c}	331.5 ± 3.8$^{c/\alpha}$	354.3 ± 7.7^{*c}	302.9 ± 14.6$^{c/\beta}$
	14	309.6 ± 2.3^{c}	485.7 ± 5.8***	312.8 ± 6.1^{c}	303.5 ± 9.0^{c}	318.4 ± 1.6^{c}	296.2 ± 3.7$^{c/\gamma}$	287.5 ± 0.4^{c}	279.2 ± 1.1$^{c/\gamma}$

Effect of *C. odorata* and coumarin administration on heart rate (HR) in HRCHFC-diet induced CMS rats. Values are expressed as mean ± SEM ($n = 6$), where $^{***}p < 0.001$, $^{**}p < 0.01$, $^{*}p < 0.05$ vs. normal control and $^{c}p < 0.001$, $^{b}p < 0.01$, and $^{a}p < 0.05$ vs. CMS control group using two-way ANOVA followed by Bonferroni *post hoc* test. ns = non-significant, $^{\gamma}p < 0.001$, $^{\beta}p < 0.01$, $^{\alpha}p < 0.05$ shows effect of low vs. high dose of *C. odorata* and coumarin in treatment period (Student's t-test).

Discussion

Due to a high mortality and morbidity rate, CMS presents a serious global health risk, thus demanding effective therapeutic alternatives (Agrawal et al., 2018). The results of the present study clearly demonstrated that *C. odorata* and coumarin improved the characteristic features of CMS by attenuating obesity, dyslipidemia, oxidative stress, insulin resistance, glucose intolerance, and hypertension in HRCHFC-fed rats. A chronic administration of a HRCHFC diet with additional cholic acid induces oxidative stress, and hemodynamic and metabolic alteration (Prasatthong et al., 2021) that mitigate the cellular metabolism of dietary ingredients, resulting in the development of obesity and related comorbidities such as hyperglycemia, glucose intolerance, dyslipidemia, arterial hypertension, insulin resistance, systemic inflammation, and hepatic steatosis (Senaphan et al., 2015).

The traditional use of *C. odorata* in the treatment of diabetes and its α-glucosidase-inhibitory activity (Abbasi M. et al., 2014) provide a sound basis to its potential use as an anti-diabetic. Furthermore, *C. odorata* has high amount of coumarin as phenolic content (Joshi et al., 2019). Thus, the beneficial effects of *C. odorata* and coumarin are attributed to its increased antioxidant activity and attenuation of excessive adipocytokine production, including TNF-α, IL-6, leptin, chemerin, and adiponectin with the regulation of body weight and feed intake. A notable improvement in hepatic steatosis and dyslipidemia is strongly related to the modulation of HMG-CoA reductase and inflammatory cytokines. *C. odorata* and coumarin reversed HRCHFC- diet induced hypertension, possibly through a NO mediated pathway.

Phytochemical analysis and the oxidative potential of plant extract were examined by HPLC, TFC, TPC, and radical scavenging activities (DPPH, H_2O_2, reducing power). The conventional FTIR spectrum of *C. odorata* showed a narrow peak at 3,245.75 cm^{-1} (O–H and N–H), while a peak at 2,938.41 cm^{-1} identifies a C–H stretch. Sharp peaks at 2,366.59, 2059.31 cm^{-1} (C≡N, C≡C) indicate the presence of a CH_2 group. The peaks present at 1,607.74, 1,521.24 cm^{-1} (C=O), 1,442.22 cm^{-1} (aromatic ring), 1,358.66 (C–H), and 1,245.68 (O–H) indicate that *C. odorata* contains flavonoids, alkaloids, and phenolics. Interval peaks at 1,014.86 and 926.32 cm^{-1} show a C–O–C group of saponins. The HPLC analysis revealed a quantitative amount of a variety of polyphenols, mainly phenolic acids, flavonoids, and their derivatives in aqueous methanolic extract of *C. odorata*: quercetin, catechin, gallic acid, caffeic acid, ferulic acid, chologenic acid, syringic acid, p-coumaric acid, sinapic acid, and a higher expression of coumarins. Many of these polyphenols are reported to have an ameliorating effect on obesity and other features of metabolic syndrome, including glucose intolerance, dyslipidemia, hypertension, and oxidative stress (Prince et al., 2021). Thus, the results obtained from this study that indicate the ability of *C. odorata* to inhibit obesity and associated metabolic alterations are attributed in part to the presence of these polyphenolic compounds—amongst these, coumarin contributes prominently to the overall effectiveness of *C. odorata* in CMS.

After the eighth week of induction with the HRCHFC diet, significant weight gain and food consumption were observed due to the addition of added vegetable oil (fat), fish meal (protein), and refined carbohydrate. This may intricate hyperplasia and hypertrophy of adipocytes (BrahmaNaidu et al., 2014).

As a result of high caloric diet intake, the energy metabolism is compromised in the liver (Gutierrez-Salmean et al., 2014). Low energy levels stimulate the hunger center, increasing food intake and resulting in the development of CMS in animals. This suggests that low hepatic energy influences feeding behavior and ultimately causes an increase in body weight (Zhang et al., 2021). This study's results clearly showed that weight gain is consistent with feed intake. The administration of *C. odorata* and coumarin significantly and in a dose-dependent manner reduced weight gain and feed intake during the experimental period. Treated groups probably increased energy consumption and enhanced fat oxidation, thus causing weight loss

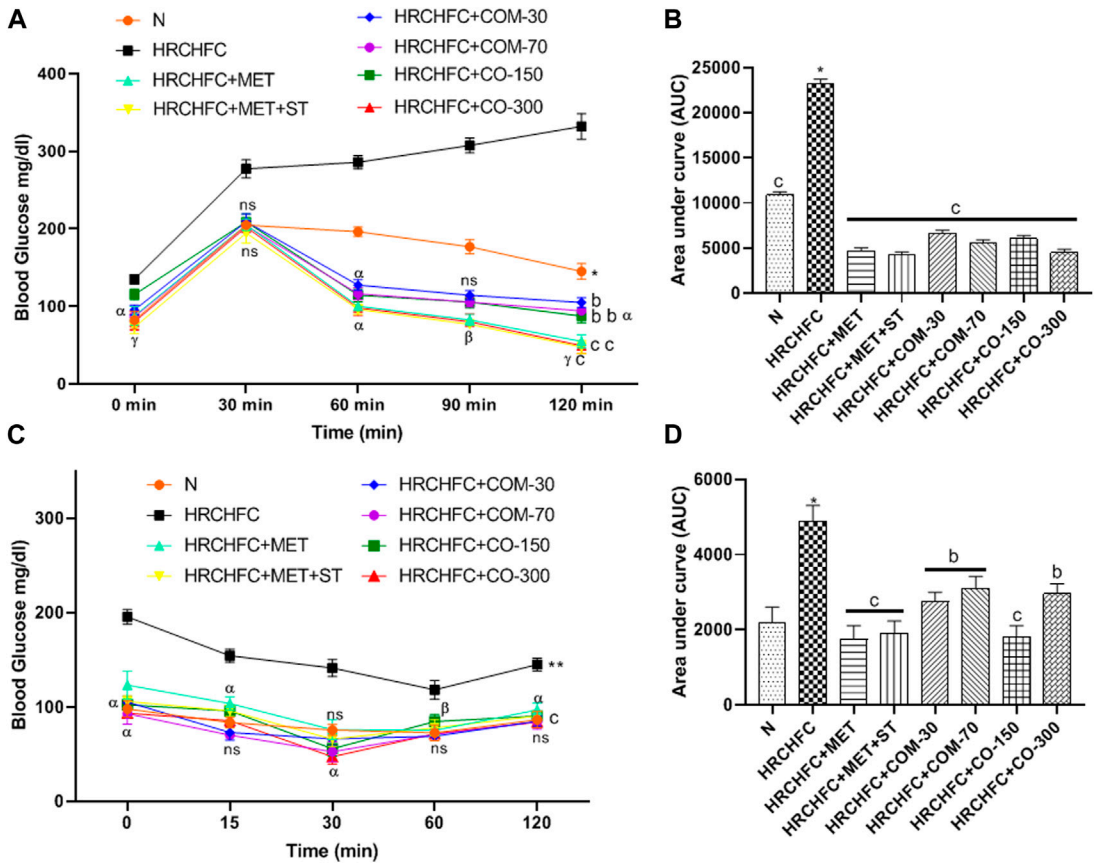

FIGURE 5
Effect of *C. odorata* and coumarin administration on **(A)** oral glucose tolerance test during 14th week of study, **(B)** AUC of blood glucose level of animals measured at end of treatment, **(C)** insulin tolerance test, and **(D)** AUC of blood glucose level of animals measured after insulin injection in HRCHFC diet induced CMS rats. N: normal control; HRCHFC: high refined carbohydrate-high fat-cholesterol loaded diet induced CMS control; HRCHFC + MET: (metformin 300 mg/kg); HRCHFC + MET + ST: (metformin and rosuvastatin 200 mg/kg +1.5 mg/kg); HRCHFC + COM-30: (coumarin 30 mg/kg); HRCHFC + COM-70: (coumarin 70 mg/kg); HRCHFC + CO-150: (*C. odorata* 150 mg/kg); HRCHFC + CO-300: (*C. odorata* 300 mg/kg). Values are expressed as mean ± SEM ($n = 6$), where ***$p < 0.001$, **$p < 0.01$, *$p < 0.05$ shows normal control vs. CMS control group (Student's t-test); $^{c}p < 0.001$, $^{b}p < 0.01$ and $^{a}p < 0.05$ show a comparison of treatment vs. CMS control group using one-way ANOVA followed by Dennett's test. ns = non-significant, $^{\gamma}p < 0.001$, $^{\beta}p < 0.01$, $^{\alpha}p < 0.05$ shows effect of low vs. high dose of *C. odorata* and coumarin (Student's t-test).

in HRCHFC-fed rats (Mabrouki et al., 2020). Organ weight increase, particularly of the liver and heart, in diseased animals might be due to inflammation, hypertrophy, and steatosis (Nwakiban-Atchan et al., 2022), while a marked decrease was observed in treated groups. These findings indicate the anti-obesity effect of *C. odorata* and coumarin. This was also confirmed by morphological examination of the adipocyte of fat pads, where a significant increase in the size and number of adipocytes were reversed to normal in the treatment groups.

It is known that metabolic complications related to obesity are prevented by inhibiting elevated adipokine levels. HRCHFC diet-induced obesity and related diseases like diabetes, insulin resistance, and increased fat mass are associated with the dysregulation of adipocytokines. These are secreted from adipocyte, in which adiponectin has anti-diabetic, anti-atherogenic, and anti-inflammatory properties (Sasso et al., 2019). Leptin is appetite regulator hormone which plays a major role in balanced feed intake and body weight control. Leptin secretion is positively correlated with the degree of triglycerides stored in adipose tissues (BrahmaNaidu et al., 2014). Elevated chemerin levels show the interlinking of metabolic syndrome and obesity by producing pathophysiological complications such as increased fat, glucose, lipid metabolism, inflammation, and elevated blood pressure that lead to hyperlipidemia and insulin resistance. Chemerin also stimulates insulin-mediated glucose uptake and improves insulin action in 3T3-L1 adipocyte to treat obesity and insulin resistance (Takahashi et al., 2008). The present study highlights *C. odorata* and coumarin treated rats as presenting high levels of adiponectin and reduced levels of leptin and chemerin. Reduced leptin may be due to decreased body fat mass and increased leptin sensitivity (BrahmaNaidu et al., 2014). These observations indicate that the regulation of adipokines in treated groups may be due to reduced lipid buildup in adipocytes, which is also consistent with the findings on the lipid profile in treated rats.

Insulin resistance is considered a hallmark for metabolic syndrome and diabetes (Senaphan et al., 2015). It causes elevated adipokine secretion, which develops hyperglycemia or glucose intolerance for metabolic adaptation. A HRCHFC diet produces

TABLE 6 Effect of *C. odorata* and coumarin administration on biochemical markers in HRCHFC-diet induced CMS rats.

Groups	Triglycerides (mg/dl)	HDL (mg/dl)	Cholesterol (mg/dl)	ALT (U/L)	AST (U/L)	Creatinine (mg/dl)	Urea (mg/dl)
N	81.4 ± 1.2^{c}	61.4 ± 1.7^{c}	70.0 ± 1.2^{c}	30.6 ± 1.3^{c}	68.6 ± 5.7^{b}	0.6 ± 0.0^{c}	32.6 ± 1.8^{c}
HRCHFC	205.0 ± 3.4***	32.8 ± 3.4***	262.6 ± 3.0***	96.1 ± 3.4***	106.2 ± 9.7**	1.8 ± 0.3***	74.7 ± 6.7***
HRCHFC + MET	97.7 ± 6.7^{*c}	68.2 ± 1.7^{c}	78.3 ± 1.7^{c}	45.7 ± 6.2^{c}	88.7 ± 0.7	0.7 ± 0.0^{c}	30.3 ± 0.7^{c}
HRCHFC + MET + ST	90.6 ± 0.5^{c}	71.3 ± 4.0^{c}	69.2 ± 2.0^{c}	35.7 ± 7.1^{c}	71.7 ± 2.9^{b}	0.5 ± 0.0^{c}	18.4 ± 0.5^{*c}
HRCHFC + COM-30	85.7 ± 1.9^{c}	55.5 ± 3.2^{b}	98.1 ± 1.7^{***c}	36.0 ± 4.1^{c}	75.7 ± 6.2^{b}	0.8 ± 0.0^{c}	34.2 ± 0.3^{c}
HRCHFC + COM-70	67.8 ± 4.1$^{c/\beta}$	68.7 ± 1.9$^{c/\beta}$	76.3 ± 3.5$^{c/\gamma}$	33.0 ± 1.2$^{c/ns}$	60.5 ± 2.6$^{c/\alpha}$	0.6 ± 0.0$^{c/\gamma}$	25.4 ± 0.7$^{c/\gamma}$
HRCHFC + CO-150	95.0 ± 1.4^{c}	45.6 ± 3.5*	71.7 ± 1.5^{c}	32.7 ± 1.8^{c}	54.5 ± 3.6^{c}	0.9 ± 0.0^{c}	34.8 ± 2.4^{c}
HRCHFC + CO-300	85.1 ± 2.1$^{c/\beta}$	63.4 ± 2.4$^{c/\beta}$	59.7 ± 3.4$^{c/\beta}$	23.8 ± 0.8$^{c/\beta}$	37.7 ± 5.6$^{**c/\alpha}$	0.7 ± 0.0$^{c/\beta}$	33.4 ± 0.8$^{c/ns}$

Effect of *C. odorata* and coumarin administration on biochemical markers in HRCHFC-diet induced CMS rats. Values are expressed as mean ± SEM ($n = 6$), where ***$p < 0.001$, **$p < 0.01$, *$p < 0.05$ vs. normal control and $^{c}p < 0.001$, $^{b}p < 0.01$, and $^{a}p < 0.05$ vs. CMS control group using one-way ANOVA followed by Dunnett's test. ns = non-significant, $^{\gamma}p < 0.001$, $^{\beta}p < 0.01$, $^{\alpha}p < 0.05$ shows effect of low vs. high dose of *C. odorata* and coumarin (Student's t-test).

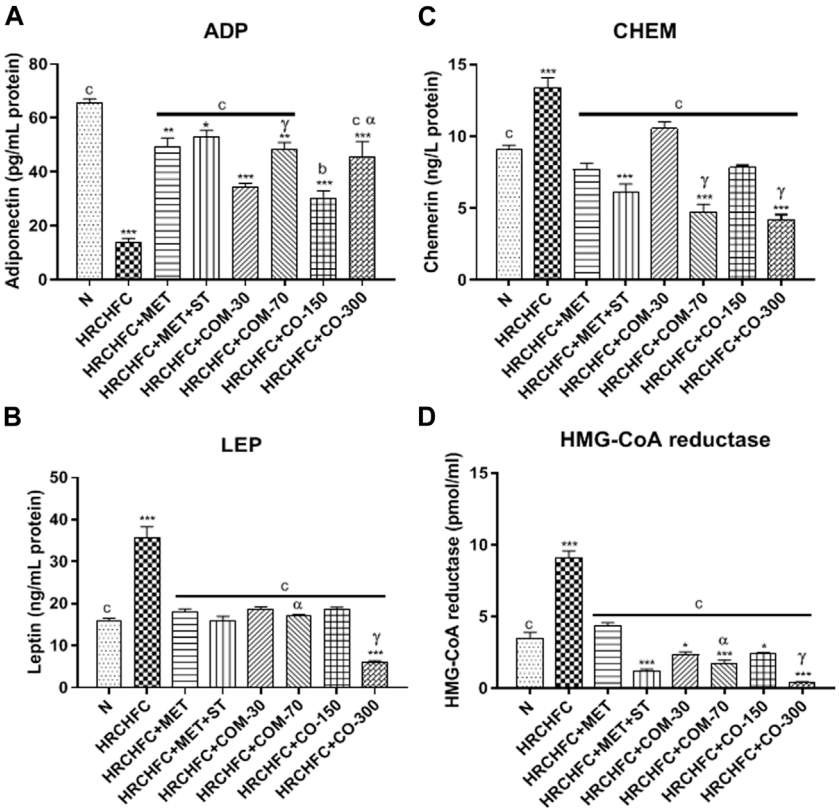

FIGURE 6
Effect of *C. odorata* and coumarin administration on serum **(A)** ADP, **(B)** LEP, **(C)** CHEM, **(D)** HMG-CoA reductase in HRCHFC-diet induced CMS rats. N: normal control; HRCHFC: high refined carbohydrate-high fat-cholesterol loaded diet induced CMS control; HRCHFC + MET: (metformin 300 mg/kg); HRCHFC + MET + ST: (metformin and rosuvastatin 200 mg/kg +1.5 mg/kg); HRCHFC + COM-30: (coumarin 30 mg/kg); HRCHFC + COM-70: (coumarin 70 mg/kg); HRCHFC + CO-150: (*C. odorata* 150 mg/kg); HRCHFC + CO-300: (*C. odorata* 300 mg/kg). Values are expressed as mean ± SEM ($n = 6$), where ***$p < 0.001$, **$p < 0.01$, *$p < 0.05$ vs. normal control, and $^{c}p < 0.001$, $^{b}p < 0.01$ and $^{a}p < 0.05$ vs. CMS control group using one-way ANOVA followed by Dunnett's test. ns = non-significant, $^{\gamma}p < 0.001$, $^{\beta}p < 0.01$, $^{\alpha}p < 0.05$ shows effect of low vs. high dose of *C. odorata* and coumarin (Student's t-test).

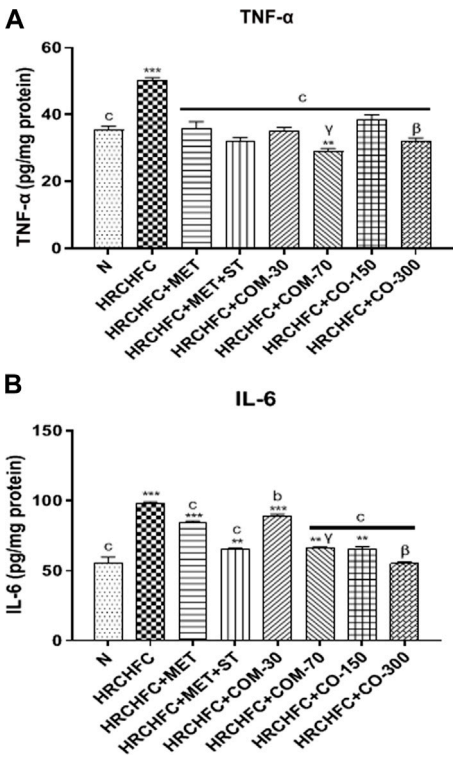

FIGURE 7
Effect of *C. odorata* and coumarin administration on serum **(A)** TNF-α, **(B)** IL-6 in HRCHFC diet induced CMS rats. Values are expressed as mean ± SEM ($n = 6$), where ***$p < 0.001$, **$p < 0.01$, *$p < 0.05$ vs. normal control and $^{c}p < 0.001$, $^{b}p < 0.01$ and $^{a}p < 0.05$ vs. CMS control group using one-way ANOVA followed by Dunnett's test. ns = non-significant, $^{\gamma}p < 0.001$, $^{\beta}p < 0.01$, $^{\alpha}p < 0.05$ shows effect of low vs. high dose of *C. odorata* and coumarin (Student's t-test).

hepatic insulin resistance, possibly by elevating the circulation of free fatty acid (FFA) levels (Prince et al., 2021). Elevated FFA in HRCHFC-fed rats leads to increased serum glucose levels that manifest obesity-induced glucose intolerance and inhibit muscle glucose uptake (Lasker et al., 2019). Excessive FFA levels also damage the pancreas to produce insulin to combat hyperglycemia (BrahmaNaidu et al., 2014). *C. odorata* and coumarin alleviate hyperglycemia by reducing FBG levels to prevent insulin resistance. The observed effects might be achieved due to the presence of a diverse nature of phytoconstituents in the plant. This effect is in line with previously reported *in vitro* α-glucosidase activity of *C. odorata* (Abbasi M. et al., 2014), which also supports the anti-diabetic action of *C. odorata*. *C. odorata* and coumarin administration caused an improvement in HRCHFC diet-induced impaired glucose tolerance in a dose-dependent manner, evident by its positive impact in the oral glucose tolerance test and assessed FBG levels. Treatment groups markedly reduced their blood glucose levels following by insulin administration, thus showing an improvement in insulin sensitivity. This effect possibly occurs due to improvement in one or more defects *viz.* insulin receptors, insulin receptor substrate, glucose transporters, or glycosylated enzymes. The liberation of inflammatory cytokines is also a strong inducer of insulin resistance (Senaphan et al., 2015). Improved insulin resistance was also shown in the pancreatic tissue of *C. odorata* and coumarin treated rats, where damaged islets of Langerhans, atrophic β-cell, reduced β-cell mass, and congested intra-lobular duct were revived to normalcy.

Atherogenic dyslipidemia is an intricate disorder related to obesity, diabetes, and metabolic syndrome that enhances the progression of CVD risk (Prince et al., 2021). HRCHFC diet-induced hypertriglyceridemia causes endothelial dysfunction, atherosclerosis, and increased oxidative stress which can be prevented by antioxidants by altering the lipid metabolism (Aziz et al., 2013). In our study, a HRCHFC diet with cholesterol and cholic acid increased TG and TC levels while decreasing HDL-C levels, possibly by increasing FFA in the liver due to insulin deficiency and/or resistance. Hence, more TGs are absorbed into adipose tissues (Nwakiban-Atchan et al., 2022). The reduced liberation of FFA results in elevated levels of VLDL (Ojetola et al., 2021). These changes were endorsed by the observed decreased HMG-CoA reductase activity (Nepal et al., 2011) and TG uptake by peripheral tissues (Sharma et al., 2012). However, reduced HDL-C levels are due to activated lipoprotein lipase and lecithin cholesterol-acyl transferase (LCAT) with reduced cholesterol catabolism (BrahmaNaidu et al., 2014). Treatment with *C. odorata* and coumarin noticeably improved the lipid profile by causing a decrease in HMG-CoA reductase activity, and TG and TC levels, while increasing HDL-C levels—possibly by inhibiting lipid synthesis—and reducing cholesterol absorption and secretion from the intestine. HMGR (3-hydroxy-3-methylglutaryl-coenzyme A reductase) limits the endogenous enzyme for cholesterol synthesis and is also used to catalyze HMG-CoA reductase conversion to mevalonate (BrahmaNaidu et al., 2014). HMG-CoA reductase inhibitors (lipid-lowering agents) are used as first line agents in treating hyperlipidemia (Javaid et al., 2021). Our study also showed increased HMGR levels in HRCHFC-fed rats, which is an established fact of obesity related to CMS (Kalaivani et al., 2019). Most therapeutic agents that decrease TC levels may also potentially block HMGR enzymes (Istvan, 2002). These findings suggest that *C. odorata* and coumarin possess anti-dyslipidemic effects.

The elevated hepatic enzymes released in HRCHFC-fed rats may be due to the modified plasma membrane permeability of hepatocytes and biliary obstruction, thus increasing the risk of developing non-alcoholic fatty liver disease (NASH) (Suman et al., 2016). Hepatocyte damage followed by oxidative damage leads to liver injury. Furthermore, higher oxidative stress, dysregulated adipocytokine production, and mitochondrial dysfunction are causative factors of NASH (Sharma et al., 2012). Administration of *C. odorata* and coumarin to rats caused a remarkable dose-dependent reduction in serum ALT and AST levels to relieve hepatic steatosis through protecting hepatic dysfunction. Increased urea and creatinine levels in CMS-developed animals were found to be strongly associated with renal damage (Bamanikar et al., 2016). Treatment with *C. odorata* and coumarin offered a significant attenuation in serum urea and creatinine levels to prevent nephropathy. Damaged renal tissues in HRCHFC-fed rats were produced by ROS production (El-Alfy et al., 2005). Intake of *C. odorata* and coumarin in CMS animals restored renal architecture in HRCHFC-fed rats, possibly by neutralizing free radicals in these tissues. Our results are in accordance with previously published data (Bhatti et al., 2022). The observed findings might be attributed to the presence of abundant phytochemicals in *C. odorata*, their antioxidant potential, and anti-inflammatory properties.

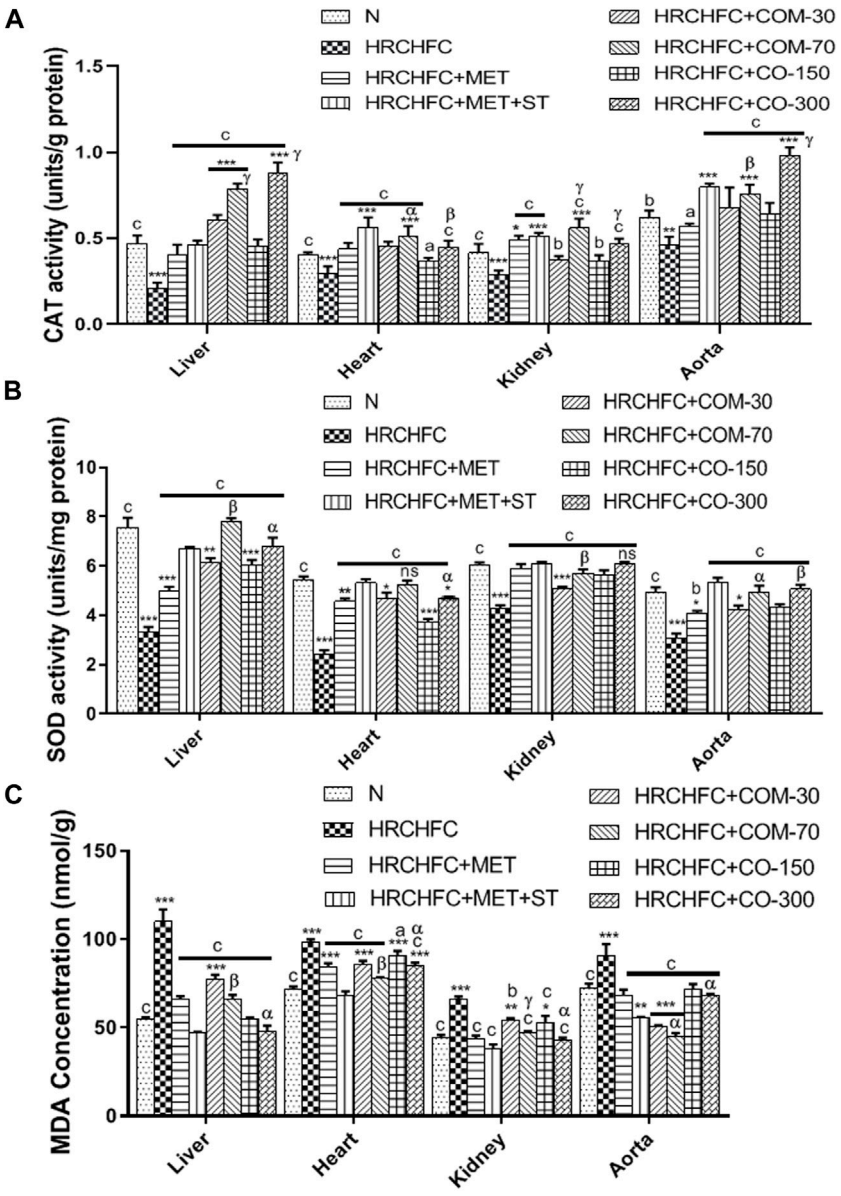

FIGURE 8
Effect of *C. odorata* and coumarin administration on **(A)** CAT, **(B)** SOD, and **(C)** MDA enzyme in various organs of HRCHFC- diet induced CMS rats. Values are expressed as mean ± SEM ($n = 6$), where ***$p < 0.001$, **$p < 0.01$, *$p < 0.05$ vs. normal control and $^{c}p < 0.001$, $^{b}p < 0.01$ and $^{a}p < 0.05$ vs. CMS control group using one-way ANOVA followed by Dunnett's test. ns = non-significant, $^{\gamma}p < 0.001$, $^{\beta}p < 0.01$, $^{\alpha}p < 0.05$ shows effect of low vs. high dose of *C. odorata* and coumarin (Student's t-test).

Manifested features of hepatic steatosis were found to be reduced in hepatic tissues of treated groups, which was evident in revived hepatocyte texture, reduced vacuolization, and congestion in the central vein as well as minimized fat deposition. Similarly, the kidney tissues of treated groups also revived congested glomerular blood vessels, necrotic tubules, inflammation, and cloudy deteriorative parts to a more normal architecture.

The administration of HRCHFC diet for 8 weeks initiated the development of obesity and low-grade chronic inflammation mediated by the liberation of pro-inflammatory cytokines like IL-6 and TNF-α (Sasso et al., 2019). The literature also showed that elevated inflammatory biomarkers and free radicals cause insulin resistance commonly associated with endothelial dysfunction, dyslipidemia, and hyperglycemia (Senaphan et al., 2015). Elevated FFAs in HRCHFC-fed rats directly activate the macrophages to secret pro-inflammatory cytokines (TNF-α primarily stimulate others) that render insulin resistant in peripheral tissues (Jung et al., 2011). This study showed that treatment with *C. odorata* and coumarin exhibited a significant dose-dependent decrease in serum TNF-α and IL-6 levels. Thus, increased antioxidant enzyme activity and the suppression of inflammatory markers show potential in treating hypertension, insulin resistance, diabetes, obesity, and hepatic steatosis.

C. odorata and coumarin-treated groups displayed significantly elevated catalase and superoxide dismutase enzyme

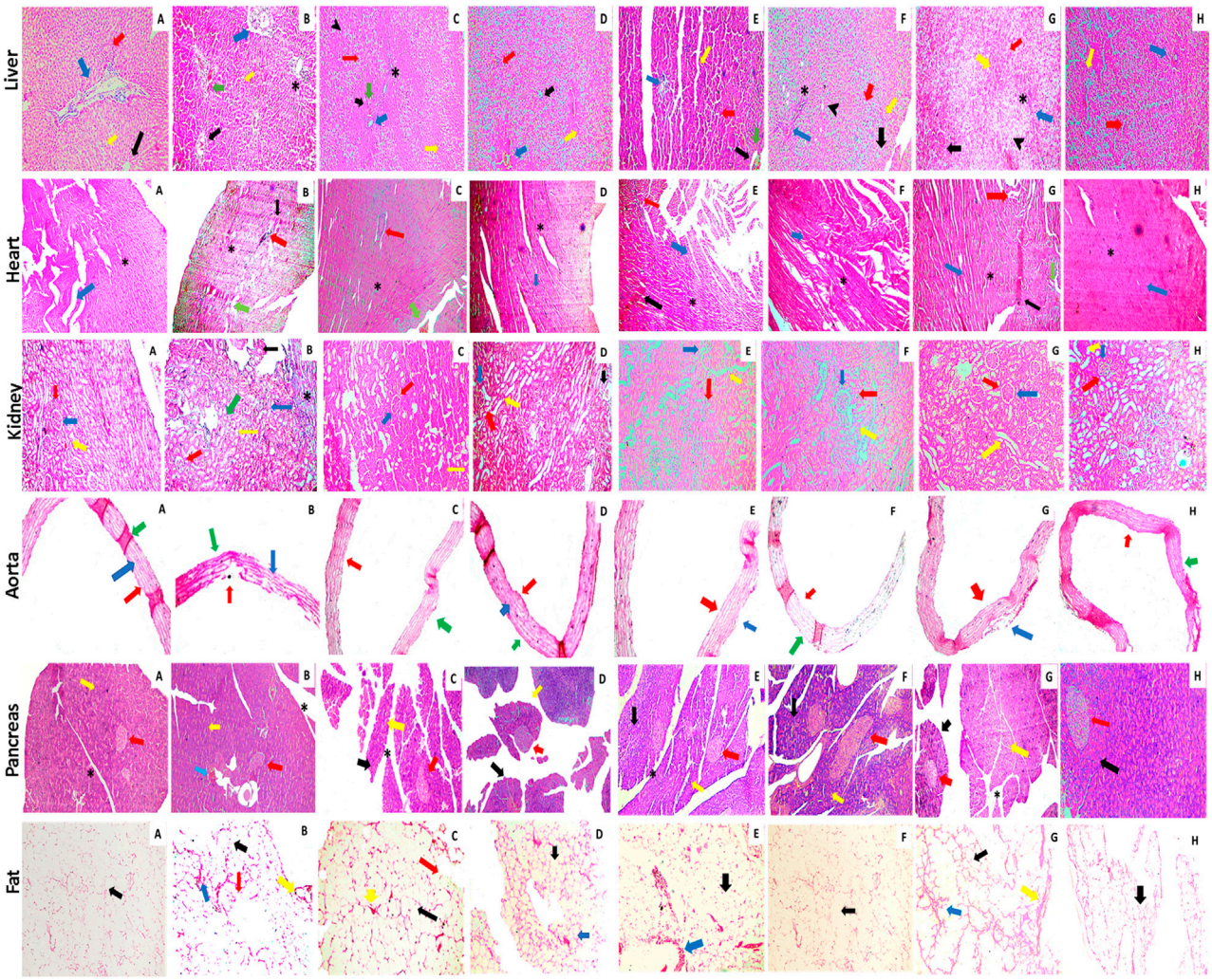

FIGURE 9
Photomicrographic illustration of liver, heart, kidney, aorta, and fat tissue sections stained with H&E dye showing effect of administration of *C. odorata*: aqueous methanolic extract of *C. odorata* (150 and 300 mg/kg) and coumarin: (30 and 70 mg/kg) in HRCHFC diet-induced CMS and normal rats. Liver: black, yellow, green, red, blue arrows, stearic, and arrow head, respectively, show central vein, sinusoids, necrosis, hepatocyte, branch of portal triad, cell infiltration, and fat collection. Heart: black, green, red, blue arrows, and stearic, respectively, show inflammation, necrosis, cell infiltration, myofibrils, and cardiomyocytes myofibrils. Kidney: red, blue, yellow, black arrows, and stearic, respectively, show Bowman's capsule, glomerulus, distal convoluted tubules, shrinkage of cortex, and cell infiltration. Pancreas: yellow, black, blue, red arrows, and stearic, respectively, show exocrine pancreas, pancreatic acinar cells, cell infiltration, islets of Langerhans, and intra lobular duct. Aorta: red, blue, and green arrows show tunica adventitia, media, and intima layers of blood vessel, respectively. Fat: yellow, green, red, and blue arrows, respectively, show collagen fiber, adipose cell, fat deposit, and inflammation.

levels compared to HRCHFC-fed rats. SOD and CAT are considered first-line defense anti-oxidant enzymes against ROS (Nepal et al., 2011). The upregulation of CAT levels prevents atherosclerosis and blocks angiotensin-II mediated aortic wall hypertrophy. Elevated SOD levels prevent the inactivation of NO and protect the liver from oxidative damage by scavenging molecular oxygen (Sharma et al., 2012). Thus, the reduction offered in CAT and SOD levels might demonstrate the cardio and hepatoprotective effects of *C. odorata* and coumarin. A HRCHFC diet administered to animals causes oxidative stress which is either enzymatically or non-enzymatically reflected as higher level of TBARS or reduced levels of SOD, CAT, GPx, GSTs, and GSH (Aziz et al., 2013). Earlier studies reported that increased oxidative stress in HRCHFC-fed rats is usually an outcome of inflammation, insulin resistance, hypertension, dysregulated adipocytokines, and NASH (Kabelova et al., 2021). Oxidative stress develops with increased ROS and reduced antioxidant enzymes, resulting in excessive molecular oxygen and hydrogen peroxide that lead to initiate lipid peroxidation (Sharma et al., 2012). *C. odorata* and coumarin administration attenuated lipid peroxidation levels, which was evident by reduced MDA levels in treated rats, and thus offers protection against hypertension. Theses finding on *C. odorata* and coumarin may highlight their therapeutic potential in treating CMS.

Hypertension is a characteristic feature of metabolic syndrome related to obesity (Suman et al., 2016). HRCHFC-fed rats show multiple

underlying mechanism(s) that mediate hypertension, including endothelium dysfunction, oxidative degradation of NO, and diminished eNOS activity (Ghibu et al., 2019). Previous studies have reported that decreased NO production in vascular endothelium accounts for impaired vascular function that can result in vascular diseases including hypertension. Endothelial cells also form active oxygen radicals in response to hyperlipidemia and inflammation, which causes destruction of NO and vasoconstriction. A growing body of evidence suggests that HRCHFC diet leads to increased levels of LDL-c and oxidative stress, which was also observed in our study. This increases the levels of oxidized LDL which has a suppressive action on endothelial NO synthase. ROS also increases cytosolic Ca^{2+} in smooth muscle as well as sensitizing the muscle contractile apparatus in vascular smooth muscle, further augmenting vasoconstriction (Roberts et al., 2000). Elevated ROS, mainly superoxide anions, can strongly inactivate NO, leading to the development of vascular damage (Sharma et al., 2012). Moreover, superoxide anions fuses to NO and tyrosine to make peroxynitrite and nitrotyrosine, respectively, which ultimately attack proteins, lipids, and DNA to cause cellular damage. It has also been reported that hyperlipidemia, insulin resistance, and inflammatory contributors in CMS have repressive effects on eNOS. These increase the wall thickness of conduit vessels, leading to deceased NO synthesis for the development of hypertension (Ojetola et al., 2021). Vasomotor tone modulation and vascular remodeling can also be managed by rendering oxidative stress biomarkers, which are known to mediate cardiovascular complications (Senaphan et al., 2015). Several studies have shown that the intake of natural agents enriched with antioxidants has proven beneficial effects against oxidative stress-augmented pathophysiological anomalies. (Nepal et al., 2011). In our study, the observed anti-hypertensive effect on the part of *C. odorata* and coumarin by reducing systolic blood pressure (SBP), diastolic blood pressure (DBP), mean blood pressure (MBP), and heart rate (HR) might be associated with its anti-oxidant, antihyperlipidemic, and/or anti-inflammatory activities.

Furthermore, treated rats showed a marked improvement in the morphological features of aortic and cardiac tissues by exhibiting restored myocardial fiber texture, reduced inflamed necrotic areas, and a repaired tunica media layer with less fat deposition, indicating the cardiovascular beneficial potential of the test materials.

Many studies have shown that the phytoconstituents of *C. odorata* account for its multiple therapeutic properties (Shahzadi et al., 2012; Abbasi M. et al., 2014; Abbasi M. A. et al., 2014; Abbasi et al., 2017; Joshi et al., 2019). Flavonoids and phenolic compounds have much biological potential due to their antioxidant and free radical scavenging properties (Prince et al., 2021). Furthermore, it is unclear which constituent is exactly responsible for attenuating the characteristic features of CMS. Hence, further investigation is needed to determine the biologically active constituent responsible for the actions of *C. odorata* against CMS.

Conclusion

C. odorata and coumarin improved obesity and dyslipidemia through the modulation of adipocytokines (leptin, adiponectin, chemerin), inhibition of HMG-CoA reductase, and attenuation of the lipid profile. Treatment with *C. odorata* and coumarin offered an anti-hypertensive effect and caused modulation in insulin resistance, possibly through its effect on amended oxidative stress biomarkers (SOD, CAT, and MDA), inflammatory mediators (TNF-α and IL-6) and improved insulin sensitivity. Its protective effect for hepatic steatosis was evident by its positive influence on hepatic function markers (LFTs). Thus, this study highlights the therapeutic potential of *C. odorata* and coumarin for treating cardiometabolic syndrome.

Data availability statement

The original contributions presented in the study are included in the article/Supplementary Material; further inquiries can be directed to the corresponding author.

Ethics statement

The animal study design was reviewed and approved by the Ethical Review committee of GCU Faisalabad [IRB:879 (Ref. No. GCUF/ ERC/2279]. Laboratory animals were used in this study as per approved protocol.

Author contributions

MHM proposed the idea and design layout of the research. He supervised this project entirely and was also involved in guidance, data acquisition and analysis, and writing, reviewing and submission of the manuscript. MGA played a role in concept design of the study, experimental performance, data acquisition and analysis, and manuscript writing. SM was involved in data analysis and manuscript writing. MF was involved in data collection and interpretation.

Funding

We acknowledge the Higher Education Commission (HEC) of Pakistan for partial financial support for publication under the NRPU project (Project# 20-9195/NRPU/R&D/HEC/2017-2018) awarded to PI, MHM, supervisor of PhD scholar MGA, HEC-PhD Indigenous Scholar [pin no: 518-77854-2MD5-014 (50043678)].

Acknowledgments

We are very obliged to HEC, Pakistan, for providing partial financial support to complete this research with the help of the indigenous fellowship program and the NRPU project. We are also grateful for the assistance of the helpers in the animal house and faculty members in the labs of the Department of Pharmacology, Faculty of Pharmaceutical Sciences, GCUF.

Conflict of interest

The authors declare that the research was conducted in the absence of any commercial or financial relationships that could be construed as a potential conflict of interest.

Publisher's note

References

Abbasi, M. A., Hussain, G., Siddiqui, S. Z., Ahmed, V. U., and Ahmad, V. U. (2017). In silico study of furocoumarins from Caryopteris odorata: Moderate inhibitors of butyryl cholinesterase and lipoxygenase. *Asian J. Chem.* 29 (4), 758–762. doi:10.14233/ajchem.2017.20241

Abbasi, M. A., Shahzadi, T., and Ahmad, V. U. (2014b). New iridoid glucosides from Caryopteris odorata with suitable antioxidant potential. *Chem. Nat. Compd.* 50 (5), 836–841. doi:10.1007/s10600-014-1095-5

Abbasi, M., Aziz-ur-RehmanAhmad, V., Riaz, T., and Khlaid, F. (2014a). Evaluation of antibacterial, antifungal, enzyme inhibition and hemolytic activities of Caryopteris odorata fractions. *Int. Res. J. Pharm.* 4, 9–15. doi:10.7897/2230-8407.041203

Abdelhafez, O. M., Amin, K. M., Batran, R. Z., Maher, T. J., Nada, S. A., and Sethumadhavan, S. (2010). Synthesis, anticoagulant and pivka-ii induced by new 4-hydroxycoumarin derivatives. *Bioorg. Amp; Med. Chem.* 18 (10), 3371–3378. doi:10.1016/j.bmc.2010.04.009

Adedapo, A. D. A., Ajayi, A. M., Ekwunife, N. L., Falayi, O. O., Oyagbemi, A., Omobowale, T. O., et al. (2020). Antihypertensive effect of phragmanthera incana (schum) balle on NG-nitro-L-arginine methyl ester (L-NAME) induced hypertensive rats. *J. Ethanopharmacology* 257, 112888. doi:10.1016/j.jep.2020.112888

Agrawal, R., Nath, V., Kumar, H., and Kumar, V. (2018). Deciphering activation in cardiometabolic syndrome: Studies by *in silico* and *in vivo* experimental assessment. *J. Recept. Signal Transduct.* 38 (2), 122–132. doi:10.1080/10799893.2018.1436560

Aziz, N., Mehmood, M. H., and Gilani, A.-H. (2013). Studies on two polyherbal formulations (ZPTO and ZTO) for comparison of their antidyslipidemic, antihypertensive and endothelial modulating activities. *BMC Complementary Altern. Med.* 13 (1), 371–379. doi:10.1186/1472-6882-13-371

Bamanikar, S., Bamanikar, A., and Arora, A. (2016). Study of Serum urea and Creatinine in Diabetic and non-diabetic patients in in a tertiary teaching hospital. *J. Med. Res.* 2 (1), 12–15. doi:10.31254/jmr.2016.2104

Basile, A., Sorbo, S., Spadaro, V., Bruno, M., Maggio, A., Faraone, N., et al. (2009). Antimicrobial and antioxidant activities of coumarins from the roots of ferulago campestris (apiaceae). *Molecules* 14 (3), 939–952. doi:10.3390/molecules14030939

Bhattarai, S. B. S., and Tamang, R. T. R. (2017). Medicinal and aromatic plants: A synopsis of makawanpur district, Central Nepal. *Int. J. Indig. Herbs Drugs*, 6–15.

Bhatti, J. S., Sehrawat, A., Mishra, J., Sidhu, I. S., Navik, U., Khullar, N., et al. (2022). Oxidative stress in the pathophysiology of type 2 diabetes and related complications: Current therapeutics strategies and future perspectives. *Free Radic. Biol. Med.* 184, 114–134. doi:10.1016/j.freeradbiomed.2022.03.019

BrahmaNaidu, P., Nemani, H., Meriga, B., Mehar, S. K., Potana, S., and Ramgopalrao, S. (2014). Mitigating efficacy of piperine in the physiological derangements of high fat diet induced obesity in sprague dawley rats. *Chemico-biological Interact.* 221, 42–51. doi:10.1016/j.cbi.2014.07.008

Bruneton, J. (1999). *Immunotoxicity of epicutaneously applied anti-coagulant rodenticide warfarin*. Hampshire, UK: Intercept Ltd., 245–263.

Cao, Z., Wang, Z., Shang, Z., and Zhao, J. (2017). Classification and identification of rhodobryum roseum limpr. And its adulterants based on fourier-transform infrared spectroscopy (FTIR) and chemometrics. *PLoS One* 12 (2), e0172359. doi:10.1371/journal.pone.0172359

Caunii, A., Pribac, G., Grozea, I., Gaitin, D., and Samfira, I. (2012). Design of optimal solvent for extraction of bio–active ingredients from six varieties of medicago sativa. *Chem. Central J.* 6 (1), 123–128. doi:10.1186/1752-153X-6-123

CeleghinI, R., Yariwake, J., and Lancas, F. (2001). Extraction and quantitative HPLC analysis of coumarin in hydroalcoholic extracts of mikania glomerata spreng: ("guaco") leaves. *J. Braz. Chem. Soc.* 12, 706–709. doi:10.1590/s0103-50532001000600003

De-Oliveira, A. M., De-Freitas, A. F. S., Costa, M. D. D. S., Torres, M. K. D. S., Castro, Y. A. D. A., Almeida, A. M. R., et al. (2021). Pilosocereus gounellei (cactaceae) stem extract decreases insulin resistance, inflammation, oxidative stress, and cardio-metabolic risk in diet-induced obese mice. *J. Ethnopharmacol.* 265, 113327. doi:10.1016/j.jep.2020.113327

Della-Vedova, M. C., Muñoz, M. D., Santillan, L. D., Plateo-Pignatari, M. G., Germano, M. J., Rinaldi Tosi, M. E., et al. (2016). A mouse model of diet-induced obesity resembling most features of human metabolic syndrome. *Nutr. Metabolic Insights* 9, 93–102. NMI-S32907. doi:10.4137/NMI.S32907

El-Alfy, A. T., Ahmed, A. A., and Fatani, A. J. (2005). Protective effect of red grape seeds proanthocyanidins against induction of diabetes by alloxan in rats. *Pharmacol. Res.* 52 (3), 264–270. doi:10.1016/j.phrs.2005.04.003

Fetni, S., Bertella, N., Ouahab, A., Zapater, J. M. M., and Fernandez, S. D. P.-T. (2020). Composition and biological activity of the Algerian plant rosa caninal. By HPLC-UV-MS. *Arabian J. Chem.* 13 (1), 1105–1119. doi:10.1016/j.arabjc.2017.09.013

Frezza, C., Venditti, A., Serafini, M., and Bianco, A. (2019). Phytochemistry, chemotaxonomy, Ethnopharmacology, and nutraceutics of lamiaceae. *Stud. Nat. Prod. Chem.* 62, 125–178. doi:10.1016/B978-0-444-64185-4.00004-6

Fylaktakidou, K. C., Hadjipavlou-Litina, D. J., Litinas, K. E., and Nicolaides, D. N. (2004). Natural and synthetic coumarin derivatives with anti-inflammatory/antioxidant activities. *Curr. Pharm. Des.* 10 (30), 3813–3833. doi:10.2174/1381612043382710

Gantimur, D., Syrchina, A. I., and Semenov, A. A. (1986). Khellactone derivatives from phlojodicarpus sibiricus. *Chem. Nat. Compd.* 22 (1), 103–104. doi:10.1007/BF00574597

Ghibu, S., Craciun, C. E., Rusu, R., Morgovan, C., Mogosan, C., Rochette, L., et al. (2019). Impact of alpha-lipoic acid chronic discontinuous treatment in cardiometabolic disorders and oxidative stress induced by fructose intake in rats. *Antioxidants* 8 (12), 636. doi:10.3390/antiox8120636

Gutierrez-Salmean, G., Pilar, O.-V., Maria, V., Leticia, G.-S., German, C.-C., Meaney, E., et al. (2014). Effects of (-)-Epicatechin on A diet-induced rat model of cardiometabolic risk factors. *Eur. J. Pharmacol.* 728, 24–30. doi:10.1016/j.ejphar.2014.01.053

Hands, J. R., Clemens, G., Stables, R., Ashton, K. M., Brodbelt, A. R., Davis, C., et al. (2016). Brain tumour differentiation: Rapid stratified serum diagnostics via attenuated total reflection fourier-transform infrared spectroscopy. *J. Neuro-Oncology* 127 (3), 463–472. doi:10.1007/s11060-016-2060-x

Hirsh, J., Dalen, J., Anderson, D. R., Poller, L., Bussey, H., Ansell, J., et al. (2001). Oral anticoagulants: Mechanism of action, clinical effectiveness, and optimal therapeutic range. *Chest* 119 (1), 8S–21s. doi:10.1378/chest.119.1_suppl.8s

Huang, G. J., Deng, J. S., Liao, J. C., Hou, W. C., Wang, S. Y., Sung, P. J., et al. (2012). Inducible nitric oxide synthase and cyclooxygenase-2 participate in anti-inflammatory activity of imperatorin from glehnia littoralis. *J. Agric. Food Chem.* 60 (7), 1673–1681. doi:10.1021/jf204297e

Inam, S., and Shah, N. (2019). Aging, obesity and unhealthy lifestyle behaviors; risk factors for the emergence of cardiometabolic diseases in Pakistani adults (P01-019-19). *Curr. Dev. Nutr.* 3 (1), nzz028. doi:10.1093/cdn/nzz028.P01-019-19

Iwase, M., Yamamoto, T., Nishimura, K., Takahashi, H., Mohri, S., Li, Y., et al. (2017). Suksdorfin promotes adipocyte differentiation and improves abnormalities in glucose metabolism via PPARγ activation. *Lipids* 52 (7), 657–664. doi:10.1007/s11745-017-4269-7

Jain, M., Surin, W. R., Misra, A., Prakash, P., Singh, V., Khanna, V., et al. (2013). Antithrombotic activity of a newly synthesized coumarin derivative 3-(5-hydroxy-2,2-dimethyl-chroman-6-yl)-N-{2-[3-(5-hydroxy-2,2-dimethyl-chroman-6-yl)-propionylamino]-ethyl}-propionamide. *Chem. Biol. Drug Des.* 81 (4), 499–508. doi:10.1111/cbdd.12000

Javaid, F., Mehmood, M. H., and Shaukat, B. (2021). Hydroethanolic *Extract of A. officinarum* hance ameliorates hypertension and causes diuresis in obesogenic feed-fed rat model. *Front. inPharmacology* 12, 670433. doi:10.3389/fphar.2021.670433

Joshi, A., Pant, A. K., Prakash, O., Stocki, M., and Isidorov, V. A. (2019). Phytochemical analysis, phenolic content and antioxidant activity of methanolic extract of Caryopteris odorata D. Don. Robin. *J. Med. Herbs* 9 (4), 189–196.

Jung, J. Y., Lim, Y., Moon, M. S., Kim, J. Y., Kwon, O., and Kwon, O. (2011). Onion peel extracts ameliorate hyperglycemia and insulin resistance in high fat diet/streptozotocin-induced diabetic rats. *Nutr. Metabolism* 8 (1), 18–8. doi:10.1186/1743-7075-8-18

Kabelova, A., Malinska, H., Markova, I., Oliyarnyk, O., Chylikova, B., and Seda, O. (2021). Ellagic acid affects metabolic and transcriptomic profiles and attenuates features of metabolic syndrome in adult male rats. *Nutrients* 13 (3), 804. doi:10.3390/nu13030804

Kumar, V., and Roy, B. K. (2018). Population authentication of the traditional medicinal plant Cassia tora l. Based on ISSR markers and FTIR analysis. *Sci. Rep.* 8 (1), 10714. doi:10.1038/s41598-018-29114-1

Lake, B. G. (1999). Coumarin metabolism, toxicity and carcinogenicity: Relevance for human risk assessment. *Food Chem. Toxicol.* 37 (4), 423–453. doi:10.1016/s0278-6915(99)00010-1

Lasker, S., Rahman, M. M., Parvez, F., Zamila, M., Miah, P., Nahar, K., et al. (2019). High-fat diet-induced metabolic syndrome and oxidative stress in obese rats are

ameliorated by yogurt supplementation. *Sci. Rep.* 9 (1), 20026. doi:10.1038/s41598-019-56538-0

Li, J., Li, X., Li, Z., Zhang, L., Liu, Y., Ding, H., et al. (2017). Isofraxidin, A coumarin component improves high-fat diet induced hepatic lipid homeostasis disorder and macrophage inflammation in mice. *Food Funct.* 8 (8), 2886–2896. doi:10.1039/C7FO00290D

Mabrouki, L., Rjeibi, I., Taleb, J., and Zourgui, L. (2020). Cardiac ameliorative effect of moringa oleifera leaf extract in high-fat diet-induced obesity in rat model. *BioMed Res. Int.* 2020, 6583603. doi:10.1155/2020/6583603

Mead, J. A., Smith, J. N., and Williams, R. T. (1958). Studies in detoxication. 72. The metabolism of coumarin and of o-coumaric acid. *Biochem. J.* 68 (1), 67–74. doi:10.1042/bj0680067

Murali, R., Srinivasan, S., and Ashokkumar, N. (2013). Antihyperglycemic effect of fraxetin on hepatic key enzymes of carbohydrate metabolism in streptozotocin-induced diabetic rats. *Biochimie* 95 (10), 1848–1854. doi:10.1016/j.biochi.2013.06.013

Najmanova, I., Dosedel, M., Hrdina, R., Anzenbacher, P., Filipsky, T., Riha, M., et al. (2015). Cardiovascular effects of coumarins besides their antioxidant activity. *Curr. Top. Med. Chem.* 15 (9), 830–849. doi:10.2174/1568026615666150220112437

Nandiyanto, A. B. D., Oktiani, R., and Ragadhita, R. (2019). How to read and interpret FTIR spectroscope of organic material. *Indonesian J. Sci. Technol.* 4 (1), 97–118. doi:10.17509/ijost.v4i1.15806

Nepal, S., Malik, S., Sharma, A., Bharti, S., Kumar, N., Siddiqui, K., et al. (2011). Abresham ameliorates dyslipidemia, hepatic steatosis and hypertension in high-fat diet fed rats by repressing oxidative stress, TNF-alpha and normalizing NO production. *Exp. Toxicol. Pathology* 64 (7-8), 705–712. doi:10.1016/j.etp.2011.01.003

Nguelefack-Mbuyo, P. E., Nguelefack, T. B., Dongmo, A. B., Afkir, S., Azebaze, A. G. B., Dimo, T., et al. (2008). Anti-hypertensive effects of the methanol/methylene chloride stem bark extract of mammea africana in L-name-induced hypertensive rats. *J. Ethnopharmacol.* 117 (3), 446–450. doi:10.1016/j.jep.2008.02.028

Nnorom, O., and Onuegbu, G. (2019). Authentication of <i>Rothmannia whitfieldii</i> Dye Extract with FTIR Spectroscopy. *J. Text. Sci. Technol.* 5 (02), 38–47. doi:10.4236/jtst.2019.52004

Nwakiban-Atchan, A. P., Shivashankara, S. T., Piazza, S., Tchamgoue, A. D., Beretta, G., Dell'Agli, M., et al. (2022). Polyphenol-rich extracts of xylopia and aframomum species show metabolic benefits by lowering hepatic lipid accumulation in diet-induced obese mice. *ACS Omega* 7 (14), 11914–11928. doi:10.1021/acsomega.2c00050

Ojetola, A. A., Adeyemi, W. J., David, U. E., Ajibade, T. O., Adejumobi, O. A., Omobowale, T. O., et al. (2021). D-ribose-L-cysteine prevents oxidative stress and cardiometabolic syndrome in high fructose high fat diet fed rats. *Biomed. Pharmacother.* 142, 112017. doi:10.1016/j.biopha.2021.112017

Pari, L., and Rajarajeswari, N. (2009). Efficacy of coumarin on hepatic key enzymes of glucose metabolism in chemical induced type 2 diabetic rats. *Chemico-Biological Interact.* 181 (3), 292–296. doi:10.1016/j.cbi.2009.07.018

Piller, N. B. (1975). A comparison of the effectiveness of some anti-inflammatory drugs on thermal oedema. *Br. J. Exp. Pathology* 56 (6), 554–560.

Prasatthong, P., Meephat, S., Rattanakanokchai, S., Bunbupha, S., Prachaney, P., Maneesai, P., et al. (2021). Hesperidin ameliorates signs of the metabolic syndrome and cardiac dysfunction via IRS/Akt/GLUT4 signaling pathway in a rat model of diet-induced metabolic syndrome. *Eur. J. Nutr.* 60 (2), 833–848. doi:10.1007/s00394-020-02291-4

Prince, M. R. U., Zihad, S., Ghosh, P., Sifat, N., Rouf, R., Al Shajib, G. M., et al. (2021). Amaranthus spinosus attenuated obesity-induced metabolic disorders in high-carbohydrate-high-fat diet-fed obese rats. *Front. Nutr.* 8, 653918. doi:10.3389/fnut.2021.653918

Roberts, C., Vaziri, N., Wang, X., and Barnard, R. (2000). Enhanced NO inactivation and hypertension induced by a high-fat, refined-carbohydrate diet. *Hypertension* 36 (3), 423–429. doi:10.1161/01.hyp.36.3.423

Sasso, S., Sampaio, E. S. P. C., Santana, L. F., Cardoso, C. A. L., Alves, F. M., Portugal, L. C., et al. (2019). Use of an extract of annona muricata linn to prevent high-fat diet induced metabolic disorders in C57bl/6 mice. *Nutrients* 11 (7), 1509. doi:10.3390/nu11071509

Senaphan, K., Kukongviriyapan, U., Sangartit, W., Pakdeechote, P., Pannangpetch, P., Prachaney, P., et al. (2015). Ferulic acid alleviates changes in a rat model of metabolic syndrome induced by high-carbohydrate, high-fat diet. *Nutrients* 7 (8), 6446–6464. doi:10.3390/nu7085283

Shahzadi, T., Abbasi, M. A., Riaz, T., Rehman, A.-U., Siddiqui, S. Z., and Ajaib, M. (2011). Caryopteris odorata: A rich source of antioxidants for protection against chronic diseases and food products. *J. Chil. Chem. Soc.* 56 (2), 678–681. doi:10.4067/s0717-97072011000200012

Shahzadi, T., Abbasi, M. A., Ur-Rehman, A., Riaz, T., Khan, K. M., Ashraf, M., et al. (2013). Antioxidant and lipoxygenase inhibiting new iridoid glucosides from Caryopteris odorata. *Nat. Prod. Res.* 27 (4-5), 302–313. doi:10.1080/14786419.2012.668692

Shahzadi, T., Abbasi, M., Aziz-ur-RehmanRiaz, T., Khan, K., Ahmad, V., et al. (2012). Characterization of chemical isolates of Caryopteris odorata. *J. Chem. Soc. Pak.* 34 (2), 442–447.

Sharma, A., Bharti, S., Bhatia, J., Nepal, S., Malik, S., Ray, R., et al. (2012). Sesamol alleviates diet-induced cardiometabolic syndrome in rats via up-regulating PPARγ, PPARα and e-NOS. *J. Nutr. Biochem.* 23 (11), 1482–1489. doi:10.1016/j.jnutbio.2011.09.011

Sharma, A., Goyal, R., and Sharma, L. (2016). Potential biological efficacy of pinus plant species against oxidative, inflammatory and microbial disorders. *BMC Complementary Altern. Med.* 16 (1), 35–11. doi:10.1186/s12906-016-1011-6

Shin, E., Choi, K. M., Yoo, H. S., Lee, C. K., Hwang, B. Y., and Lee, M. K. (2010a). Inhibitory effects of coumarins from the stem barks of fraxinus rhynchophylla on adipocyte differentiation in 3T3-L1 cells. *Biol. Pharm. Bull.* 33 (9), 1610–1614. doi:10.1248/bpb.33.1610

Shin, J. W., Seol, I. C., and Son, C. G. (2010b). Interpretation of animal dose and human equivalent dose for drug development. *J. Korean Med.* 31 (3), 1–7.

Singh, D., Mathela, C. S., Panwar, A., and Pande, V. (2014). Sesquiterpene hydrocarbon rich essential oils of Caryopteris odorata (D. Don) robin.: Chemical composition, antioxidant and antimicrobial activity. *J. Essent. Oil Res.* 26 (4), 274–281. doi:10.1080/10412905.2014.922507

Suman, R. K., Ray Mohanty, I., Borde, M. K., Maheshwari, U., and Deshmukh, Y. A. (2016). Development of an experimental model of diabetes Co-existing with metabolic syndrome in rats. *Adv. Pharmacol. Sci.* 2016, 9463476. doi:10.1155/2016/9463476

Taira, N., Nugara, R. N., Inafuku, M., Takara, K., Ogi, T., Ichiba, T., et al. (2017). *In vivo* and *in vitro* anti-obesity activities of dihydropyranocoumarins derivatives from peucedanum japonicum thunb. *J. Funct. Foods* 29, 19–28. doi:10.1016/j.jff.2016.11.030

Takahashi, M., Takahashi, Y., Takahashi, K., Zolotaryov, F. N., Hong, K. S., Kitazawa, R., et al. (2008). Chemerin enhances insulin signaling and potentiates insulin-stimulated glucose uptake in 3T3-L1 adipocytes. *FEBS Lett.* 582 (5), 573–578. 0014-5793 (Print)). doi:10.1016/j.febslet.2008.01.023

Tasdemir, E., Atmaca, M., Yldrm, Y., Bilgin, H. M., Demirtaş, B., Obay, B. D., et al. (2017). Influence of coumarin and some coumarin derivatives on serum lipid profiles in carbontetrachloride-exposed rats. *Hum. Exp. Toxicol.* 36 (3), 295–301. doi:10.1177/0960327116649675

Tatarua, L. D. (2017). ATR-FTIR spectra fingerprinting of medicinal herbs extracts prepared using microwave extraction. *Arabian J. Med. Aromatic Plants* 3 (1), 9. doi:10.48347/IMIST.PRSM/ajmap-v3i1.7985

Ullah, K., Jahan, S., Aziz, F., Khan, M. S., Rahman, K. U., Shah, Z. A., et al. (2019). Ameliorative effect of Caryopteris grata benth. Against arsenic-induced enzymatic alterations in testis of albino BALB/c mice. *Pol. J. Environ. Stud.* 28 (2), 861–866. doi:10.15244/pjoes/84831

Yaseen, G., Ahmad, M., Ahmad, M., Sultana, S., Kayani, S., Andrade Cetto, A., et al. (2015). Traditional management of diabetes in Pakistan: Ethnobotanical investigation from traditional health practitioners. *J. Ethnopharmacol.* 174, 91–117. doi:10.1016/j.jep.2015.07.041

Younis, W., AlamgeerSchini-Kerth, V. B., Junior, A. G., and Majid, M. (2018). Cardioprotective effect of Asphodelus tenuifolius cav. On blood pressure and metabolic alterations in glucose-induced metabolic syndrome rats–an ethnopharmacological approach. *J. Ethnopharmacol.* 214, 168–178. doi:10.1016/j.jep.2017.12.005

Zhang, S., Zhao, J., Xie, F., He, H., Johnston, L. J., Dai, X., et al. (2021). Dietary fiber-derived short-chain fatty acids: A potential therapeutic target to alleviate obesity-related nonalcoholic fatty liver disease. *Obes. Rev.* 22 (11), e13316. doi:10.1111/obr.13316

frontiers | Frontiers in Pharmacology

TYPE Original Research
PUBLISHED 06 April 2023
DOI 10.3389/fphar.2023.1085013

OPEN ACCESS

EDITED BY
Hai-Dong Guo,
Shanghai University of Traditional Chinese Medicine, China

REVIEWED BY
Washim Khan,
Southern Research Institute, United States
Ilhami Gulcin,
Atatürk University, Türkiye

*CORRESPONDENCE
Malik Hassan Mehmood,
malikhassan.mehmood@gmail.com,
malikhassanmehmood@gcuf.edu.pk

SPECIALTY SECTION
This article was submitted to Ethnopharmacology, a section of the journal Frontiers in Pharmacology

RECEIVED 31 October 2022
ACCEPTED 22 March 2023
PUBLISHED 06 April 2023

CITATION
Mehdi S, Mehmood MH, Ahmed MG and Ashfaq UA (2023), Antidiabetic activity of *Berberis brandisiana* is possibly mediated through modulation of insulin signaling pathway, inflammatory cytokines and adipocytokines in high fat diet and streptozotocin-administered rats. *Front. Pharmacol.* 14:1085013. doi: 10.3389/fphar.2023.1085013

Antidiabetic activity of *Berberis brandisiana* is possibly mediated through modulation of insulin signaling pathway, inflammatory cytokines and adipocytokines in high fat diet and streptozotocin-administered rats

Shumaila Mehdi[1], Malik Hassan Mehmood [1]*, Mobeen Ghulam Ahmed[1] and Usman Ali Ashfaq[2]

[1]Department of Pharmacology, Faculty of Pharmaceutical Sciences, Government College University, Faisalabad, Pakistan, [2]Department of Biotechnology and Bioinformatics, Faculty of Life Sciences, Government College University, Faisalabad, Pakistan

Medicinal plants play a key role in protection of chronic non-communicable ailments like diabetes, hypertension and dyslipidemia. *Berberis brandisiana* Ahrendt (Berberidaceae) is traditionally used to treat diabetes, liver problems, wounds, arthritis, infections, swelling and tumors. It is also known to be enriched with multiple phytoconstituents including berbamine, berberine, quercetin, gallic acid, caffeic acid, vanillic acid, benzoic acid, chlorogenic acid, syringic acid, *p*-coumaric acid, *m*-coumaric acid and ferulic acid. The efficacy of *B. brandisiana* has not been established yet in diabetes. This study has been planned to assess the antidiabetic activity of *B. brandisiana* in high fat diet and streptozotocin (HFD/STZ)-induced diabetes using animals. Administration of aqueous methanolic extract of *B. brandisiana* (AMEBB) and berbamine (Berb) for 8 weeks caused a dose dependent marked ($p < 0.01$) rise in serum insulin and HDL levels with a significant decline ($p < 0.01$) in glucose, triglycerides, glycosylated hemoglobin (HbA1c), cholesterol, LDL, LFTs and RFTs levels when compared with only HFD/STZ-administered rats. AMEBB and Berb also modulated inflammatory biomarkers (TNF-α, IL-6) and adipocytokines (leptin, adiponectin and chemerin). AMEBB (150 mg/kg and 300 mg/kg) and Berb (80 mg/kg and 160 mg/kg) treated rats showed a marked increase ($p < 0.001$) in catalase levels (Units/mg) in pancreas (42.4 ± 0.24, 47.4 ± 0.51), (38.2 ± 0.583, 48.6 ± 1.03) and liver (52 ± 1.41, 63.2 ± 0.51), (57.2 ± 0.58, 61.6 ± 1.24) and superoxide dismutase levels (Units/mg) in pancreas (34.8 ± 1.46, 38.2 ± 0.58), (33.2 ± 0.80,

Abbreviations: AMEBB, Aqueous methanolic extract of *Berberis brandisiana*; Berb, berbamine; AST, aspartate aminotransferase; ALT, alanine transaminase; RFTs, renal function tests; SOD, superoxide dismutase; CAT, catalase; MDA, melondialdehyde; HDL, high-density lipoprotein; ROS, reactive oxygen species; ELISA, enzyme-linked immunosorbent assay; HFD, high fat diet; STZ, Streptozotocin; HPLC; highperformance liquid chromatography; LDL, Low-density lipoprotein; TC, total cholesterol; TGs, Total triglycerides; TNF- α, tumor necrosis factor alpha; IL-6, interleukin –6; IR, insulin receptor; IRS-1, insulin receptor substrate –1; GLUT-4, glucose transporter –4; SIRT 1, Sirtuin- 1; ADAM 17, A disintigrin and A metalloproteinase 17; PI3K, phosphatidylinositol 3-kinase.

40.4 ± 1.96) and liver (31.8 ± 1.52, 36.8 ± 0.96), (30 ± 0.70, 38.4 ± 0.81),respectively while a significant ($p < 0.01$) decrease in serum melondialdehyde levels (nmol/g) in pancreas (7.34 ± 0.17, 6.22 ± 0.22), (7.34 ± 0.20, 6.34 ± 0.11) and liver (9.08 ± 0.31,8.18 ± 0.29), (9.34 ± 0.10, 8.86 ± 0.24) compared to the data of only HFD/STZ-fed rats. Histopathological studies of pancreas, liver, kidney, heart and aorta revealed restoration of normal tissue architect in AMEBB and Berb treated rats. When mRNA expressions of candidate genes were assessed, AMEBB and Berb showed upregulation of IRS-1, SIRT1, GLUT-4 and downregulation of ADAM17. These findings suggest that AMEBB and Berb possess antidiabetic activity, possibly due to its effect on oxidative stress, glucose metabolism, inflammatory biomarkers and adipocytokines levels. Further upregulation of IRS-1, SIRT1, GLUT-4 and downregulation of ADAM17, demonstrated its potential impact on glucose homeostasis, insulin resistance and chronic inflammatory markers. Thus, this study provides support to the medicinal use of *B. brandisiana* and berbamine in diabetes.

KEYWORDS

***Berberis brandisiana* Ahrendt, chemerin, adipocytokines, insulin receptor substrate -1, A disintigrin and A metalloproteinase 17**

Introduction

Diabetes and obesity are the paramount recurrent endocrine-metabolic disorders that are categorized by hyperglycemia and impaired insulin secretion and/or its action (Kiziltas et al., 2022; Mutlu et al., 2023). Loss of β-cells function and impaired insulin secretion in obesity and diabetes results in persistent hyperglycemia and dyslipidemia (Eguchi et al., 2021). Although the etiology of diabetes is complex, however, genetic proclivity combined with an unbalanced diet play an important role in its onset and progression. Its prevalence has been increased dramatically which might be the result of sedentary lifestyle and increased consumption of high-energy foods (Sankaranarayanan et al., 2018). As per Global Diabetes Alliance, there are 537 million grown-ups with diabetes. This figure is also projected to reach 643 million by 2030 (Miaffo et al., 2021) and will further increase to780 million by 2045. It has also become one of the top 10th global causes of death (Li et al., 2020). Persistent hyperglycemia in diabetes is crucial in the development and progression of diabetes related complications possibly through induction of pro-inflammatory cytokines, reactive oxygen species and adipocytokines (Nedosugova et al., 2022). Consumption of high fat diet (HFD) and streptozotocin (STZ) in animals leads to β-cells damage and impaired insulin secretion and/or function (Hong et al., 2021). Metabolic syndrome has usually been associated with inflammation which results due to stimulation of inflammatory cytokines (TNF-α and IL-6) and adipocytokines (leptin, adiponectin and chemerin) (Zorena et al., 2020; Matthews et al., 2021). Diabetes is exacerbated by overproduction of reactive oxygen species (ROS) which disrupts the insulin signaling pathway, resulting in the development of insulin resistance in diabetes. Multiple evidences support that oxidative stress and hyperglycemia activate serine kinase cascades, which has several possible targets in the insulin signaling pathway, including insulin receptor substrate (IRS) proteins family. Increased phosphorylation of IRS at specific threonine or serine sites, causes decreased phosphorylation of tyrosine, hence resulting in impaired action of insulin (Batista et al., 2021). Serine/threonine phosphorylated IRS molecules are less likely to interrelate with insulin receptor (IR) signaling. In this case, downregulation of target molecules, particularly, phosphatidylinositol 3-kinase (PI3K) is mainly involved in impaired insulin action and glucose transport. Phosphatidylinositol 4, 5-biphosphate (PIP2), an intracellular membrane substrate, is phosphorylated by PI3K to form phosphatidylinositol 3, 4, 5-triphosphate (PIP3), which recruits signaling proteins such as AKT (Saltiel, 2021). PI3K/AKT signaling is important in cellular physiology as it mediates critical cellular processes like lipid metabolism, protein synthesis and glucose homeostasis (Camaya et al., 2022). ROS is known to play a part in activation of intracellular stress kinases and inhibition of IRS-1, thus potentially influencing insulin signaling and to promote *via* GLUT-4 translocation and down streaming of AKT resulting in insulin resistance, obesity and diabetes mellitus (Li et al., 2022).

There are growing evidences that development of insulin resistance is related with an increase in the release of pro-inflammatory cytokines and adipocytokines (Menghini et al., 2013; Al-Mansoori et al., 2021). Stimulated production of TNF-α contributes in degradation of β-cell and increased activity of ADAM 17, a mediator of TNF- α production (Al-Kuraishy et al., 2021). Imbalance between antioxidants and reactive oxygen species in diabetes usually stimulates the production of ADAM17 and TNF-α. It has been reported that there is association between increased TNF-α levels in diabetes and impaired insulin signaling possibly by increasing IRS-1 serine phosphorylation. This inhibits tyrosine kinase IR activity and thus intervening signal down streaming (Lee et al., 2022).

Sirtuin-1 (SIRT1) modulates insulin signaling through IRS after IR tyrosine phosphorylation stimulated by insulin, continues to activate AKT, resulting in positive regulation of insulin secretion in pancreatic β-cells, protection from inflammation and oxidative stress and plays important roles in the metabolic pathway through modulation of insulin signaling (Lee et al., 2009). The overexpression of SIRT 1 in diabetic animal represents significantly amelioration of glucose intolerance and insulin resistance. As a result, SIRT1 is a promising therapeutic

target for the treatment of insulin resistance and diabetes (Feng et al., 2021).

Despite the availability of multiple therapeutic treatment options for treatment of diabetes, the disease progression spectra are increasing day by day. The currently available treatment options are either introducing exogenous insulin or to increase the sensitivity of insulin. These therapeutic options remain unable to provide sustained glycemic control or halt the disease progression (Bhatti et al., 2022). Herbal products have recently received a lot of attention as a complementary and/or adjuvant therapies (Abdulghafoor et al., 2021; Gall et al., 2021; Ayaz et al., 2022). The use of traditional medicinal plants in the treatment of diseases including diabetes is endorsed by WHO. Diabetes has been managed by using a variety of medicinal plants including *Zingiber officinale, Allium sativum, Elephantopus scaber, Areca catechu, Elephantopus scaber, Ricinus communis* and *Ocimum sanctum* since ancient times (Aumeeruddy and Mahomoodally, 2021).

Research findings have been published by various labs on the phytochemical and pharmacological properties of Berberis species. *Berberis brandisiana* Ahrendt is member of Berberidaceae family, a dicotyledonous genus mainly woody, spiny, evergreen shrubs and flowers (Khan and Khatoon, 2007). It consists of 17 Genera and 650 species. Berberis species belonging to this family are originated from the mountainous regions in Pakistan at sea level of above 1400–3500 m and are also used both in modern system of medicines and traditionally as well. Its vernacular names are "Ishkeen and Shugloo". It has been traditionally used in various disorders like diabetes, kidney stones, liver problems, wounds, arthritis, infections, tumors, leucorrhoea and swellings (Khan et al., 2016). Berberis species have been widely used in Ayurveda as raw materials or as ingredients for wound healing, arthritis, eye infections, hemorrhoids, piles, reducing obesity, treating dysentery and indigestion (Khan and Khatoon, 2007; Bhardwaj and Kaushik, 2012). A number of clinical and pharmacological studies on various Berberis species have been published, demonstrating their significance as medicinal plants with great therapeutic potential (Rahimi-Madiseh et al., 2017). *Berberis aristata, Berberis chitria* and *Berberis lycium* extracts have been used as a home remedy for diabetes, bleeding piles, conjunctivitis, skin diseases, ophthalmic problems, ulcers, jaundice, inflamed spleen and liver since ancient times (Khan et al., 2016). From various parts of the Berberis plants, phytochemicals including alkaloids, phenolic acids, sterols, lignins, anthocyanins, flavanoids, carotenoids, terpenoids, vitamins, lipids and proteins were isolated (Khan et al., 2016). Berberis plants were used to extract alkaloids like berberine, berbamine, baluchistanamine, thalifoline, isotetrandrine and flavonoids rich in polyphenols like caffeic acid, quercetin, meratin, rutin, chlorogenic acid and other nutrients and minerals such as β-carotene, anthocyanin, and ascorbic acid (Khan et al., 2016). Berberis plants contain two important alkaloids, berberine and berbamine (Chander et al., 2017).

Berbamine (Berb) is a bis-benzylisoquinoline alkaloid reported to be present in Berberis plants including *Berberis aristata, Berberis vulgaris, Berberis poiretil schneid, Berberis amurensis* and *Berberis brandisiana* (Wang et al., 2009; Khan et al., 2016) belongs to Berberidaceae family. Berb has long been used in clinical settings for variety of ailments due to its reported anti-inflammatory effect by inhibiting (NF-κB, ERK1/2 and JNK signaling pathways) through the activation of macrophages and neutrophils (Jia et al., 2017), anticancer (Farooqi et al., 2022), antioxidant (Sithuraj and Viswanadha, 2018), immunomodulatory (Zhang et al., 2020), hepatoprotective (Sharma et al., 2021), cardioprotective (Sun et al., 1998; Zhang et al., 2012; Han et al., 2018; Sankaranarayanan et al., 2018) and antihypercholesterolemic effects.

Considering the therapeutic potential of *B. brandisiana* in diverse health ailments and the availability of limited data on this botanical herb, this study has been designed to investigate the antidiabetic properties of *B. brandisiana* and its metabolite, berbamine with an insight into its modulatory effects on insulin signaling pathway, inflammatory cytokines and adipocytokines using HFD/STZ-administered diabetic rats. Further quantitative expression of mRNA of diabetic candidate genes like, IRS-1, GLUT-4, SIRT 1 and ADAM17 were also studied for their role on the part of protective potential of *B. brandisiana* and berbamine in diabetes.

Materials and methods

Chemicals

Streptozotocin (STZ) and berbamine (Berb) were purchased from Glenthem life sciences, United Kingdom. Metformin, cholesterol and formalin were sourced from Sigma-Aldrich. ELISA kits for the assessment of TNF-α, IL-6, adiponectin insulin, leptin and chemerin; (E-EL-H0109), (E-EL-H0102), (E-EL-R3034), (E-EL-H 6122), (E-EL-R 0582) and (E-0864Ra) were purchased from Elabscience, United States. In this study, all chemicals were of analytical quality and obtained from Glenthem life sciences, United Kingdom. Other ingredients including powdered milk, vegetable oil, wheat bran, fishmeal, black treacle, wheat flour and table salt were purchased from local supplier at clock tower market, Faisalabad, Pakistan. Nutrivet-V and potassium metabisulfite were purchased from local veterinary pharmacy in Faisalabad.

Animals

Wister rats, of either sex, weighing 180–250 g were obtained from University of Veterinary Sciences, Lahore. All animals were kept in ventilated cages (23°C temperature, 55% humidity and light/dark cycle 12 h) with free access to water *ad libitum*. The animals were acclimatized for 1 week. The studies were performed according to methods approved by The Ethical Review Committee (ERC) at GCUF (Ref. No. GCUF/ERC/50).

Plant collection and extraction

In March 2019, the plant material was collected from Gilgit-Baltistan, Pakistan. The plant was identified and authenticated by a botanist, Prof. Dr. Mansoor Hameed, Department of Botany, University of Agriculture, Faisalabad, Pakistan. The specimen sample was submitted at Herbarium, University of Agriculture with voucher number (31-21-01) for future reference. The plant specie has also been validated using online resources like https://powo.science.kew.org/taxon/urn:lsid:ipni.org:names:106475-1 http://www.theplantlist.org/tpl1.1/record/kew-2673508; https://

www.ipni.org/n/106475-1 https://sites.google.com/site/efloraofindia/system/app/pages/search?scope=search-site&q=berberis+brandisiana; http://www.efloras.org/florataxon.aspx?flora_id=5&taxon_id=242420734). To prepare the crude extract, 1.5 kg powdered plant material was soaked in methanol and distilled water (70:30, v/v) for 7 days with occasional shaking. The maceration process was repeated thrice to obtain sufficient extract. The first filtrate was obtained by using muslin cloth and Whatman filter paper No. 1. The procedure was carried out three times. A rotary evaporator (Model: RE300 Stuart® United Kingdom) was used to evaporate filtrates and to obtain extract. The percentage yield of AMEBB was obtained 13% wt/wt.

Quantitative analysis

Estimation of total phenolic content (TPC)

To determine the total phenolic content (TPC) of AMEBB, Folin Ciocalteu spectrophotometric method was used (Kiziltas et al., 2022b; Topal and Gulcin, 2022). Around 40 µL AMEBB and gallic acid (standard) were mixed with 1.8 mL of Folin–Ciocalteu reagent and allowed to stand at room temperature for 5 min and then sodium bicarbonate (1.2 mL, 7.5%) was added to the mixture. The mixture was allowed to stand for 60 min at room temperature and absorbance was measured at 765 nm. For each sample, measurements were carried out triplicate. Gallic acid was used as a standard. TPC were calculated as mg of gallic acid in milligram equivalent (GAE)/g of dry extract.

Estimation of total flavonoid content (TFC)

TFC of AMEBB were estimated by using calorimetric assay. A 4 mL of distilled water was added to 1 mL of AMEBB. Then, 0.3 mL of 5% sodium nitrite ($NaNo_2$) solution was added, followed by 0.3 mL of 10% aluminum chloride ($AlCl_3$) solution in test tubes. Test tubes were incubated for 5 min followed by addition of 2 mL of 1 M sodium hydroxide (NaOH) in the mixture. The volume of reaction mixture was made up to 10 mL with distilled water. The mixture was thoroughly vortexed. The absorbance was measured at 510 nm. A calibration curve was prepared with catechin and the results were expressed as mg catechin equivalent (CEQ)/100 g sample (Bilgari et al., 2008).

DPPH (1, 1-diphenyl-2picryl-hydrazyl) radical scavenging assay of AMEBB

The DPPH has been widely used for the measurement of free radical scavenging activity of samples (Durmaz et al., 2022; Gülçin et al., 2022). To prepare stock solution, 4 mg of DPPH was mixed in 100 mL of methanol. Around 2800 µL of DPPH solution was mixed with various concentrations of AMEBB. A 3 mL aliquot was filled with 200 mL of AMEBB concentrations (200, 100, 50, 25, 12.5, and 6.25 µg/mL) and DPPH. The mixture was carefully shaken before being stored at room temperature for 60 min. The OD (optical density) was measured at 517 nm using a UV spectrophotometer (Hitachi, Japan). For negative control, 2800 µL DPPH and 200 mL of methanol were used. On the other hand, methanol was used as a control. Following equation was used to calculate % age inhibition or scavenging effect:

$$\%\ \text{age inhibition or scavenging effect} = \left[(AC - AS) / AC \right] \times 100$$

Where AC denotes absorbance of negative control and AS denotes absorbance of test samples. IC_{50} values were calculated using Graph pad prism (8.4.3).

HPLC analysis of AMEBB for detection of alkaloids

The aqueous methanolic extract of *B. brandisiana* (AMEBB) was evaluated using HPLC fingerprinting and content determination method. HPLC (Perkin Elmer, United States) was attached with Flexer Binary LC pump and UV/VS LC detector (Shelton City, 06484 United States). HPLC column (C_{18}) with dimensions of 260 × 4.6 mm and a thickness of 5 µm was used. Temperature of column was 36°C. A 10 µL was injected volume of the sample. The mobile phase was methanol-water (water containing 4% acetic acid) and methanol: water ratio was 66:34 v/v. The flow rate was 1 mL/min and detectors were used at the wavelength of 290 and 250 nm. Whereas, berbamine standardization was carried out with methanol (60%) and water (40%); v/v. Quantification of berbamine in AMEBB was performed by standard method using berbamine ≥98% HPLC (Batch #. 066AZF, Glenthem Life Sciences, United Kingdom) as standard. The stock solution of plant sample was prepared by mixing 50 mg of the dry extract in a 1000 mL solution of methanol/water (70:30, v/v). The HPLC chromatogram was obtained using same mobile phase and detection wavelength as used for berbamine (Dar et al., 2014). For data analysis, software version 4.2.6410 was used.

HPLC analysis of AMEBB for detection of Flavonoids and Phenolics

AMEBB sample was prepared for high performance liquid chromatography analysis by mixing 50 mg sample in 24 mL of methanol, 16 mL of distilled water and 10 mL of 6 M HCl. The mixture was incubated at 95°C for 2 h. Solution was filtered through membrane filter (0.45 µm nylon). Gradient HPLC (Shimadzu, Japan; SPD 10AV) was used for separation of phenolics and flavonoids from AMEBB using C_{18} (shim-pack CLC-ODS), 5 µm column (25 cm × 4.6 mm) linked with UV- visible spectrophotometer detector at wavelength of 280 nm and injector for sampling. Separation was carried out on gradient mobile phase (A: Water and acetic acid, B: Acetonitrile). Flow rate was 1 mL/min. The gradient used for solvent B was 15% for 0–15 min, 45% for 15–30 min and 100% for 35–45 min compounds were interpreted by comparing the retention time (Rt) and the UV visible peaks previously obtained by standards. External standardization was used for quantification (Shaukat et al., 2022).

Design of experiments

Wister rats were divided into nine groups (n = 6, each) prior to dietary manipulation. For 4 weeks, six groups of animals were fed

high fat diet composed of 5 kg refined wheat flour, 5 kg wheat bran, 2.25 kg fish meal, 75 g table salt, 33 g multivitamin, 150 g black treacle, 2 kg powdered milk, 500 g vegetable oil, 15 g potassium metabisulphate and 2% cholesterol/15 kg feed (Aziz et al., 2013). Following that, freshly prepared intraperitoneal injection of streptozotocin (40 mg/kg) was administered after dissolving in citrate buffer (0.1 M and pH 4.5). After 1 week, fasting blood glucose levels were measured and rats with glucose levels more than 250 mg/dL were classified as diabetic. Diabetic animals were treated as follows for 56 days. Normal control rats were fed standard diet in group I. Diabetic rats were fed high fat diet in group II. Diabetic rats were given metformin (200 mg/kg) in group III as positive control. In group IV and V: diabetic rats were treated with Berb (80 and 160 mg/kg), respectively. Group VI and VII: diabetic + AMEBB (150 and 300 mg/kg) respectively. Normal animals were given Berb (80 and 160 mg/kg) and AMEBB (160 and 300 mg/kg) in Group VIII and IX, respectively. The doses of *B. brandisiana* extract (150 and 300 mg/kg) were finalized on the basis of effective doses of similar species of same genera used in animal models (Singh and Kakkar, 2009; Pareek and Suthar, 2010; Rahimi-Madiseh et al., 2017) and, by translation of human administered dose to animal dose. In traditional system of medicine, *B. brandisiana* has been used as decoction (one teaspoon per cup) (Khan and Khatoon, 2007; Jan et al., 2008; Khan et al., 2016). One teaspoon thrice a day which is equivalent to 15g/day or 250 mg/kg. The % yield of *B. brandisiana* was found 13%, as per material to yield conversion, it became1.95 g/day/kg. For translation from human to animal dose, human dose factor 7 has been multiplied with human dose for its conversion to its respective animal dose (Nair and Jacob, 2016). It resulted as 195 mg/kg. Based on aforementioned references and calculations, we have selected lower dose as 150 mg/kg and higher dose as 300 mg/kg of *B. brandisiana*. Similarly, the doses (80 and 160 mg/kg) of berbamine were chosen from the results of our preliminary pilot experiment, performed on small number of animals (data not shown) and the results of previous animal studies (Sankaranarayanan et al., 2018; Sharma et al., 2021; Yin et al., 2022) where berbamine has been used in range of 50–200 mg/kg in different studies.

Acute toxicity research

In accordance with OECD 425 guidelines, doses of 1000 and 2000 mg/kg were used for assessment of acute toxicity of AMEBB. After 24 h, rats were observed for toxicity indicators like agitation, lacrimation, general behavior and respiration as well as mortality (Shaukat et al., 2022).

Estimation of body weight, food intake and fluid intake

During the experimental period, an electronic weighing balance (Sartorius-Power™, United States) was used to measure the increase in body weight of animals in each group to determine the effect of HFD feed intake. To assess the impact of diet, food intake of each rat in all groups was calculated daily. Water was provided in graduated drinking bottles and daily consumption was recorded (Sholikhah and Ridwan, 2021).

Biochemical analysis

At 12th week of experiment, animals were starved for 18 h before being euthanized followed by achievement of deep anesthesia with isoflurane (5%–10% v/wt) through inhalation in a closed chamber. For the assessment of glucose levels in blood and glycosylated hemoglobin (HbA1c) levels, blood samples were drawn through cardiac puncture in EDTA tubes (EDTA, sodium citrate, heparin). Tissues were dissected, washed in ice-cold normal saline and homogenized with phosphate buffer (0.1 M, pH 7.5). The supernatant was collected after centrifugation at 3000 /rpm for 10 min. The blood was centrifuged at 4000 /rpm for 10 min to obtain serum. The serum and tissue homogenates were stored at −80°C. Serum and homogenates were preserved for further biochemical analysis (Javaid et al., 2021).

Estimation of glucose, insulin and glycosylated hemoglobin

Blood glucose levels were measured using a digital glucometer (EVOCHECK GM700S), while serum insulin levels were measured by ELISA kit (E-EL-R3034) sourced from Elabscience, USA, with sensitivity range of 3.75 pg/mL, and a detection range of 6.25–400 pg/mL. The reaction was observed at 450 nm wavelength. HbA1c levels were determined using a commercial kit (A1C EZ 2.0 ™) sourced from Wuxi Bio Hermes Biomedical Technology Co., Ltd. Beijing, China (Sankaranarayanan et al., 2018).

Determination of inflammatory biomarkers

Pro-inflammatory cytokines (TNF-α, IL-6) levels were measured with ELISA kits (E-EL-H0109) and (E-EL-H0102) sourced from Elabscience, United States, with sensitivity and detection ranges are of 4.69 pg/mL and 7.81–500 pg/mL, respectively. The reaction was observed at 450 ± 2 nm wavelength. The mixture reaction was provided with 100 ul of serum in already coated wells in the ELISA plate reader (DIA source, Germany). Following the recommendations of manufacturer, TNF-α and IL-6 concentrations were calculated using the standard markers included in the assay kits. The results are presented in ng/mL (Shaukat et al., 2022).

Estimation of adipocytokines levels in serum

The obesity biomarkers in serum, adiponectin (E-EL-H 6122), leptin (E-EL-R 0582), Elabscience, United States, and chemerin (E0864Ra), BT LAB, Birmingham, United Kingdom, levels were estimated using ELISA kits according to the instructions of manufacturer with sensitivity ranges of 0.1 ng/mL and 0.52 ng/mL, respectively. The ELISA plates were pre-coated with antibodies specific to rat LEP, ADP and CHEM maintained at

37°C. The reaction was observed at 450 ± 10 nm wavelength. Serum leptin, adiponectin and chemerin levels were measured in ng/mL (Shaukat et al., 2022).

Determination of lipid profile, LFTs and RFTs

Lipid profile including triglycerides (TGs), total cholesterol (TC) and high-density lipoprotein (HDL) levels were measured in serum samples (Rabbi et al., 2021). To carry out standardized enzymatic procedures, commercial kits (CAT # ETI10150100-4, CAT # ETI11630100-3) sourced from Humen, Germany were used. The fraction of low-density lipoprotein (LDL) was obtained through subtracting high-density lipoprotein from total cholesterol. LFTs (ALT, AST) and RFTs (creatinine and urea) levels were measured in isolated samples of serum. The results were shown in U/L and mg/dL.

Antioxidant studies on tissue homogenates

The antioxidant activities of tissue homogenates were determined by assessing the levels of catalase (CAT), superoxide dismutase (SOD) and melondialdehyde (MDA). All animals were euthanized followed by achievement of deep anesthesia with isoflurane (5%–10% v/wt) through inhalation in a closed chamber. The pancreas, kidney, liver, aorta and heart were removed and kept at −80°C after being washed with ice-cold normal saline. The experiments were carried out according to pre-established procedures (Javaid et al., 2021).

Histopathological analysis

Histopathological analysis was performed using formalin (10%) to preserve the liver, pancreas, kidney, aorta and heart of rats. Organs were stained with hematoxylin and eosin followed by harvesting with a microtome (Leica, Germany) and observed under light microscope (ACCU-SCOPE 3001- LED Digital Microscope, USA) (Madić et al., 2021).

Quantitative reverse transcription polymerase chain reaction (q RT-PCR)

q RT-PCR was used to estimate the mRNA expression of IRS-1, GLUT-4, SIRT 1, ADAM 17 and β-actin. Trizol reagent (Tri Quick Reagent, Cat #R1100) was used to homogenize frozen liver tissues and to extract total RNA. Reverse transcriptase kit of cDNA was used to acquire cDNA from approximately 2 µg of total RNA/sample (Molecular Biology, Thermoscientific, Lithuania). Amplification of cDNA was carried out using SyberGreen PCR (Molecular Biology, Thermoscientific, Lithuania). The primer stock solutions were used in accordance with the protocol of manufacturer (Macrogen, Korea). With a total volume of 20 µL, PCR for IRS-1, GLUT-4, SIRT 1, ADAM 17 and β-actin was performed in the presence of 2.5 µL of cDNA template, Sybergreen (10 µL), RNAase free water (4.5 µL), forward primer (1.5 µL) and reverse primer (1.5 µL) into each sets of the primers (The primer sequence is listed in Table 1). The annealing temperatures used for all primers were (58°C–60°C for 60 s). The $2^{-\Delta\Delta Ct}$ method was used to calculate the relative mRNA levels of candidate genes, which were normalized to β-actin levels and compared to untreated control group (Aljohani et al., 2022).

Results

Total flavonoid content (TFC) and total phenolic content (TPC)

Total flavonoid and phenolic equivalent contents of AMEBB were calculated using catechin and gallic acid standard regression lines, respectively. TFC and TPC contents were found to be 77.76 mg CEQ/g dry extract weight and 89.69 mg GAE/g dry extract, respectively.

Antioxidant activities of AMEBB

AMEBB inhibited DPPH in a concentration-dependent manner with maximum of 78.15% scavenging activity at 200 µg/ml. The IC_{50} value of AMEBB was 40.32 µg/mL with 95% CI of 20.46–80.38, n = 3, similar to the IC_{50} value of ascorbic acid which was 87.09 µg/mL (51.72–156.7, n = 3) (Figure 1).

HPLC analysis of AMEBB for detection of alkaloids

The HPLC chromatogram of the aqueous methanolic extract of *B. brandisiana* (AMEBB) displayed different metabolites with respective concentrations like, berbamine (74.95 mg) and berberine (52.15 mg) [Figures 2A, B].

HPLC analysis of AMEBB for detection of Flavonoids and Phenolics

The HPLC chromatogram of the aqueous methanolic extract of *B. brandisiana* (AMEBB) revealed various metabolites with different concentrations in ppm like quercetin (11.14), gallic acid (23.68), caffeic acid (8.53), vanillic acid (14.43), benzoic acid (15.49), chlorogenic acid (19.89), syringic acid (13.41), *p*-coumaric acid (1.9 m), *m*-coumaric acid (15.54) and ferulic acid (25.96) [Figure 2C].

Acute toxicity study

At highest administered dose of 2000 mg/kg of AMEBB, animals showed no signs of toxicity. All the animals were survived with no disability or deaths.

Effect of AMEBB and Berb on body weight, food and fluid intake

Body weight of rats in groups 2–7 significantly ($p < 0.001$) increased after 28 days of high fat diet consumption. Only high fat diet and

TABLE 1 List of Primers used in q RT- PCR.

Genes	Forward/reverse	Sequences	Gene accession no.
IRS-1	Forward	5′CCAAGGGCTTAGGTCAGACA 3′	2011202-005_E7
	Reverse	5′CCACTTGCATCCAGAACTCG 3′	
GLUT-4	Forward	5′ TTGCCCTTCTGTCCTGAGAG 3′	2011202-005_D9
	Reverse	5′CGCTCTCTTTCCAACTTCCG 3′	
ADAM17	Forward	5′AAGACCCCAGCACAGATTCA 3′	2011202-005_D11
	Reverse	5′GGCTCCCACTAACACTCTGT 3′	
SIRT 1	Forward	5′GCAGTAACAGTGACAGTGGC 3′	2011202-005_E4
	Reverse	5′AACTGCCTCTTGATCCCCTC 3′	
β-actin	Forward	5′CACCATGTACCCAGGCATTG 3′	2011202-005_E10
	Reverse	5′ACAGTCCGCCTAGAAGCATT 3′	

Bold values are represent as IRS-1: Insulin receptor substrate- 1, GLUT-4: Glucose transporter-4, SIRT1: Sirtuin-1, ADAM 17: A disintegrin and A metalloproteinase 17, β-actin: ACTB gene.

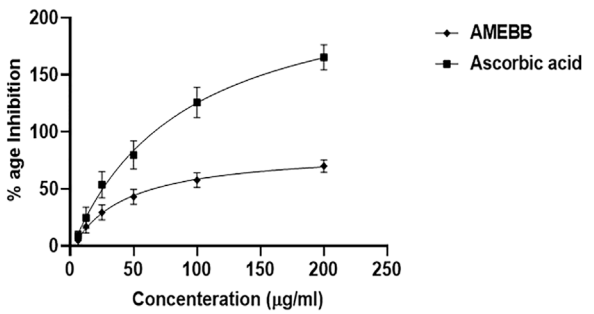

FIGURE 1
Aqueous methanolic extract *Berberis brandisiana* (AMEBB) has antioxidant DPPH radical scavenging activity *in vitro*. The values are depicted as Mean ± S.E.M. (n = 3).

streptozotocin administered rats for 56 days, showed a noticeable ($p < 0.01$) attenuation in the body weights when compared with normal animals (Table 2). Similarly, diabetic rats consumed significantly ($p < 0.001$) more food and fluids throughout the experiment. Oral administration of AMEBB (150 and 300 mg/kg) and Berb (80 and 160 mg/kg) for 8 weeks significantly ($p < 0.01$) reduced food intake (grams) (39.20 ± 0.80, 40 ± 0.70), (40.60 ± 1.03, 39.60 ± 1.91) and fluid intake (mL) (220.2 ± 1.93, 217.6 ± 1.03), (224.4 ± 0.51, 216.8 ± 0.91) in diabetic animals compared to control (30 ± 1.73) and (179.2 ± 0.37), respectively. These findings were found similar to those on the part of metformin, a standard antidiabetic drug, administered group (Figure 3).

Effect of AMEBB and berb on glucose, insulin and HbA1c levels

Serum insulin levels (5.54 ± 0.22 µU/mL) were significantly ($p < 0.001$) reduced in high fat diet and streptozotocin-fed diabetic rats, while blood glucose levels (346 ± 13.27 mg/dL) were significantly ($p < 0.001$) increased compared to normal control (87 ± 1.09) animals (Table 3). Administration of AMEBB (150 and 300 mg/kg) and Berb (80 and 160 mg/kg) for 8 weeks caused a significant ($p < 0.01$) improvement in serum insulin levels in µU/mL (12.11 ± 0.14, 13.08 ± 0.24) (8.3 ± 0.27, 12.92 ± 0.09) and blood glucose levels in mg/dL (156.4 ± 1.83, 135.6 ± 2.62) (242.4 ± 2.66, 158 ± 4.57), respectively compared to HFD/STZ-induced diabetic rats. HbA1c (%) levels were found significantly ($p < 0.001$) enhanced (7.66 ± 0.18) in HFD/STZ-induced diabetic rats vs. normal rats. AMEBB (150 and 300 mg/kg) and Berb (80 and 160 mg/kg) considerably ($p < 0.01$) reduced HbA1c levels (5.22 ± 0.04, 6.22 ± 0.05), (5.24 ± 0.14, 5.26 ± 0.07), respectively. However, AMEBB and Berb caused no significant changes in normal rats. AMEBB and Berb also showed marked effect at higher dose vs. its effect at lower dose in insulin and glucose levels as depicted in Table 3.

Effect of AMEBB and Berb on inflammatory biomarkers

When AMEBB (150 and 300 mg/kg) and Berb (80 and 160 mg/kg) were given to HFD/STZ-induced diabetic rats, these presented marked ($p < 0.001$) decline in serum TNF-α (20.39 ± 0.17, 19.20 ± 0.37) (20.43 ± 0.39, 19.95 ± 0.27) and IL-6 (ng/mL) levels compared to only HFD/STZ-exposed rats. Administration of AMEBB and Berb showed no marked difference in serum TNF-α and IL-6 levels of normal rats. AMEBB and Berb also showed marked effect at higher dose vs. its effect at lower dose in serum IL-6 levels as depicted in Figure 4.

Effect of AMEBB and Berb on adipocytokines levels

HFD/STZ-induced diabetic rats exhibited marked ($p < 0.001$) increase in serum leptin (20.38 ± 0.11) and chemerin (1.48 ± 0.15) levels compared to normal rats. In treated animals, AMEBB (150 and 300 mg/kg) and Berb (60 and 180 mg/kg) significantly ($p < 0.01$) decreased leptin (18.27 ± 0.15, 15.52 ± 0.10) (18.21 ± 0.04, 17.71 ± 0.19) and chemerin (0.76 ± 0.03, 0.62 ± 0.04), (0.80 ± 0.04, 0.60 ± 0.03) levels, respectively, compared to only HFD/STZ-exposed rats. However, a noticeable ($p < 0.001$)

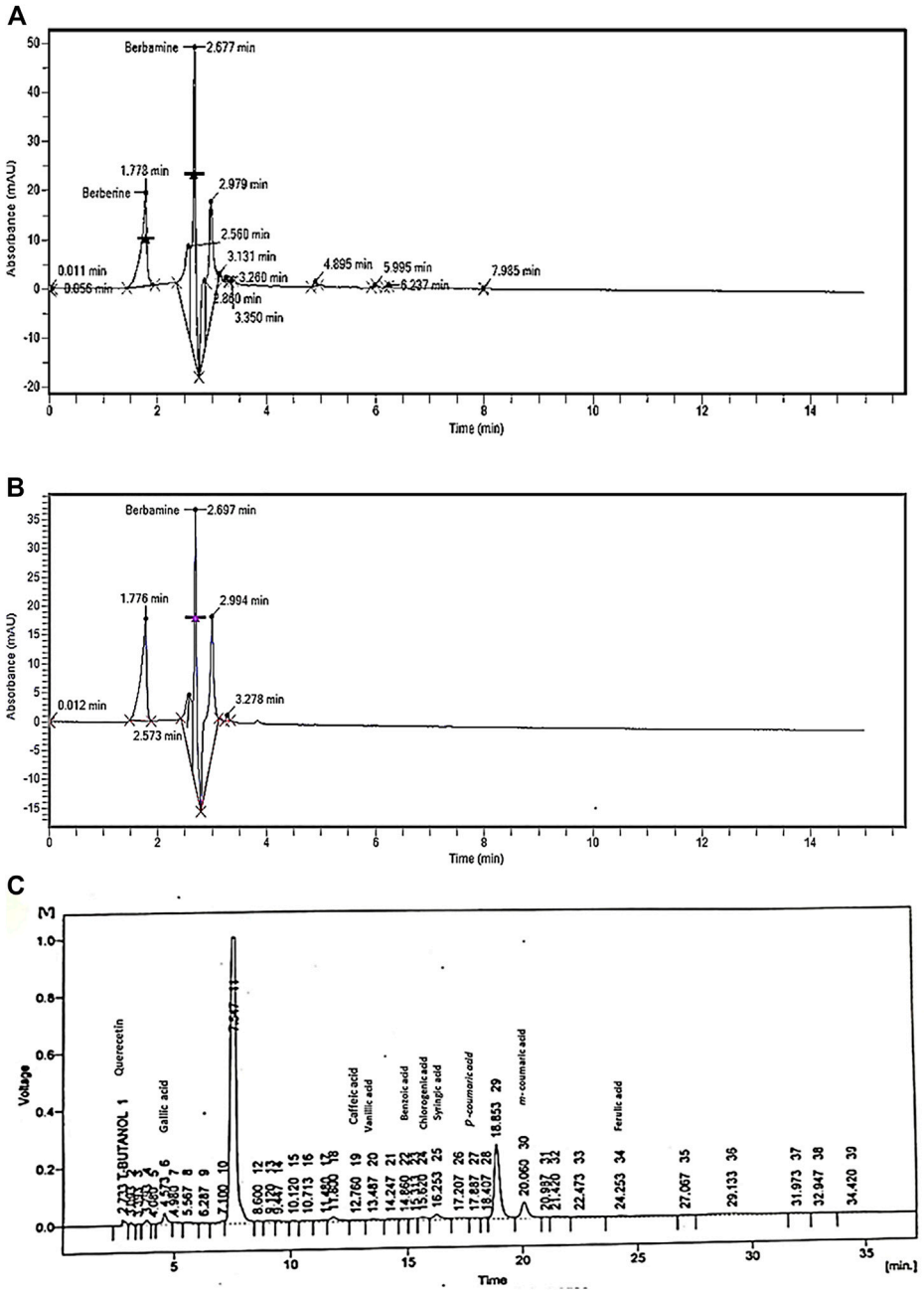

FIGURE 2
(A) HPLC chromatogram of aqueous methanolic extract of *Berberis brandisiana* (AMEBB) for detection of Alkaloids **(B)** HPLC fingerprints of standard (Berbamine). **(C)** HPLC chromatogram of aqueous methanolic extract of *Berberis brandisiana* (AMEBB) for detection of Flavonoids and Phenolics.

decrease in adiponectin (0.21 ± 0.04) levels in ng/mL were recorded in HFD/STZ-exposed rats compared to control animals. Treatment with AMEBB and Berb at both doses caused improvement in adiponectin (0.53 ± 0.01, 0.55 ± 0.01), (0.52 ± 0.01, 0.56 ± 0.01) levels respectively, similar to the effect of metformin. There was no significant modification in normal rats when treated with AMEBB and Berb. AMEBB and Berb also showed marked effect at higher dose vs. its effect at lower dose effects in serum, leptin, chemerin and adiponectin levels as displayed in Figure 5.

Effect of AMEBB and Berb on oxidative stress

Figure 6 depicts oxidative damage markers in liver, pancreas, kidney, aorta and heart tissue homogenates. Treatment of AMEBB and Berb to HFD/STZ-induced diabetic rats showed a noticeable ($p < 0.001$) increase in serum antioxidant enzymes (CAT and SOD in Units/mg) in pancreas (42.4 ± 0.24,47.4 ± 0.51), (38.2 ± 0.583, 48.6 ± 1.03) and liver (52 ± 1.41, 63.2 ± 0.51), (57.2 ± 0.58, 61.6 ± 1.24) and superoxide dismutase levels in pancreas (34.8 ± 1.46,38.2 ± 0.58), (33.2 ± 0.80, 40.4 ± 1.96) and liver (31.8 ± 1.52,36.8 ± 0.96),

10.3389/fphar.2023.1085013

TABLE 2 Effect of administration of *Berberis brandisiana* and berbamine on body weight in high fat diet and streptozotocin-fed diabetic rats.

	Weight (gm)		
	0 week	4th week	12th week
Control (NPD)	155.6 ± 2.32	158.4 ± 1.81	158.2 ± 1.53
Diabetic (HFD + STZ)	156.6. ± 2.48	256 ± 2.821^{+++}	140.8 ± 2.04^{+++}
Diabetic + MET (200 mg/kg)	150.4 ± 12.01	172.8 ± 7.21^{ab}	153.2 ± 5.81^{ab}
Diabetic + Berb (80 mg/kg)	163 ± 0.84	189.4 ± 4.72^{ab}	175.4 ± 2.68^{ab}
Diabetic + Berb (160 mg/kg)	155.4 ± 1.57	180.4 ± 5.39^{ab}	166.2 ± 4.99$^{ab/ns+}$
Diabetic + AMEBB (150 mg/kg)	155.2 ± 1.16	185.2 ± 4.97^{ab}	171 ± 4.92^{ab}
Diabetic + AMEBB (300 mg/kg)	147.8 ± 6.42	178 ± 4.92^{ab}	162 ± 4.56$^{ab/ns+}$
Control + Berb (160 mg/kg)	152 ± 5.78	189.8 ± 3.17^{ns}	201.2 ± 3.54^{ns}
Control + AMEBB (300 mg/kg)	156 ± 11.31	188.6 ± 4.98^{ns}	195.4 ± 4.82^{ns}

The values are depicted as Mean ± S.E.M. (n = 6); $+++p < 0.001$ shows comparisons of normal vs. diabetic animals (student t-test); ^{ab} $p < 0.01$ shows comparison of treatment vs diseased animals (Two Way ANOVA, followed by Dunnett's test); ns = non-significant; Where NPD: normal pallet diet; Diabetic: High fat diet/streptozotocin; MET: metformin; Berb: berbamine; AMEBB: aqueous methanolic extract of *Berberis brandisiana*; ns^{+} (non-significant)shows the comparison between the effect of low vs. high dose of *Berberis brandisiana* and berbamine (student t-test).

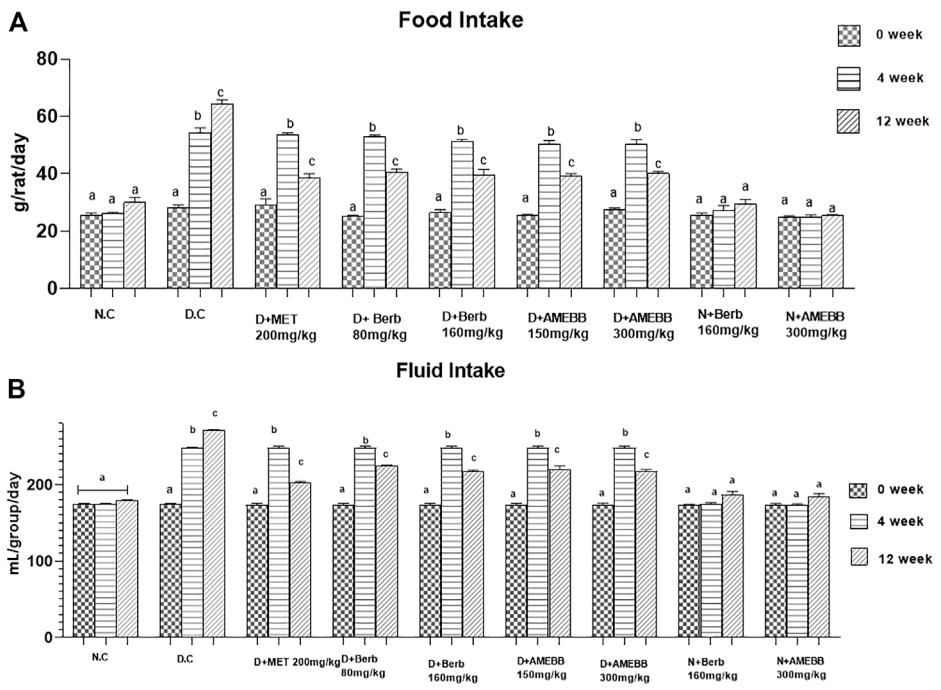

FIGURE 3
Effect of administration of *Berberis brandisiana* and berbamine on and food intake **(A)** fluid intake **(B)** in high fat diet and streptozotocin fed diabetic rats. Mean ± S.E.M (n = 6); are used to express the bars. Where N.C- Normal control, D.C- disease control, D + AMEBB–diabetic rats treated with aqueous methanolic extract of *Berberis brandisiana* (150 and 300 mg/kg), D + Berb–diabetic rats treated with aqueous solution of berbamine (80 and 160 mg/kg), D + MET-diabetic rats treated with metformin (200 mg/kg). $^{a, b, c}$ $p < 0.001$ shows comparisons of normal vs diabetic animals (student t-test) treatment vs diseased animals (Two Way ANOVA followed by Dunnett's test).

(30 ± 0.70, 38.4 ± 0.81), kidney, heart and aorta homogenates when compared with only HFD/STZ-exposed animals. Administration of AMEBB (150 and 300 mg/kg) and Berb (80 and 160 mg/kg) to HFD/STZ-fed diabetic rats caused significant ($p < 0.01$) decrease in MDA (nmol/g) levels in pancreas (7.34 ± 0.17, 6.22 ± 0.22), (7.34 ± 0.20, 6.34 ± 0.11) and in liver (9.08 ± 0.31, 8.18 ± 0.29), (9.34 ± 0.10, 8.86 ± 0.24) homogenates compared to the control group of animals. AMEBB and Berb also showed marked ($p < 0.001$) effect at higher dose vs. its effect at lower dose in tissue homogenates of pancreas, liver, kidney, heart and aorta (Figure 6).

10.3389/fphar.2023.1085013

TABLE 3 Effect of administration of *Berberis brandisiana* and berbamine on glucose insulin, and glycated hemoglobin levels in high fat diet and streptozotocin fed diabetic rats.

Groups	Diabetic parameters		
	Glucose (mg/dL)	Insulin (μU/mL)	HbA1c (%)
Control (NPD)	87 ± 1.09	16.6 ± 0.68	4.7 ± 0.05
Diabetic (HFD + STZ)	346 ± 13.27^{+++}	5.5 ± 0.22^{+++}	7.6 ± 0.18^{+++}
Diabetic + MET (200 mg/kg)	116.2 ± 1.07^{ab}	12.9 ± 0.39^{ab}	4.9 ± 0.02^{ab}
Diabetic + Berb (80 mg/kg)	242.4 ± 2.66^{ab}	8.3 ± 0.27^{ab}	5.3 ± 0.14^{ab}
Diabetic + Berb (160 mg/kg)	158 ± 4.57$^{ab/***}$	13 ± 0.09$^{ab/***}$	5.3 ± 0.07$^{ab/ns+}$
Diabetic + AMEBB (150 mg/kg)	156.4 ± 1.83^{ab}	12.1 ± 0.14^{ab}	5.2 ± 0.04^{ab}
Diabetic + AMEBB (300 mg/kg)	135.6 ± 2.62$^{ab/***}$	13.1 ± 0.24$^{ab/**}$	5 ± 0.05$^{ab/**}$
Control + Berb (160 mg/kg)	86.4 ± 0.75 ^{ns}	16.3 ± 0.04^{ns}	5.5 ± 0.08^{ns}
Control + AMEBB (300 mg/kg)	84 ± 0.78^{ns}	16.2 ± 0.22^{ns}	4.5 ± 0.06^{ns}

The values are depicted as Mean ± S.E.M. (n = 6); $+++p < 0.001$ shows comparisons of normal vs diabetic animals (student t-test); $^{a}p < 0.05$ and; ^{ab} $p < 0.01$ show comparison of treatment vs diseased animals (Dunnett's test followed One Way ANOVA); ns = non-significant; Where NPD: normal pallet diet; Diabetic: High fat diet/streptozotocin; MET: metformin; Berb: berbamine; AMEBB: aqueous methanolic extract of *berberis brandisiana*; HbA1c: glycosylated hemoglobin; ns^{+} (non-significant), $***p < 0.001$ and $** p < 0.01$ show the comparison between the effect of low vs. high dose of *Berberis brandisiana* and berbamine (student t-test).

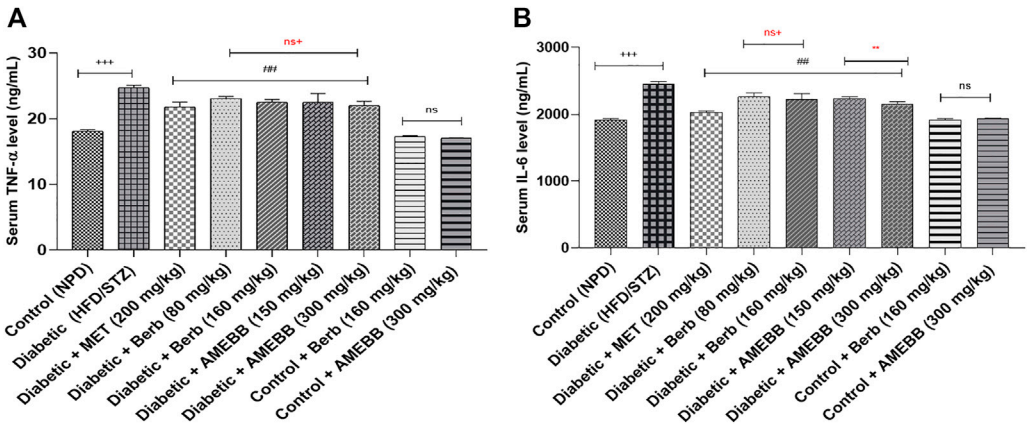

FIGURE 4
Effect of administration of *Berberis brandisiana* and berbamine on TNF- α **(A)** and IL-6 **(B)** in high fat diet and streptozotocin fed diabetic rats. The values are given as Mean ± S.E.M. (n = 6); $^{+++}p < 0.001$ shows comparisons of normal vs diabetic animals (student t-test); $^{###}p < 0.001$ shows comparison of treatment vs diseased animals (Dunnett's test followed One Way ANOVA); ns = non-significant; Where NPD: normal pallet diet; Diabetic: High fat diet/streptozotocin; MET: metformin; Berb: berbamine; AMEBB: Aqueous methanolic extract of *Berberis brandisiana*; IL-6: interleukin 6: TNF-α: Tumor necrosis factor alpha. ns^{+} (non-significant) and $**p < 0.01$ show the comparison between the effect of low vs. high dose of *B. brandisiana* and berbamine (student t-test).

Effect of AMEBB and Berb on serum biochemical parameters

Administration of AMEBB (150 and 300 mg/kg) and Berb (80 and 160 mg/kg) in hyperglycemic rats revealed a marked ($p < 0.001$) attenuation in triglycerides (TG), total cholesterol (TC), low-density lipoprotein (LDL), aspartate aminotransferase (AST), alanine transaminase (ALT), urea and creatinine levels compared to only HFD/STZ-exposed rats, similar to the effect of metformin. When AMEBB and Berb were administered to HFD/STZ-exposed diabetic rats, it caused a marked ($p < 0.001$) increase in HDL levels compared to only HFD/STZ challenged rats (Tables 4, 5).

Effect of AMEBB and Berb on histopathology of organs

The histopathological analysis of pancreas, liver, kidney, heart, and aortic sections from normal control and HFD/STZ-induced diabetic rats are presented in Figure 7.

Administration of AMEBB and Berb displayed an improvement in texture of islets of Langerhans in pancreas, betterment in disarray of hepatocytes, accumulation of fat droplets and inflammation of sinusoids in lives tissues. Restoration of normal glomerulus and absence of inflammatory cells was observed in kidney tissues. Isolated heart tissue of treated rats showed effective restoration of

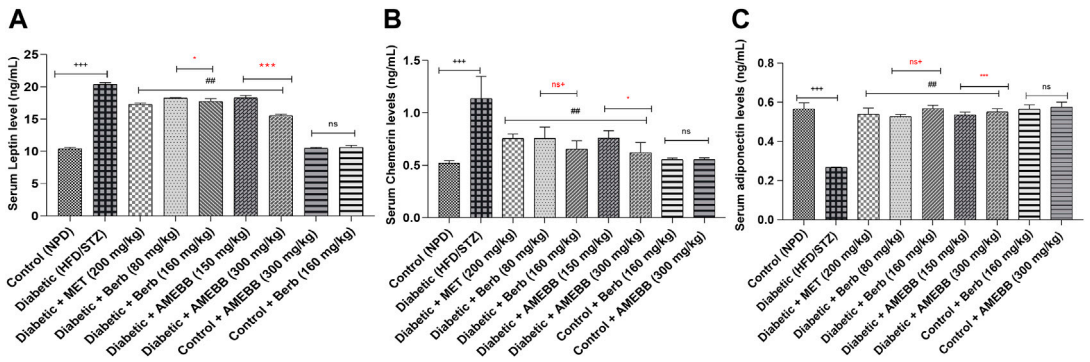

FIGURE 5
Effect of administration of *Berberis brandisiana* and berbamine on leptin **(A)**, Adiponectin **(B)** and Chemerin **(C)** in high fat diet and streptozotocin fed diabetic rats. The values are given as Mean ± S.E.M. (n = 6); $^{+++}p < 0.001$ shows comparisons of normal vs diabetic animals (student t-test); $^{\#\#}p < 0.01$ shows comparison of treatment vs diseased animals (One Way ANOVA followed by Dunnett's test); ns = non-significant; Where NPD: normal pallet diet; Diabetic: High fat diet/streptozotocin; MET: metformin; Berb: berbamine; AMEBB: Aqueous methanolic extract of *Berberis brandisiana*; ns^{+} (non-significant), $^{***}p < 0.001$ and $p < 0.05$ show the comparison between the effect of low vs. high dose of *B. brandisiana* and berbamine (student t-test).

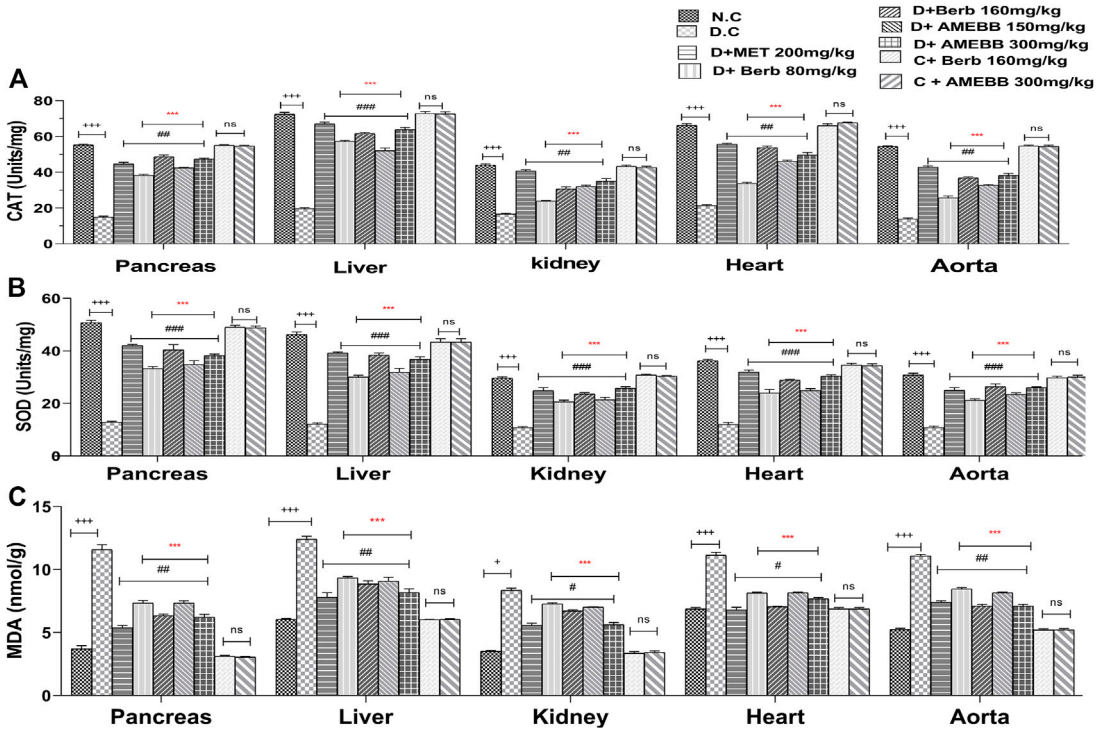

FIGURE 6
Effect of administration of *Berberis brandisiana* and berbamine on CAT **(A)**, SOD **(B)** and MDA **(C)** in high fat diet and streptozotocin-fed diabetic rats The values are given as Mean ± S.E.M. (n = 6); $^{+++}p < 0.001$ shows comparisons of normal vs diabetic animals (student t-test); $^{\#}p < 0.05$, $^{\#\#}p < 0.01$ and $^{\#\#\#}p < 0.001$, ns = non-significant show comparison of treatment vs diseased animals and comparison of normal vs normal treated animals (One Way ANOVA followed by Dunnett's test); Where NPD: normal pallet diet; Diabetic: High fat diet/streptozotocin; MET: metformin; Berb: berbamine; AMEBB: Aqueous methanolic extract of *Berberis brandisiana*; Catalase (CAT), superoxide dismutase (SOD), malondialdehyde (MDA); $^{***}p < 0.001$ shows the comparison between the effect of low vs. high dose of *B. brandisiana* and berbamine (student t-test).

myocytes and attenuation of inflammation. Whereas, aortic tissue sections of treated animals, showed significant upgrading in the deposition of elastic fibers and reduction in lipid deposition in tunica intima as detailed in Figure 7.

Effect on gene expression

The mRNA expressions of IRS-1, GLUT-4, SIRT 1, and ADAM 17 were assessed using Real time qPCR. The mRNA levels of ADAM

10.3389/fphar.2023.1085013

TABLE 4 Effect of administration of *Berberis brandisiana* and berbamine on Lipid Profile in high fat diet and streptozotocin-fed diabetic rats.

Groups	Lipid profile			
	TC (mg/dL)	TG (mg/dL)	HDL (mg/dL)	LDL (mg/dL)
Control (NPD)	121.6 ± 0.51	103.2 ± 0.97	46.6 ± 0.81	75 ± 0.20
Diabetic (HFD + STZ)	315.2 ± 4.49^{+++}	204.2 ± 0.66^{+++}	23 ± 0.58^{+++}	292 ± 0.40^{+++}
Diabetic + MET (200 mg/kg)	174.6 ± 1.21 ^{ab}	116.6 ± 0.68 ^{ab}	32.60 ± 0.40 ^{ab}	142 ± 0.20 ^{ab}
Diabetic + Berb (80 mg/kg)	183.6 ± 0.87 ^{ab}	124.8 ± 0.37 ^{ab}	35.8 ± 0.66 ^{ab}	148 ± 0.37 ^{ab}
Diabetic + Berb (160 mg/kg)	172.8 ± 1.53 $^{ab/***}$	117.4 ± 0.93 $^{ab/***}$	32.4 ± 0.25 $^{ab/***}$	140 ± 0.32 $^{ab/***}$
Diabetic + AMEBB (150 mg/kg)	185 ± 1.30 ^{ab}	125.8 ± 0.74 ^{ab}	36 ± 0.55 ^{ab}	149 ± 0.25 ^{ab}
Diabetic + AMEBB (300 mg/kg)	175.8 ± 1.07 $^{ab/***}$	115.2 ± 0.58 $^{ab/***}$	32.8 ± 0.66 $^{ab/***}$	143 ± 0.51 $^{ab/***}$
Control + Berb (160 mg/kg)	121 ± 0.32 ^{ns}	105.2 ± 0.37 ^{ns}	44.6 ± 1.44^{+}	76.4 ± 1.24 ^{ns}
Control + AMEBB (300 mg/kg)	121 ± 0.22 ^{ns}	105.8 ± 0.37 ^{ns}	45 ± 0.71^{+}	76 ± 0.92 ^{ns}

The values are depicted as Mean ± S.E.M. (n = 6); $+++p < 0.001$ shows comparisons of normal vs diabetic animals (student t-test); ^{a} $p < 0.05$ and ^{ab} $p < 0.01$ show comparison of treatment vs diseased animals (One Way ANOVA, followed by Dunnett's test); ns = non-significant; Where NPD: normal pallet diet; Diabetic: High fat diet/streptozotocin; MET: metformin; Berb: berbamine; AMEBB: aqueous methanolic extract of *Berberis brandisiana*; total cholesterol (TC) triglycerides (TGs), high-density lipoprotein (HDL) low-density lipoprotein (LDL); $***p < 0.001$ shows the comparison between the effect of low vs. high dose of *B. brandisiana* and berbamine (student t-test).

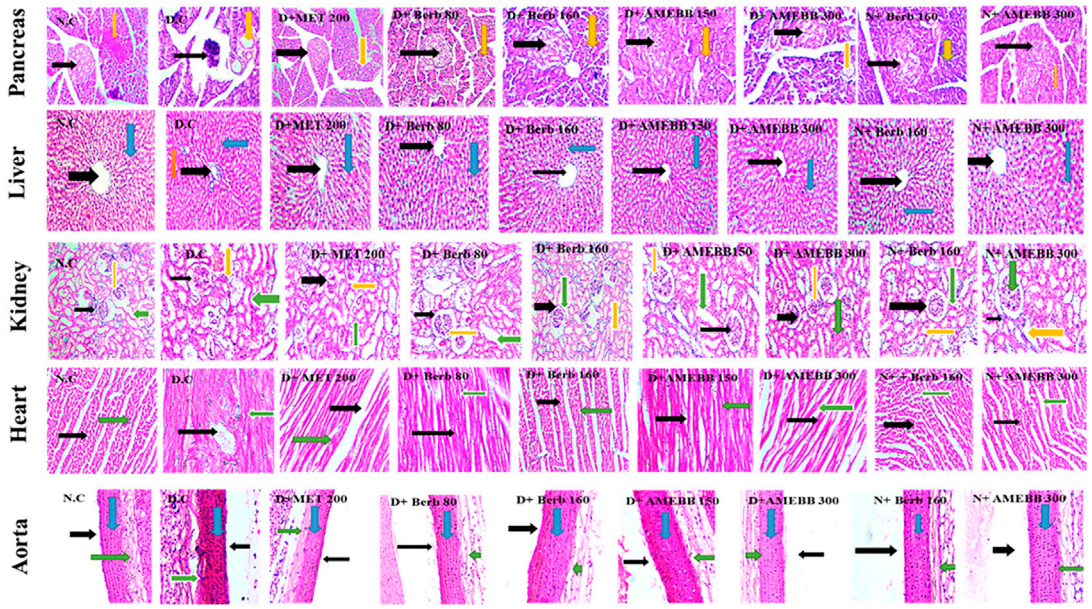

FIGURE 7
Photomicrographic representation of pancreatic tissue, Liver, kidney, heart and aorta sections showing the influence of administration of Berb: Berbamine (80 and 160 mg/kg body weight) and AMEBB: Aqueous methanolic extract of *Berberis brandisiana* (150 and 300 mg/kg body weight) respectively in HFD/STZ-induced diabetic (D.C) and normal rats (N.C). Pancreas: Black and yellow arrows respectively show pancreatic islets and exocrine parts of pancreas. Liver: Black, red and blue arrows respectively show: central vein, plates of hepatic cells and sinusoids. Kidney: Black, yellow and green arrows respectively show bowman capsule, glomerulus and distil proximal convoluted tubule. Heart: Black, and green arrows respectively show nuclei of cardiomyocytes and myofibers. Aorta: Black, blue and green arrows respectively show lumen, tunica intima, and tunica adventia.

17 gene were markedly ($p < 0.001$) upregulated by 3.33 fold compared to data of control animals. When compared to the normal control group, IRS-1, GLUT-4, and SIRT 1 were significantly ($p < 0.001$) downregulated by 1.5, 1.9, and 0.33 fold, respectively, in HFD/STZ-exposed groups. In comparison to HFD/STZ-induced diabetic groups, administration of AMEBB and Berb upregulated IRS-1, GLUT-4, and SIRT 1, while caused downregulation of ADAM 17 in liver tissues, results in restoration of the expression of genes of interest towards normal. AMEBB and Berb also showed marked effect at higher dose vs. its

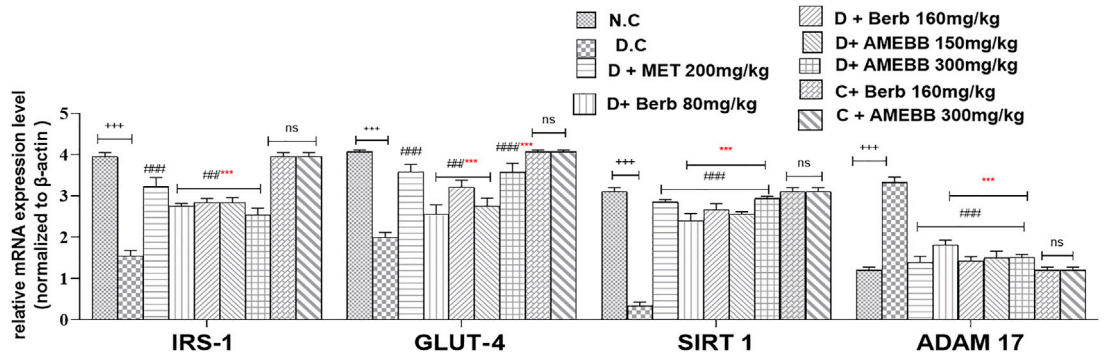

FIGURE 8
Effect of administration of *Berberis brandisiana* and berbamine on IRS-1, GLUT-4, SIRT 1, ADAM 17 mRNA level in high fat diet and streptozotocin fed diabetic rats. Values are expressed as Mean ± S.E.M, n = 6; $^{+++}p < 0.001$ shows comparisons of normal vs diabetic animals (student t-test). $^{\#\#}p < 0.01$ and $^{\#\#\#}p < 0.001$ show comparison of treatment vs diseased animals (One Way ANOVA followed by Dunnett's test); ns = non-significant; Where NPD: normal pallet diet; Diabetic: High fat diet/streptozotocin; MET: metformin; Berb: berbamine; AMEBB: Aqueous methanolic extract of *Berberis brandisiana;* IRS-1: insulin receptor substrate-1; GLUT-4: glucose transporter −4; SIRT 1; sirtuin 1; ADAM 17: A disintegrin and A metalloproteinase 17; $^{***}p < 0.001$ shows the comparison between the effect of low vs. high dose of *B. brandisiana* and berbamine (student t-test).

TABLE 5 Effect of administration of *Berberis brandisiana* and berbamine on LFTs and RFTs in high fat diet and streptozotocin-fed diabetic rats.

Groups	LFTs and RFTs			
	AST (U/L)	ALT (U/L)	Urea (mmol/L)	Creatinine (μmol/L)
Control (NPD)	113.8 ± 0.58	81.4 ± 0.510	12.3 ± 0.20	34.6 ± 0.25
Diabetic (HFD + STZ)	271 ± 1.11^{+++}	181 ± 0.45^{+++}	36.2 ± 1.24^{+++}	73.8 ± 1.46^{+++}
Diabetic + MET (200 mg/kg)	166.4 ± 0.82 ^{ab}	104.4 ± 0.68 ^{ab}	14.6 ± 0.40 ^{ab}	38.8 ± 0.37 ^{ab}
Diabetic + Berb (80 mg/kg)	175.4 ± 0.25 ^{ab}	132.8 ± 0.37 ^{ab}	17.8 ± 0.12 ^{ab}	52.2 ± 0.38 ^{ab}
Diabetic + Berb (160 mg/kg)	173.2 ± 0.37 $^{ab/***}$	120.6 ± 1.40 $^{ab/***}$	16.2 ± 0.12 $^{ab/***}$	41 ± 0.45 $^{ab/***}$
Diabetic + AMEBB (150 mg/kg)	177.6 ± 1.08 ^{ab}	132 ± 0.55 ^{ab}	18 ± 0.32 ^{ab}	51.6 ± 0.51^{ab}
Diabetic + AMEBB (300 mg/kg)	175.6 ± 0.51 $^{ab/ns+}$	121.8 ± 156 $^{ab/***}$	16.2 ± 0.242$^{ab/***}$	42.3 ± 0.54 ^{ab***}
Control + Berb (160 mg/kg)	114.2 ± 0.37 ^{ns}	80.8 ± 0.37 ^{ns}	12.2 ± 0.20 ^{ns}	34 ± 0.55 ^{ns}
Control + AMEBB (300 mg/kg)	114 ± 0.32 ^{ns}	80 ± 0.37 ^{ns}	12.6 ± 0.25 ^{ns}	34 ± 0.55 ^{ns}

The values are depicted as Mean ± S.E.M. (n = 6); $+++p < 0.001$ shows comparisons of normal vs diabetic animals (student t-test); ^{ab} $p < 0.01$ shows comparison of treatment vs. diseased animals (One Way ANOVA, followed by Dunnett's test); ns = non-significant; Where NPD: normal pallet diet; Diabetic: High fat diet/streptozotocin; MET: metformin; Berb: berbamine; AMEBB: aqueous methanolic extract of *berberis brandisiana*; aspartate transaminase (AST) alkaline phosphatase (ALT); ns^{+} (non-significant) and $^{***}p < 0.001$ show the comparison between the effect of low vs. high dose of *B. brandisiana* and berbamine (student t-test).

effect at lower dose in mRNA levels of IRS-1, GLUT-4 and SIRT1 (Figure 8).

Statistical analysis

Graph Pad Prism 8.4.3 was used for analysis and graphical presentation of the data. Values were displayed as mean ± standard error of the mean (SEM). For comparison of the data in different groups One-way analysis of variance (ANOVA) followed by Dunnett's test or Two-way analysis of variance (ANOVA) followed by Dunnett's test for multiple comparisons were used. $p < 0.05$ was considered significantly different.

Discussion

Diabetes related morbidity and mortality are posing a continuous harmful impact on health systems around the globe. Additionally, nutritional fat consumption reduces glucose utilization mediated by insulin and endorses insulin resistance in diabetics. Further, 40 mg/kg streptozotocin administration to HFD-fed rats cause β-cells necrosis, resulting in deficiency of insulin and development of diabetes (Pratiwi et al., 2021). To assess the efficacy of a test material for its insulin sensitizing and/or insulin secretory properties, high fat and streptozotocin-fed animal model is considered appropriate. Similar models have been used in numerous labs (Sakashita et al., 2021). Traditional use of *B. brandisiana* in the treatment of diabetes (Jan et al., 2008) provide basis for further studies to strengthen its potential use as

antidiabetic agent. *B. brandisiana* has also been found enriched with berbamine (Khan et al., 2016). *B. brandisiana* and berbamine are known for their antioxidant, anti-inflammatory, hepatoprotective and cardiovascular beneficial effects (Sankaranarayanan et al., 2018). This study has been designed to assess the ameliorating potential of the aqueous methanolic extract of *B. brandisiana* (AMEBB) and berbamine in HFD/STZ-induced diabetic rats.

The HPLC analysis showed variety of phenolic acids and flavonoids in AMEBB including, quercetin, gallic acid, caffeic acid, benzoic acid, ferulic acid, chologenic acid, syringic acid, m-coumaric acid, p-coumaric acid and ferulic acid. Most of these metabolites (flavonoids, m-coumaric acid, p-coumaric acid, quercetin, gallic acid) are known to boost insulin sensitivity, slow down the rate, digestion and absorption of sugar, hence supporting their protective effects in diabetes (Mihaylova et al., 2018; Sankaranayanan et al., 2018).

Administration of high fat diet for 56 days along with streptozotocin develop glucose intolerance, insulin resistance, β-cell destruction, alterations in inflammatory biomarkers (TNF-α, IL-6), adipocytokines (leptin, chemerin and adiponectin) levels, oxidative stress biomarkers (CAT,SOD and MDA) and diabetic candidate genes like IRS-1. GLUT-4, SIRT 1 and ADAM 17. Treatment with AMEBB and Berb to HFD/STZ-administered rats from 28th day of induction period, resulted in weight gain, increased food consumption and fluid intake compared to non-diabetic rats during the experimental period. Although the food intake of diabetic rats was increased during the experimental period, the weight gain was significantly reduced. It has been reported that diabetes is associated with weight loss, polydipsia, polyphagia and polyuria (Peng et al., 2021). Energy metabolism is compromised in hepatic tissue, thus a low energy state is stimulated for satiety center and food consumption is increased in diabetes mellitus. As hepatic energy influences feeding behavior, hence in turn affects body weight (Rawlinson and Andrews, 2021). High fat diet-fed rats showed increase in body weight over a 4-week period due to its deposition in a variety of body fat packs. Weight gain was significantly ($p < 0.01$) reduced during the experimental period while food intake of diabetic rats was increased. In diabetic rats, the inability to use carbohydrates as an energy source, combined with poor glycemic control, causes extreme protein catabolism in order to supply amino acids for gluconeogenesis, resulting in muscle deterioration and weight loss during insulin deficiency (Kumar et al., 2021). Flavonoids have previously been identified as active metabolites of AMEBB, and are known for their slimming properties (Yin et al., 2022). In comparison to normal control, osmotic diuresis increases fluid consumption only in high fat diet (HFD) and streptozotocin (STZ) exposed rats. Oral administration of AMEBB and Berb considerably ($p < 0.01$) improved body weight and normalized food and fluid consumption in treated rats, indicating an improvement in glycemic control as previously reported (Sankaranarayanan et al., 2018).

Persistent hyperglycemia causes non-enzymatic glycation of proteins, including lens crystalline protein and hemoglobin. In uncontrolled diabetes, glycosylation of hemoglobin occurs gradually and is proportional to fasting blood glucose levels. According to Babaya et al. (2021), a persistent increase in HbA1c level was related with failure of β-cell function. Under hyperglycemic condition due to HFD/STZ-exposure, levels of HbA1c were higher in diabetic rats vs. normal control rats. When compared to only HFD/STZ-exposed rats, Berb and AMEBB administration decreased glucose and HbA1c levels in diabetic rats. Earlier reports have revealed that antioxidant constituents are known to inhibit glycation of protein associated with diabetes (Sarmah and Roy, 2021). These aspects offer support to the antidiabetic effect of AMEBB and Berb. HPLC analysis confirmed the presence of flavonoids such as gallic acid, quercetin and polyphenols as active plant metabolites. The presence of such advantageous metabolites contributes to the assessed benefits of AMEBB as well.

Present study showed administration of AMEBB and Berb significantly ($p < 0.01$) decreased serum TNF-α and IL-6 levels compared to only HFD/STZ-administered rats. Administration of HFD for 4 weeks helps in progression of obesity (Leite et al., 2021). Obese adipose tissues secrete a number of pro-inflammatory cytokines, including TNF-α and IL-6. There is emerging evidence that increased pro-inflammatory cytokine release is linked to development of insulin resistance because of β-cell degradation and has been reported to increase diabetes related complication (Heo et al., 2021). The AMEBB and Berb significantly modified TNF-α and IL-6 levels which is also supported by earlier studies on the part of other botanical drugs (Zheng et al., 2021).

Adipocytokines are secreted by adipose tissues and are known to contribute in defective insulin secretion and action, resulting in peripheral insulin resistance (Deng et al., 2021). Obesity-related diseases have been linked to the deficiency of adiponectin, such as diabetes, insulin resistance and cardiovascular diseases. Findings of our study are in line with earlier study of Achari and Jain. (2017). Leptin, also known as "anorexigenic" hormone, promotes oxidation of fatty acids and lipolysis while preventing lipogenesis. Other than obesity, hyperleptinemia has been linked to insulin resistance. Chronic hyperlipidemia imparts negative impact on leptin function as decribed by López-Jaramillo et al. (2014). Chemerin is a relatively new adipokine that has been discovered to have endocrine, paracrine, and autocrine functions. It also plays important role in lipid and glucose homeostasis, angiogenesis, inflammation, immune modulation and blood pressure regulation (Roman et al., 2012). The current study found a link between AMEBB and Berb supplementation and adipocytokines levels in diabetic rats. Lower levels of leptin and chemerin and higher level of adiponectin were observed in diabetic rats treated with AMEBB and Berb. AMEBB and Berb showed dose dependent effects.

The CAT and SOD levels were markedly ($p < 0.01$) increased in AMEBB (150 and 300 mg/kg) and Berb (80 and 160 mg/kg) treated groups compared to HFD/STZ-exposed rats. SOD and CAT are antioxidant enzymes that serve as the first line of defense against ROS in cells, scavenging the toxic intermediate of partial oxidation. Decrease in the levels of these antioxidant enzymes results in an additional molecular oxygen and hydrogen peroxide, which produces reactive hydroxyl free radicals and leads to the lipid peroxidation (Repetto et al., 2012). Superoxide dismutase enzyme protects cells from reactive oxygen species by scavenging molecular oxygen, which causes damage to membrane and biological structure (Ighodaro and Akinloye, 2018). The decrease in catalase activity happens due to the enzyme being inactivated by glycation. AMEBB and Berb treatment increased the levels of SOD and CAT in diabetic rats compared to only HFD/STZ-induced diabetic rats. Indeed, the return of SOD levels promoted by AMEBB and Berb may hasten the superoxide dismutation to hydrogen peroxide, which is rapidly

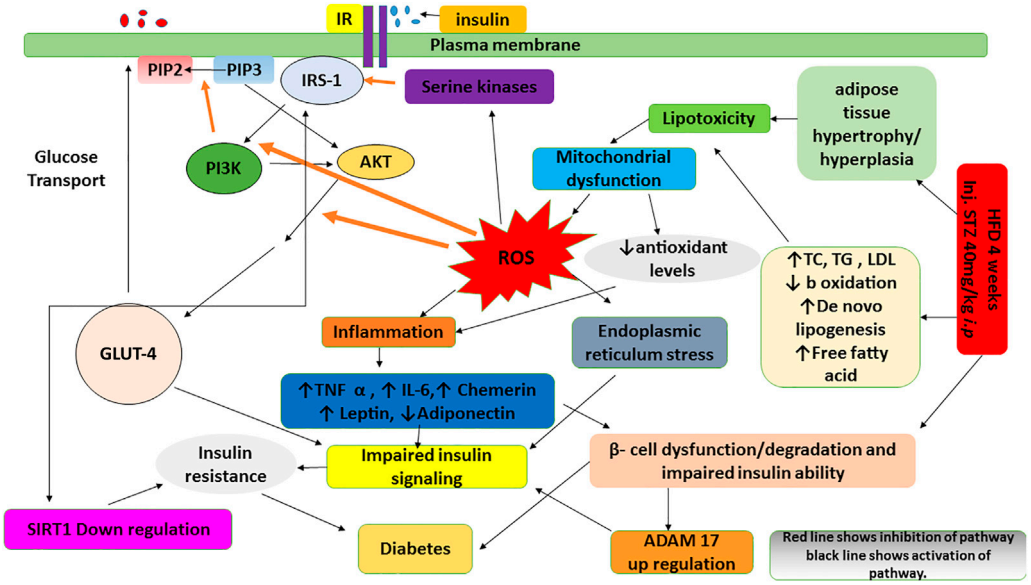

FIGURE 9
A flow diagram highlighting the effect of administration of high fat diet and streptozotocin on the production of reactive oxygen species and the cross talk of insulin signaling pathway (IRS-1, GLUT4, SIRT1 and ADAM 17) with PI3K/AKT pathway.

detached by CAT, protecting diabetic animal tissues from highly toxic hydroxyl ion free radicals, result in avoiding lipid peroxidation. These results are also in line with earlier study of Aboonabi et al. (2014).

An abnormal blood lipid profile is another symptom of insulin resistance. The current study found that diabetic rats had higher total cholesterol (TC), triglycerides (TG), low-density lipoprotein (LDL), and lower HDL levels. These changes are endorsed to an increase in free fatty acid flux into the liver as a result of insulin deficiency or insulin resistance which results in an excess accumulation of fatty acid in liver and conversion to triglycerides (Adiels et al., 2008). The inability of insulin to inhibit the liberation of free fatty acids results in increased VLDL production in the liver (Pilz and März, 2008). When VLDL and TG levels rise, the activation of lipoprotein lipase and lecithin acyl-cholesterol transferase, results in decrease HDL and an increase in the concentration of LDL particles (Sharma et al., 2010). High levels of cholesterol in HFD/STZ-induced diabetic animals may be due to increased dietetic cholesterol captivation from the small intestine succeeding high fat diet consumption in the diabetic condition (Naidu et al., 2015). Furthermore, hypertriglyceridemia may increase triglycerides absorption in the form of chylomicrons as a result of over consumption of fat-rich diet. The AMEBB and Berb treatment showed noticeable ($p < 0.01$) decrease in, TG, TC, LDL and increase in HDL levels. Dietary polyphenols, on the other hand, effectively reduce the amount of lipoprotein rich in triglycerides and are linked to oxidative stress in postprandial and fasting conditions (Vries et al., 2014).

High concentrations of AST, ALT are typical indicators of liver dysfunction often observed in HFD-fed and STZ induced diabetic animals. Observed increase in AST and ALT levels may be due to the outflow of enzymes from cytosol of hepatocytes into the blood stream. The AMEBB and Berb treatment significantly ($p < 0.01$) decreased levels of these elevated enzymes and subsequently relieved liver injury. Increased levels of creatinine and urea in the serum of diabetic animals were found to be strongly correlated with renal damage. Renal tissue depletion in diabetic rats was caused by the production of reactive oxygen species as a result of elevated free radical concentrations in these tissues (El-Alfy et al., 2005). In our study, diabetic rats treated with AMEBB and Berb had significant ($p < 0.01$) reduction in serum urea and creatinine levels and restored renal structural parameters in diabetic rats, possibly by neutralizing free radicals in biological systems.

The histopathological data revealed that treatment with AMEBB and Berb improved in β-cell mass and islets of Langerhans in pancreatic tissues when compared with only HFD/STZ-exposed rats. Histograms of diabetic rat hepatic sections showed hepatocytes degeneration and inflamed sinusoids. Treatment with AMEBB and Berb protected hepatic lesions and inflammation. In diabetic group, kidney tissue sections showed degenerated renal tubules and inflammation, whereas AMEBB and Berb treatment resulted in revival of renal tubules damage and inflammation. Heart tissue of treated rats showed effective restoration of myocytes and attenuation of inflammation. Whereas, aortic tissues of treated groups showed significant upgrading in deposition of elastic fibers and reduction in lipid deposition in tunica intima.

Administration of HFD/STZ causes activation PI3K/AKT pathway through production of reactive oxygen species (ROS). ROS and PI3K/AKT pathway is indirectly involved in mediation of insulin signaling *via* IRS-1, GLUT-4, SIRT 1 and ADAM 17. The observed antidiabetic effects of *B. brandisiana* and berbamine were found in line with the estimated expression of mRNA of IRS-1, GLUT-4, SIRT 1 and ADAM 17 as elaborated in Figure 9.

IRS-1 plays important role in the signal transduction pathway stimulated by insulin and connecting receptor of insulin to its ultimate biological actions through intermediate effectors. IRS-1 regulation differs in the liver as it has been observed in diabetic animals,

which may result in distinctive changes in insulin levels in liver tissue and contribute to insulin resistance in liver. mRNA expression of IRS-1 was found lower in the livers of HFD/STZ-induced diabetic rats while the treatment of AMEBB and Berb upregulated mRNA expression of IRS-1, a key contributor in insulin resistance. Our finding is also in line with an earlier study (Zheng et al., 2011). ROS is known to play a part in activation of intracellular stress kinases and inhibition of IRS-1, thus potentially influencing insulin signaling and to promote *via* GLUT-4 translocation and down streaming of AKT resulting in insulin resistance, obesity and diabetes mellitus (Li et al., 2022). mRNA expression of GLUT-4 is downregulated in HFD/STZ-induced diabetic rats, indicating that insulin acts as a positive regulator of gene expression and explains the impaired glucose disposal. Administration of AMEBB and Berb upregulated mRNA expression of GLUT-4, thus offering protective potential of the treatment in insulin resistance and diabetes. SIRT1 controls insulin secretion by preserving pancreatic β-cells, improves insulin resistance, inflammation, mitochondrial function, controls oxidation of fatty acid and regulates hepatic glucose production. Therefore, for the treatment of insulin resistance and diabetes, SIRT1 is a favorable pharmacological target (Kitada and Koya, 2013). In our study, mRNA expression of SIRT 1 in hepatic tissues was found upregulated in HFD/STZ–exposed rats, while treatment showed is downregulation, hence supporting its protective potential against high fat diet-induced hepatic steatosis (Li et al., 2011), insulin sensitivity and oxidative stress possibly mediated through AKT pathway. These findings are also supported by earlier study of Abedimanesh et al. (2022). Similarly, medicinally active plants containing flavonoids are known to reduce SIRT 1 expression in hepatocytes (Sung et al., 2015). Diabetes is known to cause an increase in ADAM 17 overexpression due to a decrease in antioxidants and/or rise in ROS. It is reported that TNF-α has been linked to signaling pathway of insulin impairment by increasing serine phosphorylation of IRS-1, which inhibits activity of tyrosine kinase resulting in impaired downstream signaling and development of insulin resistance. Administration of AMEBB and Berb caused downregulation of mRNA expression of ADAM17 in hepatic tissues, thus offering it potential utility for the treatment of diabetes. These findings are also in line with earlier findings on another medical plant (Matthews et al., 2021). In current study, the decreased levels of mRNA of IRS-1, GLUT-4, SIRT1 and increased levels of mRNA of ADAM17 in diabetic animals, while treatment groups showed increased levels of mRNA of IRS-1, GLUT-4, SIRT1 and decreased level of mRNA of ADAM17. This helps to correlate that observed efficacy of test materials might have been achieved because of the improved insulin action which is an outcome of insulin signaling ultimately through modulation of mRNA levels of IRS-1, GLUT-4, SIRT1 and ADAM17. Our findings are also in line with earlier studies (Balbaa et al., 2016).

Conclusion

This study demonstrates that *B. brandisiana* and Berb possess antidiabetic effects possibly mediated through attenuation of oxidative stress, glucose metabolism, inflammatory biomarkers and adipocytokines levels. Further the downregulation of IRS-1, SIRT1 and GLUT-4 and upregulation of ADAM 17 demonstrates its potential impact on glucose homeostasis, insulin resistance and chronic inflammatory markers. Thus, this study provides scientific basis to the medicinal use of *B. brandisiana* and berbamine in diabetes.

Innovation

- It is the pioneer study showing the anti-diabetic potential of *B. brandisiana* Ahrendt in HFD and STZ-fed animals.
- Quantitative expression of mRNA of diabetic candidate genes like, IRS-1, SIRT 1, GLUT-4 and ADAM17 were studied for their role on the part of protective potential of AMEBB and Berb in diabetes.
- AMEBB and Berb demonstrated anti-inflammatory and antioxidant potential, thus providing additional support to the anti-diabetic effects of AMEBB and Berb.

Data availability statement

The original contributions presented in the study are included in the article/supplementary materials, further inquiries can be directed to the corresponding author.

Ethics statement

The animal study design was reviewed and approved by the Ethical Review committee of Government College University, Faisalabad, Pakistan (Ref.No. GCUF/ERC/50). Laboratory animals were used in this study as per approved protocol.

Author contributions

MHM developed the concept of study and layout of the project. He has supervised this project completely and has also been involved in data acquirement and analysis, writing, reviewing and submission of the manuscript. SM has been involved in concept design, performance of experiments, data collection, analysis and manuscript writing. MGA has been involved in data collection, analysis, manuscript writing and reviewing. UAA has been involved in quantitative analysis of candidate genes of diabetes studied in this manuscript and has also been involved in reviewing of the manuscript.

Acknowledgments

We are thankful to the animal house assistants and Department of Pharmacology, Faculty of Pharmaceutical Sciences, Government College University, Faisalabad, for support from conduction to conclusion of the study.

Conflict of interest

The authors declare that the research was conducted in the absence of any commercial or financial relationships that could be construed as a potential conflict of interest.

Publisher's note

References

Abdulghafoor, H. A., Ramadhan, S. J., and Nawfal, A, J. (2021). Therapeutic effects of allicin against the diabetes mellitus induced by streptozotocin in male rats. *Nveo-natural volatiles Essent. oils Journal| NVEO* 8, 8934–8945.

Abedimanesh, N., Nouri, M., Mohammadnejad, K., Barati, M., Dabardani, E., Kakavand, E., et al. (2022). Vinca herbacea extract suppresses NF-kB signaling and modulates SIRT1/AMPK/PGC1α Axis to exert antidiabetic effects in streptozotocin-induced diabetic rats. *Res. J. Pharmacogn.* 9, 1–15.

Aboonabi, A., Rahmat, A., and Othman, F. (2014). Antioxidant effect of pomegranate against streptozotocin-nicotinamide generated oxidative stress induced diabetic rats. *Toxicol. Rep.* 1, 915–922.

Achari, A. E., and Jain, S. K. (2017). Adiponectin, a therapeutic target for obesity, diabetes, and endothelial dysfunction. *Int. J. Mol. Sci.* 18, 1321. doi:10.3390/ijms18061321

Adiels, M., Taskinen, M. R., and Borén, J. (2008). Fatty liver, insulin resistance, and dyslipidemia. *Curr. diabetes Rep.* 8, 60–64. doi:10.1007/s11892-008-0011-4

Al-Mansoori, L., Al-Jaber, H., Prince, M. S., and Elrayess, M. A. (2021). Role of inflammatory cytokines, growth factors and adipokines in adipogenesis and insulin resistance. *Inflammation* 45, 1–14. doi:10.1007/s10753-021-01559-z

Aljohani, A. S., Ahmed, A. A., Althwab, S. A., Alkhamiss, A. S., Rasheed, Z., Fernández, N., et al. (2022). Gene expression of glutathione S-transferase alpha, glutathione S-transferase rho, glutathione peroxidase, uncoupling protein 2, cytochrome P450 1a, heat shock protein 70 in liver of Oreochromis niloticus upon exposure of microcystin-Lr, microcystin-rr and toxic cyanobacteria crude. *Gene Rep.* 26, 101498. doi:10.1016/j.genrep.2022.101498

Al-Kuraishy, H. M., Al-Gareeb, A. I., Alblihed, M., Cruz-Martins, N., and Batiha, G. E. S. (2021). COVID-19 and risk of acute ischemic stroke and acute lung injury in patients with type ii diabetes mellitus: The anti-inflammatory role of metformin. *Front. Med.* 110.

Aumeeruddy, M. Z., and Mahomoodally, M. F. (2021). Ethnomedicinal plants for the management of diabetes worldwide: A systematic review. *Curr. Med. Chem.* 28 (23), 4670–4693.

Ayaz, M., Nawaz, A., Ahmad, S., Mosa, O. F., Eisa Hamdoon, A. A., Khalifa, M. A., et al. (2022). Underlying anticancer mechanisms and synergistic combinations of phytochemicals with cancer chemotherapeutics: Potential benefits and risks. *J. Food Qual.* 2022, 1–15. doi:10.1155/2022/1189034

Aziz, N., Mehmood, M. H., and Gilani, A. H. (2013). Studies on two polyherbal formulations (ZPTO and ZTO) for comparison of their antidyslipidemic, antihypertensive and endothelial modulating activities. *BMC Complementary Altern. Med.* 13 (1), 371–379. doi:10.1186/1472-6882-13-371

Babaya, N., Noso, S., Hiromine, Y., Taketomo, Y., Niwano, F., Yoshida, S., et al. (2021). Relationship of continuous glucose monitoring-related metrics with Hba1c and residual B-cell function in Japanese patients with type 1 diabetes. *Sci. Rep.* 11, 4006–4009. doi:10.1038/s41598-021-83599-x

Balbaa, M., El-Zeftawy, M., Ghareeb, D., Taha, N., and Mandour, A. W. (2016). Nigella sativa relieves the altered insulin receptor signaling in streptozotocin-induced diabetic rats fed with a high-fat diet. *Oxidative Med. Cell. Longev.* 2016, 2492107. doi:10.1155/2016/2492107

Batista, T. M., Haider, N., and Kahn, C. R. (2021). Defining the underlying defect in insulin action in type 2 diabetes. *Diabetologia* 64, 994–1006. doi:10.1007/s00125-021-05415-5

Bhardwaj, D., and Kaushik, N. (2012). Phytochemical and pharmacological studies in genus Berberis. *Phytochem. Rev.* 11, 523–542. doi:10.1007/s11101-013-9272-x

Bhatti, J. S., Sehrawat, A., Mishra, J., Sidhu, I. S., Navik, U., Khullar, N., et al. (2022). Oxidative stress in the pathophysiology of type 2 diabetes and related complications: Current therapeutics strategies and future perspectives. *Free Radic. Biol. Med.* 184, 114–134. doi:10.1016/j.freeradbiomed.2022.03.019

Biglari, F., AlKarkhi, A. F., and Easa, A. M. (2008). Antioxidant activity and phenolic content of various date palm (Phoenix dactylifera) fruits from Iran. *Food Chem.* 107 (4), 1636–1641. doi:10.1016/j.foodchem.2007.10.033

Camaya, I., Donnelly, S., and O'Brien, B. (2022). Targeting the pi3k/akt signaling pathway in pancreatic β-cells to enhance their survival and function: An emerging therapeutic strategy for type 1 diabetes. *J. Diabetes* 14, 247–260. doi:10.1111/1753-0407.13252

Chander, V., Aswal, J., Dobhal, R., and Uniyal, D. (2017). A review on pharmacological potential of berberine; an active component of himalayan Berberis aristata. *J. Phytopharm.* 6, 53–65. doi:10.31254/phyto.2017.6108

Dar, O., Lawrence, R., and Dar, S. (2014). HPLC, antioxidant and antibacterial activities of methanolic extract of Berberis aristata stem. *Int. J. Sci. Res.* 3 (11), 1137–1141.

Deng, Y., Li, N., Wu, Y., Wang, M., Yang, S., Zheng, Y., et al. (2021). Global, regional, and national burden of diabetes-related chronic kidney disease from 1990 to 2019. *Front. Endocrinol.* 12, 672350.

Durmaz, L., Kiziltas, H., Guven, L., Karagecili, H., Alwasel, S., and Gulcin, İ. (2022). Antioxidant, antidiabetic, anticholinergic, and antiglaucoma effects of magnofluorine. *Molecules* 27 (18), 5902. doi:10.3390/molecules27185902

Eguchi, N., Vaziri, N. D., Dafoe, D. C., and chii, H. (2021). The role of oxidative stress in pancreatic B cell dysfunction in diabetes. *Int. J. Mol. Sci.* 22, 1509. doi:10.3390/ijms22041509

El-Alfy, A. T., Ahmed, A. A., and Fatani, A. J. (2005). Protective effect of red grape seeds proanthocyanidins against induction of diabetes by alloxan in rats. *Pharmacol. Res.* 52, 264–270. doi:10.1016/j.phrs.2005.04.003

Farooqi, A. A., Wen, R., Attar, R., Taverna, S., Butt, G., and Xu, B. (2022). Regulation of cell-signaling pathways by berbamine in different cancers. *Int. J. Mol. Sci.* 23 (5), 2758. doi:10.3390/ijms23052758

Feng, L., Chen, M., Li, Y., Li, M., Hu, S., Zhou, B., et al. (2021). SIRT1 deacetylates and stabilizes P62 to promote hepato-carcinogenesis. *Cell. death Dis.* 12, 405–413. doi:10.1038/s41419-021-03666-z

Gall, A., Butler, T. L., Lawler, S., and Garvey, G. (2021). Traditional, complementary and integrative medicine use among indigenous peoples with diabetes in Australia, Canada, New Zealand and the United States. *Aust. N. Z. J. Public Health* 45, 664–671. doi:10.1111/1753-6405.13120

Gülçin, İ., Bingöl, Z., Taslimi, P., Gören, A. C., Alwasel, S. H., and Tel, A. Z. (2022). Polyphenol contents, potential antioxidant, anticholinergic and antidiabetic properties of mountain mint (cyclotrichium leucotrichum). *Chem. Biodivers.* 19 (3), e202100775. doi:10.1002/cbdv.202100775

Han, B., Kou, S., He, K., Han, Y., Wang, Y., Huang, T., et al. (2018). Anti-hypercholesterolemic effect of berbamine isolated from *Rhizoma Coptidis* in hypercholesterolemic zebrafish induced by high-cholesterol diet. *Iran. J. Pharm. Res. IJPR* 17 (1), 292–306.

Heo, E., Kim, E., Jang, E. J., and Lee, C. H. (2021). The cumulative dose-dependent effects of metformin on the development of tuberculosis in patients newly diagnosed with type 2 diabetes mellitus. *BMC Pulm. Med.* 21, 303–311. doi:10.1186/s12890-021-01667-4

Hong, H., Xu, Y., Xu, J., Zhang, J., Xi, Y., Pi, H., et al. (2021). Cadmium exposure impairs pancreatic β-cell function and exaggerates diabetes by disrupting lipid metabolism. *Environ. Int.* 149, 106406. doi:10.1016/j.envint.2021.106406

Ighodaro, O. M., and Akinloye, O. A. (2018). First line defence antioxidants-superoxide dismutase (SOD), catalase (CAT) and glutathione peroxidase (GPX): Their fundamental role in the entire antioxidant defence grid. *Alexandria J. Med.* 54 (4), 287–293.

Jan, G., Khan, M., and Gul, F. (2008). Ethnomedicinal plants used against diarrhea and dysentery in Dir Kohistan valley (NWFP), Pakistan. *Ethnobot. Leafl.* 12, 620–637.

Javaid, F., Mehmood, M. H., and Shaukat, B. (2021). Hydroethanolic extract of A. Officinarum hance ameliorates hypertension and causes diuresis in obesogenic feed-fed rat model. *Front. Pharmacol.* 1437, 670433. doi:10.3389/fphar.2021.670433

Jia, X. J., Li, X., Wang, F., Liu, H. Q., Zhang, D. J., and Chen, Y. (2017). Berbamine exerts anti-inflammatory effects via inhibition of NF-κB and MAPK signaling pathways. *Cell. Physiology Biochem.* 41 (6), 2307–2318. doi:10.1159/000475650

Khan, I., Najeebullah, S., Ali, M., and Shinwari, Z. K. (2016). Phytopharmacological and ethnomedicinal uses of the genus Berberis (berberidaceae): A review. *Trop. J. Pharm. Res.* 15, 2047–2057. doi:10.4314/tjpr.v15i9.33

Khan, S. W., and Khatoon, S. (2007). Ethnobotanical studies on useful trees and shrubs of haramosh and bugrote valleys in Gilgit northern areas of Pakistan. *Pak J. Bot.* 39, 699–710.

Kitada, M., and Koya, D. (2013). SIRT1 in type 2 diabetes: Mechanisms and therapeutic potential. *Diabetes and metabolism J.* 37, 315–325. doi:10.4093/dmj.2013.37.5.315

Kiziltas, H., Bingol, Z., Goren, A. C., Pinar, S. M., Ortaakarsu, A. B., Alwasel, S. H., et al. (2022a). Comprehensive metabolic profiling of acantholimon caryophyllaceum using LC–HRMS and evaluation of antioxidant activities, enzyme inhibition properties and molecular docking studies. *South Afr. J. Bot.* 151, 743–755. doi:10.1016/j.sajb.2022.10.048

Kiziltas, H., Goren, A. C., Alwasel, S. H., and Gulcin, İ. (2022b). Sahlep (dactylorhiza osmanica): Phytochemical analyses by LC-HRMS, molecular docking, antioxidant activity, and enzyme inhibition profiles. *Molecules* 27 (20), 6907. doi:10.3390/molecules27206907

Kumar, S., Kumar, R., Rohilla, L., Jacob, N., Yadav, J., and Sachdeva, N. (2021). A high potency multi-strain probiotic improves glycemic control in children with new-onset

type 1 diabetes mellitus: A randomized, double-blind, and placebo-controlled pilot study. *Pediatr. Diabetes* 22, 1014–1022. doi:10.1111/pedi.13244

Lee, H. A., Lee, J. K., and Han, J. S. (2022). Betulinic acid improves tnf-A-induced insulin resistance by inhibiting negative regulator of insulin signalling and inflammation-activated protein kinase in 3T3-L1 adipocytes. *Archives Physiology Biochem.* 2022, 1–8. doi:10.1080/13813455.2022.2120503

Lee, J. H., Song, M. Y., Song, E. K., Kim, E. K., Moon, W. S., Han, M. K., et al. (2009). Overexpression of SIRT1 protects pancreatic beta-cells against cytokine toxicity by suppressing the nuclear factor-kappaB signaling pathway. *Diabetes* 58, 344–351. doi:10.2337/db07-1795

Leite, P., Belo, I., and Salgado, J. M. (2021). Co-Management of agro-industrial wastes by solid-state fermentation for the production of bioactive compounds. *Industrial Crops Prod.* 172, 113990. doi:10.1016/j.indcrop.2021.113990

Li, M., Chi, X., Wang, Y., Setrerrahmane, S., Xie, W., and Xu, H. (2022). Trends in insulin resistance: Insights into mechanisms and therapeutic strategy. *Signal Transduct. Target Ther.* 7 (1), 216.

Li, J. Q., Welchowski, T., Schmid, M., Letow, J., Wolpers, C., Pascual-Camps, I., et al. (2020). Prevalence, incidence and future projection of diabetic eye disease in europe: A systematic review and meta-analysis. *Eur. J. Epidemiol.* 35, 11–23. doi:10.1007/s10654-019-00560-z

Li, Y., Xu, S., Giles, A., Nakamura, K., Lee, J. W., Hou, X., et al. (2011). Hepatic overexpression of SIRT1 in mice attenuates endoplasmic reticulum stress and insulin resistance in the liver. *FASEB J.* 25, 1664–1679. doi:10.1096/fj.10-173492

López-Jaramillo, P., Gómez-Arbeláez, D., López-López, J., López-López, C., Martínez-Ortega, J., Gómez-Rodríguez, A., et al. (2014). The role of leptin/adiponectin ratio in metabolic syndrome and diabetes. *Hormone Mol. Biol. Clin. investigation* 18, 37–45. doi:10.1515/hmbci-2013-0053

Madić, V., Petrović, A., Jušković, M., Jugović, D., Djordjević, L., Stojanović, G., et al. (2021). Polyherbal mixture ameliorates hyperglycemia, hyperlipidemia and histopathological changes of pancreas, kidney and liver in A rat model of type 1 diabetes. *J. Ethnopharmacol.* 265, 113210. doi:10.1016/j.jep.2020.113210

Matthews, J., Villescas, S., Herat, L., Schlaich, M., and Matthews, V. (2021). Implications of ADAM17 activation for hyperglycaemia, obesity and type 2 diabetes. *Biosci. Rep.* 41, BSR20210029. doi:10.1042/BSR20210029

Menghini, R., Fiorentino, L., Casagrande, V., Lauro, R., and Federici, M. (2013). The role of ADAM17 in metabolic inflammation. *Atherosclerosis* 228, 12–17. doi:10.1016/j.atherosclerosis.2013.01.024

Miaffo, D., Ntchapda, F., Mahamad, T. A., Maidadi, B., and Kamanyi, A. (2021). Hypoglycemic, antidyslipidemic and antioxydant effects of vitellaria paradoxa barks extract on high-fat diet and streptozotocin-induced type 2 diabetes rats. *Metab. Open* 9, 100071. doi:10.1016/j.metop.2020.100071

Mihaylova, D., Popova, A., Alexieva, I., Krastanov, A., and Lante, A. (2018). Polyphenols as suitable control for obesity and diabetes. *Open Biotechnol. J.* 12 (1), 219–228. doi:10.2174/1874070701812010219

Mutlu, M., Bingol, Z., Uc, E. M., Köksal, E., Goren, A. C., Alwasel, S. H., et al. (2023). Comprehensive metabolite profiling of cinnamon (cinnamomum zeylanicum) leaf oil using LC-HR/MS, GC/MS, and GC-FID: Determination of antiglaucoma, antioxidant, anticholinergic, and antidiabetic profiles. *Life* 13 (1), 136. doi:10.3390/life13010136

Naidu, P. B., Ponmurugan, P., Begum, M. S., Mohan, K., Meriga, B., RavindarNaik, M. R., et al. (2015). Diosgenin reorganises hyperglycaemia and distorted tissue lipid profile in high-fat diet–streptozotocin-induced diabetic rats. *J. Sci. Food Agric.* 95, 3177–3182. doi:10.1002/jsfa.7057

Nair, A. B., and Jacob, S. (2016). A simple practice guide for dose conversion between animals and human. *J. Basic Clin. Pharmacol.* 7 (2), 27.

Nedosugova, L. V., Markina, Y. V., Bochkareva, L. A., Kuzina, I. A., Petunina, N. A., Yudina, I. Y., et al. (2022). Inflammatory mechanisms of diabetes and its vascular complications. *Biomedicines* 10 (5), 1168.

Pareek, A., and Suthar, M. (2010). Antidiabetic activity of extract of Berberis aristata root in streptozotocin induced diabetic rats. *Pharmacologyonline* 2, 179–185.

Peng, W., Yuan, J., Chiavaroli, V., Dong, G., Huang, K., Wu, W., et al. (2021). 10-year incidence of diabetic ketoacidosis at type 1 diabetes diagnosis in children aged less than 16 Years from A large regional center (hangzhou, China). *Front. Endocrinol.* 12, 653519. doi:10.3389/fendo.2021.653519

Pilz, S., and März, W. (2008). Free fatty acids as A cardiovascular risk factor. *Clin. Chem. laboratory Med.* 46, 429–434. doi:10.1515/CCLM.2008.118

Pratiwi, R. Y., Elya, B., Setiawan, H., and Solawati, A.(2021). Alterations in body weight, blood glucose levels, and lipid profiles in high-fat diet-low dose streptozotocin-induced diabetic rats. *Pharmacogn. J.* 13, 1562–1567. doi:10.5530/pj.2021.13.199

Rabbi, F., Zada, A., Nisar, A., Sohail, M., Khalil, S. K., and Ahmad, M. M. (2021). *In vivo* laxative, anti-diarrheal, hepatoprotective and diuretic investigations of sterculia diversifolia and its isolated compounds. *J. Traditional Chin. Med.* 41, 717.

Rahimi-Madiseh, M., Lorigoini, Z., Zamani-Gharaghoshi, H., and Rafieian-Kopaei, M. (2017). Berberis vulgaris: Specifications and traditional uses. *Iran. J. Basic Med. Sci.* 20, 569–587. doi:10.22038/IJBMS.2017.8690

Rawlinson, S., and Andrews, Z. B. (2021). Hypothalamic insulin signalling as a nexus regulating mood and metabolism. *J. Neuroendocrinol.* 33, e12939. doi:10.1111/jne.12939

Repetto, M., Semprine, J., and Boveris, A. (2012). Lipid peroxidation: Chemical mechanism, biological implications and analytical determination. *Lipid peroxidation* 1, 3–30.

Roman, A. A., Parlee, S. D., and Sinal, S. J. (2012). Chemerin: A potential endocrine link between obesity and type 2 diabetes. *Endocrine* 42, 243–251. doi:10.1007/s12020-012-9698-8

Sakashita, M., Tanaka, T., and Inagi, R. (2021). Metabolic changes and oxidative stress in diabetic kidney disease. *Antioxidants* 10 (7), 1143.

Saltiel, A. R. (2021). Insulin signaling in health and disease. *J. Clin. Investig.* 131 (1).

Sankaranarayanan, C., Nishanthi, R., and Pugalendi, P. (2018). Ameliorating effect of berbamine on hepatic key enzymes of carbohydrate metabolism in high-fat diet and streptozotocin induced type 2 diabetic rats. *Biomed. Pharmacother.* 103, 539–545. doi:10.1016/j.biopha.2018.04.066

Sarmah, S., and Roy, A. S. (2021). A review on prevention of glycation of proteins: Potential therapeutic substances to mitigate the severity of diabetes complications. *Int. J. Biol. Macromol.* 195, 565–588. doi:10.1016/j.ijbiomac.2021.12.041

Sharma, A., Anand, S. K., Singh, N., Dwarkanath, A., Dwivedi, U. N., and Kakkar, P. (2021). Berbamine induced activation of the SIRT1/LKB1/AMPK signaling axis attenuates the development of hepatic steatosis in high-fat diet-induced NAFLD rats. *Food and Funct.* 12 (2), 892–909. doi:10.1039/d0fo02501a

Sharma, N., Garg, V., and Paul, A. (2010). Antihyperglycemic, antihyperlipidemic and antioxidative potential of prosopis cineraria bark. *Indian J. Clin. Biochem.* 25, 193–200. doi:10.1007/s12291-010-0035-9

Shaukat, B., Mehmood, M. H., Shah, S., and Anwar, H. (2022). Ziziphus oxyphylla hydro-methanolic extract ameliorates hypertension in L-name induced hypertensive rats through No/cgmp pathway and suppression of oxidative stress related inflammatory biomarkers. *J. Ethnopharmacol.* 285, 114825. doi:10.1016/j.jep.2021.114825

Sholikhah, A. M., and Ridwan, M. (2021). Swimming training on moderate intensity significantly reduces total cholesterol and bodyweight on hypercholesterolemic rat model. *J. Keolahragaan* 9, 51–58. doi:10.21831/jk.v9i1.33362

Sithuraj, S., and Viswanadha, V. P. (2018). Berbamine protects the heart from isoproterenol induced myocardial infarction by modulating eNOS and iNOS expressions in rats. *J. Appl. Biomed.* 16 (4), 301–310. doi:10.1016/j.jab.2018.06.001

Singh, J., and Kakkar, P. (2009). Antihyperglycemic and antioxidant effect of *Berberis aristata* root extract and its role in regulating carbohydrate metabolism in diabetic rats. *J. Ethnopharmacol.* 123 (1), 22–26.

Sun, S. W., Lee, S. S., Wu, C. A., and Chen, C. K. (1998). Determination of bisbenzylisoquinoline alkaloids by high-performance liquid chromatography. *J. Chromatogr. A* 799 (1), 337–342. doi:10.1016/s0021-9673(97)01065-0

Sung, B., Chung, J. W., Bae, H. R., Choi, J. S., Kim, C. M., and Kim, N. D. (2015). Humulus japonicus extract exhibits antioxidative and anti-aging effects via modulation of the AMPK-SIRT1 pathway. *Exp. Ther. Med.* 9, 1819–1826. doi:10.3892/etm.2015.2302

Topal, M., and Gulcin, İ. (2022). Evaluation of the *in vitro* antioxidant, antidiabetic and anticholinergic properties of rosmarinic acid from rosemary (rosmarinus officinalis L.). *Biocatal. Agric. Biotechnol.* 43, 102417. doi:10.1016/j.bcab.2022.102417

Vries, M. A. d., Klop, B., Janssen, H. W., Njo, T. L., Westerman, E. M., and Castro Cabezas, M. (2014). Postprandial inflammation: Targeting glucose and lipids. *Adv. Exp. Med. Biol.* 824, 161–170. doi:10.1007/978-3-319-07320-0_12

Wang, S., Liu, Q., Zhang, Y., Liu, K., Yu, P., Liu, K., et al. (2009). Suppression of growth, migration and invasion of highly-metastatic human breast cancer cells by berbamine and its molecular mechanisms of action. *Mol. cancer* 8, 81–15. doi:10.1186/1476-4598-8-81

Yin, L., Zhang, L., Luo, L., Liu, Y., Wang, F., Feng, Y., et al. (2022). Berbamine reduces body weight via suppression of small GTPase Rab8a activity and activation of paraventricular hypothalamic neurons in obese mice. *Eur. J. Pharmacol.* 916, 174679. doi:10.1016/j.ejphar.2021.174679

Zhang, H., Zhu, T., Fu, R., Peng, Y., Jing, P., Xu, W., et al. (2020). Combination of detoxified pneumolysin derivative ΔA146Ply and berbamine as a treatment approach for breast cancer. *Mol. Therapy-Oncolytics* 18, 247–261. doi:10.1016/j.omto.2020.06.015

Zhang, Y., Hu, G., Yuan, Z., and Chen, L. (2012). Glycosylated hemoglobin in relationship to cardiovascular outcomes and death in patients with type 2 diabetes: A systematic review and meta-analysis.

Zheng, H., Sun, W., Zhang, Q., Zhang, Y., Ji, L., Liu, X., et al. (2021). Proinflammatory cytokines predict the incidence of diabetic peripheral neuropathy over 5 Years in Chinese type 2 diabetes patients: A prospective cohort study. *EClinicalMedicine* 31, 100649. doi:10.1016/j.eclinm.2020.100649

Zheng, X. K., Zhang, L., Wang, W., Wu, Y, Y., Zhang, Q, B., and Feng, W. S. (2011). Anti-diabetic activity and potential mechanism of total flavonoids of Selaginella tamariscina (Beauv.) Spring in rats induced by high fat diet and low dose STZ. *J. Ethnopharmacol.* 137, 662–668. doi:10.1016/j.jep.2011.06.018

Zorena, K., Jachimowicz-Duda, O., Ślęzak, D., Robakowska, M., and Mrugacz, M. (2020). Adipokines and obesity. Potential link to metabolic disorders and chronic complications. *Int. J. Mol. Sci.* 21 (10), 3570. doi:10.3390/ijms21103570

frontiers | Frontiers in Pharmacology

TYPE Review
PUBLISHED 30 May 2023
DOI 10.3389/fphar.2023.1122969

OPEN ACCESS

EDITED BY
Hai-Dong Guo,
Shanghai University of Traditional Chinese Medicine, China

REVIEWED BY
Peng Zhou,
Anhui University of Chinese Medicine, China
Wei Zhou,
China Pharmaceutical University, China

*CORRESPONDENCE
Min Wu,
wumin19762000@126.com
Longtao Liu,
liulongtao1976@126.com

RECEIVED 13 December 2022
ACCEPTED 10 April 2023
PUBLISHED 30 May 2023

CITATION
Li X, Sun C, Zhang J, Hu L, Yu Z, Zhang X, Wang Z, Chen J, Wu M and Liu L (2023), Protective effects of paeoniflorin on cardiovascular diseases: A pharmacological and mechanistic overview.
Front. Pharmacol. 14:1122969.
doi: 10.3389/fphar.2023.1122969

Protective effects of paeoniflorin on cardiovascular diseases: A pharmacological and mechanistic overview

Xiaoya Li[1], Changxin Sun[2], Jingyi Zhang[2], Lanqing Hu[1], Zongliang Yu[1], Xiaonan Zhang[1], Zeping Wang[2], Jiye Chen[1], Min Wu[3]* and Longtao Liu[1]*

[1]Xiyuan Hospital, China Academy of Chinese Medical Sciences, Beijing, China, [2]Beijing University of Chinese Medicine, Beijing, China, [3]Guang'anmen Hospital, China Academy of Chinese Medical Sciences, Beijing, China

Background and ethnopharmacological relevance: The morbidity and mortality of cardiovascular diseases (CVDs) are among the highest of all diseases, necessitating the search for effective drugs and the improvement of prognosis for CVD patients. Paeoniflorin (5beta-[(Benzoyloxy)methyl] tetrahydro-5-hydroxy-2-methyl-2,5-methano-1H-3,4-dioxacyclobuta [cd] pentalen-1alpha (2H)-yl-beta-D-glucopyranoside, $C_{23}H_{28}O_{11}$) is mostly derived from the plants of the family Paeoniaceae (a single genus family) and is known to possess multiple pharmacological properties in the treatment of CVDs, making it a promising agent for the protection of the cardiovascular system.

Aim of the study: This review evaluates the pharmacological effects and potential mechanisms of paeoniflorin in the treatment of CVDs, with the aim of advancing its further development and application.

Methods: Various relevant literatures were searched in PubMed, ScienceDirect, Google Scholar and Web of Science. All eligible studies were analyzed and summarized in this review.

Results: Paeoniflorin is a natural drug with great potential for development, which can protect the cardiovascular system by regulating glucose and lipid metabolism, exerting anti-inflammatory, anti-oxidative stress, and anti-arteriosclerotic activities, improving cardiac function, and inhibiting cardiac remodeling. However, paeoniflorin was found to have low bioavailability, and its toxicology and safety must be further studied and analyzed, and clinical studies related to it must be carried out.

Conclusion: Before paeoniflorin can be used as an effective therapeutic drug for CVDs, further in-depth experimental research, clinical trials, and structural modifications or development of new preparations are required.

KEYWORDS

paeoniflorin, cardiovascular diseases, mechanism, pharmacology, traditional Chinese medicine

1 Introduction

Cardiovascular diseases (CVDs), a chronic non-communicable disease, refer to a group of disorders of the heart or blood vessels. Common CVD types include coronary heart disease, aortic disease, peripheral arterial disease, and stroke (Olvera Lopez et al., 2022). Ischemic heart disease and ischemic stroke are collectively referred to as atherosclerotic cardiovascular disease (ASCVD), which is the most prevalently encountered CVD (Arnett et al., 2019; Wong et al., 2022). Several risk factors for CVDs have been identified, such as dyslipidemia, diabetes, metabolic syndrome, hypertension, chronic kidney disease, smoking, age, and genetic history (Yusuf et al., 2020; O'Sullivan et al., 2022). At present, the mainstream therapy of CVDs is medication, including antiplatelet drugs, anticoagulants, statins, anti-thrombotic drugs, beta receptor blockers, antiarrhythmic agent and nitrates (Leong et al., 2017). Despite the availability of a wide range of drugs for clinical use, the morbidity and mortality of CVDs are the highest among all diseases, which not only pose a severe challenge to human health but also bring a huge economic burden to individuals, families, and society (Kalogeropoulos and Butler, 2022; Townsend et al., 2022). As an important problem that must be faced and solved, it is pivotal to seek effective drugs for treating CVDs, and improve the prognosis and quality of life of CVDs patients.

Paeoniflorin ($C_{23}H_{28}O_{11}$, PubChem CID: 442534), with its chemical name as 5beta-[(Benzoyloxy)methyl] tetrahydro-5-hydroxy-2-methyl-2,5-methano-1H-3,4-dioxacyclobuta [cd] pentalen-1alpha (2H)-yl-beta-D-glucopyranoside, is a pinane monoterpene bitter glucoside distributed in the roots of Paeonia albiflora Pall, P. suffrsticosa Andr, P. delarayi Franch and other Paeoniaceae (Paeonia L.). Paeoniflorin is mostly derived from plants of Paeoniaceae (a single genus family). In 1963, paeoniflorin was first isolated from the roots of Paeonia albiflora and named by Shibata and Nakahara (1963). Further studies showed that the basic skeleton of paeoniflorin is a pinane derivative, which is chemically stable and is a water-soluble monoterpene glycoside (Xia et al., 2007; Sun B et al., 2017). As shown in Figure 1, β-d-glucopyranosyl, benzoyl, and semi-ketal-acetal structures are linked to the backbone, which formed the complete chemical structure of paeoniflorin (Zhang et al., 2022).

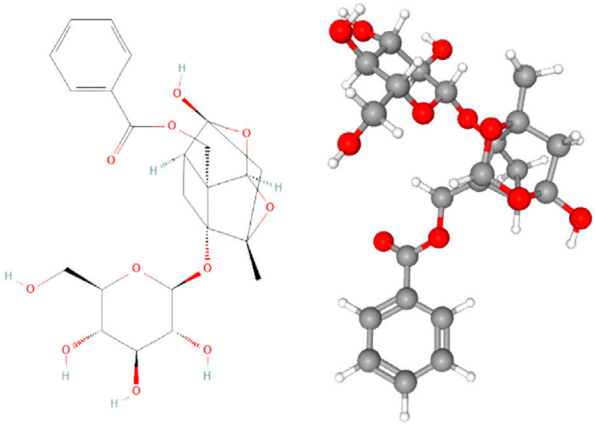

FIGURE 1
Chemical structure of paeoniflorin.

Studies have shown that the paeoniflorin can regulate glucose and lipid metabolism, exert anti-inflammatory, anti-oxidative stress, and anti-arteriosclerotic activities, improve cardiac function, and inhibit cardiac remodeling, thus making it a promising candidate for the treatment of CVDs and protection of the cardiovascular system (Figure 1). Whilst several previous reviews have approached the usage of paeoniflorin for neurological disorders and neurodegeneration (Jiao et al., 2021; Hong et al., 2022), analgesia (Lin et al., 2019; Ruan et al., 2021), antidepressants (Zhang et al., 2021a; Lei et al., 2022), neuroprotection (Chen et al., 2020; Guo et al., 2021), and immunomodulation (Chen et al., 2016; Yang and Wei, 2020), a review specific to paeoniflorin's protective effect on the cardiovascular system is notably lacking. At present, no review articles about paeoniflorin protecting the cardiovascular system have been found in PubMed or other relevant databases. This article is thus dedicated to providing an overview of the pharmacological effects and possible mechanisms of paeoniflorin in the treatment of CVDs, in the hopes of further advancing its development and application (Figure 2).

2 Plant sources of paeoniflorin

Paeoniaceae is a monofamily consisting of 34 species, mainly distributed in temperate Eurasia, northwest Africa and western North Americ (Hong, 2011). In China, plants of the Paeoniaceae family are widely cultivated and used for their special medicinal benefits and ornamental value, which makes China the region with the highest concentration of Paeoniaceae in the world (Zhou et al., 2021). The most representative plant in Paeoniaceae is Paeonia lactiflora Pall (Shaoyao in Chinese). As a medicinal plant, Shaoyao was first recorded in the book Shennong's Herbal Classic of Materia Medica and has a history of more than 2000 years (Xu et al., 2021). In Zhang Zhongjing's book "Treatise on Febrile Diseases," there are 113 prescriptions, 33 of which contain Shaoyao, accounting for 29% of all prescriptions. In the northern and southern dynasties, Tao Hongjing pointed out that Shaoyao can be divided into Chishao (Paeoniae Radix Rubra) and Baishao (Paeoniae Radix Alba) in Chinese, which are included in modern Chinese pharmacopoeia (Committee, 2020).

As the traditional Chinese medicines in China, Chishao and Baishao are all processed from the roots of Paeoniaceae plants. The Chinese Pharmacopoeia records that Chishao is the dried root of Paeonia lactiflora Pall or Paeonia veitchii Lynch, while Baishao is the dried root of Paeonia lactiflora Pall (Committee, 2020). Paeoniflorin is the main active ingredient of Chishao and Baishao (Zhang et al., 2022). Chishao and Baishao derive from the same species or closely related plants, which contain similar chemical components, but the paeoniflorin content in Chishao is slightly higher than that in Baishao. According to the Chinese Pharmacopoeia, the paeoniflorin content in dried Baishao should be higher than 1.6%, and in Chishao should be higher than 1.8% (Committee, 2020). In addition to the roots of Paeoniaceae, paeoniflorin is distributed throughout the plant including flowers, stems, leaves, fruits, seeds and rhizomes (Zhang et al., 2022). Since the biosynthetic pathway of paeoniflorin has not been fully elucidated, the chemical

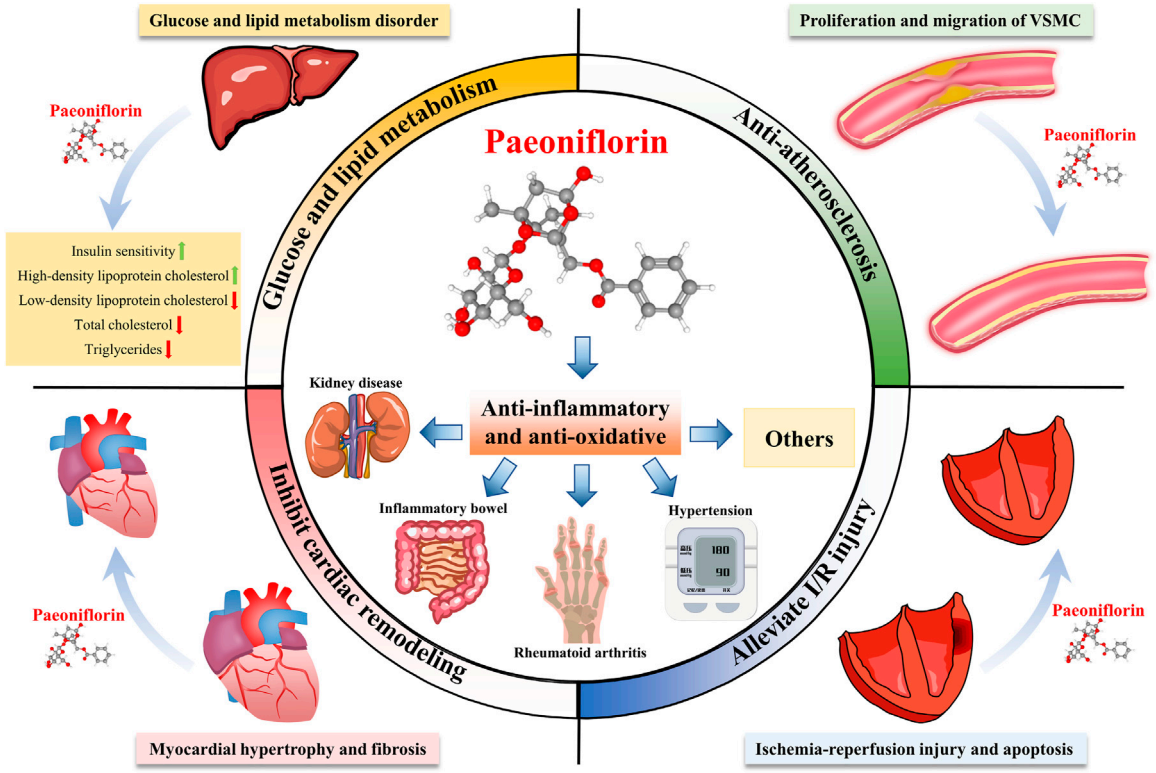

FIGURE 2
Multi-system pharmacological effects of paeoniflorin. Paeoniflorin has therapeutic effects on many diseases, and can prevent and treat kidney diseases, inflammatory bowel disease, rheumatoid arthritis, hypertension and other diseases through anti-inflammatory and anti-oxidant effects. In addition, paeoniflorin can improve glucose and lipid metabolism, resist atherosclerosis, inhibit myocardial remodeling, and improve ischemia-reperfusion injury.

synthesis process is complicated and the production cost is high, therefore, the currently applied paeoniflorin is mainly extracted from Paeoniaceae plants (SUN L C et al., 2017). However, the low yield of this generation method does not allow for economical mass production and is increasingly difficult to meet the current increasing demand in pharmaceutical formulations. In the next stage, we should further study the specific modification stage of paeoniflorin in structure and function, further clarify the biosynthesis pathway, and increase the production of paeoniflorin on the basis of environmental protection.

3 Pharmacological effects of paeoniflorin on the cardiovascular system

3.1 Regulation of glucose and lipid metabolism

Dyslipidemia, obesity, and overweight are risk factors for hypertension, coronary heart disease, and peripheral vascular disease (Seravalle and Grassi, 2017; Pirillo et al., 2021). Paeoniflorin has been shown to reduce body weight, regulate lipid metabolism and serum glucose levels, increase insulin sensitivity in obese mice, and improve the accumulation of ectopic lipids (Zhang et al., 2015; Ma et al., 2017a). It has also been reported to significantly reduce the levels of total cholesterol, low-density lipoprotein, and triglycerides in hyperlipidemic rats (Yang et al., 2004; Li et al., 2017a). However, other studies suggest that the effect of paeoniflorin is mainly achieved by lowering cholesterol, with only a limited impact on triglyceride levels (Zhang et al., 2015). Thus, further investigation and discussion on the effects of paeoniflorin on triglyceride metabolism is warranted. The identification of lipid metabolism genes targeted by paeoniflorin has indicated it can regulate lipid synthesis and metabolism through several signaling pathways, such as the *de novo*, lipid oxidation, cholesterol synthesis and output pathways (Zhang et al., 2015). It has been suggested that paeoniflorin can reduce lipid synthesis by inhibiting SREBP-1c via the *de novo* pathway and decreasing the expression of FAS, ACC-α, and other proteins (Ma et al., 2017a). It has been found that enzyme 3-hydroxy-3-methylglutaryl coenzyme A reductase (HMG-COAR) is an important enzyme for cholesterol synthesis, and cytochrome P4507A1 (CYP7A1) is a rate-limiting enzyme in the classical pathway of bile acid synthesis. The two enzymes are the key enzymes to regulate the metabolic balance of cholesterol in the body (Osaki et al., 2015). Studies have shown that paeoniflorin can regulate cholesterol synthesis and metabolism by decreasing HMG-CoAR activity and increasing CYP7A1 expression (Zhang et al., 2015; Ma et al., 2017a). Furthermore, Paeoniflorin can attenuate the

TABLE 1 Summary of pharmacological effects of paeoniflorin (PF).

Type	Model	Dose (PF)	Group	Duration	Method	Effect (PF group)	References
vitro	LPS-exposed microglia model	48 μg/mL (100 μM), 96 μg/mL (200 μM)	(1) Control (intact cells); (2) An LPS-treated group (100 ng/mL); (3) Low-dose group (LPS + PF 100 μM); (4) High-dose group (LPS + PF 200 μM).	1 h	ELISA kits, Western blotting analyses, qRT-PCR.	NF-κB↓, TNF-α↓, IL-1β↓, IL-6↓, IFNγ↓, IL-4↑, IL-10↑, ROS↓, MOD↓, SOD↑, GSH↑	Chen et al. (2020)
vivo	Non-alcoholic fatty liver disease model (HFD-fed C57BL/6J mice)	Corresponding diet supplemented with 0.05% PF	(1) Control (normal control mice); (2) Control + PF; (3) High-fat diet-fed mice; (4) High-fat diet-fed mice + PF.	24 weeks	Biochemical analysis, histologcal analysis, qRT-PCR.	TC↓, TG↓, LDL-C↓, HDL-C↓, ALT↓, AST↓, FAS↓, PPARα ↑, HMGCR↓, PPARγ↓, ABCA-1↓, TNF-α↓, IL-1↓, IL-6↓, MCP-1↓	Zhang et al. (2015)
vivo	Non-alcoholic fatty liver disease model (HFD-fed male Sprague-Dawley rats)	20 mg/kg	(1) Control; (2) HFD group; (3) HFD + PF (PF 20 mg/kg).	4 weeks	Biochemical analysis, histologcal analysis, Western blotting analyses.	TC↓, TG↓, ALT↓, AST↓, SREBP-1c↓, FAS↓, ACCα↓, HMGCR↓, CYP7A1↑, p-IRS-1↓, p-Akt↑, p-GSK3β↑, ROS↓, MOD↓, CYP2E1↓, HOMA-IR index↓	Ma et al. (2017a)
vivo + vitro	Atherosclerosis rat model was established by administration of excessive vitamin D and cholesterol. Cell model of atherosclerosis (VSMCs)	vivo: 10, 20 mg/kg;	Vivo: (1) Control (SD rats + saline); (2) Atherosclerotic group (vitamin D3 + fat emulsion); (3) Low-dose group (PF 10 mg/kg/day); (4) High-dose group (PF 20 mg/kg/day); (5) Simvastatin group (simvastatin 5 mg/kg).	vivo: 15 weeks;	Histopathologic evaluation of aortas, MTT assay, ELISA kits, qRT-PCR, Western blot analysis.	TLR4↓, MyD88↓, IκBα↓, NF-κB↓, TC↓, TG↓, LDL-C↓, IL-1β↓, TNF-α↓, IL-6↓	Li et al. (2017a)
		vitro: 5, 10, 30, 60, 100 μmol/L	vitro: (1) Control; (2) Atherosclerotic group (palmitic acid 100 μmol/L); (3) Low-dose group (PF 60 μmol/L); (4) High-dose group (PF 100 μmol/L).	vitro:1 h			
vitro	3T3-L1 adipocyte insulin resistance model	12.5, 25, 50, 100 mg/L	(1) Control; (2) TNFα group (10 ng/mL); (3) Insulin group (10 nM); (4) PF group; (5) PF + TNFα group; (6) TNFα + insulin group.	24 h	ELISA kits, BCA protein assay, MTT assay, Western blot analysis, qRT-PCR.	TNF-α↓, PPARγ↓, IL-6↓, MCP-1↓	Kong et al. (2013)
vivo	Apolipoprotein E null mice	10, 20, 30 mg/kg	(1) Control (C57BL/6J); (2) Untreated ApoE −/− group; (3) PF + ApoE −/−group (10, 20, 30 mg/kg).	6 weeks	T-AOC detection kit, qRT-PCR, Western blot analysis.	ANGPTL3↓, GALNT2↑, LPL↑, TC↓, LDL-C↓, TG↓, HDL-C↑	Xiao et al. (2017)
vivo + vitro	Experimental DIC mouse model; cell inflammation model (RAW 264.7 murine macrophages)	15, 30, 60 mg/kg	vivo: (1) Control; (2) LPS (60 mg/kg); (3) Heparin (10 IU/kg); (4) low-PF treatment (15 mg/kg); (5) Medium-PF treatment (30 mg/kg); (6) High-PF treatment (60 mg/kg). Thereafter mice in each group were randomly divided into three groups: 0-h group, 2 h group, and 8 h group.	vivo: every 2 h	MTT assay, ELISA kits, Western blot analysis.	NF-κB↓, TNF-α↓, IL-6↓, TLR4↓, IκBα↓	Fang et al. (2020)

(Continued on following page)

10.3389/fphar.2023.1122969

TABLE 1 (*Continued*) Summary of pharmacological effects of paeoniflorin (PF).

Type	Model	Dose (PF)	Group	Duration	Method	Effect (PF group)	References
			vitro: (1) Control, (2) LPS (10 μg/mL), (3) PF treatment groups (30, 60, 120 μm).	vitro: 30 min			
vitro	Coculture of differentiated 3T3-L1 adipocytes and RAW 264.7 macrophages	6.25, 12.5, 25, 50, 100 mg/L	(1) Vehicle (0.1% DMSO); (2) Negative control (TNF α or MCP-1 levels released by macrophages alone, FFA from adipocytes alone); (3) PF treatment (1–100 mg/L).	24 h	MTT assay, ELISA kits, acyl-coenzyme A oxidase-based colorimetric assay kit, BCA protein assay, Western blot analysis, qRT-PCR.	MAPKs↓, NF-κB↓, ERK1/2↓, p38↓, JNK↓, IKK↓, TNF-α↓, MCP-1↓, FFA↓	Jiang et al. (2012)
vitro	Lysophosphatidylcholine-induced inflammatory factor production in HUVECs	1, 10, 100 μmol/L	(1) Control; (2) LPC, (1 μg/mL); (3) PF + LPC group (PF: 1, 10, 100 μmol/L); (4) PF group (100 μmol/L); (5) ethanol (less than 0.1% v/v).	2 h	MTT assay, ELISA kits, qRT-PCR, Western blot analysis.	HMGB1↓, RAGE↓, TLR-2↓, TLR-4↓, NF-κB↓, ICAM-1↓, MCP-1↓, IL-6↓, TNF-α↓	Li et al. (2013)
vitro	LPS-stimulated RAW264.7 macrophages	25, 50, 100, 200, 400 μM	(1) Control; (2) LPS (1 μg/mL); (3) PF + LPS group. (PF: 100, 200, 400 μg/mL)	24 h	ELISA kits, Western blot analysis, qRT-PCR.	NF-κB↓, ERK1/2↓, MAPKs↓, COX-2↓, iNOS↓, ROS↓	Li et al. (2022)
vitro	LPS-stimulated RAW264.7 macrophages	11, 33, 100 μM	(1) Control; (2) LPS (60 mg/kg); (3) PF + LPS group (PF: 11, 33, 100 μM); (4) DXM + LPS group (DXM: 33 μM).	2 h	Microplate reader, ELISA kits.	NO↓, TNF-α↓, IL-6↓	Bi et al. (2017)
vitro	M1/M2 cells differentiated from bone marrow progenitor cells of male Balb/c mice	1, 10, 100 μg/mL	(1) Control; (2) LPS (100 ng/mL); (3) PF + LPS group (PF: 1, 10, 100 μg/mL); (4) IL-4 group (20 ng/mL); (5) IL-4 + PF group (PF: 1, 10, 100 μg/mL).	24 h	CCK-8, ELISA kits, Western blot analysis, qRT-PCR, NO assay kit, arginase assay Kit, immunofluorescence analysis.	NF-κB↓, iNOS↓, NO↓, STAT6↑, IL-4↑, M1↓, M2↑	Zhai et al. (2016)
vivo + vitro	Male C57/BL6 mice, RAW264.7 macrophages	vivo: 1, 5, 25 mg/kg	vivo: (1) Control; (2) LPS (200 ng); (3) PF + LPS group (PF: 1, 5, 25 mg/kg).	vivo: 1 week	MTT assay, ELISA kits, qRT-PCR, Western blot analysis, calcium imaging, protein kinase C activity assay kit.	TNF-α↓, IL-1β↓, IL-33↓, NF-κB↓, TLR4↓, MAPKs↓, IκBα↓, Ca2+ influx↓	Li et al. (2020)
		vitro: 0–25 μM	vitro: (1) Control; (2) LPS (1 μg/mL); (3) PF group (10 μg/mL) (4) PF + LPS group.	vitro: 24 h			
vivo + vitro	vivo: Diabetic mice model (8–10 weeks males WT- C57BL/6J and TLR4−/− mice);	vivo: 25, 50, 100 mg/kg	vivo: (1) WT; (2) WT + STZ; (3) WT + STZ + PF (PF:25, 50, 100 mg/kg); (4) TLR4−/− mice; (5) TLR4−/− + STZ.	vivo: 12 weeks	Pathology and immunohistochemistry analysis, CCK-8 kit, cell migration assay, flow cytometry analyses, confocal microscopy analysis, ELISA kits, Western blotting analyses, qRT-PCR.	TLR4↓, IL-1β↓, MCP-1↓, iNOS↓, MyD88↓, IκBα↓, NF-κB↓, p-IRAK1↓, Trif ↓, p-IRF3↓, TNF-α↓, IL-1β↓, MCP-1↓	Shao et al. (2019)
	vitro: BMDM (6–8 weeks old male TLR4−/− and C57BL/6JWT).	vitro: 10^{-8}–10^{-3} mol/L	vitro: (1) Normal glucose concentration control group (LG), (2) Normal glucose concentration + PF intervention group (LG + PF), (3) High-glucose stimulation group (HG), (4) PF intervention group (HG + PF), (5) Normal glucose	vitro: 24 h			

(Continued on following page)

10.3389/fphar.2023.1122969

TABLE 1 (*Continued*) Summary of pharmacological effects of paeoniflorin (PF).

Type	Model	Dose (PF)	Group	Duration	Method	Effect (PF group)	References
			concentration TLR4 knockout group (TLR4−/−), (6) TLR4 knockout macrophages + high-glucose stimulation group (TLR4−/− + HG), and (7) TLR4 knockout macrophages + high-glucose stimulation + PF intervention group (TLR4−/− + HG + PF).				
vitro	LPS-stimulated HUVECs	20, 50, 80 μM	(1) Control; (2) LPS (1 μg/mL); (3) PF group (PF: 20, 50, 80 μM) (4) PF + LPS + 4-PBA (PF: 20, 50, 80 μM; PBA: 5 mM).	24 h	MTT assay, ELISA kits, qRT-PCR, Western blot analysis, transmission electron microscope assay, immunofluorescence staining.	IL-6↓, MCP-1↓, GRP78↓, CCAAT↓, IRE1α↓, NF-κB↓	Chen et al. (2018a)
vivo + vitro	vivo: A mouse model of cutaneous Arthus reaction;	vivo: 25, 50 mg/kg	vivo: (1) Control; (2) IC (IgG 40 μg/30 μL in PBS); (3) PF + IC group (PF: 25, 50 mg/kg);	vivo: 0.5 h	Immunohistochemistry, analysis of myeloperoxidase activity, ELISA kits, Western blotting analyses, qRT-PCR, adhesion assay.	E-selectin↓, ICAM-1↓, TNF-α↓, p38↓, JNK↓	Chen et al. (2013)
	vitro: TNF-α-induced HDMECs	vitro: 125, 250, 500 μM	vitro: (1) Control; (2) TNF-α(10 ng/mL); (3) PF + TNF-α group (PF: 125, 250, 500 μM).	vitro: 0.5 h			
vivo + vitro + vivo	vivo: ANIT-induced cholestatic liver injury model (C57BL/6 mice)	vivo: 75, 150, 300 mg/kg	vivo: (1) Control; (2) ANIT (80 mg/kg); (3) PF + ANIT (PF 75, 150, 300 mg/kg); (4) Red Tuihuang particles (3.9 g/kg) + ANIT.	vivo: 10 days	Uridine diphospho-glucuronosyltransferase assay, MDA assay kit, Western blotting analyses, MTT assay.	ALT↓, AST↓, TBIL↓, DBIL↓, TBA↓, ALP↓, MDA↓, GSH↑, Nrf2↑, Ntcp↑, Nox4↓, NTCP↑, NOX4↓, NQO1↑	Mao et al. (2022)
	vitro: Nrf2 plasmid or siRNA-Nrf2 transfection on LO2 cells	vitro: 4, 20, 100, 500 μM	vitro: (1) Control; (2) ANIT (50 μM); (3) PF + ANIT (PF 100 μM)	vitro: 24 h			
	vivo: ANIT-induced cholestatic liver injury model ($Nrf2^{-/-}$ mice)		vivo: (1) Control; (2) ANIT (80 mg/kg); (3) PF + ANIT (PF 300 mg/kg).	vivo: 10 days			
vivo	SAP lung injury rat model	40 mg/kg	(1) Sham operation group; (2) SAP group (5% sodium taurocholate (1 mL/kg) was retrogradely injected into the biliopancreatic duct at a rate of 0.1 mL/min); (3) PF treatment group (40 mg/kg); (4) Dexamethasone-positive control group (2 mg/kg).	24 h	H&E Staining, biochemical indicators, ELISA kits, Western blotting analyses.	AMY↓, lipase activity↓, LDH↓, MDA↓, SOD↑, TNF-α↓, IL-6↓, IL-10↑, Cyt-Nrf2↑, HO-1↑, NQO1↑	Hu and Yang (2022)
vivo	A hyperlipidemic rat model	500 mg/kg, 300 mg/kg, and 100 mg/kg	(1) Normal control group; (2) High cholesterol group; (3) High cholesterol + simvastatin group; (4) High cholesterol + PF group (PF: 500 mg/kg, 300 mg/kg, 100 mg/kg).	12 weeks	Rat liver histology and immunohistochemical analysis, Western blotting analyses.	HMG-CoAR↓, LDLR↑, PPAR-α↑, CYP7A1↑, SOD↑, MDA↓, Nrf2↑	Hu et al. (2017)

(Continued on following page)

10.3389/fphar.2023.1122969

TABLE 1 (*Continued*) Summary of pharmacological effects of paeoniflorin (PF).

Type	Model	Dose (PF)	Group	Duration	Method	Effect (PF group)	References
vitro	Oxidative damage model induced by advanced oxidation protein products (AOPPs) in HUVECs	50–200 μM	(1) Control; (2) BSA (200 μg/mL); (3) AOPPs (200 μg/mL); (4) PF (200 μM); (5) Different inhibitors (RAGE blocking agent FPS-ZM1, NADPH oxidase inhibitor Apocynin, ROS scavenger NAC, NF-κB inhibitor BAY11-7082).	1 h	MTT assay, DCFH-DA staining, flow cytometry, confocal microscopy, ATP determination kit, Western blotting analyses.	MMP↑, ATPz↑, NF-κB p65↓, Nox1↓, Nox2↓, HIF-4α↓, VEGF↓, RAGE↑	Song et al. (2017)
vitro	DOX-induced cardiomyocyte apoptosis model (H9c2 cell)	100 μmol/L	(1) Control (cultured in normal condition); (2) DOX group (incubated with 5 μmol/L DOX for 24 h); (3) PF + DOX group (cells were treated with 100 μmol/L PF for 2 h prior to exposure to 5 μmol/L DOX for 24 h); (4) PF group (incubated with 100 μmol/L PF for 26 h).	26 h	MTT assay, cardiomyocyte apoptosis assay, intracellular ROS assay, Western blotting analyses, qRT-PCR.	ROS↓, microRNA-1↓, Bcl-2↑	Li et al. (2016)

Abbreviations: AMY, serum amylas; ANIT, α-naphthalene isothiocya-nate; AOPPs, advanced oxidation protein products; ApoE −/−, apolipoprotein E null; ALT, alanine aminotransferase; ALP, alkaline phosphatase; AST, aspartate aminotransferase; ATP, adenosine triphosphate; BMDMs, bone marrow-derived macrophages; BSA, bovine serum albumin; CCK-8, cell counting kit-8; COX, cyclooxygenase; DBIL, direct bilirubin; DCFH-DA. 2′, 7′-dichlorofluorescein-diacetate; DOX, doxorubicin; DXM, dexamethasone; ELISA, enzyme-linked immunosorbent assay; ERK, extracellular signal-regulated kinase; FFA, free fatty acid; HDL-C, high-density lipoprotein cholesterol; HDMECs, human dermal microvascular endothelial cells; HFD, high-fat diet; HMG-CoAR, 3-hydroxy-3-methylglutharyl-coenzyme A reductase; HO-1, heme oxygenase-1; HOMA-IR, homeostasis model of insulin resistance; HUVECs, human umbilical vein endothelial cells; IC, immune complex; iNOS, inducible nitric oxide synthase; ICAM, inter cellular adhesion molecule; IL, interleukin; JNK, c-Jun N-terminal kinase; LDL-C, low-density lipoprotein cholesterol; LPC, lysophosphatidylcholine; LPS, lipopolysaccharide; MAPK, mitogen-activated protein kinase; MMP, matrix metalloproteinase; MTT, thiazolyl blue tetrazolium bromide; NF-E2 p45-related factor 2 (Nrf2); NF-κB, nuclear factor-kappa B; Nqo1 (NRF2 downstream gene); NTCP, sodium taurocholate co-transporting polypeptide; PBA, phenylbutric acid; ROS, reactive oxygen species; RT-qPCR, reverse transcription polymerase chain reaction; SAP, severe acute pancreatitis; SOD, superoxide dismutase; STZ, streptozotocin; TBA, total bile acid; TBIL, total bilirubin; TC, total cholesterol; TG, triglycerides; TLR, Toll-like receptor; TNF, tumor necrosis factor; TPG, total paeony glucosides VEGF, vascular endothelial growth factor; WT, Wild-type.

↑ represents upregulation of expression andid ↓ represents downregulation of expression.

10.3389/fphar.2023.1122969

lipolysis in adipocytes and ameliorate tumor necrosis factor-α (TNF-α) -induced dysfunction of adipocytes (Kong et al., 2013). In addition, the N-acetylgalactosamine transferase 2-angiopoietin like protein 3-lipoprotein lipase (GALNT2-ANGPTL3-LPL) pathway, which is closely related to dyslipidemia and able to directly affect HDL metabolism, has been reported to be effectively regulated by paeoniflorin (Khetarpal et al., 2016; Xiao et al., 2017). A study by Xiao and colleagues showed that 6-week paeoniflorin treatment was able to significantly reduce ANGPTL3 expression, promote GALNT2 and LPL expression, increase serum HDL cholesterol levels, and regulate lipid metabolism in ApoE (−/−) mice (Xiao et al., 2018) (Table 1).

3.2 Anti-inflammatory effect

Inflammation is a major pathological factor contributing in the occurrence and progression of CVDs such as atherosclerosis, thrombosis, myocardial infarction, and ischemia-reperfusion injury (Kim and Conte, 2020). Paeoniflorin has prominent anti-inflammatory effects, which can act by regulating a variety of signalling pathways, such as the GPCR, MAPKs/NF-κB, PI3K/Akt/mTOR, JAK2/STAT3, and TGFβ/Smad pathways (Tu et al., 2019; Xin et al., 2019; Zhang and Wei, 2020). Paeoniflorin can achieve the regulation of anti-inflammatory effects on macrophages and endothelial cell dysfunction by regulating upstream and downstream molecules of NF-κB signaling pathway, which may indicate that paeoniflorin can treat and alleviate cardiovascular diseases from anti-inflammatory mechanism (Table 1).

TNF-α, a prototype member of the tumor necrosis factor superfamily, is predominantly secreted by macrophages and monocytes. Being a major proinflammatory cytokine, it triggers a series of inflammatory processes (Aggarwal et al., 2012). Paeoniflorin can attenuate TNF-α expression by suppressing the activation of the NF-κB signaling pathway (Fang et al., 2020). The paracrine loops of free fatty acids (FFA) and TNF-α present between adipocytes and macrophages form a vicious cycle of inflammation that increases inflammatory changes and insulin resistance in adipose tissue of obese individuals (Suganami et al., 2005). Meanwhile, paeoniflorin is capable of lowering FFA and TNF-α levels by interfering in the interaction between adipocytes and macrophages, thereby impeding the occurring of related inflammatory reactions (Jiang et al., 2012). Research has also demonstrated its capacity to inhibit TNF-α-stimulated phosphorylation at ERK, JNK, and IKK subunits, as well as reduce the expression of pro-inflammatory factors such as IL-6 and MCP-1 in adipocytes (Kong et al., 2013). Pathogen pattern recognition receptors, such as Toll-like receptors (TLRs), can regulate the cytokine response to various inflammatory stimuli (de Kleijn and Pasterkamp, 2003). TLR4 can mediate the activation of the downstream factors MyD88 and NF-κB and induce a surge in proinflammatory cytokines like Il-1β, IL-6, and TNF-α (Fitzgerald et al., 2001). Moreover, paeoniflorin has been found to effectively regulate TLR-2 and TLR-4 expression, thereby decreasing inflammation by suppression of the TLR4/MyD88/NF κB pathway (Li et al., 2013; Li et al., 2017a) (Table 1).

Macrophages are key effectors of inflammation and the innate immune response, and play an pivotal role in the pathogenesis of many CVDs (Xu et al., 2022). The study found that paeoniflorin can reduce the inflammatory response of LPS-stimulated RAW264.7 macrophages by inhibiting the NF-κB/ERK1/2/p38 MAPK signaling pathway (Bi et al., 2017; Li et al., 2022). Linked to that, macrophages show the capability to polarize to M1 and M2 phenotypes (Murray, 2017). Paeoniflorin can decrease the pro-inflammatory activities of M1 macrophages by downregulating inducible nitric oxide synthase (iNOS) expression and NO production through the NF-κB signaling pathway, while simultaneously facilitating the anti-inflammatory function of M2 macrophages by upregulating Arg-1 activity attainable by modulation of the IL-4/STAT6 signaling pathway (Zhai et al., 2016). In addition, Interleukin 33 (IL-33) is a newly identified member of the interleukin family that macrophages, such as M2 macrophages, can secrete (Furukawa et al., 2017). When tissue or cell injury occurs, the release of IL-33 increases, and further adjusts macrophage function by controlling chemokine expression and triggering macrophage polarization (Joshi et al., 2010). Paeoniflorin can regulate macrophage polarization and inhibit IL-33 production by macrophages by regulating the TLR4/NF-κB/P38 MAPK signaling pathway (Chen et al., 2020; Li et al., 2020). However, other studies have suggested that paeoniflorin cannot directly inhibit the activation of macrophages but affects macrophages by inhibiting the expression of iNOS and the production of TNF-α, IL-1β, and MCP-1 (Shao et al., 2019). Therefore, the specific action mode of paeoniflorin in regulating the function of macrophages deserves further study and discussion (Table 1).

Endothelial dysfunction is the primary pathological manifestation of several CVDs (Badimon et al., 2012). On a molecular level, inflammation associated with endoplasmic reticulum (ER) stress appears to be the primary culprit of endothelial dysfunction (ED) (Battson et al., 2017). Paeoniflorin has been reported to be able to restrain the inositol enzyme 1alpha (IRE1α)/NF-κB pathway, eventually diminishing vascular inflammation related to endoplasmic reticulum stress and subsequently reducing endothelial dysfunction (Chen et al., 2018a). Additionally, endothelial cell injury can lead to increased inter cellular adhesion molecule-1 (ICAM-1) expression, which further induces monocyte migration, adhesion, activation, and the ensuing intensify of inflammatory response locally (Most et al., 1992; Frank and Lisanti, 2008). Studies have unveiled that paeoniflorin has the capacity to reduce ICAM-1 expression and inhibit vascular damage (Chen et al., 2013) (Table 1).

By combing through the above research literature, we found that currently, there is limited evidence to directly verify the anti-inflammatory role of paeoniflorin in cardiovascular disease. However, the results of the *in vitro* studies do demonstrate a remarkable anti-inflammatory effect for paeoniflorin, which can regulate macrophages and endothelial cells, the two vital cell types in the cardiovascular system. Therefore, its potential anti-inflammatory role in cardiovascular disease warrants further exploration and examination. Notwithstanding, there are a few shortcomings visible in the above research. For example, the highest dose of paeoniflorin used by studies conducting cell experiments stands in great disparity, with some suggesting a maximum dose of 100 μM (Bi et al., 2017), while others pointing out that 15 μM paeoniflorin could show obvious cytotoxicity

when cultured for 48 h (Li et al., 2020). Since dose concentration is the essential information in pharmacology, it may significantly hamper forward fundamental and clinical studies and, therefore, subsequent researches should focus on precisely figuring out the maximum efficacious dose of paeoniflorin *in vivo* or *in vitro* studies and provide detailed, experimental data for further studies (Table 1).

3.3 Anti-oxidative effect

In addition to hypertension, diabetes, dyslipidemia, overweight, obesity, and inflammation, increased oxidative stress i is considered to be a major contributing factor to the increased incidence of certain CVDs (Senoner and Dichtl, 2019; Shaito et al., 2022). Oxidative stress refers to the excessive generation or accumulation of free radical species, such as the oxygen reactive species (ROS) (Di Meo and Venditti, 2020). Previous studies have shown that paeoniflorin can not only downregulate ROS-producing systems, but also intensifying antioxidant enzyme systems, which helps in managing ROS levels and ameliorating the pathological damage induced by oxidative stress (Han et al., 2022; Hu and Yang, 2022; Mao et al., 2022). For instance, paeoniflorin can increase superoxide dismutase (SOD) levels, reduce malondialdehyde (MDA) concentration, and upregulate nuclear factor erythroid factor 2-related factor 2 (Nrf2) expression, thereby augmenting liver antioxidant capacity and protecting the liver from oxidative stress (Hu et al., 2017). At present, At the moment, there is only a limited number of studies regarding the antioxidant effects of paeoniflorin on CVDs. Elevated ROS levels can induce inflammation and mitochondrial dysfunction, thereby affecting endothelial cell and macrophage function and ultimately accelerating the occurrence of CVDs (Forstermann et al., 2017). Paeoniflorin can suppress the secretion of cytokines and the expression of cyclooxygenase-2 (COX-2) and iNOS in a dose-dependent manner, at the same time diminish ROS accumulation in cells without experiencing any effect on macrophage phagocytosis (Li et al., 2022). ROS can be generated in cells via the NADPH oxidase system, which consists of multiple membrane-associated and cytosolic components (Vignais, 2002). NADPH oxidase 2 (Nox2) and Nox4 are highly expressed in endothelial cells and play a role in endothelial cell-cell adhesion and motility, which represent crucial elements in the oxidative stress-induced arteriosclerosis (Van Buul et al., 2005). Paeoniflorin can reduce ROS production by inhibiting the ROS-NF-κB axis and reducing Nox2/Nox4 expression, resulting in downregulation of HIF-1alpha/VEGF levels, alleviation of mitochondrial dysfunction, and protection of human umbilical vein endothelial cells from oxidative damage induced by AOPP (Song et al., 2017). Furthermore, paeoniflorin is capable of diminishing ROS levels in cardiomyocytes by downregulating the expression of microRNA-1, thereby improving cardiomyocyte viability and restraining cardiomyocyte apoptosis induced by doxorubicin (a highly potent anthracycline antitumor antibiotic) (Li et al., 2016) (Table 1).

4 Roles of paeoniflorin in various models of cardiac diseases

4.1 Anti-atherosclerotic effect

ASCVD is defined as an unequivocally diagnosed arteriosclerosis disease that includes acute coronary syndrome, stable coronary artery disease, post-revascularization, ischemic cardiomyopathy, ischemic stroke, transient cerebral ischemia, and peripheral arteriosclerosis disease. Factors such as dyslipidemia, impaired insulin sensitivity, inflammatory state, intense oxidative stress, endothelial dysfunction and other related factors may contribute to the initiation and progression of arteriosclerosis processes (Hill et al., 2021; Pirillo et al., 2021). Most ASCVD events can be avoided by preventing the formation of risk factors and by controlling traditional cardiovascular factors (Arnett et al., 2019). In case of ASCVD, adequate drug treatment is exceptionally critical to impede the progression of the disorder, and a combination of drugs instead of augmenting the amount of a single medication can create greater efficacy and decrease risks (Kim et al., 2022). Paeoniflorin, having multiple pharmacological actions, has great utilization potentiality in managing ASCVD. The regulatory effects of paeoniflorin on glucose and lipid metabolism, inflammation, and oxidative stress suggest its remarkable anti-arteriosclerotic characteristics, as is documented in 3.1–3.4. Equally, paeoniflorin can improve the pathological morphology of the aorta in atherosclerotic rats and alleviate atherosclerosis-related inflammation by inhibiting the TLR4/MyD88/NF-κB pathway (Li et al., 2017a). The underlying pathological mechanism of arteriosclerosis involves the proliferation, migration and inflammatory response of vascular smooth muscle cells (VSMCs) (Bennett et al., 2016). It was found that paeoniflorin could activate HO-1, induce cell cycle arrest, inhibit the p38/ERK1/2/MAPK/NF-κB signaling pathway, inhibit VSMC proliferation and migration induced by ox-LDL in a dose-dependent manner, and reduce the expression of inflammatory cytokines and chemokines (Li et al., 2018a). Paeoniflorin can also promote VSMC apoptosis by upregulating caspases (Guo et al., 2017). Furthermore, paeoniflorin made distinctive anti-platelet effects, counteracting platelet aggregation and clotting and significantly deterring intra-arterial thrombosis (Koo et al., 2010; Xie et al., 2017; Ngo et al., 2019). However, there is a lack of relevant mechanistic studies, so *in vivo* or *in vitro* experiments should be designed to investigate the specific mechanism behind paeoniflorin's anticoagulant and anti-platelet aggregation effects (Table 2).

4.2 Improvement of cardiac function and inhibition of cardiac remodeling

Many studies have shown that paeoniflorin has pharmacological effects which improve cardiac function and inhibit cardiac remodeling. Paeoniflorin ameliorates cardiac dysfunction and regulates the levels of inflammatory cytokines (e.g., IL-1β, IL-6, IL-12, MCP-1, IFN-γ, and iNOS), by affecting the PI3K/AKT signaling pathway and reducing inflammation-related damage (Zhai and Guo, 2016). What is more, paeoniflorin has been proven to be effective in inhibiting cardiac remodeling and

TABLE 2 Roles of paeoniflorin (PF) in various models of cardiac diseases.

Disease	Type	Model	Dose (PF)	Group	Duration	Mechanism	References
AS	Vitro	Ox-LDL-induced VSMCs	20, 40, 80 μM	(1) Control; (2) Ox-LDL-induced VSMCs (100 μg/mL); (3) Ox-LDL + PF group (PF: 20, 40, 80 μM).	24 h	PF inhibits VSMCs proliferation and migration by arresting cell cycle and activating HO-1 through MAPKs and NF-κB pathway.	Li et al. (2018a)
AS	Vitro	Non-alcoholic fatty liver disease model (HFD-fed C57BL/6J mice)	25, 50, 100 μg/mL	(1) Control; (2) Low-PF group (25 μg/mL); (3) Medium-PF group (50 μg/mL); (4) High-PF group (100 μg/mL).	12, 24, 48 h	PF inhibits VSMCs proliferation by down-regulating proteins associated with the nuclear factor-κB signaling pathway and promotes VSMCs apoptosis by up-regulating the expression of cystathione aspartase.	Guo et al. (2017)
Cardiac dysfunction	Vivo	LPS-induced cardiac dysfunction in C57BL/6 mice	15 mg/kg	(1) Control; (2) PF group (15 mg/kg; sterile saline dissolved with 0.5% Tween 80); (3) LPS group (10 mg/kg, sterile saline dissolved); (4) LPS + PF group.	3 days	PF attenuates cardiac dysfunction in endotoxemic mice via the inhibition of NF-κB pathway.	Tomek and Bub (2017)
Cardiac remodeling	Vivo	Cardiac remodeling in spontaneous hypertensive rats (SHR)	2.25, 4.50, 9.00 mg/kg	(1) Control (Wistar-Kyoto rats); (2) SHR group; (3) Low-PF treatment (2.25 mg/kg/d); (4) Medium-PF treatment (4.50 mg/kg/d); (5) High-PF treatment (9.00 mg/kg/d); (6) Captopril treatment (13.5 mg/kg/d).	8 weeks	PF improves pressure overload-induced cardiac remodeling by modulating the MAPK signaling pathway.	Liu et al. (2019a)
Cardiac remodeling	Vivo	Pressure overload-induced cardiac remodeling	20 mg/kg	(1) Sham operated control (saline); (2) Sham + PF (20 mg/kg); (3) AB (saline); (4) AB+ PF.	7 weeks	PF attenuates pressure overload-induced cardiac remodeling via inhibition of TGFBβ/Smads and NF-κB pathways.	Zhou et al. (2013)
Acute myocardial infarction	Vivo	Ventricular remodeling in AMI rats	2.25, 4.50, 9.00 mg/kg	(1) Sham operated control; (2) Model control; (3) Captopril group (4.50 mg/kg/d); (4) Low-PF treatment (2.25 mg/kg/d); (5) Medium-PF treatment (4.50 mg/kg/d); (6) High-PF treatmen (9.00 mg/kg/d).	28 days	PF decreases BNP, TNF-α and IL-6 levels, increases IL-10 levels and further inhibits the expression of cystathionin-3 and cystathionin-9.	Chen et al. (2018b)
Acute myocardial infarction	Vivo	Myocardial ischemic damage in AMI rats	5, 10, 20 mg/kg	(1) Sham operated control; (2) Vehicle group (saline + AMI); (3) PF treatment groups (AMI + PF 5, 10, 20 mg/kg).	7 days	PF ameliorates acute myocardial infarction of rats by inhibiting inflammation and inducible nitric oxide synthase signaling pathways.	Chen et al. (2015)
I/R	Vivo	Myocardial I/R induced injury in	10 mg/kg	(1) Sham rats underwent surgical	1 h	PF can reduce myocardial damage in	Nizamutdinova et al. (2008)

(Continued on following page)

TABLE 2 (*Continued*) Roles of paeoniflorin (PF) in various models of cardiac diseases.

Disease	Type	Model	Dose (PF)	Group	Duration	Mechanism	References
		Sprague-Dawley rats		operation, but without occlu-sion of LAD; (2) Ischemia (25 min) and subsequent reperfusion (24 h) and the treatment with placebo (saline 0.3 mL); (3) Pretreatment with PF (10 mg/kg) before I/R injury.		rat through protection from apoptosis.	
I/R	Vivo	Myocardial I/R model	15, 30, 60 mg/kg	(1) Sham group; (2) Model group; (3) Low-PF group (15 mg/kg); (4) Medium-PF group (30 mg/kg); (5) High-PF group (60 mg/kg).	7 days	PF can reduce oxidative stress and apoptosis by inhibiting the expression of apoptosis-related signaling pathway.	Wu et al. (2020)
Hypertension	vitro	Blocking effect of compounds on calcium channels by live-cell imaging analysis (HEK 293 and H9C2)	Moutan Cortex: 1, 0.1, 0.01 mg/mL	(1) Control group; (2) Model group; (3) nifedipine group (10–5 mol/L); (4–6) Three Moutan Cortex groups with different concentrations (1, 0.1, 0.01 mg/mL).	6 h	PF can effectively block voltage-operated Ca^{2+} channels (VOCCs) to exert calcium antagonism.	Lu et al. (2019)
Arrhythmic	vitro	Isolated rat ventricular myocytes or transfected human embryonic kidney 293 (HEK293) cells	10 mmol/L	(1) control; (2) PF group (10 mmol/L).	2 h	PF can block I(Ca-L), I(Na), and I(K1) without affecting I(to1), I(Ks), or I(Kr).	Wang et al. (2011)
Angiogenesis	Vivo + vitro	Vivo: A vascular insufficiency model in the Tg(fli-1: EGFP)y1 transgenic zebrafish	Vivo: 6.25–100 μmol/L	Vivo: (1) vehicle control (embryo water containing 0.1% DMSO); (2) VRI group (300 ng/mL) (2) VRI + PF group (6.25, 12.5, 25, 50, 100 μmol/L);	Vivo: 24 h	The mechanism of PF pro-angiogenic action may be related to the activation of VEGF signaling pathway.	Xin et al. (2018)
		Vitro: HUVECs	Vitro: 0.001, 0.003, 0.01, 0.03, μmol/L; 0.3, 1, 10 μmol/L; 0.3–10 μmol/L	vitro: (1) Vehicle control (DMSO 0.1%); (2) Positive control (VEGF 20 ng/mL); (3) PF group.	vitro: MTT assay—24 h; wound healing assay - 10 h; tube formation assay—4 h		
Vascular remodeling	vitro	PDGF-BB - induced proliferation of primary cultured rat VSMCs	50, 100, 200 μM	(1) Control; (2) PDGF-BB group (1 ng/mL); (3) PDGF-BB + PF group (50, 100, 200 μM); (4) PF group.	Flow cytometry analysis of cell cycle progression—20 h; Scratch migration test—24 h; ROS measurement—1 h;	PF suppresses PDGF-BB-induced VSMC proliferation through the ROS-mediated ERK1/2 and p38 signaling pathways.	Fan et al. (2018)
Angiogenesis	vitro	Angiogenesis in ox-LDL-induced HUVECs	10, 1, 0.1, 0.01 μmol/L	(1) Control; (2) Ox-LDL group (20 μg/mL); (3) Ox-LDL + PF group (10, 1, 0.1, 0.01 μmol/L).	24 h	PF suppresses ox-LDL-induced angiogenesis in HUVECs by inhibiting both the VEGF/VEGFR2 and the Jagged1/Notch1 signaling pathways.	Yuan et al. (2018)

(Continued on following page)

TABLE 2 (*Continued*) Roles of paeoniflorin (PF) in various models of cardiac diseases.

Disease	Type	Model	Dose (PF)	Group	Duration	Mechanism	References
Insulin resistance	vitro	Human HepG2 cells	3, 30, 100 mM	(1) Control; (2) PA group (0.25 mM); (3) PA + PF group (3, 30, 100 mM).	1 h	PF suppresses lipid accumulation and alleviates insulin resistance by regulating the Rho kinase/IRS-1 pathway in palmitate-induced HepG2Cells.	Ma et al. (2017b)
Insulin resistance	vivo	Fructose-induced insulin resistance and hepatic steatosis in Sprague-Dawley rats	10, 20, 40 mg/kg	(1) Control group (Saline); (2) Fructose group (20% Fructose drink); (3–5) Fructose + PF group (10, 20, 40 mg/kg); (6) Fructose + pioglitazone group (10 mg/kg).	8 weeks	PF ameliorates fructose-induced insulin resistance and hepatic steatosis by activating LKB1/AMPK and AKT pathways.	Li et al. (2018c)
Diabetes	vitro	Rat insulin-secreting beta-cell line (INS-1)	20, 40, 80 μM	(1) Control; (2) STZ group (3 mmol/L); (3) STZ + PF group (20, 40, 80 μM).	2 h	PF protects pancreatic beta cells from STZ-induced damage through inhibition of the p38 MAPK and JNK signaling pathways.	Liu et al. (2019c)

Abbreviations: AB, aortic banding; AMI, acute myocardial infarction; AS, atherosclerosis; HEK 293, human embryonic kidney cells; HUVECs, human umbilical vein endothelial cells; H9C2, rat myocardial cells; SHR, spontaneous hypertensive rats; VSMCs, vascular smooth muscle cells; MAPK, mitogen-activated protein kinase; NF-κB, nuclear factor-kappa B; PDGF-BB, platelet derived growth factor-BB; STZ, streptozotocin; VRI, VEGF receptor tyrosine kinase inhibitor II.

alleviating myocardial infarction and ischemia-reperfusion injury. It should be noted that cardiac remodeling denotes an alteration in the size, shape, and function of the heart, which is triggered by gene expression changes induced by cardiac injury or hemodynamic stress and is drastically correlated to hypertension as well as other cardiovascular abnormalities (Tomek and Bub, 2017). Of all these alterations, myocardial hypertrophy and fibrosis are the most predominant, and the severity of myocardial hypertrophy and fibrosis is closely related to the mortality of patients following heart failure (Heinzel et al., 2015; Shenasa and Shenasa, 2017). Paeoniflorin attenuates cardiac hypertrophy, fibrosis, and inflammation in spontaneously hypertensive rats by inhibiting MAPK signaling, and ameliorates pressure overload-induced cardiac remodelling (Liu et al., 2019a). Moreover, to validate the efficacy of paeoniflorin, a model of cardiac remodeling was established by aortic band (AB)-induced pressure overload in mice. The findings demonstrated that treatment with paeoniflorin decreased the heart weight to body weight ratio (HW/BW), reduced the expression of hypertrophic genes, inhibited the apoptosis of cardiomyocytes, alleviated myocardial fibrosis and improved ventricular function by suppressing the activity of the TGF-β/Smads/NF-κB pathways (Zhou et al., 2013). Strikingly, another study also demonstrated that paeoniflorin inhibited the TGF-β1/Smad signaling pathway to reduce cardiac remodeling in an isoproterenol (Iso)-induced rat cardiac remodeling model (Liu et al., 2019b) (Table 2).

Ischemic heart disease, myocardial infarction (MI), hypertension, and valvular heart disease (VHD) are common causes of heart failure (Heidenreich et al., 2022). In China, the occurrence and development of ventricular remodeling after myocardial infarction are the main causes of heart failure. To test this, a rat model of acute myocardial infarction (AMI) was established by ligation of the anterior descending coronary artery, and paeoniflorin was administered orally for 4 weeks post-surgery. Subsequent examination of doppler ultrasonography showed significantly increased left ventricular ejection fraction (LVEF), decreased left ventricular end-diastolic diameter (LVIDd), and decreased left ventricular end-systolic diameter (LVIDs). Furthermore, pathological results from myocardial samples (pericardium tissue) taken from within a 2 mm radius from the visible edge of the infarct showed that paeoniflorin treatment decreased myocardial degeneration in rats. Collectively, these results highlight the ability of paeoniflorin to enhance cardiac function and mitigate the adverse remodeling of the left ventricle post-infarction (Chen et al., 2018b). Additionally, an additional study attributed paeoniflorin's cardioprotective effects to its ability to reduce inflammation and inhibit the iNOS signaling pathway (Chen et al., 2015) (Table 2).

4.3 Alleviation of ischemia-reperfusion injury

Early access to coronary intervention following myocardial infarction is a crucial measure for improving prognosis, yet it is paramount to not underestimate ischemia-reperfusion (I/R) injury that may occur after revascularization (Yellon and Hausenloy, 2007). To assess the effects of Paeoniflorin on I/R injury, a rat study was conducted, in which 10 mg per kilogram (mg/kg) of Paeoniflorin was intraperitoneally injected 1 h before I/R injury. The results of this study demonstrated that Paeoniflorin significantly improved hemodynamic parameters and reduced myocardial infarction size, as well as downregulated the expression of caspase-3 and Bax, while upregulating the expression of Bcl-2,

thus indicating that Paeoniflorin can protect against I/R injury through its anti-apoptotic action (Misao et al., 1996). Another study also revealed the potential of Paeoniflorin to have immediate effects on I/R injury (Nizamutdinova et al., 2008). As the occurrence times of acute cardiac events cannot be predicted during clinical diagnosis and treatment, a course of traditional Chinese medicine preparations are usually taken orally for a certain period of time in order for its therapeutic properties to be adequatelyeffective. Prior to constructing the I/R rat model, Wu et al. orally administered Paeoniflorin for seven consecutive days to the experimental animals, with the last dose being 30 min prior to the induction of ischemia (Wu et al., 2020). It was shown that paeoniflorin pretreatment significantly reduced the size of myocardial infarction, the degree of myocardial injury, apoptosis, and oxidative stress. The specific mechanism of action may be related to the regulation of the MAPK signaling pathway (Wu et al., 2020) (Table 2).

4.4 Improvement of hypertension and arrhythmia

Paeoniflorin also has the pharmacological effect of improving hypertension and arrhythmia. Studies have found that, compared with its single use, the combination of Paeoniflorin-enriched extract and metoprolol can enhance the bioavailability of Paeoniflorin and contribute to a greater anti-hypertensive effect; it can concurrently reduce systolic and diastolic blood pressure in spontaneously hypertensive rats (SHR), increase NOS expression in vascular endothelium, improve the arrangement of elastic fibers and cell hypertrophy in the vascular wall, as well as limit aortic vascular damage and other organ damages (Li et al., 2017b; Li et al., 2018b). Yu et al. suggested that the anti-hypertensive mechanism of paeoniflorin may be related to the effective blocking of voltage-controlled calcium channels (VOCCs) (Lu et al., 2019). This hypothesis is further supported by research which suggests that Paeoniflorin not only blocks L-type calcium current (I(Ca-L)), inward rectifier potassium current (I(K1)) and sodium current (I(Na)) in rat cardiomyocytes, but does so without affecting the instantaneous outward potassium current (I(to1)), slow delayed rectifier current (I(Ks)) and HERG current (I(Kr)), which may partly explain its anti-arrhythmic effects with minimal pro-arrhythmic potential (Wang et al., 2011) (Table 2).

4.5 Regulation of angiogenesis

Angiogenesis has been shown to be beneficial in patients with cardiac insufficiency or myocardial infarction (Oka et al., 2014). Paeoniflorin has been demonstrated to bidirectionally regulate angiogenesis, and its angiogenic effect has been demonstrated in a zebrafish model of vascular insufficiency, as well as in human umbilical vein endothelial cells (HUVECs) (Xin et al., 2018). When Platelet-derived growth factor BB (PDGF-BB) is released in the context of vascular injury, it binds to the cell membrane receptor PDGFR-β and activates NADPH oxidase to generate large amounts of ROS. This leads to aberrant proliferation and migration of vascular smooth muscle cells (VSMCs), and consequently to arteriosclerosis and restenosis (Rivard and Andres, 2000; Lee et al., 2007; Ding et al., 2015). In such cases, it is important to limit angiogenesis. Paeoniflorin has been shown to inhibit PDGF-BB-induced VSMC proliferation by modulating ERK12 and p38 signaling pathways, suggesting the potential of paeoniflorin to act as a therapeutic for arteriosclerosis and restenosis following a percutaneous coronary intervention (Fan et al., 2018). In addition, paeoniflorin can stabilize arteriosclerosis plaques, by inhibiting both the VEGF/VEGFR2 and Jagged1/Notch1 signaling pathways (Yuan et al., 2018) (Table 2).

4.6 Improvement of insulin resistance

The contribution of insulin resistance and diabetes to the pathogenesis of CVDs has already been established (Fox et al., 2007; Hill et al., 2021). CVDs is considered to be the leading cause of death and complications in type 1 diabetes (T1D) mellitus and type 2 diabetes (T2D) mellitus (Cheng et al., 2018). The main pathological feature of T2D mellitus is chronic insulin resistance (Madsbad, 1992). The gradual decline in pancreatic β cell function is the main cause of impaired insulin sensitivity (Shoemaker et al., 2015). Recent studies have shown that paeoniflorin can improve insulin resistance and protect β cells, by inhibiting the activation of Rho kinase (ROCK) and serine phosphorylation of INSR substrate (IRS)-1, and promoting AKT and glycogen synthase kinase (GSK)-3β phosphorylation (Ma et al., 2017b). Additionally, paeoniflorin can also reduce serum insulin and glucagon levels and improve insulin sensitivity by activating the LKB1/AMPK signaling pathway (Li et al., 2018c). Furthermore, paeoniflorin also can significantly ameliorate pancreatic beta cell injury, and regulate glucose metabolism by inhibiting the p38 MAPK and JNK signaling pathways (Liu et al., 2019c) (Table 2).

5 Pharmacokinetics of paeoniflorin

Since 1985, research on paeoniflorin pharmacokinetics has gradually deepened and its effects become better understood (Hattori et al., 1985; Shen et al., 2021). Researchers have delved into studying of the processes of absorption, distribution, biochemical conversion (or metabolism), and excretion of paeoniflorin in the body, particularly its changes in blood concentration over time, which is of great help for the further development and application of paeoniflorin. The usual bioavailability of paeoniflorin absorbed by oral or intestinal perfusion is approximately at 2%–4% (Fei et al., 2016; Wang et al., 2016; Yu et al., 2019). Poor fat solubility of paeoniflorin, P-glycoprotein (P-gp)-mediated transport mechanism, and degradation by gut microbiota enzymes are causes that impede its bioavailability (Liu et al., 2006; Yu et al., 2019).

After absorption, paeoniflorin is widely distributed in various tissues, such as the heart, liver, spleen, lung, kidney, stomach, and intestines (Luo et al., 2014). Additionally, paeoniflorin can pass the blood-brain barrier by passive diffusion (Luo et al., 2014; Hu et al., 2016). Many researchers think it is the metabolite of paeoniflorin, benzoic acid, that actually reaches the barrier mentioned above (Yu et al., 2019). Most paeoniflorin is mainly eliminated in the urine via

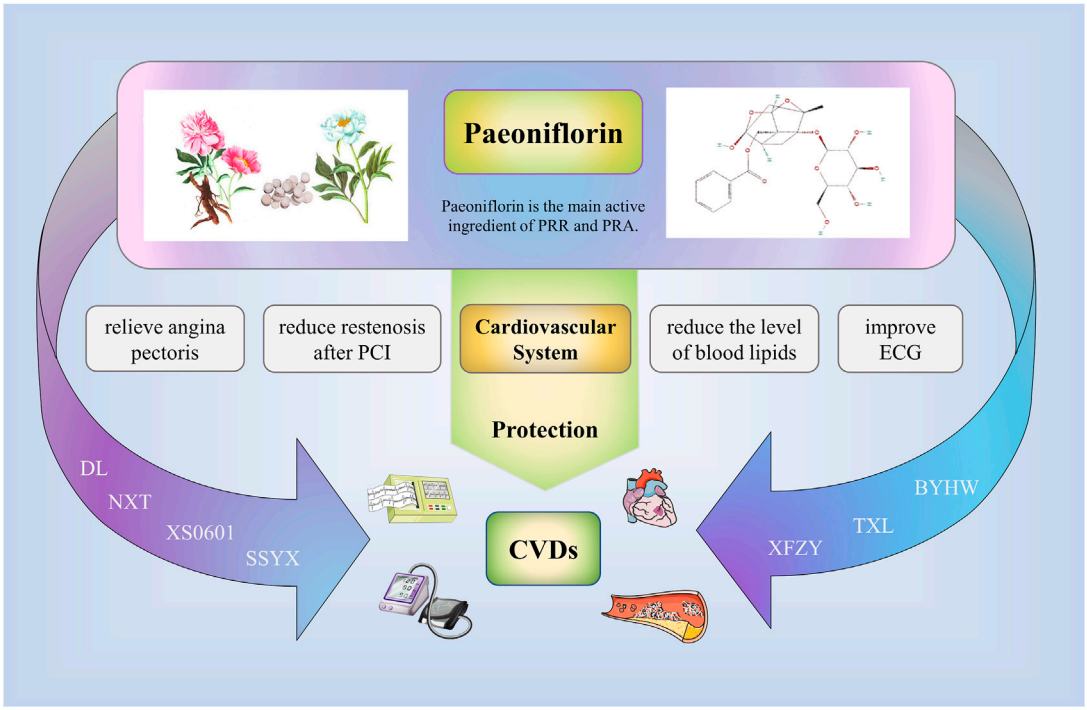

FIGURE 3
Clinical application of paeoniflorin. Some Chinese patent medicines or preparations containing Peony or paeoniflorin showed good cardiovascular protection; for example, XS0601, Naoxintong (NXT), Buyang Huanwu (BYHW), Xuefu Zhuyu (XFZY), Shensong Yangxin (SSYX), Tongxinluo (TXL), Danlou (DL). The above drugs can reduce the symptoms of angina pectoris, reduce the restenosis after PCI, reduce the level of blood lipids, improve ECG, and effectively treat the related cardiovascular diseases.

glomerular filtration of the renal system (Cheng et al., 2016). As experimental data collected from rats show, the serum concentration of paeoniflorin is dose-dependent, with a half-life (T1/2) of approximately 1.8 h (Fei et al., 2016; Chen et al., 2021). In traditional Chinese medicine, Chinese herbal preparations made by combinations of various kinds of botanical drugs can usually achieve the role of synergistic effect and attenuation of toxicity. Moreover, studies show that the compatibility of such botanical drugs or the combination of their active ingredients can play a role in altering paeoniflorin's pharmacokinetic parameters: when combined with Angelica sinensis, its absorption rate is accelerated, peak time (T max) is shortened, T1/2 is increased, mean residence time (MRT) is prolonged, and its distribution within said tissues is widened (Luo et al., 2014). Conversely, when combined with glycyrrhizic acid, it has been noticed that the T1/2 of paeoniflorin reduces, while its drug clearance and metabolism in rats speed up (Sun et al., 2019). In addition, paeoniflorin displays distinct effects when used in combination with other pharmaceuticals such as quinidine, verapamil, sinomenine, and cyclosporine A (Chan et al., 2006; Liu et al., 2006; Gong et al., 2015; Xu et al., 2016; He et al., 2017).

6 Clinical application

At present, the clinical application of paeoniflorin in traditional Chinese medicine is seldom studied by searching the relevant databases (Figure 3). Peony is the main source of paeoniflorin, especially Chishao (Zhang et al., 2022). Some Chinese patent medicines or preparations containing Peony or paeoniflorin showed good cardiovascular protection; for instance, XS0601 consists of active ingredients (Paeoniflorin and Chuangxiongol) that have been shown through animal studies to inhibit neointimal hyperplasia arteries (Xu et al., 2001). Notably, a multicenter, randomized, double-blind, placebo-controlled trial involving 335 patients has confirmed that administering of XS0601 for 6 months significantly reduces restenosis after percutaneous coronary intervention (PCI) (Chen et al., 2006). Naoxintong is composed of Chishao and 15 additional botanical drugs (Han et al., 2019). It has been proved through clinical trials to protect endothelial cells and treat coronary artery disease (Lv et al., 2016; Long-Tao, 2018). Supplementing aspirin with NXT has further been revealed to heighten the antiplatelet effect in cerebrovascular disease patients (Chen et al., 2008a). Buyang Huanwu (BYHW) decoction containing Chishao is also a traditional Chinese medicine compound preparation. Relevant clinical studies and meta-analysis have proved that its therapeutic effect on stable angina pectoris (SAP)and stroke (Zhang et al., 1995; Gao et al., 2021; Wang et al., 2022a). Recently, Wang et al. (2022b) designed a randomized, blinded, parallel controlled, multicenter clinical trial to compare the efficacy and safety of NXT and BYHW in the treatment of SAP. The results of the trial have yet to be published. Xuefu Zhuyu (XFZY) decoction is composed of Chishao and 10 additional botanical drugs (Li et al., 1998). It has great

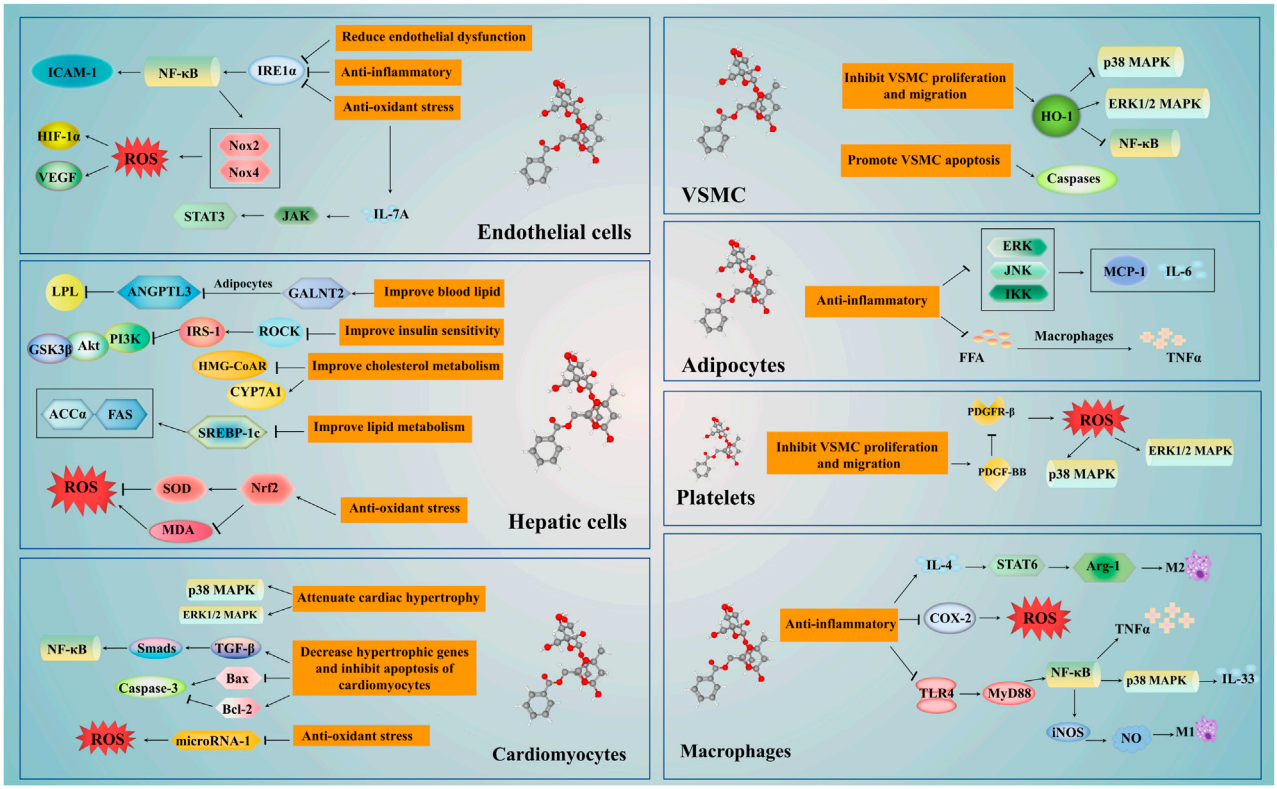

FIGURE 4
The mechanism of Paeoniflorin in the treatment of cardiovascular disease. The treatment of paeoniflorin has the advantage of multi-targets and multi-pathways. It regulates the NF-κB, p38 MAPK, ERK 1/2 MAPK and other signaling pathways in the liver, macrophages, adipocytes, vascular endothelial cells, smooth muscle cells and myocardial cells. Paeoniflorin can regulate insulin sensitivity and liver activity, and improve glucose and lipid metabolism. Moreover, paeoniflorin can improve the proliferation and migration of VSMCs, regulate the levels of blood lipids, protect the vascular endothelium and achieve the goal of anti-atherosclerosis through exerting anti-inflammatory and antioxidant stress. In addition, paeoniflorin can inhibit cardiomyocyte apoptosis and myocardial remodeling, reduce ischemia-reperfusion damage, and improve cardiac function. Abbreviations: ANGPTL3, angiopoietin like protein 3; COX-2, cyclooxygenase-2; CYP7A1, cytochrome P4507A1; FFA, free fatty acids; GALNT-2, N-acetylgalactosaminyltransferase 2; GSK3β, glycogen synthase kinase (GSK)-3β; HMG-CoAR, 3-hydroxy-3-methylglutaryl coenzyme A reductase; ICAM-1, inter cellular adhesion molecule-1; IL, interleukin; iNOS, nitric oxide synthase; IREα, inositol enzyme 1alpha; IRS, INSR substrate; LPL, lipoprotein lipase; MCP-1, monocyte chemoattractant protein-1; MDA, malondialdehyde; NF-κB, ; Nrf2, nuclear factor erythroid factor 2-related factor 2; Nox, NADPH oxidase; PDGF-BB, platelet-derived growth factor BB; ROCK, Rho kinase; ROS, reactive oxygen species; SOD, superoxide dismutase; TGF-β, transforming growth factor-β; TLR, toll like receptors; TNF-α, tumor necrosis factor-α; VSMCs, vascular smooth muscle cells.

advantage in treating coronary heart disease. It can effectively relieve symptoms of angina pectoris, improve ECG, reduce the level of blood lipids, and improve endothelial function, among others (Wang and Qiu, 2019; Zhang et al., 2021b). Additionally, Shensong Yangxin (SSYX) capsule consists of Chishao and 11 additional botanical drugs. A randomized, double-blind, controlled, multicenter trial demonstrated a significant effect of SSYX capsules in reducing the number of premature ventricular contractions (PVC) and relieving symptoms associated with PVC compared with placebo or mexiletine (Zou et al., 2011). Furthermore, Tongxinluo (TXL) capsule contains radix paeoniae rubra and 11 additional botanical drugs (Hao et al., 2015). Related clinical studies have shown that TXL can anti arteriosclerosis, reduce blood lipid levels, improve angina pectoris, reduce the incidence of restenosis, and significantly reduce the incidence of no-reflow and myocardial infarction area after primary PCI (Chen et al., 2008b; Chen et al., 2011; Zhang et al., 2019). Danlou (DL) tablets are also a kind of Chinese patent medicine composed of Chishao and other botanical drugs. It has been widely used to treat coronary artery disease in China for a long time. Relevant clinical research demonstrated that DL can treat stable angina pectoris, alleviate adverse left ventricular remodeling after myocardial infarction, and reduce the peri-procedural myocardial injury among patients undergoing PCI for non-ST elevation acute coronary syndrome (Wang et al., 2015; Mao et al., 2016; Yang et al., 2020; Zhao et al., 2021).

7 Conclusion and future directions

Paeoniflorin, an effective component of natural plants, protects the cardiovascular system through multiple pharmacological actions (Figure 4). It can regulate lipid synthesis and metabolism via numerous processes, such as the *de novo* synthesis, lipid oxidation, cholesterol synthesis, and output. Also, it can inhibit the inflammatory response induced by the NF-κB signaling pathway through multiple targets, regulate macrophage function, and inflammation-induced endothelial dysfunction. Additionally,

paeoniflorin decreases oxidative stress-induced cellular dysfunction by decreasing the excessive production or accumulation of ROS. It can also stymie atherosclerosis by decreasing cholesterol deposition, and eradicating inflammatory, oxidative and platelet aggregation effects. Besides, it ameliorates cardiac dysfunction by regulating the PI3K/Akt signalling pathway, attenuating cardiac remodeling, and alleviating ischemia-reperfusion injury inspired by inhibition of the MAPK signaling pathway. Not only this, but paeoniflorin also has various pharmacological benefits, such as reduction in blood pressure, arrhythmia improvement, angiogenesis regulation, and lucubration of insulin resistance.

In summary, paeoniflorin is a natural drug with high potential development. However, pharmacokinetic studies have shown that its low bioavailability, and therefore necessitating combining it with other traditional Chinese medicines to significantly improve its pharmacokinetic parameters. It has been shown that the esterified derivatives of paeoniflorin could improve the bioavailability and have beneficial pharmacodynamics. Consequently, how to further develop paeoniflorin, improve its bioavailability and extend its medicinal applications is the next focus in pharmaceutics. In regards to safety, certain basic experiments have revealed hepatoprotective effects of paeoniflorin, such as its ability to interfere with bile acid metabolism and pivotal inflammation-related targets, as well as its capacity to ameliorate cholestatic liver injury (Wei et al., 2020; Liu et al., 2022). Despite this, whether paeoniflorin could cause liver injury has not been declared yet. In addition, paeoniflorin is mainly excreted in urine through glomerular filtration, and its effect on renal function has not been reported. In attempts to promote paeoniflorin application, it is essential to analyze its possible toxicity and safety.

At present, the protective effects of paeoniflorin on CVDs are mainly based on animal or cell experimental model. Most of the corresponding clinical studies mainly address Chinese herbal compound preparations containing paeoniflorin or Chishao, with popular treatments including NXT, BYHW, XFZY, Shensong Yangxin, TXL,DL, and so on. Although most studies have proved that paeoniflorin has a wide range of effects on the prevention and treatment of CVDs, but the above studies inevitably have some objective limitations, which is not enough for the scientific research and clinical application of paeoniflorin. Therefore, the next step is to carefully design multicenter, large-scale, and randomized controlled trial studies to assess the efficacy and toxicological characteristics of paeoniflorin alone for CVDs. In addition, paeoniflorin's basic research, including metabonomics, proteomics, genomics and network pharmacology, should be carried out to fully understand its pharmacological effects and molecular mechanisms. As a therapeutic agent with significant medical application potential, paeoniflorin is worthy of further development and utilization in the foreseeable future.

Author contributions

LL and MW contributed to the conception and design of the study. XL wrote the first draft of this manuscript. CS and XL contributed to drawing relevant diagrams and tables. JZ, LH, and ZY critically revised the article. XZ, ZW, and JC contributed to the identification of relevant references. All authors have contributed to the manuscript and approved the submitted version.

Funding

This study was financially supported by the National Natural Science Foundation of China (Grant No. 81973689), Beijing Natural Science Foundation (7202176), Capital Health Development Scientific Research Program (2022-2-4172), and State Administration of Traditional Chinese Medicine young scholars of Qi Huang (No. 7 [2020]).

Conflict of interest

The authors declare that the research was conducted in the absence of any commercial or financial relationships that could be construed as a potential conflict of interest.

Publisher's note

All claims expressed in this article are solely those of the authors and do not necessarily represent those of their affiliated organizations, or those of the publisher, the editors and the reviewers. Any product that may be evaluated in this article, or claim that may be made by its manufacturer, is not guaranteed or endorsed by the publisher.

References

Aggarwal, B. B., Gupta, S. C., and Kim, J. H. (2012). Historical perspectives on tumor necrosis factor and its superfamily: 25 years later, a golden journey. *Blood* 119 (3), 651–665. doi:10.1182/blood-2011-04-325225

Arnett, D. K., Blumenthal, R. S., Albert, M. A., Buroker, A. B., Goldberger, Z. D., Hahn, E. J., et al. (2019). 2019 ACC/AHA guideline on the primary prevention of cardiovascular disease: Executive summary: A report of the American college of cardiology/American heart association task force on clinical practice guidelines. *Circulation* 140 (11), e563–e595. doi:10.1161/CIR.0000000000000677

Badimon, L., Romero, J. C., Cubedo, J., and Borrell-Pagès, M. (2012). Circulating biomarkers. *Thromb. Res.* 130 (1), S12–S15. doi:10.1016/j.thromres.2012.08.262

Battson, M. L., Lee, D. M., and Gentile, C. L. (2017). Endoplasmic reticulum stress and the development of endothelial dysfunction. *Am. J. Physiol. Heart Circ. Physiol.* 312 (3), H355–H367. doi:10.1152/ajpheart.00437.2016

Bennett, M. R., Sinha, S., and Owens, G. K. (2016). Vascular smooth muscle cells in atherosclerosis. *Circ. Res.* 118 (4), 692–702. doi:10.1161/CIRCRESAHA.115.306361

Bi, X., Han, L., Qu, T., Mu, Y., Guan, P., Qu, X., et al. (2017). Anti-inflammatory effects, SAR, and action mechanism of monoterpenoids from radix paeoniae Alba on LPS-stimulated RAW 264.7 cells. *Molecules* 22 (5), 715. doi:10.3390/molecules22050715

Chan, K., Liu, Z. Q., Jiang, Z. H., Zhou, H., Wong, Y. F., Xu, H. X., et al. (2006). The effects of sinomenine on intestinal absorption of paeoniflorin by the everted rat gut sac model. *J. Ethnopharmacol.* 103 (3), 425–432. doi:10.1016/j.jep.2005.08.020

Chen, C., Du, P., and Wang, J. (2015). Paeoniflorin ameliorates acute myocardial infarction of rats by inhibiting inflammation and inducible nitric oxide synthase signaling pathways. *Mol. Med. Rep.* 12 (3), 3937–3943. doi:10.3892/mmr.2015.3870

Chen, D. K., Zhang, H. Q., and Zhang, J. H. (2008). Intervening effect of naoxintong on anti-platelet treatment with aspirin. *Zhongguo Zhong Xi Yi Jie He Za Zhi* 28 (9), 843–846.

Chen, D., Li, Y., Wang, X., Li, K., Jing, Y., He, J., et al. (2016). Generation of regulatory dendritic cells after treatment with paeoniflorin. *Immunol. Res.* 64 (4), 988–1000. doi:10.1007/s12026-015-8773-7

Chen, H., Dong, Y., He, X., Li, J., and Wang, J. (2018). Paeoniflorin improves cardiac function and decreases adverse postinfarction left ventricular remodeling in a rat model of acute myocardial infarction. *Drug Des. Devel Ther.* 12, 823–836. doi:10.2147/DDDT.S163405

Chen, J., Zhang, M., Zhu, M., Gu, J., Song, J., Cui, L., et al. (2018). Paeoniflorin prevents endoplasmic reticulum stress-associated inflammation in lipopolysaccharide-stimulated human umbilical vein endothelial cells via the IRE1α/NF-κB signaling pathway. *Food Funct.* 9 (4), 2386–2397. doi:10.1039/c7fo01406f

Chen, K. J., Shi, D. z., Xu, H., Lü, S. z., Li, T. c., Ke, Y. n., et al. (2006). XS0601 reduces the incidence of restenosis: A prospective study of 335 patients undergoing percutaneous coronary intervention in China. *Chin. Med. J. Engl.* 119 (1), 6–13. doi:10.1097/00029330-200601010-00002

Chen, Q., Liu, Y., Zhang, Y., Jiang, X., Zhang, Y., and Asakawa, T. (2020). An *in vitro* verification of the effects of paeoniflorin on lipopolysaccharide-exposed microglia. *Evid. Based Complement. Altern. Med.* 2020, 5801453. doi:10.1155/2020/5801453

Chen, Q., Yin, C., Li, Y., Yang, Z., and Tian, Z. (2021). Pharmacokinetic interaction between peimine and paeoniflorin in rats and its potential mechanism. *Pharm. Biol.* 59 (1), 129–133. doi:10.1080/13880209.2021.1875013

Chen, T., Guo, Z. P., Wang, L., Qin, S., Cao, N., Li, M. M., et al. (2013). Paeoniflorin suppresses vascular damage and the expression of E-selectin and ICAM-1 in a mouse model of cutaneous Arthus reaction. *Exp. Dermatol* 22 (7), 453–457. doi:10.1111/exd.12174

Chen, W., Sun, X., Wang, W. j., Fu, X. d., Fu, D. y., Zhou, J. m., et al. (2008). Effects of tongxinluo capsule on cardiac ventricle remodeling after myocardial infarction: A multicentre clinical research. *Zhonghua Yi Xue Za Zhi* 88 (32), 2271–2273.

Chen, Z. Q., Hong, L., and Wang, H. (2011). Effect of tongxinluo capsule on platelet activities and vascular endothelial functions as well as prognosis in patients with acute coronary syndrome undergoing percutaneous coronary intervention. *Zhongguo Zhong Xi Yi Jie He Za Zhi* 31 (4), 487–491.

Cheng, C., Lin, J. z., Li, L., Yang, J. l., Jia, W. w., Huang, Y. h., et al. (2016). Pharmacokinetics and disposition of monoterpene glycosides derived from Paeonia lactiflora roots (Chishao) after intravenous dosing of antiseptic XueBiJing injection in human subjects and rats. *Acta Pharmacol. Sin.* 37 (4), 530–544. doi:10.1038/aps.2015.103

Cheng, Y. J., Imperatore, G., Geiss, L. S., Saydah, S. H., Albright, A. L., Ali, M. K., et al. (2018). Trends and disparities in cardiovascular mortality among U.S. Adults with and without secf-reported diabetes, 1988-2015. *Diabetes Care* 41 (11), 2306–2315. doi:10.2337/dc18-0831

Committee, N. P. (2020). *Pharmacopoeia of the people's Republic of China*. Part 1, 108–165.

de Kleijn, D., and Pasterkamp, G. (2003). Toll-like receptors in cardiovascular diseases. *Cardiovasc Res.* 60 (1), 58–67. doi:10.1016/s0008-6363(03)00348-1

Di Meo, S., and Venditti, P. (2020). Evolution of the knowledge of free radicals and other oxidants. *Oxid. Med. Cell Longev.* 2020, 9829176. doi:10.1155/2020/9829176

Ding, Z., Liu, S., Wang, X., Deng, X., Fan, Y., Sun, C., et al. (2015). Hemodynamic shear stress via ROS modulates PCSK9 expression in human vascular endothelial and smooth muscle cells and along the mouse aorta. *Antioxid. Redox Signal* 22 (9), 760–771. doi:10.1089/ars.2014.6054

Fan, X., Wu, J., Yang, H., Yan, L., and Wang, S. (2018). Paeoniflorin blocks the proliferation of vascular smooth muscle cells induced by plateletderived growth factorBB through ROS mediated ERK1/2 and p38 signaling pathways. *Mol. Med. Rep.* 17 (1), 1676–1682. doi:10.3892/mmr.2017.8093

Fang, Y., Wu, L. C., Ma, K., Pan, G., Yang, S., Zheng, Y., et al. (2020). Paeoniflorin alleviates lipopolysaccharide-induced disseminated intravascular coagulation by inhibiting inflammation and coagulation activation. *Drug Dev. Res.* 81 (4), 517–525. doi:10.1002/ddr.21647

Fei, F., Yang, H., Peng, Y., Wang, P., Wang, S., Zhao, Y., et al. (2016). Sensitive analysis and pharmacokinetic study of the isomers paeoniflorin and albiflorin after oral administration of Total Glucosides of White Paeony Capsule in rats. *J. Chromatogr. B Anal. Technol. Biomed. Life Sci.* 1022, 30–37. doi:10.1016/j.jchromb.2016.04.005

Fitzgerald, K. A., Palsson-McDermott, E. M., Bowie, A. G., Jefferies, C. A., Mansell, A. S., Brady, G., et al. (2001). Mal (MyD88-adapter-like) is required for Toll-like receptor-4 signal transduction. *Nature* 413 (6851), 78–83. doi:10.1038/35092578

Forstermann, U., Xia, N., and Li, H. (2017). Roles of vascular oxidative stress and nitric oxide in the pathogenesis of atherosclerosis. *Circ. Res.* 120 (4), 713–735. doi:10.1161/CIRCRESAHA.116.309326

Fox, C. S., Coady, S., Sorlie, P. D., D'Agostino, R. B., Pencina, M. J., Vasan, R. S., et al. (2007). Increasing cardiovascular disease burden due to diabetes mellitus: The framingham heart study. *Circulation* 115 (12), 1544–1550. doi:10.1161/CIRCULATIONAHA.106.658948

Frank, P. G., and Lisanti, M. P. (2008). ICAM-1: Role in inflammation and in the regulation of vascular permeability. *Am. J. Physiol. Heart Circ. Physiol.* 295 (3), H926–H927. doi:10.1152/ajpheart.00779.2008

Furukawa, S., Moriyama, M., Miyake, K., Nakashima, H., Tanaka, A., Maehara, T., et al. (2017). Interleukin-33 produced by M2 macrophages and other immune cells contributes to Th2 immune reaction of IgG4-related disease. *Sci. Rep.* 7, 42413. doi:10.1038/srep42413

Gao, L., Xiao, Z., Jia, C., and Wang, W. (2021). Effect of buyang huanwu decoction for the rehabilitation of ischemic stroke patients: A meta-analysis of randomized controlled trials. *Health Qual. Life Outcomes* 19 (1), 79. doi:10.1186/s12955-021-01728-6

Gong, C., Yang, H., Wei, H., Qi, C., and Wang, C. H. (2015). Pharmacokinetic comparisons by UPLC-MS/MS of isomer paeoniflorin and albiflorin after oral administration decoctions of single-herb Radix Paeoniae Alba and Zengmian Yiliu prescription to rats. *Biomed. Chromatogr.* 29 (3), 416–424. doi:10.1002/bmc.3292

Guo, K., Zhang, Y., Li, L., Zhang, J., Rong, H., Liu, D., et al. (2021). Neuroprotective effect of paeoniflorin in the mouse model of Parkinson's disease through α-synuclein/protein kinase C δ subtype signaling pathway. *Neuroreport* 32 (17), 1379–1387. doi:10.1097/WNR.0000000000001739

Guo, Y., Zhao, Y., Li, L., Wei, X., Gao, P., Zhou, Y., et al. (2017). Concentrationdependent effects of paeoniflorin on proliferation and apoptosis of vascular smooth muscle cells. *Mol. Med. Rep.* 16 (6), 9567–9572. doi:10.3892/mmr.2017.7776

Han, J., Tan, H., Duan, Y., Chen, Y., Zhu, Y., Zhao, B., et al. (2019). The cardioprotective properties and the involved mechanisms of NaoXinTong Capsule. *Pharmacol. Res.* 141, 409–417. doi:10.1016/j.phrs.2019.01.024

Han, X., Hu, S., Yang, Q., Sang, X., Tang, D., and Cao, G. (2022). Paeoniflorin ameliorates airway inflammation and immune response in ovalbumin induced asthmatic mice: From oxidative stress to autophagy. *Phytomedicine* 96, 153835. doi:10.1016/j.phymed.2021.153835

Hao, P. P., Jiang, F., Chen, Y. G., Yang, J., Zhang, K., Zhang, M. X., et al. (2015). Traditional Chinese medication for cardiovascular disease. *Nat. Rev. Cardiol.* 12 (2), 115–122. doi:10.1038/nrcardio.2014.177

Hattori, M., Shu, Y. Z., Shimizu, M., Hayashi, T., Morita, N., Kobashi, K., et al. (1985). Metabolism of paeoniflorin and related compounds by human intestinal bacteria. *Chem. Pharm. Bull. (Tokyo)* 33 (9), 3838–3846. doi:10.1248/cpb.33.3838

He, R., Xu, Y., Peng, J., Ma, T., Li, J., and Gong, M. (2017). The effects of 18β-glycyrrhetinic acid and glycyrrhizin on intestinal absorption of paeoniflorin using the everted rat gut sac model. *J. Nat. Med.* 71 (1), 198–207. doi:10.1007/s11418-016-1049-2

Heidenreich, P. A., Bozkurt, B., Aguilar, D., Allen, L. A., Byun, J. J., Colvin, M. M., et al. (2022). 2022 AHA/ACC/HFSA guideline for the management of heart failure: Executive summary: A report of the American college of cardiology/American heart association joint committee on clinical practice guidelines. *Circulation* 145 (18), e876–e894. doi:10.1161/CIR.0000000000001062

Heinzel, F. R., Hohendanner, F., Jin, G., Sedej, S., and Edelmann, F. (2015). Myocardial hypertrophy and its role in heart failure with preserved ejection fraction. *J. Appl. Physiol.* 119 (10), 1233–1242. doi:10.1152/japplphysiol.00374.2015

Hill, M. A., Yang, Y., Zhang, L., Sun, Z., Jia, G., Parrish, A. R., et al. (2021). Insulin resistance, cardiovascular stiffening and cardiovascular disease. *Metabolism* 119, 154766. doi:10.1016/j.metabol.2021.154766

Hong, D.-Y. (2011). *Peonies of the world*. Kew Pub.

Hong, H., Lu, X., Wu, C., Chen, J., Chen, C., Zhang, J., et al. (2022). A review for the pharmacological effects of paeoniflorin in the nervous system. *Front. Pharmacol.* 13, 898955. doi:10.3389/fphar.2022.898955

Hu, H., Zhu, Q., Su, J., Wu, Y., Zhu, Y., Wang, Y., et al. (2017). Effects of an enriched extract of paeoniflorin, a monoterpene glycoside used in Chinese herbal medicine, on cholesterol metabolism in a hyperlipidemic rat model. *Med. Sci. Monit.* 23, 3412–3427. doi:10.12659/msm.905544

Hu, P. Y., Liu, D., Zheng, Q., Wu, Q., Tang, Y., and Yang, M. (2016). Elucidation of transport mechanism of paeoniflorin and the influence of ligustilide, senkyunolide I and senkyunolide A on paeoniflorin transport through mdck-mdr1 cells as blood-brain barrier *in vitro* model. *Molecules* 21 (3), 300. doi:10.3390/molecules21030300

Hu, Y., and Yang, W. (2022). Paeoniflorin can improve acute lung injury caused by severe acute pancreatitis through Nrf2/ARE pathway. *Comput. Math. Methods Med.* 2022, 5712219. doi:10.1155/2022/5712219

Jiang, B., Qiao, J., Yang, Y., and Lu, Y. (2012). Inhibitory effect of paeoniflorin on the inflammatory vicious cycle between adipocytes and macrophages. *J. Cell Biochem.* 113 (8), 2560–2566. doi:10.1002/jcb.22173

Jiao, F., Varghese, K., Wang, S., Liu, Y., Yu, H., Booz, G. W., et al. (2021). Recent insights into the protective mechanisms of paeoniflorin in neurological, cardiovascular, and renal diseases. *J. Cardiovasc Pharmacol.* 77 (6), 728–734. doi:10.1097/FJC.0000000000001021

Joshi, A. D., Oak, S. R., Hartigan, A. J., Finn, W. G., Kunkel, S. L., Duffy, K. E., et al. (2010). Interleukin-33 contributes to both M1 and M2 chemokine marker expression in human macrophages. *BMC Immunol.* 11, 52. doi:10.1186/1471-2172-11-52

Kalogeropoulos, A. P., and Butler, J. (2022). Worsening cardiovascular disease epidemiology in the United States: The time for preparation is now. *J. Am. Coll. Cardiol.* 80 (6), 579–583. doi:10.1016/j.jacc.2022.05.035

Khetarpal, S. A., Schjoldager, K. T., Christoffersen, C., Raghavan, A., Edmondson, A. C., Reutter, H. M., et al. (2016). Loss of function of GALNT2 lowers high-density lipoproteins in humans, nonhuman primates, and rodents. *Cell Metab.* 24 (2), 234–245. doi:10.1016/j.cmet.2016.07.012

Kim, A. S., and Conte, M. S. (2020). Specialized pro-resolving lipid mediators in cardiovascular disease, diagnosis, and therapy. *Adv. Drug Deliv. Rev.* 159, 170–179. doi:10.1016/j.addr.2020.07.011

Kim, B. K., Hong, S. J., Lee, Y. J., Hong, S. J., Yun, K. H., Hong, B. K., et al. (2022). Long-term efficacy and safety of moderate-intensity statin with ezetimibe combination therapy versus high-intensity statin monotherapy in patients with atherosclerotic cardiovascular disease (RACING): A randomised, open-label, non-inferiority trial. *Lancet* 400 (10349), 380–390. doi:10.1016/S0140-6736(22)00916-3

Kong, P., Chi, R., Zhang, L., Wang, N., and Lu, Y. (2013). Effects of paeoniflorin on tumor necrosis factor-alpha-induced insulin resistance and changes of adipokines in 3T3-L1 adipocytes. *Fitoterapia* 91, 44–50. doi:10.1016/j.fitote.2013.08.010

Koo, Y. K., Kim, J. M., Koo, J. Y., Kang, S. S., Bae, K., Kim, Y. S., et al. (2010). Platelet anti-aggregatory and blood anti-coagulant effects of compounds isolated from Paeonia lactiflora and Paeonia suffruticosa. *Pharmazie* 65 (8), 624–628.

Lee, C. K., Lee, H. M., Kim, H. J., Park, H. J., Won, K. J., Roh, H. Y., et al. (2007). Syk contributes to PDGF-BB-mediated migration of rat aortic smooth muscle cells via MAPK pathways. *Cardiovasc Res.* 74 (1), 159–168. doi:10.1016/j.cardiores.2007.01.012

Lei, C., Chen, Z., Fan, L., Xue, Z., Chen, J., Wang, X., et al. (2022). Integrating metabolomics and network analysis for exploring the mechanism underlying the antidepressant activity of paeoniflorin in rats with CUMS-induced depression. *Front. Pharmacol.* 13, 904190. doi:10.3389/fphar.2022.904190

Leong, D. P., Joseph, P. G., McKee, M., Anand, S. S., Teo, K. K., Schwalm, J. D., et al. (2017). Reducing the global burden of cardiovascular disease, Part 2: Prevention and treatment of cardiovascular disease. *Circ. Res.* 121 (6), 695–710. doi:10.1161/CIRCRESAHA.117.311849

Li, B., Yang, Z. B., Lei, S. S., Su, J., Jin, Z. W., Chen, S. H., et al. (2018). Combined antihypertensive effect of paeoniflorin enriched extract and metoprolol in spontaneously hypertensive rats. *Pharmacogn. Mag.* 14 (53), 44–52. doi:10.4103/pm.pm_483_16

Li, B., Yang, Z. B., Lei, S. S., Su, J., Pang, M. X., Yin, C., et al. (2017). Beneficial effects of paeoniflorin enriched extract on blood pressure variability and target organ damage in spontaneously hypertensive rats. *Evid. Based Complement. Altern. Med.* 2017, 5816960. doi:10.1155/2017/5816960

Li, H., Jiao, Y., and Xie, M. (2017). Paeoniflorin ameliorates atherosclerosis by suppressing TLR4-mediated NF-κB activation. *Inflammation* 40 (6), 2042–2051. doi:10.1007/s10753-017-0644-z

Li, J. Z., Tang, X. N., Li, T. T., Liu, L. J., Yu, S. Y., Zhou, G. Y., et al. (2016). Paeoniflorin inhibits doxorubicin-induced cardiomyocyte apoptosis by downregulating microRNA-1 expression. *Exp. Ther. Med.* 11 (6), 2407–2412. doi:10.3892/etm.2016.3182

Li, J. Z., Wu, J. H., Yu, S. Y., Shao, Q. R., and Dong, X. M. (2013). Inhibitory effects of paeoniflorin on lysophosphatidylcholine-induced inflammatory factor production in human umbilical vein endothelial cells. *Int. J. Mol. Med.* 31 (2), 493–497. doi:10.3892/ijmm.2012.1211

Li, W., Tao, W., Chen, J., Zhai, Y., Yin, N., and Wang, Z. (2020). Paeoniflorin suppresses IL-33 production by macrophages. *Immunopharmacol. Immunotoxicol.* 42 (3), 286–293. doi:10.1080/08923973.2020.1750628

Li, W., Zhi, W., Liu, F., Zhao, J., Yao, Q., and Niu, X. (2018). Paeoniflorin inhibits VSMCs proliferation and migration by arresting cell cycle and activating HO-1 through MAPKs and NF-κB pathway. *Int. Immunopharmacol.* 54, 103–111. doi:10.1016/j.intimp.2017.10.017

Li, Y., Chen, K., and Shi, Z. (1998). Effect of xuefu zhuyu pill on blood stasis syndrome and risk factor of atherosclerosis. *Zhongguo Zhong Xi Yi Jie He Za Zhi* 18 (2), 71–73.

Li, Y. C., Qiao, J. Y., Wang, B. Y., Bai, M., Shen, J. D., and Cheng, Y. X. (2018). Paeoniflorin ameliorates fructose-induced insulin resistance and hepatic steatosis by activating LKB1/AMPK and AKT pathways. *Nutrients* 10 (8), 1024. doi:10.3390/nu10081024

Li, Y., Yin, S., Chen, X., Shi, F., Wang, J., and Yang, H. (2022). The inhibitory effect of paeoniflorin on reactive oxygen species alleviates the activation of NF-κB and MAPK signalling pathways in macrophages. *Microbiol. Read.* 168 (8). doi:10.1099/mic.0.001210

Lin, Y. T., Huang, W. S., Tsai, H. Y., Lee, M. M., and Chen, Y. F. (2019). *In vivo* microdialysis and *in vitro* HPLC analysis of the impact of paeoniflorin on the monoamine levels and their metabolites in the rodent brain. *Biomed. (Taipei)* 9 (2), 11. doi:10.1051/bmdcn/2019090211

Liu, M., Ai, J., Feng, J., Zheng, J., Tang, K., Shuai, Z., et al. (2019). Effect of paeoniflorin on cardiac remodeling in chronic heart failure rats through the transforming growth factor β1/Smad signaling pathway. *Cardiovasc Diagn Ther.* 9 (3), 272–280. doi:10.21037/cdt.2019.06.01

Liu, T., Zhang, N., Kong, L., Chu, S., Zhang, T., Yan, G., et al. (2022). Paeoniflorin alleviates liver injury in hypercholesterolemic rats through the ROCK/AMPK pathway. *Front. Pharmacol.* 13, 968717. doi:10.3389/fphar.2022.968717

Liu, X., Chen, K., Zhuang, Y., Huang, Y., Sui, Y., Zhang, Y., et al. (2019). Paeoniflorin improves pressure overload-induced cardiac remodeling by modulating the MAPK signaling pathway in spontaneously hypertensive rats. *Biomed. Pharmacother.* 111, 695–704. doi:10.1016/j.biopha.2018.12.090

Liu, Y., Han, J., Zhou, Z., and Li, D. (2019). Paeoniflorin protects pancreatic beta cells from STZ-induced damage through inhibition of the p38 MAPK and JNK signaling pathways. *Eur. J. Pharmacol.* 853, 18–24. doi:10.1016/j.ejphar.2019.03.025

Liu, Z. Q., Jiang, Z. H., Liu, L., and Hu, M. (2006). Mechanisms responsible for poor oral bioavailability of paeoniflorin: Role of intestinal disposition and interactions with sinomenine. *Pharm. Res.* 23 (12), 2768–2780. doi:10.1007/s11095-006-9100-8

Long-Tao, L. (2018). Chinese experts consensus on clinical application of naoxintong capsule. *Chin. J. Integr. Med.* 24 (3), 232–236. doi:10.1007/s11655-018-2981-6

Lu, Y., Deng, Y., Liu, W., Jiang, M., and Bai, G. (2019). Searching for calcium antagonists for hypertension disease therapy from Moutan Cortex, using bioactivity integrated UHPLC-QTOF-MS. *Phytochem. Anal.* 30 (4), 456–463. doi:10.1002/pca.2828

Luo, N., Li, Z., Qian, D., Qian, Y., Guo, J., Duan, J. A., et al. (2014). Simultaneous determination of bioactive components of Radix Angelicae Sinensis-Radix Paeoniae Alba herb couple in rat plasma and tissues by UPLC-MS/MS and its application to pharmacokinetics and tissue distribution. *J. Chromatogr. B Anal. Technol. Biomed. Life Sci.* 963, 29–39. doi:10.1016/j.jchromb.2014.05.036

Lv, P., Peng, Q., Liu, Y., Jin, H., Liu, R., et al. (2016). Treatment with the herbal medicine, naoxintong improves the protective effect of high-density lipoproteins on endothelial function in patients with type 2 diabetes. *Mol. Med. Rep.* 13 (3), 2007–2016. doi:10.3892/mmr.2016.4792

Ma, Z., Chu, L., Liu, H., Wang, W., Li, J., Yao, W., et al. (2017). Beneficial effects of paeoniflorin on non-alcoholic fatty liver disease induced by high-fat diet in rats. *Sci. Rep.* 7, 44819. doi:10.1038/srep44819

Ma, Z., Liu, H., Wang, W., Guan, S., Yi, J., and Chu, L. (2017). Paeoniflorin suppresses lipid accumulation and alleviates insulin resistance by regulating the Rho kinase/IRS-1 pathway in palmitate-induced HepG2Cells. *Biomed. Pharmacother.* 90, 361–367. doi:10.1016/j.biopha.2017.03.087

Madsbad, S. (1992). Hypoglycemia in diabetes mellitus. Symptoms, epidemiology, physiopathology, causes and treatment. *Ugeskr. Laeger* 154 (5), 246–250.

Mao, L., Chen, J., Cheng, K., Dou, Z., Leavenworth, J. D., Yang, H., et al. (2022). Nrf2-Dependent protective effect of paeoniflorin on α-naphthalene isothiocyanate-induced hepatic injury. *Am. J. Chin. Med.* 50 (5), 1331–1348. doi:10.1142/S0192415X22500562

Mao, S., Wang, L., Ouyang, W., Zhou, Y., Qi, J., Guo, L., et al. (2016). Traditional Chinese medicine, Danlou tablets alleviate adverse left ventricular remodeling after myocardial infarction: Results of a double-blind, randomized, placebo-controlled, pilot study. *BMC Complement. Altern. Med.* 16 (1), 447. doi:10.1186/s12906-016-1406-4

Misao, J., Hayakawa, Y., Ohno, M., Kato, S., Fujiwara, T., and Fujiwara, H. (1996). Expression of bcl-2 protein, an inhibitor of apoptosis, and Bax, an accelerator of apoptosis, in ventricular myocytes of human hearts with myocardial infarction. *Circulation* 94 (7), 1506–1512. doi:10.1161/01.cir.94.7.1506

Most, J., Schwaeble, W., and Dierich, M. P. (1992). Expression of intercellular adhesion molecule-1 (ICAM-1) on human monocytes. *Immunobiology* 185 (2-4), 327–336. doi:10.1016/S0171-2985(11)80650-9

Murray, P. J. (2017). Macrophage polarization. *Annu. Rev. Physiol.* 79, 541–566. doi:10.1146/annurev-physiol-022516-034339

Ngo, T., Kim, K., Bian, Y., Noh, H., Lim, K. M., Chung, J. H., et al. (2019). Antithrombotic effects of paeoniflorin from Paeonia suffruticosa by selective inhibition on shear stress-induced platelet aggregation. *Int. J. Mol. Sci.* 20 (20), 5040. doi:10.3390/ijms20205040

Nizamutdinova, I. T., Jin, Y. C., Kim, J. S., Yean, M. H., Kang, S. S., Kim, Y. S., et al. (2008). Paeonol and paeoniflorin, the main active principles of Paeonia albiflora, protect the heart from myocardial ischemia/reperfusion injury in rats. *Planta Med.* 74 (1), 14–18. doi:10.1055/s-2007-993775

O'Sullivan, J. W., Raghavan, S., Marquez-Luna, C., Luzum, J. A., Damrauer, S. M., Ashley, E. A., et al. (2022). Polygenic risk scores for cardiovascular disease: A scientific statement from the American heart association. *Circulation* 146 (8), e93–e118. doi:10.1161/CIR.0000000000001077

Oka, T., Akazawa, H., Naito, A. T., and Komuro, I. (2014). Angiogenesis and cardiac hypertrophy: Maintenance of cardiac function and causative roles in heart failure. *Circ. Res.* 114 (3), 565–571. doi:10.1161/CIRCRESAHA.114.300507

Olvera Lopez, E., Ballard, B. D., and Jan, A. (2022). *Cardiovascular disease*. Treasure Island (FL: StatPearls.

Osaki, Y., Nakagawa, Y., Miyahara, S., Iwasaki, H., Ishii, A., Matsuzaka, T., et al. (2015). Skeletal muscle-specific HMG-CoA reductase knockout mice exhibit rhabdomyolysis: A model for statin-induced myopathy. *Biochem. Biophys. Res. Commun.* 466 (3), 536–540. doi:10.1016/j.bbrc.2015.09.065

Pirillo, A., Casula, M., Olmastroni, E., Norata, G. D., and Catapano, A. L. (2021). Global epidemiology of dyslipidaemias. *Nat. Rev. Cardiol.* 18 (10), 689–700. doi:10.1038/s41569-021-00541-4

Rivard, A., and Andres, V. (2000). Vascular smooth muscle cell proliferation in the pathogenesis of atherosclerotic cardiovascular diseases. *Histol. Histopathol.* 15 (2), 557–571. doi:10.14670/HH-15.557

Ruan, Y., Ling, J., Ye, F., Cheng, N., Wu, F., Tang, Z., et al. (2021). Paeoniflorin alleviates CFA-induced inflammatory pain by inhibiting TRPV1 and succinate/SUCNR1-HIF-1α/NLPR3 pathway. *Int. Immunopharmacol.* 101, 108364. doi:10.1016/j.intimp.2021.108364

Senoner, T., and Dichtl, W. (2019). Oxidative stress in cardiovascular diseases: Still a therapeutic target? *Nutrients* 11 (9), 2090. doi:10.3390/nu11092090

Seravalle, G., and Grassi, G. (2017). Obesity and hypertension. *Pharmacol. Res.* 122, 1–7. doi:10.1016/j.phrs.2017.05.013

Shaito, A., Aramouni, K., Assaf, R., Parenti, A., Orekhov, A., Yazbi, A. E., et al. (2022). Oxidative stress-induced endothelial dysfunction in cardiovascular diseases. *Front. Biosci. (Landmark Ed.* 27 (3), 105. doi:10.31083/j.fbl2703105

Shao, Y. X., Gong, Q., Qi, X. M., Wang, K., and Wu, Y. G. (2019). Paeoniflorin ameliorates macrophage infiltration and activation by inhibiting the TLR4 signaling pathway in diabetic nephropathy. *Front. Pharmacol.* 10, 566. doi:10.3389/fphar.2019.00566

Shen, C., Shen, B., Zhu, J., Wang, J., Yuan, H., and Li, X. (2021). Glycyrrhizic acid-based self-assembled micelles for improving oral bioavailability of paeoniflorin. *Drug Dev. industrial Pharm.* 47 (2), 207–214. doi:10.1080/03639045.2020.1862178

Shenasa, M., and Shenasa, H. (2017). Hypertension, left ventricular hypertrophy, and sudden cardiac death. *Int. J. Cardiol.* 237, 60–63. doi:10.1016/j.ijcard.2017.03.002

Shibata, S., and Nakahara, M. (1963). Studies on the constituents of Japanese and Chinese crude drugs. VIII. Paeoniflorin, A glucoside of Chinese paeony root.(1). *Chem. Pharm. Bull.* 11 (3), 372–378. doi:10.1248/cpb.11.372

Shoemaker, R., Yiannikouris, F., Thatcher, S., and Cassis, L. (2015). ACE2 deficiency reduces beta-cell mass and impairs beta-cell proliferation in obese C57BL/6 mice. *Am. J. Physiol. Endocrinol. Metab.* 309 (7), E621–E631. doi:10.1152/ajpendo.00054.2015

Song, S., Xiao, X., Guo, D., Mo, L., Bu, C., Ye, W., et al. (2017). Protective effects of Paeoniflorin against AOPP-induced oxidative injury in HUVECs by blocking the ROS-HIF-1α/VEGF pathway. *Phytomedicine* 34, 115–126. doi:10.1016/j.phymed.2017.08.010

Suganami, T., Nishida, J., and Ogawa, Y. (2005). A paracrine loop between adipocytes and macrophages aggravates inflammatory changes: Role of free fatty acids and tumor necrosis factor alpha. *Arterioscler. Thromb. Vasc. Biol.* 25 (10), 2062–2068. doi:10.1161/01.ATV.0000183883.72263.13

Sun, B., Dai, G., Bai, Y., Zhang, W., Zhu, L., Chu, J., et al. (2017). Determination of paeoniflorin in rat plasma by ultra-high performance liquid chromatography-tandem mass spectrometry and its application to a pharmacokinetic study. *J. Chromatogr. Sci.* 55 (10), 1006–1012. doi:10.1093/chromsci/bmx066

Sun, H., Wang, J., and Lv, J. (2019). Effects of glycyrrhizin on the pharmacokinetics of paeoniflorin in rats and its potential mechanism. *Pharm. Biol.* 57 (1), 550–554. doi:10.1080/13880209.2019.1651876

Sun, L.-C., Li, S., Wang, F., and Xin, F. (2017). Research progresses in the synthetic biology of terpenoids. *Biotechnol. Bull.* 33 (1), 64.

Tomek, J., and Bub, G. (2017). Hypertension-induced remodelling: On the interactions of cardiac risk factors. *J. Physiol.* 595 (12), 4027–4036. doi:10.1113/JP273043

Townsend, N., Kazakiewicz, D., Lucy Wright, F., Timmis, A., Huculeci, R., Torbica, A., et al. (2022). Epidemiology of cardiovascular disease in Europe. *Nat. Rev. Cardiol.* 19 (2), 133–143. doi:10.1038/s41569-021-00607-3

Tu, J., Guo, Y., Hong, W., Fang, Y., Han, D., Zhang, P., et al. (2019). The regulatory effects of paeoniflorin and its derivative paeoniflorin-6'-O-benzene sulfonate CP-25 on inflammation and immune diseases. *Front. Pharmacol.* 10, 57. doi:10.3389/fphar.2019.00057

Van Buul, J. D., Fernandez-Borja, M., Anthony, E. C., and Hordijk, P. L. (2005). Expression and localization of NOX2 and NOX4 in primary human endothelial cells. *Antioxid. Redox Signal* 7 (3-4), 308–317. doi:10.1089/ars.2005.7.308

Vignais, P. V. (2002). The superoxide-generating NADPH oxidase: Structural aspects and activation mechanism. *Cell Mol. Life Sci.* 59 (9), 1428–1459. doi:10.1007/s00018-002-8520-9

Wang, C., Yuan, J., Zhang, L. L., and Wei, W. (2016). Pharmacokinetic comparisons of Paeoniflorin and Paeoniflorin-6'O-benzene sulfonate in rats via different routes of administration. *Xenobiotica* 46 (12), 1142–1150. doi:10.3109/00498254.2016.1149633

Wang, L., Mao, S., Qi, J. y., Ren, Y., Guo, X. f., Chen, K. j., et al. (2015). Effect of Danlou tablet on peri-procedural myocardial injury among patients undergoing percutaneous coronary intervention for non-ST elevation acute coronary syndrome: A study protocol of a multicenter, randomized, controlled trial. *Chin. J. Integr. Med.* 21 (9), 662–666. doi:10.1007/s11655-015-2284-1

Wang, R., Ren, J., Li, S., Bai, X., Guo, W., Yang, S., et al. (2022). Efficacy evaluation of buyang huanwu decoction in the treatment of ischemic stroke in the recovery period: A systematic review of randomized controlled trials. *Front. Pharmacol.* 13, 975816. doi:10.3389/fphar.2022.975816

Wang, R. R., Zhang, Y. H., Ran, Y. Q., and Pu, J. L. (2011). The effects of paeoniflorin monomer of a Chinese herb on cardiac ion channels. *Chin. Med. J. Engl.* 124 (19), 3105–3111.

Wang, S., and Qiu, X. J. (2019). The efficacy of xue fu zhu Yu prescription for hyperlipidemia: A meta-analysis of randomized controlled trials. *Complement. Ther. Med.* 43, 218–226. doi:10.1016/j.ctim.2019.02.008

Wang, Y., Xu, Y., Zhang, L., Huang, S., Dou, L., Yang, J., et al. (2022). Comparison of buyang huanwu granules and naoxintong capsules in the treatment of stable angina pectoris: Rationale and design of a randomized, blinded, multicentre clinical trial. *Trials* 23 (1), 65. doi:10.1186/s13063-021-05914-1

Wei, S., Ma, X., Niu, M., Wang, R., Yang, T., Wang, D., et al. (2020). Mechanism of paeoniflorin in the treatment of bile duct ligation-induced cholestatic liver injury using integrated metabolomics and network pharmacology. *Front. Pharmacol.* 11, 586806. doi:10.3389/fphar.2020.586806

Wong, N. D., Budoff, M. J., Ferdinand, K., Graham, I. M., Michos, E. D., Reddy, T., et al. (2022). Atherosclerotic cardiovascular disease risk assessment: An American Society for Preventive Cardiology clinical practice statement. *Am. J. Prev. Cardiol.* 10, 100335. doi:10.1016/j.ajpc.2022.100335

Wu, F., Ye, B., Wu, X., Lin, X., Li, Y., Wu, Y., et al. (2020). Paeoniflorin on rat myocardial ischemia reperfusion injury of protection and mechanism research. *Pharmacology* 105 (5-6), 281–288. doi:10.1159/000503583

Xia, S. M., Shen, R., Sun, X. Y., Shen, L. L., Yang, Y. M., Ke, Y., et al. (2007). Development and validation of a sensitive liquid chromatography-tandem mass spectrometry method for the determination of paeoniflorin in rat brain and its application to pharmacokinetic study. *J. Chromatogr. B Anal. Technol. Biomed. Life Sci.* 857 (1), 32–39. doi:10.1016/j.jchromb.2007.06.022

Xiao, H. B., Liang, L., Luo, Z. F., and Sun, Z. L. (2018). Paeoniflorin regulates GALNT2-ANGPTL3-LPL pathway to attenuate dyslipidemia in mice. *Eur. J. Pharmacol.* 836, 122–128. doi:10.1016/j.ejphar.2018.08.006

Xiao, H. B., Wang, J. Y., and Sun, Z. L. (2017). ANGPTL3 is part of the machinery causing dyslipidemia majorily via LPL inhibition in mastitis mice. *Exp. Mol. Pathol.* 103 (3), 242–248. doi:10.1016/j.yexmp.2017.11.003

Xie, P., Cui, L., Shan, Y., and Kang, W. Y. (2017). Antithrombotic effect and mechanism of radix paeoniae rubra. *Biomed. Res. Int.* 2017, 9475074. doi:10.1155/2017/9475074

Xin, Q. Q., Yang, B. R., Zhou, H. F., Wang, Y., Yi, B. W., Cong, W. H., et al. (2018). Paeoniflorin promotes angiogenesis in A vascular insufficiency model of zebrafish *in vivo* and in human umbilical vein endothelial cells *in vitro*. *Chin. J. Integr. Med.* 24 (7), 494–501. doi:10.1007/s11655-016-2262-2

Xin, Q., Yuan, R., Shi, W., Zhu, Z., Wang, Y., and Cong, W. (2019). A review for the anti-inflammatory effects of paeoniflorin in inflammatory disorders. *Life Sci.* 237, 116925. doi:10.1016/j.lfs.2019.116925

Xu, H., Shi, D. Z., and Chen, K. J. (2001). Effect of xiongshao capsule on vascular remodeling in porcine coronary balloon injury model. *Zhongguo Zhong Xi Yi Jie He Za Zhi* 21 (8), 591–594.

Xu, J. X., Cao, Y., Zhu, Y. J., Li, X. Y., Ge, D. Z., et al. (2021). Modern research progress of traditional Chinese medicine Paeoniae Radix Alba and prediction of its Q-markers. *Zhongguo Zhong Yao Za Zhi* 46 (21), 5486–5495. doi:10.19540/j.cnki.cjcmm.20210818.201

Xu, W., Zhao, Y., Qin, Y., Ge, B., Gong, W., Wu, Y., et al. (2016). Enhancement of exposure and reduction of elimination for paeoniflorin or albiflorin via Co-administration with total Peony glucosides and hypoxic pharmacokinetics comparison. *Molecules* 21 (7), 874. doi:10.3390/molecules21070874

Xu, X., Wang, Y., Li, Y., Zhang, B., and Song, Q. (2022). The future landscape of macrophage research in cardiovascular disease: A bibliometric analysis. *Curr. Probl. Cardiol.* 47 (10), 101311. doi:10.1016/j.cpcardiol.2022.101311

Yang, G., He, H., Li, H., Shen, Z., Zhou, S., Lu, B., et al. (2020). Effects of Danlou tablet for the treatment of stable angina pectoris: A study protocol of a randomized, double-blind, and placebo-controlled clinical trial. *Med. Baltim.* 99 (49), e23416. doi:10.1097/MD.0000000000023416

Yang, H. O., Ko, W. K., Kim, J. Y., and Ro, H. S. (2004). Paeoniflorin: An antihyperlipidemic agent from Paeonia lactiflora. *Fitoterapia* 75 (1), 45–49. doi:10.1016/j.fitote.2003.08.016

Yang, X. Z., and Wei, W. (2020). CP-25, a compound derived from paeoniflorin: Research advance on its pharmacological actions and mechanisms in the treatment of inflammation and immune diseases. *Acta Pharmacol. Sin.* 41 (11), 1387–1394. doi:10.1038/s41401-020-00510-6

Yellon, D. M., and Hausenloy, D. J. (2007). Myocardial reperfusion injury. *N. Engl. J. Med.* 357 (11), 1121–1135. doi:10.1056/NEJMra071667

Yu, J. B., Zhao, Z. X., Peng, R., Pan, L. B., Fu, J., Ma, S. R., et al. (2019). Gut microbiota-based pharmacokinetics and the antidepressant mechanism of paeoniflorin. *Front. Pharmacol.* 10, 268. doi:10.3389/fphar.2019.00268

Yuan, R., Shi, W., Xin, Q., Yang, B., Hoi, M. P., Lee, S. M., et al. (2018). Tetramethylpyrazine and paeoniflorin inhibit oxidized LDL-induced angiogenesis in human umbilical vein endothelial cells via VEGF and notch pathways. *Evid. Based Complement. Altern. Med.* 2018, 3082507. doi:10.1155/2018/3082507

Yusuf, S., Joseph, P., Rangarajan, S., Islam, S., Mente, A., Hystad, P., et al. (2020). Modifiable risk factors, cardiovascular disease, and mortality in 155 722 individuals from 21 high-income, middle-income, and low-income countries (PURE): A prospective cohort study. *Lancet* 395 (10226), 795–808. doi:10.1016/S0140-6736(19)32008-2

Zhai, J., and Guo, Y. (2016). Paeoniflorin attenuates cardiac dysfunction in endotoxemic mice via the inhibition of nuclear factor-κB. *Biomed. Pharmacother.* 80, 200–206. doi:10.1016/j.biopha.2016.03.032

Zhai, T., Sun, Y., Li, H., Zhang, J., Huo, R., Li, H., et al. (2016). Unique immunomodulatory effect of paeoniflorin on type I and II macrophages activities. *J. Pharmacol. Sci.* 130 (3), 143–150. doi:10.1016/j.jphs.2015.12.007

Zhang, H., Liang, M. J., and Ma, Z. X. (1995). Clinical study on effects of buyang huanwu decoction on coronary heart disease. *Zhongguo Zhong Xi Yi Jie He Za Zhi* 15 (4), 213–215.

Zhang, L., and Wei, W. (2020). Anti-inflammatory and immunoregulatory effects of paeoniflorin and total glucosides of paeony. *Pharmacol. Ther.* 207, 107452. doi:10.1016/j.pharmthera.2019.107452

Zhang, L., Yang, B., and Yu, B. (2015). Paeoniflorin protects against nonalcoholic fatty liver disease induced by a high-fat diet in mice. *Biol. Pharm. Bull.* 38 (7), 1005–1011. doi:10.1248/bpb.b14-00892

Zhang, M., Liu, Y., Xu, M., Zhang, L., Liu, Y., Liu, X., et al. (2019). Carotid artery plaque intervention with tongxinluo capsule (capital): A multicenter randomized double-blind parallel-group placebo-controlled study. *Sci. Rep.* 9 (1), 4545. doi:10.1038/s41598-019-41118-z

Zhang, S., Chen, Z. L., Tang, Y. P., Duan, J. L., and Yao, K. W. (2021). Efficacy and safety of xue-fu-zhu-yu decoction for patients with coronary heart disease: A systematic review and meta-analysis. *Evid. Based Complement. Altern. Med.* 2021, 9931826. doi:10.1155/2021/9931826

Zhang, S., Jiang, M., Yan, S., Liang, M., Wang, W., Yuan, B., et al. (2021). Network pharmacology-based and experimental identification of the effects of paeoniflorin on major depressive disorder. *Front. Pharmacol.* 12, 793012. doi:10.3389/fphar.2021.793012

Zhang, X. X., Zuo, J. Q., Wang, Y. T., Duan, H. Y., Yuan, J. H., and Hu, Y. H. (2022). Paeoniflorin in Paeoniaceae: Distribution, influencing factors, and biosynthesis. *Front. Plant Sci.* 13, 980854. doi:10.3389/fpls.2022.980854

Zhao, X., Chen, Y., Li, L., Zhai, J., Yu, B., Wang, H., et al. (2021). Effect of DLT-SML on chronic stable angina through ameliorating inflammation, correcting dyslipidemia, and regulating gut microbiota. *J. Cardiovasc Pharmacol.* 77 (4), 458–469. doi:10.1097/FJC.0000000000000970

Zhou, H., Yang, H. X., Yuan, Y., Deng, W., Zhang, J. Y., Bian, Z. Y., et al. (2013). Paeoniflorin attenuates pressure overload-induced cardiac remodeling via inhibition of TGFβ/Smads and NF-κB pathways. *J. Mol. Histol.* 44 (3), 357–367. doi:10.1007/s10735-013-9491-x

Zhou, S.-L., Xu, C., Liu, J., Yu, Y., Wu, P., Cheng, T., et al. (2021). Out of the pan-himalaya: Evolutionary history of the Paeoniaceae revealed by phylogenomics. *J. Syst. Evol.* 59 (6), 1170–1182. doi:10.1111/jse.12688

Zou, J. G., Zhang, J., Jia, Z. H., and Cao, K. J. (2011). Evaluation of the traditional Chinese medicine shensongyangxin capsule on treating premature ventricular contractions: A randomized, double-blind, controlled multicenter trial. *Chin. Med. J. Engl.* 124 (1), 76–83.

Frontiers in Pharmacology

Explores the interactions between chemicals and living beings

The most cited journal in its field, which advances access to pharmacological discoveries to prevent and treat human disease.

Discover the latest Research Topics

See more →

Frontiers

Avenue du Tribunal-Fédéral 34
1005 Lausanne, Switzerland
frontiersin.org

Contact us

+41 (0)21 510 17 00
frontiersin.org/about/contact